DESIGN GUIDELINES FOR TEST LEVEL 3 (TL-3) THROUGH TEST LEVEL 5 (TL-5) ROADSIDE BARRIER SYSTEMS PLACED ON MECHANICALLY STABILIZED EARTH (MSE) RETAINING WALL

A Dissertation

by

DEEYVID OSCAR SAEZ BARRIOS

Submitted to the Office of Graduate Studies of
Texas A&M University
in partial fulfillment of the requirements for the degree of

DOCTOR OF PHILOSOPHY

Approved by:

Chair of Committee,	Jean-Louis Briaud
Committee Members,	Charles Aubeny
	Stefan Hurlebaus
	Alan Palazzolo
Head of Department,	John Niedzwecki

December 2012

Major Subject: Civil Engineering

ABSTRACT

The use of Mechanically Stabilized Earth (MSE) wall structures has increased dramatically in recent years. Traffic barriers are frequently placed on top of the MSE wall to resist vehicular impact loads. The barrier systems are anchored to the concrete in case of rigid pavement. Nevertheless, in case of flexible pavement, the barriers are constructed in an L shape so that the impact load on the vertical part of the L can be resisted by the inertia force required to uplift the horizontal part of the L. The barrier must be designed to resist the full dynamic load but the size of the horizontal part of the L (moment slab) is determined using an equivalent static load.

Current design practice of barriers mounted on top of MSE retaining wall is well defined for passenger cars and light trucks. However, the information of this impact level is extrapolated to heavy vehicle impact. Therefore, the bases of this research is to develop design procedure and to help understand the dynamic behavior of a barrier-moment slab system on top of an MSE wall when subjected to heavy vehicle impact loads.

In a first part, numerical analyses were conducted to better understand the behavior of the barrier-moment slab system when subjected to heavy vehicle impact loads. The full-scale impact simulations were used to develop the recommendation for designing and sizing the barrier-moment slab system.

In a second part, the barrier-moment slab systems defined to contain heavy vehicle impact loads were placed on top of an MSE wall model to study the kinematic

behavior of the system. Loads in the soil reinforcing strips and displacements on the barriers and wall components are evaluated to define recommendation for design of strip reinforcements against pullout and yielding.

In a third part, a full-scale crash test on a barrier-moment slab system on top of an instrumented 9.8 ft (3 m) high MSE wall is described and analyzed. The MSE wall and barrier system were adequate to contain and redirected the vehicle and, therefore, it served as verification of the proposed recommendation.

Finally, conclusions are drawn on the basis of the information presented herein.

ACKNOWLEDGEMENTS

This research proposal is part of a project sponsored by the National Cooperative Highway Research Program (NCHRP). The author wishes to thank the NCHRP panel members for their input. The assistantship of Mark McClelland and Mr. Charles W. Niessner is particularly noted.

I would like to express my deepest gratitude to my adviser, Dr. Jean-Louis Briaud and to Dr. Roger Bligh, for their guidance, support and giving me the opportunity to work in this research project. In addition, many thanks to the research team of this project, Dr. Akram Abu-Odeh and Dr. Kang-mi Kim, and to all the Texas Transportation Institute staff at Riverside Campus.

The author also wishes to sincerely thank the Reinforced Earth Company, Mr. Pete Anderson, Mr. Carl Sanders, and Mr. David Hutchinson, for their help on answering many questions and for providing the material for the construction of the full-scale MSE test wall.

The author acknowledges the assistance of Dr. Jose Roesset, Dr. Gene Buth, Dr. Chuck Plaxico, Dr. Chiara Silvestri, Mr. Dusty Arrington, Mr. Nauman Sheikh, Mr. Gary Gerke, Mr. Dick Zimmer and Dr. Robert Warden for their input in many topics related to this research.

The author wants to thanks the committee member of this thesis dissertation, Dr. Charles Aubeny, Dr. Stefan Hurlebaus and Dr. Alan Palazzolo.

Finally, the author acknowledges the Texas A&M Supercomputing Facility (http://sc.tamu.edu/) for providing computing resources used in conducting the numerical simulations.

TABLE OF CONTENTS

Page

Page

Page

Page

Page

LIST OF FIGURES

Page

Page

Page

Page

Page

Page

Page

Page

Page

Page

Page

Page

Page

LIST OF TABLES

Page

Page

Page

Page

Page

1 INTRODUCTION

1.1 Problem Statement

The use of Mechanically Stabilized Earth (MSE) retaining walls in highway applications has increased over the last decades. According to the Federal Highway Administration (FHWA), it is estimated that more than 9,000,000 ft^2 (850,000 m^2) of MSE retaining walls with precast facing are constructed on average every year in the United States. This may represent more than half of all retaining wall usage for transportation applications *(1).*

One major use of MSE wall systems constitutes its application as fill-retaining structures in conjunction with bridges. These MSE walls are typically constructed with a roadside barrier system supported on the edge of the wall. This barrier system generally consists of a traffic barrier or bridge rail placed on a structural slab (e.g., rigid pavement) or on a continuous footing (e.g., flexible pavement). In the case of a rigid pavement, the structural slab of the pavement provides the resistance to anchor the barrier to the concrete slab and resist the impact of an errant vehicle. However, in the case of a flexible pavement, that resistance does not exist and a moment slab is required to anchor the barrier and provide the required inertial resistance to withstand a vehicle impact.

The design practices of MSE retaining walls moved from an Allowable Stress Design (ASD) method to a Load and Resistance Factor Design (LRDF) method. This

change includes consideration of new design parameters that has not been properly defined for use of the LFRD design approach. Therefore, extensive research has been conducted over the last decade to help improve the design procedure of MSE wall structures. Part of this research effort has been focused on calibration of the load and resistance factors used in the LRFD design procedure. However, the majority of these studies have been focused on gravity wall and little work had been conducted on L shaped barrier-foundation system on top of MSE wall prior the publication of NCHRP Report 663 *(2)*.

Vehicular impact loads also generate forces in the MSE wall reinforcement and wall panels in addition to the static loads due to gravity. The design loads for evaluation of barriers placed on top of MSE retaining wall are based on the current design loads presented in AASHTO LRFD Table A13.2-1 "Design Forces for Traffic Railings" *(3)*. These design forces correspond to test levels defined in NCHRP Report 350, "Recommended Procedures for the Safety Performance Evaluation of Highway Features" *(4)*. However, this document was updated after AASHTO published the AASHTO Manual for Assessing Safety Hardware (MASH) in 2009 *(5)*. MASH incorporated some changes in the test vehicles and test matrices that ultimately will increase the dynamic load imposed to the system. Since the ultimate capacity of the barrier must be compared to the design load defined in AASHTO LRFD for a given test level, the AASHTO LRFD design forces must be updated according to MASH.

The NCHRP Report 350 and MASH documents define six different test levels of increasing impact severity (IS) that incorporate varying impact speeds and vehicle types.

These test levels provide a basis for establishing warrants for the application of roadside barriers for roadway facilities with different levels of use (i.e., service levels). Test Level 1 through 3 (TL-1 to TL-3) relate to passenger vehicles and vary by impact speed and angle. Test Level 4 through 6 (TL-4 to TL-6) retain consideration of passenger cars, but also incorporate consideration of heavy trucks. Table 1.1 summarizes the test levels with their corresponding nominal weight, impact velocity and impact angle defined in the new MASH specifications.

The NCHRP Report 663, "Design of Roadside Barrier Systems Placed on MSE Retaining Walls" *(2)*, presents guidelines for designing barrier-moment slab and MSE wall to withstand vehicle impact loads. However, the scope of this project was limited to passenger vehicle and light truck impacts (Figure 1.1) and did not include consideration of large trucks. Highways with a significant percentage of truck traffic often employ higher test level barriers.

Consequently, additional research is needed to enhance our understanding of the behavior of an MSE wall and barrier foundation system when subjected to large truck impacts. Developing guidelines for the use of truck barriers on MSE walls will permit the development of more relevant and cost-effective designs for the barrier-foundation system and MSE wall. This research will extend the work accomplished under NCHRP Report 663 and eliminate the need to extrapolate knowledge from a TL-3 impact to a TL-4 and TL-5 impact.

1.2 Objectives

The objectives of this study are divided into general and specific objectives as describe below.

The general objective of this research is:

- Develop recommended guidelines for designing roadside barrier-foundation systems placed on MSE retaining wall to resist vehicular impact loadings varying from passenger vehicles to heavy trucks (Test Levels 3 through 5) (Figure 1.1). The design guideline will be developed in a format suitable for consideration by the American Association of State High and Transportation Officials (AASHTO) LRFD Bridge Design Specifications *(3)*. The loading condition must be in accordance with the evaluation criteria defined in MASH.

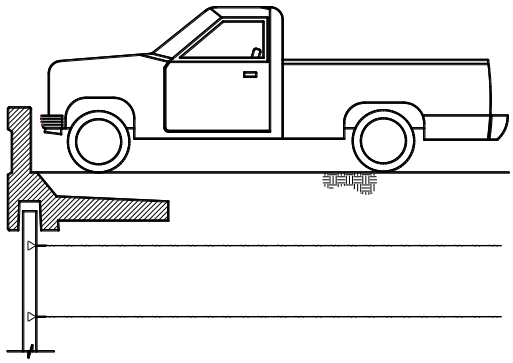

Figure 1.1 Sketch of an MSE retaining wall with a barrier-moment slab system *(2)*

Table 1.1 MASH designation and impact conditions *(5)*.

Test Level	Test Vehicle, Designation and Type	Test Conditions		
		Total Vehicle Weight, lb.	Impact Speed, mph	Impact Angle, degrees
1	1100C (Passenger Car)	2,420	31	25
	2270P (Pickup Truck)	5,000	31	25
2	1100C (Passenger Car)	2,420	44	25
	2270P (Pickup Truck)	5,000	44	25
3	1100C (Passenger Car)	2,420	62	25
	2270P (Pickup Truck)	5,000	62	25
4	1100C (Passenger Car)	2,420	62	25
	2270P (Pickup Truck)	5,000	62	25
	10000S (Single-Unit Truck)	22,000	56	15
5	1100C (Passenger Car)	2,420	62	25
	2270P (Pickup Truck)	5,000	62	25
	36000V (Tractor-Van Trailer)	79,300	50	15
6	1100C (Passenger Car)	2,420	62	25
	2270P (Pickup Truck)	5,000	62	25
	36000V (Tractor-Tank Trailer)	79,300	50	15

The specific objectives of this research are:

a) Estimate design impact loads for TL-3 through TL-5 impact for design and evaluation of longitudinal barriers. These recommendations must include magnitude, longitudinal distribution and height of application of the impact load in the vertical direction. In addition, they must address the effect of barrier height on the magnitude of the lateral load, especially for articulated vehicles.
b) Develop a proposed traffic barrier and foundation system to withstand a TL-4 and a TL-5 impact. The proposed traffic barrier and foundation system for TL-5 impact must include the effect of change on impact load due to the effect of barrier height.
c) Estimate an equivalent static load for designing a barrier-foundation system placed on top of an MSE retaining wall to resist a TL-4 and a TL-5 impact. Analyses shall include a study of parameters affecting magnitude and distribution of forces into the traffic barrier, traffic barrier foundation, and MSE wall system at the various test levels
d) Develop a design diagram shown the variation of the Dynamic Amplification Factor (DAF) associated with vehicle impact against barrier-foundation systems on top of MSE walls. Analyses shall include a study of the parameters affecting the magnitude of DAF and its variation with impact conditions for TL-3 through TL-5.

e) Develop a finite element (FE) model representative of a TL-4 barrier-moment slab system on top of an MSE wall to evaluate the proposed system under a TL-4 full-scale impact simulation.

f) Develop a FE model representative of a TL-5 barrier-moment slab system on top of an MSE wall to evaluate the proposed system under a TL-5 full-scale impact simulation. The model must include dimensions similar to the proposed full-scale TL-5 test installation. In addition, the analyses shall include the effect of change on impact load due to the effect of barrier height.

g) Conduct a full-scale TL-5 crash testing according to the specifications defined in MASH. Instrumentation of the barrier, barrier-foundation, MSE wall test installation and test vehicle shall be installed to validate the impact loading.

h) Conduct a full-scale TL-5 quasi-static test on the same barrier-foundation system used in the TL-5 crash test. Instrumentation of the barrier-foundation system shall be installed to validate the quasi-static loading.

i) Finalize the equivalent static design loads, DAF study, and design guidelines for TL-3 through TL-5 impacts to be used in the design of MSE retaining walls and traffic barrier foundations (Figure 1.2).

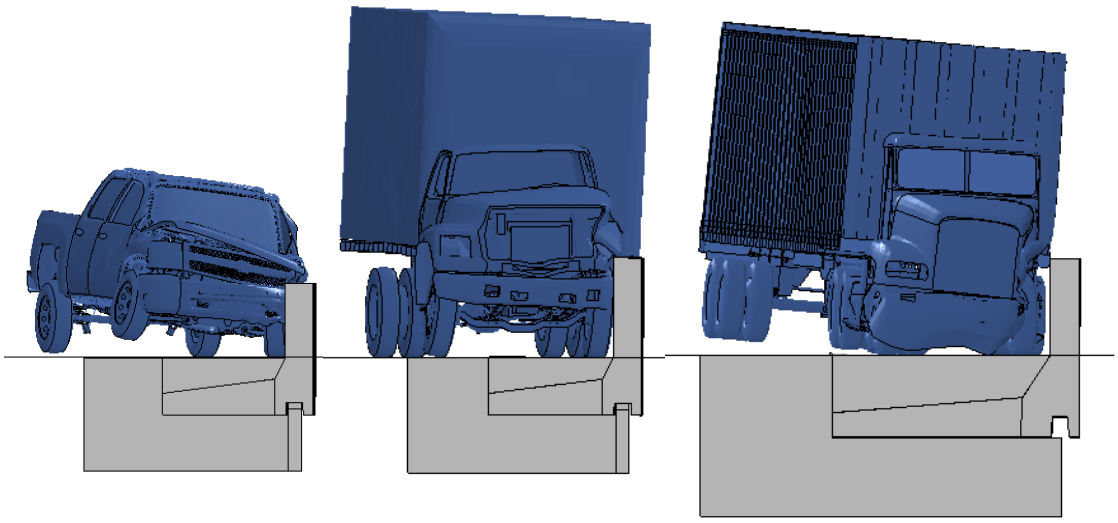

a) TL-3 **b) TL-4** **c) TL-5**

Figure 1.2 Sketch of FE models on barrier-moment slab systems

1.3 Research Approach

The research plan for developing, analyzing, and validating procedures for designing roadside barrier systems placed on MSE walls, subjected to TL-4 and TL-5 impact conditions, consists of eight tasks divided into two distinct phases, as outlined below:

1.3.1 Phase I: Analytical Study

The phase one of the project includes the following tasks:

a) Task 1

Conduct an extensive literature review of current design practices of design of MSE retaining wall, design and evaluation of longitudinal barriers, crash test impact reports and barrier-foundation system placed on MSE retaining walls. Critically, review the AASHTO LRFD, MASH Specifications, TL-4 and TL-5 roadside barrier crash test reports and the NCHRP Report 663.

b) Task 2

Conduct engineering analyses and computer simulations of TL-4 and TL-5 impacts on rigid barriers. The engineering analyses consist of estimating the TL-4 and TL-5 impact loads using existing data from pervious full-scale crash tests. The computer simulations consist of conducting a barrier-height variation analysis for full-scale TL-4 and TL-5 impact on a longitudinal barrier using the commercially available FE program LS-DYNA *(6).* The FE analyses will also help to capture the distribution of the load in the longitudinal and vertical direction.

c) Task 3

Develop a FE model of a barrier-moment slab system capable to withstand a TL-4 and TL-5 impact within a tolerable limiting permanent displacement of 1 in. (25 mm). The

FE model shall include representation of material properties that are typically used for construction of these systems. Simulations shall include both dynamic and static analyses for the systems evaluated. The dynamic analyses will consist of a full-scale impact simulation in accordance to the MASH specifications. The static analyses consist of a quasi-static FE analyses on the same barrier-moment slab. This analysis will help to estimate an equivalent static load for TL-4 and TL-5 impact. The final barrier-moment slab system configuration will be placed on top of an MSE wall model to evaluate the behavior of the system under these load impact conditions

d) Task 4

Conduct engineering analyses and computer simulations of TL-4 impact on barrier-moment slab systems and MSE retaining walls. The analyses consist of a full-scale impact simulation using an SUT vehicle model weighing 22,000 lb. (9,982 kg) impacting the system at 56 mph (90 km/hr.) at 15 degrees angle. The barrier and the width of the moment slab system will be based on the TL-4 analyses conducted in task 3. The results of the analyses will help to draft the preliminary guideline for barrier-foundation systems and MSE wall for TL-4 impact.

e) Task 5

Conduct engineering analyses and computer simulations of TL-5 impact on barrier-moment slab systems and MSE retaining walls. Simulations shall include both dynamic and static analyses for the system evaluated. The analyses consist of a full-scale impact simulation of a tractor-van-trailer vehicle model weighing 79,366 lb. (36,000 kg) impacting the system at 50 mph (80 km/hr.) at 15 degrees angle. The barrier and the width of the moment slab system will be based on the TL-5 analyses conducted in task 3. The results of the analyses will help to draft the preliminary guideline for designing barrier-foundation systems and MSE wall for TL-5 impact. In addition, the results of the TL-5 analyses will be used to propose and plan the TL-5 test installation for the full-scale crash test.

f) Task 6

Conduct a parametric study to evaluate the different variables affecting the magnitude of the DAF for designing barrier-foundation systems subjected to vehicular impact. The analyses shall include dimensional analyses using variables from the impacting vehicle (e.g., impact speed) and from the barrier-moment slab system (e.g., mass moment of inertia).

g) Task 7

Develop a proposed traffic barrier and foundation system for TL-4 and TL-5 impacts. Additionally, propose a preliminary pressure distribution for analyses of the soil reinforcement of MSE walls against pullout and yielding. The proposed guideline will be based on the results of the simulation analyses conducted for TL-4 and TL-5 impact. The guideline must address stability analyses of the system, design of the soil reinforcement for pullout and yielding and structural adequacy of the barrier and wall components.

1.3.2 Phase II: Experimental Study

The phase two of the project includes the following tasks:

a) Task 8

Conduct a full-scale TL-5 crash testing on the proposed barrier-moment slab system placed on top of an MSE wall. The design of the wall shall be based on the preliminary proposed design guidelines. Construction of the wall shall be in accordance with current deign practice of MSE wall construction. Instrumentation of the barrier, barrier foundation, MSE wall, and test vehicle shall be installed to validate impact loading. Revised and, if necessary, modify the final recommendation for design of the wall reinforcement against pullout and yielding and barrier-moment slab system.

b) Task 9

Conduct a full-scale quasi-static test on the proposed barrier-moment slab system placed on top of an MSE wall. Instrumentation of the barrier foundation shall be installed to validate impact the finding from the FE analyses.

c) Task 10

Finalize the equivalent static design loads, DAF study and design guidelines for TL-3 through TL-5 impacts to be used in design of MSE walls and traffic barrier foundations.

1.4 Organization of Dissertation

Following this introduction, this report contains nine additional sections, summarized as follow:

- Section 2 summarizes the state of the practice used in the design of MSE retaining walls, design and evaluation of longitudinal barriers and prior full-scale test impact on barrier-moment slab systems placed on top of MSE retaining walls.
- Section 3 investigates the magnitude and distribution of the impact loads imposed by heavy vehicle collision against traffic barriers. Recommendation of design loads for TL-4 and TL-5 impact are also included in this section.

- Section 4 evaluates the kinematic behavior of a barrier-moment slab system subjected to vehicle collisions for TL-4 and TL-5 impact. Recommendation of traffic barrier and foundation systems and equivalent static loads for TL-4 and TL-5 are also included in this section.
- Section 5 investigates the phenomenon of DAF associated with vehicle impact against barrier-moment slab system placed on top of MSE walls.
- Section 6 evaluates the dynamic behavior of the barrier-moment slab system and the underlying MSE wall when the barrier system is subjected to a vehicular impact. The analysis is conducted using soil reinforcement of different lengths.
- Section 7 reports the results of the FE analyses conducted on the TL-5 test installation and the full-scale crash test used to verify the preliminary design guideline for TL-5 impact.
- Section 8 reports the results of the FE analyses and TL-5 full-scale static load test on the same barrier-moment slab system used to evaluate the TL-5 full-scale impact test.
- Section 9 presents the final design guideline of roadside barrier system and MSE retaining walls for TL-3 through TL-5 impact.
- Section 10 contains the summary and overall conclusions of this research.

2 STATE OF PRACTICE FOR BARRIERS AND MSE WALLS

This section includes background regarding MSE wall design and construction methods, design practice of roadside barriers, roadside barrier crash testing criteria, and design of barrier atop of MSE walls.

2.1 Design of Mechanically Stabilized Earth (MSE) Wall System

MSE walls are composed of three major elements: soil, reinforcing elements and facing. The individual facing units independently restrained by the soil reinforcements, allow the structure to be nearly as flexible as the soil embankment itself. This inherent flexibility allows the structure to be built on sites where significant total and differential settlement is anticipated *(7)*.

Some of the major applications include the solution of problems in location of restricted right-of-way, site with difficult subsurface soil conditions, steepened-slope problems, and other environmental constraints. Another major use of a MSE wall system constitutes its application as fill-retaining structures in conjunction with bridges. These MSE walls are typically constructed with a roadside barrier system supported on the edge of the wall. This barrier system generally consists of a traffic barrier or bridge rail placed on a continuous footing (e.g., flexible pavement) or structural slab (e.g., rigid pavement).

This increase in the use of MSE retaining walls has lead the FHWA and State Department of Transportations (DOTs) to conduct extensive research to improve current understanding of the analysis, design, and construction of MSE walls *(1,8,9,10).* One of the most significant advances of this area is related to the change of MSE walls design procedure from an allowable stress design procedure (ASD) to the load and resistance factor design approach (LRFD). The LRFD design procedure is now mandated in AASHTO for the design of retaining structures *(3).* This section provides an explanation of the uses of the LRFD method on MSE wall design methodology.

2.1.1 Design and Construction Methods

Current methods for designing an MSE wall consist of determining the geometry and the soil reinforcement of the structure to maintain internal and external stability. The analysis can be divided into two main components: external stability and internal stability. The external stability analysis addresses failure modes such as sliding, overturning, bearing capacity, and slope stability failure. Figure 2.1 shows a schematic representation of each failure mode considered for external stability. Each failure mode can be described as follow:

- The sliding design ensures that the active force does not overcome the frictional resistance of the system.

- The overturning design ensures that the moment generated by the active force does not represent an unreasonable risk of overcoming the resisting moment due to the weight of the wall mass.
- The bearing capacity design ensures that the pressure impose to the soil due to the self-weight of the structure does not overcome the ultimate bearing capacity of the soil.
- The slope stability design ensures that there is not a reasonable risk of generating failures surface due general deep seated rotation.

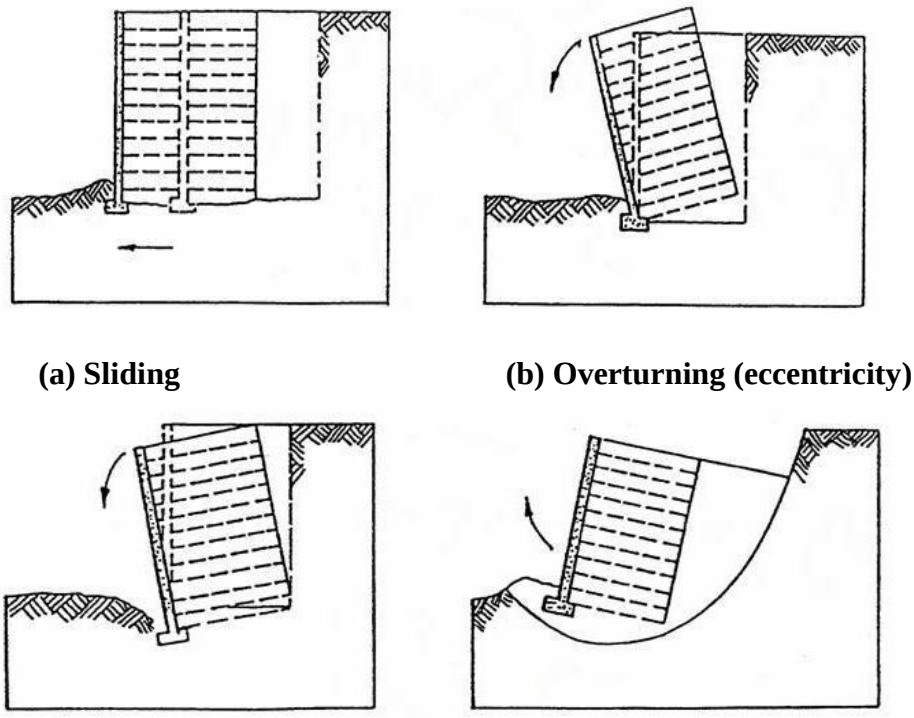

(a) Sliding **(b) Overturning (eccentricity)**

(c) Bearing capacity **d) Deep seated stability (rotational)**

Figure 2.1 External stability considerations *(11)*

The internal stability design of the MSE wall should address a series of potential internal failure modes such as the soil reinforcement yielding and soil reinforcement pullout. The internal stability design of an MSE wall ensures that the system will behave as solid block with tensile resistance as shown in Figure 2.2. In this analysis, the geometry of the reinforcement (strips, bar mats, geogridss, etc.) should be appropiatly selected to ensures that the system is not going to fail due to rupture of the soil reinforcement or soil reinforcement pullout.

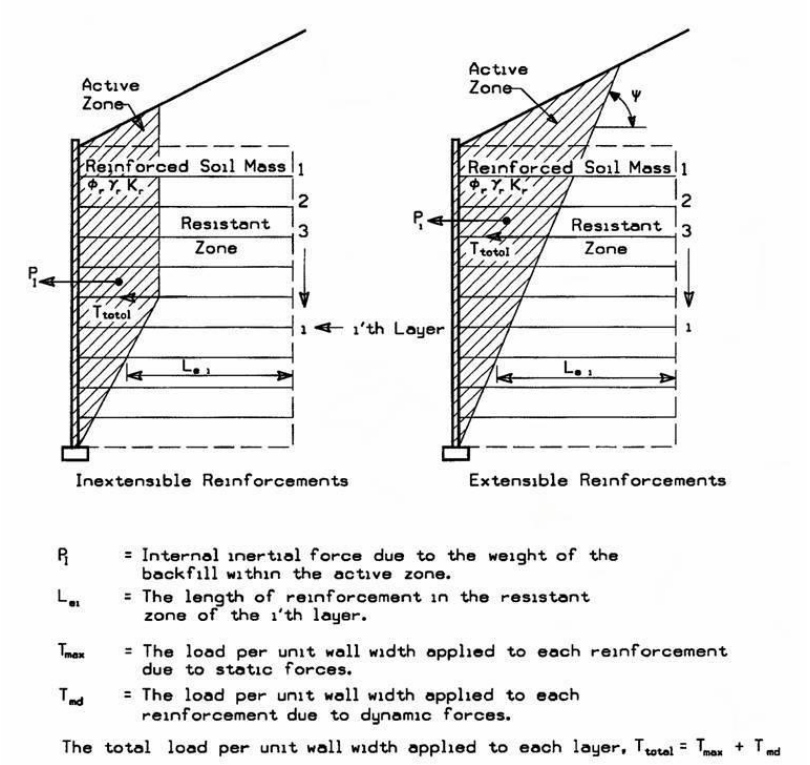

Figure 2.2 Internal stability considerations *(*AASHTO LRFD Figure 11.10.7.2.-1*) (3)*

The maximum tensile load in the reinforcement can be computed by multiplying the vertical earth pressure at the reinforcement level by the lateral earth pressure coefficient. The resulting lateral pressure shall be applied to the correspondent tributary area. Then, the load in the reinforcement is computed as (AASHTO LRFD Eq. 11.10.6.2.1-2):

$$T_{\max} = \sigma_h \times S_v \tag{2-1}$$

where

σ_h = horizontal stress due to the soil, $\sigma_h = \sigma_V K_r$

σ_v = vertical earth pressure

K_r = horizontal pressure coefficient (AASHTO LRFD Figure 11.10.6.2.1-3)

S_v = vertical spacing of the reinforcement

The pullout resistance design of the reincorcement ensures that the system will not fail against pullout failure due to the maximun static load (T_{max}). Only the effective length of the reinforcent (located outside of the failure wedge (0.7 the height of the wall)) is considered for the computation of the pullout failure. Then, the total reinforcement length consist of the effective length (L_e) and the active length of the reinfocement (L_a). The equation for computing the pullout resistance is written as (AASHTO LRFD Eq. 11.10.6.3.2-1):

$$P = F^* \times \alpha \times \sigma_v \times C \times b \times L_e \quad (2\text{-}2)$$

where

F^* = pullout friction factor as shown in Figure 2.3

α = scale effect correction factor (AASHTO LRFD Table 11.10.6.3.2-1)

$\sigma_v = \gamma \times h$, h: height of the strip from the roadside

C = overall reinforcement surface area geometry factor based on the gross perimeter of the reinforcement and is equal to 2 for strip, grid and sheet-type reinforcements.

b= width of the soil reinforcement

L_e = length of reinforcement in the resisting zone (effective length).

Additional information regarding the external and internal stability analysis of MSE wall is presented in AASHTO LRFD.

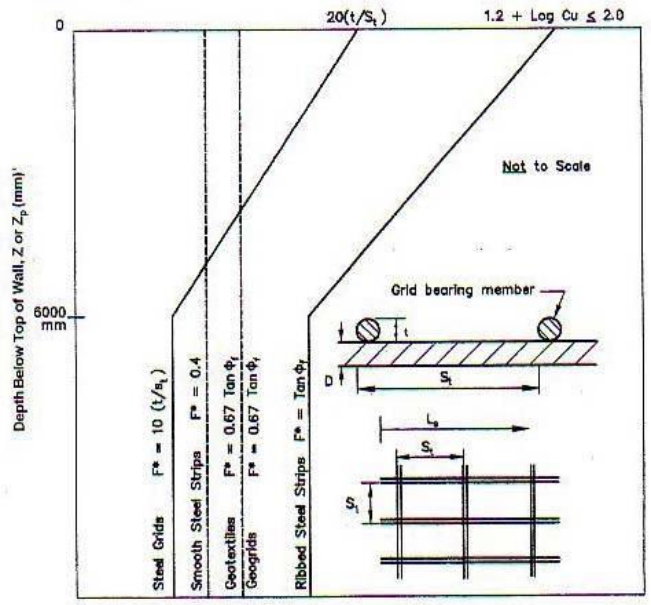

Figure 2.3 Default values for the pullout friction factor, F*(AASHTO LRFD Figure 11.10.6.3.2-1) ***(3)***

The rupture analysis of the soil reinforcement ensures that the reinforcement does not rupture (yield) during the service life (e.g., 75 years) of the structure or during an impact event. The analyses is conducted at every level within the wall and its computation depends on the type of reinforcement being used.

Beside the soil reinforcing strips, there are other important components of the MSE walls such as the conrete laveling pad, precast concrete facing panels and the backfill material. The concrete leveling pad serve as a flat, level working surface for placement of the concrete panels. The precast concrete facing panels usually fabricated in nominal dimensions depending of the design and functionality of the wall (eg., 5 ft

(1.52 m) wide by 5 ft (1.52 m) high). Typically, panels are placed with a joint gap in the vertical and in the horizonatal direction. The principal objetives of these joints are to ensure proper alignment of the panels, provide adequate permeability and maximize the flexibility of the wall. The ideal backfill material should be a well-graded granular material with no more than 15% fines and a maximum particle size of 4 in. (102 mm). The material should have some important properties such as durability, workability, good electromechanical properties and good permeability. Electromechanical properties is in particular important as they determine the rate at which corrosion of the soil reinfocement may occur.

2.1.2 LRFD vs. ASD Design Approach

The MSE walls are being designed on the basis of the LRFD approach. Prior to the development of the LRFD design procedure, also called limit state design (LSD), MSE walls were designed on the basis of the ASD approach, also called working stress design approach (WSD). The WSD approach consist of applying a global factor of safety to each of the failure modes considered in the design. Typically, these global factors of safety are based on gathered experience or developed "intuition". In LRFD, the external and internal stability of the MSE wall is evaluated at all appropriate strength limit states and overall stability and lateral/vertical wall movement are evaluated at the service limit state. The collision force generated during a vehicle impact is analyzed as an extreme event.

The use of LRFD in MSE wall design provides many advantages over the use of ASD. LRFD separately accounts for uncertainty in both resistance and load, and, when appropriately calibrated, it can provide more consistent levels of safety in the design of superstructure and substructure components in terms of reliability index. The general formulation of the LRFD design methods can be expressed as:

$$\sum_{i=1}^{n} \gamma_i L_i = \sum_{i=1}^{n} \varphi_i R_i \qquad (2\text{-}3)$$

where

γ = load factor

L = load

φ = resistance factor

R = resistance

One of the drawbacks inherent in the application of the LRFD design method for MSE wall is that values of γ and φ are difficult to estimate with good precision. This is because large databases are necessary to establish the risk levels. In some cases, those values are calibrated to match the factor of safety use on the ASD design method. Table 2.1 shows some of the resistance and load factors used in the LRFD design approach and the global factor of safety (FS) used in the former ASD design approach. The AASHTO LRFD Specifications *(3)* provide additional information of LRFD factors for earth retaining structures including MSE walls.

Table 2.1 Comparison between LRFD factors and ASD factors for designing MSE wall.

Typical Application of Load Factors (AASHTO LRFD)[1]				
Load Factor, γ	Bearing Resistance	Sliding and Eccentricity	Bearing Resistance and	Sliding, Exc. and Reinforc. Pullout
Vertical Earth Pressure, γ_{EV}	1.35	1.00	--	--
Horizontal Earth pressure, γ_{EH}	1.50	1.50	--	--
Death Load of Structural Components, γ_{DC}	1.25	0.90	--	--
Water Load, γ_{WA}	1.00	1.00	--	--
Live Load Surcharge, γ_{LS}	--	--	1.75	1.75

Typical Application of Resistance Factors (AASHTO LRFD)[1]		
Resistance Factor, φ	Static Loading	Combined Static and Impact Loading
Tensile Resistance of the Strip Reinforcement, φ	0.75	1.0
Pullout Resistance of the Strip Reinforcement, φ	0.90	1.0

Typical Factor of Safety on ASD Approach[2]	
Failure Analyses	Global Factor of Safety
Sliding	≈1.5
Overturning	≈2.0
Bearing Resistance	≈2.5

[1] *AASHTO LRFD Bridge Design Specification, Section 11.*

[2] *Average values used for factor of safety for different failure modes in ASD methodology (11).*

2.2 Design and Evaluation of Longitudinal Barrier and Bridge Rails

This section includes background regarding roadside barrier design and crash testing criteria, analyses of crash test data for TL-4 and TL-5 impact, and a history of the design loads for heavy trucks.

2.2.1 Guidelines for Barrier Evaluation

Guidelines for testing and evaluation of roadside barriers systems started in 1962 with Highway Research Circular 482 entitled “Proposed Full-Scale Testing Procedures for Guardrails” *(12).* This one-page document contained only one test vehicle, six test articles and three evaluation criteria.

NCHRP Report 350, "Recommended Procedures for the Safety Performance Evaluation of Highway Feature" was published in 1993 *(4).* This 132-page document represented a comprehensive update to crash tests and evaluation procedures. It incorporated significant changes and additions to procedures for safety-performance evaluation. Also, it included updates reflecting the changing character of the highway network and the fleet characteristics of the vehicles using it *(2)*. This report contains six test levels for longitudinal barriers. Test levels 1 through 3 (TL-1 to TL-3) relate to passenger vehicles (820C to 2000P) and vary by impact speed and impact angle. Test levels 4 through 6 (TL-4 to TL-6) retain consideration of passenger cars, but also incorporate consideration of heavy trucks. The research presented in this paper covers

TL-4 and TL-5 impacts. The TL-4 and TL-5 impacts refer to a collision with a single unit truck (SUT) and a tractor-van-trailer vehicle, respectively.

The AASHTO Manual for Assessing Safety Hardware (MASH) published in October 2009 is an update to NCHRP Report 350. This document was developed under NCHRP Project 22-14(2), 'Improvement Procedures for Safety-Performance Evaluation of Roadside Feature" by researchers at the University of Nebraska. Changes include new design test vehicles, revised test matrices, and revised impact conditions. Table 2.2 compares the design test vehicles specified by NCHRP Report 350 and MASH.

As shown in Table 2.2, the primary parameters that define a full-scale crash test are the impact speed, impact angle and test vehicle mass. These impact conditions are selected to represent a "practical worst case" scenario. While the impact conditions for passenger vehicles have their foundation in real-world crash data, such data does not exist for large trucks. Therefore, they are based on engineering judgment. Each of the test levels places increasing structural demand on the barrier, therefore, they are designed to assess one or more of the three principal evaluating criteria: occupant risk, vehicle trajectory, and structural adequacy.

Two of the most important changes incorporated in MASH that are of interest to this project are summarized as follow*:*

- The impact velocity of the single-unit truck (Test Designation 4-12) changed from 50 mph (80 km/hr.) in NCHRP Report 350 to 56 mph (90 km/hr.) in MASH. This change in impact speed and mass of the test vehicle increases the kinetic energy (also called impact severity (IS)) of the of the impact by 56%.

- The height of the ballast center of mass of the SUT test vehicle was decreased from 67 in. (1.7 m) in NCHRP Report 350 to 63 in. (1.60 m) in MASH.

Table 2.2 Vehicle description incorporated in NCHRP Report 350 and MASH *(4,5)*.

Test Level	NCHRP Report 350		MASH	
	Test Vehicle Designation and Type	Weight (lb.)/ Speed (mph)/ Angle (deg.)	Test Vehicle Designation and Type	Weight (lb.)/ Speed (mph)/ Angle (deg.)
TL-1	700C (Small Car)	1540/31/20	1100C (Passenger Car)	2420/31/25
TL-2	820C (Small Car)	1848/44/20	1500A (Passenger Car)	3300/44/25
TL-3	2000C (Pickup Truck)	4400/62/25	2270P (Pickup Truck)	5000/62/25
TL-4	8000S (Single-Unit Van Truck)	17600/50/15	10000S (Single-Unit Truck)	22000/56/15
TL-5	36000V (Tractor-Van Trailer)	79300/50/15	36000V (Tractor-Van Trailer)	79300/50/15
TL-6	36000T (Tractor-Tank Trailer)	79300/50/15	36000T (Tractor-Tank Trailer)	79300/50/15

Note: 1 kg=2.2 lb.

Even when the speed and impact angle are within the acceptable tolerances, the IS could be unacceptably low. Therefore, MASH has incorporated an additional limiting condition to the IS of full-scale crash tests. According to MASH, the IS criteria for tests involving vehicular redirection must be no more than 8% below the target value. The test planned to be performed under this research project corresponds to Test Designation 5-12. This test involves an 79,300 lb. (36,000 kg) tractor-van-trailer (36000V) impacting the barrier at a velocity of 50 mph (80 km/hr.) at angle of 15 degrees. The IS is 404 kip-ft (548 kJ), therefore, the limiting value is 372 kip-ft (504 kJ).

2.2.2 Barrier Design

Current design forces for bridge rails are presented in AASHTO LRFD Table A13.2-1 "Design Forces for Traffic Railings" *(3)*. These design forces correspond to test levels defined in NCHRP Report 350, "Recommended Procedures for the Safety Performance Evaluation of Highway Features" *(4)*. For instance, the design loads for TL-4 and TL-5 barriers are 54 kips (240 kN) and 124 kips (552 kN), respectively. These loads were derived using data from the instrumented wall testing program conducted at TTI during the 1980's *(13,14)*. The principal objective of that research project was to construct an instrumented rigid wall capable of measuring the impact forces associated with light and heavy vehicle impacts. The wall was 40 ft (12.2 m) long, 7.5 ft (2.3 m) tall and 2 ft (0.6 m) wide. Load cells and accelerometers were mounted on the wall to capture the magnitude and location of the impact load applied to the wall.

The forces were determined by direct measurement using load cells and also computed using the acceleration data. Longitudinal and vertical forces and the load distribution in the wall were not measured. If necessary, the measured forces were adjusted to account for differences in impact conditions and/or rail geometry. The information also served as bases to define the minimum barrier height required for stability of the vehicle during an impact event. Minimum barrier heights of 32 in. (0.81 m) and 42 in. (1.07 m) were recommended for TL-4 and TL-5 impacts, respectively.

After the instrumented wall testing program, it was observed that the measured dynamic load from full-scale vehicle crash tests were substantially larger than the static loads used in the design of bridge rails following ASD design procedure. This finding does not necessarily mean that railings designed for a static load of 10 kips (44.5 kN) following the AASHTO Standard Specifications for Highway Bridges are inadequate. This is because a railing system will generally have an ultimate strength well above that indicated by ASD procedures. However, the amount of reserve capacity will vary depending on materials and design details, and is not predicted when allowable stress design methods are used. Ultimate strength design procedures provide a more accurate indication of the actual strength of a rail *(2).*

In 1984, Buth et al. *(15)* recommended that bridge rails be designed based on ultimate strength procedures using yield strength of the material with a factor of safety equal to 1.0. The capacity determined in this manner is compared to the dynamic impact loads determined from data measured in the instrumented wall testing program. Such a design procedure is intended to produce yielding, but not ultimate failure/fracture when a

design impact collision occurs. This premise should hold true provided the materials and structural elements have sufficient ductility and ultimate strength substantially greater than yield strength.

Ultimate strength design procedures were widely used by roadside safety researchers in the 1980s to develop bridge rails capable of containing buses and trucks. In most cases, the impact performance of the rail was verified through full-scale crash testing. In 1989, these procedures were incorporated into the AASHTO Guide Specifications for Bridge Rails and subsequently into the AASHTO LRFD Bridge Design Specifications published in 1994 *(3,16,17)*.

The capacity of the barrier is evaluated using the yield line analyses procedure, described in chapter 13 of the AASHTO LRFD Bridge Design Specification *(3)*. The yield line theory considers the plastic strength of all the railing system components with consideration given to barrier geometry, material strengths, applied loading, and strength of the supporting bridge structure. Steel rail systems, concrete rail systems or a combination rail comprised of a steel rail on a concrete parapet can be evaluated using these design procedures. The limiting ultimate capacity of the railing system is calculated based on the yield line theory. This ultimate capacity is then compared to design forces derived from vehicular loads measured from actual crash testing presented in AASHTO LRFD. Typically, capacities of the railing system are calculated at both mid-span of the railing system and at a joint or end of the rail system, as shown on Figure 2.4.

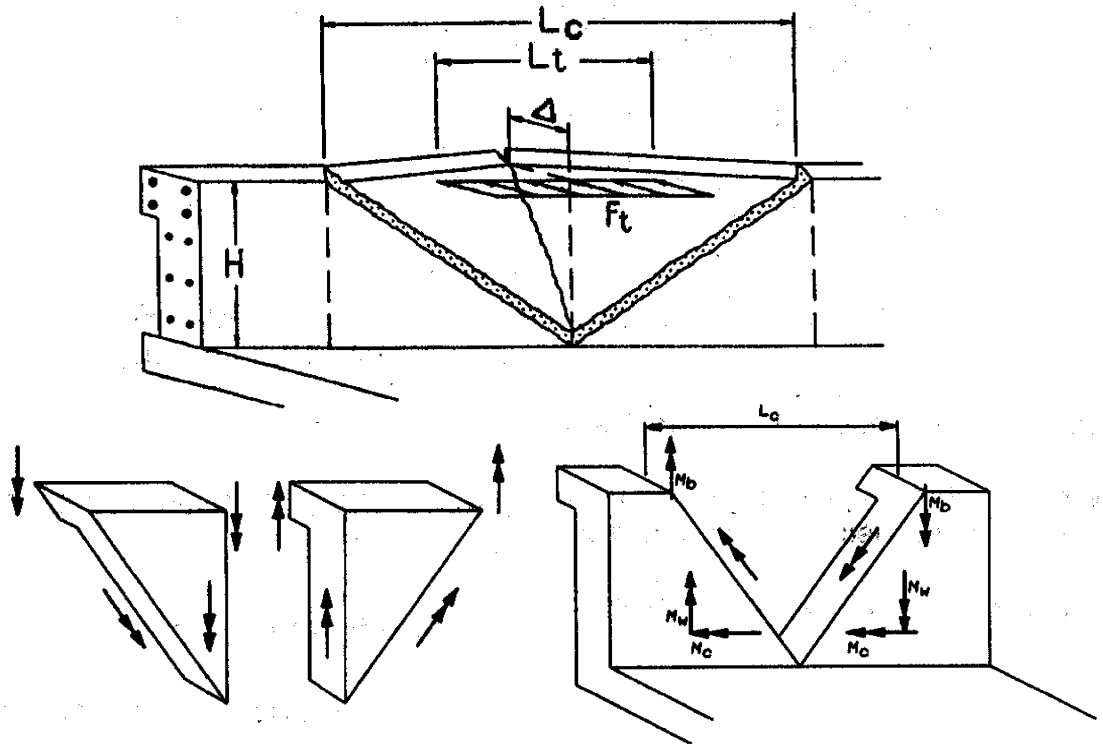

a) Analyses within wall segment

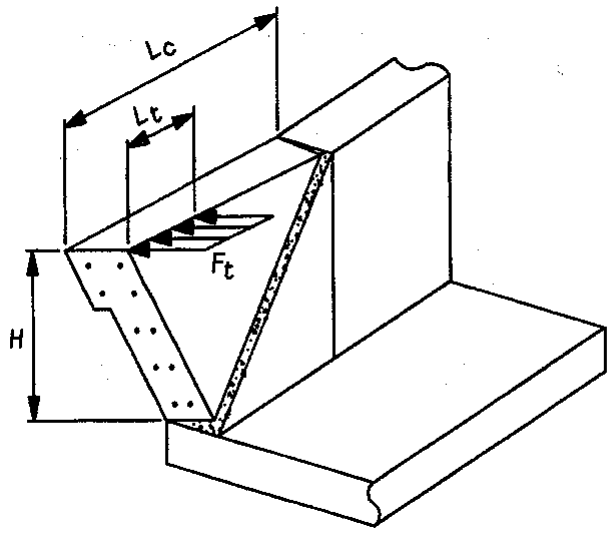

b) Analyses near end of wall segment

Figure 2.4 Idealized mid-span failure mechanism *(3)*.

2.2.3 Full-Scale Crash Testing for TL-4

Extensive literature exists for designing, analyzing, testing, and evaluating bridge rails and other roadside barriers system. It was found that most of the research conducted on rail impact has focused on full-scale crash tests. While design impact forces have been defined and design procedures have been developed for bridge rails (AASHTO LRFD), evaluation and assessment of rail impact performance continues to be primarily performance based (i.e., determined through full-scale crash testing) rather than analysis based (i.e., determined through compliance with a design specification).

Numerous TL-4 full-scale crash tests were conducted in accordance with NCHRP Report 350 Specifications. A minimum rail height of 32 in. (0.812 m) was required to contain and redirect the TL-4 test vehicle (8000S) specified in that report. However, due to the recent incorporation of MASH, a limited number of TL-4 full-scale crash tests have been conducted using this guideline. The new changes in vehicle properties and impact conditions concluded that the current minimum barrier height of 32 in. (0.81 m) for TL-4 impact does not meet the requirement to contain and redirect the MASH 10000S test vehicle. This was proved in a MASH TL-4 full-scale crash test conducted by TTI researchers in a 32 in. (0.81 m) tall N.J. Safety Shape bridge rail as part of NCHRP Project 20-14 *(18).* The length of the test installation was 100 ft (30.5 m). The vehicle impacted the barrier at a speed of 57.4 mph (92.3 km/hr.) at an angle of 14.4 degrees. The weight of the test vehicle was 22,090 lb. (10,030 kg) and the ballast center of gravity (C.G.) height was 63 in. (1.6 m). The calculated IS was 150.4 kip-ft (204 kN-

m), 97.5 percent of the target IS. The maximum 50 millisecond (msec.) average accelerations in the longitudinal and lateral direction were -2.6 g and 4.1 g, respectively. The maximum roll angle of the SUT was 101 degrees (the vehicle rolled over the barrier). The test failed the structural adequacy criteria specified in MASH. This bridge rail had previously met TL-4 impact performance criteria under NCHRP Report 350.

Based on the above result, TTI researchers conducted another research project with the objective of estimating the minimum barrier height required to contain and redirect a MASH 10000S test vehicle *(19)*. The results of the FE analyses showed that a 36 in. (0.91 m) tall barrier meet the MASH requirements of structural adequacy. The FE results were then verified through a full-scale crash test. The total weight of the vehicle, the impact velocity and the impact angle were 22,000 lb. (9,982 kg), 57.2 mph (92 km/hr.) and 16.1 degrees, respectively. The 36 in. (0.91 m) tall Single Slope Barrier (SSB) contained and redirected the TL-4 MASH test vehicle. The measured maximum 50 msec. average lateral acceleration was 4.5 g's. The results of the TL4 crash tests are summarized in Table 2.3.

Table 2.3 Summary of the TL-4 crash tests

Test No. / Agency Ref. No.	Guideline Specification	Vehicle Weight (lb.) Speed (mph) Angle (deg.)	Max. 50 msec. Ave. Lateral Accel. g's (a_{lat})	Barrier Height (in.)	Barrier Type	Remarks of the Test
476460-1/ TTI *(18)*	MASH	22,090 57.4 14.4	4.1	32	N.J Safety Shape	Vehicle rollover/ Fail
420020-9B/ TTI *(19)*	MASH	22,000 57.2 16.1	4.5	36	Single Slope Barrier	Test Pass

2.2.4 Full-Scale Crash Testing for TL-5

Some of the early work on bridge rail design with full-scale crash tests was conducted at TTI during the 70's and 80's. During this time, the majority of the full-scale tests performed on bridge rails and medium barriers were with passenger cars. However, some tests were conducted using large trucks with weights ranging from 50,000 lb. (22,680 kg) to 80,000 lb. (36,288 kg).

Bridge rails with increasing structural demands received significant attention during the 1980's. In 1981, a modification of the Texas traffic rail type C202 concrete parapet was crash-tested with a fully loaded tractor-van-trailer *(20)*. The total height of the barrier was 54 in. (1.37 m). The bridge rail did not sustain significant damage but the deck received some cracking.

Additional full-scale crash tests with fully loaded tractor trailers were conducted by TTI in 1984 and 1986 *(21,22).* In the first test (1984), the standard Texas rail T5 was modified to contain and redirect an 80,000 lb. (36,288 kg) tank type tractor trailer. The final height of the barrier was 90 in. (2.3 m). In the second test (1986), a 32 in. (0.81 m) concrete median barrier (CMB) was modified to contain and redirect large trucks. The selected combination rail was a modification of the Texas type T5 traffic rail with an 18 in. (0.46 m) tall modified Texas type C4 metal traffic rail mounted on the top, giving a total height of 50 in. (1.27 m). In both tests, the bridge rail received moderate impact damage.

Barrier profiles do not have a considerable effect for impacts associated with large trucks. However, it does for light trucks and passenger cars. Therefore, the shape of the barrier remains important as evaluation of higher test level (TL-4 through TL-6) retain consideration of small cars. Table 6-1 of the 2011 AASHTO Roadside Design Guide *(23)* presents four reinforced CMB design for TL-5 impact conditions. The barriers include a vertical wall, N.J. shape, single slope and an F-shape barrier. All these barriers have a minimum height requirement of 42 in. (1.07 m).

The reinforced N.J. shape barrier was successfully crash tested with a tractor-van-trailer under TL-5 impact conditions by TTI in 1982 and 1986 *(24,25)*. The research report, "Performance Limits of Longitudinal Barrier Systems"*(25),* indicates that the barriers were capable of containing and redirecting a fully loaded 80,000 lb. (36,288 kg) tractor-van-trailer. The report does not present considerable details about the barrier and vehicle damage. It was stated that the barrier received tire marks and gouging. There

was no measurable deformation of the barrier during or after the test. The non-reinforced N.J. barrier, commonly referred to as the Ontario Tall wall, was successfully tested by TTI in 1990. The vertical concrete parapet was also successfully crash tested by TTI in 1993 *(26).* No record could be found of a TL-5 crash test of the single slope barrier.

Two TL-5 full-scale crash tests have been conducted by the Midwest Roadside Safety Facility (MwRSF) at the University of Nebraska. The objective of the first project was to develop an aesthetic, open concrete bridge railing to meet TL-5 safety performance criteria *(27).* The objective of the second project was to design a new CMB to safely redirect vehicles ranging from small cars to fully loaded tractor-trailers, as specified in NCHRP Report 350 for TL-5 safety performance conditions *(28).* Both designs addressed issues such as vehicle stability, rollover, and passenger car occupant safety (head ejection).

The most recent TL-5 crash tests have been conducted by TTI researchers in 2010 and 2011. The purpose of the tests was to assess the performance of the Schöck ComBAR parapet *(29)* and the Ryerson/Pultrall parapet *(30)* according to the safety-performance evaluation guidelines specified in MASH. Although no revision was included in MASH for TL-5, these tests represent the first TL-5 crash test conducted under the MASH specification. The Schöck ComBAR parapet and the Ryerson/Pultrall parapet contained and redirected the 36000V test vehicle. There was no measurable deformation during the tests and the parapet sustained only minor damage.

Table 2.4 summarizes the impact conditions, maximum 50 msec. average lateral acceleration and barrier geometry of the crash tests with large trucks reviewed as part of this study. These tests were conducted on a variety of barriers with different heights and geometries. Based on the performance of the different barriers, the AASHTO LRFD Bridge Design Specification *(3)* has defined the 42 in. (1.07 m) rail height as the minimum recommended for TL-5 test designation.

Table 2.4 also shows that many of the early tests conducted with tractor-van-trailers used sand bags and hay bales for ballast. Because ballast was not rigidly secured to the floor of the trailer, it was able to shift during impact resulting in lower forces on the barrier. While these are still acceptable type of ballast, MASH states that "Ballast should be firmly secured to prevent movement during and after the test". This results in higher impact loads.

Table 2.4 Summary of full-scale crash test conducted with tractor-trailer vehicles

Test No. / Agency/ Ref. No.	Tractor Type	Vehicle Weight (lb.)/ Speed (mph)/ Angle (degrees)	Max. 50 msec. Ave. Lateral Accel. in g's (a_{lat})	Barrier Height (in.)	Barrier/ Ballast
4348-2, TTI *(24)*	Van	80,180/52.8/15	11.4	42	CMB/Sand bags
4798-13, TTI *(25)*	Van	80,180/52.1/16.5	3.1	42	CMB/ Sand bags
416-1, TTI (*22*)	Van	80,080/48.4/15	5.5	50	Modified TX C202 Bridge Rail /Sand bags
230-6, TTI *(20)*	Van	79,770/49.1/15	5.94	54	Modified TX C202 Bridge Rail/Sand bags
911-1, TTI *(21)*	Tank	80,120/51.4/15	5.54	90	Conc. Parapet/ Smooth Red/Water
7046-3/ TTI *(13)*	Van	80,080/55/15.3	N.A	90	Rigid wall/Sand bags
7046-4, TTI *(13)*	Tank	79,900/54.8/16	N.A	90	Rigid wall/Water
7046-9, TTI *(13)*	Van	50,000/50.4/14.6	N.A	90	Rigid wall/Bales of hay
7069-10, TTI *(31)*	Van	50,000/52.2/14.0	4.7	42	F-Shape/Sand bags and bales of hay
7069-13, TTI *(32)*	Van	50,000/50.4/14.6	3.7	42	Concrete Parapet/N.S.
405511-2, TTI *(26)*	Van	79,286/49.8/14.5	5.9	42	Concrete Parapet/N.S.
ACBR-1-TL-5, MwRSF *(27)*	Van	78,975/49.4/16.3	N.A	42	OBR/Steel Panels, concrete barriers and foam blocks
TL5-CMB-2, MwRSF *(28)*	Van	79,705/52.7/15.4	N.A	42	CMB/ Steel panels, concrete barrier and foam
401761-SBG1/ TTI *(29)*	Van	79,220/50.5/15.6	18.6	42	Schöck ComBAR parapet/Sand bags
510605-RYU1/ TTI *(30)*	Van	79,650/49.1/14.6	9.4	42	Ryerson-Pultrall Parapet/concrete

N.A. = Not Available; CMB=Concrete Medium Barrier; N.S. = Not Specified; OBR= Open Bridge Rail

2.3 Background on Design Impact Load for Heavy Vehicles

Early tests showed that the principal force involved in redirecting articulated trucks was generated by the rear tandem axles of the tractor. A relatively small percentage of the lateral kinetic energy was expended in the redirection of the front axles of the tractor and the rear tandem axles of the trailer.

The prediction of impact forces for collisions involving tractor trailers started with the work conducted by TTI researchers in the 1970s. The first attempt was the application of the equations presented in NCHRP Report 86 to articulated vehicles *(33)*. This 42-page document contained different service levels for evaluating longitudinal barriers whose test matrices included vehicles ranging from small passenger cars to intercity buses. In addition, it incorporated a series of mathematical equations for predicting the impact loads for different vehicle-barrier impacts. These equations assume that, at the instant of impact, the vehicle motion can be defined by an impact velocity (V_I) and an impact angle (θ), as shown in Figure 2.5. The equations can be written as:

$$AvgG_{lat} = \frac{V_I^2 \sin^2(\theta)}{2g[AL\sin(\theta) - B[1-\cos(\theta)] + D]} \quad (2\text{-}4)$$

$$AvgG_{long} = G_{lat}\left[\cot(\theta) - \frac{V_E}{V_I}\csc(\theta)\right] \quad (2\text{-}5)$$

$$AveF_{lat} = W(AvgG_{lat}) \quad (2\text{-}6)$$

$$F_{lat,\max} = \left(AveF_{lat}\right)\frac{\pi}{2} \tag{2-7}$$

$$F_{long,\max} = \mu\left(AveF_{lat}\right)\frac{\pi}{2} \tag{2-8}$$

where

$AvgG_{lat}$ = average acceleration in the lateral direction (g's)

$AvgG_{long}$ = average acceleration in the longitudinal direction (g's)

$AvgF_{lat}$ = average impact force in the lateral direction

F_{latmax} = maximum impact force in the lateral direction

$F_{longmax}$ = maximum impact force in the longitudinal direction

V_I = impact velocity

V_E = exit velocity

θ = impact angle (degrees)

g = acceleration of gravity

AL = distance from vehicle's front end to center of mass

B = half of vehicle width

D = lateral displacement of the barrier

W = vehicle weight

μ = coefficient of friction between vehicle body and barrier railing

Figure 2.6 shows a summary of this work. The mathematical model used to compute dynamic impact forces assumes a sine wave force distribution. The results indicate that the average and the maximum impact forces generated by an 80,000 lb.

(36,288 kg) tractor trailer are approximately 110 kips (489.3 kN) and 168 kips (747.3 kN), respectively. However, these forces were estimated based on an impact speed of 60 mph (96.6 km/hr.) and an impact angle of 15 degrees. If these forces are scaled to an impact speed of 50 mph (80.5 km/hr.) to meet the current MASH criterion for TL-5, the results of the average and maximum impact force would be approximately 75 kips (333.6 kN) and 117 kips (520.4 kN), respectively. The correction is made based on the kinetic energy of the impact, as shown on Figure 2.6.

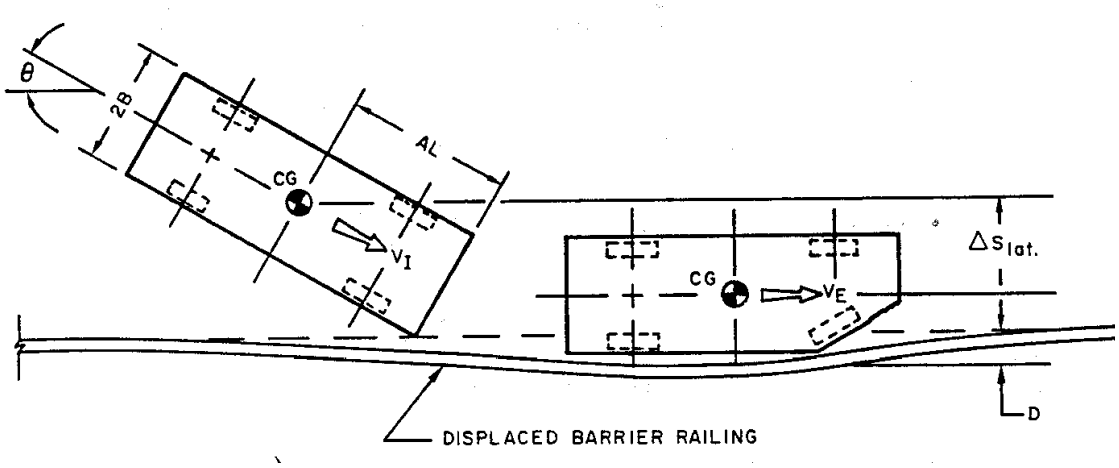

Figure 2.5 Mathematical model of vehicle-barrier railing collision *(33)*.

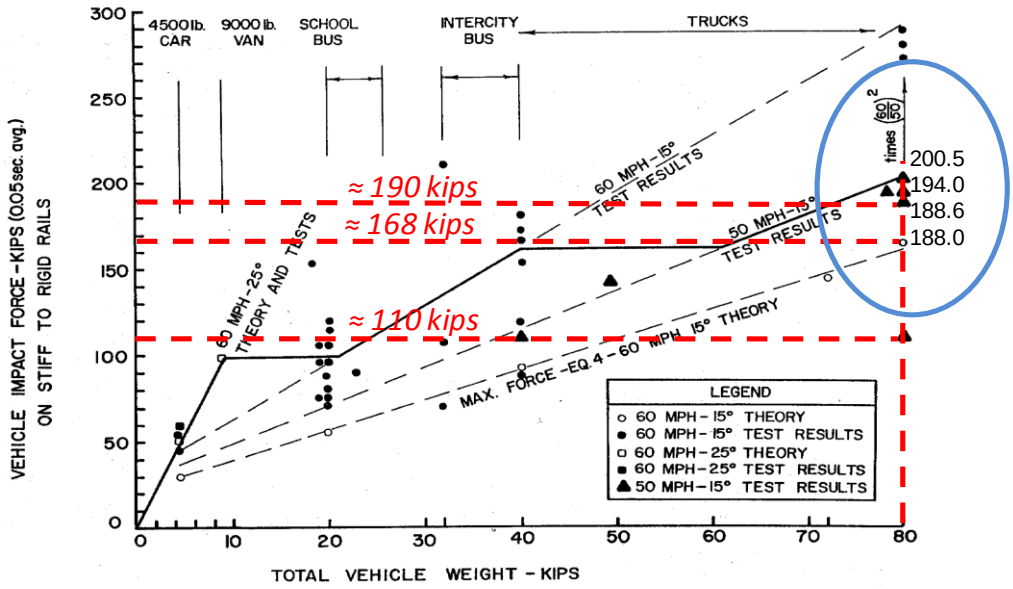

Figure 2.6 Impact force prediction based on NCHRP Report 86 mathematical models *(34)*.

Another method used to estimate the impact force is to partially apply the equation of motion at the central axles of the articulated vehicle. It was understood that the largest impact load associated with articulated vehicles occurs during redirection of the axles of the tractor. Therefore, this methodology requires measurements of the lateral acceleration close to the rear tandem of the tractor and the reaction mass associated with it.

In the late 1980's, researchers at TTI conducted a research project to measure the impact forces generated by collisions of large trucks against barriers *(13)*. The principal objective of this research project was to construct an instrumented rigid wall capable of

measuring the impact forces associated with heavy vehicle impacts. The rigid wall was constructed by modifying an existing instrumented wall that was developed to measure the impact forces associated with light vehicles. The load measuring face of the original instrumented wall consisted of four long reinforced concrete segments. Each segment was 3.5 ft (1.07 m) height, 2 ft. (0.61 m) thick and 10 ft (3.05 m) long. Since the original wall was too short to allow a smooth redirection of heavy vehicles, the wall was modified by increasing its height from 3.5 ft (1.07 m) to 7.5 ft (2.29 m). The rest of the dimensions remain unchanged.

Each segment of the wall was instrumented with four strain gage load cells and one accelerometer located at its center of gravity (C.G.). The outputs derived from this instrumentation were used to compute the magnitude and location of the impact force using principals of structural dynamics.

Groups of accelerometers were mounted slightly ahead of the C.G. of both vehicle units to capture the acceleration at the C.G. of the tractor and the trailer during the test. These accelerometer groups were located behind the anticipated areas of permanent deformation. In addition, accelerometer groups were mounted near the rear of each unit. The information captured by these accelerometers was used to calculate the acceleration associated with the C.G. of the tractor-trailer. In these analyses, the tractor and the trailer were considered as single rigid bodies undergoing centric impacts. Therefore, the impact force was determined by simply multiplying the mass of each vehicle unit by the component of the acceleration perpendicular to the face of the wall. The total force was found by summing the impact forces for each vehicle unit.

The research consisted of three full-scale crash tests with tractor-trailers *(13)*. The first test (Test 7046-3) was a collision of a tractor-van-trailer with a weight of 80,080 lb. (36,324 kg), the second test (Test 7046-4) was a collision of a tractor-tank-trailer with a weight of 79,900 lb. (36,243 kg), and the third test (Test 7046-9) was a collision of a tractor-van-trailer with a weight of 50,000 lb. (22,680 kg). There were three primary peaks of the measured impact force. The first peak force was associated with the initial impact of the tractor, the second peak force was associated with the impact of the rear tandem axles of the tractor and the front of the trailer, and the third peak force was associated with the final impact of the van trailer. Table 2.5 summarizes the impact conditions, impact loads and resultant height of the maximum impact load and the load associated with the impact of the rear tandem axles of the tractor (second peak load). The time history of the impact load of the three tests is shown in Figure 2.7 through Figure 2.9.

Table 2.5 Summary of the instrumented wall test program with tractor trailers *(13)*

Test No.	Impact Conditions			First Peak Load (kips)	Second Peak Load (kips)	Third Peak Load (kips)	Height of Maximum Resultant Force (in.)	Resultant Height of the Second Peak Force (in.)
	Weight (lbs.)	Speed (mph)	Angle (degrees)					
7046-3	80,080	55.0	15.3	66	176	220	70.0	44.0
7046-4	79,900	54.8	16.0	91	212	408	56	40.5
7046-9	50,000	50.4	14.6	39	150	70	70.0	35

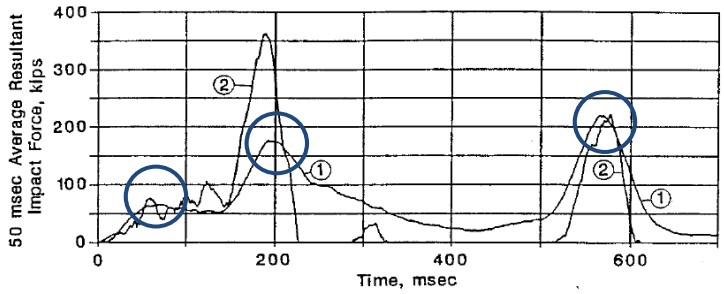

① Load measured from load cell
② Load from accelerometer data ($F = m \times a$)

Figure 2.7 50 msec. average acceleration impact force-Test 7046-3 *(13)*

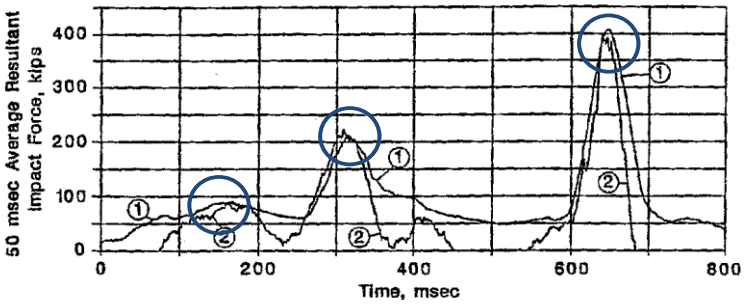

① Load measured from load cell
② Load from accelerometer data ($F = m \times a$)

Figure 2.8 50 msec. average acceleration impact force-Test 7046-4 *(13)*

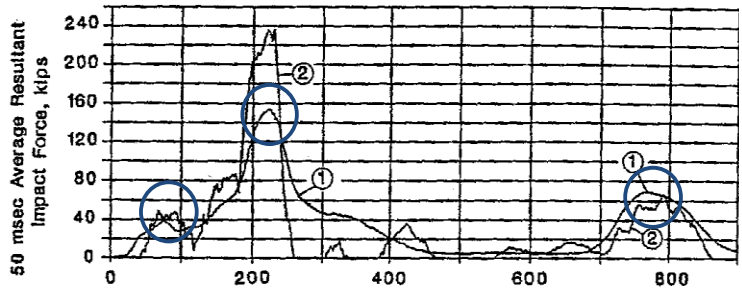

① Load measured from load cell
② Load from accelerometer data ($F = m \times a$)

Figure 2.9 50 msec. average acceleration impact force -Test 7046-9 *(13)*

Data collected from the instrumented wall was used to derive barrier design loads for various impact conditions included in the AASHTO Guideline Specification for Bridge Rails *(35)* and subsequently in Section 13 of the AASHTO LRFD Bridge Design Specification *(3)*. The AASHTO LRFD specified a design impact force of 54 kips (240 kN) and 124 kips (551.6 kN) for TL-4 and TL-5, respectively. The TL-5 design force of 124 kips (551.6 kN) was scaled for a 42 in. (1.07 m) tall barrier.

Recent work associated with lateral impact forces imparted into common barrier system due to the collision of tractor-trailers has been conducted by researchers at the MwRSF at the University of Nebraska *(36)*. Linear regression analyses was conducted for a selected number of large trucks crash tests based on the assumption that the lateral impact force is approximately proportional to the kinetic energy (or impact severity (IS)) of a given test. The analysis was conducted using the total mass of the vehicle and the reaction mass at the central axles of the tractor-trailer vehicle. The results of this analytical investigation yield two equations:

$$Y = 0.5543\,X_{TV} \tag{2-9}$$

$$Y = 1.2988 X_{RT} \tag{2-10}$$

where

Y = design impact load (kips)

X_{TV} = total vehicle IS (kips-ft)

X_{RT} = IS of the rear tandem axles of the tractor (kips-ft)

Using these correlations, researchers at the MwRSF estimated a TL-5 peak design load ranging from 243 kips (1,081 kN), based on the IS of the total vehicle, to 248 kips (1,103 kN), based on the IS of the tractor's rear tandem axle.

In a second analysis, MwRSF researchers determined the redirective capacity of four existing barrier designs using the yield-line analysis procedure. The analysis showed that the standard yield-line analytical procedure likely underestimates the redirective capacity of solid, reinforced concrete parapets. They concluded that this may be due to the fact that other factors (e. g., torsional resistance), that likely contribute to the barrier redirective capacity, are not accounted for in the analyses. However, since a "modified" yield-line analysis is currently unavailable for use in combination with the linear regression analyses, the researchers used a standard yield line-line analysis procedure in combination with a scaled-down design impact load procedure.

The scaled-down procedure estimated the design impact load based on the redirective barrier capacity and the vehicle IS from a successfully crash tested 42 in. (1.07 m) vertical wall (Test No. 405511-2). The MwRSF researchers determined the redirective capacity of this rigid wall to be 210 kips (934 kN), which compares well with the 198 kips (881 kN) reported by TTI researchers. Since the IS of the crash test was 6.5% below the nominal value (439 kip-ft (596 kJ)), researchers at the MwRSF considered it appropriate to increase the required redirective capacity of the barrier by 6.5%. The results indicated that the impact design load would be 211 kips (939 kN) and 224 kips (996 kN) based on TTI and MwRSF calculations, respectively. Consequently, the

revised TL-5 design impact load recommended by the MwRSF researchers was 217 kips (965 kN).

2.4 Roadside Barrier System Atop of MSE Walls

A roadside barrier system must be designed to contain and safely redirect a vehicle during an impact event. Therefore, the ultimate strength capacity of the barrier component must be compared to the impact loads defined in AASHTO LRFD *(3).* When a MSE wall structure required a barrier-foundation system atop, the resulting moment slab dimension must be determined using an equivalent static load and not the dynamic load. This equivalent-static load is well defined for TL-3 impact (10 kips (44.5 kN)) but it has not been yet defined for TL-4 and TL-5 impact.

The impact load also generates forces in the supporting MSE wall reinforcement and wall panels in addition to the static loads due to gravity. This load is transferred to the reinforced soil by shear stresses that develop beneath the barrier slab or by direct contact of the barrier with the wall panels (if any exist). Therefore, to preclude the transfer of high impact loads to the MSE wall panels below the barrier, a horizontal gap (usually ¾ in. (19 mm)) is provided between the throat of the precast barrier and the back side of the facing panels.

2.4.1 Full-Scale Crash Tests of Barriers on Top of MSE Walls

The first full-scale crash test on a precast barrier section atop of an MSE wall was conducted in 1982 by the Terre Armee Interantionale (TAI) in France. This company is closely related to the Reinforced Earth Company (RECO) in the USA. The test vehicle was a 26,500 lbs. (12,024 kg) bus which impacted the barrier at 44 mph (70.8 km/hr.) at 20 degrees. The precast barrier section used in the test was a 32 in. (0.81 m) tall New Jersey (NJ) shape. The barrier had minimal reinforcement (No. 4 longitudinal bars) and each/h precast unit was 5 ft (1.52 m) long. The 4.1 ft (1.25 m) wide moment slab was cast in place with a joint every 30 ft (9.14 m). The MSE wall was 10 ft (3.05 m) high with two courses of 5 ft (1.52 m) panels with normal strip reinforcement 16.4 ft (5 m) long and a density of 4 strips per 9.84 ft (3 m) of wall. The first and second layer of soil reinforcements were at depth of 15 in. (0.38 m) and 45 in. (1.14 m) below the bottom of the moment slab. The results of the test indicated that the MSE wall panels were not damage and had minimal movement. All the damage was concentrated to the barrier sections. The maximum recorded strip load was 6.5 kips (28.91 kN). In 1995, RECO wrote a report outlining the results of this test and it was concluded that the minimum density of soil reinforcement was adequate to resist the impact load.

In 2004, researchers at Texas A&M University and TTI initiated an extensive research program to study and evaluate the performance of barriers mounted on top of MSE walls when subjected to light truck impact. The results of this research effort are summarized in the NCHRP Report 663, “Design of Roadside Barriers Systems Placed

on MSE Retaining Walls" *(2).* The report presents a comprehensive study of the load transfer mechanism, barrier stability analyses, dynamic pullout resistance tests of steel reinforcing strips and full-scale impact tests of barriers mounted on top of MSE walls. The results of these tests were used to develop a complete design guideline using the LRFD approach.

The barrier stability study included a static load test and two dynamic impact tests with a 5,000 lb. (2,268 kg) bogie vehicle impacting a concrete parapet (Texas T201). The static load test was conducted prior to the dynamic bogie impact tests. The purpose of this test was to quantify the magnitude of the force required to initiate movement of the barrier-moment slab system. The test installation was 10 ft (3.05 m) long and the moment slab was 4.5 ft (1.37 m) wide. The measured static load, including soil resistance, was about 9 kips (40 kN). The magnitude of the measured static load was comparable to the recommended static load presented in the AASHTO Guidelines Specification for Bridge Design *(35).*

Upon completion of the static load test, the soil on and around the moment slab was recompacted for the dynamic bogie impact tests. The purpose of these tests was to estimate the forces required to initiate sliding and overturning in the system. In the first dynamic test, the bogie vehicle impacted the barrier at a speed of 13 mph (20.9 km/hr.). The estimated impact load, computed from the measured acceleration data at the C.G. of the bogie, was 42.5 kips (189 kN). In the second dynamic test, the impact speed was increased to 18 mph (28.9 km/hr.). The estimated impact load was 54 kips (240 kN). The results of these tests are shown in Figure 2.10.

According to the results of the dynamic and static tests, the ratio of dynamic load to static load of the 13 mph (20.9 km/hr.) and the 18 mph (28.94 km/hr.) bogie test are 4.2 and 4.9, respectively. These dynamic amplification factors (DAF) are associated with a tolerable displacement of 1 in. (25.4 mm) measured at the top of the barrier. The difference in this ratio is attributed to the inertial resistance of the system. The results are shown in Figure 2.10.

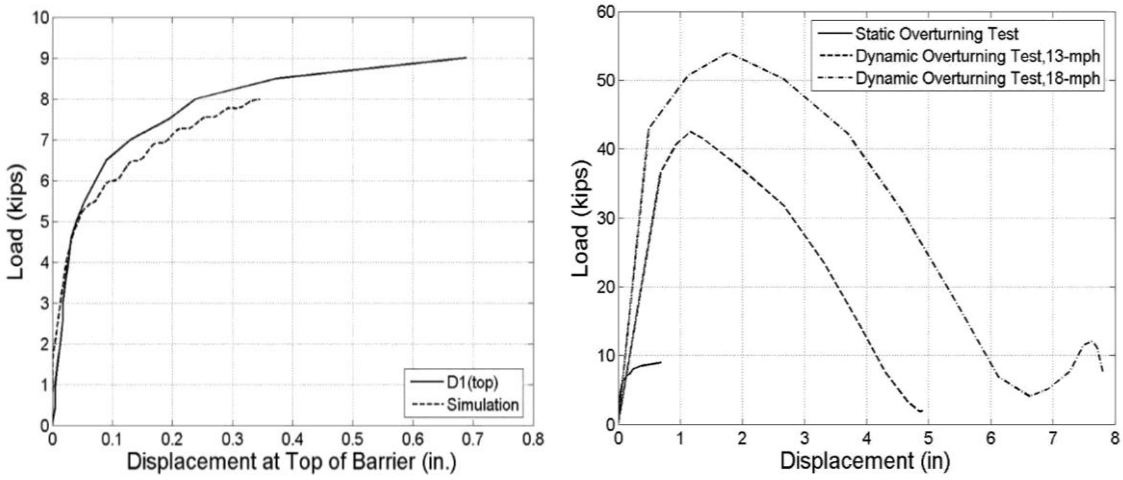

a) Static Test and FEM **b) Static Test and Overturning Test**

Figure 2.10 Comparison of static and dynamic overturning tests *(2)*

In addition, four full-scale tests were conducted on a 5 ft (1.52 m) high MSE wall with a barrier-moment slab system. The main objectives of these tests were to quantify the movement of the barrier-moment slab system as well as the force distribution in the reinforcement strips due to the impact. The tests were conducted using two different

reinforcement lengths commonly used in design practice, 8 ft (2.44 m) long (minimum length in construction) and 16 ft (4.88 m) long. The impact speed of the bogie vehicle varied from 20.2 mph (32.5 km/hr.) to 21.8 mph (35.08 km/hr.). The barrier types were a 32 in. (0.81 m) tall N.J. shape barrier (Test 1) and a 27 in. (0.69 m) tall vertical wall barrier (Test 2 through Test 4). Figure 2.11 shows the setup for the four impact tests. The maximum 50 msec. average impact load on the barriers varied from 64.4 kips (286.6 kN) to 73.4 kips (326.5 kN), which are all higher than the 54 kips (240 kN) design force associated with AASHTO LRFD for TL-3.

Data collected from the results of the barrier-stability analyses and the bogie impact tests on the 5 ft (1.52 m) high MSE wall served as a basis to draft a TL-3 design guideline in AASHTO LRFD. A full-scale crash test on a barrier mounted on top of a 10 ft (3.05 m) tall MSE wall served as the final verification of the guidelines. This test performed acceptably and the impact test met the evaluation criteria specified for MASH test designation 3-11. Figure 2.12 shows the set-up for the full-scale crash test with pickup truck prior to testing. The summary of the crash test is presented in Figure 2.13. A summary of the results of the stability tests, bogie tests, and full-scale crash test is presented in Table 2.6. Although the wall systems were subjected to loads higher than design conditions in some tests, movement of the wall was considered acceptable in all instances.

(a) Test 1

b) Test 2

(c) Test 3

(d) Test 4

Figure 2.11 Full-scale test for 5 ft high MSE wall with a bogie *(2)*

Figure 2.12 Barrier on MSE wall prior to testing *(2)*

0.000 s

0.086 s

0.171 s

0.340 s

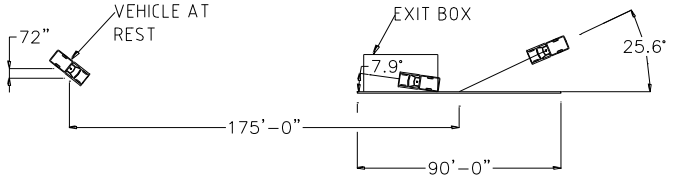

General Information
- Test Agency ..... Texas Transportation Institute
- Test No. 475350-1
- Date..... 2008-09-25

Test Article
- Type ..... 32 in. Vertical Barrier (T-221)
- Name..... MSE Wall
- Installation Length..... 90 ft
- Material or Key Elements...

Soil Type and Condition..... TxDOT Type B Backfill, Dry

Test Vehicle
- Type/Designation..... 2270P
- Make and Model ..... 2004 Dodge Ram 1500 Quad-Curb ..... Cab
- Test Inertial..... 4794 lb.
- Dummy..... 4951 lb.
- Gross Static..... No. Dummy 4951 lb.

Impact Conditions
- Speed.....63.2 mi/h
- Angle.....25.6 degrees
- Location/Orientation .....4.3 ft upstream of 4th joint

Exit Conditions
- Speed.....54.9 mi/h
- Angle.....7.9 degrees

Occupant Risk Values
- Impact Velocity
  - Longitudinal.....12.8 ft/s
  - Lateral.....29.2 ft/s
- Ridedown Accelerations
  - Longitudinal.....-4.4 Gs
  - Lateral..... 9.2 Gs
- THIV.....34.6 km/hr.
- PHD .....9.3 Gs

Max. 0.050-s Average
- Longitudinal..... -6.5 Gs
- Lateral.....15.7 Gs
- Vertical..... -3.7 Gs

Post-Impact Trajectory
- Stopping Distance.....175 ft downstream 6 ft toward traffic

Vehicle Stability
- Maximum Yaw Angle ..... 42 degrees @ 1.04 s
- Maximum Pitch Angle .....-10 degrees @ 1.64 s
- Maximum Roll Angle.....-39 degrees @ 0.58 s
- Vehicle Snagging.....No
- Vehicle Pocketing .....No

Test Article Deflections
- Dynamic.....0.84 in. (top of barrier)
- Permanent.....0.37 in. (bot. of barrier)
- Working Width 0

Vehicle Damage
- VDS.....11LFQ5
- CDC.....11FLEW4
- Max. Exterior Deformation .....15.75 inches
- Max. Occupant Compartment Deformation.....2.1 inches
- OCDI LF0000100

Figure 2.13 Summary of results for MASH test 3-11 on the MSE wall *(2)*.

Table 2.6 Summary of the stability tests, bogie tests, and full-scale crash test conducted under NCHRP Project 22-20 *(2)*.

		Stability Test 1	Stability Test 2	Bogie Test 1	Bogie Test 2	Bogie Test 3	Bogie Test 4	TL-3
Test Installation	Barrier Type	27 in. tall Vertical Wall	27 in. tall Vertical Wall	32 in. tall New Jersey	27 in. tall Vertical Wall	27 in. tall Vertical Wall	27 in. tall Vertical Wall	32 in. tall Vertical Wall
	Reinforcement	NA	NA	16 ft long Strip (4 per panel)	8 ft long Bar Mat	8 ft long Strip (6 per panel)	16 ft long Strip (4 per panel)	10 ft long Strip (6 per panel)
	Speed of Bogie	13 mph	18 mph	21.8 mph	20.3 mph	20.19 mph	20.19 mph	63.2 mph
Test Results								
Peak Acceleration	Bogie or Truck	-8.5 g	-10.9 g	-14.45 g	-13 g	-13.82g	-12.69 g	-6.5 g (long.) 15.67 g (lateral)
	Barrier	2.8 g	2.5g	7.36 g	10.71 g	10.16 g	13.04 g	1.5 g
	Moment Slab	2.2 g	3.9 g	1.84 g	N/A	1 g	N/A	0.52 g
Impact Force		42.5 kips	54.1 kips	73.4 kips	66.1 kips	70.17 kips	64.42 kips	83.3 kips
Displacement	Top of Barrier							
	Dynamic	4.9 in.	7.81 in.	6.14 in.	6.04 in.	5.17 in.	6.02 in.	0.86 in.
	Permanent	2.4 in.	4.02 in.	3.0 in.	4.0 in.	2.5 in.	3.0 in.	0.37 in.
	Bottom of Coping							
	Dynamic	0.3 in.	0.32 in.	1.12 in.	0.93 in.	1.16 in.	0.69 in.	0.55 in.
	Permanent	0 in.	0.1in.	0.55 in.	0.5 in.	0.6 in.	0.22 in.	0.68 in.
	Panel (Upper Layer)							
	Dynamic	N/A	N/A	0.63 in.	0.37 in.	0.92 in.	0.3 in.	0.42 in.
	Permanent	N/A	N/A	0.24 in.	0.2 in.	0.55 in.	0.07 in.	0.16 in.
	Panel (Second Layer)							
	Dynamic	N/A	N/A	0.0 in.	0.1 in.	0.19 in.	0.07 in.	0.26 in.
	Permanent	N/A	N/A	0.0 in.	0.02 in.	0.18 in.	0.0 in.	0.04 in.
Loads in Strip	Upper Layer							
	Max. 50-msec	N/A	N/A	7.19 kips	1.54 kips	2.13 kips	7.46 kips	1.94 kips
	Design Load	N/A	N/A	5.29 kips	1.68 kips	1.64 kips	6.25 kips	N/A
	Design Load (kip/ft)	N/A	N/A	2.15 kip/ft	1.023 kip/ft	1.01 kip/ft	2.57 kip/ft	N/A
	Second Layer							
	Max. 50-msec	N/A	N/A	-1.2 kips	0.08 kips	1.19 kips	0.15 kips	0.66 kips
	Design Load	N/A	N/A	-0.88 kips	0.083 kips	0.92 kips	0.13 kips	N/A
	Design Load (kip/ft)	N/A	N/A	-0.36 kip/ft	0.05 kips/ft	0.57 kips/ft	0.05 kips/ft	N/A

N/A= not applicable

2.4.2 Design of Barriers and MSE Walls for Vehicle Impact

Section 11 of the AASHTO LRFD Bridge Design Specification *(3)* outlines the procedure to design a barrier on top of an MSE wall. The equation presented to calculate the horizontal stress due to the soil weight and the impact load can be written as follow:

$$\sigma_H = \sigma_h + \Delta\sigma_{h,\max} \tag{2-11}$$

where

σ_h = horizontal stress due to the soil weight ($\sigma_h = k_r \times \sigma_v$),

k_r = horizontal earth pressure coefficient given by 1.7 k_a,

$\Delta\sigma_{h,\max}$ = horizontal stress due to the impact load P_{h1} on the barrier ($\Delta\sigma_{h,\max} = 2P_{h1}/l_1$)

l_1 = depth of influence of the impact load down the wall face as shown in Figure 2.14.

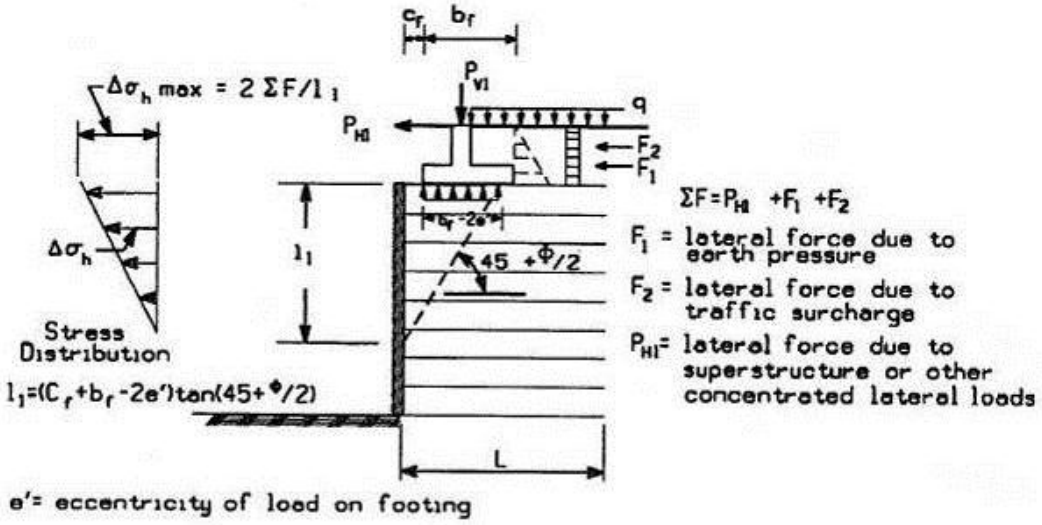

Figure 2.14 Distribution of stress from concentrated horizontal loads (AASHTO LRFD Figure 3.11.6.3-2 a) ***(3)***

AASHTO LRFD makes use of pseudo static impact load (P_{h1}) of 10 kips (44.5 kN) to be distributed into the soil reinforcement layer using a simplified vertical distribution described in Figure 2.14. This procedure was formerly inhered from the AASHTO ASD design procedure.

NCHRP Report 663 presents a comprehensive guideline for design of barrier and MSE walls for TL-3 impact. The guideline addresses barrier stability, pullout and yielding of the soil reinforcement. The barrier stability analysis is conducted using equilibrium equations for overturning and sliding of the barrier-moment slab system. The applied equivalent static load is 10 kips (44.5 kN). A pressure distribution diagram was developed by mean of full-scale impact tests for design of the soil reinforcement

against pullout and yielding failure (Figure 2.15). The pullout and yielding resistance of the reinforcing strips are calculated according to AASHTO LRFD. The expected dynamic load for pullout and yielding can be computed as:

$$\phi P \geq \gamma_s p_s A_t + \gamma_d p_d A_t \quad (2\text{-}12)$$

$$\phi R \geq \gamma_s p_s A_t + \gamma_d p_d A_t \quad (2\text{-}13)$$

where

ϕ = resistance factor and equal to 1.0 (extreme event)

ϕP= factored static resistance according to AASHTO LRFD Eq. 11.10.6.3.2-1

γ_s = load factor for static load and is equal to 1.0 (extreme event)

γ_d = load factor for the impact load and is equal to1.0 (extreme event)

p_s = earth pressure

A_t = tributary area of the reinforcing strip

p_d = dynamic pressure for pullout or yielding analyses as shown in Figure 2.15.

ϕR= factored resistance to yielding

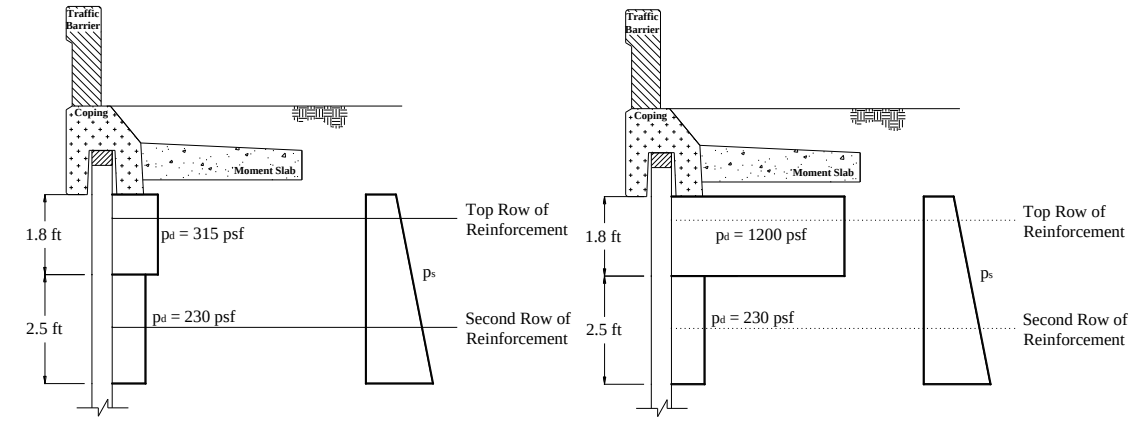

a) Pullout of soil reinforcement **b) Yielding of soil reinforcement**

Figure 2.15 Soil reinforcement pressure distribution (NCHRP Report 663) ***(2)***

3 HEAVY VEHICLE IMPACT LOADS FOR DESIGN OF TRAFFIC BARRIERS

The objectives of this study are to quantify the design impact loads for TL-4 and TL-5 impacts. The analyses efforts include prediction of impact loads based on measured test data and FE impact analyses using the commercial finite element (FE) software LS-DYNA *(6).* The results of the FE analyses were used to quantify the magnitude and distribution of the loads for TL-4 and TL-5 impacts.

3.1 Impact Load Study for TL-4 Impact

The principal objective of this section is to estimate the magnitude and distribution of the MASH TL-4 impact load on barriers of different heights. In addition, the distributions of the lateral impact load in the longitudinal and vertical direction are also investigated using finite element (FE) analyses techniques. The MASH TL-4 impact involves a SUT (10000S) vehicle weighing 22,036 lb. (10,000 kg) impacting a barrier at a speed of 56 mph (90 km/hr.) at 15 degree angle. The nominal IS of the impact is 154.7 kip-ft (209.6 kJ).

3.1.1 Analytical Study

When a SUT impacts a barrier there are two distinct impacts. The first impact occurs when the front of the vehicle contacts the barrier. The vehicle rotates as "yaw" forward to the barrier and the second impact occurs when the rear of the vehicle contacts the barrier. This second impact is sometimes referred to as the "back slap". Normally, the second impact transmits most of the kinetic energy to the system and generates the largest impact force.

The new changes in vehicle properties and impact conditions incorporated in the MASH TL-4 test vehicle concluded that the current minimum barrier height of 32 in. (0.81 m) is no longer adequate for TL-4 impact. This was proved in a MASH TL-4 full-scale crash test conducted by TTI researchers in a 32 in. (0.81 m) N.J. Safety Shape bridge rail *(18).* The vehicle rolled over the barrier and it did not pass the structural adequacy of MASH. Based on this result, TTI researchers conducted another research project with the objective of estimating the minimum barrier height required to contain and redirect a MASH 10000S test vehicle *(19).* The results of the FE analyses and a full-scale crash test shows that 36 in. (0.91 m) tall barrier meet the MASH requirements of structural adequacy. The total weight of the vehicle, the impact velocity and the impact angle were 22,000 lb. (9,982 kg), 57.2 mph (92 km/hr.) and 16.1 degrees, respectively. The measured maximum 50 msec. average lateral acceleration was 4.5 g's.

A first level approximation of the MASH TL-4 impact load was obtained using a simulated mass-spring model in combination with the mathematical model described in

NCHRP Report 86 *(33).*The procedure employs a dimensional analyses to estimate the influence of a change in impact velocity, impact angle, vehicle dimensions, weight and stiffness of the system on the magnitude of the impact load. This approach, which is shown in Eq. (3-1) through Eq. (3-3), was used by TTI researchers to help derive the current impact loads presented in AASHTO LRFD *(3)* using force measured with an instrumented rigid wall *(13)*. A series of assumptions must be considered in order to apply the mathematical models shown in Eq. (3-2). For example, the lateral and longitudinal accelerations are considered constants, the vertical rotation of the vehicle is neglected, the vehicle is not snagged by the barrier, the center of mass moves with the entire mass of the vehicle, the forces generated between the vehicle tires and the roadway surface are neglected, and the lateral force is represented by a sine wave distribution *(33).*

$$\frac{F_2}{F_1} = \frac{a_2}{a_1} = f\left[\sqrt{\frac{K_2}{K_1}}; \sqrt{\frac{W_2}{W_1}}\right] \tag{3-1}$$

$$\frac{F_2}{F_1} = \frac{a_2}{a_1} = f\left[\left(\frac{V_2}{V_2}\right)^2; \left(\frac{\sin\theta_2}{\sin\theta_1}\right); \left(\frac{A_1 L_1}{A_2 L_2}\right)\right] \tag{3-2}$$

$$F_2 = F_1 x\left[\frac{V_2}{V_1}\right]^2\left[\frac{Sin\,\theta_2}{Sin\,\theta_1}\right]\left[\frac{A_1 L_1}{A_2 L_2}\right]\left[\sqrt{\frac{K_2}{K_1}}\right]\left[\sqrt{\frac{W_2}{W_1}}\right] \tag{3-3}$$

where

F = impact load

a= lateral acceleration

V= impact velocity of the vehicle

θ = impact angle of the vehicle

AL = distance from the front of the vehicle to its center of mass

K = stiffness of the system (vehicle and the barrier)

W= mass of the vehicle

The subindex 1 refers to a NCHRP Report 350 TL-4 test vehicle and the subindex 2 refers to a MASH TL-4 test vehicle. The ratio of A_1L_1/A_2L_2 was assumed to be equal to 1 because the dimensions of the SUT test vehicle did not change. The ratio K_2/K_1 accounts for the relative stiffness of a 10000S vehicle impacting a 36 in. (0.91 m) tall barrier compared to an 8000S test vehicle impacting a 32 in. (0.81 m) tall barrier. Since the two vehicles and the two barrier are considered to be the same material, the difference in stiffness between the two impacts can be only associated with the change in height of the barrier and resulting change in contact area. Therefore, K_2/K_1 can be written as h_2/h_1. Then, Eq. (3-3) was used to update the 54 kips (240 kN) impact load from NCHRP Report 350 to MASH TL-4 impact conditions. The result shows a MASH TL-4 impact load of 80.3 kips (357.5 kN). This load accounts for the changes in impact speed, vehicle weight, and barrier height.

Another way of estimating the impact load of single body vehicles is using the equation of motion. In this procedure, the total mass of the vehicle is used and multiplied by the lateral vehicle acceleration measured at the center of gravity of the vehicle. Using

this approach, the impact load of the successful MASH TL-4 test *(19)* can be estimated using Eq. (3-4):

$$F_{impact} = m_{total} \times a_{lat} = \frac{22050}{32.2} \times \left(4.5 \times 32.2\right) = 99\ kips \tag{3-4}$$

These methods can be used to approximate the lateral impact force transmitted to a barrier when the impacting vehicle is a single body. However, they cannot provide information regarding longitudinal distribution or resultant height of the lateral load, nor the impact load in the longitudinal and vertical direction.

3.1.2 Finite Element Analyses for MASH TL-4 Impact

The complex nonlinear interaction that occurs during the collision of a heavy vehicle into a longitudinal barrier is difficult to analyze using conventional analysis techniques. Therefore, an explicit nonlinear FE analyses was conducted to capture the impact force generated during the collision of a MASH 10000S vehicle model into rigid barriers of different heights. The numerical simulations were performed using the commercially available FE software LS-DYNA *(6)*. The variation of the lateral, longitudinal, and vertical impact forces with barrier height and the horizontal and vertical distribution of the lateral impact load were also investigated.

a) Validation of the TL- 4 Vehicle Model

The MASH SUT vehicle model was modified by TTI researchers. The original SUT vehicle model was developed by the National Crash Analysis Center (NCAC) *(37)* and further modified by the National Transportation Research Center (NTRCI) *(38).* The Ford F800 Series Truck meets the NCHRP Report 350 *(4)* criteria of the 8000S test vehicle specification. The SUT model needed to be modified to reflect the MASH 10000S test vehicle specification to account for the changes in mass, vehicle dimensions, and ballast height. The ballast height changed from 67 in. (1.7 m) in NCHRP Report 350 to 63 in. (1.25 m) in MASH. Some important changes to the vehicle model include decrease in the wheel base and overall length, increase in mass and changes in some structural components to match the test vehicle used for verification.

Researchers at TTI performed validation of the MASH SUT vehicle model using crash test results conducted on a 32 in. (0.81 m) tall New Jersey profile concrete barrier *(18).* Figure 3.1 shows the sequential photographs of the test and the FE model. The simulation results with the modified SUT vehicle correlate reasonably well with the test results as shown in Figure 3.2. Detailed information about the modifications and validation of the MASH SUT vehicle model can be found in reference *(19).*

a) Test t=0 sec.

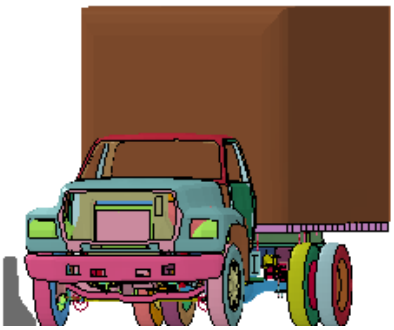

b) Simulation t=0 sec.

c) Test t=0.246 sec.

d) Simulation t=246 sec.

e) Test t=0.366 sec.

f) Simulation t=366 sec.

Figure 3.1 Comparison front view sequential photographs for test *(18)* and simulation

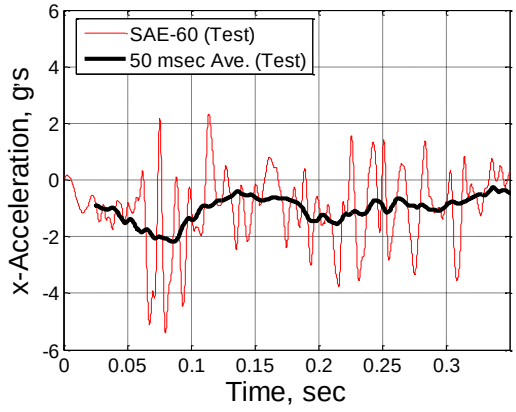

a) x-acceleration (Test 476460-1b)

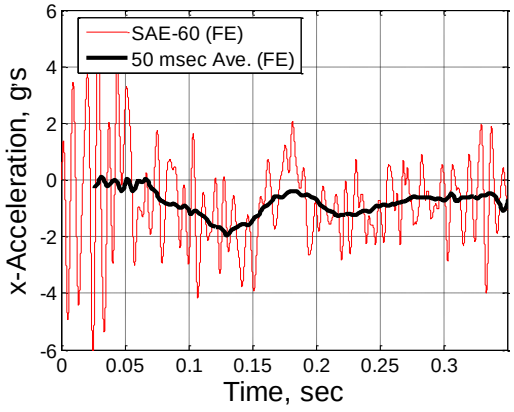

b) x-acceleration (MASH SUT Model)

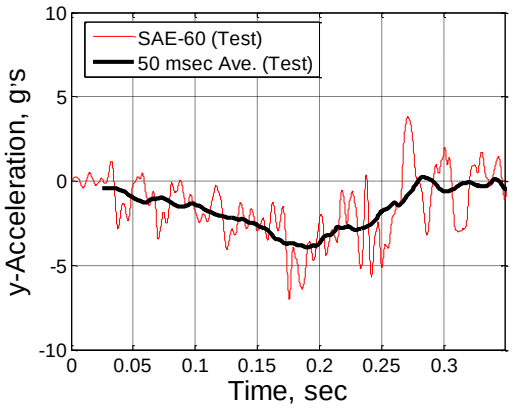

c) y-acceleration (Test 476460-1b)

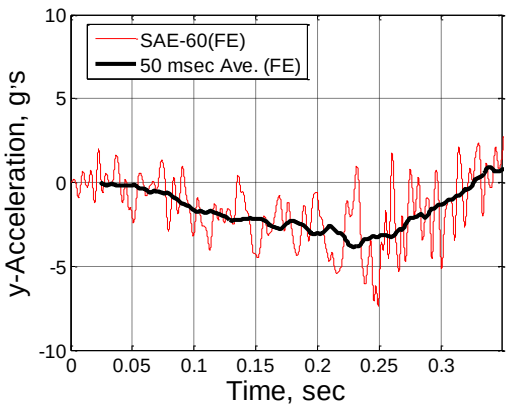

d) y-acceleration (MASH SUT Model)

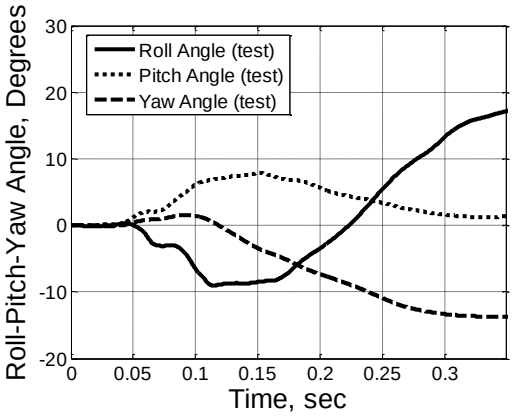

e) Angular Displacement (Test 476460-1b)

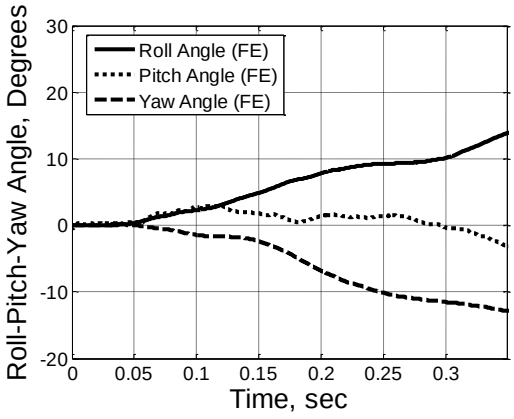

f) Angular Displacement (Model)

Figure 3.2 Comparison of acceleration and angular displacement of test 476460-1b *(18)* and simulation data.

b) Barrier Height Variation Analyses

FE analyses are conducted on rigid barriers of different heights (36 in. (914 mm), 39 in. (991 mm), 42 in. (1067 mm), and a tall rigid wall). The objective of the analyses is to estimate the magnitude, distribution and location of the dynamic forces associated with a MASH TL-4 impact of an SUT vehicle. The selection of the heights of these barriers is in accordance with current design practice in highway application. The tall rigid wall analysis is conducted to determine the maximum impact force associated with a MASH TL-4 impact into a rigid wall. The analyses have been conducted using vertical wall barriers; however, the results should be applicable to other barrier types. Figure 3.3 shows the lower bound model (36 in. (914 mm)) and the upper bound model (tall rigid wall) right before impact and at the time of maximum load.

The distribution of the impact force in the longitudinal and vertical directions of each barrier was studied. The rigid barriers were discretized into multiples segments. The impact force was output over 1 ft (304.8 mm) increments in the longitudinal direction and 6 in. (152.4 mm) increments in the vertical direction. The maximum 50 msec. average impact force in each segment was determined and distributed along each segment length. The LS-DYNA *CONTACT FORCE TRANSDUCER PENALTY *(6)* was used to capture the total contact forces applied during the impact. The discrete impact load in each section of the barrier was computed and the total load was estimated using Eq. (3-5). The vertical location of the impact force was determined by summing moments about the base of the barrier. Eq. (3-6) was used to determine the application

height of the total impact load. This calculation was conducted at the time of maximum lateral impact load determined from the time history of the impact load.

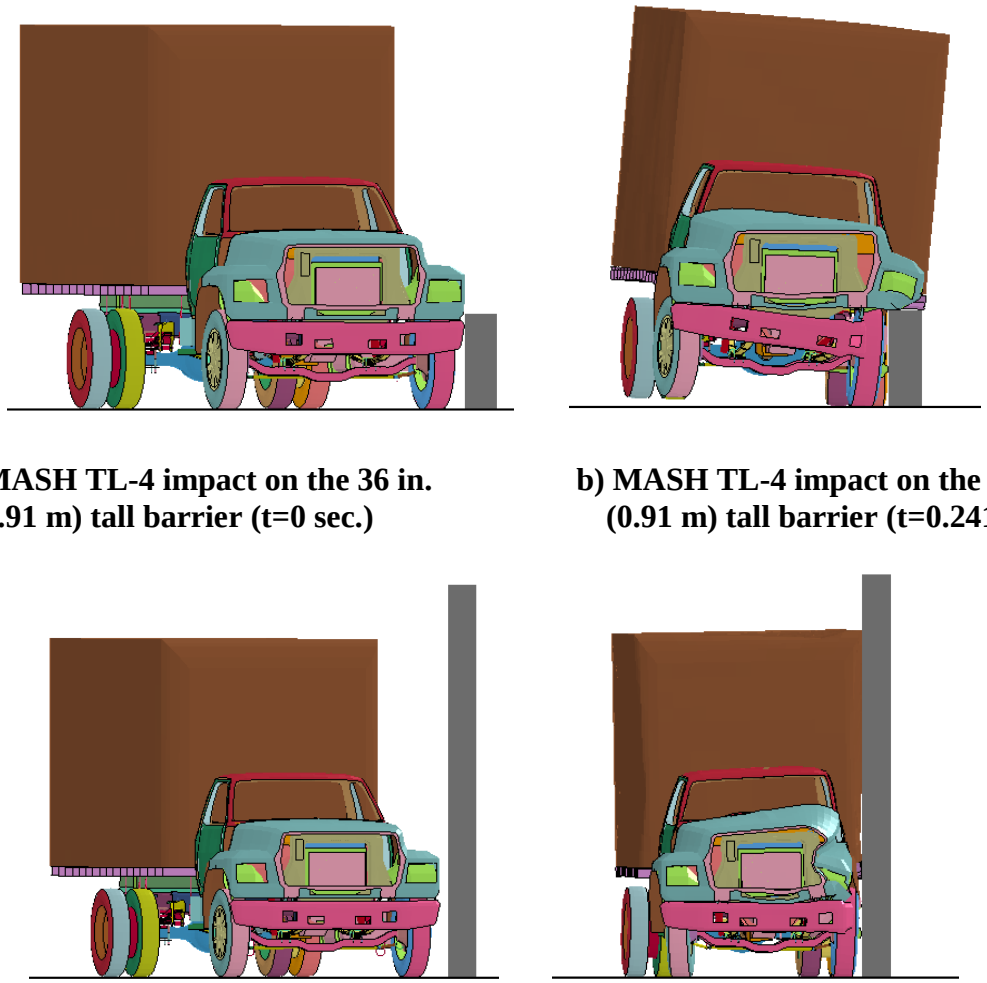

a) MASH TL-4 impact on the 36 in. (0.91 m) tall barrier (t=0 sec.)

b) MASH TL-4 impact on the 36 in. (0.91 m) tall barrier (t=0.241 sec.)

c) MASH TL-4 impact on the tall vertical wall (t=0 sec.)

d) MASH TL-4 impact on the tall vertical wall (t=0.237 sec.)

Figure 3.3 MASH TL-4 FE model for the 36 in. (0.91 m) tall barrier and the tall vertical wall

$$F_{impact} = \Sigma F_i \tag{3-5}$$

$$Z = \frac{Z_i(F_i)}{F_{impact}} \tag{3-6}$$

where

F_{impact} = maximum 50 msec. average impact load

F_i= discrete impact load in each segment of the barrier

Z= vertical location of F_{impact} from the base of the barrier,

Z_i= vertical location of F_i from the base of the barrier.

The magnitude and distribution of the MASH TL-4 impact forces obtained from the impact simulation on the different barriers are presented from Figure 3.4 through Figure 3.7. For the specific case of the 36 in. (0.891 m) tall barrier, the maximum 50 msec. average impact force in the lateral (F_t), longitudinal (F_L) and vertical (F_v) directions are 67.2 kips (299 kN), 21.6 kips (96.1 kN) and 37.8 kips (168.2 kN), respectively. Figure 3.4(c) shows that F_v is significantly larger than the weight of the vehicle, which corresponds to the current criterion specified in AASHTO LRFD for bridge rail design. This is due to the acceleration of the vehicle box as it rolls on top of the barrier during its redirection. A similar analysis was conducted for the other barrier heights. Figure 3.7(a) and Figure 3.7(b) compares the magnitude of F_t using the MASH and the NCHRP 350 test vehicle model. As shown in these figures, the magnitude of F_t increased from 76 kips (338.2 kN) in NCHRP Report 350 specification to 93.3 kips (415.2 kN) in MASH specification.

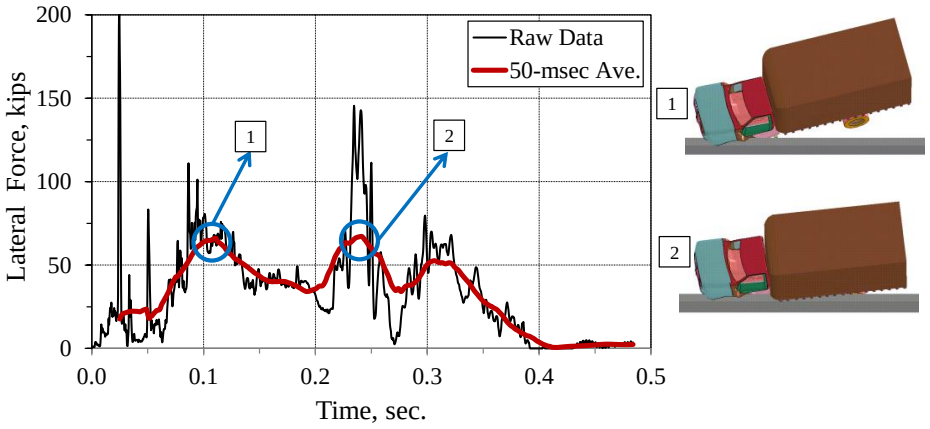

a) Lateral impact force (F_t)

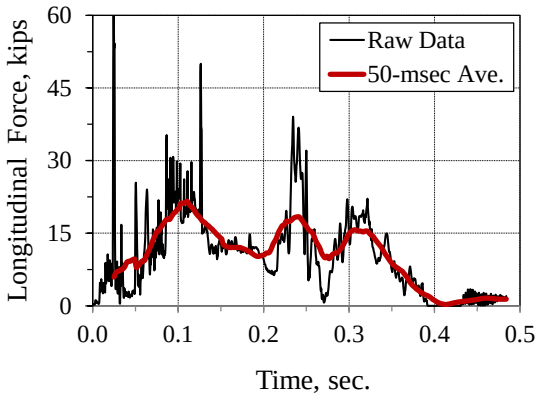

b) Longitudinal impact force (F_L)

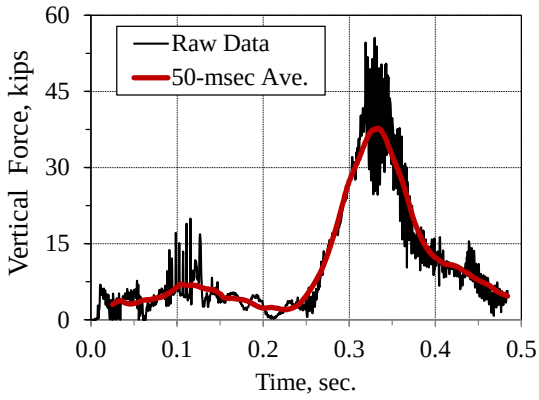

c) Vertical impact force (F_v)

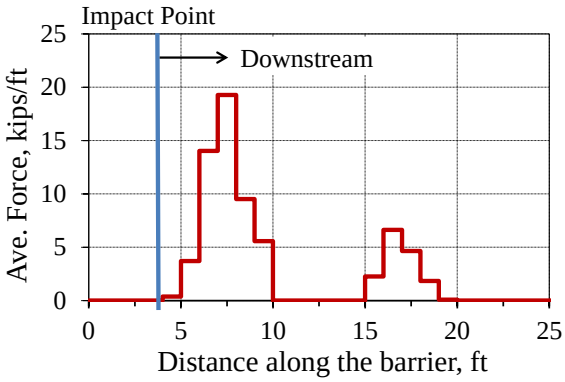

d) Longitudinal distribution, L_L (t=0.241 sec.)

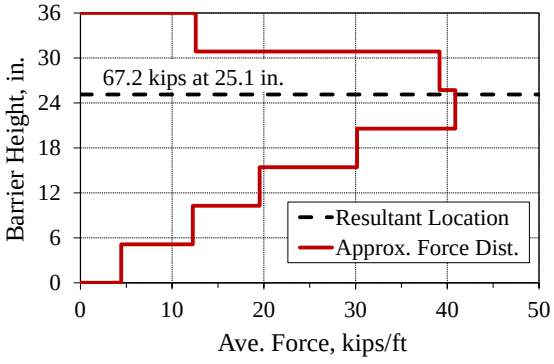

e) Transverse distribution and application H_e (t=0.241 sec.)

Figure 3.4 Results of the TL-4 impact simulation on the 36 in. (0.91 m) tall vertical wall.

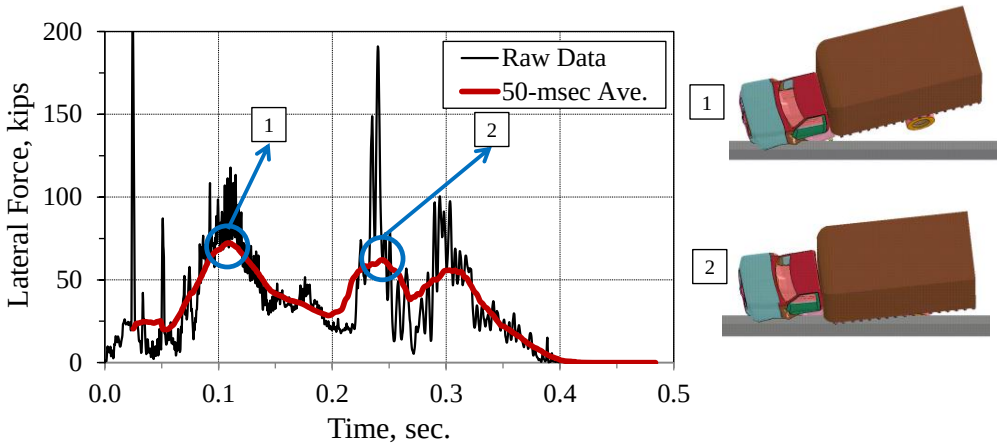

a) Lateral impact force (F_t)

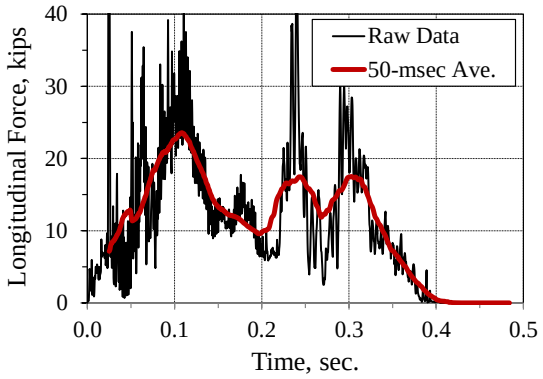

b) Longitudinal impact force (F_L)

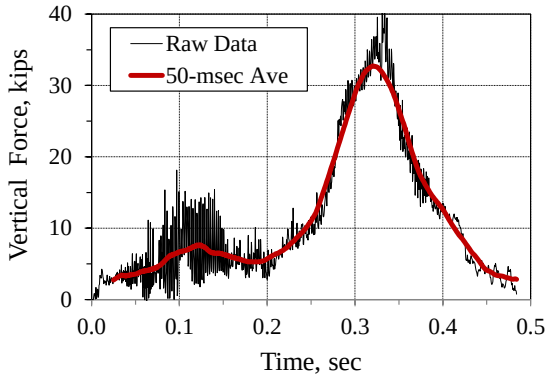

c) Vertical impact force (F_v)

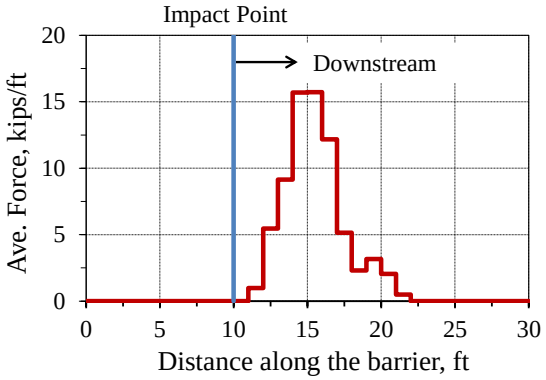

d) Longitudinal distribution, L_L (t=0.109 sec.)

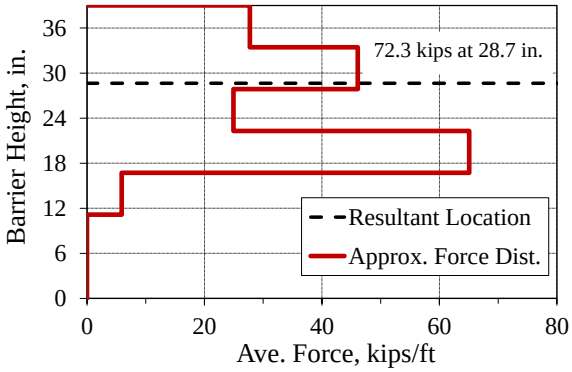

e) Transverse distribution and application H_e (t=0.109 sec.)

Figure 3.5 Results of the TL-4 impact simulation on the 39 in. (0.99 m) tall vertical wall.

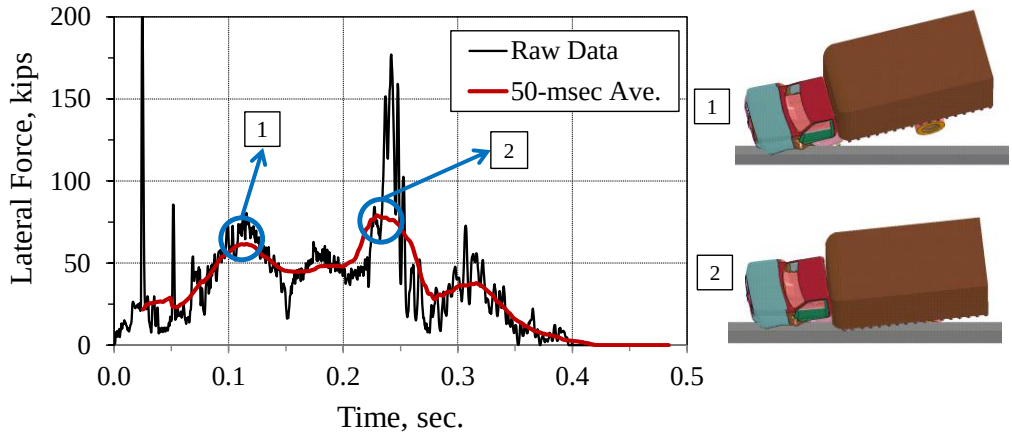

a) Lateral impact force (F_t)

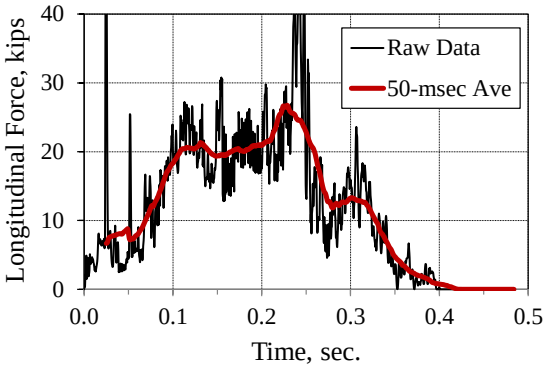

b) Longitudinal impact force (F_L)

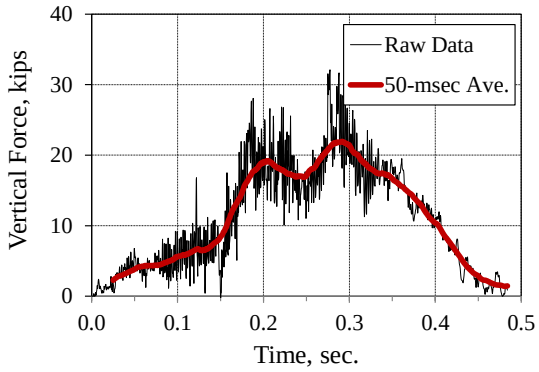

c) Vertical impact force (F_v)

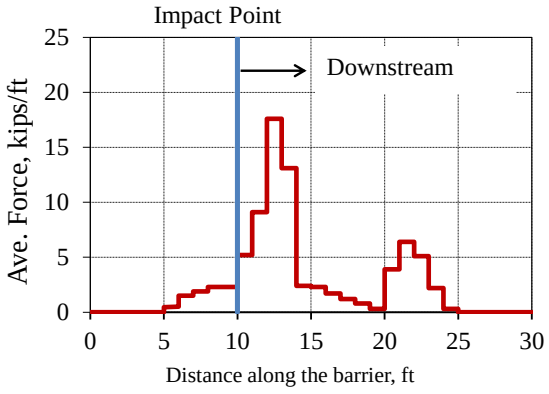

d) Longitudinal distribution, L_L (t=0.229 sec.)

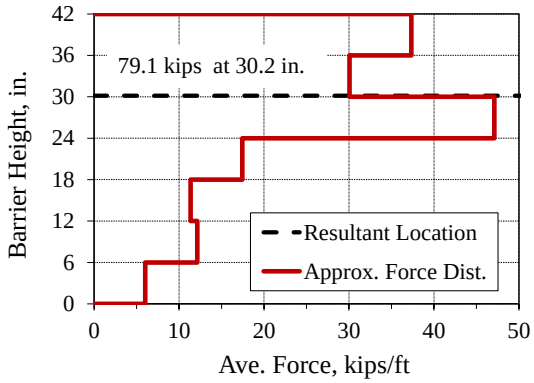

e) Transverse distribution and application H_e (t=0.229 sec.)

Figure 3.6 Results of the TL-4 impact simulation on the 42 in. (1.07 m) tall vertical wall.

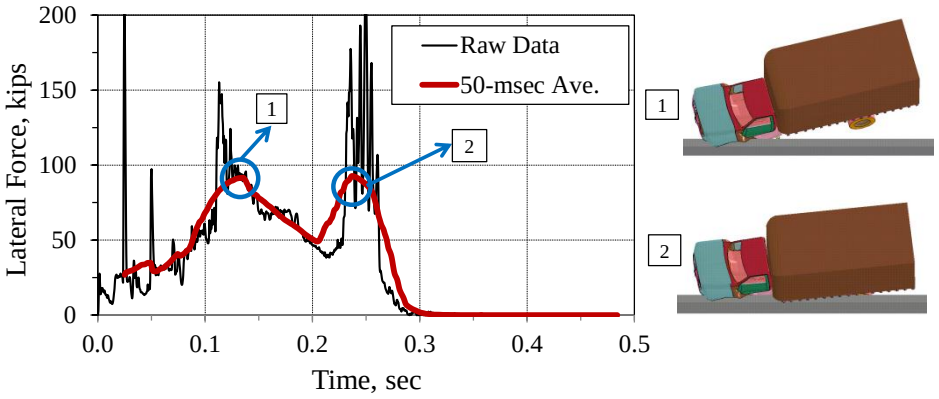

a) MASH lateral impact force (F_t)

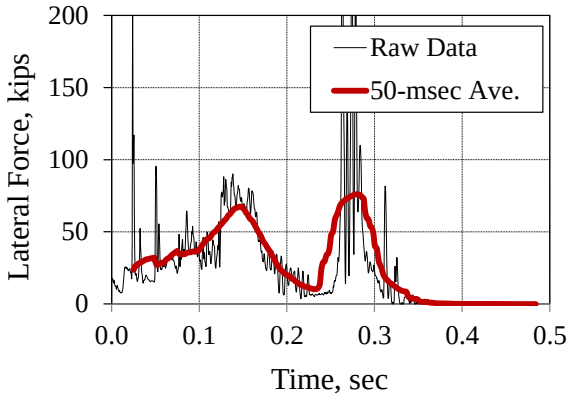

b) NCHRP 350 Lateral impact force (F_t)

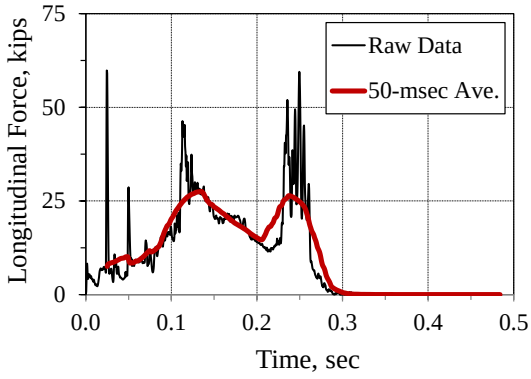

c) MASH Longitudinal load (F_L)

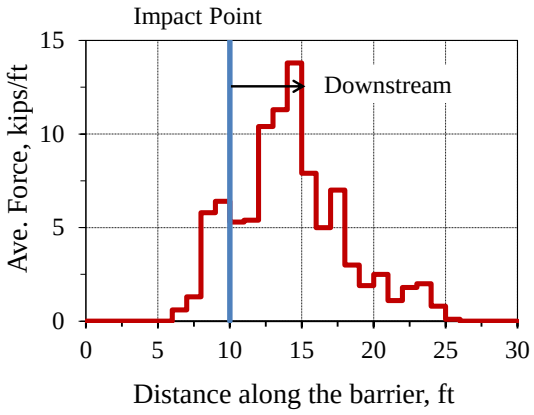

d) MASH longitudinal distribution, L_L and (t=0.237 sec.)

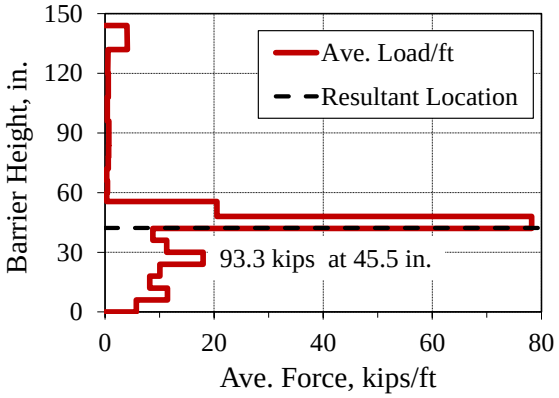

e) MASH transverse distribution and application H_e (t=0.237 sec.)

Figure 3.7 Results of the TL-4 impact simulation on the tall vertical wall.

A summary of the magnitude, distribution and application of the resultant MASH TL-4 impact loads for the different barriers is presented in Table 3.1. Although the impact conditions are the same, it is noted that F_t increases as the barrier height increases as shown in Figure 3.8. This is due to the increase in relative stiffness between impacts, which is controlled by the contact area between the vehicle and the barrier (Figure 3.9). Additionally, as the height of the barrier increases, there is less vehicle roll and more mass is engaged in the impact, thereby increasing the impact load.

The F_L for the 36 in. (914 mm) and the 39 in. (991 mm) tall barriers are controlled by the contact of the front tire and the crushable zone during the front impact. For the 42 in. (1067 mm) tall barrier and the tall rigid wall, F_L is controlled by the second impact, which is associated with the contact of the rear tandem axle and the bottom of the box of the SUT vehicle. However, in general these loads are similar in magnitude and they are not very influenced by the change in height of the barrier.

The F_v is highly influenced by barrier height. The F_v decreases as the barrier height increases as shown in Table 3.1. This is associated with a reduction in vertical deceleration of the SUT box on top of the barrier due to a decrease in roll.

The influence of the barrier height is also evident in the longitudinal and vertical distribution of the impact load. At a 36 in. (814 mm) barrier height, the box overrides the barrier and only the rear tandem axle contacts the barrier. Therefore, L_L and H_e of the peak load correspond to approximately the diameter of the tire (3.5 ft (1067 mm)) and the rear axle height (21 in. (533 mm)), respectively. The analyses of the 39 in. (914 mm) and 42 in. (1067 mm) tall barriers show a slightly more distributed peak load (6 ft (1.83

m)) than the 36 in. (814 mm) tall barrier. In addition, the resultant height of the load is greater, which increases the dynamic moment imposed at the deck or foundation. The longitudinal distribution of the peak load for the tall wall is controlled by the contact area between the box of the SUT vehicle and the wall. The peak load is distributed over a distance of approximately 14 ft (4.3 m), close to the length of the SUT box. The resultant height of the impact load is also higher (45.5 in. (1.16 m)).

Table 3.1 Summary of magnitude, distribution and application of the MASH TL-4 impact loads

Design Forces and Designations	Barrier Height (in.)			
	36	39	42	Tall
F_t Transverse (kip)	67.2	72.3	79.1	93.3
F_L Longitudinal (kip)	21.6	23.6	26.8	27.5
F_v Vertical (kip)	37.8	32.7	22	N/A
L_L (ft)	4	5	5	14
H_e (in.)	25.1	28.7	30.2	45.5

N/A= not applicable

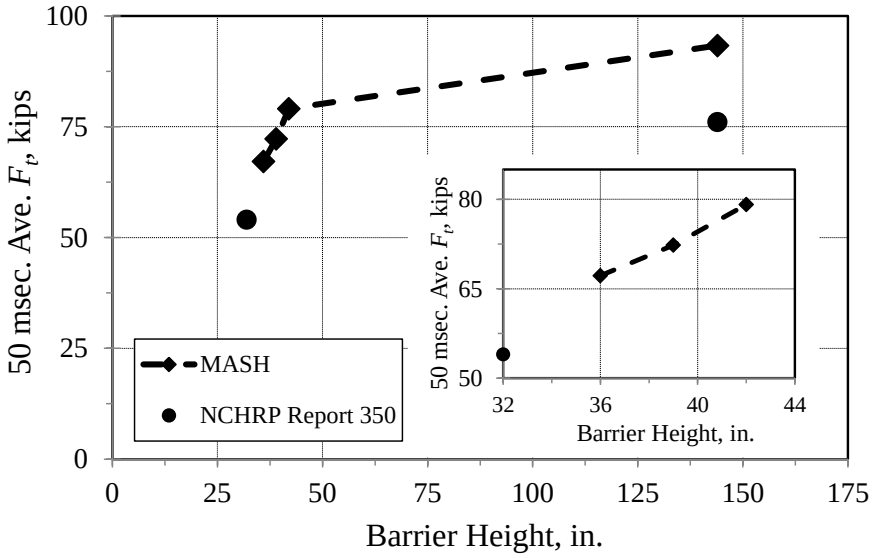

Figure 3.8 Variation of impact force for different barrier heights for MASH TL-4

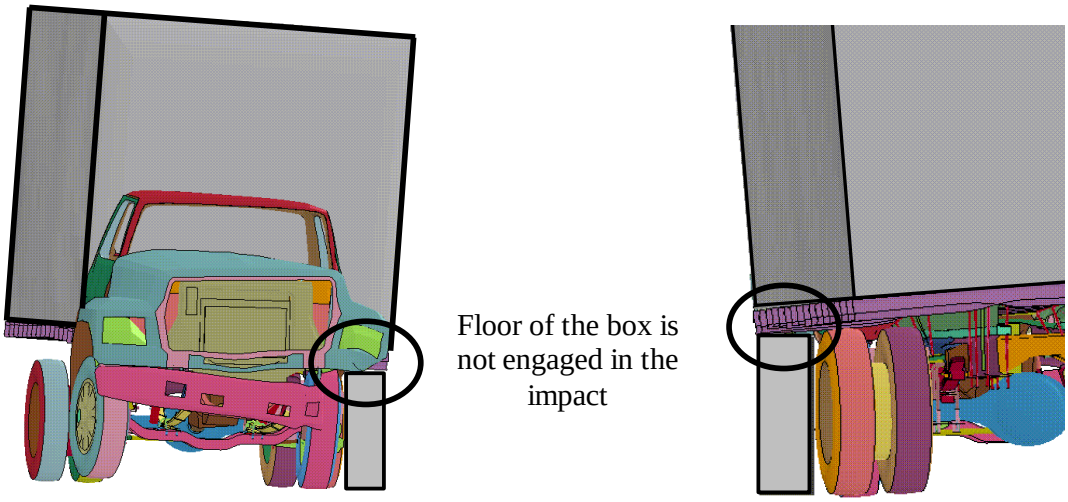

a) 36 in. (0.81 m) tall barrier (front view)

b) 36 in. (0.81 m) tall barrier (back view)

Figure 3.9 Comparison of contact area between barriers for MASH TL-4 impact.

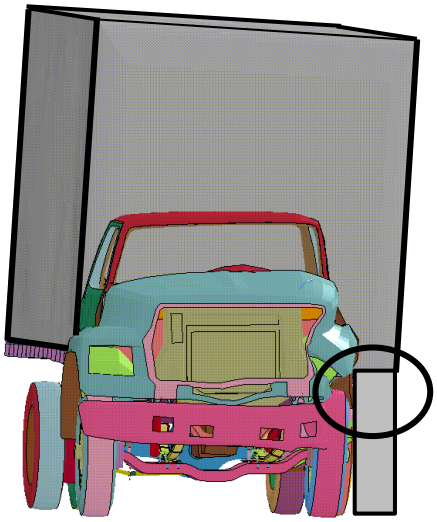

Floor of the box is engaged in the impact

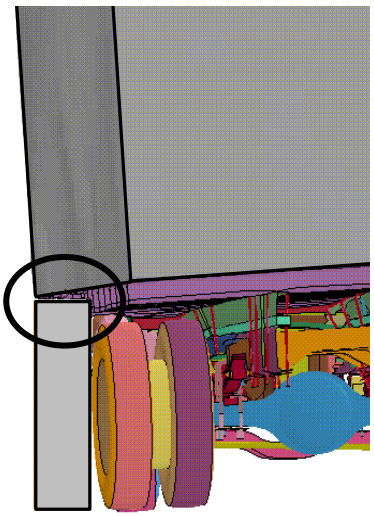

c) 42 in. (0.81 m) tall barrier (front view)

d) 42 in. (1.07 m) tall barrier (back view)

Figure 3.9 Continued

3.2 Impact Load Study for Test Level 5 Impact

The objective of these analyses is to estimate the magnitude, distribution, and location of the dynamic forces associated with a MASH TL-5 impact into a rigid barriers. The influence of the height of the barrier on the impact load is also addressed. MASH TL-5 impact involves a collision with a 79,300 lb. (36,000 kg) tractor-van-trailer (36000V) impacting the barrier at a speed of 50 mph (80 km/hr.) at an angle of 15 degrees. The nominal IS of the impact is 447.5 kip-ft (606.3 kJ).

3.2.1 Analytical Study

Articulated vehicles such as a tractor-van-trailer vehicle typically experience three distinct impacts. The first impact occurs when the front of the tractor impacts the barrier. The redirection of the tractor starts after this impact. The second impact occurs when the rear tandem axles of the tractor and the front of the trailer contacts the barrier. This impact transmits most of the kinetic energy into the system and it can create the largest impact force depending on the geometry of the system. The third impact occurs when the rear tandem axles of the trailer strike the barrier. This complex kinematic behavior makes the estimation of the impact load imposed by a tractor-trailer vehicle difficult to estimate using conventional analyses.

In 1989, researchers at TTI measured the load associated with an 80,080 lb. (36,334 kg) tractor-van-trailer impacting a 90 in. (2.29 m) tall instrumented rigid wall at 55 mph (84.5 km/hr.) and 15.3 degrees angle *(13).* The results showed that the first, second and third peak load were 66 kips (293.6 kN), 176 kips (782.9 kN), and 220 kips (978.6 kN), respectively. The resultant heights of the second and third peak loads were 44 in. (1.12 m) and 70 in. (1.78 m), respectively. These loads were scaled down for application to a 42 in. (1.07 m) tall barrier using procedures similar to the one described by Eq. (3-3). However, some of the assumptions used to develop Eq. (3-3) do not hold for articulated vehicles.

Alternatively, Eq. (3-4) can be partially applied to approximate the load due to a specific impact. Data collected from previous TL-5 full-scale crash tests indicates that

the critical impact load (maximum load/unit length) is generated by contact of the rear tandem axles of the tractor and the front of the trailer. These assumptions are based on acceleration data measured at the rear tandem axles of the tractor and the trailer. Therefore, Eq. (3-7) was applied for the impact of the central axles of the tractor-trailer which is expected to impose the critical impact load to the system. The acceleration data used in these analyzes was collected from accelerometers located at the rear tandem axles of the tractor. The mass was assumed as the reaction mass at the central axles of the tractor-trailer.

$$F_{impact} = m_{ca} \times a_{lat} \tag{3-7}$$

where

F_{impact}= estimated impact load

m_{ca}= total reaction mass at the central axles of the tractor-van-trailer

a_{lat}= lateral acceleration measured at the rear tandem axles of the tractor

The results of this analysis, presented in Table 3.2, shows a range of impact loads between 108.5 kips (488.3 kN) to 202 kips (899 kN). A relationship between impact load and barrier height is not well defined using this approach. One limitation is the difficulty of estimating the effect of the trailer on the impact load imposed to barriers taller than 42 in. (1.07 m). For barriers taller than 42 in. (1.07 m), the front of the trailer interacts with the barrier at the same time as the rear tandem axle of the tractor. This mobilizes more mass and increases the impact load. As a result, the assumption of using the reaction

mass at the central axles of the vehicle is not valid for barriers taller than 42 in. (1.07 m). Therefore, FE analyses were conducted to provide a more in-depth study of TL-5 loading.

Table 3.2 Computation of impact dynamic forces using the equation of motion

Test No (Refer. No.).	Test Condition. Weight (lb.), Speed (mph), Angle (deg.)	ReactionWeight at the Central axles, m_{ca} (lb.)	Max.50 msec. Ave. Lateral Accel., a_{lat} (g's)	Barrier Height (in.)	Barrier Type	Computed Force $F_{lat}=m_{ca} \times a_{lat}$ (kips)
4348-2 *(24)*	80,180 52.8 15	34,030	5.70	42	CMB (N.J.)	194.0
4798-13, *(25)*	80,180 52.1 16.5	30,010	3.1	42	CMB.	108.5
416-1 *(22)*	80,080 48.4 15	34,170	5.50	50	CMB and Metal Rail	188.0
230-6 *(20)*	79,770 49.1 15	33,760	5.94	54	Modified TX C202 Bridge Rail	200.5
911-1 *(21)*	80,120 51.4 15	34,050	5.54	90	Concrete Parapet	188.6
405511-2 *(26)*	79,286 49.8 14.5	34,239	5.90	42	Concrete Parapet	202.0

CMB= concrete medium barrier

3.2.2 Finite Element Analyses for MASH TL-5 Impact

FE analyses were conducted to capture the impact loads associated with the collision of a MASH 36000V vehicle model into rigid barriers of different. The simulation data is used to determine the average dynamic load in the lateral, longitudinal and vertical direction. The distribution of the lateral impact load in the longitudinal and vertical directions of the barrier is also studied.

a) Validation of the TL-5 Vehicle Model

A FE model of a tractor-trailer was recently released by the NTRCI *(39)*. The tractor FE model was modified from an existing model developed by the NCAC *(37).*The modifications included improvements to the element mesh, changes in material properties and their characterization, geometry, suspension components, connections, failure modes, and others.

The NTRCI research team developed a new FE semi-trailer model. The new model meets all the geometric requirements specified in NCHRP Report 350 and MASH, and is considered representative of typical trailers currently seen in service. The FE trailer model developed by the NTRCI was based on a 53 ft (16.2 m), dual-tire, tandem axle 2004 Stoughton box trailer *(40,41).*

The tractor semi-trailer FE model used in the analyses reported herein corresponds to the tractor version 10-0520 (day-cab model) and trailer version 10-0521

(39,40,41). The FE model was validated by the NTRCI research team using test TL5-CMB-2 *(28)* conducted by the MwRSF researchers at the University of Nebraska. The overall geometry of the FE model was modified to meet the geometry of the tractor-trailer used in the crash test. The overall length of the tractor and the semi-trailer are 21.2 ft (6.5 m) and 48 ft (14.63 m), respectively.

The tractor-trailer FE model has 583 parts with a total of 378,915 elements. The total mass of the empty tractor trailer FE model is 28,819 lb. (23,098 kg) and it is ballasted to 79,741 lb. (36,170 kg) using concrete median barriers (Figure 3.10). The validation of the tractor-trailer model was conducted by NTRCI researchers. Details of the validation results of this model can be found in reference *(40,41).*

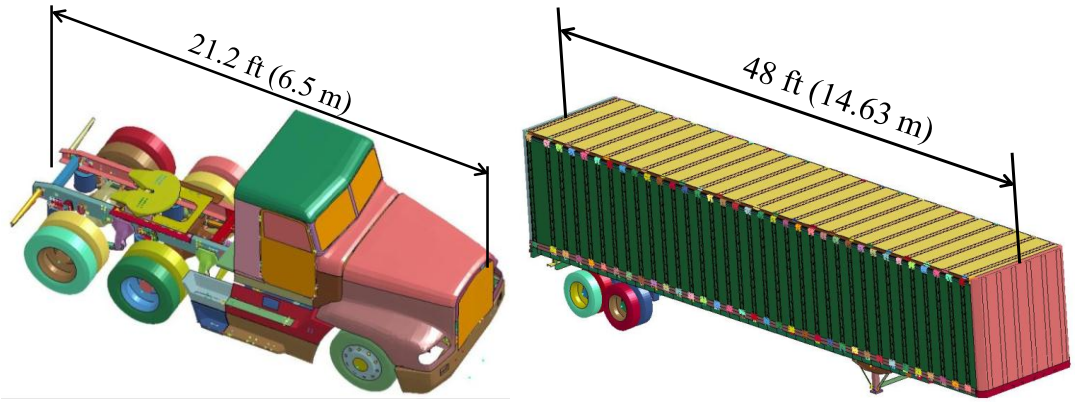

a) FE tractor model **b) FE trailer model**

Figure 3.10 Enhanced FE tractor-trailer model developed by NTRC *(39)*

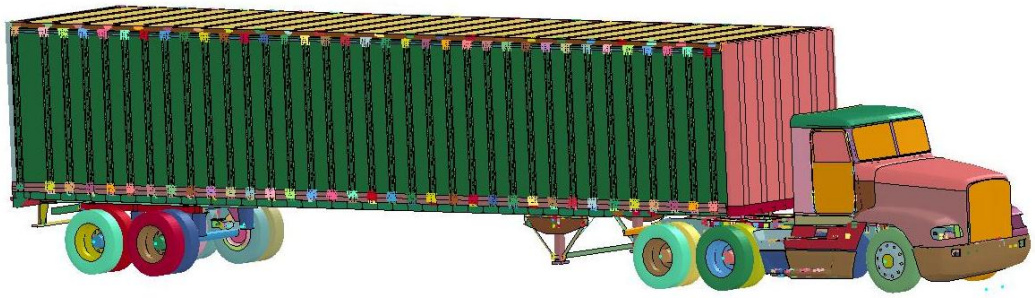

c) FE tractor-van-trailer model

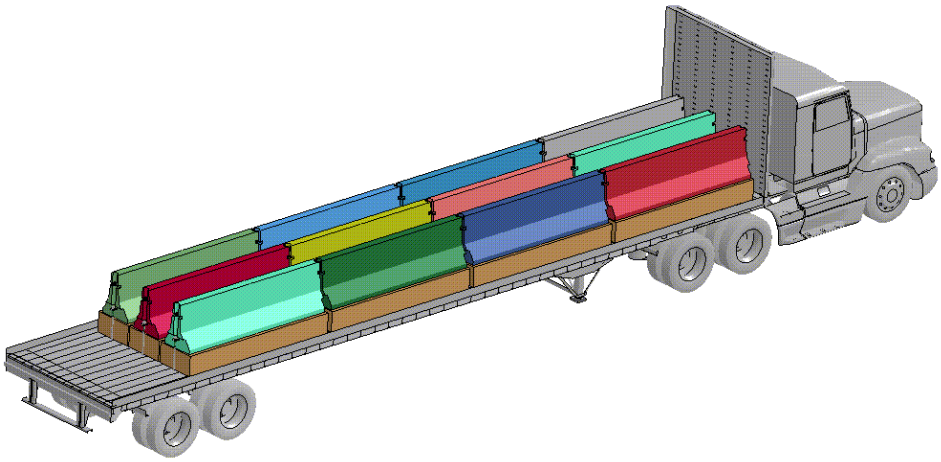

d) FE tractor-van-trailer and ballast model

Figure 3.10 Continued

b) Barrier Height Variation Analyses

Four barriers were subjected to TL-5 impacts. The heights of the barriers were: 42 in. (1.07 m), 48 in. (1.22 m), 54 in. (1.37 m), and 157.5 in. (4.0 m). The barriers were selected to cover the range of heights of previously crash tested TL-5 barriers. The tall rigid wall provides information regarding the maximum impact load associated with a

TL-5 impact. Figure 3.11 shows the lower bound model (42 in. (1.07 m)) and the upper bound model (tall rigid wall) right before impact and at the time of maximum load. The procedure followed to capture the impact load in the longitudinal and vertical direction was similar to the procedure described for MASH TL-4.

The results of the analyses on the 42 in. (1.07 m) tall barrier are presented in Figure 3.12. The time history of the lateral impact load indicates that the load associated with the first, second and third impact are 54.6 kips (243 kN), 123 kips (547.3 kN) and 159 kips (707.6 kN), respectively. These loads also include the component of the frictional load on top of the barrier, which is significant for this barrier height.

Note that the load due to the second impact (123 kips (547.3 kN)) compares very well with the TL-5 design load presented in AASHTO LRFD *(3)*. However, the controlling load is associated with the third impact, which has a magnitude of 159 kips (707.6 kN). The moment imposed by this load into the deck or barrier foundation is 454 kips-ft (616 kN-m). This moment is similar to the moment imposed by the current AASHTO load (434 kip-ft (589 kN-m)) due to a different resultant height. The longitudinal distribution was selected to be 10 ft (3.05 m), which roughly corresponds to the width of the tandem axles. A similar analysis was conducted for the other barriers. The results of the 48 in. (1.22 m) and the 54 in. (1.37 m) tall barrier and the tall rigid wall are presented from Figure 3.13 through Figure 3.15.

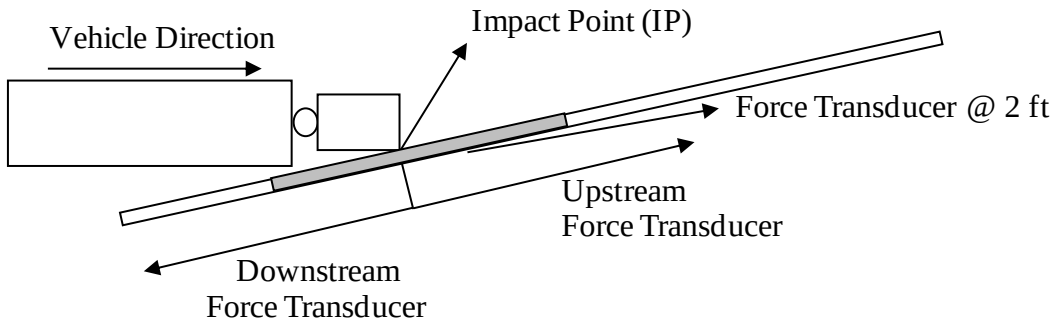

a) Sketch of force transducer location

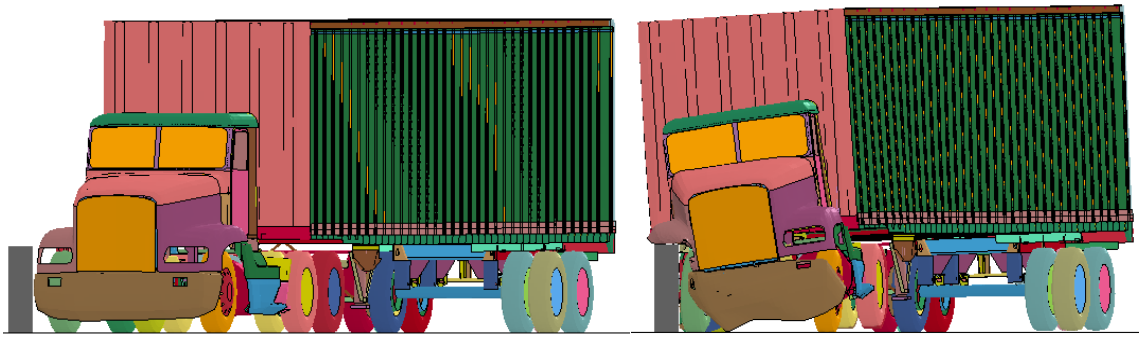

b) MASH TL-5 impact on the 42 in. (1.07 m) (1.07) tall barrier (t=0 sec.)

c) MASH TL-5 impact on the 42 in. barrier (t=0.245 sec.)

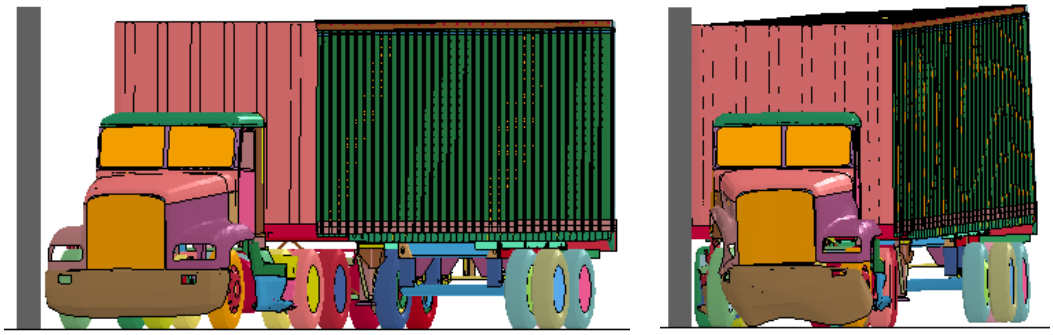

d) MASH TL-5 impact on the tall rigid rigid wall (t=0 sec.)

e) MASH TL-5 impact the tall (t=0.7 sec.)

Figure 3.11 MASH TL-5 FE model for the 42 in. (1.07 m) tall barrier and the tall vertical wall

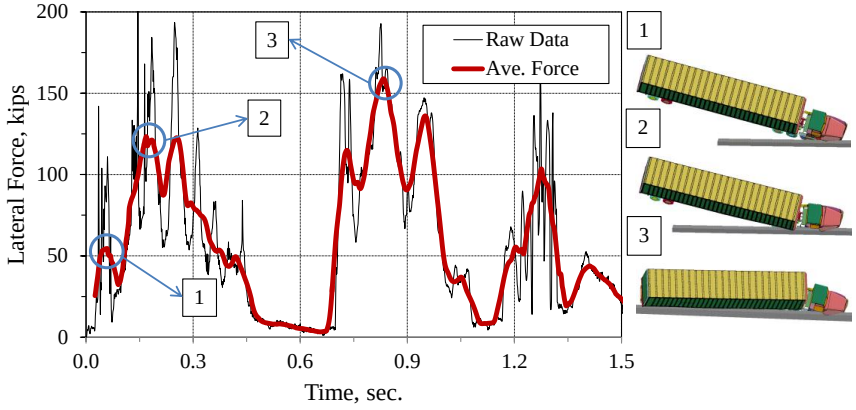

a) Lateral impact force (F_t)

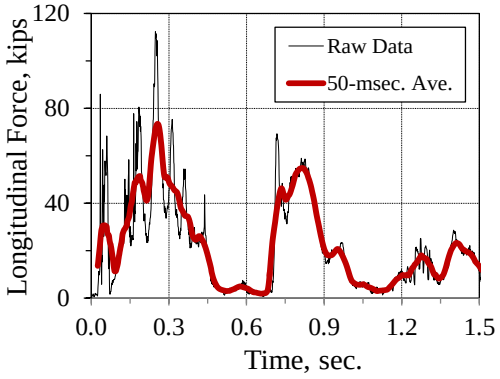

b) Longitudinal impact force (F_L)

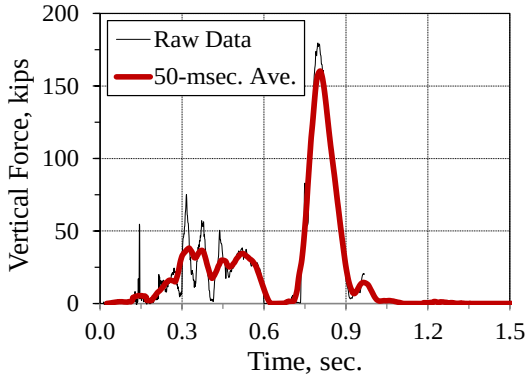

c) Vertical impact force (F_v)

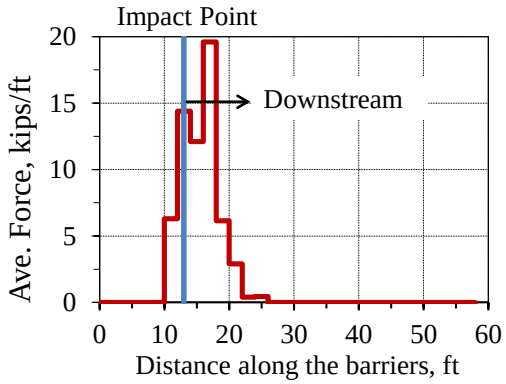

d) Longitudinal distribution, L_L (t=0.254 sec.)

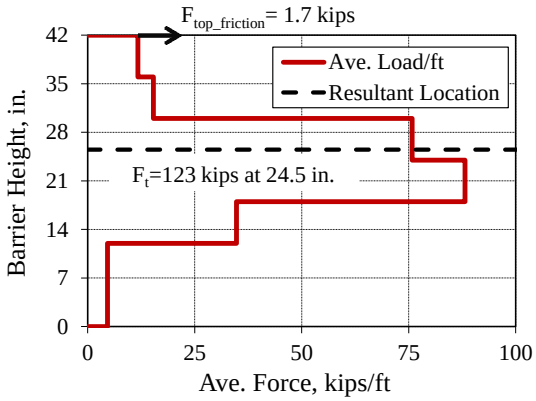

e) Transverse distribution and application H_e (t=0.254 sec.)

Figure 3.12 TL-5 impact force and distribution on the 42 in. (1.07 m) tall vertical barrier.

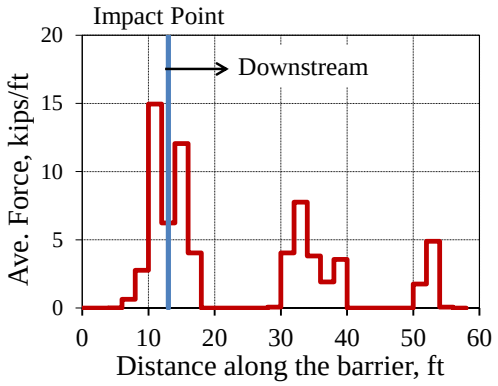

f) Longitudinal distribution, L_L (t=0.832 sec.)

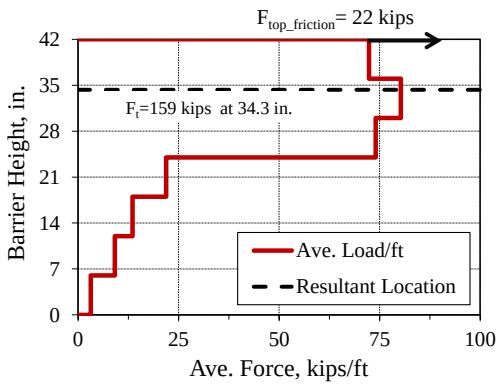

g) Transverse distribution and application H_e (t=0.832 sec.)

Figure 3.12 Continued

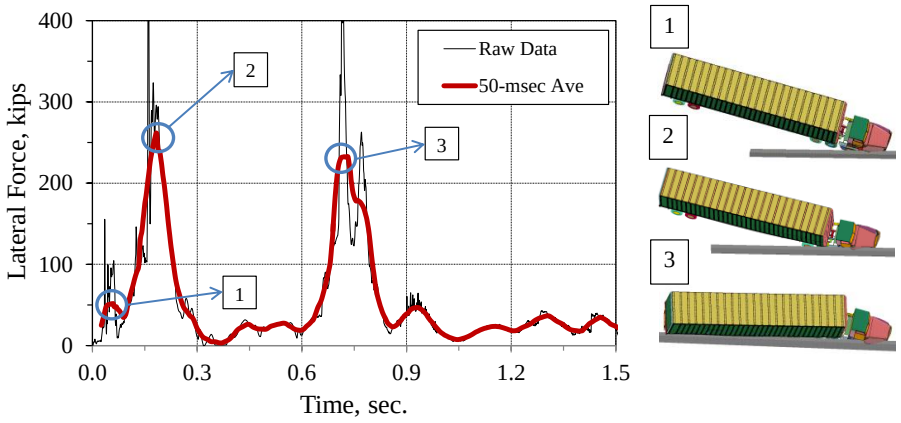

a) Lateral impact force (F_t)

Figure 3.13 TL-5 impact force and distribution on the 48 in. (1.22 m) tall vertical barrier

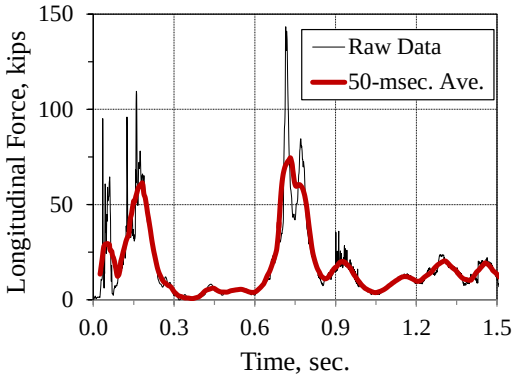

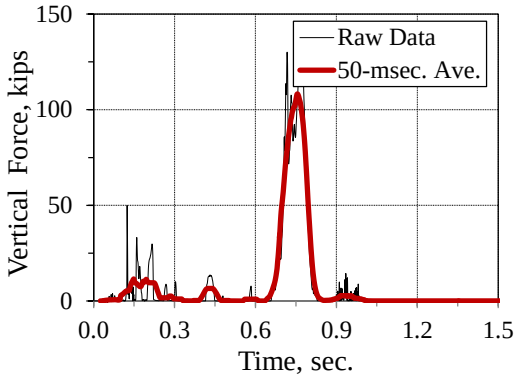

b) Longitudinal impact force (F_L)

c) Vertical impact force (F_v)

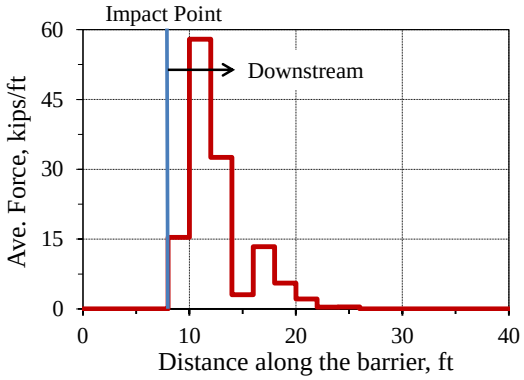

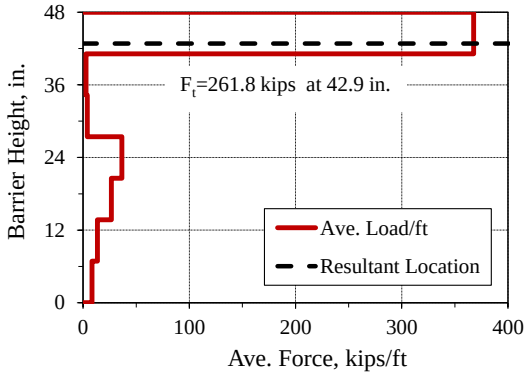

d) Longitudinal distribution, L_L (t=0.183 sec.)

e) Transverse distribution and application H_e (t=0.183 sec.)

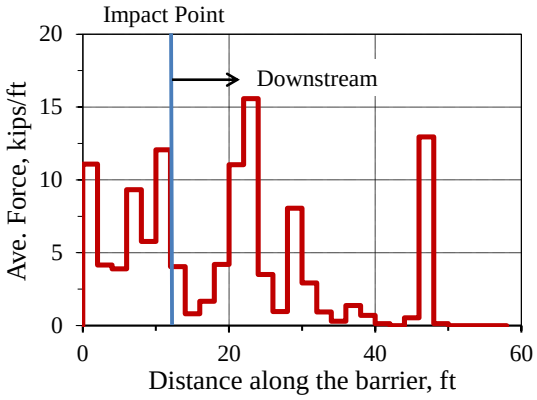

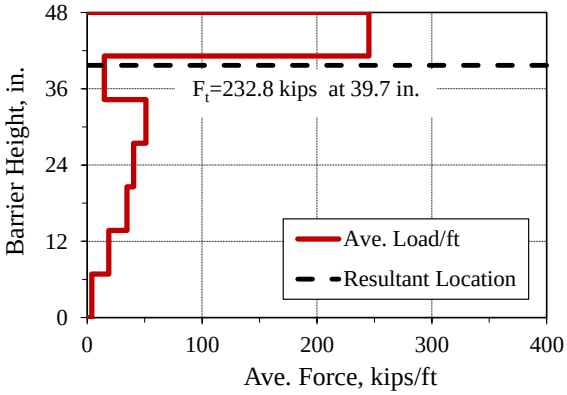

f) Longitudinal distribution, L_L (t=0.731 sec.)

g) Transverse distribution and application H_e (t=0.731 sec.)

Figure 3.13 Continued

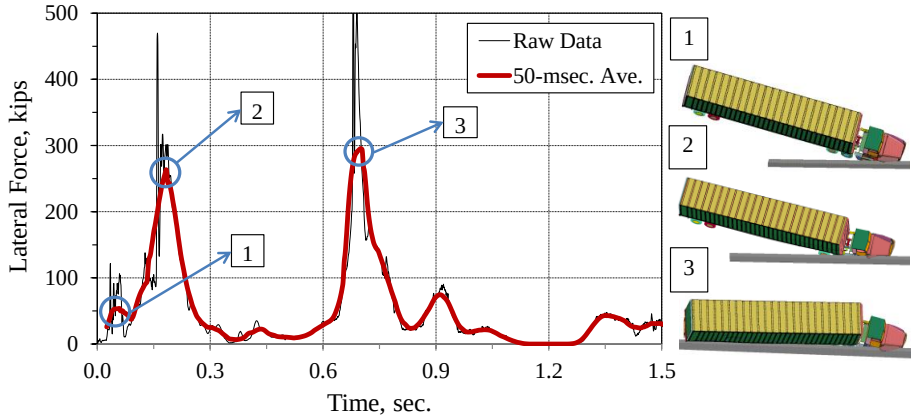

a) Lateral impact force (F_t)

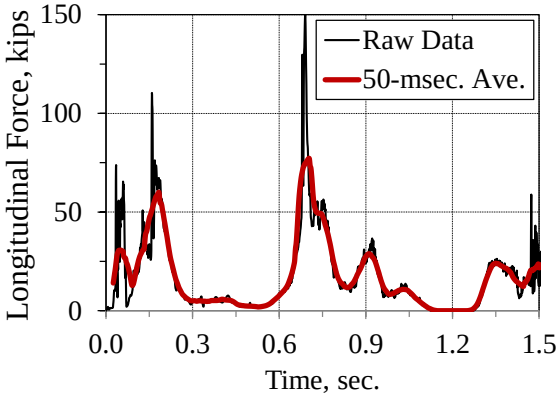

b) Longitudinal impact force (F_L)

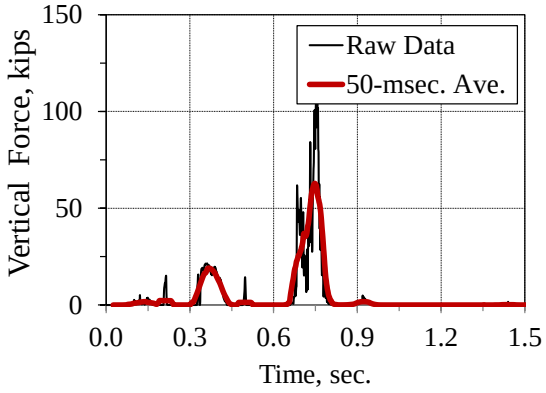

c) Vertical impact force (F_v)

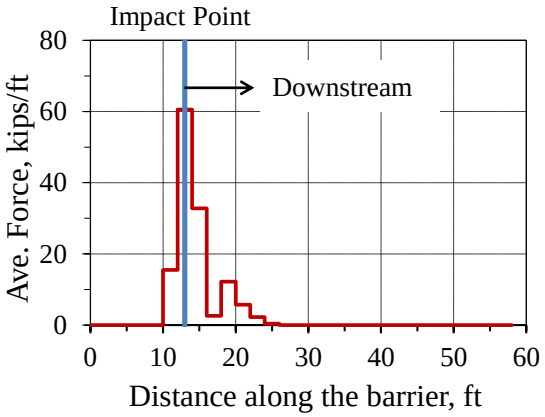

d) Longitudinal distribution, L_L (t=0.183 sec.)

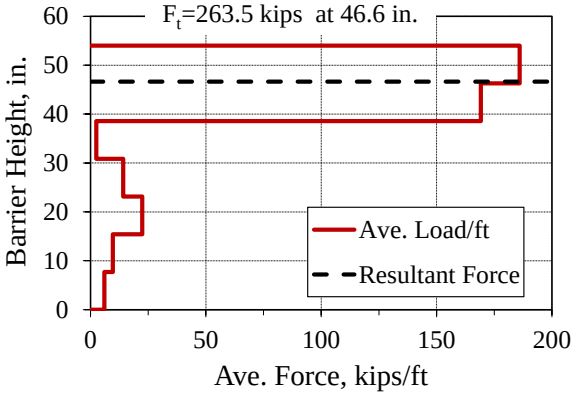

e) Transverse distribution and application H_e (t=0.183 sec.)

Figure 3.14 TL-5 impact force and distribution on the 54 in. (1.37 m) tall vertical barrier

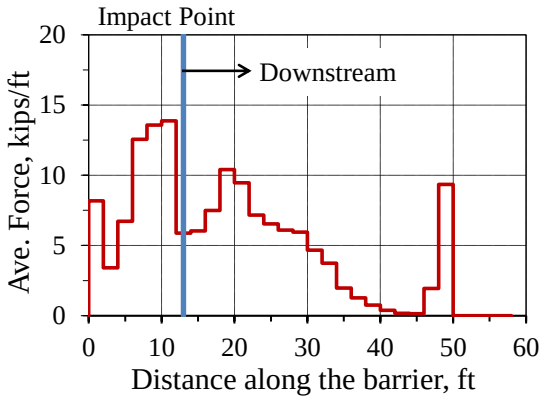

f) Longitudinal distribution, L_L (t=0.183 sec.)

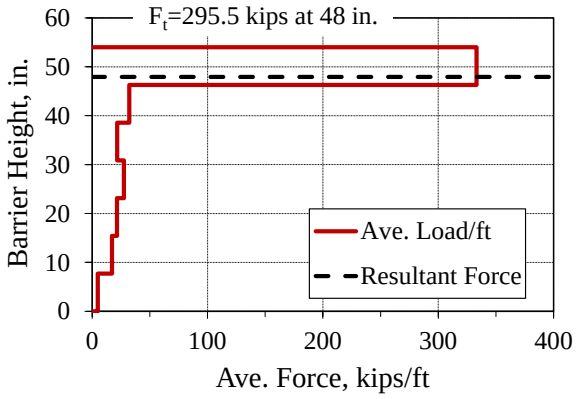

g) Transverse distribution and application H_e (t=0.183 sec.)

Figure 3.14 Continued

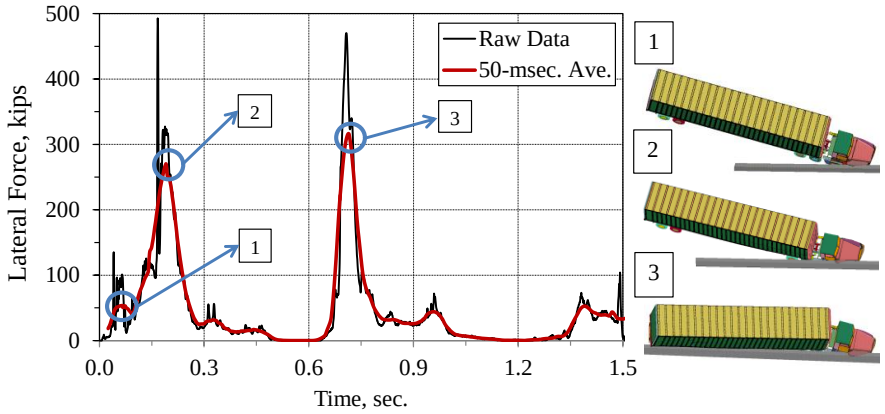

a) Lateral impact force (F_t)

Figure 3.15 TL-5 impact force and distribution on the tall vertical barrier

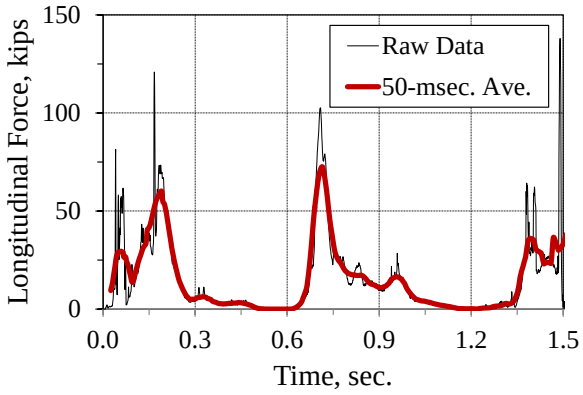

b) Longitudinal impact force (F_L)

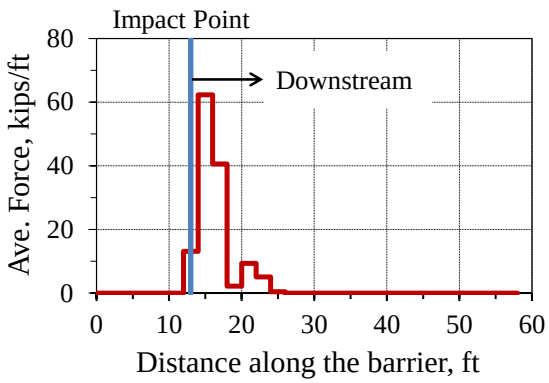

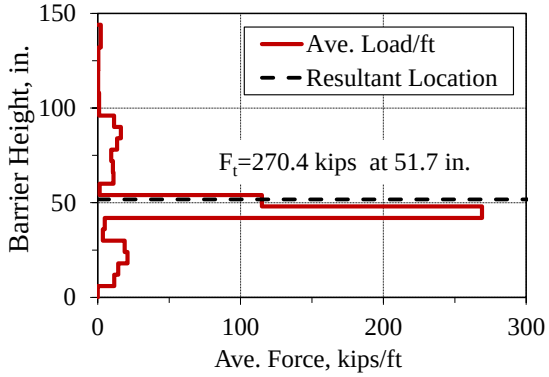

c) Longitudinal distribution, L_L (t=0.191 sec.)

d) Transverse distribution and application H_e (t=0.191 sec.)

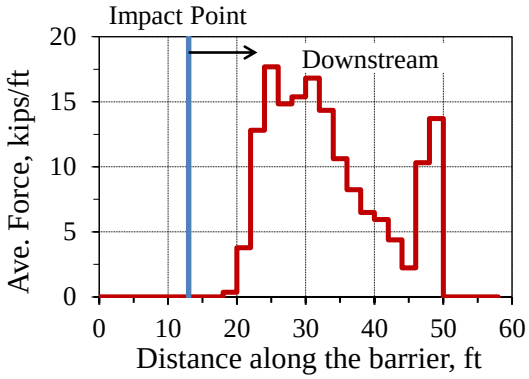

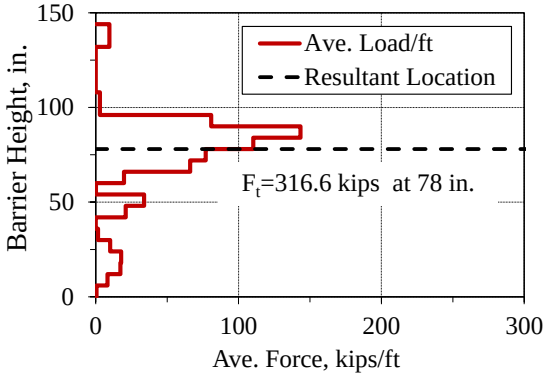

e) Longitudinal distribution, L_L (t=0.70 sec.)

f) Transverse distribution and application H_e (t=0.70 sec.)

Figure 3.15 Continued

The results of the different barriers analyzed in this section are summarized in Table 3.3 and Figure 3.16. The dash lines in Figure 3.16 is not intended to show a linear behavior of the impact load but the trace of the three impacts.

Table 3.3 Summary of magnitudes, distributions and applications of dynamic loads for MASH TL-5 impact

Design Forces and Designations	Barrier Height (in.)			
	42	48	54	Tall
F_t Transverse (kips) (First Impact)	54.6	51.7	53.8	53.7
F_t Transverse (kips) (Second Impact)	123	261.8	263.5	270.4
F_t Transverse (kips) (Third Impact)	159	232.8	295.5	316.6
F_L Longitudinal (kips)	73.5	74.6	77.2	72.6
F_v Vertical (kips)	160	108	62.8	N/A
L_L (ft) (Second Impact)	10	10	10	10
H_e (in.)	34.3	42.9	46.6	51.7

N/A= not applicable

Barrier height has a dramatic effect on the peak lateral load. Above a height of 42 in. (1.07 m), the trailer floor engages the barrier, resulting in a significant increase in force applied to the barrier. For example, the lateral load associated with the second impact on the 48 in. (1.22 m) tall barrier increases to 262 kips (1166 kN). This represent

a 213% increase over the 123 kips (547.4 kN) lateral load for the 42 in. (1.07 m) tall barrier. This is due to the impact of the front corner of the trailer as shown in Figure 3.17.

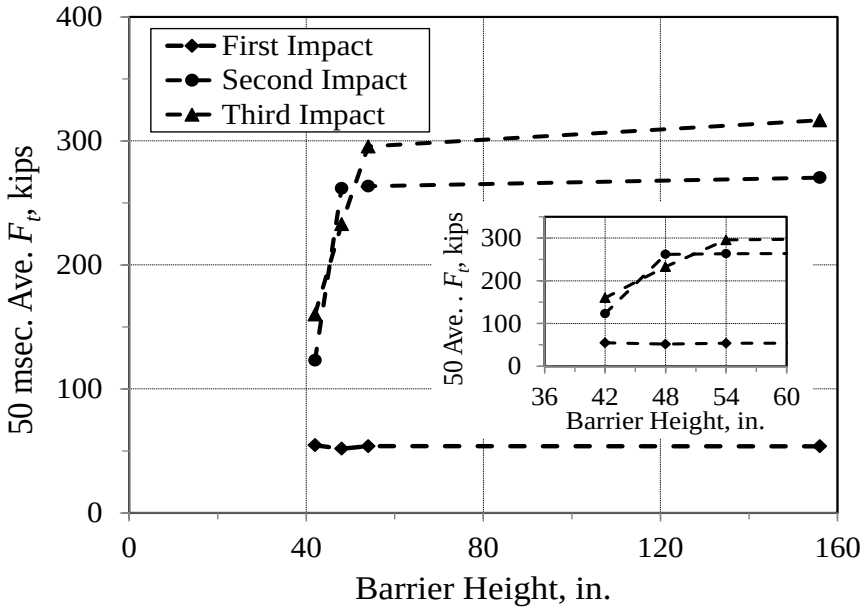

Figure 3.16 Variation of impact force for different barrier heights for MASH TL-5

The peak lateral loads associated with the taller barriers are greater than the load measured in the instrumented wall tests conducted by TTI researchers in the 1980's. The primary reason for this is the difference in the ballast. Many of the early tests conducted with tractor-van-trailers used sand bags and hay bales for ballast. Because ballast was not rigidly secured to the floor of the trailer, it was able to shift during impact resulting

in lower forces on the barrier. While these are still acceptable type of ballast, MASH states that "Ballast should be firmly secured to prevent movement during and after the test" *(5)*. This results in higher impact loads.

As shown in Table 3.3, the dynamic load due to the first impact is similar for all barriers. F_L, which is controlled by the frictional contact between the tires and the barrier, is also similar in all cases. Similar to the TL-4 study, F_v decreases as the barrier height increases. This is due to a reduction in roll of the tractor-trailer.

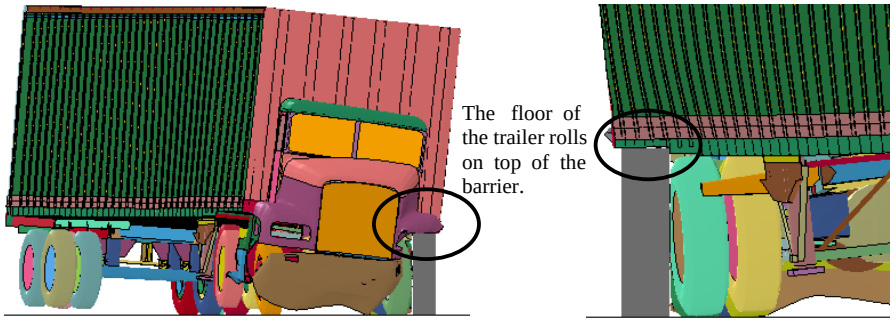

a) 42 in. (1.07 m) tall barrier (front view) **b) 42 in. (1.07 m) tall barrier (front view)**

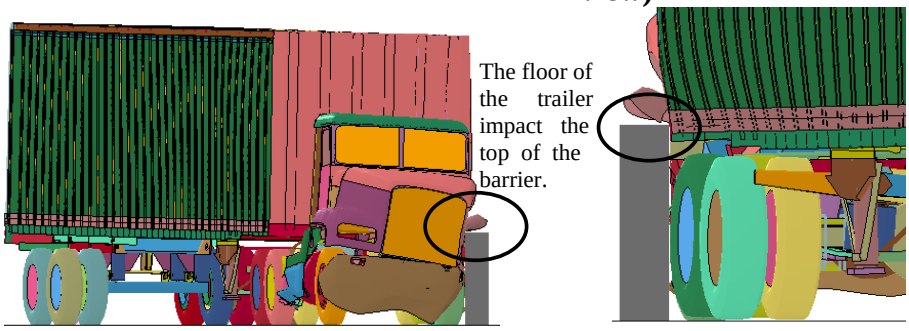

c) 48 in. (1.22 m) tall barrier (front view) **d) 48 in. (1.22 m) tall barrier (front view)**

Figure 3.17 Comparison of contact area between barriers for MASH TL-5 impact.

3.3 Recommendation of Design Impact Loads in Traffic Barriers for Mash TL-4 and TL-5 Impact

The FE analyses results were used to define the recommended design impact loads for MASH TL-4 and TL-5 impacts. The distribution of the critical impact load and the height of load application are also recommended. The recommendations of L_L were analyzed by considering the maximum load/unit length as well as the total length of load application. These two criteria were used to study the practical effect on the final design of the barrier (structural and practicality) and used to select the final recommendation of $L_{L.}$ The information is presented in Table 3.4.

The recommendations for MASH TL-4 impacts accounts for changes in impact condition, vehicle properties, and barrier height. The recommendations for MASH TL-5 accounts for the highest of the three impact loads imposed by the tractor-trailer on a barrier of a given height. Also, the final recommendation for MASH TL-5 has been split into two recommendations (TL-5-1 and TL-5-2) in order to assess the effect of the trailer and ballast in the magnitude of the impact load.

Table 3.4 Recommended design loads for TL-4 and TL-5 impact

Design Forces and Designations	TL-4	TL-5-1	TL-5-2
Rail Height, H (in.)	≥36	42	>42
F_t Transverse (kips)	80	160	260
F_L Longitudinal (kips)	27	75	75
F_v Vertical (kips)	38	160	80
L_L (ft)	4	10	10
L_v (ft)	18	40	40
H_e (in.)[1]	30	34	43[2]

[1] Vertical height of the resultant load.
[2] If barriers taller than 54 in. are used, use H_e=52 in.

4 BARRIER-MOMENT SLAB SYSTEM ANALYSES FOR TEST LEVEL 4 AND TEST LEVEL 5

The FE models of the TL-4 and TL-5 barrier-moment slab system (BMS) were developed to evaluate the kinematic response of the system when subjected to impact loading. The analyses were performed using the commercially available FE software LS-DYNA *(6).* The results of these analyses were used to study the dynamic behavior of the selected system on top of an MSE wall.

4.1 Dynamic Finite Element Analyses Model

The objective of these analyses are to determine the optimum barrier-moment slab system for TL-4 and TL-5 impact level under a limiting permanent displacement of 1.0 in. (25.4 mm). The study includes quantification of the barrier capacity, minimum width of the moment slab and movement of the barrier and the coping system.

4.1.1 Modeling Methodology

The methodology followed to model the barrier-moment slab system and then simulate their performance under impact consisted of the following steps:

- Design a barrier-moment slab system capable to withstand the impact of the corresponding test level (TL-4 and TL-5).
- Develop a FE model of the selected barrier-foundation system.
- Initialize the barrier-moment slab system model to account for gravitational loading.
- Simulate the impact test against the barrier. The prescribed impact conditions were based on the nominal conditions specified in MASH for TL-4 and TL-5 impact level.
- Quantify the displacement of the barrier and the magnitude of the impact forces. The optimum system should have a maximum permanent displacement of 1 in. (25.4 mm) at the coping section of the barrier. An iterative process was conducted until the displacement criterion was met.

a) Overview of the BMS Model

The finite element representation of the barrier-moment slab system model consists of the following components:

- Precast concrete barrier section and cast-in-place moment slab
- Backfill soil and overburden soil material
- Steel reinforcement connecting the precast barrier section to the moment slab
- Steel reinforcement shear dowels connecting the moment slab sections.
- Concrete leveling pad

The components of the BMS model (precast barrier, leveling pad, cast in place moment slab and soil) were modeled using solid elements. The steel reinforcement (rebars and shear dowels) were modeled using beam elements with six degrees of freedom at each end.

The elements of the barrier surrounding the impact location were meshed with an element characteristic size of 1.5 in. (38.1 mm) to capture the barrier deformation with improved accuracy. The rest of the barriers were coarsely meshed to reduce computational cost of the simulation. The soil elements located beneath the barrier and moment slab and at the shearing face were finely meshed using element characteristic size ranging from 1.5 in. (38.1 mm) to 4 in. (101.4 mm). This help to increase the robustness of the contact between the coping, moment slab and the soil. Figure 4.1 shows the components of a typical BMS model used for these analyses.

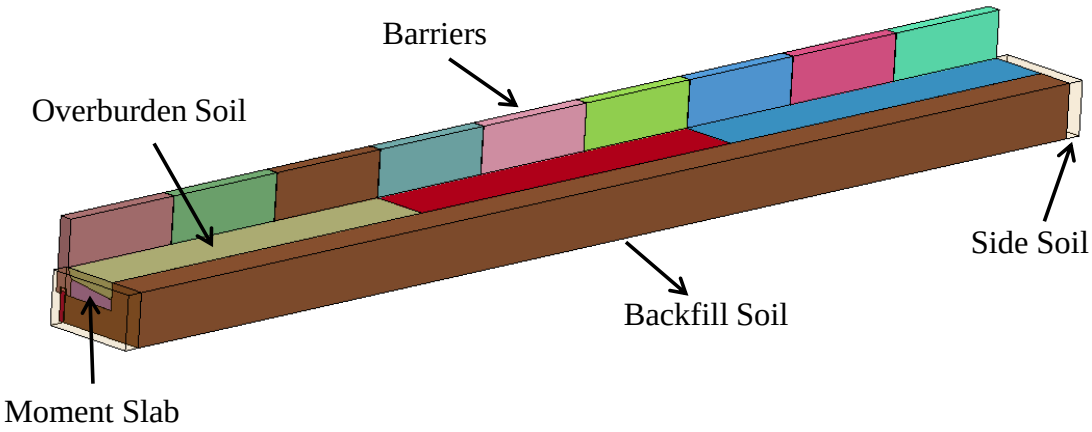

a) Three dimensional view

Figure 4.1 Details of a typical section of a BMS model

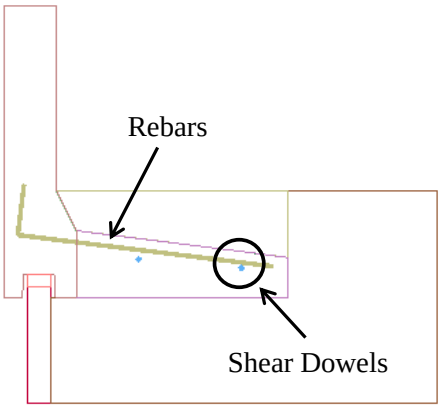

b) Rebar connection detail and shear dowels

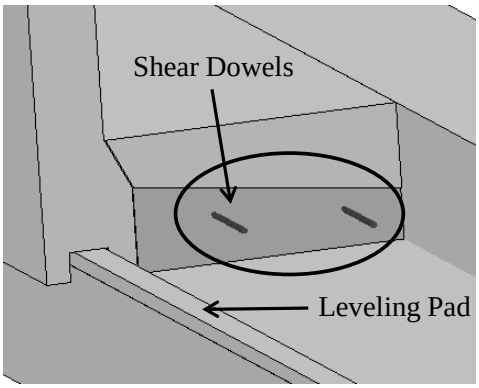

c) Shear dowels details and leveling pad

Figure 4.1 Continued

b) Contact Algorithm

Modeling large deformation problem required the implementation of advanced contact algorithms to successfully capture the interaction between all free surfaces. The LS-DYNA FE code offers some of the most advance features for modeling contact in crash analyses involving full-scale vehicles with different material properties and complex geometry. There are two ways of modeling the interaction between the beam elements and the solid elements (e.g., rebars and concrete). One method requires commons nodes between the rebars and the concrete. This will lead to the creation of unnecessary small element sizes and poor aspect ratio which will impact the time step and consequently the computational time. The other method is to couple the rebars to the concrete by using a

coupling algorithm. This mitigates the problem of having excessive small elements and poor aspect ratio *(42).* This last methodology was used to model the contact between the rebars to the concrete and the soil reinforcement to the soil.

The steel reinforcing bars were coupled (rather than merged) to the concrete using the LS-DYNA feature *CONSTRAINED_LAGRANGE_IN_SOLID. This coupling algorithm permits the reinforcement bars (treated as a slave) to be placed anywhere inside the concrete (treated as a master) without any mesh accommodation *(2,43,44).*

The interface between the soil and the structural slab was modeled using surface contact in order to represent the interaction between them. The contact friction was based on an angle of internal friction of the backfill material of 35 degrees (ϕ=35^o), measured using the Direct Shear Test *(45,46).*

c) Material Model and Model Parameters

The LS-DYNA FE code has several material models that can be implemented to evaluate the response of concrete structures. These material options range the very simple elastic material to a nonlinear damage material model including rate effects *(2).* The elastic material option was used to study the dynamic response of the concrete barriers and moment slabs (LS-DYNA *MAT_001). In this case, the tensile capacity of the concrete was checked to prevent it to exceed the failure threshold of the concrete.

The steel rebars were modeled using a piecewise linear isotropic plasticity model that is representative of an actual stress-strain relationship of a steel grade 60 (LS-DYNA *MAT_24). This is an elastic plastic material model which uses the young modulus if stresses are below the yield stress and the measured stress-strain-curve if the stresses are above the yield stress *(47)*. After yielding, the steel rebars exhibit rate effects and yield in a ductile manner until it breaks at an ultimate strain greater than approximately 20% *(2)*.

The backfill soil and the overburden soil material were modeled using the LS-DYNA two invariant geologic cap models (LS-DYNA *MAT_25) *(6)*. This soil-cap constitutive model is defined by a convex yield surface consisting of a failure enveloped (f_1), an elliptic cap (f_2), and a tension cutoff region (f_3), as shown in Figure 4.2. The three yield surfaces are given as follows *(6)*:

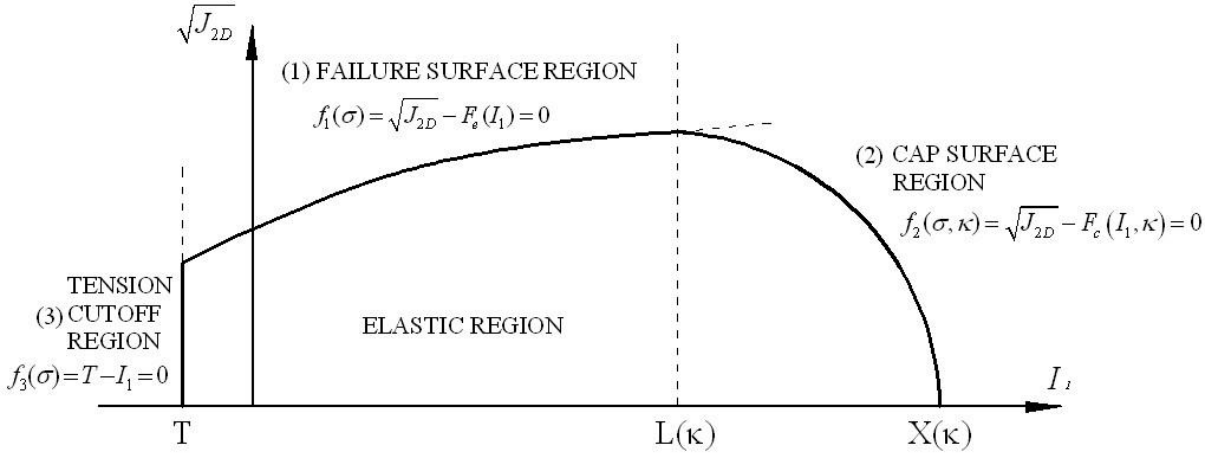

Figure 4.2 Yield surface of the cap model *(6)*.

1. Failure envelope region:

$$f_1(\sigma) = \sqrt{J_{2D}} - F_e(I_1) = 0 \text{, for } T \le I_1 < L(\kappa) \tag{4-1}$$

$$F_e(I_1) = \alpha - \gamma e^{-\beta I_1} + \theta I_1 \tag{4-2}$$

2. Cap region:

$$f_2(\sigma, \kappa) = \sqrt{J_{2D}} - F_c\left(I_1, \kappa\right) = 0 \text{, for } L(\kappa) \le I_1 < X(\kappa) \tag{4-3}$$

$$F_c\left(I_1, \kappa\right) = \frac{1}{R}\sqrt{\left[X(\kappa) - L(\kappa)\right]^2 - \left[I_1 - L(\kappa)\right]^2} \tag{4-4}$$

$$X(\kappa) = \kappa + RF_e(\kappa) \tag{4-5}$$

$$L(\kappa) = \begin{cases} \kappa & if\ \kappa > 0 \\ 0 & if\ \kappa \le 0 \end{cases} \tag{4-6}$$

3. Tension cutoff region: $f_3(\sigma) = T - I_1 = 0$, for $I_1 = T$ (4-7)

The above equations shows that the failure surface of the cap model is defined in term of the first stress invariant (I_1) and the second deviatoric stress invariant ($J_{2D}=1/2S_{ij}S_{ji}$), where σ = stress tensor. The parameter T is the maximum hydrostatic tension sustainable by the material (value of I_1 at the tension cutoff location); $L(\kappa)$ is the intersection point between the shear failure surface and the ellipsoidal cap. The parameters α, θ, γ, α and β are used to evaluate the yield surface at the elastic range. They are usually evaluated by fitting a curve through failure data taken from a set of triaxial compression tests *(6)*.

The value of *R* is the ratio of the major to minor axes of the elliptical cap. The parameter *X(κ)* defines the intersection of the cap with the I_1; κ is the hardening parameter which is equal to the plastic volumetric strain ($\kappa=\varepsilon_v^p$). The plastic volumetric strain is evaluated using the hardening law function, as follow:

$$\varepsilon_v^p = W\left\{1-\exp\left[-D(X(\kappa)-X_0\right]\right\} \tag{4-8}$$

The parameters *W, D* and X_o, shown in Eq. (4-8), are material constants. The value of *W* represents the maximum plastic volumetric strain that the material can developed, *D* is the initial slope of loading in hydrostatic compression and X_o in the hardening law coefficient (defines the initial location of the cap).

The implementation of the cap model exhibits two major advantages over other classical models such as the Drucker-Prager and Mohr-Coulomb. The first advantage is the ability to control dilatency produced under shear loading and the second advantage in the ability to model plastic compaction *(6).* Therefore, these properties make this model suitable to study the dynamic behavior of the backfill and overburden soil material during impact and shear loading.

The soil material properties implemented in the cap model in this study is described in Table 4.1. The values of the parameters were successfully implemented during the study conducted in NCHRP Report 663.

Table 4.1 Soil cap material properties used in the simulation *(2)*.

Elasticity	K (MPa)	22.219
	G (MPa)	7.407
Plasticity	α (MPa)	4.154
	β (MPa^{-1})	0.0647
	γ (MPa)	4.055
	θ (radian)	0.0
Hardening Law	W	0.08266
	D (MPa^{-1})	0.239
	R	28
	X_0 (MPa)	-2.819
Tension Cut	T (MPa)	0.0

4.1.2 Analyses for Test Level 4 Impact

A nonlinear FE analyses is performed to theoretically explain the dynamic performance of a BMS system when subjected to a MASH TL-4 impact. The principal objective is to obtain the optimum width of moment slab required to contain a MASHT TL-4 test vehicle with a limiting permanent displacement of 1.0 in. (25.4 mm). The study is conducted using a 42 in. (1.07 m) tall vertical wall as it develops the largest impact load for TL-4.

a) Description of the Barrier and the Moment Slab

The design load for a MASH TL-4 impact is 80 kips (356 kN), as recommended in section 3. This load was estimated based on a 42 in. (1.07 m) tall rigid barrier study

using full-scale impact simulation. Therefore, the barrier section used in this study is a concrete vertical wall barrier of 42 in. (1.07 m) tall, as shown in Figure 4.3.

The end section ultimate capacity of this barrier was computed to be 89.8 kips (399.6 kN) using the yield line failure mechanism described in AASHTO LRFD *(3).* The length of the failure mechanism calculated for the 42 in. (1067 mm) tall barrier section analyzed was 4.2 ft (1.3 m) (in end section). The moment and shear capacity at the coping section (section B-B) was computed to be 424 kip-ft (575 kN-m) and 133 kips (591.8 kN), respectively. Since the coping provides enough capacity to resist the impact load, this indicates that the 10 ft (3.05 m) section length selected for evaluation of the TL-4 impact is sufficient to develop the primary failure mechanism for the barrier.

The TL-4 BMS system model was composed of three sections of 30 ft (9.15 m) long each. Each section was composed of three 10 ft (3.05 m) long barriers (Figure 4.3). The width of the moment slab was 4.5 ft (1.37 m) measured from the face of the panels. The width of the moment slab was estimated using equilibrium analyses, simulated and re-designed, if necessary, until it meets the displacement criterion. Two #9 shear dowel bars were used to connect the joints between the moment slabs. The shear dowels were embedded 18 in. (457 mm) at each side of the moment slab.

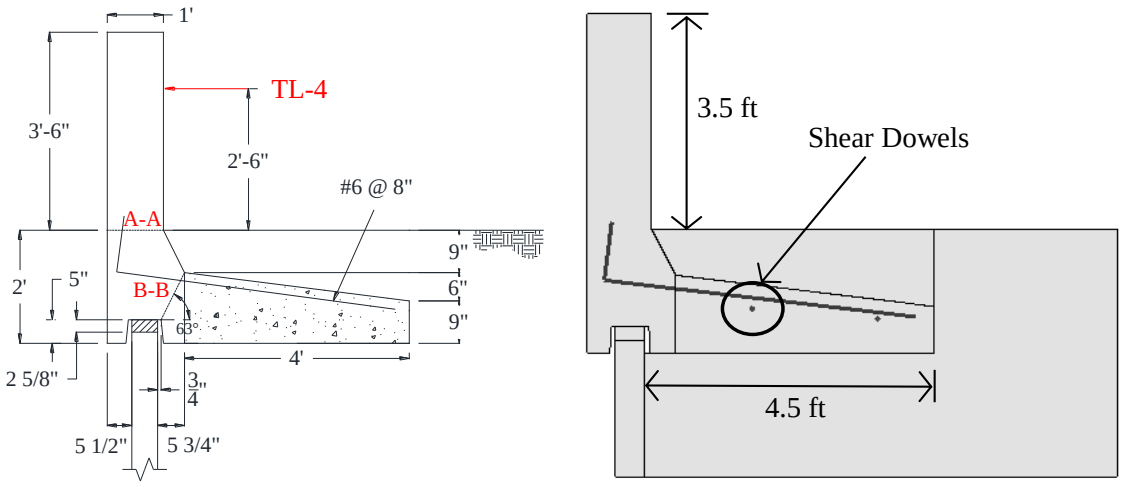

a) Concrete barrier detail **b) Concrete barrier detail in the model**

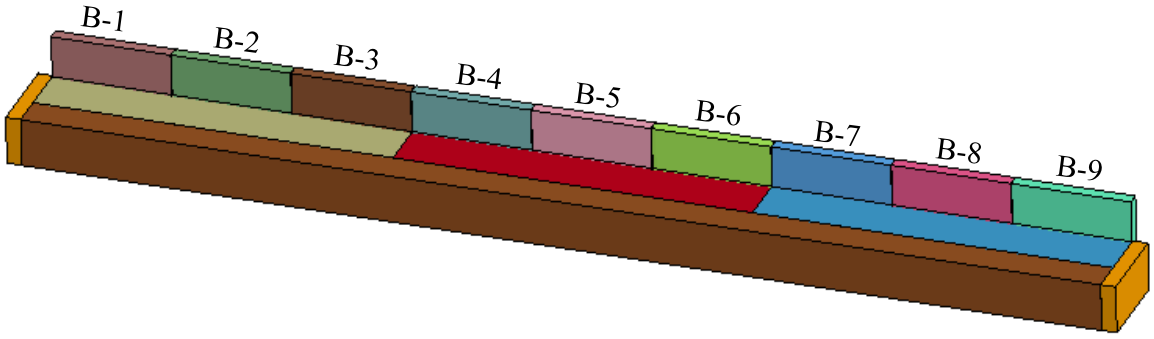

c) Alphanumeric designator for the barriers

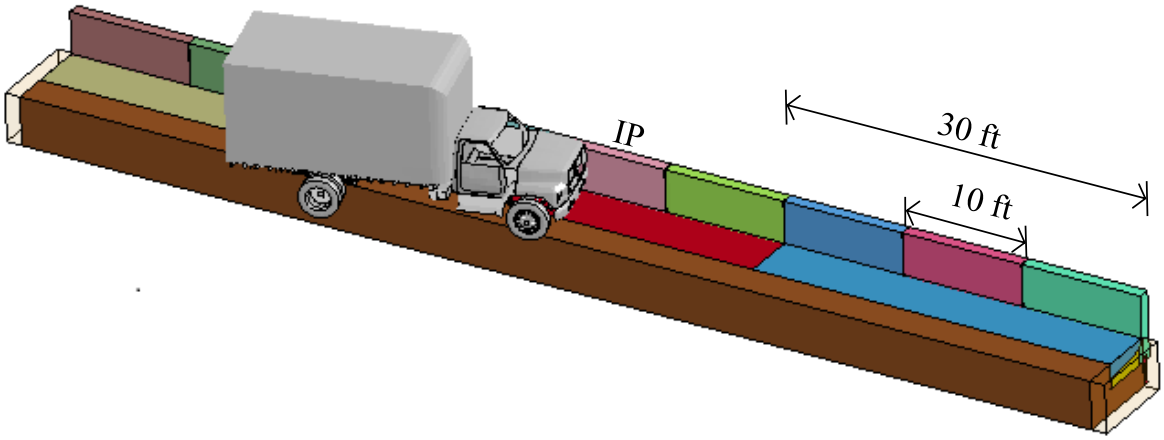

d) Three dimensional view

Figure 4.3 Barrier-moment slab system details for TL-4 analyses

b) Loads and Displacements of the Barrier-Moment Slab System

The simulated SUT vehicle model impacted barrier 5 (B-5) at a speed of 56 mph (90 km/hr.) at 15 degrees angle. Sequential images from the simulation are shown in Figure 4.4. These images are associated with the time of the peak load due to the front impact Figure 4.4(b)), the time of maximum load in the barrier Figure 4.4(c)), and the time of maximum longitudinal load Figure 4.4(c)).

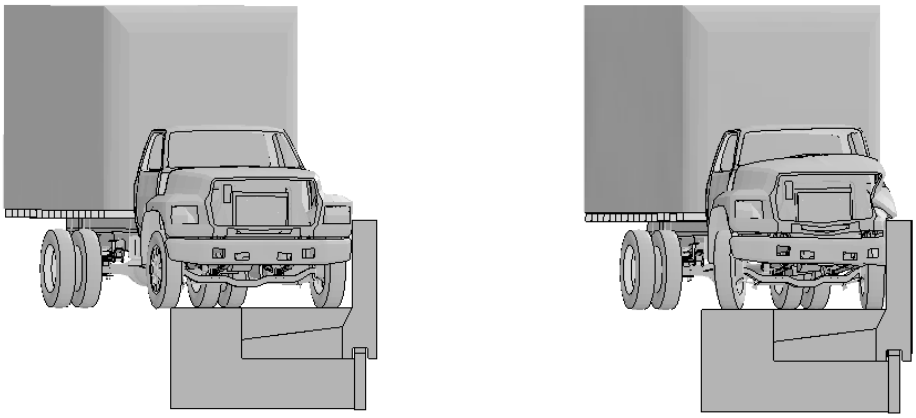

a) t=0.0 sec. **b) t=0.1l sec.**

Figure 4.4 TL-4 SUT vehicle position at each significant moment

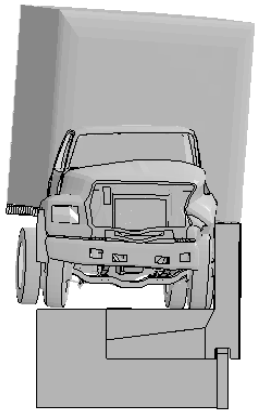

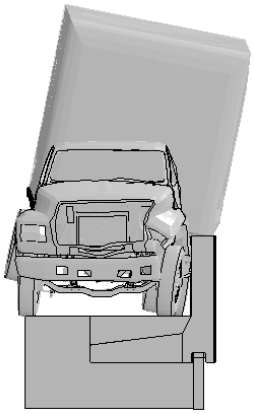

c) t=0.235 sec. **d) t=0.365 sec.**

Figure 4.4 Continued

The calculated maximum 50-msec. average impact load F_t was 70.3 kips (312.8 kN) at 0.235 sec. and it was due to the back slap impact (Figure 4.5). In the longitudinal and vertical direction, the maximum 50-msec. average impact load were 38.8 kips (172.7 kN) at 0.365 sec. and 20.5 kips (91.2 kN) at 0.30 sec., respectively. The simulation results indicate that the concrete barrier did not exceed the tensile capacity threshold of the concrete (approximately 400 psi (2.76 MPa)).

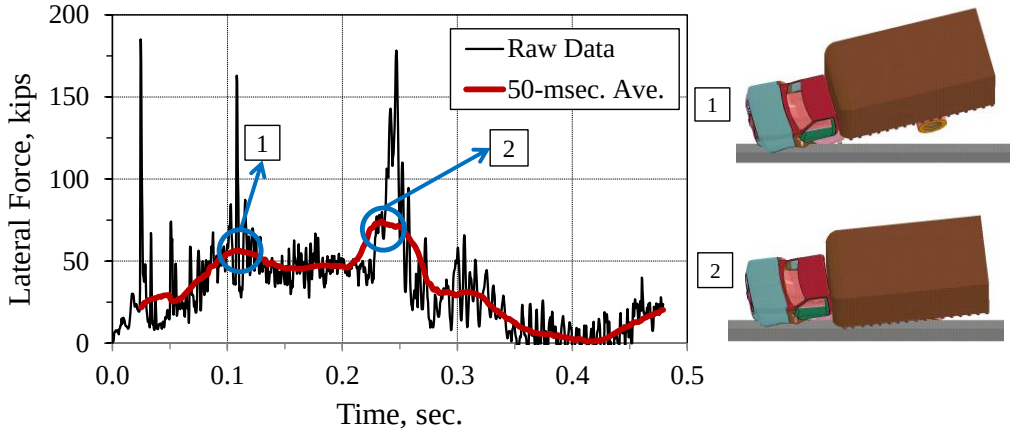

a) Lateral impact force (F_t)

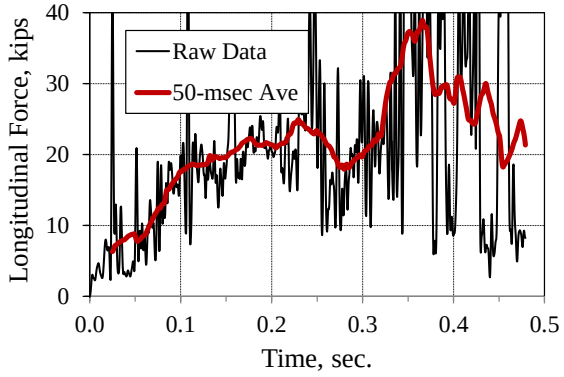

b) Longitudinal impact force (F_L)

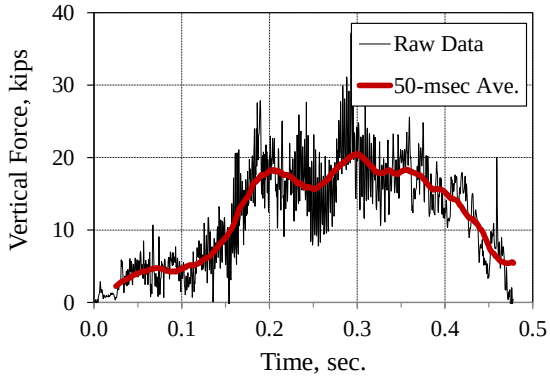

c) Vertical impact force (F_V)

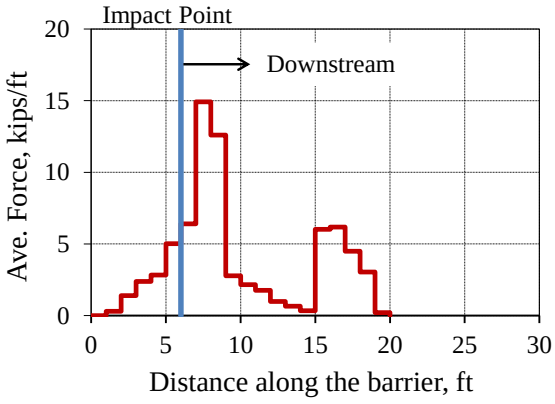

d) Longitudinal impact force (F_L)

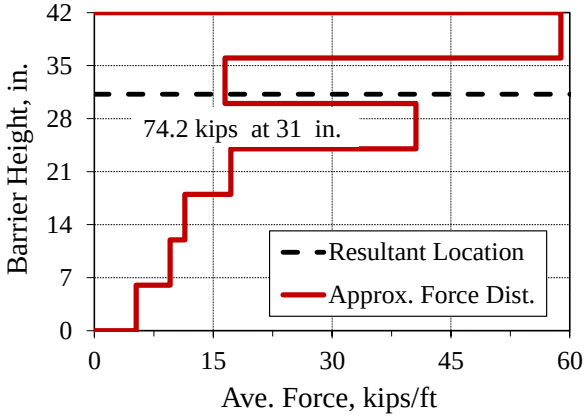

e) Vertical impact force (F_V)

Figure 4.5 TL-4 time history load in the barrier and load distribution.

The maximum displacement at the top of the barrier occurred close to the impact point (IP) (barrier section "B-5") and it was 1.6 in. (40.6 mm). The displacement-time history at the IP is shown in Figure 4.6(a). Figure 4.6(b) shows that about 2/3 of this displacement is associated with rotation of the barrier while 1/3 is associated with sliding. The total permanent displacement at the coping section was 0.75 in. (19 mm).

Figure 4.6(c) through Figure 4.6(e) show the relative displacement at the upstream joint ("B3-B4") of IP, barrier section "B5-B6" and downstream joint ("B6-B7") of IP. In all cases, the relative displacement at the coping is very small which indicates that the shear dowels and the connection between the barrier and the moment slab are adequate to withstand this impact level. At the top of the barrier, the relative displacement is more appreciable. However, this relative displacement is associated with the rotation of the barrier and therefore most of it is recoverable. The vertical displacement of the middle moment slab was also captured from the simulation. Figure 4.6(f) shows that the maximum vertical movement of the upstream joint edge and the downstream joint edge of moment slab is 0.69 in. (17.3 mm) and 0.6 in. (15.2 mm), respectively. This indicates that the 30 ft (9.15 m) long barrier-moment slab section is behaving with a close rigid body motion and the connection between the moment slabs and barriers is also adequate.

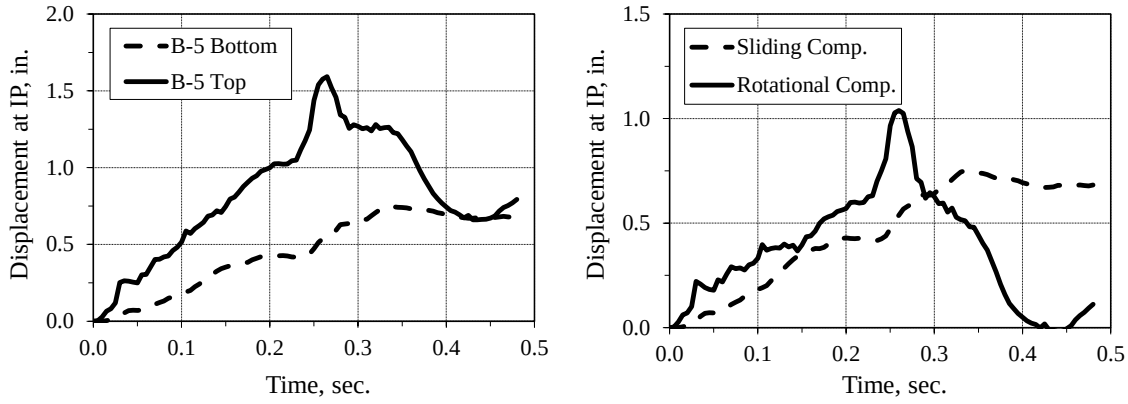

a) Displacement at impact point (IP) **b) Sliding and rotational comp.**

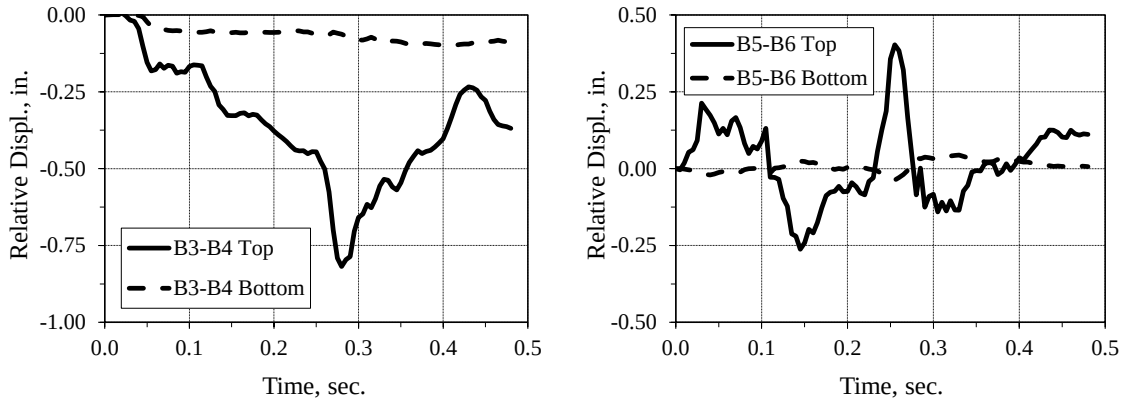

c) Relative displacement at B3-B4 **d) Relative displacement at B5-B6**

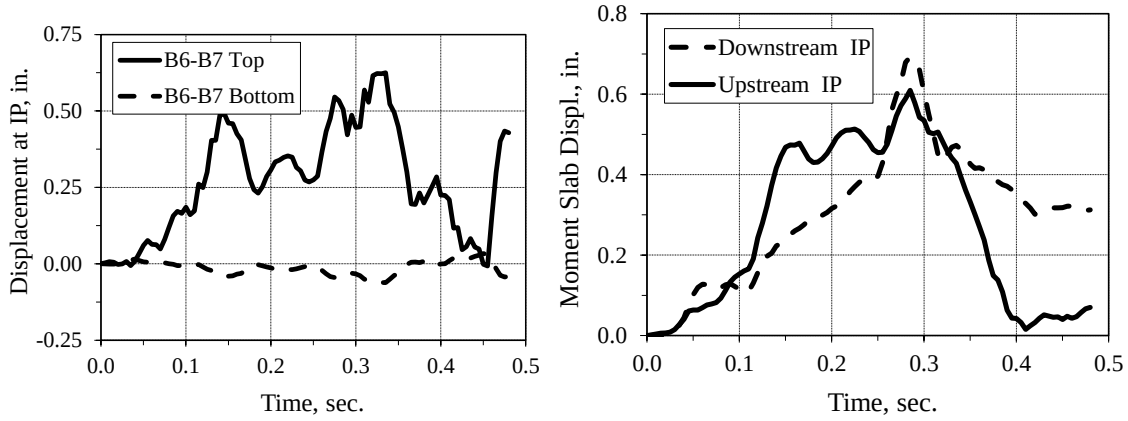

e) Relative displacement at B6-B7 **f) Vertical displacement of moment slab**

Figure 4.6 Displacement of the barriers and the moment slab for TL-4 impact

4.1.3 Analyses for Test Level 5 Impact with 42 in. (1.07 m) Tall Barrier (TL-5-1)

In section 3 it was found that the impact load associated with a fully-loaded tractor trailer is highly influenced by the height of the barrier. Consequently, the analyses conducted in this section for MASH TL-5 was divided into a TL-5-1 (MASH TL-5 test vehicle impacting a 42 in. (1067 mm) tall barrier) and a TL-5-2 (MASH TL-5 test vehicle impacting a 48 in. (1219 m) tall barrier).

A nonlinear FE analyses was developed to theoretically explain the dynamic performance of a BMS system when subjected to a MASH TL-5-1 impact. The principal objectives are to obtain the optimum width of moment slab and the length of the barrier section required to contain a MASHT TL-5 test vehicle with a limiting permanent displacement of 1.0 in. (25.4 mm). The TL-5-1 study is conducted using a 42 in. (1.07 m) tall vertical wall barrier.

a) Description of the Barrier and the Moment Slab

Figure 4.7 shows the cross section of the 42 in. (1.07 m) tall barrier-moment slab system used to withstand a MASH TL-5 impact. The barrier-section was designed to contain a dynamic load of 160 kips (712 kN), as recommended in section 3. The end section ultimate capacity of the barrier was computed to be 161.1 kips (716.9 kN) using the yield line failure mechanism described in AASHTO LRFD *(3).* The length of the failure mechanism calculated for the barrier section analyzed was 10.3 ft (3.14 m) in end

section. The moment and shear capacity at the coping section (section B-B) was 1175 kip-ft (1593.3 kN-m) and 255 kips (1134.8 kN), respectively. The results indicate that the coping section provides enough capacity to resist the impact load. Therefore, the 15 ft (4.57 m) section length selected for evaluation of the TL-5-1 impact is sufficient to develop the primary failure mechanism of the barrier.

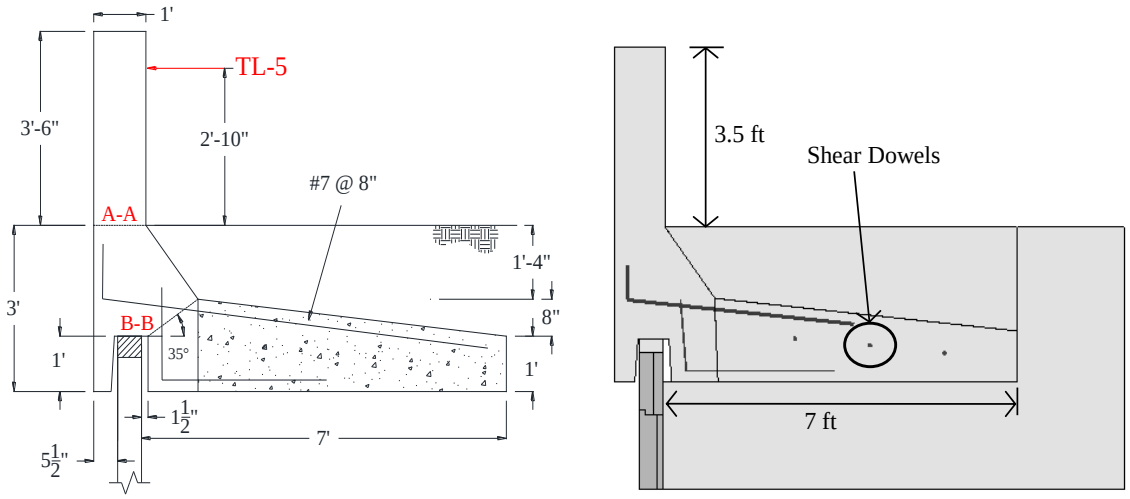

a) Concrete barrier detail **b) Concrete barrier detail in the model**

Figure 4.7 Barrier-moment slab system details for TL-5-1 analyses

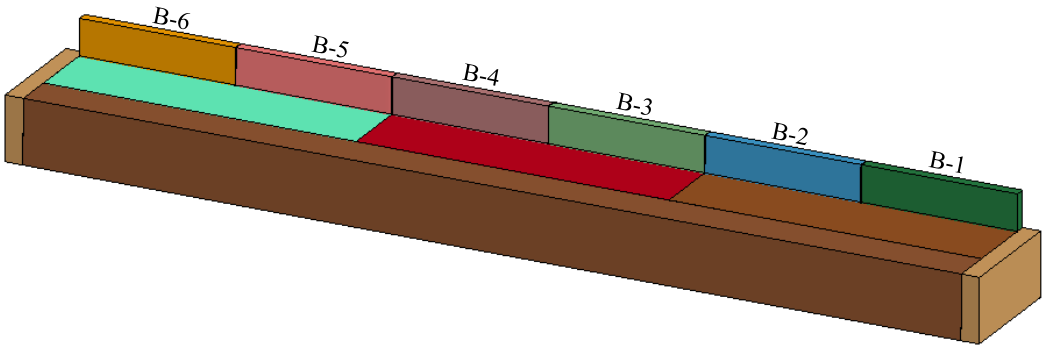

c) Alphanumeric designator for the barriers

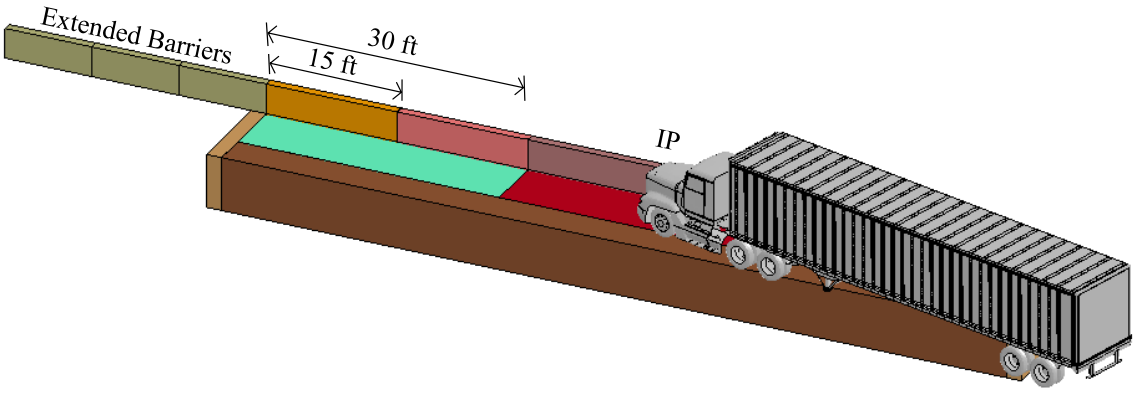

d) Three dimensional view

Figure 4.7 Continued

The TL-5-1 BMS system model was composed of three sections of 30 ft (9.15 m) long each. Each section was composed of two 15 ft (4.57 m) long barriers (Figure 4.7). The width of the moment slab was 7 ft (2.13 m) measured from the face of panels. The procedure used to estimate the optimum width of the moment slab was similar to the procedure described for MASH TL-4 impact.

Since the impulse load applied by a fully loaded tractor trailer is significant larger than a MASH TL-4 impact, therefore, the number of shear dowels were increased from two #9 steel bars to three #11 steel bars. The shear dowels were embedded in the moment slabs about 18 in. (457 mm) at each side. These shear dowels will ensure a good connection between the impacted moment slab to its neighbors. The extension of the vertical wall barriers (Figure 4.7(d)) beyond the BMS model have the purpose of helping redirect the tractor-trailer vehicle model downstream the impact point.

b) Loads and Displacements of the Barrier-Moment Slab System

The simulated tractor-trailer vehicle model impacted the joint between barrier 3 (B-3) and barrier 4 (B-4) at a speed of 50 mph (80 km/hr.) at 15 degrees angle. Sequential images from the simulation are shown in Figure 4.8. These images are associated with the time of peak load due to the front impact of the tractor (Figure 4.8(b)), the time of peak load due to the impact of the rear tandem axles of the tractor and the front of the trailer (Figure 4.8(c)) and the time of peak load associated with the impact of the rear tandem axles of the trailer (Figure 4.4 (c)).

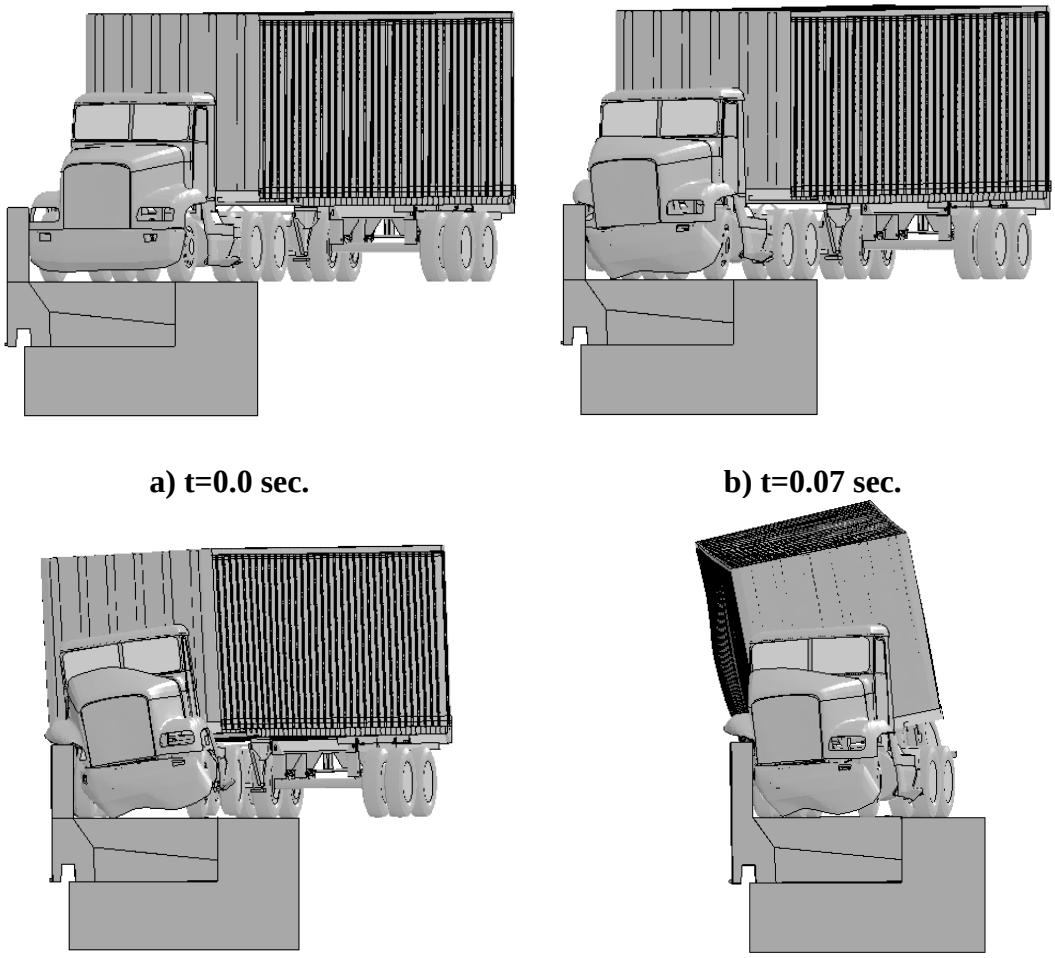

a) t=0.0 sec. **b) t=0.07 sec.**

c) t=0.261 sec. **d) t=0.809 sec.**

Figure 4.8 TL-5-1 tractor-trailer vehicle position at each significant moment

The time history of the impact load shows that the maximum 50-msec. average load (F_t) was 168.8 kips (751.2 kN) at 0.808 sec. and it was associated with the impact of the rear tandem axles of the trailer (Figure 4.9 (a)). This load also includes the lateral component of the friction load imposed while it is riding on top of the barrier. The friction load on top of the barrier might not have a significant effect for designing the

strength capacity of a concrete barrier but it has a significant influence on the overall stability of the barrier-moment slab system.

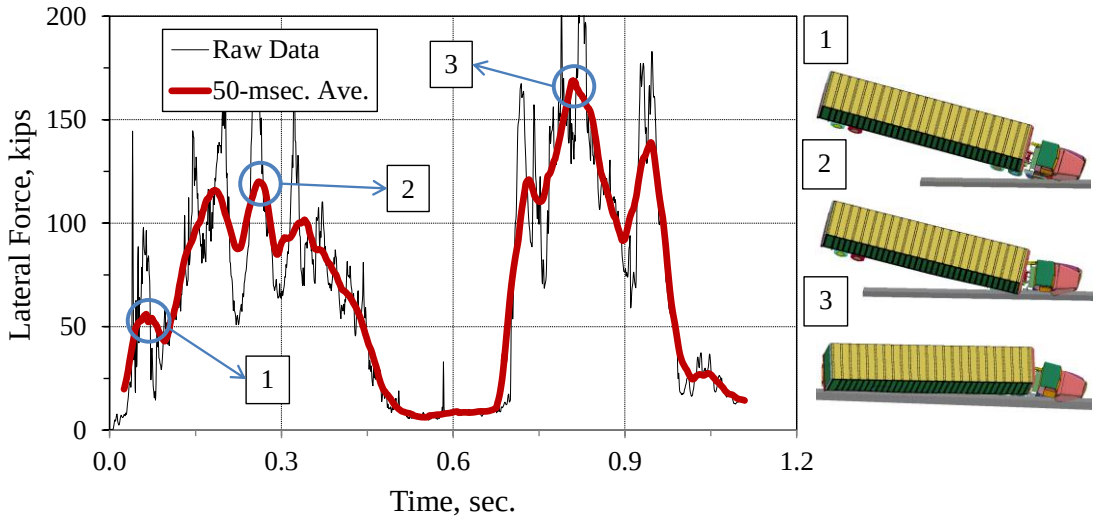

a) Lateral impact force (F_t)

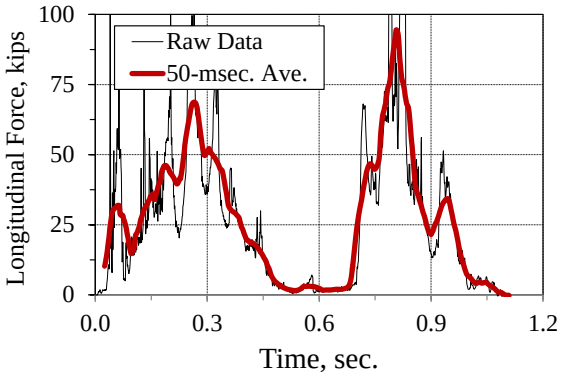

b) Longitudinal impact force (F_L)

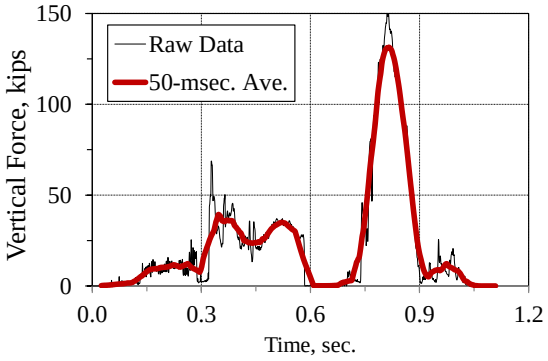

c) Vertical impact force (F_V)

Figure 4.9 TL-5 time history load in the barrier and load distribution on the 42 in. (1.07 m) BMS system

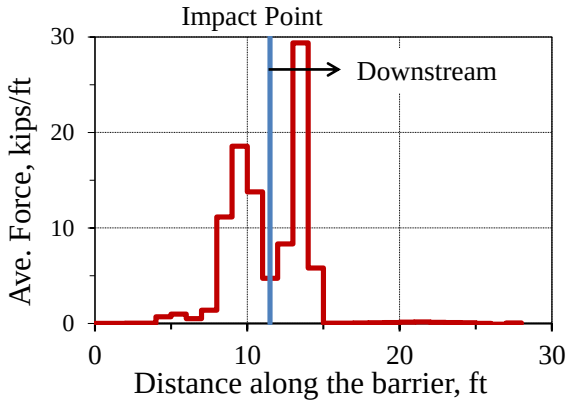

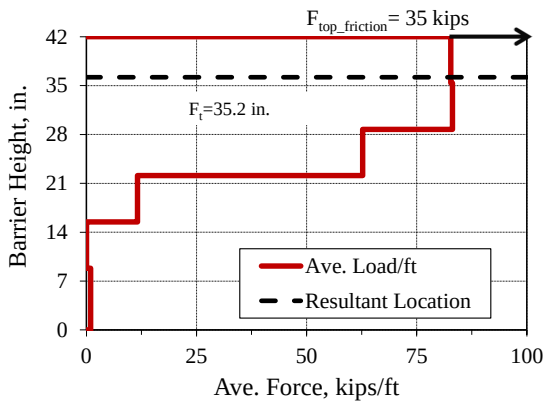

d) Longitudinal distribution (L_L) of F_t **e) Vertical distribution of F_t**

Figure 4.9 Continued

In the longitudinal and vertical direction, the maximum 50-msec. average impact load were 94.4 kips (420.1 kN) at 0.807 sec. and 131.4 kips (584.7 kN) at 0.816 sec., respectively. The simulation results indicate that the concrete barrier did not exceed the tensile capacity threshold of the concrete (approximately 400 psi (2.76 MPa)).

The maximum displacement of the barriers occurred close to the IP and it was 1.73 in. (43.9 mm) at the top and 0.55 in. (14 mm) at the coping section. The displacement-time history at the IP is shown in Figure 4.10(a). Figure 4.10(b) shows that the impact associated with the rear tandem axles of the tractor displaces the barrier about 0.75 in. (19.1 mm) in rotation and 0.25 in. (6.4 mm) in sliding. Then, the barrier rebounds back and it is impacted by the rear tandem axles of the trailer which displaces it about 1.25 in. (31.8 mm) in rotation and slide the system 0.3 in. (7.6 mm) more.

The relative displacements at the upstream joint ("B2-B3"), barrier section "B3-B4" and downstream joint ("B4-B5") are very small as shown in Figure 4.10(c), Figure 4.10(d) and Figure 4.10(e), respectively. This small movement at the coping indicates that the shear dowels and the connection between the barrier and the moment slab are appropriate to withstand this impact level.

At the top of the barriers, the relative displacement is more appreciable. However, this relative displacement is associated with the rotation of the barriers and, therefore, most of it is recoverable. Figure 4.10(f) shows the vertical displacement of the middle moment slab section. The kinematic behavior of the moment slab when impacted by the tractor-van-trailer model was similar to the behavior observed in the MASH TL-4 impact simulation analyses. The rotational displacement at the top of the barrier and the vertical movement of the moment slab shows similar trace indicating a rigid body motion and little bending deformation.

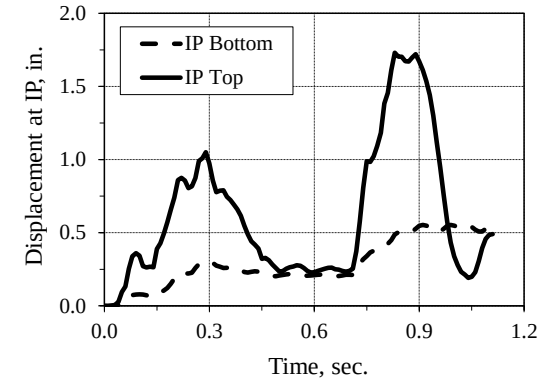

a) Displacement at impact point (IP)

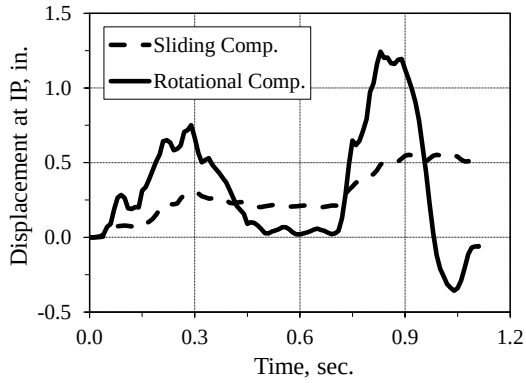

b) Sliding and rotational comp.

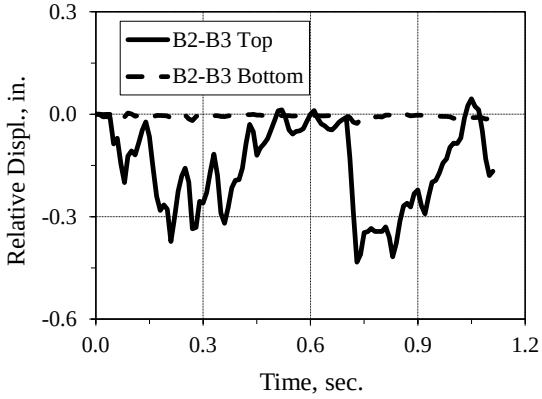

c) Relative displacement at B2-B3

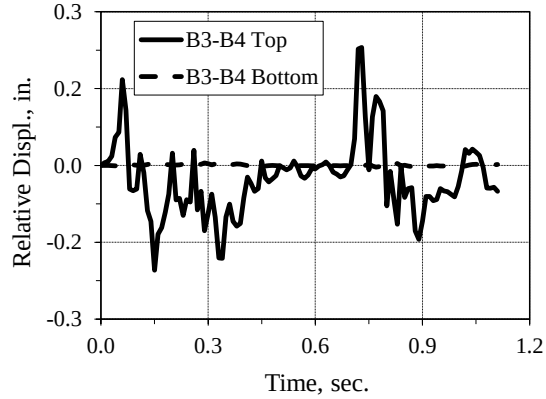

d) Relative displacement at B3-B4

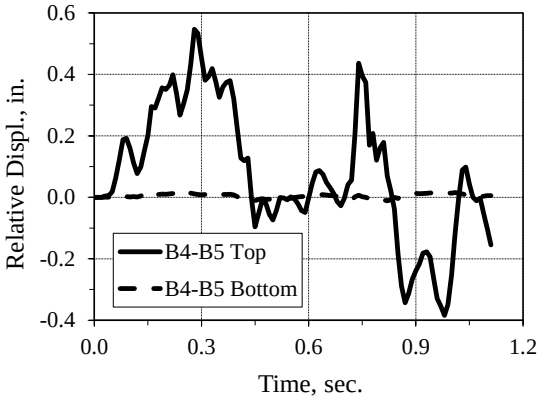

e) Relative displacement at B4-B5

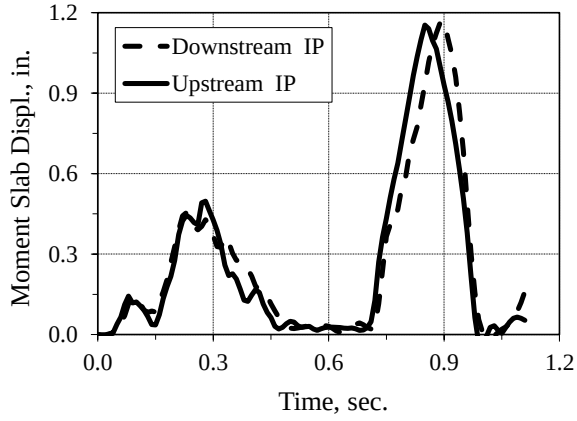

f) Vertical displacement of moment slab

Figure 4.10 Displacement of the barriers and the moment slab for TL-5-1 impact

4.1.4 Analyses for Test Level 5 Impact with 48 in. (1.22 m) Tall Barrier (TL-5-2)

The 48 in. (1219 mm) tall barrier was selected to study the dynamic response of a BMS when it is impacted by a fully-loaded tractor trailer. As previously mentioned, at this barrier height the floor of the trailer impacts the face of the barrier imposing larger dynamic loads than those associated with a barrier height of 42 in. (1067 mm). Therefore, the objectives of this analysis are similar to those described in the previous section but using a prescribed barrier height of 48 in. (1219 mm).

a) Description of the Barrier and the Moment Slab

The cross section of the 48 in. (1219 mm) tall BMS system used in this analysis is presented in Figure 4.11. To study the response of this system, a FE model of 90 ft (27.4 m) long was developed for use in LS-DYNA (Figure 4.11(b)). The model consisted of three sections of 30 ft (9.15 m) long. The moment slab was 9 ft (2.74 m) wide and it was composed of two 15 ft (4.57 m) long barriers. The moment slabs were connected using three #11 shear dowels embedded 18 in. (457 mm) at each section of the moment slabs.

The methodology followed to design and model the 48 in. (1219 mm) BMS system, and then simulates the tractor-trailer impact, is similar to that used on the 42 in. (1067 mm) tall barrier model. However, the barriers used in this model were designed to withstand an impact load of 260 kips (1157 kN). The end section ultimate capacity of the

barrier was 323 kips (1437.4 kN) with a failure length of 10.2 ft (3.12 m). The moment and shear capacity at the coping section (section B-B) was 1728 kip-ft (2343.2 kN-m) and 364 kips (1620 kN), respectively. The results indicate that the coping section provides enough capacity to resist the impact load. Therefore, the 15 ft (4.57 m) section length selected for evaluation of the TL-5-2 impact is sufficient to develop the primary failure mechanism of the barrier.

b) Loads and Displacements of the Barrier-Moment Slab System

The tractor-trailer impacted the system at the joint between B-3 and B-4 at a speed of 50 mph (80 km/hr.) at an angle of 15 degrees. Sequential images from the simulation are shown in Figure 4.12. These images are associated with the time of peak load due to the front impact of the tractor (Figure 4.12(b)), the time of peak load due to the impact of the rear tandem axles of the tractor and the front of the trailer (Figure 4.12(c)) and the time of peak load associated with the impact of the trailer (Figure 4.12(c)).

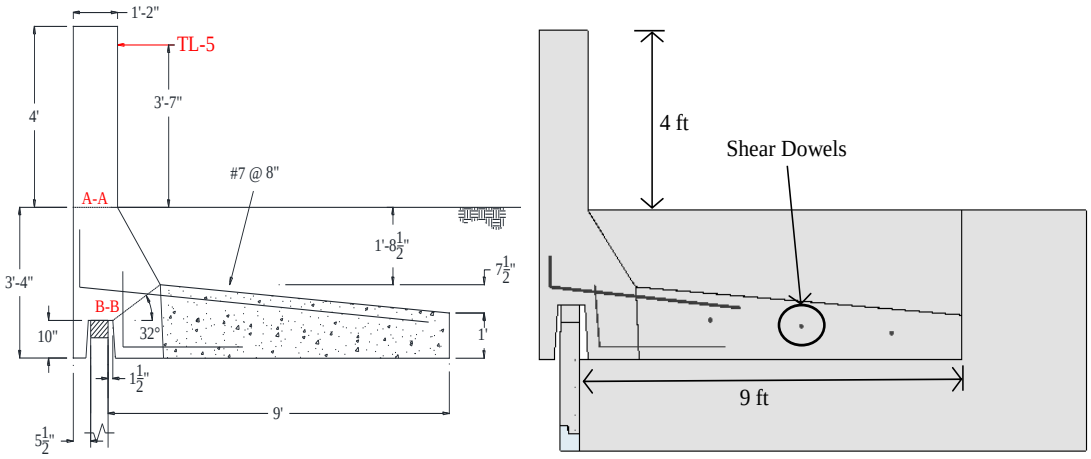

a) Concrete barrier detail **b) Concrete barrier detail in the model**

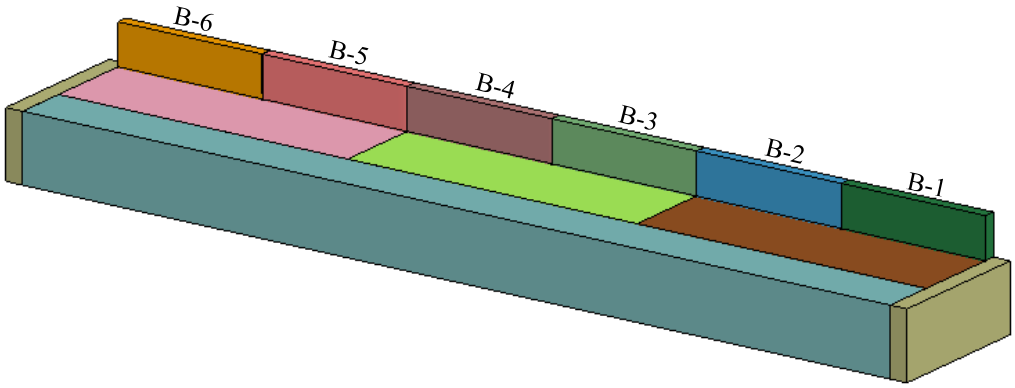

c) Alphanumeric designator for the barriers

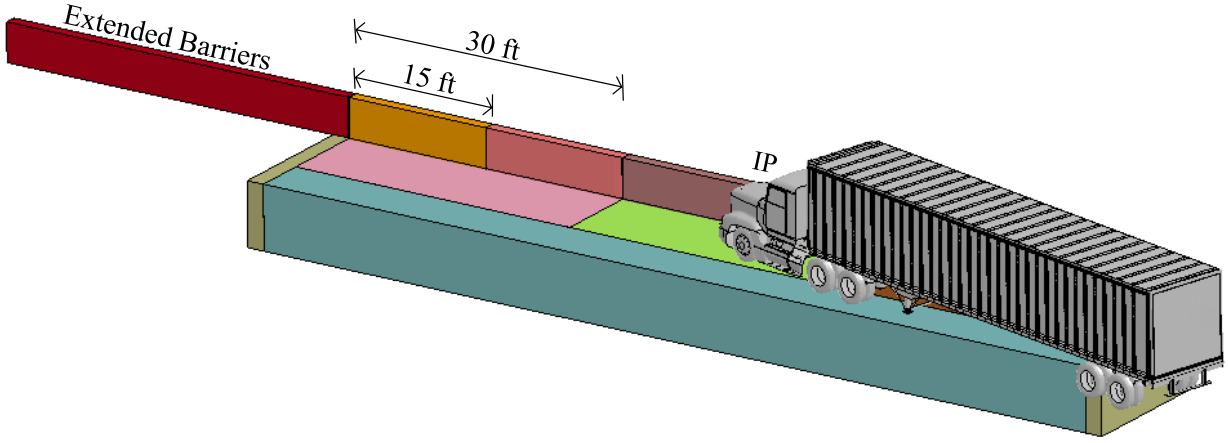

d) Three dimensional view

Figure 4.11 Barrier-moment slab system details for TL-5-2 analyses

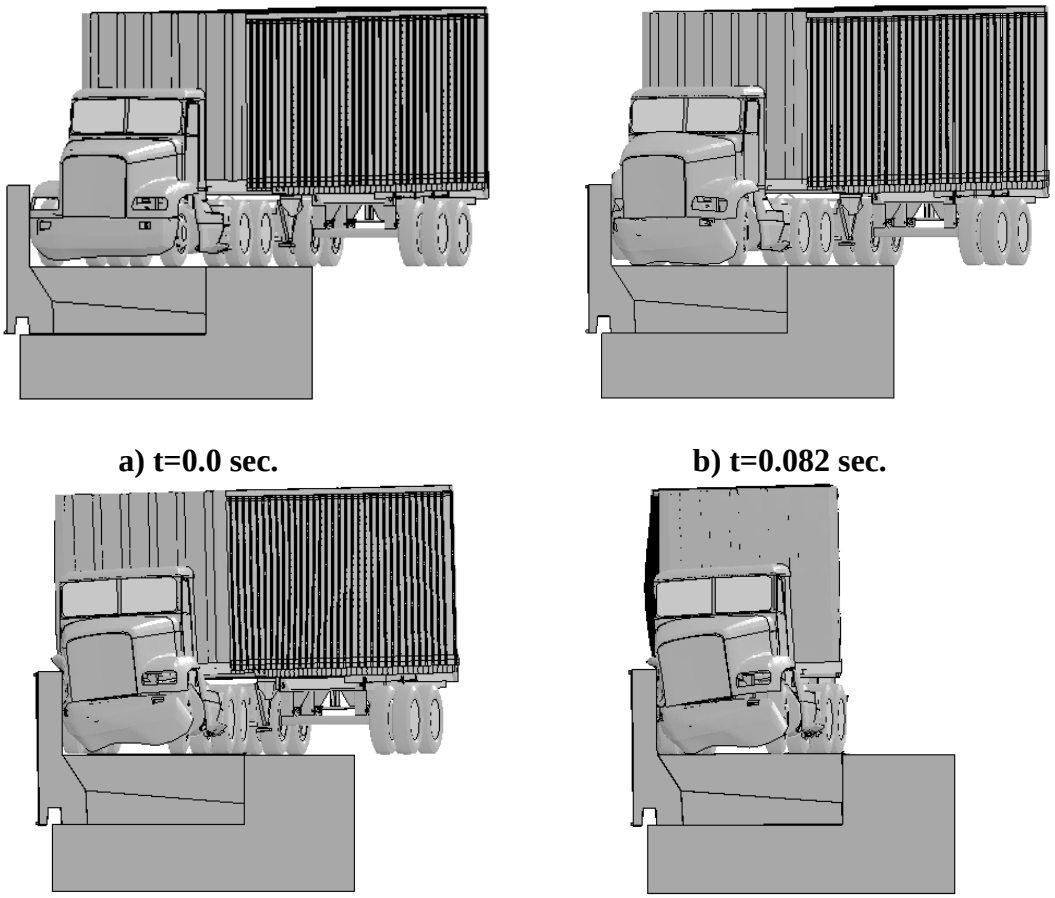

a) t=0.0 sec. **b) t=0.082 sec.**

c) t=0.212 sec. **d) t=0.813 sec.**

Figure 4.12 TL-5-2 tractor-trailer vehicle position at each significant moment

The time history force of the impact load indicates that maximum 50 msec. average force (F_t) is 251 kips (1117 kN) at 0.813 sec, as shown in Figure 4.13. This load is associated with the impact of the trailer. In the longitudinal and vertical direction, the maximum 50-msec. average impact load were 69.1 kips (307.5 kN) at 0.811 sec. and 131.4 kips (584.7 kN) at 0.796 sec., respectively. Similar to the previous analyses, the

results indicate that the concrete barrier did not exceed the tensile capacity threshold of the concrete.

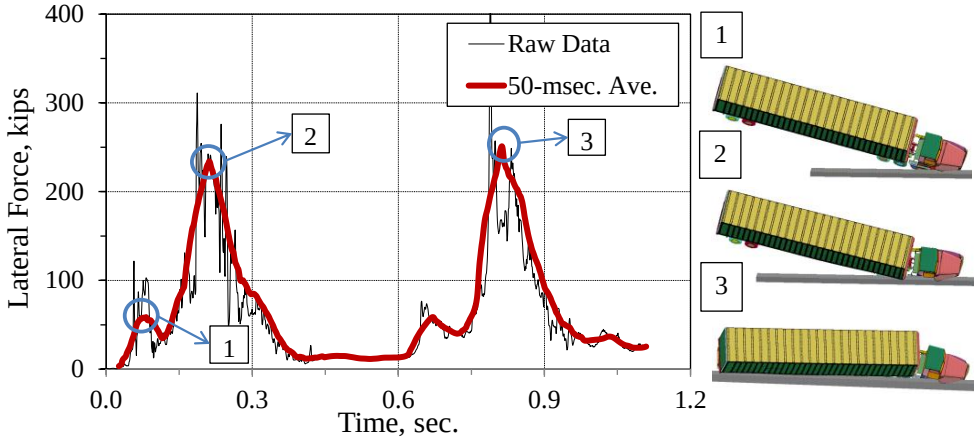

a) Lateral impact force (F_t)

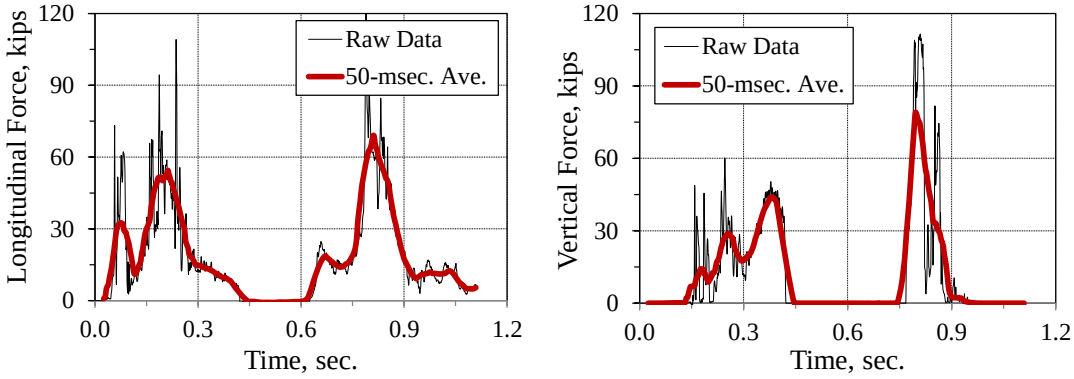

b) Longitudinal impact force (F_L) **c) Vertical impact force (F_V)**

Figure 4.13 TL-5 time history load in the barrier and load distribution on the 48 in. (1.22 m) tall BMS system

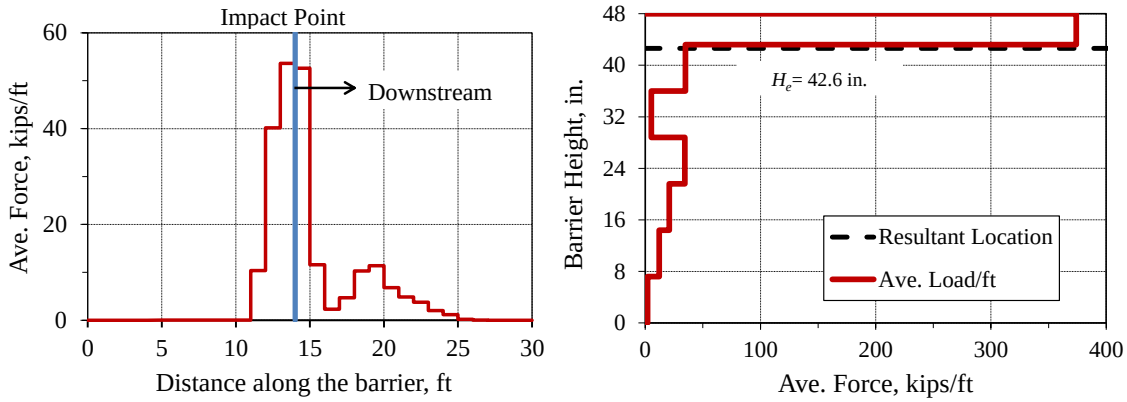

d) Longitudinal distribution (L_L) of F_t **e) Vertical distribution of F_t**

Figure 4.13 Continued

The maximum displacement of the barriers occurred close to the IP and it was 2.12 in. (53.8 mm) at the top and 0.7 in. (17.8 mm) at the coping section. The displacement-time history at the IP is shown in Figure 4.14(a).

The dynamic behavior of the 48 in. (1219 mm) tall barrier is different from that observed in a 42 in. (1067 mm) tall barrier. Figure 4.14(b) shows that the impact associated with the rear tandem axles of the tractor and the front of the trailers generates the largest displacement at the top of the barrier while at 42 in. (1.07 m) tall barrier the largest displacement is associated with the impact of the rear tandem axles of the trailer. This is because of the location of the impact load. While at 42 in. (1067 mm) tall barrier the floor of the trailer travels on top of the barrier at the height of 48 in. (1219 mm) the trailer impacts the face of the barrier at the top. This generates a larger rotational displacement than the load transmitted through the tractor axles. The permanent

displacement associated with this impact is 0.35 in. (8.9 mm). Then, the barrier rebounds back and it is impacted by the rear tandem axles of the trailer which displaces it about 1.25 in. (31.8 mm) in rotation and slide the system 0.3 in. (7.6 mm) more.

The relative displacement between the barriers is more significant for this test level as shown in Figure 4.14(c) through Figure 4.14(e). However, the barriers rebounds back to its vertical position with little residual displacement between them. The relative displacement at the coping section is also negligible, as shown in previous analyses. Figure 4.14(f) shows the vertical displacement of the moment slab at the central section. A comparison between the rotational displacement at the top of the barrier and the vertical movement of the moment slab indicates that the 30 ft (9.15 m) long barrier-moment slab section is also behaving rigidly.

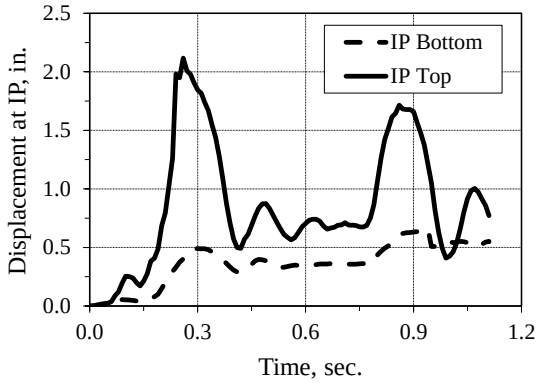

a) Displacement at impact point (IP)

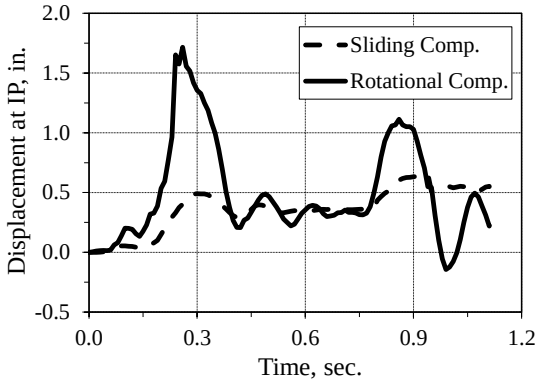

b) Sliding and rotational comp.

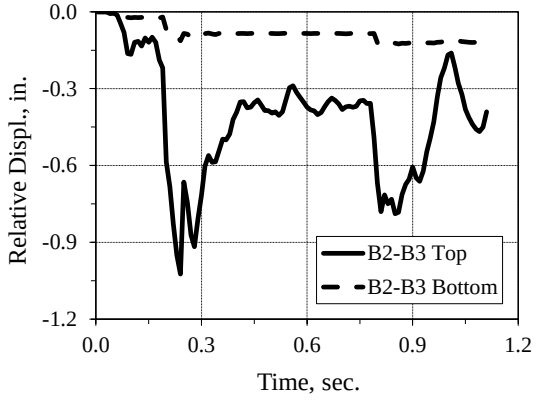

c) Relative displacement at B2-B3

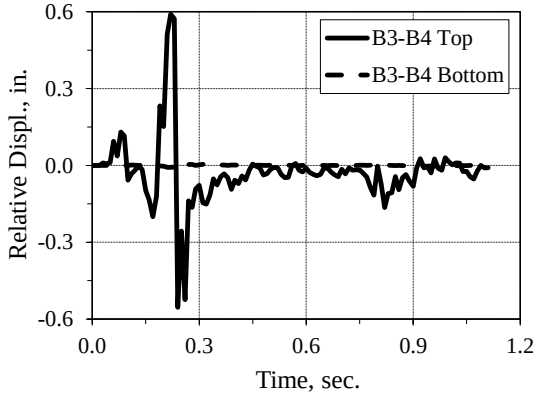

d) Relative displacement at B3-B4

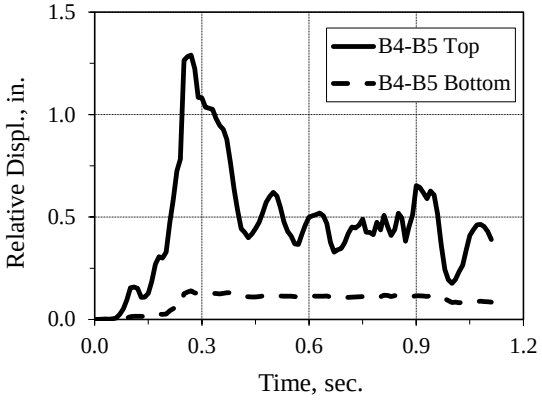

e) Relative displacement at B4-B5

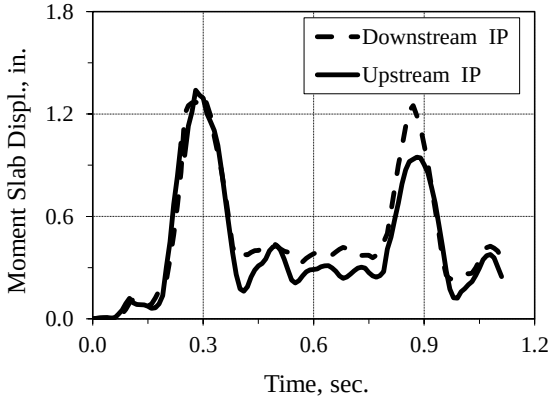

f) Vertical displacement of moment slab

Figure 4.14 Displacement of the barriers and the moment slab for TL-5-2 impact

4.2 Static Analyses of the Barrier-Moment Slab System

The BMS system analyzed in the previous sections were used to perform static analyses and a quasi-static FE analyses. The purpose of these studies is to quantify the equivalent static load and the dynamic amplification factor (DAF) associated with TL-4 and TL-5 impacts. The analyses are conducted in a 30 ft (9.15 m) long barrier-moment slab section. The shear dowels were removed from the model in order to isolate the moment slab section.

4.2.1 Static Analytical Solution

The static analyses for sliding and overturning are conducted using equilibrium equations. The static force required to initiate motion of the system (F_s) in sliding is:

$$F_s = W \tan\phi_r + f_r A_s \tag{4-9}$$

where

W= weight of the barrier, moment slab and soil of the section

ϕ= angle of the internal friction of the soil

$\tan\phi_r$= interface friction between the soil and the moment slab (ϕ_r is taken as ϕ if the interface is rough (cast in place) and $^2/_3\phi$ if the interface is smooth (precast concrete)).

f_r= shear strength resistance of the soil

A_s= interface area of the surrounding soil

For this analysis, it is assumed that the moment slab interface is rough (cast in place concrete). The strength resistance of the soil (f_r) was backcalcuated using the results of the static test presented in NCHRP Report 663, summarized in section 2 *(2).* The results of the test indicated that the average shear strength resistance of the concrete soil interface (f_r) was 126 psf (6.3 kPa) *(2).*

The static force required to initiate motion of the system (F_o) in overturning is:

$$F_o = \frac{Wl + f_r A_s \times x_s}{h} \quad (4\text{-}10)$$

where

W= weight of the barrier, moment slab and soil of the section

l= moment arm of the weight of the system

h= moment arm of the equivalent static load applied to the system to the rotation point.

x_s= moment arm of the force associated with the shear strength of the soil

The static analysis was conducted using as a reference the rotation point at the toe of the barrier (rotation point A) and the rotation point on top of the panel (rotation point B), as shown in Figure 4.15. Table 4.2 summarizes the results of the static analytical solution for sliding and overturning of the barrier-moment slab system for TL-4, TL-5-1 and TL-5-2. According to the results, the rotation point B offers more

resistance to overturning than rotation point A. This increment in rotation is associated with the reduction of the moment arm of the overturning load and the increase of the moment arm associated with the resistance moment.

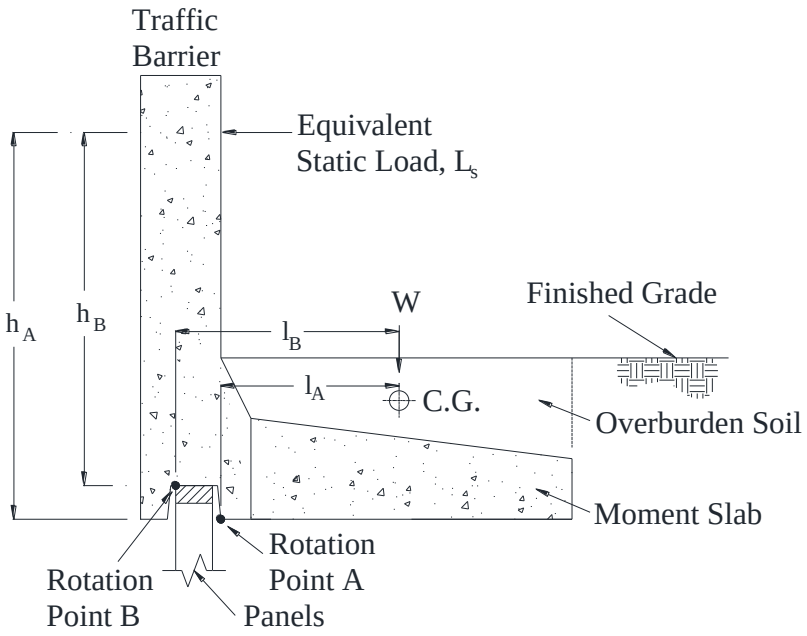

Figure 4.15 Detail of the rotation points on the barrier-moment slab system

Table 4.2 Summary of the static forces using equilibrium equation

Test Level	W (kips)	Moment Arms				Sliding Analyses		Overturning Analyses			
		Rotation Point A		Rotation Point B				Rotation Point A		Rotation Point B	
		l_A (in.)	h_A (in.)	l_B (in.)	h_B (in.)	F_S (kips)	F_{s+soil} (kips) (1)	F_o (kips)	F_{o+soil} (kips)	F_o (kips)	F_{o+soil} (kips)
TL-4	59.8	13.6	54.0	20.3	48.8	40.3	42.4	15.1	23.4	24.9	35.6
TL5-1	112.4	29.5	70.0	36.8	60.0	75.8	78.4	47.4	62.6	69.0	88.3
TL5-2	149.5	42.0	83.0	47.0	73.0	100.8	104.7	75.6	94.7	96.2	119.9

(1) Strength of the soil was only considered at the side faces of the moment slab and not at the front.

4.2.2 Quasi-Static FE Analyses

In order to conduct the quasi-static FE analyses, the shear dowels were removed from the model to isolate the moment slab sections. The interface between the soil and the moment slab were modeled using contact to capture the force generated between the soil and the moment slab.

The analyses was conducted by applying a prescribed displacement to a wood block that was used as a means of providing distribution of the applied controlled quasi-static loading definition. The displacement was applied at a very low rate to reduce the inertia effects. The length of the wood block was 4 ft (1.22 m) for TL-4 and 10 ft (3.05 m) for TL-5-1 and TL-5-2. The loads were applied at an effective height of 30 in. (762

mm), 34 in. (864 mm) and 43 in. (1092 mm) for TL-4, TL-5-1 and TL-5-2, respectively. These dimensions match the longitudinal distribution and application point of the lateral impact load associated with TL-4, TL-5-1 and TL-5-2 impact.

The FE model was initialized to account for gravitational loading on the mass before the application of the quasi-static load. The set-ups of the quasi-static FE models are shown in Figure 4.16. The analyses were conducted using as a reference the point of rotation at the toe of the barrier coping (rotation point A) and at the point of contact between the barriers and the panels (rotation point B).

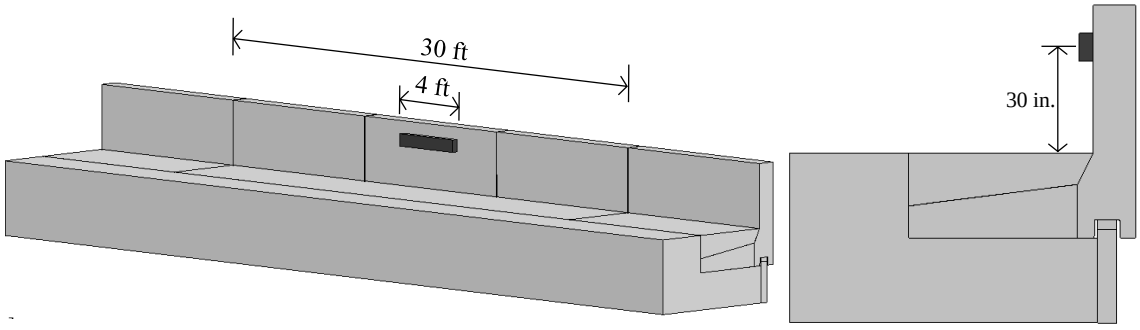

a) TL-4 barrier-moment slab system model

Figure 4.16 Load distribution and application point of the quasi-static FE models

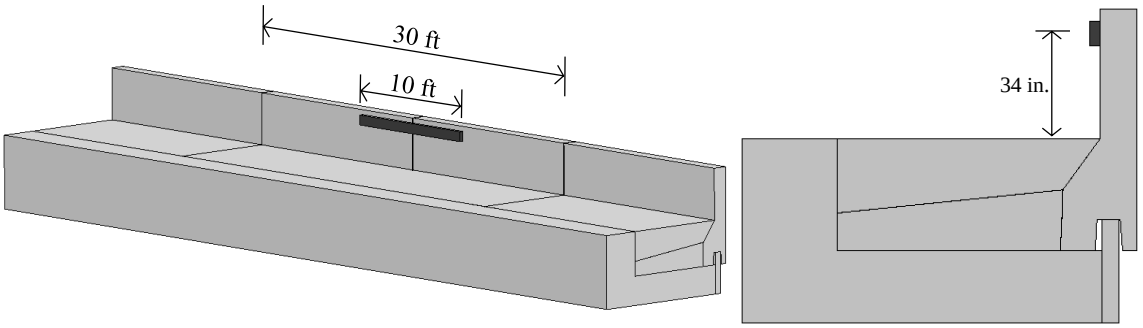

b) TL-5-1 barrier-moment slab system model

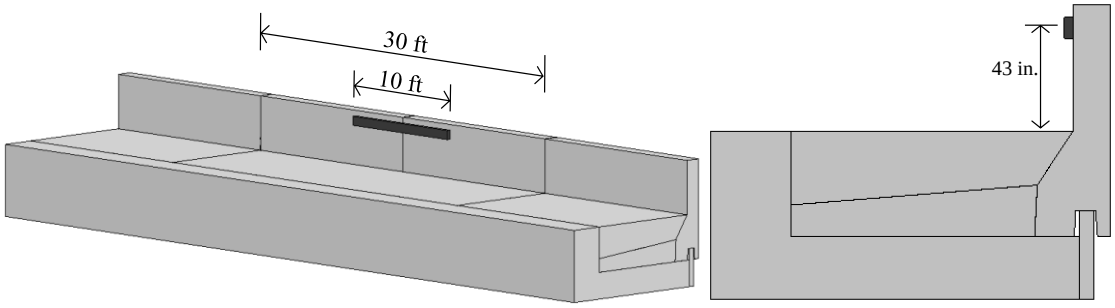

c) TL-5-2 barrier-moment slab system model

Figure 4.16 Continued

The results of the numerical simulation showed that the barrier-moment slab system failed by overturning, not by sliding. Figure 4.17 presents the results as a load displacement curve and compares them with the analytical solution using equilibrium equations. The information is also summarized in Table 4.3.

Table 4.3 Comparison between analytical solution and FE analyses

Test Level	Rotation Point A			Rotation Point B		
	Analytical Solution		FEA	Analytical Solution		FEA
	F_o (kips)	F_{o+soil} (kips)	F_o (kips)	F_o (kips)	F_{o+soil} (kips)	F_{o+soil} (kips)
TL-4	15.1	23.4	15.7	24.9	35.6	37.0
TL-5-1	47.4	62.6	49.2	69.0	88.3	78.0
TL-5-2	75.6	94.7	78.6	96.2	119.9	115.7

The FEA compares well with the hand calculation analyses when the barrier system rotates around point B. This is because the location of the rotation point B remains fixed as the barriers move (Figure 4.18(a)). However, when the barrier system rotates around point A, the toe of the barriers start punching the soil underneath them, therefore, it breaks the soil interface at an early loading stage. In addition, due to this behavior, the point of rotation A changes as the barriers rotates (Figure 4.18(b)). This behavior decreases the resistance moment arm (d) reducing the static resistance to overturning. These phenomena cannot be captured using equilibrium analysis. Consequently, the difference between both analyses gets more significant.

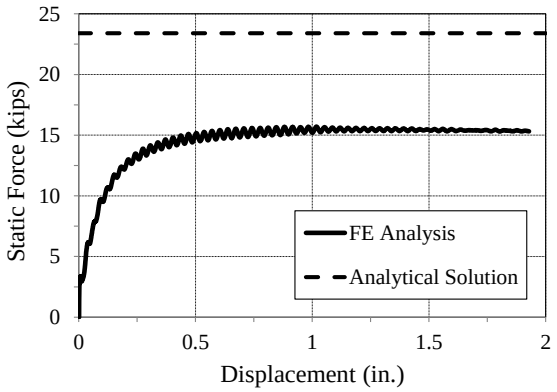

a) TL-4 (Rotation Point A)

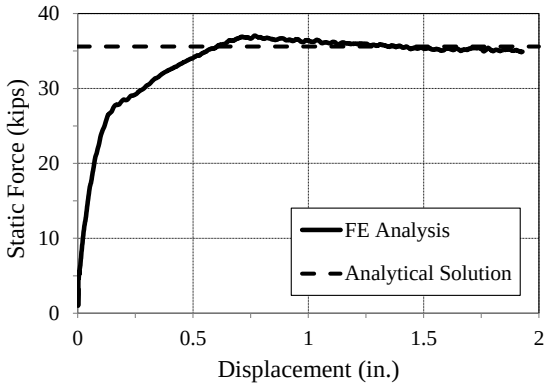

b) TL-4 (Rotation Point B)

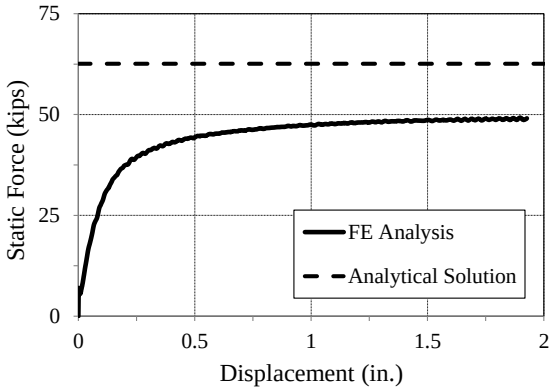

c) TL-5-1 (Rotation Point A)

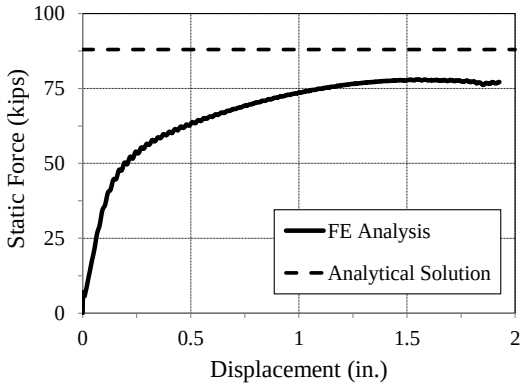

d) TL-5-1 (Rotation Point B)

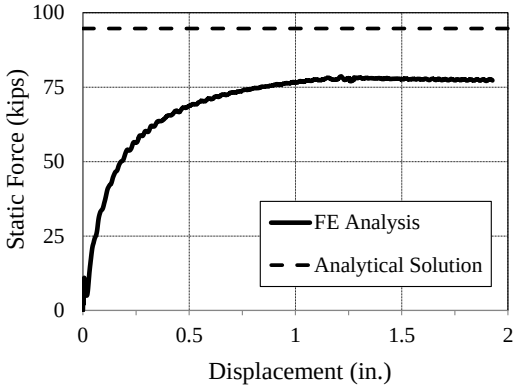

e) TL-5-2 (Rotation Point A)

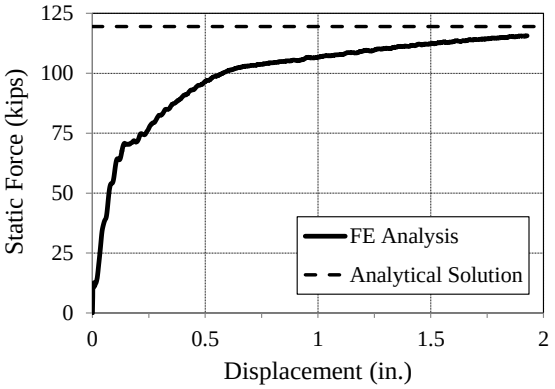

f) TL-5-2 (Rotation Point B)

Figure 4.17 Result of the quasi-static FE analyses for the barrier-moment slab system

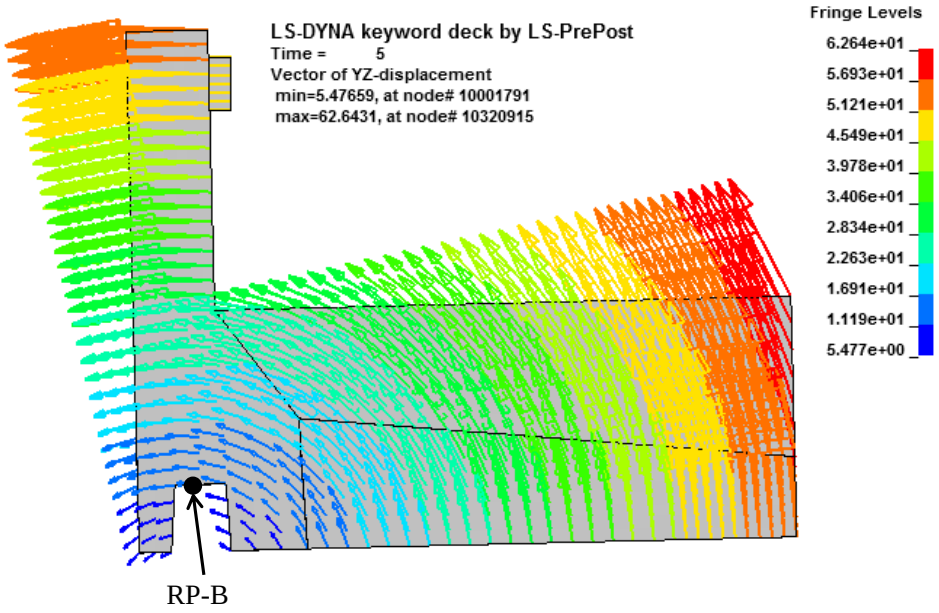

a) Rotation Point B (RP-B)

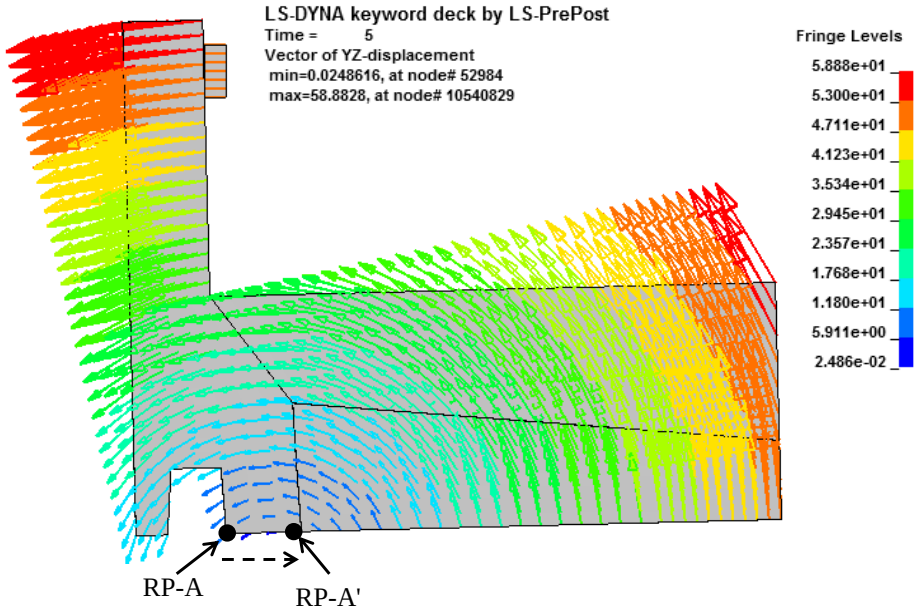

b) Rotation Point A (RP-A)

Figure 4.18 Displacement vector during rotation of the barrier system

4.3 Conclusions

The following conclusions are based on and limited to the content of this chapter:

1. A set of full-scale impact simulations were conducted on a barrier-moment slab system for MASH TL-4 and TL-5 impact. The TL-5 study addresses the effect of barrier heights on the impact load. Therefore, the analysis was performed on a 42 in. (1067 mm) tall barrier (TL5-1) and a 48 in. (1219 mm) tall barrier.
2. The results of the full-scale impact simulations shows that the width of the moment slab to contain a MASH TL-4 and MASH TL-5 impact with a limiting permanent displacement of 1 in. (25.4 mm) at the coping section are:
    - 4.5 ft (1.37 m) wide and 30 ft (9.15 m) long for MASH TL-4 impact
    - 7.0 ft (2.13 m) wide and 30 ft (9.15 m) long for MASH TL-5-1 impact
    - 9.0 ft (2.74 m) wide and 30 ft (9.15 m) long for MASH TL-5-2 impact
3. A set of static analytical calculations and quasi-static FE analyses were conducted on the same barrier-moment slab system used for the impact simulations. The results show that overturning of the system occurs before sliding. However, both criteria should be checked.
4. The static load associated with TL-4 and TL-5 impact varies significantly between point of rotation A and B. For rotation point B, the FEA indicates that the quasi-static load, including soil resistance, to resist overturning due to a TL-4, TL-5-1 and TL-5-2 impact are 37 kips (164.6 kN), 78 kips (347 kN) and 115.7 kips (514.9 kN), respectively. This point of rotation was selected as a reference

because the barrier system rotated around point B during the full-scale impact simulation.

5. The static analytical solution indicates that the quasi-static load, without soil resistance, to resist overturning around rotation point B due to a TL-4, TL-5-1 and TL-5-2 impact are 23.4 kips (104.1 kN), 62.6 kips (278.6 kN) and 96.2 kips (428.1 kN), respectively.
6. The ratio between the dynamic load and the static load (DAF) vary from the different test levels. For example, using as a reference the rotation point B and the quasi-static load of the system without soil resistance, the DAF is 3.0 (70/23.4) for TL-4 impact, 2.68 (168/62.6) for TL-5-1 impact and 2.61 (251/96.2) for TL-5-2 impact. The difference of DAF for the various test levels obeys to the difference in inertia resistance of the system and impulse load applied by the test vehicle.

5 DYNAMIC AMPLIFICATION FACTOR (DAF) STUDY

The previous analyses of dynamic and quasi-static loading showed that there is a difference between the magnitude and application time of the impact load imposed by small cars, large trucks and the static load. Analytic expressions of the dynamic amplification factor (DAF) and the characteristic response of the system do not exist for design and evaluation of barrier-moment slab system when subjected to impact loading. In this case, these coefficients should typically be given as a function of the impact conditions and the inertia resistance of the system. They allow a rapid estimation of the dynamic loads induced by the errant vehicle. These results are particularly useful in the context of barrier-moment slab system preliminary design and assessment of the system response under high-speed impact. Therefore, the objective of this chapter is to theoretically explain the DAF concept associated with evaluation of barrier-moment slab system when subjected to vehicle impact loads.

5.1 Theoretical Background

It is important in the design of barrier-moment slab system that adequate consideration is given to the level of system excitation resulting from the dynamic component of a barrier-vehicle interaction during an impact event. The concept of a dynamic amplification factor (DAF) is used to describe the ratio between the load effect when the system is loaded dynamically and statically. The general expression is written as:

$$DAF = 1 + DA \tag{5-1}$$

$$DAF = \frac{F_s + F_d}{F_s} \tag{5-2}$$

where

1+DA= dynamic amplification factor

DA = dynamic amplification computed as the ratio of dynamic to static load

F_s = static load computed using equilibrium analyses

F_d = dynamic load imposed by the vehicle impact

For example, a DAF value of 1.75 corresponds to a dynamic amplification of 75%. There are many ways of interpreting this simple definition of the DAF from test data. Therefore, for design purposes of a barrier-moment slab system, the DAF is used to help predict the vehicular impact load by knowing the static load, as shown in Eq. (5-3). This has a particular utility to help evaluate the barrier component and level of displacements associated with the impact load.

$$F_d = F_s \times \left(DAF - 1 \right) \tag{5-3}$$

Due to the complex interaction in a barrier-moment slab-vehicle impact, there is a large number of parameter that affects the magnitude of DAF. However, not all of

them play an important role when selecting a DAF value. The parameters affecting DAF are:

- Barrier-moment slab system-related: location of the rotation point, width of the moment slab, embedment depth of the coping section, height of the barrier, mass-moment of inertia of the system, presence of shear dowels between sections and the length of moment slab.
- Vehicle-related: impact speed, impact angle and vehicle mass.

5.1.1 Dimensional Analyses

Figure 5.1 shows a simple model to help study the magnitude of the impact load and the DAF with different barrier-moment slab system properties and vehicle impact conditions. The analysis gives consideration to the kinetic energy of the impacting vehicle (E_k), rotational stiffness of the system (k_φ), mass moment of inertia of the system (I_o), overturning moment arm of the impact load (h), location of the center of gravity of the system (c.g.) and resistant moment of the system (M_R). These variables were used to first conduct a dimensional analysis and then a FE analyses.

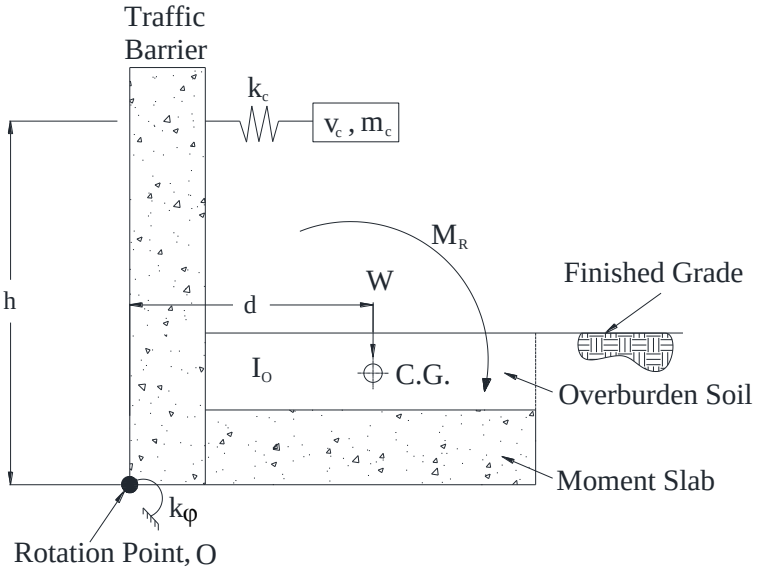

Figure 5.1 Barrier-moment slab system model to study the DAF

Using the k_φ, h and m_c as the repeating variables, the result of the dimensional analyses yield the following expression:

$$\frac{F_d h}{k_\varphi} = f\left[\frac{m_c V_c^2}{k_\varphi}; \frac{h^2 k_c}{k_\varphi}; \frac{I_o}{m_c h^2}; \frac{M_R}{k_\varphi}\right] \tag{5-4}$$

where

k_c= stiffness of the car (kip/ft or kN/m)

m_c= mass of the vehicle (lb.-sec.^{2}/ft of kg)

V_i= impact velocity (ft/sec. or m/sec.)

h = height of load application (ft or m)

I_o= mass moment of inertia of the barrier-moment slab around the point of rotation "O" (lb.-sec.^{2}-ft or kg-m^2)

M_R= resisting moment (kip-ft or kN-m)

k_φ= rotational stiffness of the foundation system (kip-ft or kN-m).

The first term of Eq. (5-4) refers to the ratio of kinetic energy, the second term refers to the spring ratio of the impacting vehicle and the rotational stiffness of the system, the third term refers to mass ratio between the barrier-moment slab system and the vehicle, and the last term refer to rotational capacity ratio of the barrier-moment slab system.

If the last term of Eq.(5-4) (M_R/k_φ) is moved to left-hand side of the expression, the dimensional analyses show that the DA will be a function of the magnitude of the ratios expressed in the following expression:

$$\frac{F_d h_e}{M_R} = f\left[\frac{m_c V_c^2}{k_\varphi}; \frac{h_e^2 k_c}{k_\varphi}; \frac{I_o}{m_c h_e^2}\right] \tag{5-5}$$

The major drawback in applying Eq. (5-5) is the difficulty to accurately estimate the ratio of stiffness (second term). A literature review has shown that the car stiffness associated with an oblique impact event is difficult to estimate due to the large number of variables involve in the analyses and no reliable record was found with these conditions. On the other hand, the rotational capacity of the barrier-foundation system

can be estimated using the expression of the torsional stiffness of a strip footing foundation. However, k_{φ} depends on the contact area underneath the footing and, therefore, it is negligible once the system start rotating.

5.1.2 Change in Momentum Analyses

A second analysis was conducted to help determine the variables that influence the magnitude of the impact load and the DAF associated with a barrier-vehicle collision. The procedure is outlined below and it refers to the impulse equation and the change in total linear momentum of two colliding objects. The equations are written as:

$$F_d \Delta t = mV_i - mV_f \tag{5-6}$$

$$\Delta(mV)_i = \Delta(mV)_f \tag{5-7}$$

where

F_d = magnitude of the impact load

Δt = total duration of the impulse load

m = mass of the colliding object

V_i = velocity of the colliding object before impact

V_f = velocity of the colliding object after impact

$\Delta(mV)$ = change in momentum

Applying Eq. (5-7) to an impact event associated with a vehicle-barrier-moment slab system, the final velocity at the time of maximum compression phase can be estimated as:

$$\left(m_c V_i + m_w \cancel{V_i}\right) = m_c V_f + m_w V_f \tag{5-8}$$

$$V_f = \frac{m_c V_i}{\left(m_c + m_w\right)} \tag{5-9}$$

where

m_c = mass of the car

m_w= mass of the barrier-moment slab system section (mass of the wall)

V_i = velocity of the car

V_f = velocity of the car and the barrier-moment slab system section at the end of the compression phase.

The information expressed in Eq. (5-9) assumes that the velocity of the system and the vehicle is the same at the end of the compression phase. This assumption is reasonable since the maximum lateral impact load occurs during redirection of the vehicle while it is leaning toward the barrier. In addition, the information obtained from these analyses will only serve as a reference to identify potential variables that are going to be analyzed in the parametric study described in the next section. Based on these assumptions, Eq. (5-9) can be used in combination with the Eq. (5-6) to estimate the peak load generated by the colliding vehicle, as shown below:

$$F_d \Delta t \propto m_c \left[V_i - \frac{m_c V_i}{\left(m_c + m_w \right)} \right] \tag{5-10}$$

$$F_d \Delta t \propto m_c \left[\frac{m_c V_i + m_w V_i - m_c V_i}{\left(m_c + m_w \right)} \right] \tag{5-11}$$

$$F_d \Delta t \propto \frac{m_c m_w V_i}{\left(m_c + m_w \right)} \tag{5-12}$$

$$F_d \propto \frac{m_c m_w V_i}{\Delta t \left(m_c + m_w \right)} \tag{5-13}$$

Eq. (5-13) requires the input of the impulse load duration. This variable is difficult to estimate and its magnitude depends on the vehicle mass, velocity and type of vehicle (single of articulated). Eq. (5-13) also requires input of the mass of the barrier-moment slab system to assess the influence of the stiffness of the system in the magnitude of the impact load. The mass of the barrier-moment slab system associated with the impact can be estimated with the help of the dimensional analyses conducted in the previous section, using I_o and the theorem of parallel axis. The expression can be written as:

$$m_w = \frac{I_o}{h^2} \tag{5-14}$$

$$F_d \propto \frac{m_c\left(\frac{I_o}{h^2}\right)V_i}{\Delta t\left(m_c + \frac{I_o}{h^2}\right)} \tag{5-15}$$

$$F_d \propto \frac{m_c V_i}{\Delta t} \times \frac{I_o}{\left(I_o + m_c h^2\right)} \tag{5-16}$$

The Eq. (5-16) has similarities with Eq. (5-5), as shown in Eq. (5-18). The first term relates the impact speed and vehicle mass associated with the vehicle collision and the second term is associated with the ratio of inertia resistance before and at the time of maximum impact load. If these equations are written in a similar manner, we have:

$$F_d = f\left[\frac{m_c V_i}{\Delta t}; \frac{I_o}{\left(I_o + m_c h_e^2\right)}\right] \quad ; \quad F_d = f\left[\frac{m_c V_c^2}{h_e}; \frac{I_o}{m_c h_e^2}\right] \tag{5-17}$$

5.2 Parametric Study

The analyses conducted in the previous section served as a basis to determine the most relevant variables that influence the impact load and, therefore, the DAF. This section summarizes a parametric study conducted using a simple FE model that characterizes the schematic representation illustrated in Figure 5.1.

5.2.1 Impactor and Barrier-Moment Slab System Model

The impactor model was configured with three 12 in. (304.8 mm) crushable steel cylinders on its nose assembly, as shown in Figure 5.2 . A spreader beam is attached across the three cylinders. A wood block is attached to the face of the spreader beam to help dampen high-frequency noise during an impact. The body mass of the impactor was made of shell and solid components. The total weight of the impact was varied from 2205 lb. (1000 kg) to 44092 lb. (20000 kg). The speed of the impact was selected such that the dynamic displacement at the top of the barrier was 1.0 in. (25.4 mm).

The methodology followed to model the barrier-moment slab system was the same used in the analyses conducted in section 4. The different components of the system such as barrier height, moment slab width and length of moment slab were varied in order to capture the influence of each on the variables in the magnitude of the impact load, static load and the DA.

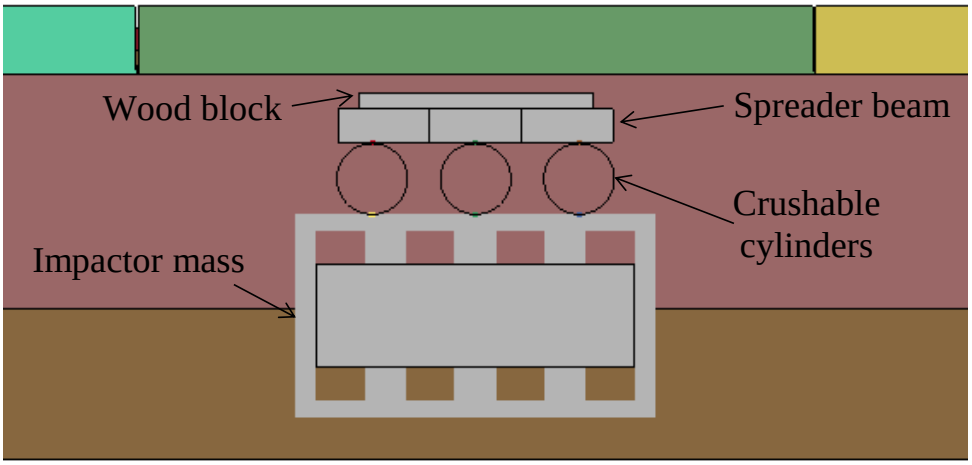

a) Barrier-moment slab system model

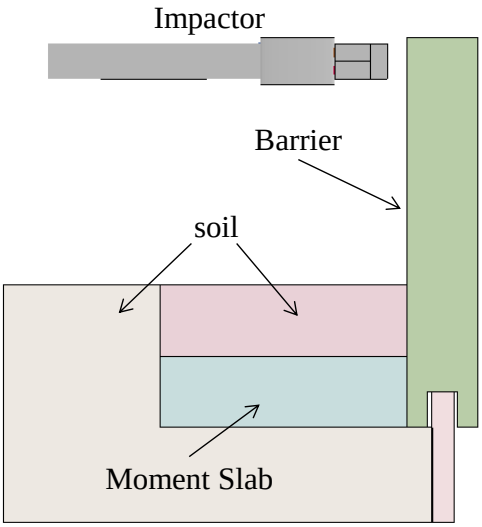

b) Detailed crushable cylinders of the impactor

Figure 5.2 Detailed of the impactor and barrier-moment slab system model

5.2.2 Results of the Impact Simulation

This section summarizes the results of the impact simulation conducted on the prototype barrier-moment slab system to study the influence of the different variables associated with the magnitude of DA.

a) Influence of Moment Slab Length (L)

A total of five models with moment slab lengths of 20 ft (6.1 m), 30 ft (9.15 m), 40 ft (12.2), 50 ft (15.25 m) and 60 ft (18.3 m) were developed to study the influence of this variable in the impact load (F_d) and DA. The rest of the variables (e.g., moment slab width, barrier height, impact mass) were constant. The velocity of the impactor was changed such as the dynamic displacement at the top of the barrier was approximately 1.0 in. (25.4 mm). Figure 5.3 shows the variation of the dynamic and static load (L_s) and the DA as the length of the moment slab increases.

Figure 5.3(a) shows that the effect of L in the magnitude of the impact load diminishes as L increases. This is because the impact load gets localized around the impact point and the upstream and downstream end of the system does not have a significant effect on the magnitude of F_d. The presence of shear dowels also contribute to this effect as they engage their neighbor sections increasing the inertia resistance of the system. Consequently, the increase in L reduces the magnitude of DA, as shown in Figure 5.3(b). This behavior seems to be irrational as one may think that stiffer systems

should have a larger DA. However, there are two primary reasons for that: 1) the rate at which the impact load increases with L becomes nearly asymptotic after a 40 ft (12.2 m) long moment slab section, and 2) the static load increases linearly with L and at a higher rate than the impact load. Consequently, stiffer systems have larger static resistance than a lighter system requiring a smaller DAF to predict the impact load.

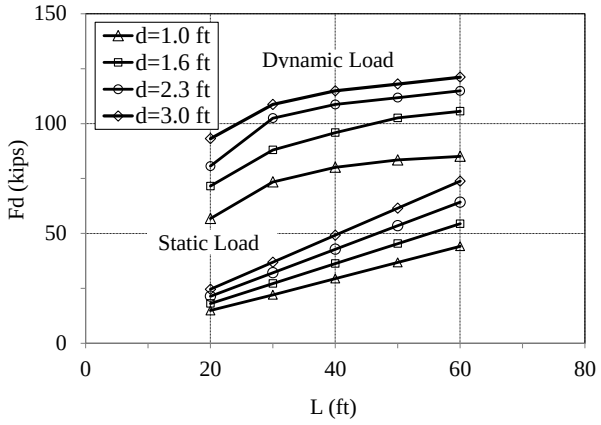

a) Influence of L on F_d and L_s

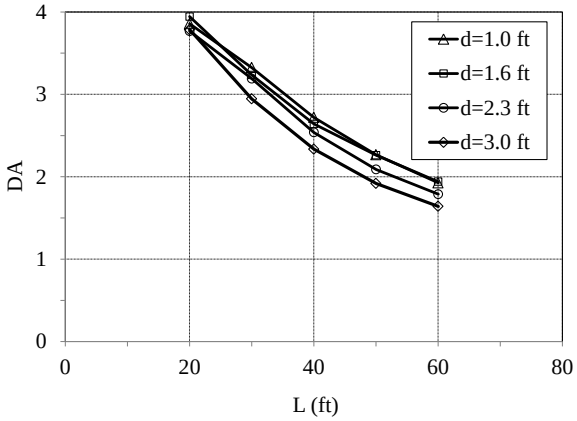

b) Influence of L on DA

Figure 5.3 Influence of moment slab in the impact load and the DA

b) Influence of the Resisting Moment Arm (d)

The influence of the resisting moment arm was studied using four models with d values of 1.5 ft (0.45 m), 2.1 ft (0.65 m), 2.8 ft (0.85 m), and 3.4 ft (1.05 m). These values of resisting moment arm corresponds to a width of moment slab of the reference model of 3.75 ft (1.14 m), 5.22 ft (1.6 m), 6.6 ft (2.02 m) and 8 ft (2.44 m), respectively. The length of the moment slab and the height of the barrier were 30 ft (9.15 m) and 42 in. (1.07 m), respectively. The weight of the impactor varied from 2.2 kips. (9.81 kN) to 44.1 kips (196.2 kN). The velocity of the impactor was changed such as the dynamic displacement at the top of the barrier was 1.0 in. (25.4 mm). The results of this analysis are shown in Figure 5.4.

The effect of the resisting moment arm on the impact load is similar to the effect of L. Both variables, d and L, increase the static load drastically while the excess dynamic load associated with the increase in stiffness of the system decreases as d increases (e.g., asymptotic behavior). Therefore, the increase in d reduces the magnitude of DA, as shown in Figure 5.4(b). Again, this behavior seems to be irrational as stiffer systems might be related to larger values of DA. Consequently, the same two reasons that explain the reduction of DA with L also applied for d.

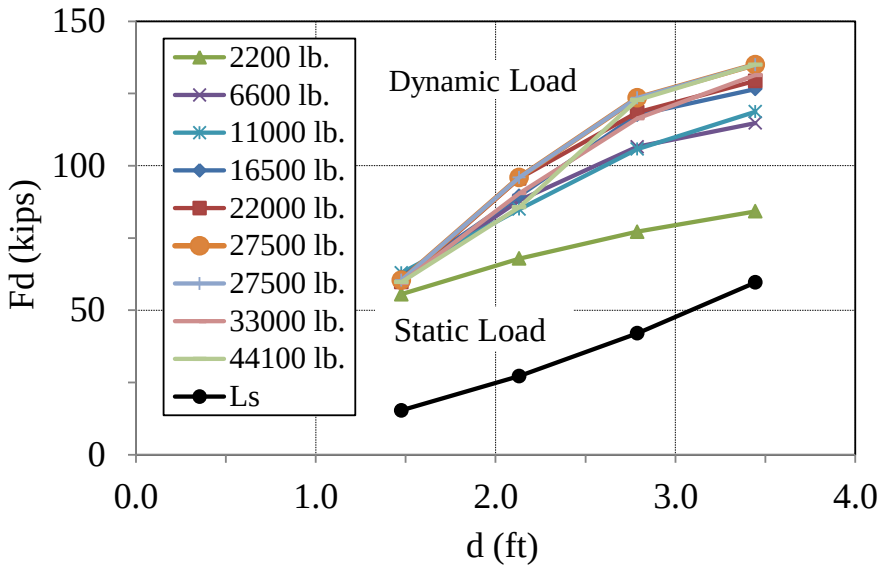

a) Influence of d on F_d and L_s

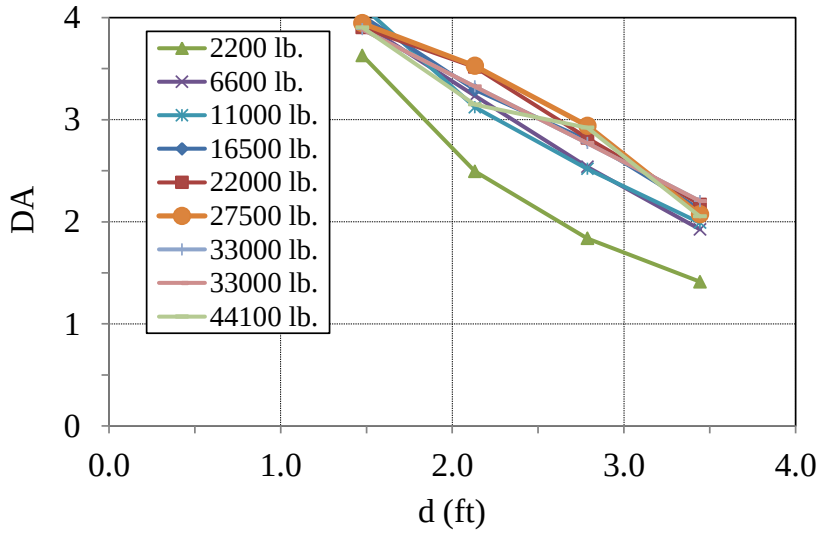

b) Influence of d on the DA

Figure 5.4 Influence of the resisting moment arm in the impact load and the DA

c) Influence of the Overturning Moment Arm (h)

The influence of the overturning moment arm was studied using nine models with different h values ranging from 3.8 ft (1.16 m) to 9 ft (2.74 m) with increments of 7.9 in. (200 mm). The values of overturning moment arm cover all barrier heights that have been previously crash-tested. The length and width of the moment slab were 30 ft (9.15 m) and 5.2 ft (1.59 m), respectively. The weight of the impactor varied from 2.2 kips. (9.81 kN) to 44.1 kips (196.2 kN). The velocity of the impactor was changed such as the dynamic displacement at the top of the barrier was 1.0 in. (25.4 mm). The results of this analysis are shown in Figure 5.5.

The increase in overturning moment arm reduces the impact load required to displace the top of the barrier 1.0 in. (25.4 mm) dynamically. This result is reasonable since h increases the flexibility of the system requiring less load to displace the system. Similarly, the static load is also affected by h but at a smaller rate since the inertia rate effect is not considered in the equilibrium analysis.

The effect of h in the magnitude of DA is not consistent. At low values of h, the magnitude of DA increases slightly up to a maximum value which is reached at an h of approximately 5.2 ft (1.59 m). Beyond this height, the system becomes more flexible due to the increase of the overturning moment. On the other hand, the total weight of the system also increases due to the added mass associated with the extension of the barrier portion. However, this mass increment moves the center of gravity of the system in the direction of the rotation point reducing the resistant moment arm (d). This combined

effect results in a change in resistant moment that is basically negligible when compared with the change in overturning moment.

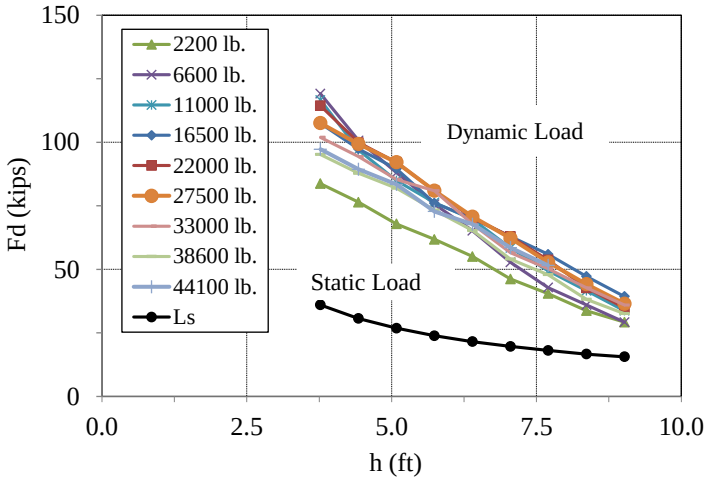

a) Influence of h on F_d and L_s

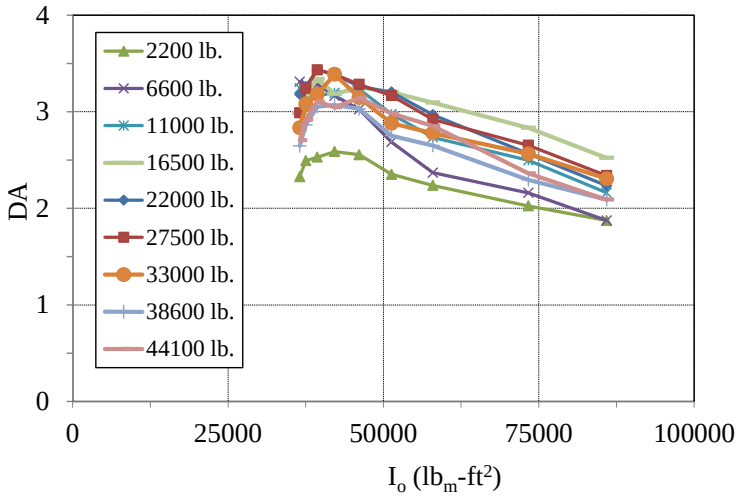

b) Influence of h on the DA

Figure 5.5 Influence of the overturning moment arm in the impact load and the DA

d) Influence of the Mass Moment of Inertia (I_o)

Unlike other variables, the magnitude of DA does not vary linearly with I_o. The analysis conducted in this section shows that DA decreases logarithmically with an increasing I_o. The study was performed using moment slab section of different widths and lengths. The height of the barrier was constant (3.5 ft (1.07 m)) as well as the weight of the impactor (6.6 kips. (29.4 kN)). The velocity of the impactor was changed such as the dynamic displacement at the top of the barrier was 1.0 in. (25.4 mm).

The results of this analysis are shown in Figure 5.6. Clearly, I_o is related to the geometry and mass of the system as well as the location of the center of gravity, as shown in Eq. (5-18). Therefore, I_o is a key variable which represents the inertia resistance of the barrier-moment slab system during an impact event.

$$I_o = \sum_i \frac{1}{12} m_i \left(x_i^2 + y_i^2 \right) + m_{total} d^2 \qquad (5\text{-}18)$$

where

I_o= total mass-moment of inertia around the rotation point

m_i= mass of the discrete components of the system

x_i= horizontal distance from the c.g. of the individual components to the c.g. of the total system.

y_i= vertical distance from the c.g. of the individual components to the c.g. of the total system.

m_{total}= total mass of the system

d= distance from the c.g. axis of the system to the rotation point axis.

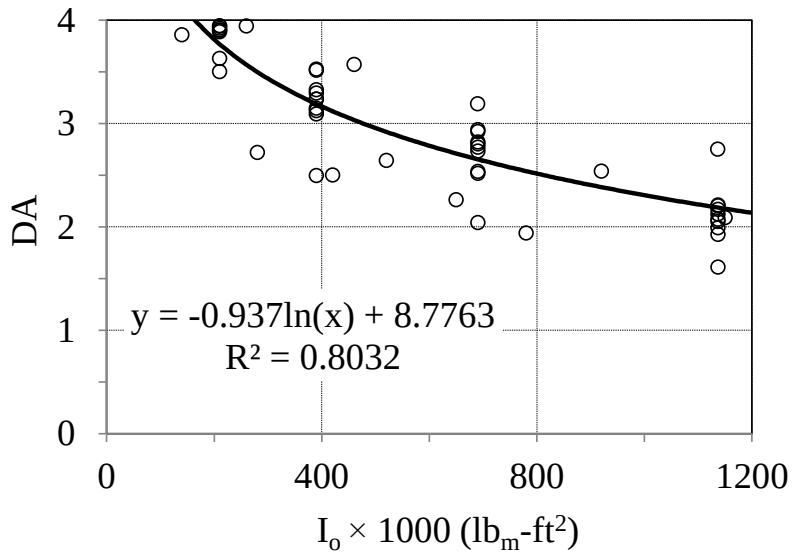

Figure 5.6 Influence of the mass moment of inertia in the DA

e) Influence of the Kinetic Energy (E_k) - Impactor Mass (m_c) and Velocity (V_c)

The effect of the kinetic energy on the impact load and the system excitation is difficult to interpret independently. Therefore, it seems more appropriate to study its global effect by also analyzing the individual influence of the impactor mass and the impact velocity. In order to accomplish this objective, a prototype system of 42 in. (1.07 m) tall barrier and 5.2 ft (1.59 m) wide and 30 ft (9.15 m) long moment slab was used with no

restriction of displacement at the top of the barrier. This helps to better understand the role of the mass and the velocity on the magnitude of the impact load and the kinematic behavior of the system. For example, Figure 5.7(a) and Figure 5.7(b) show the variation of the impact load and barrier displacement when E_k is increased by either changing the impact speed or the total mass of the impactor.

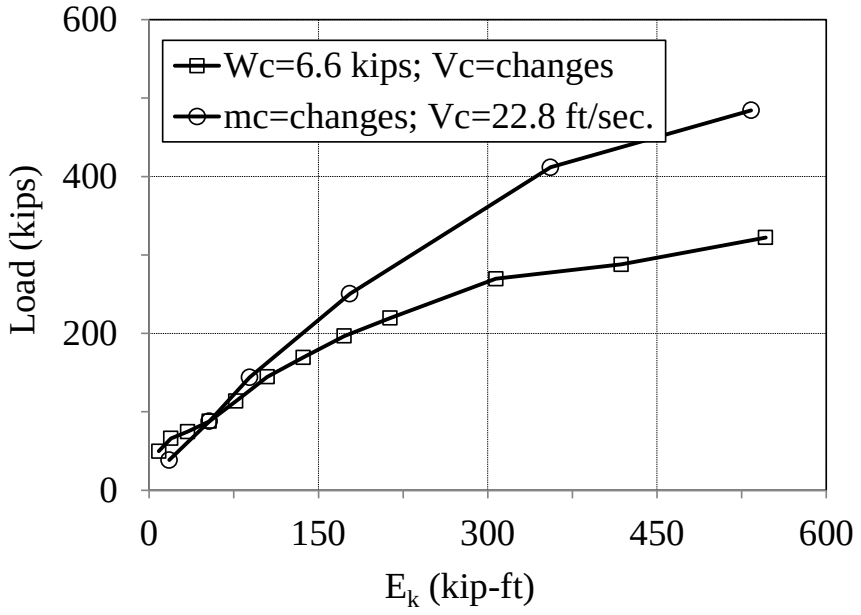

a) Effect of E_k on the impact load

Figure 5.7 Effect of kinetic energy on the magnitude of DA

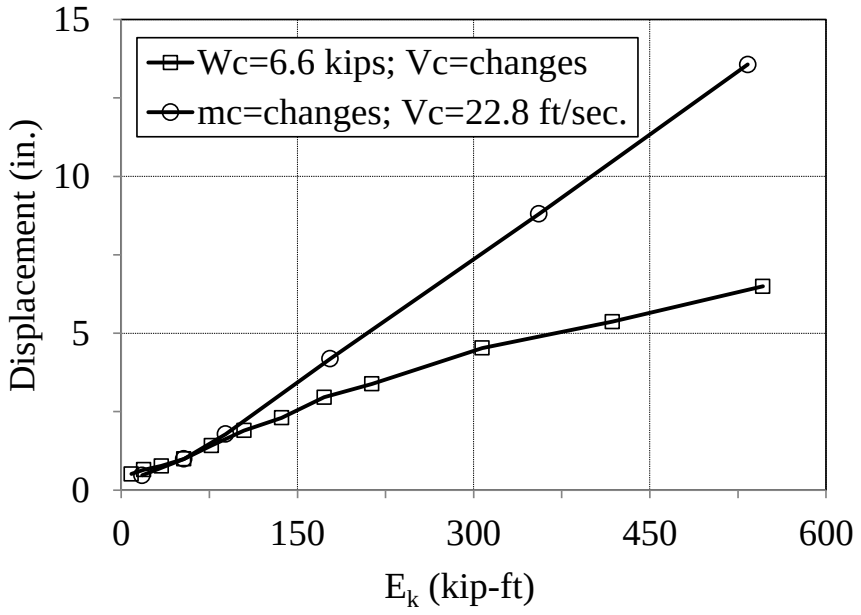

b) Effect of E_k on the barrier displacement

Figure 5.7 Continued

In is observed that the behavior of the system is similar up to a value of E_k value of 125 kip-ft (169.5 kN-m). After further loading, the imposed load and the barrier displacement is larger when E_k increases due to an increment in the impactor mass. This obey to two primary reasons: 1) the impulse load duration increases as the impacting mass increases, and 2) the damping effect associated with the crushable zone of the vehicle body is smaller when the moving mass is larger.

The effect of the impulse load duration is perhaps the most influencing factor of the two. This conclusion is supported by Figure 5.8 which shows that the change in impulse time due to the vehicle mass is more significant than the effect associated with the impact speed. Certainly, this contributes to reduce the magnitude of DA.

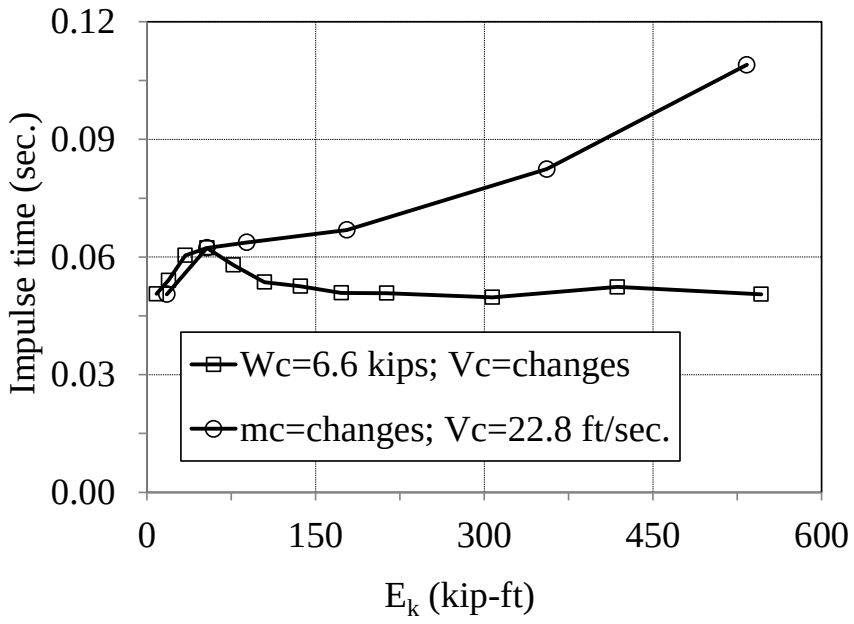

Figure 5.8 Variation of impulse load duration with kinetic energy

The analyses presented in Figure 5.7 and Figure 5.8 is only intended to provide a more comprehensive understanding of the effect of the mass and the impact speed in the magnitude of the impact load and barrier displacement. These results are not used to develop the final recommendation since they do not follow the displacement criterion specified in previous sections.

Consequently, a further analysis was conducted using the same prototype system but now displacing the barrier only 1.0 in. (25.4 mm) as presented in previous sections. The impacting weight was varied from 2.2 kips (9.81 kN) to 44.1 kips (196.2 kN). The velocity of the impactor was changed such as the dynamic displacement at the top of the barrier was 1.0 in. (25.4 mm). Figure 5.9(a) show the variation of the DA and the impulse time associated with the impacting weight.

Figure 5.9(b) shows the variation of the impulse time with the impactor weight and impact speed when the displacement at the top of the system is approximately 1.0 in. (25.4 mm).These results indicate that the time of load application increases linearly with the weight of the impactor and decreases exponentially with the impactor speed. However, the effect of these variables in the magnitude of DA is difficult to interpret.

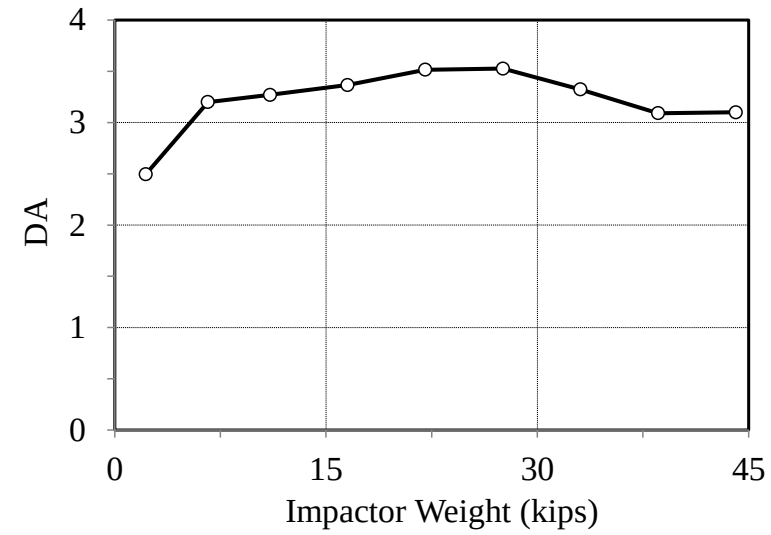

a) Influence in the DA

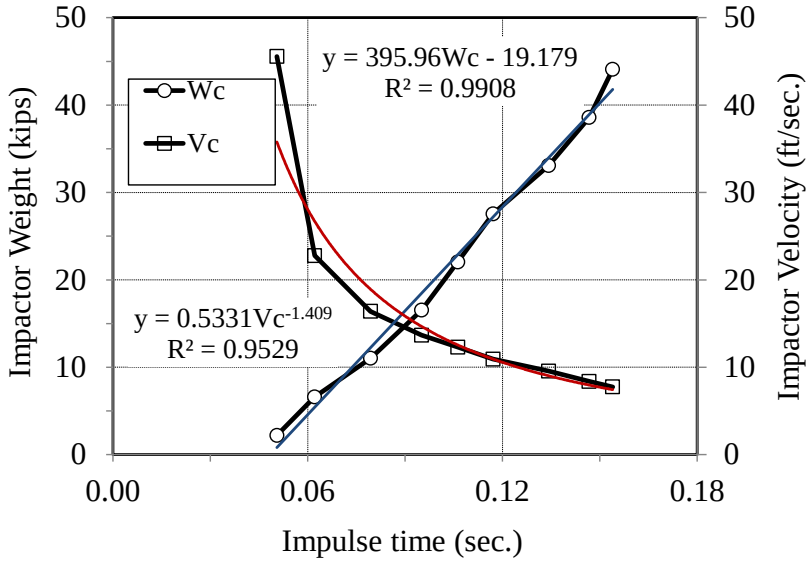

b) Influence in the impulse time

Figure 5.9 Influence of the impactor weight in the magnitude of DA and the impulse load duration

5.3 DAF for Barrier-Moment Slab System

The theoretical analyses and the results of the parametric study were used to further developed a general diagram capable of predicting the DAF for a given barrier-moment slab system and impact conditions. Recalling the definition of the DAF:

$$DAF = 1 + \frac{F_{d,f(m_c.V_c,I_o)}}{F_{s,f(I_o,L,h,d)}} \tag{5-19}$$

The information shown in Eq. (5-19) indicates that the impact load is primarily a function of the impact conditions and the inertia resistance of the system (I_o), as shown in the parametric study. However, this last variable has little contribution to the impact load when compared to the kinetic energy. The static resistance of the system is defined by equilibrium analyses in overturning assuming a rigid body motion. The overturning analyses was selected as it is the primary failure mode of the system. Including these variables into Eq. (5-20) and using as a reference Eq. (5-16), the dynamic amplification (DA) can be described as shown Eq. (5-20):

$$DA = \frac{F_d}{F_s} \propto \left[\frac{m_c V_c}{\Delta t_{f(m_c,v_c)}}\right] \times \left[\frac{I_o}{\left(I_o + m_c h^2\right)}\right] \times \left[\frac{h}{W_w d}\right] \tag{5-20}$$

$$\Delta t_{f(m_c,v_c)} \propto \alpha \times m_c \times V_c^{-b} \tag{5-21}$$

where

Δt= associated impulse time

V_c= velocity of the car in the lateral direction

α= coefficient that defined the magnitude of Δt

b= regression coefficient that defined the slope of Δt

W_w= total weight of the barrier-moment slab system

The first component of Eq. (5-20) accounts for the impact conditions and the effect of impulse time. However, this last variable was also found to be a function of the vehicle mass and impact speed. The second component was previously analyzed using a dimensional analysis and conservation of momentum. It relates the ratio of masses between the system and the vehicle around the rotation point at the time of maximum load. The last component refers to the static load of the system. Using the above information as a reference and the results of the numerical analyses, Eq. (5-20) is re-written as:

$$DA = \frac{F_d}{F_s} \propto \sqrt{\frac{V_c^2}{gd}} \times \ln\left[\frac{\left(I_o + m_c h^2\right)}{I_o}\right] \qquad (5\text{-}22)$$

The total mass of the system was removed from Eq.(5-21) since it is already considered in I_o. The location of d at the bottom of Eq.(5-22) indicates that DA decreases with d. This is due to the effect of d on the static resistance of the system as previously

demonstrated. The variable h also plays an important role in the magnitude of DA. However, its influence is more significant when the values of h are either very small or very large which, in most cases, are out of the range of the common barrier heights seen in service. Nevertheless, its influence is already taken into consideration in the second component. A summary of the global effect on DA of each component of Eq. (5-22) is presented in Table 5.1.

Table 5.1 Summary of the variables influencing the DA

Variable	Change in Variable	Effect on DA
Overturning moment arm, h	↑	↓
Resistant moment arm, d	↑	↓
Section Length of the System, L	↑	↓
Mass Moment of Inertia, I_o	↑	↓
Kinetic Energy of the Vehicle, E_k	↑	↑
Duration of the Impact Load, Δt	↑	↓

The data collected from the numerical analyses was then used to develop the diagram of the DAF (DAF=1+DA) for various conditions. Since this method does not take into account the dynamic characteristics of the barrier system, soil and pavement resistance, presence of vehicle articulation, road and barrier profile or their interaction, DAF values are conservative and they produce maximum dynamic effects that might not necessarily correspond to the maximum static effects. This level of conservatism is acceptable for new construction due to the low marginal cost of adding capacity and

uncertainty about future traffic loading growth. The final results of the analyses are shown in Figure 5.10. The x-axis indicates that at zero velocity or zero vehicle mass, the amplification factor DA) is zero and the dynamic amplification factor (DAF) is one; therefore, the total load is equal to the static load as shown in Eq. (5-3).

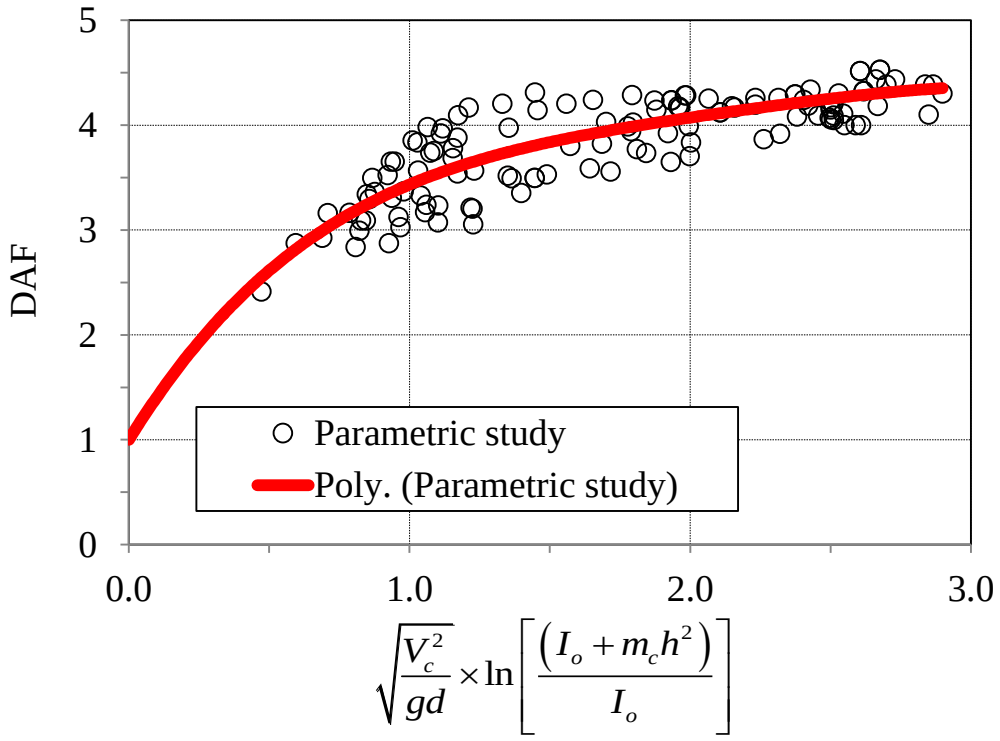

Figure 5.10 DAF diagram for barrier-moment slab system subjected to traffic loading

5.4 Comparison with Full-Scale Impact Simulation and Full-Scale Tests

The result obtained from the parametric study was then compared to the results obtained from the full-scale impact simulation and the TL-3 and TL-5 full-scale crash tests. The information is summarized in Table 5.2, Table 5.3. The four square data points show in Figure 5.11 compares the DAF values measured from the full-scale impact simulation conducted in section 4 with the DAF-diagram. These results compares well with the analyses conducted in this section.

The analysis was conducted using the nominal impact condition for the different test levels (impact velocity, angle and vehicle mass). The vehicle mass inputted into Eq. (5-22) was considered as follow:

- TL-3= total vehicle mass
- TL-4= 3/4 the total vehicle mass (mass associated with the rear axles)
- TL-5-1= 1/3 of total vehicle mass (mass associated with the central axles of the vehicle).
- TL-5-2= 2/3 of total vehicle mass (mass associated with the rear axles of the trailer)

The TL-3 and TL-4 impacts involve single body vehicles, pick-up truck and Single Unit Truck, respectively. Therefore, it is reasonable to consider that most of their mass contributes to the impact load. The TL-5-1 is associated with a minimum barrier height of 42 in. (1067 mm); therefore, it allows the trailer to roll on top of the barrier without hitting it directly. Therefore, the mass used for TL-5-1 was 1/3 of the total mass

which is also equivalent to the reaction mass at the central axles of the tractor-van-trailer. For the TL-5-2 impact, the trailer strikes the barrier directly and more mass is engage in the impact. Therefore, the analyses are conducted with approximately 2/3 of the total mass of the vehicle which is equivalent to the ballast mass carry by the trailer.

Table 5.2 Summary of the impact conditions and the barrier-moment slab system for TL-3 through TL-5

Test Level	Impact Conditions		Barrier-Moment Slab System Properties						Impact Load and Displacements		
	W_c (lb.)	$V_{c\text{-lateral}}$ (ft/sec.)	L (ft)	d (ft)	h (ft)	W_w (kips)	I_o (lbm-ft^2)	L_s (kips)	F_d [2] (kips)	Disp. Top (in.)	Disp. Bottom (in.)
TL-3[1]	5000	38.5	30	1.57	4.23	52.2	8684	19.4	62	1.0	0.50
TL-4	16500	21.2	30	1.71	5.08	60.1	12314	20.2	70	1.0	0.75
TL-5-1	26500	18.9	30	3.05	5.74	113.3	53683	60.2	125	1.0	0.80
TL-5-2	53000	18.9	30	3.84	6.49	151.2	108238	89.3	215	1.0	0.80

[1] Full-scale TL-3 scaled load to 1.0 in. displacement at the top of the barrier.
[2] Dynamic load for 1 in. dynamic displacement at the top.

Table 5.3 Comparison between the DAF obtained from the diagram and the DAF obtained from full-scale test or Impact Simulation

Test Level	$\sqrt{\frac{V_c^2}{gd}}$	$\ln\left[\frac{(I_o + m_c h^2)}{I_o}\right]$	$\sqrt{\frac{V_c^2}{gd}} \times \ln\left[\frac{(I_o + m_c h^2)}{I_o}\right]$	DAF (Diagram)	DAF (Sim./Test)
TL-3	5.41	0.36	1.96	4.1	4.2
TL-4	2.87	0.90	2.58	4.3	4.5
TL-5-1	1.90	0.52	0.99	3.3	3.1
TL-5-2	1.70	0.63	1.06	3.5	3.4

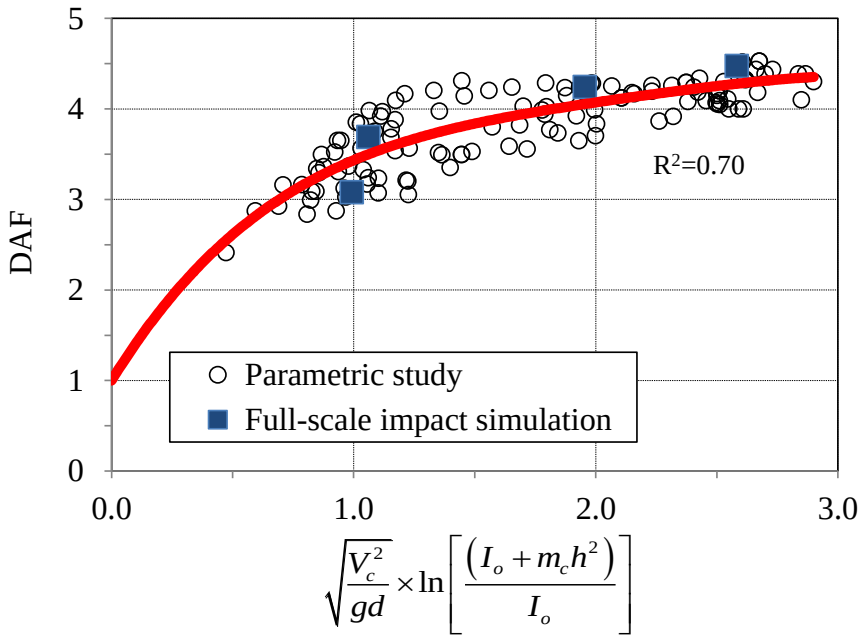

Figure 5.11 DAF diagram for barrier-moment slab system subjected to traffic loading

5.5 Conclusions

The following conclusions are based on and limited to the content of this chapter:

1. FE analyses and simple analytical expressions were used to help estimate the magnitude of the DAF using the barrier-moment slab system properties and the vehicle impact conditions. Using the results of this study, it was possible to define a more realistic design value for DAF, which may result in considerable savings and rehabilitation costs.
2. The impact simulation was conducted using a displacement criterion of 1.0 in. (25.4 mm) at the top of the barrier. It was found that the magnitude of DAF is a function of several variables from which the impact speed, vehicle mass and the inertial resistance of the barrier-moment slab system are the most influencing factors.
3. The values of DAF, computed using the proposed method, compares well with the results of the TL-3 full-scale crash test presented in NCHRP Report 663 and the results of the full-scale impact simulation conducted in section 4. The absolute difference between both approaches varies from 3% to less than 10%.

6 MSE WALL STUDY FOR TEST LEVEL 4 AND TEST LEVEL 5 IMPACT

The barrier-moment slab systems designed and evaluated in section 4 were placed on top of an approximately 9.8 ft (3 m) tall MSE wall model. The purpose of these analyses includes quantification of the movement of the barrier, coping, and moment slab system and measurement of the force distributions in the reinforcement strips due to a TL-4 and TL-5 impact. These results are used to help draft a preliminary design guideline for barrier stability, pullout and yielding of the soil reinforcement. I addition, the results obtained for the TL-5 analyses help to design and plan the TL-5 full-scale test installation.

6.1 Full-Scale MSE Wall FE Analyses

A total of three MSE wall models with different soil reinforcement lengths (standard cross section of 2 in. (50 mm) × 0.16 in. (4 mm)) were developed for evaluation of TL-4, TL-5-1, and TL-5-2 impact. The first model was developed using 10 ft (3.05 m) long strip reinforcement. This strip length is commonly used in practice for short-height wall segments and therefore constitutes the critical case for assessing wall displacement during a barrier impact. The second and third wall models were developed using a 16 ft (4.88 m) and 24 ft (7.31 m) long soil strip reinforcement, respectively. This length of reinforcement is used in practice in many MSE wall installations as the wall height increases. The increased soil reinforcement length also strengthens the bond safety of the

reinforcement. Therefore, a wall section with 24 ft (7.31 m) long strip reinforcement constitutes the critical case for assessing the magnitude and distribution of impact loads in the reinforcement. In the first two cases, a density of three strips per panel per layer was considered. The 24 ft (7.32 m) long strips had a density of 2 strips per panel per layer. A summary of the full-scale impact simulation is shown in Table 6.1.

Table 6.1 Summary of the full-scale impact simulation for TL-4 and TL-5

Simulation Sequence	Barrier Type (Length of Section (ft))	Barrier Capacity (kips)	Length of Failure (ft)	Moment Slab Width (ft)	Strip Reinforcement Length (ft)
TL-4	Vertical Wall (10)	89.8	4.2	4.5	10 16 24
TL-5-1	Vertical Wall (15)	161.1	10.3	7.0	10 16 24
TL-5-2	Vertical Wall (15)	323	10.2	9.0	10 16 24

6.1.1 MSE Wall Capacity

The forces expected in the soil strip reinforcements due to the gravity load were computed according to AASHTO LRFD *(3)*. The MSE wall design guideline presented in NCHRP Report 663 was adjusted to help estimate the dynamic loads in the strip

reinforcement resulted from a TL-4 and TL-5 impact. The scaled factors were based on the ratio of impact loads of TL-4 and TL-5 to TL-3. Therefore, the pressure distribution to pullout and yielding failure were increased accordingly. For example, the pullout and yielding pressure distributions of the strip reinforcements shown in Figure 2.15 are increased by factor of 1.48 (80 kips/54 kips), 2.96 (160 kips/(54 kips), and 4.81 (260 kips/54 kips) for TL-4, TL-5-1 and TL-5-2, respectively. These pressure distributions are preliminary and they will be verified and modified, if necessary, after the full-scale impact simulation.

The detailed calculations for designing the MSE wall are presented in Appendix A. The information is also summarized in Table 6.2 . In these analyses, the traffic surcharge was not considered. This information ultimately was compared to the forces estimated through numerical simulation. Table 6.2 shows that the expected pullout forces in the first layer of reinforcement for TL-5 impact exceeds the calculated static resistance for pullout. This might indicate that the 10 ft (3.05 m) long strips reinforcements are not sufficient to contain a TL-5-1 or TL-5-2 impact.

However, the expected loads in the soil reinforcement were computed using an estimated pressure diagram which might not represent the true value. In addition, the barrier-moment slab system placed on top of the wall is designed to resist the impact load over the full-length of barrier-slab between joints and not to transfer high impact forces into the precast concrete panels of the wall. Based on that, the actual expected load transferred into the soil reinforcement should not be sufficient to cause pullout failure. This premise will be evaluated through the conclusion of this section.

Barrier-foundation systems on top of MSE walls should be designed as a permanent structure (e.g., service life of 75 years). Therefore, the reinforcement elements shall be designed to have an adequate corrosion resistance-durability to ensure a minimum design life of 75 years.

To guarantee that, it is important to provide adequate sacrificial metal thickness for corrosion losses, in addition to the required structural thickness, to ensure that reinforcement stresses do not exceed the yielding stresses for the full service life of the structure. For example, using the AASHTO LRFD recommended rates and the standard galvanization thickness of 86 µm *(3)*, a sacrificial thickness of 0.06 in. (1.42 mm) is computed for a service life of 75 year. Therefore, for a standard reinforcing strip (2 in. (50 mm) × 0.16 in. (4 mm)) Grade-60, the unfactored tensile capacity at the end of the service life is 12.02 kips (53.5 kN).

Table 6.2 Unfactored resistance and force in the reinforcing strips for TL-5 MSE wall

Test Level	Strips Length (ft)	Layer	Depth (ft)	T_{static}[(1)] (kips)	$T_{dynamic}$[(2)] (kips)	$T_{total}=T_{static}+T_{dynamic}$ (kips)	Resistance to Pullout[(1)] (kips)
TL-4	10	Top	3.0	0.69	1.37	2.06	2.05 (F*=1.67)
	10	Second	5.5	1.20	1.36	2.56	3.41 (F*=1.52)
	16	Top	3.0	0.69	1.37	2.06	3.28 (F*=1.67)
	16	Second	5.5	1.20	1.36	2.56	5.46 (F*=1.52)
	24	Top	3.0	1.03	2.05	3.08	4.93 (F*=1.67)
	24	Second	5.5	1.80	2.04	3.85	8.20 (F*=1.52)
TL-5-1	10	Top	3.6	0.82	2.72	3.54	2.43 (F*=1.63)
	10	Second	6.1	1.35	2.72	4.07	3.78 (F*=1.49)
	16	Top	3.6	0.82	2.72	3.54	3.89 (F*=1.63)
	16	Second	6.1	1.35	2.72	4.07	6.04 (F*=1.49)
	24	Top	3.6	1.24	4.07	5.31	5.83 (F*=1.63)
	24	Second	6.1	2.03	4.07	6.11	9.06 (F*=1.49)
TL-5-2	10	Top	3.7	0.84	4.43	5.27	2.48 (F*=1.63)
	10	Second	6.2	1.37	4.42	5.79	3.82 (F*=1.49)
	16	Top	3.7	0.84	4.43	5.27	3.96 (F*=1.63)
	16	Second	6.2	1.37	4.42	5.82	6.11 (F*=1.49)
	24	Top	3.7	1.26	6.65	7.91	5.94 (F*=1.63)
	24	Second	6.2	2.06	4.42	8.69	9.17 (F*=1.49)

(1) AASHTO LRFD Eq. 11.10.6.3.2-1

(2) Modified based on NCHRP Report 663

6.1.2 Modeling Methodology

The BMS models used in the stability analyses for TL-4 and TL-5 impact were modified and placed on top of an 9.8 ft (3 m) tall MSE wall model. The modifications included improvements to the element mesh, changes in material properties and their characterization, incorporation of the MSE wall model and modeling the barrier, the moment slab and the panels with explicit reinforcement details.

The first phase of the simulation process is to account for the steady-state conditions of the system due to gravitational load. The initialized model is set up with the SUT or the tractor-trailer vehicle model in order to conduct the impact simulation. Figure 6.1 and Figure 6.2 show general details of the model MSE wall model and the precast concrete panels.

a) Overview of the MSE Wall Model

The finite element representation of the barrier-moment slab system on top of an MSE wall consists of the following components:

- Precast concrete barrier sections and cast-in-place moment slabs with explicit reinforcement details
- Backfill and overburden soil material
- Precast concrete panels with explicit reinforcement details
- Unreinforced concrete bearing pad and concrete leveling pad

- Steel reinforcement shear dowels connecting the moment slab sections.
- Soil reinforcing strips

The elements of the barrier, the panels and soil surrounding the impact location were re-meshed with an element characteristic size ranging from 0.8 in. (20.3 mm) to 1.5 in. (38.1 mm) to capture the deformation and expected damage the barriers and the panels with improve accuracy. Figure 6.1 shows detail of the components of the MSE wall model.

b) Contact Algorithm

The methodology followed to model the interface contact between all components of the MSE wall was similar to that used in the BMS models. The soil reinforcing strips were also modeled using the LS-DYNA feature *CONSTRAINED_LAGRANGE_IN_SOLID. This coupling algorithm permits the strip reinforcement (treated as a slave) to be placed anywhere inside the backfill material (treated as a master) without any mesh accommodation. This contact card can be used to model the interaction between the soil and the strip because the relative movement between them is not significantly. Therefore, it also help to simulate the passive resistance associated with ribbed reinforcing strips. The connection between the strips and the panels was defined using another LS-DYNA coupling mechanism, *CONTACT_TIED_EDGE_TO_SURFACE.

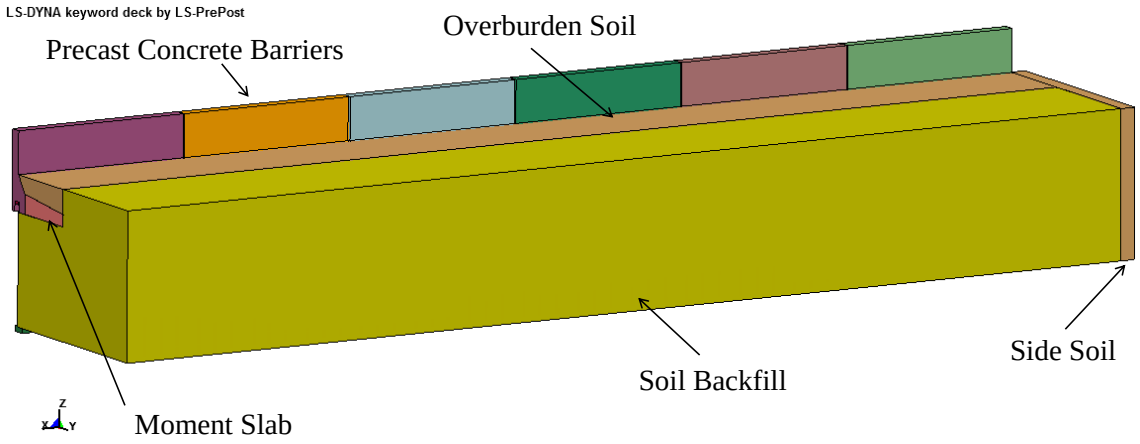

a) Three dimensional view of the MSE wall model

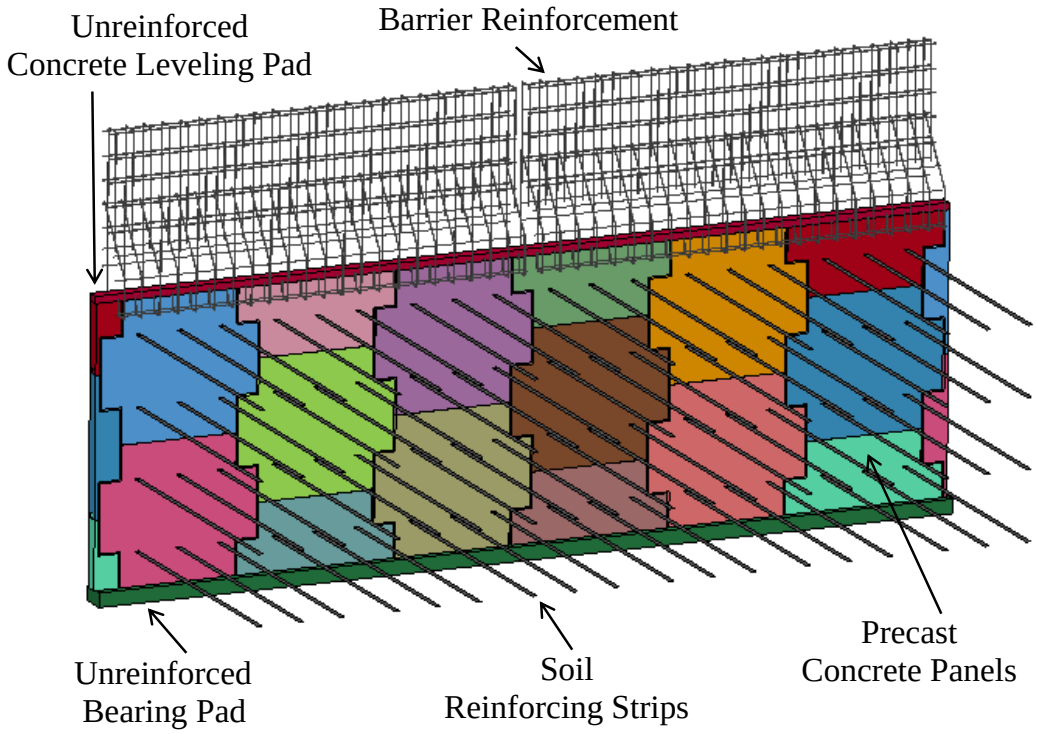

b) Three dimensional view showing barrier and soil reinforcement

Figure 6.1 Components of the MSE wall model

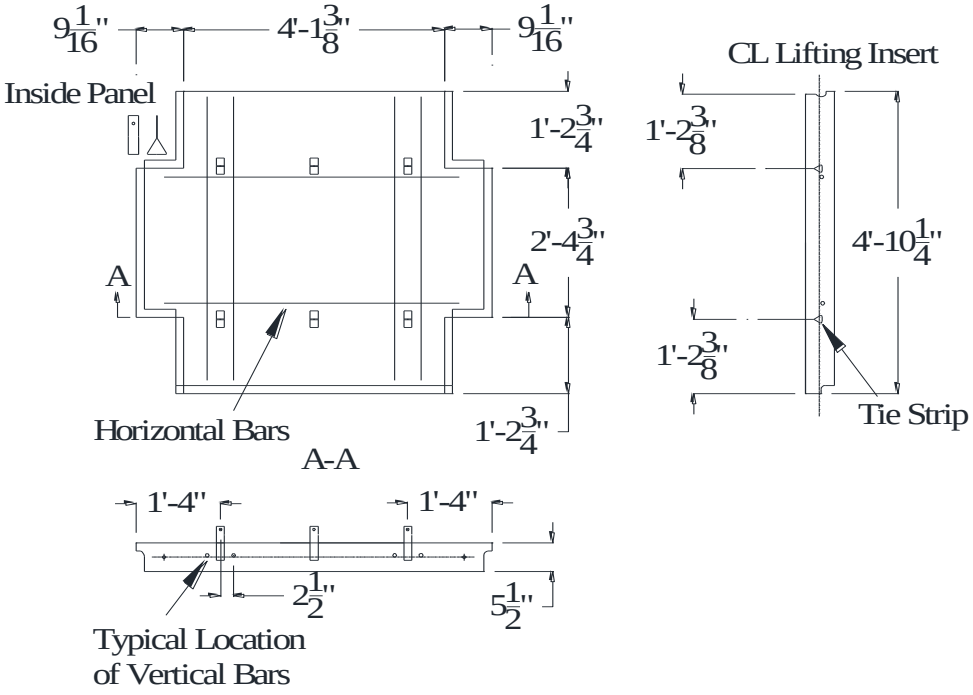

a) Detail of the panels from RECO

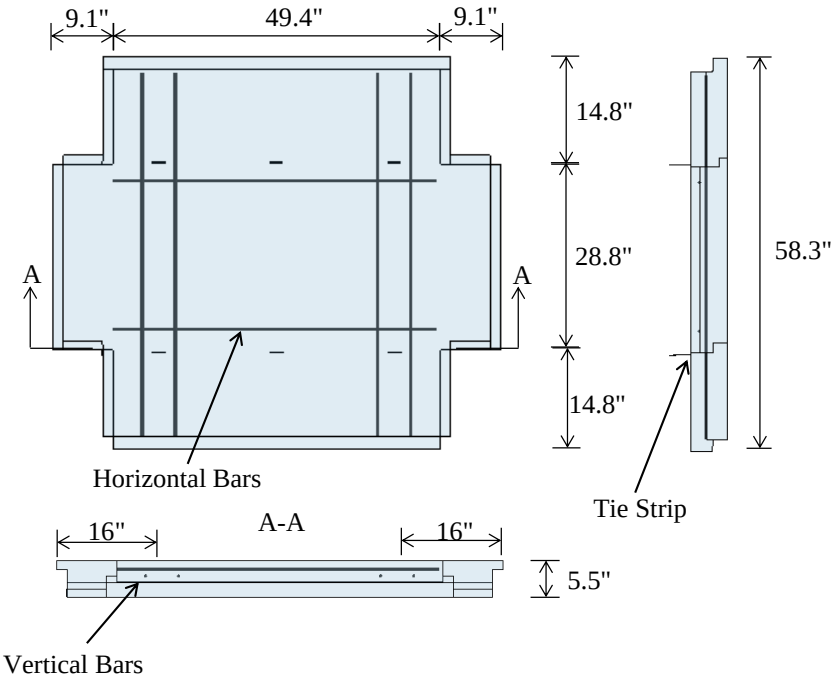

b) Detail of the panels FE model

Figure 6.2 Precast concrete panel details

c) Material Model and Model Parameters

The precast concrete barriers connected to the middle moment slab section and the precast concrete panels were modeled using a nonlinear response concrete material model (LS-DYNA *MAT_159). This material model captures the softening behavior of the barrier and the panels in the tensile regime due to the impact load. A damage formulation allows the concrete to loss its ability to carry loads after the failure threshold is reached *(42).* The strip reinforcements were modeled using a piecewise linear isotropic plasticity model (LS-DYNA *MAT_24) that is representative of an actual stress-strain relationship of a steel grade 60. The failure criterion was 20%, which means the strips will break at an ultimate strain greater than approximately 20%. The backfill material was modeled with the same material model used in the previous analyses (Modified Cap Soil Model (LS-DYNA *MAT_25)).

6.2 MSE Wall FE Analyses for TL-4 Impact

The BMS system model used in the MASH TL-4 barrier-stability analysis was placed on top of a 10 ft (3 m) tall, 90 ft (27.4 m) long MSE wall model (Figure 6.3 (a) and Figure 6.4). Three impact simulations were conducted using soil reinforcing length of 10 ft (3.05 m), 16 ft (4.88 m), and 24 ft (7.3 m), as shown in Figure 6.3. The information collected from the FE analyses includes: impact force, barrier displacement and loads and displacements in the reinforcing strips. To enable comparison of forces and

displacements, the barriers and selected strip locations were assigned an alphanumeric designator that describes their horizontal and vertical position as shown in Figure 6.5. The vehicle was aligned to impact at the middle of barrier section 5 (B5) with a speed of 56 mph (90 km/hr.) at an angle of 15 degrees.

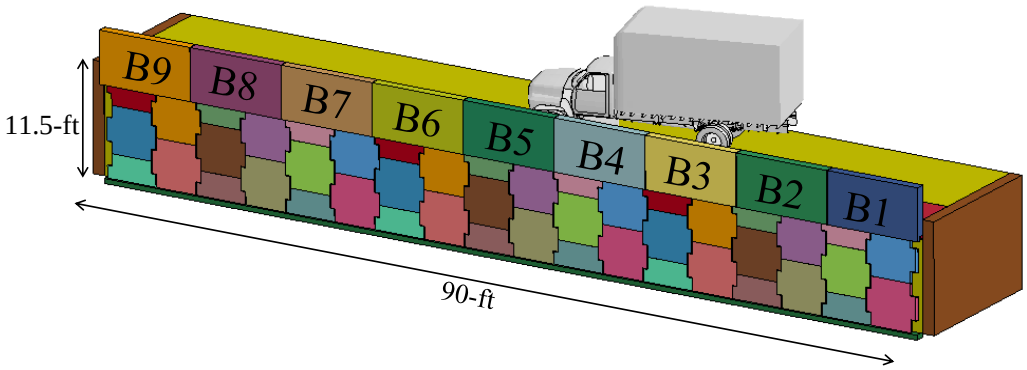

a) Three dimensional view of the TL-4 MSE wall model

Figure 6.3 TL-4 MSE wall model with different soil reinforcement lengths

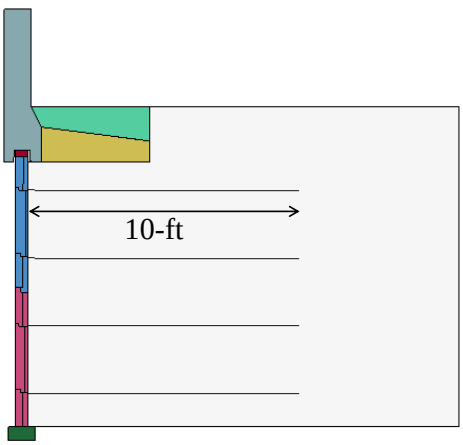

b) 10 ft long strip model

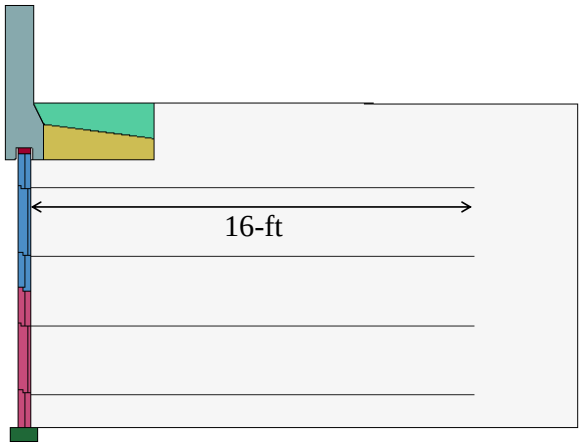

c) 16 ft long strip model

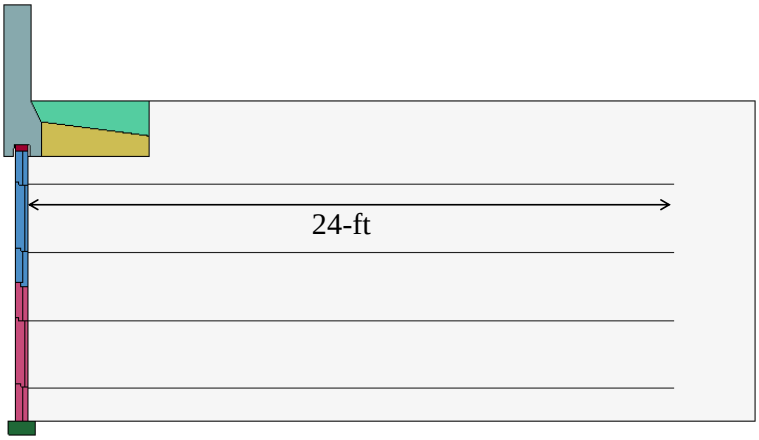

d) 24 ft long strip model

Figure 6.3 Continued

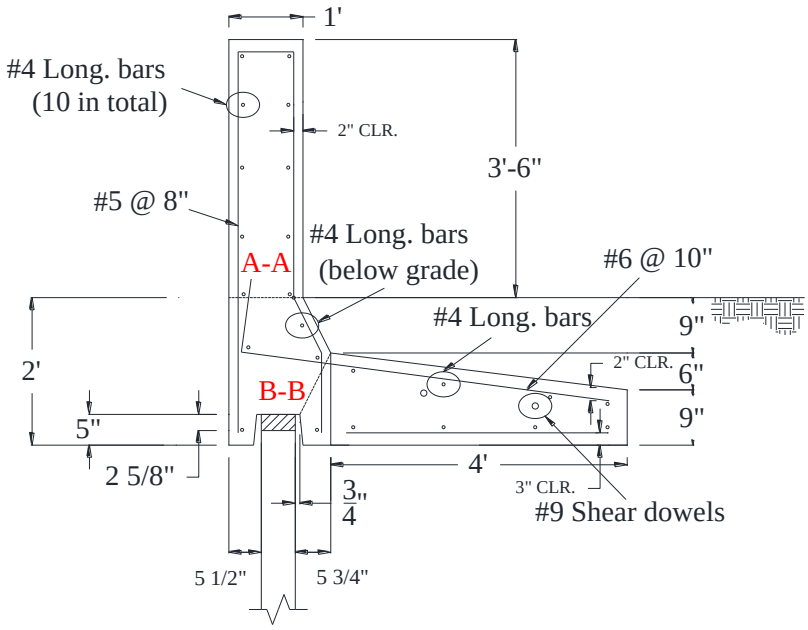

a) TL-4 barrier-moment slab system details

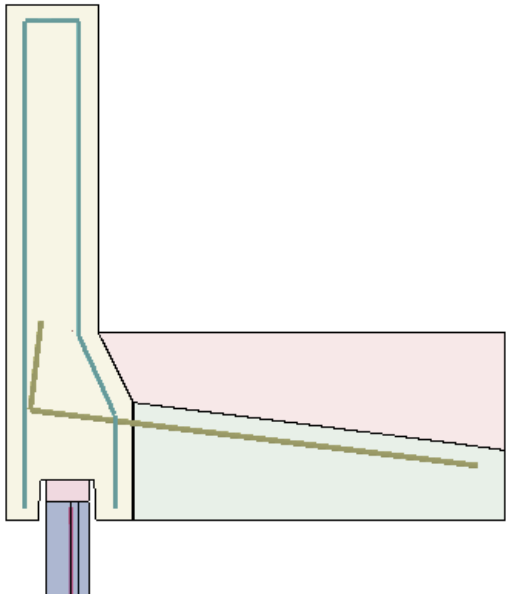

b) TL-4 barrier-moment slab system model

Figure 6.4 Rebar detail in the barrier and panel for TL-4 impact

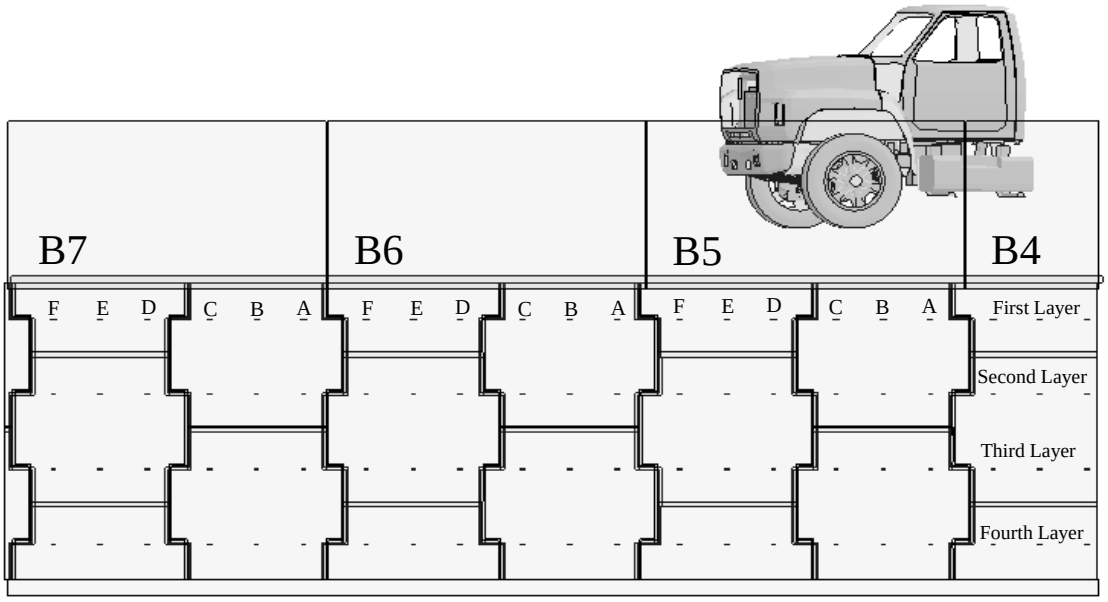

Figure 6.5 Elevation view of the MSE wall showing the strip distribution (TL-4 Impact)

6.2.1 Loads and Displacements in the Barrier

The impact load captured from the FE analyses was on average 73.8 kips (328.6 kN), as shown in Figure 6.6 and Table 6.3. This peak load was due to the back slap impact of the vehicle and its magnitude was similar in all the analyses. The damage profile of the concrete barrier at the time of maximum impact load is shown in Figure 6.7. This barrier damage profile is typically observed in barrier joints or at the end section of the barrier as described by the AASHTO LRFD yield line analyses *(3)*. The damage profile is limited to the surface elements and it does not indicate structural failure of the precast

concrete barrier. It might indicate cosmetic marks due to the frictional loads imposed by the tires and the vehicle box.

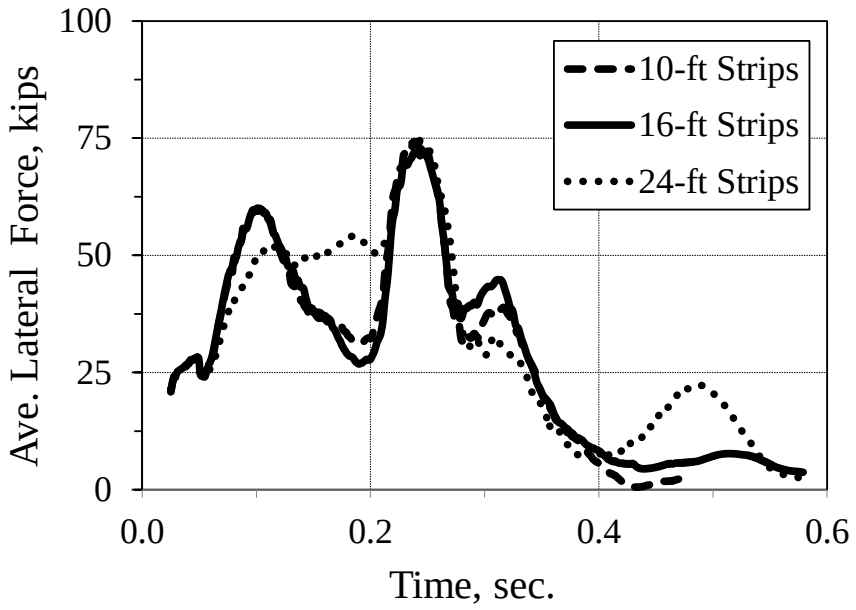

Figure 6.6 Time history of MASHT TL-4 impact load on barriers (50 msec. average)

Table 6.3 Summary of the impact loads and barrier displacements for the MASH TL-4 impact simulation

Strip Length (ft)	Impact Load (kips)	Approximate Barrier Displacement (in.)	
		Top (dynamic)[1]	Bottom (permanent)[2]
10	74.7	1.14	0.74
16	72.8	1.23	0.68
24	74.0	1.27	0.61
Average	73.8	1.21	0.68

[1] Measured at the top of the barrier at the impact point location
[2] Measured at the coping level of the barrier at the impact point location

The maximum displacements at the top and bottom of the barrier were on average 1.21 in. (30.7 mm) and 0.68 in. (17.3 mm), respectively. The information is summarized in Table 6.3 and Figure 6.8. These displacements are associated with the back slap impact of the vehicle which causes most of the sliding and rotational displacement in the barrier systems. The moment slab joints show little relative displacements indicating an adequate load transfer to the neighbor sections through the shear dowels.

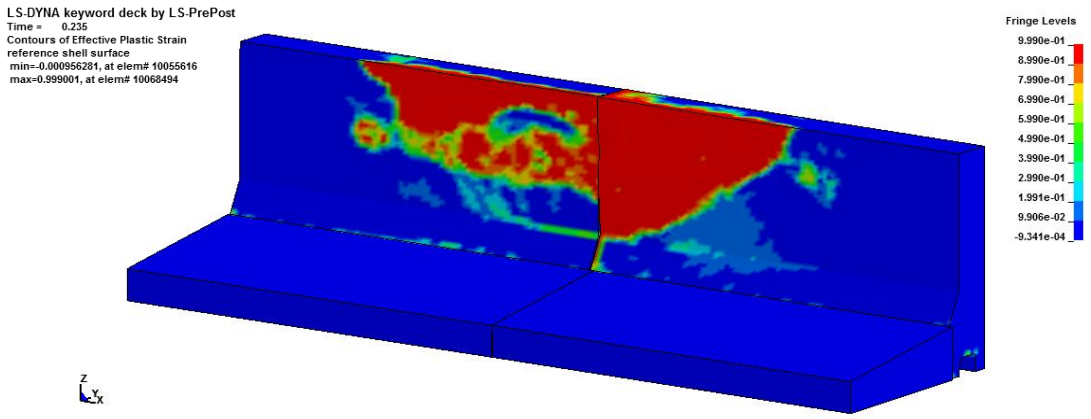

a) Front view of the barrier (back slap impact)

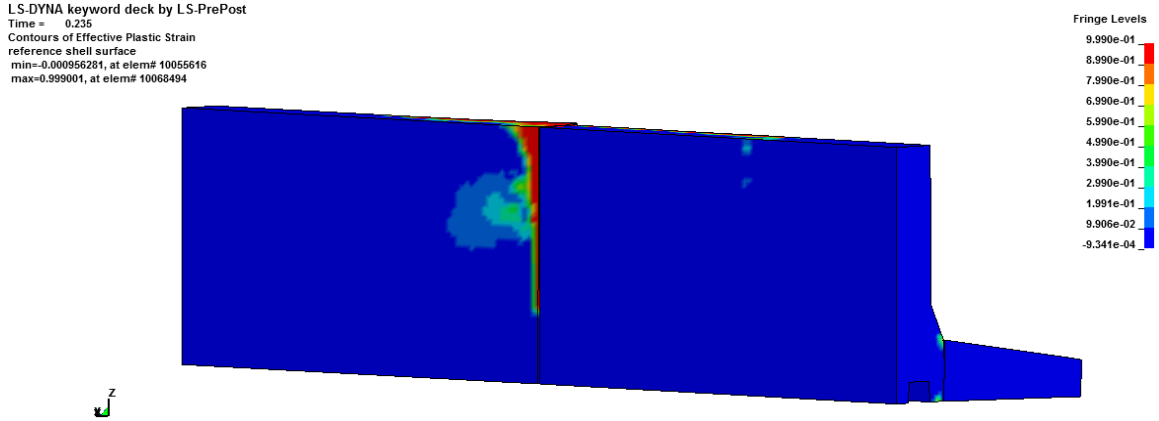

b) Back view of the barrier (back slap impact)

Figure 6.7 Damage to the 42 in. (1.07 m) tall concrete barrier (TL-4)

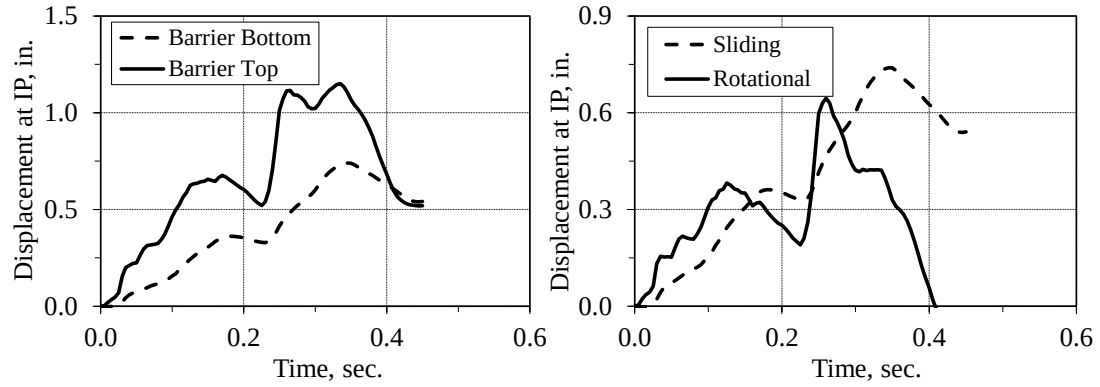

a) 10 ft long strips

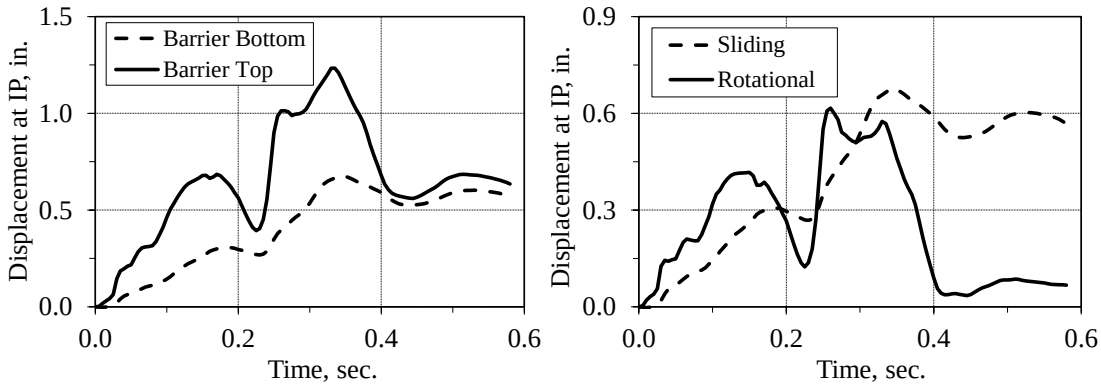

b) 16 ft long strips

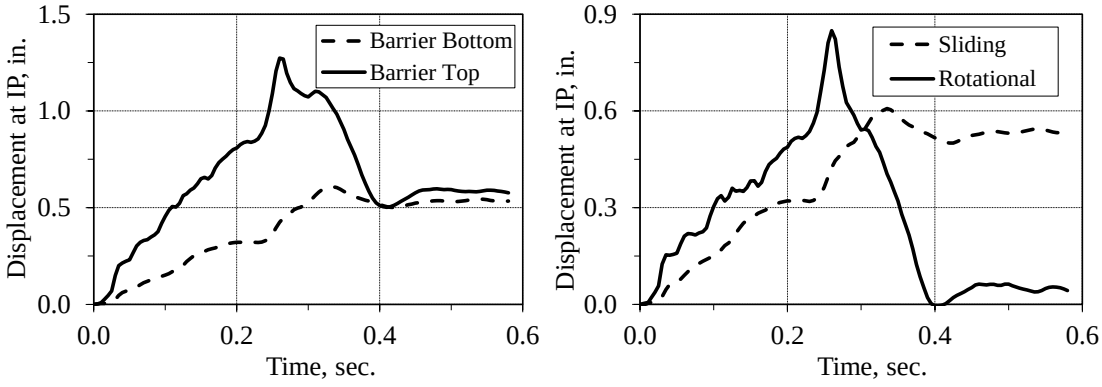

c) 24 ft long strips

Figure 6.8 Displacement of the 42 in. (1.07 m) at IP for TL-4 impact

6.2.2 Loads and Displacement in the Soil Reinforcements

The loads in the strips reinforcement were captured at two locations, 7 in. (178 mm) and 36 in. (914 mm) from the wall face (Table 6.4). The first location provides information of the maximum tension load experienced in the strips while the second location is associated with the maximum tension load due to the gravitational loading according to AASHTO LRFD. Table 6.4 shows the total load in a selected number of reinforcing strips. The results indicates that strip B6-C-1st was subjected to the highest tension load and it was 4.4 kips (19.6 kN), 5.8 kips (25.8 kN) and 7.0 kips (31.2 kN) for the 10 ft (3.05 m) long, 16 ft (4.9 m) long and 24 ft (7.3 m) long strip models, respectively.

The second layer of reinforcement was not significantly stressed as shown in Table 6.4. According to the simulation results, the maximum load in the second layer of reinforcement for the 10 ft (3.05 m) long, 16 ft (4.9 m) long and 24 ft (7.3 m) long strip models were 2.24 kips (10 kN) at strip section B6-D-2nd, 1.9 kips (8.5 kN) at strip section B5-E-2nd, and 1.6 kips (7.6 kN) at strip section B3-F-2nd, respectively. The load time-history of the selected strips are presented in Figure 6.9.

The displacements in the strips were minimal. The maximum displacement in the uppermost layer was captured at section B6_C_1st and it was 0.17 in. (4.3 mm), 0.15 in. (3.8 mm) and 0.14 in. (3.5 mm) for the 10 ft (3.05 m), 16 ft (4.9 m) and 24 ft (7.3 n) long strip models, respectively. In the second layer of soil reinforcement, the maximum displacements were 0.04 in. (1.0 mm) at section B3_C_2nd , 0.04 in. (1.0 mm) at section

B3_C_2nd and 0.04 in. (1.1 mm) at section B6_C_2nd for the 10 ft (3.05 m), 16 ft (4.9 m) and 24 ft (7.3 m) long strip models, respectively.

Table 6.4 Summary of the total load for the selected strip location (TL-4 impact)

Section	50 msec. Average Strip Load (kips)						AASHTO Pullout Resistance[(1)] (kips)		
	Strip Length								
	10-ft	16-ft	24-ft	10-ft	16-ft	24-ft			
	At 7 in. from panels			At 7 in. from panels			10-ft	16-ft	24-ft
B4_A_1st	3.8	4.8	4.9	3.0	3.6	4.0	2.05	3.25	4.93
B4_C_1st	2.4	1.9	2.2	2.0	1.7	2.1	2.05	3.25	4.93
B4_D_1st	1.5	1.2	1.3	1.4	1.2	1.3	2.05	3.25	4.93
B4_F_1st	2.0	2.9	1.9	1.7	2.3	1.8	2.05	3.25	4.93
B5_A_1st	3.5	4.6	3.3	2.7	3.5	2.8	2.05	3.25	4.93
B5_C_1st	2.9	3.9	3.1	2.4	3.1	2.8	2.05	3.25	4.93
B5_D_1st	2.6	3.4	3.3	2.2	2.8	2.8	2.05	3.25	4.93
B5_F_1st	3.8	4.5	4.3	3.0	3.5	3.6	2.05	3.25	4.93
B6_A_1st	2.8	3.9	4.6	2.4	3.1	3.8	2.05	3.25	4.93
B6_B_1st	3.4	4.5	5.4	2.8	3.6	4.5	2.05	3.25	4.93
B6_C_1st	4.4	5.8	7.0	3.5	4.2	5.2	2.05	3.25	4.93
B6_D_1st	3.7	5.4	5.6	2.7	4.1	4.4	2.05	3.25	4.93
B5_D_2nd	2.2	1.7	1.6	1.5	1.0	1.5	3.48	5.56	8.34
B5_E_2nd	1.5	1.9	1.5	1.6	1.0	1.4	3.48	5.56	8.34
B3_F_2nd	1.6	1.5	1.7	1.3	1.3	1.7	3.48	5.56	8.34

[(1)] AASHTO LRFD Eq. 11.10.6.3.2-1

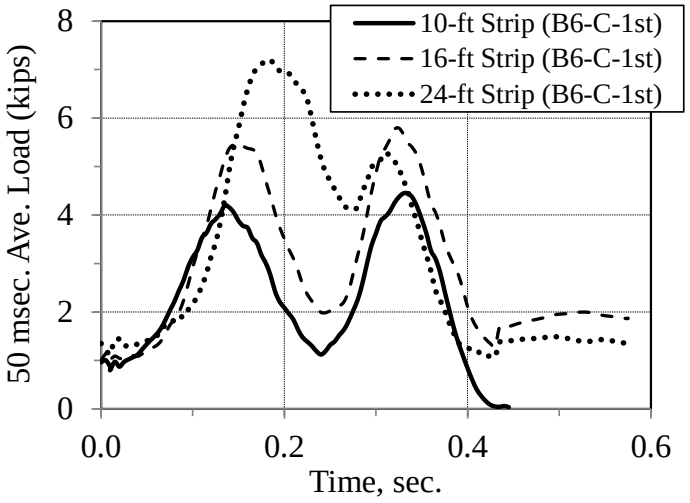

a) First layer of soil reinforcement

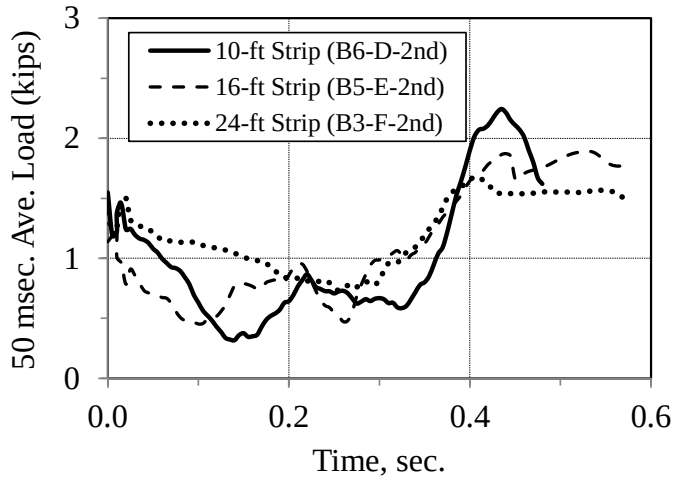

b) Second layer of soil reinforcement

Figure 6.9 Time-history of the total load in the maximum stressed strips (TL-4)

The distribution of the total load in the highest stressed soil reinforcing strip (B6-C-1st) was also studied. Based on the results shown in Figure 6.10, the load distribution appears to be linear for shorter strips with a slight increasing nonlinear behavior as the

strip length increases. It is also clear that the strips tend to be at failure at the time of maximum load. However, due to the instantaneous nature of the loading conditions, the skin friction developed at the soil-reinforcing strips interface and the apparent coefficient of friction becomes virtually large. Therefore, the strips only move a small fraction and pullout failure does not have time to occur. Assuming a linear distribution along the strip length and zero load at the end of the strip, the average skin friction developed at the interface soil-strip is 1.02 kip/ft^2 (48.8 kPa), 0.9 kip/ft^2 (43.1 kPa), and 0.71 kip/ft^2 (34 kPa) for the 10 ft (3.05 m), 16 ft (4.88 m) and 24 ft (7.32 m) long strip model, respectively.

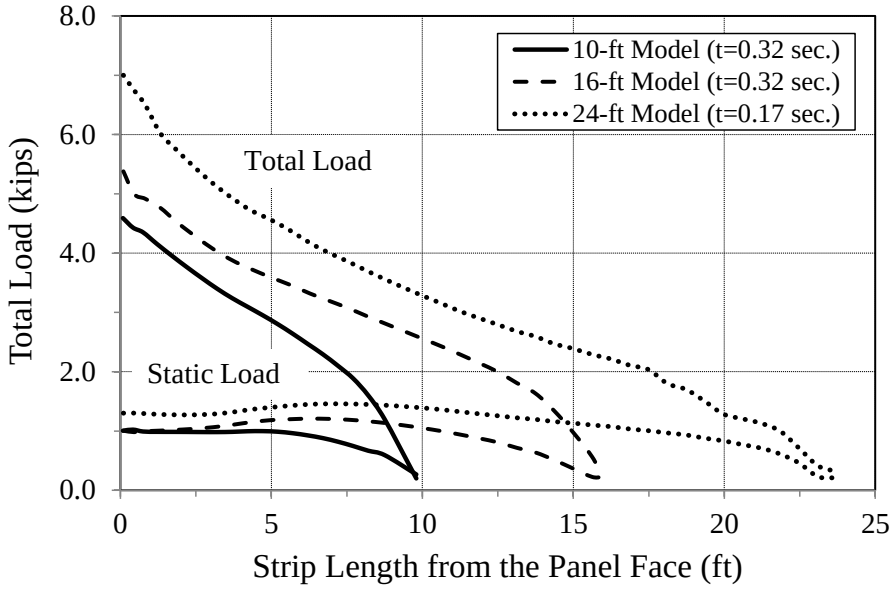

Figure 6.10 Distribution of the total load at section B6-C-1st (TL-4)

6.2.3 Wall Panel Analyses

The results of the numerical analyses show that the wall panels did not experience any damage for the TL-4 impact analyses. The compressive strains were minimal and they do not represent any risk of structural failure of the wall panels due to the impact load. The dynamic and permanent displacement of the wall panels at the impact region for the three models is shown in Figure 6.11.

It is observed that the wall displacement decreases as the strip length increases. The maximum dynamic and permanent displacement at the top of the wall panels was 0.37 in. (9.4 mm) and 0.13 in. (3.3 mm), respectively. These displacements are associated with the soil reinforcement length of 10 ft (3.05 m).

The permanent displacement of the 24 ft (7.3 m) long strip is almost zero. The increase in wall stiffness due to a large strip length (24 ft (7.3 m)) decreases the wall displacement considerable but also increases the load in the strips as shown before.

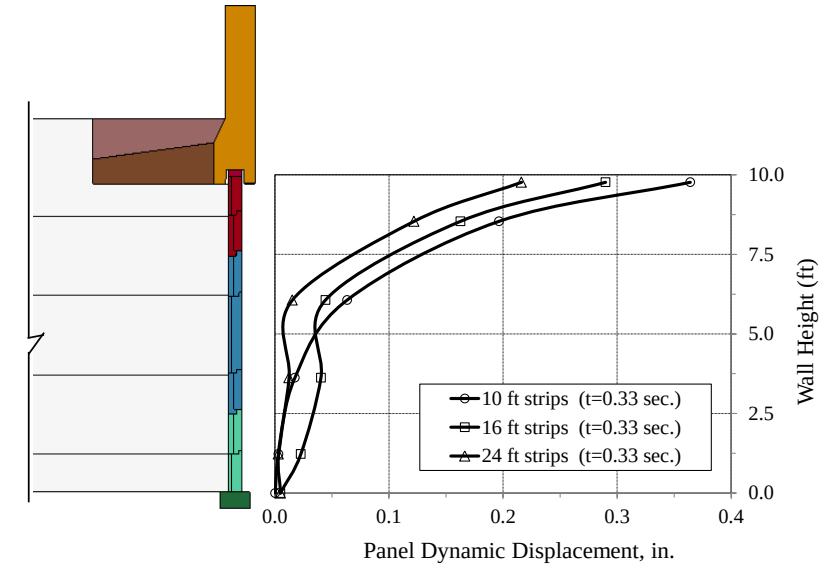

a) Dynamic displacement (impact region)

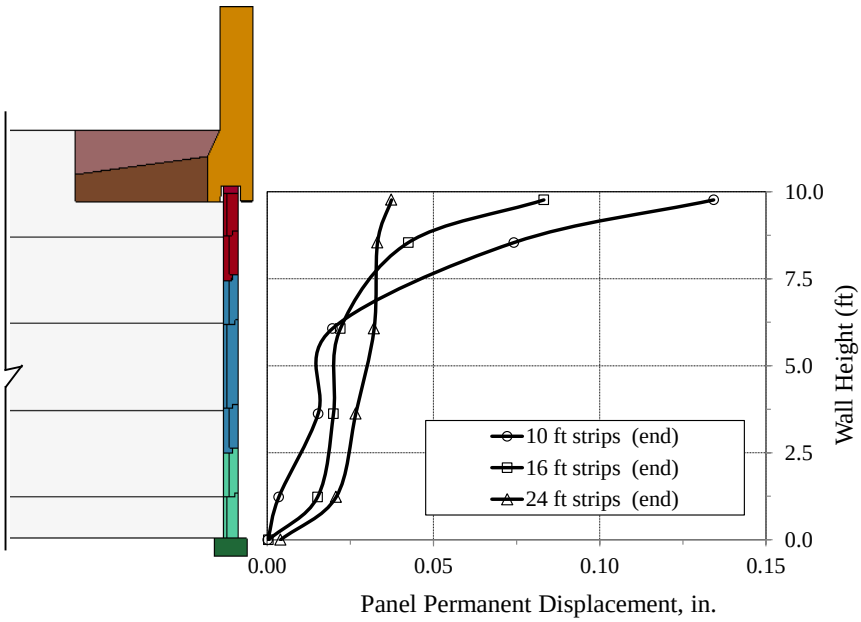

b) Permanent displacement (impact region)

Figure 6.11 Displacements at the wall panels (TL-4)

6.3 MSE Wall FE Analyses for TL-5 Impact on a 42 in. (1.07 m) Tall Barrier (TL-5-1)

The 42 in. (1.07 m) tall vertical wall barriers and the 7 ft (2.13 m) wide moment slab evaluated in the stability analyses were placed on top of the same MSE wall models used for TL-4 impact. The objectives of the analyses include quantification of the impact force, barrier displacement, loads and displacements in the reinforcing strips and understanding of the load-transfer mechanism of the impact load. The alphanumeric designator that describes the horizontal and vertical position of the reinforcing strips is shown in Figure 6.12. The vehicle was aligned to impact at the middle of barrier section 3 (B3) with a speed of 50 mph (80 km/hr.) at an angle of 15 degrees. Figure 6.13 and Figure 6.14 show details of the vertical wall barrier and the MSE wall showing the impact point and the downstream section.

To preclude the transfer of high impact load into the MSE wall panels, a 1.5 in. (38.1 mm) gap is provided between the throat of the precast barrier and the back face of the panels. The moment slab were connected using three No.11 steel bars embedded 18 in. (457 mm) at each side of the slab joint. The vertical wall barrier was extended 45 ft (13.7 m) beyond the MSE wall to help redirect the vehicle downstream.

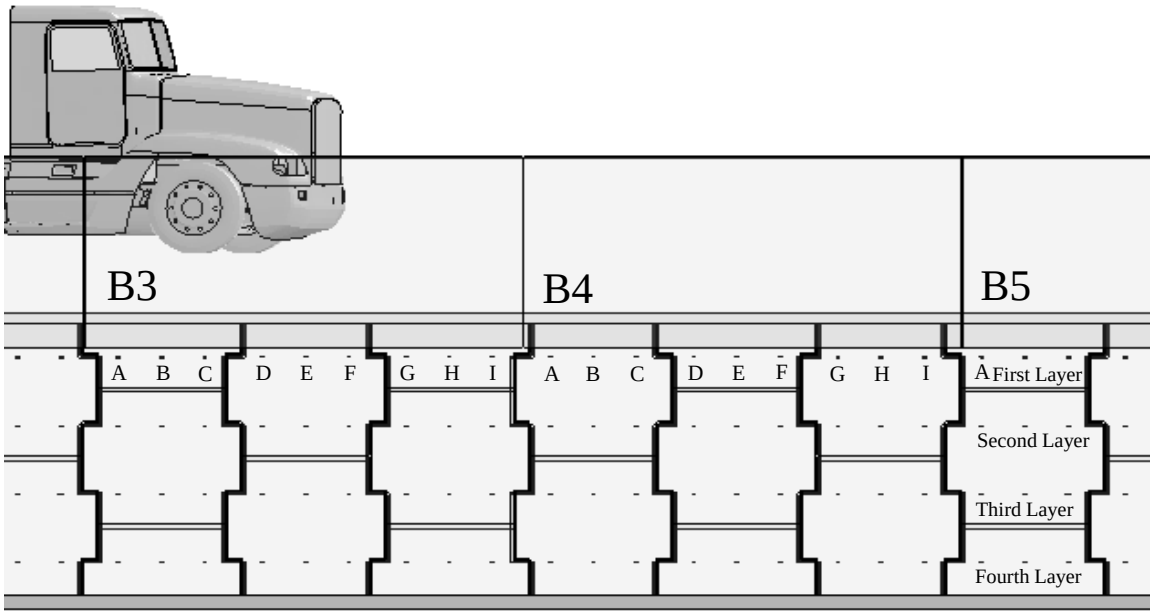

Figure 6.12 Elevation view of the MSE wall showing the strip distribution (TL-5 Impact)

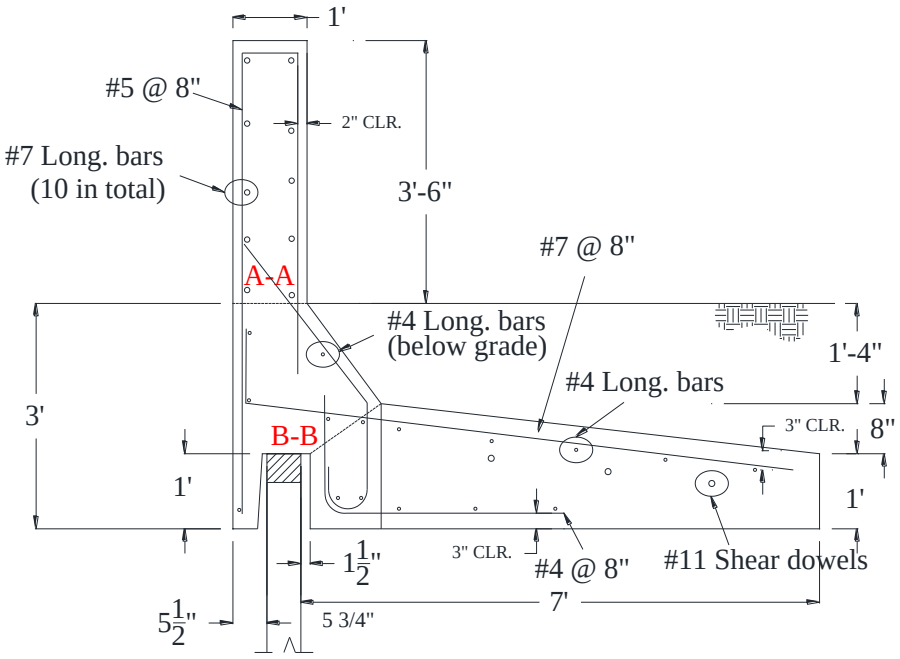

a) TL-5-1 barrier-moment slab system details

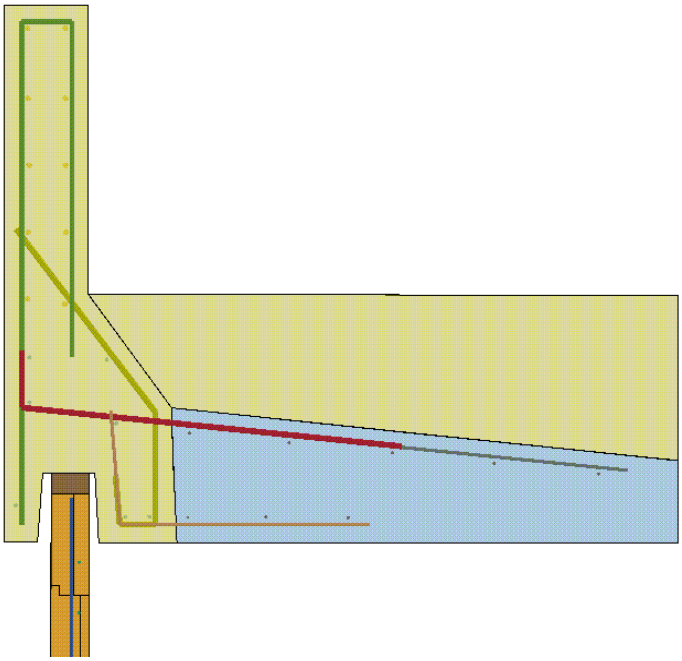

b) TL-5-1 barrier-moment slab system model

Figure 6.13 Rebar detail in the barrier and panel for TL-5-1 impact

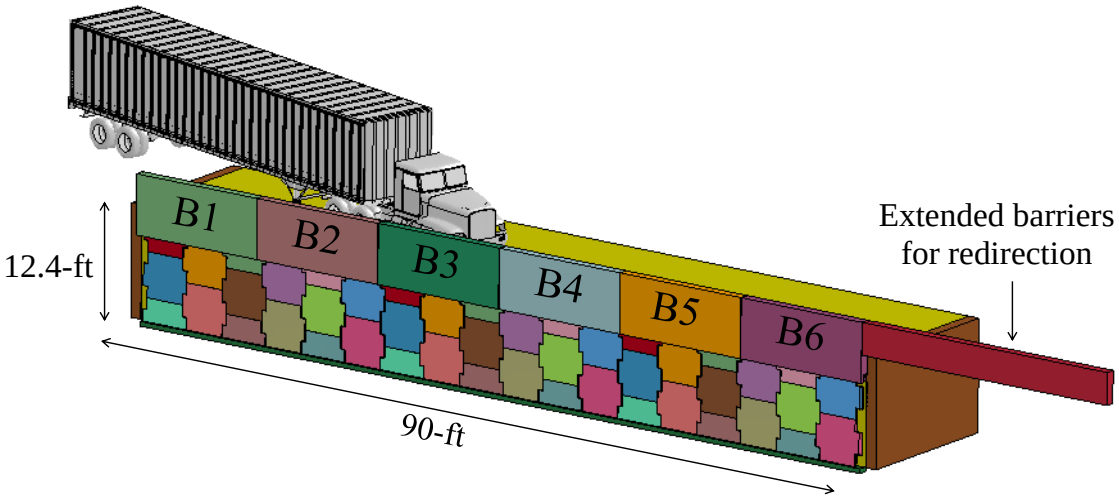

a) Three dimensional view of the TL-5-1 MSE wall model

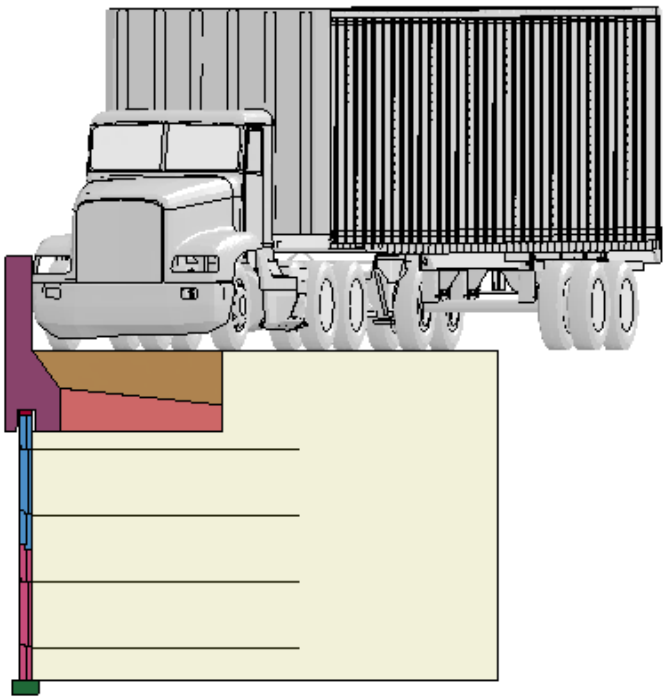

b) Downstream view

Figure 6.14 TL-5 MSE wall model showing the profile of the 42 in. (1.07 m) tall barrier and embedded soil strip

6.3.1 Loads and Displacements in the Barrier

The magnitude of the lateral impact load for the three models is shown in Figure 6.15. The time history of the impact load indicates that, in average, the first peak load is 48.6 kips (216.3 kN), the second peak load is 118.6 kips (527.8 kN) and the third peak load is 167.3 kips (744.5 kN). Note that these loads also include the component of the frictional load on top of the barrier, which is significant for this barrier height.

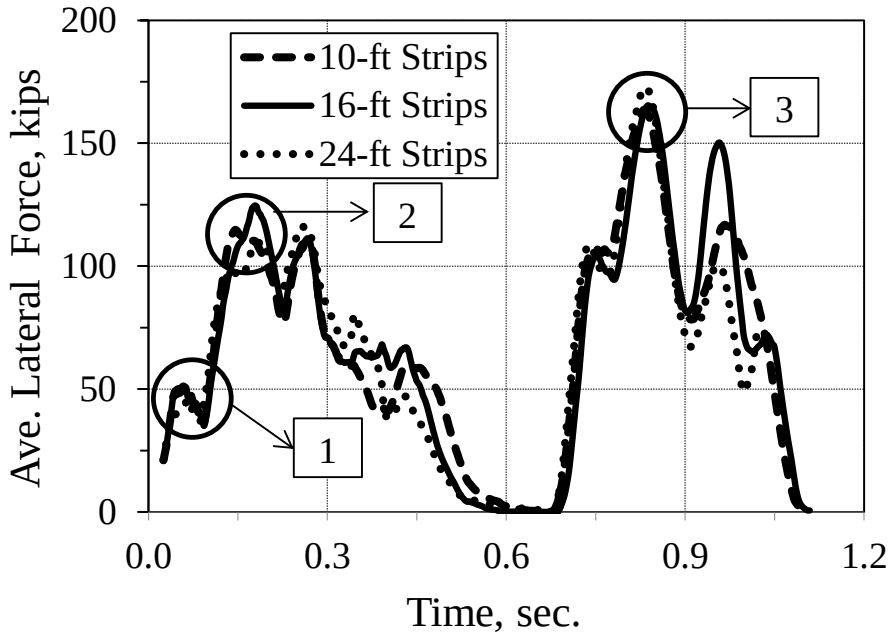

Figure 6.15 Time history of MASHT TL-5-1 impact load on barriers (50 msec. average)

Damage to the 42 in. (1.07 m) tall concrete barriers and the moment slab is shown in Figure 6.16. The damage exhibited by the barrier is typical of an end section failure mechanism and it is due to the impact load imposed by the rear tandem axles of the trailer. The length of the end section damage profile is approximately 9.4 ft (2.9 m), which is slightly smaller than the theoretical failure length computed using the yield line analyses procedure (10.4 ft (3.2 m)). The damage profiles shown in Figure 6.16(a) and Figure 6.16(b) are limited to the surface element and they do not indicates failure of the barrier.

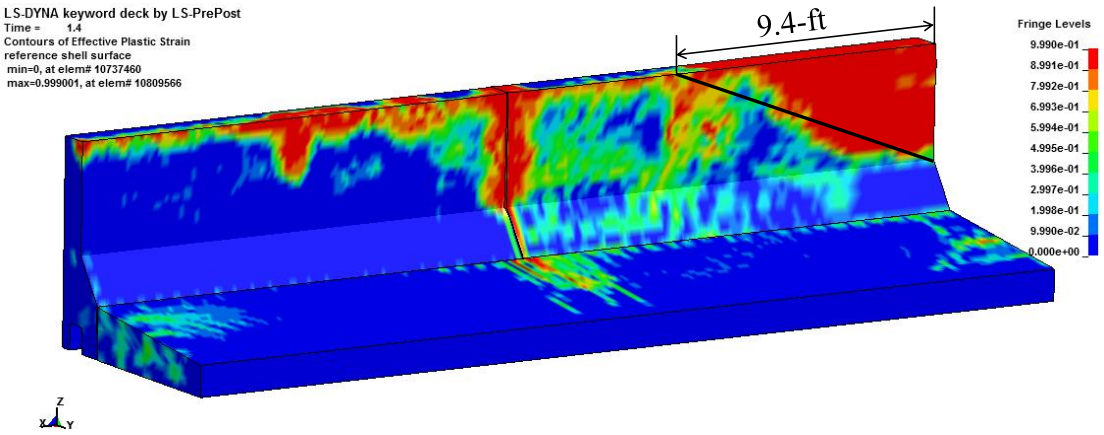

a) Front view of the barrier (impact of the rear axle of the trailer)

Figure 6.16 Damage to the 42 in. (1.07 m) tall concrete barrier (TL-5-1)

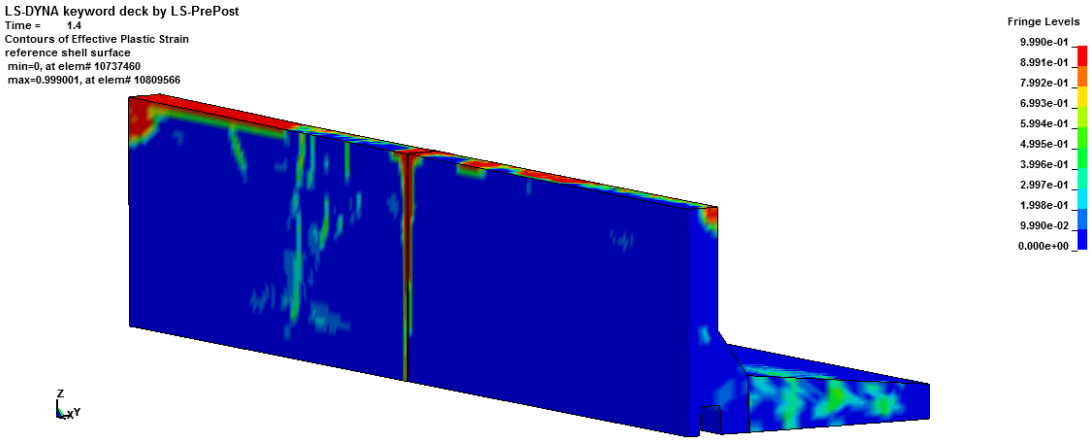

b) Back view of the barrier (impact of the rear axle of the trailer)

Figure 6.16 Continued

The maximum displacement at the top and bottom of the 42 in. (1.07 m) tall barrier was on average 1.48 in. (37.6 mm) and 0.81 in. (20.6 mm), respectively. The information of the three models is summarized in Table 6.5 and the displacement–time history is shown in Figure 6.17. The permanent displacement of the barrier at the coping section meets the criterion specified for these analyses (1 in. (25.4 mm)). Figure 6.17 shows that most of the rotational displacement at the top of the barrier is recoverable after impact reducing the risk of snagging due to small car impacts.

Table 6.5 Summary of the impact loads and barrier displacements for the MASH TL-5-1 impact simulation

Strip Length (ft)	Impact Load (kips)	Approximate Barrier Displacement (in.)	
		Top (dynamic)[1]	Bottom (permanent)[2]
10	163.6	1.60	0.87
16	165.4	1.53	0.95
24	172.8	1.31	0.61
Average	167.3	1.48	0.81

[1] Measured at the top of the barrier at the impact point location
[2] Measured at the coping level of the barrier at the impact point location

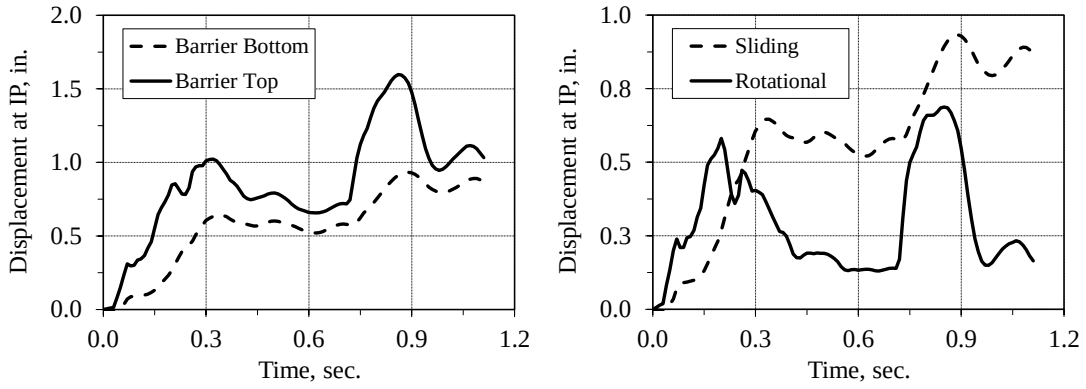

a) 10 ft model

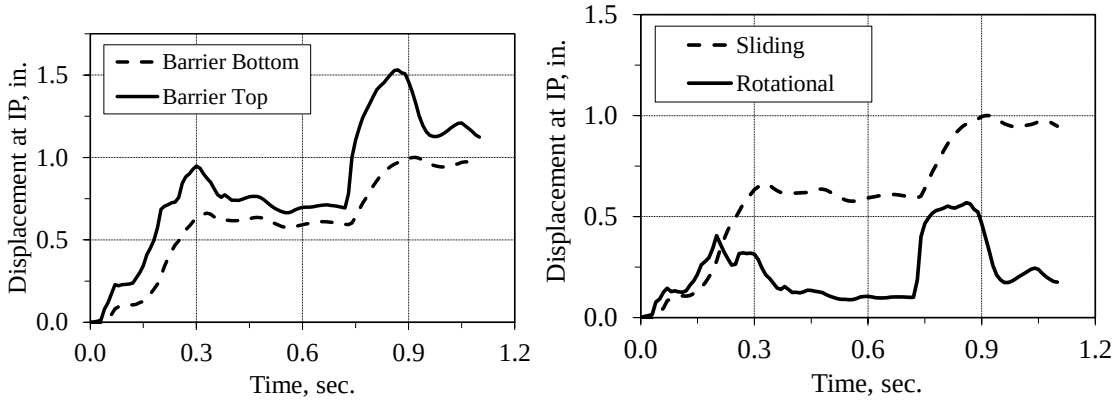

b) 16 ft model

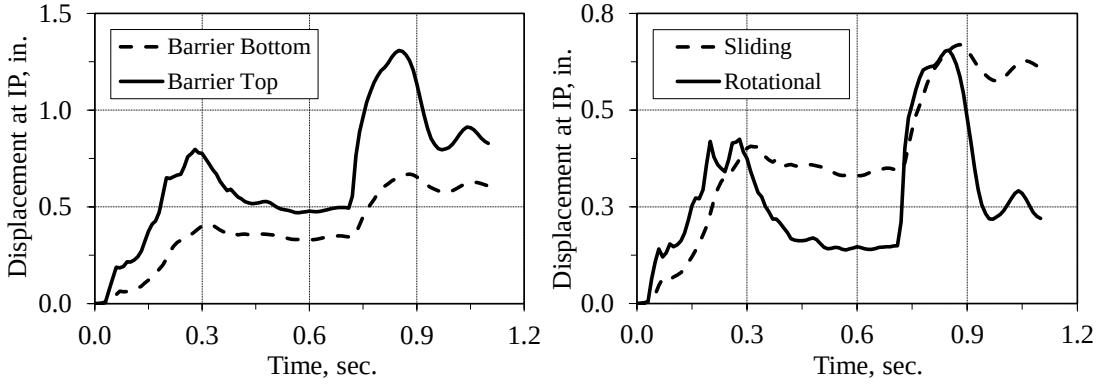

c) 24 ft model

Figure 6.17 Displacement of the 42 in. (1.07 m) at IP for TL-5-1 impact

6.3.2 Loads and Displacement in the Soil Reinforcement

Table 6.6 summarizes the maximum tension load in the first and second layer of soil 5.5 kips (24.5 kN), 8.5 kips (37.8 kN) and 9.46 kips (42.1 kN) for the 10 ft (3.05 m) long, 16 ft (4.9 m) long and 24 ft (7.3 m) long strip model, respectively. The largest peak load in the strips is being imposed by the impact of the trailer and it occurred slightly later (t=0.84 sec.) than maximum impact load in the barrier (t=0.80 sec.) (Figure 6.18). Contributions to the dynamic load component in the reinforcing strips obeys to two primary factor: a) horizontal and vertical loads transfer to the wall panels through the barrier-coping section, and b) shearing force in the soil and top of the panel due to sliding of the system.

The total loads in the second layer of soil reinforcement were 2.95 kips (13.1 kN) at section B4_I_2nd, 3.21 kips (14.28 kN) at section B4_G_2nd and 3.47 kips (14.6 kN) at section B4_G_2nd for the 10 ft (3.05 m) long, 16 ft (4.9 m) long and 24 ft (7.3 m) long strip models, respectively. These loads are significantly smaller than the total loads experienced at the uppermost layer of strips. This behavior is typical of these systems as it had been demonstrated before through full-scale crash tests *(2, 45*). The time-history of the selected strips are presented in Figure 6.18.

The maximum displacement at the uppermost layer was captured at section B3_D_1st and it was 0.30 in. (7.6 mm), 0.26 in. (6.6 mm) and 0.20 in. (5.1 mm) for the 10 ft (3.05 m), 16 ft (4.9 m) and 24 ft (7.3 m) long strip models, respectively. In the second layer of soil reinforcement, the maximum displacements were 0.12 in. (3.1 mm)

at section B4_I_2nd , 0.09 in. (2.3 mm) at section B3_F_2nd and 0.08 in. (2 mm) at section B4_G_2nd for the 10 ft (3.05 m), 16 ft (4.9 m) and 24 ft (7.3 m) long strip models, respectively.

Table 6.6 Summary of the total load for the selected strip location (TL-5-1impact)

Section	50 msec. Average Strip Load (kips)						AASHTO Pullout Resistance[(1)] (kips)		
	Strip Length								
	10-ft	16-ft	24-ft	10-ft	16-ft	24-ft			
	At 7 in. from panels			At 7 in. from panels			10-ft	16-ft	24-ft
B3_A_1st	3.55	2.29	2.89	3.38	2.22	2.56	2.45	3.90	5.86
B3_C_1st	3.82	4.28	3.54	3.63	4.10	3.11	2.45	3.90	5.86
B3_D_1st	5.36	8.41	9.46	4.66	8.25	6.15	2.45	3.90	5.86
B3_E_1st	5.52	8.52	-	5.16	8.51	6.23	2.45	3.90	5.86
B3_F_1st	5.33	8.45	8.30	4.89	8.10	6.53	2.45	3.90	5.86
B3_G_1st	4.63	4.42	5.60	4.27	3.96	4.89	2.45	3.90	5.86
B3_I_1st	5.48	5.74	6.82	4.47	4.38	5.09	2.45	3.90	5.86
B4_A_1st	4.01	3.13	4.34	3.41	2.84	3.72	2.45	3.90	5.86
B4_C_1st	3.72	3.06	2.78	3.27	2.92	2.86	2.45	3.90	5.86
B4_D_1st	4.15	3.83	2.73	3.64	3.52	2.78	2.45	3.90	5.86
B4_F_1st	4.92	4.85	3.38	4.62	4.70	6.20	2.45	3.90	5.86
B4_I_2nd	2.95	2.76	2.49	2.32	2.27	2.01	3.80	6.07	9.10
B4_G_2nd	2.50	3.21	3.47	2.07	2.62	2.09	3.80	6.07	9.10
B3_D_2nd	2.35	2.78	2.78	1.83	2.18	1.68	3.80	6.07	9.10

[(1)] AASHTO LRFD Eq. 11.10.6.3.2-1

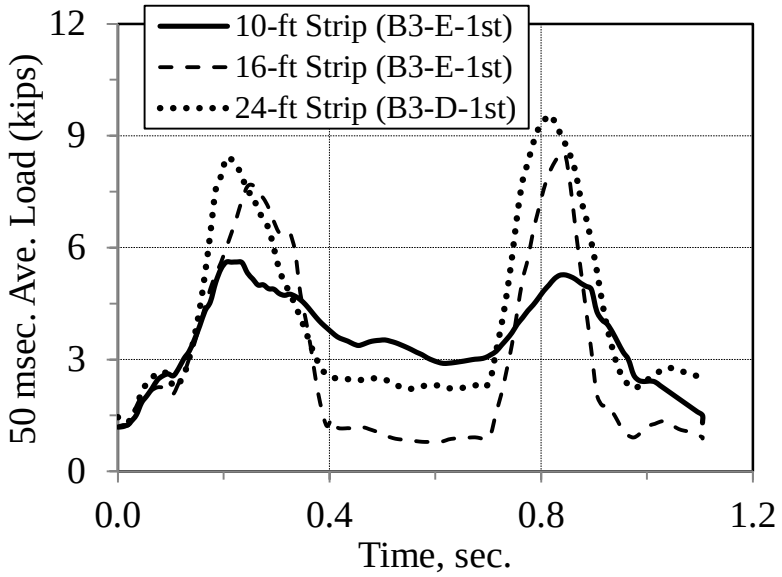

a) First layer of soil reinforcement

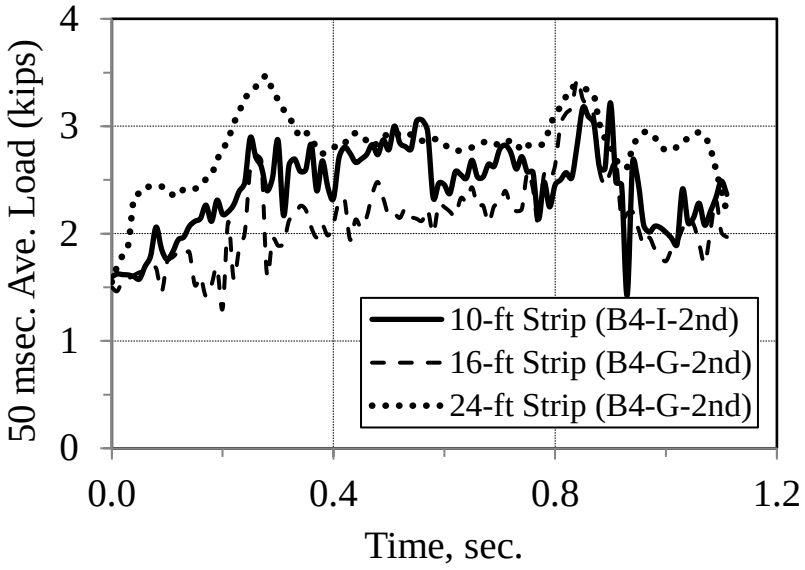

b) Second layer of soil reinforcement

Figure 6.18 Time-history of the total load in the maximum stressed strips (TL-5-1)

The distribution of the total load in strip section B3-E-1st (10 ft (3.05 m) and 16 ft (4.88 m) long strip) and strip section B3-D-1st (24 ft (7.32 m) long strip) are shown in Figure 6.19. The nonlinear behavior of the load distribution is more pronounced than the MASH TL-4 impact. This can be related to the multiple impacts associated with the articulated tractor-trailer vehicle model. Similar to the previous analyses, the strips tends to be at failure at the time of maximum load. However, the strip movements are not significant and pullout failure does not occur. Assuming a linear distribution along the strip length, the average skin friction developed at the interface soil-strip is 1.35 kip/ft^2 (64.6 kPa), 1.40 kip/ft^2 (67 kPa), and 1.05 kip/ft^2 (20.3 kPa) for the 10 ft (3.05 m), 16 ft (4.88 m) and 24 ft (7.32 m) long strip model, respectively.

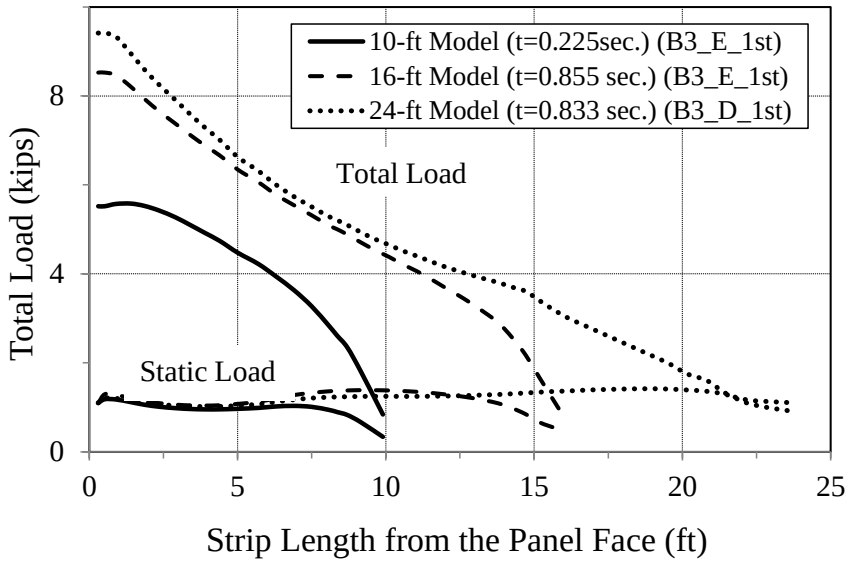

Figure 6.19 Distribution of the total load at section B3-E-1st and B3-D-1st (TL-5-1)

6.3.3 Wall Panel Analyses

The results of the numerical analyses showed that the wall panels located underneath the impact point were significantly stressed at the level of the first layer of soil reinforcement, as shown in Figure 6.20. Since the wall panels do not have sufficient steel reinforcement to prevent tension cracks due to excessive bending moment, they might experience some small cracks when subjected to high impact loads. This information will be verified after the conduction of the TL-5 full-scale crash test.

The dynamic and permanent displacement of the wall panels at the impact region of the three models are shown in Figure 6.21. The maximum dynamic and permanent displacement at the top of the wall panels for the 10 ft (3.05 m) long strip model was 0.45 in. (11.4 mm) and 0.27 in. (6.9 mm), respectively. The permanent displacement of the wall panels for the 24 ft (7.3 m) long strip decreases to almost zero due to the increase in wall stiffness.

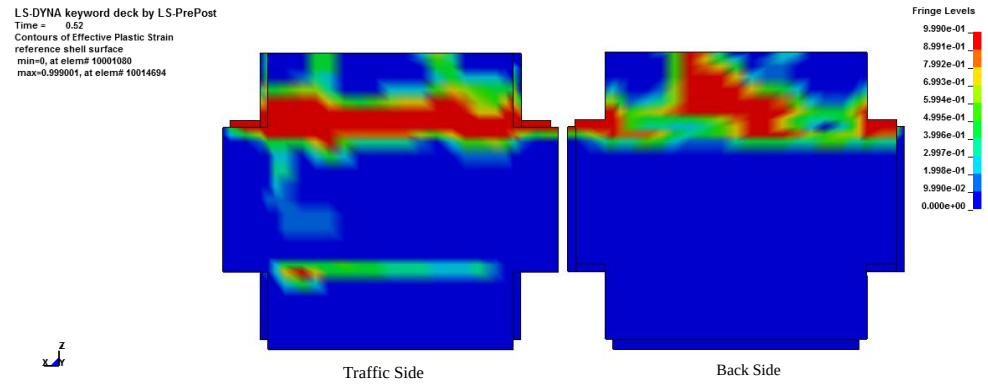

Figure 6.20 Damage profile of the panel at B3 (below IP) for TL-5-1 impact

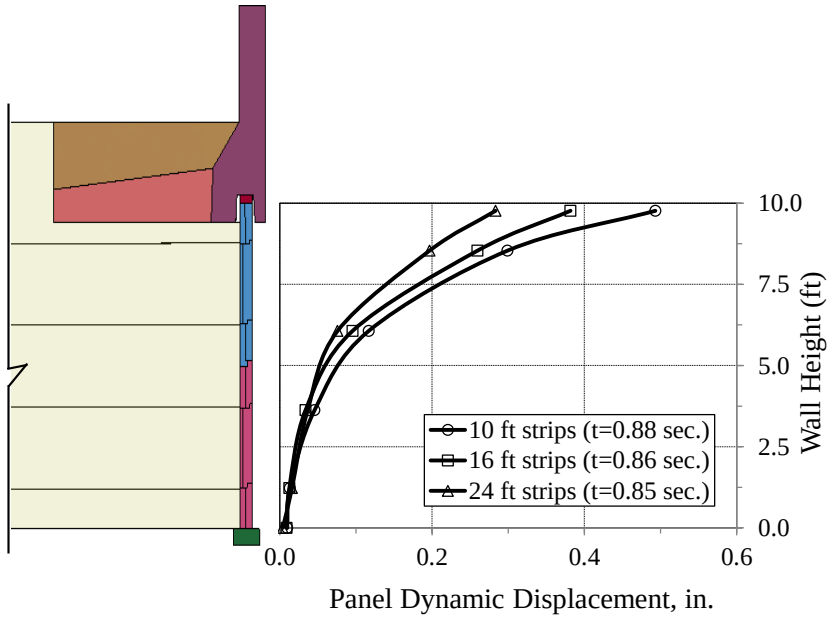

a) Dynamic displacement (impact region)

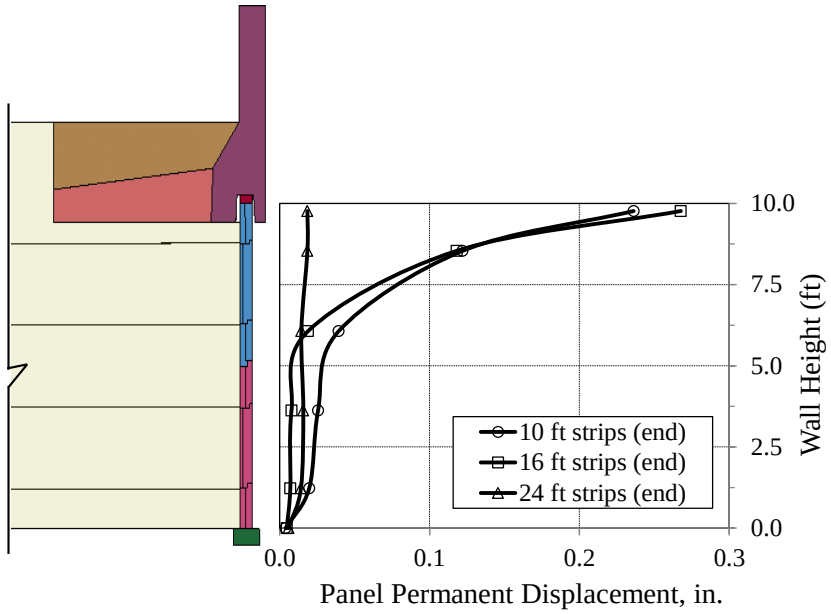

b) Permanent displacement (impact region)

Figure 6.21 Displacements at the wall panels (TL-5-1)

6.4 MSE Wall FE Analyses for TL-5 Impact on a 48 in. (1.22 m) Tall Barrier (TL-5-2)

The 48 in. (1.22 m) tall vertical wall barriers and the 9 ft (2.74 m) wide moment slab were placed on top of an MSE wall model with strips reinforcing lengths of 10 ft (3.05 m), 16 ft (4.88 m) and 24 ft (7.32 m). The objectives of the analyses include quantification of the impact force, barrier displacement, loads and displacements in the reinforcing strips and understanding of the load-transfer mechanism of the impact load associated with the trailer of the vehicle. The alphanumeric designator used in this analysis was similar to that used for the TL-5-1 impact. The vehicle was aligned to impact the middle point of barrier section 3 (B3) with a speed of 50 mph (80 km/hr.) at an angle of 15 degrees. Figure 6.22 and Figure 6.23 show details of the vertical wall barrier and the MSE wall showing the impact point and the downstream section.

A horizontal gap of 1.5 in. (38.1 mm) between the throat of the precast barrier and the back face of the panels was also provided. The moment slabs were connected using three No.11 steel bars embedded 18 in. (457 mm) at each side of the slab joint. The vertical wall barriers were also extended 45 ft (13.7 m) beyond the MSE wall to help redirect the vehicle downstream.

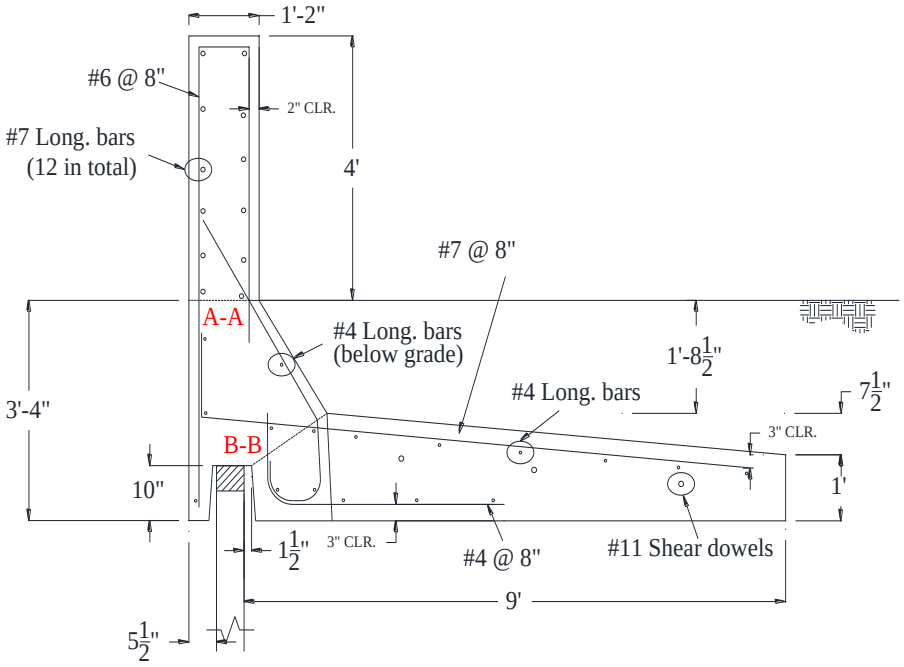

a) TL-5-2 barrier-moment slab system details

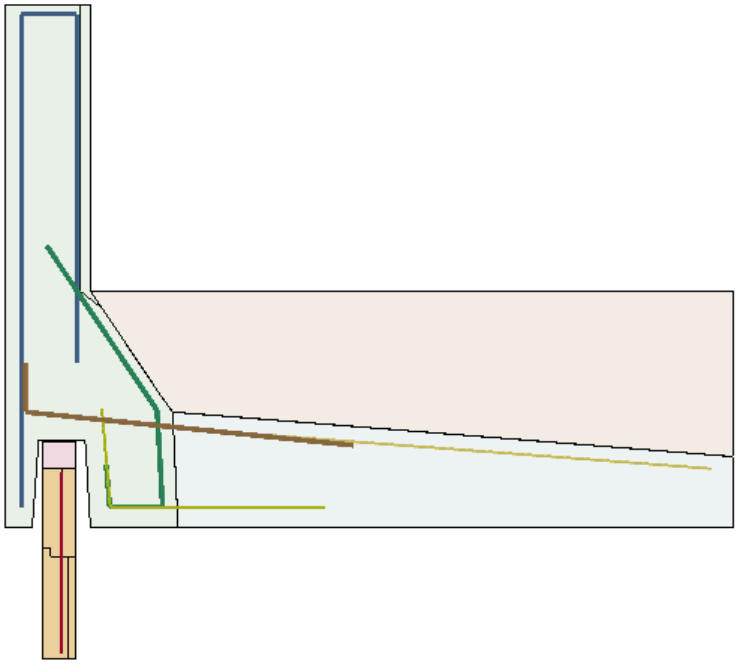

b) TL-5-2 barrier-moment slab system model

Figure 6.22 Rebar detail in the barrier and panel for TL-5-2 impact

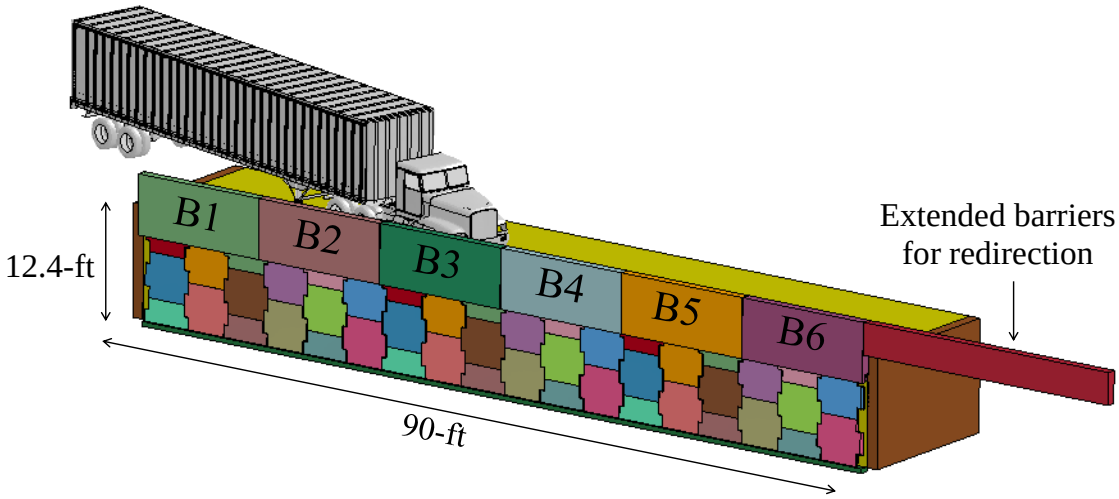

a) Three dimensional view of the TL-5-2 MSE wall model

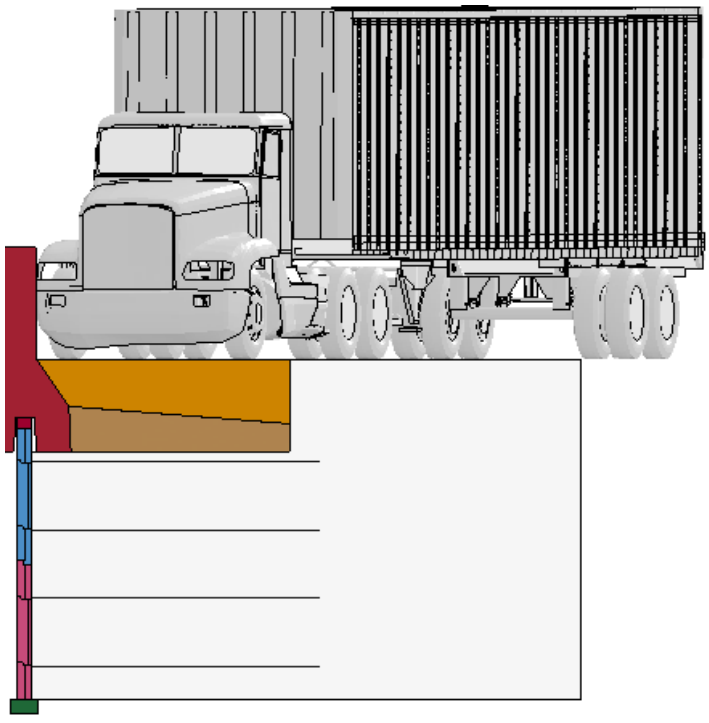

b) Downstream view

Figure 6.23 TL-5 MSE wall model showing the profile of the 48 in. (1.22 m) tall barrier and embedded soil strip

6.4.1 Loads and Displacements in the Barrier

The magnitude of the lateral impact load for the three models is shown in Figure 6.24. The average peak load of the first, second and third impact are 64 kips (285 kN), 232 kips (1032.4 kN) and 257 kips (1143.7 kN), respectively.

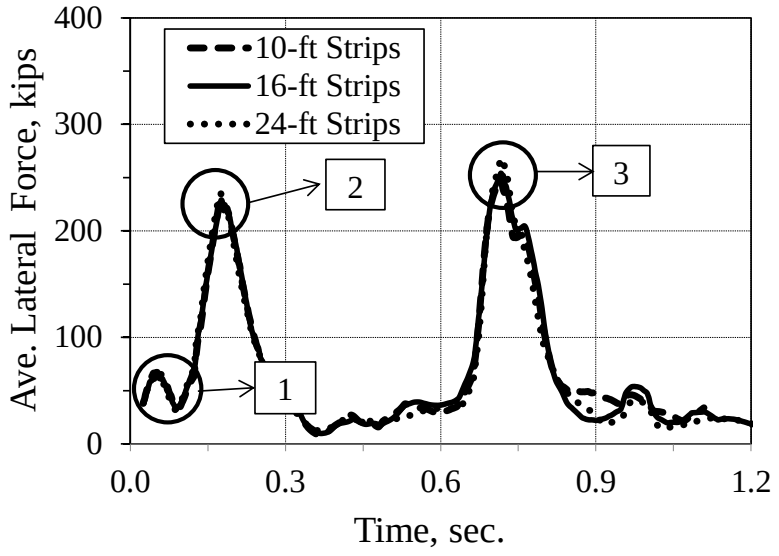

Figure 6.24 Time history of MASHT TL-5-2 impact load on barriers (50 msec. average)

Damage to the 48 in. (1.22 m) tall concrete barriers and the moment slab is shown in Figure 6.25. Similar to the previous analyses, the damage exhibited by the barrier is typical of an end section failure mechanism and it is due to the impact load

imposed by the trailer. The length of the end section damage profile is approximately 11.5 ft (3.5 m). The end section ultimate capacity of the barrier was 323 kips (1437.4 kN) with a theoretical failure length of 10.2 ft (3.1 m) computed using the yield line analyses procedure. The damage profiles shown in Figure 6.25(a) and Figure 6.25(b) are limited to the surface element and they do not indicates failure of the barrier.

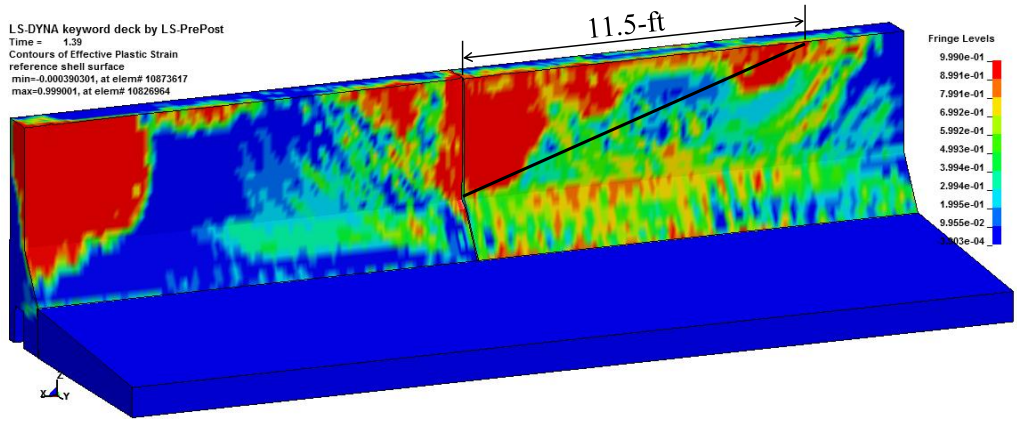

a) Front view of the barrier (impact of the trailer)

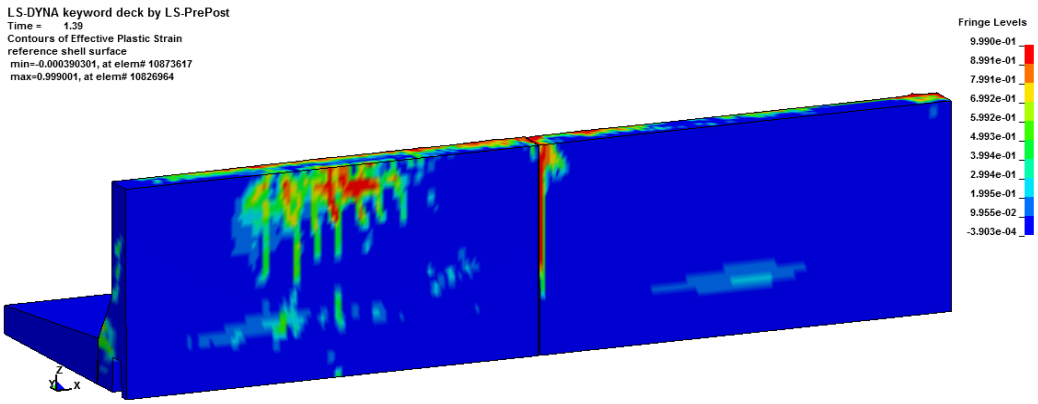

b) Back view of the barrier (impact of the trailer)

Figure 6.25 Damage to the 48 in. (1.22 m) tall concrete barrier (TL-5-2)

The maximum displacement at the top and bottom of the 48 in. (1.22 m) tall barrier was on average 2.64 in. (67.1 mm) and 1.42 in. (36.1 mm), respectively. The information of the three models is summarized in Table 6.7 and the displacement–time history is shown in Figure 6.26. The permanent displacement of the barrier at the coping section overcomes the threshold criterion specified for these analyses (1 in. (25.4 mm)). This increment on permanent displacement of the barrier obeys to several reason such as: a) increase in impact load over the entire 30 ft (9.15 m) barrier section b) increase in flexibility of the system associated with the MSE wall components, and c) decrease in sliding resistance of the system due to a potential failure of the weak-concrete leveling pad material model. Figure 6.26 and Table 6.7 shows the sliding and rotational component of the displacement associated with barrier section 3 (B3). As shown before, the displacement at the top of the barrier is not critical since most of the rotational component is recoverable after impact reducing the risk of snagging for small car impacts.

Table 6.7 Summary of the impact loads and barrier displacements for the MASH TL-5-2 impact simulation

Strip Length (ft)	Impact Load (kips)	Approximate Barrier Displacement	
		Top (dynamic)[1]	Bottom (permanent)[2]
10	249	2.61	1.60
16	254	2.50	1.32
24	268	2.36	1.35
Average	257	2.64	1.42

[1] Measured at the top of the barrier at the impact point location
[2] Measured at the coping level of the barrier at the impact point location

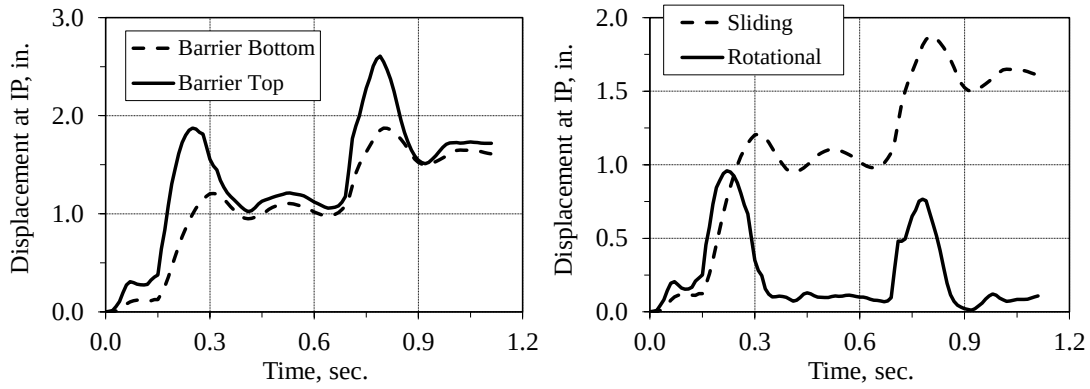

a) 10 ft model

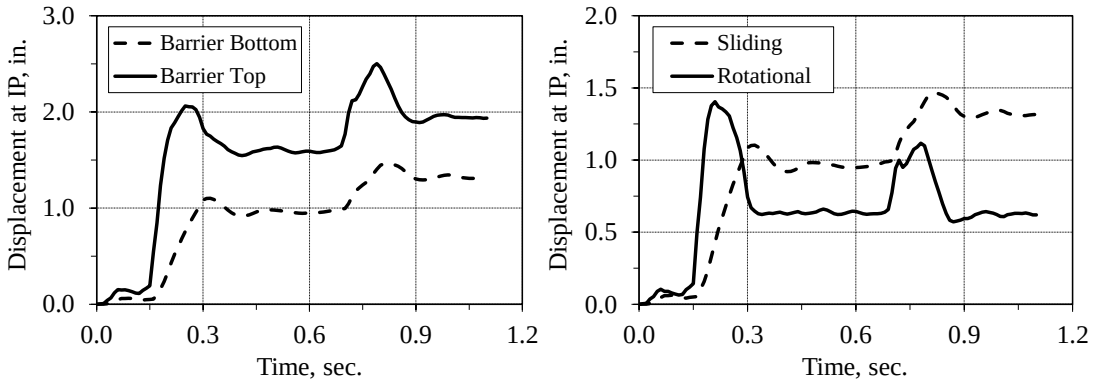

b) 16 ft model

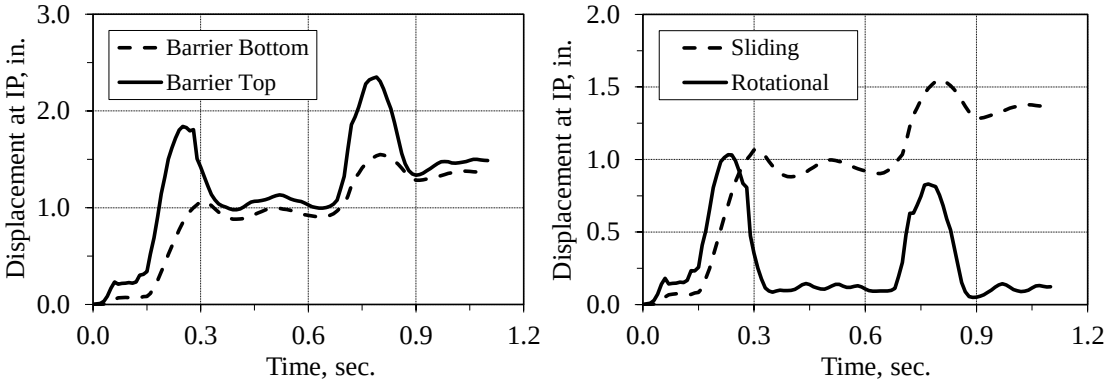

c) 24 ft model

Figure 6.26 Displacement of the 48 in. (1.22 m) at IP for TL-5-2 impact

The previous analyses indicated that a 9 ft (2.74 m) long moment slab section is not sufficient to contain a TL-5-2 impact with a tolerable permanent displacement of 1.0 in. (25.4 mm). Therefore, a further analysis was conducted using a 12 ft (3.66 m) wide moment slab section on top of the MSE wall with soil reinforcing length of 16 ft (4.88 m). The results of the analyses are presented in Figure 6.27. The barrier system contained the TL-5-2 impact with a permanent displacement at the coping section of 0.5 in. (12.7 mm). This permanent displacement is only 38% of the one observed with the 9 ft (2.74 m) wide moment slab section and 16 ft (4.88 m) long reinforcing strips. The additional inertial resistance is associated to two primary factors: 1) contribution of the additional weight of the system to the sliding and overturning capacity, and 2) contribution of the neighbor sections through the shear dowels. This information will be further analyzed in conjunction with the behavior of the wall panels and the results of the full-scale TL-5-1 crash test.

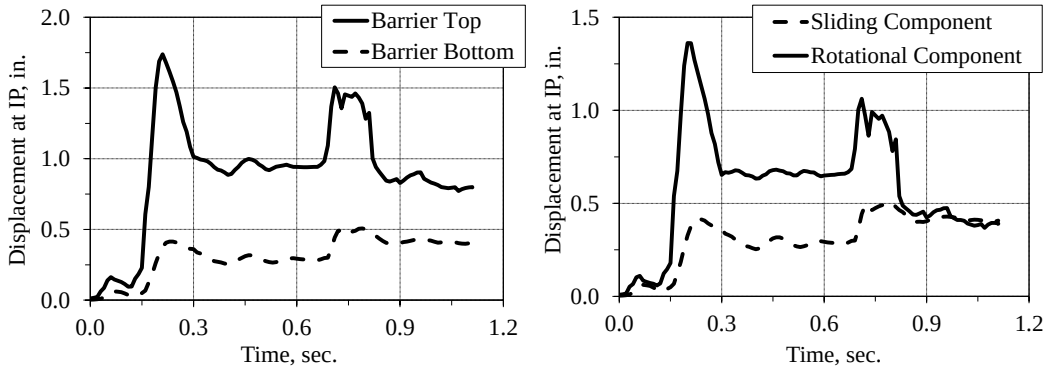

Figure 6.27 Displacement at IP for TL-5-2 impact (12 ft (3.66 m) and 16 ft (4.88 m) long strip)

6.4.2 Loads and Displacement in the Soil Reinforcement

Table 6.8 summarizes the maximum loads in the first and second layer of soil reinforcements for the TL-5-2 impact simulation. The maximum load in the reinforcing strips were measured in the 24 ft (7.31 m) long strip model at section B4_F_1st and it was 10.55 kips (46.95 kN). The maximum load in the 10 ft (3.05 m) and 16 ft (4.88 m) long strip models were 7.16 kips (31.9 kN) at strip section B3_I_1st and 9.02 kips (41.14 kN) at strip section B3_A_1st, respectively. The maximum tension load in the 10 ft (3.05 m) long strip model occurred when the corner of the trailer and the rear tandem axles of the tractor hit the barrier at t=0.225 sec. (second peak load in the barrier). For the longer strips, the maximum tension load was due to the impact of the trailer at 0.76 sec. (third peak load in the barrier). Figure 6.28 shows the time-history load for the selected strips.

The total loads in the second layer of soil reinforcement were 3.99 kips (17.8 kN) at section B4_I_2nd, 2.90 kips (12.9 kN) at section B3_A_2nd and 2.70 kips (15.71 kN) at section B3_D_2nd for the 10 ft (3.05 m) long, 16 ft (4.9 m) long and 24 ft (7.3 m) long strip models, respectively. The time-history of the selected strips are presented in Figure 6.28.

The maximum dynamic and permanent displacement at the uppermost layer were computed at section B3_D_1st of the 10 ft (3.05 m) long strip model and they were 0.63 in. (16 mm) and 0.55 in. (14 mm), respectively. The maximum strip permanent displacement in the 16 ft (4.88 m) and 24 ft (7.32 m) long strip model were 0.51 in. (13 mm) at section B3_A_1st and 0.08 in. (2.03 mm) at section B3_G_1st, respectively. In

the second layer of strips, the maximum dynamic displacements were 0.18 in. (4.5 mm) at section B3_E_2nd (10 ft (3.05 m)), 0.12 in. (3 mm) at section B4_I_2nd (16 ft (4.9 m)) and 0.08 in. (2 mm) at section B4_G_2nd (24 ft (7.3 m)). The permanent displacement of the second layer was minimal.

Table 6.8 Summary of the total load for the selected strip location (TL-5-2 impact)

Section	50 msec. Average Strip Load (kips)						AASHTO Pullout Resistance(1) (kips)		
	Strip Length								
	10-ft	16-ft	24-ft	10-ft	16-ft	24-ft			
	At 7 in. from panels			At 36 in. from panels			10-ft	16-ft	24-ft
B3_A_1st	6.12	9.02	6.88	4.77	8.24	5.96	2.47	3.95	5.93
B3_C_1st	5.39	4.42	8.09	4.37	3.75	7.25	2.47	3.95	5.93
B3_D_1st	6.93	3.37	10.46	7.67	3.15	10.18	2.47	3.95	5.93
B3_F_1st	6.23	2.81	10.55	7.89	2.76	9.46	2.47	3.95	5.93
B3_G_1st	6.76	6.97	10.31	6.48	5.66	9.40	2.47	3.95	5.93
B3_I_1st	7.16	7.19	10.37	5.79	5.75	8.65	2.47	3.95	5.93
B4_A_1st	5.59	4.40	6.01	3.95	4.25	5.61	2.47	3.95	5.93
B4_C_1st	4.74	1.84	5.80	3.76	1.56	5.40	2.47	3.95	5.93
B4_D_1st	4.27	1.96	5.19	4.02	1.79	4.89	2.47	3.95	5.93
B4_F_1st	4.87	3.46	6.73	4.62	3.21	6.30	2.47	3.95	5.93
B4_G_1st	6.38	8.25	8.60	7.88	7.55	10.05	2.47	3.95	5.93
B4_I_1st	6.09	7.82	8.33	6.28	9.00	8.54	2.47	3.95	5.93
B4_I_2nd	3.99	2.88	2.34	2.47	2.46	2.21	3.81	6.09	9.14
B3_A_2nd	2.89	2.90	2.40	1.99	2.80	2.23	3.81	6.09	9.14
B3_D_2nd	3.50	1.92	2.70	2.16	1.79	2.36	3.81	6.09	9.14

(1) AASHTO LRFD Eq. 11.10.6.3.2-1

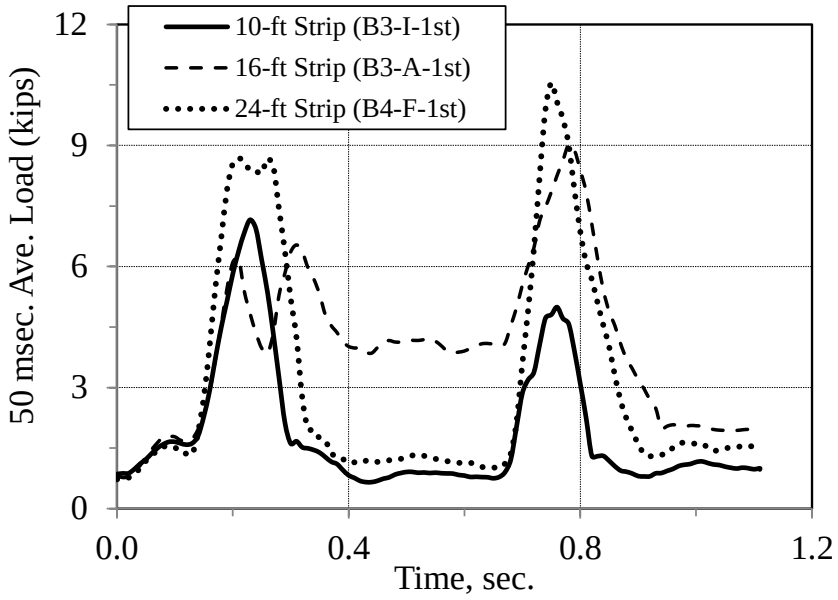

a) First layer of soil reinforcement

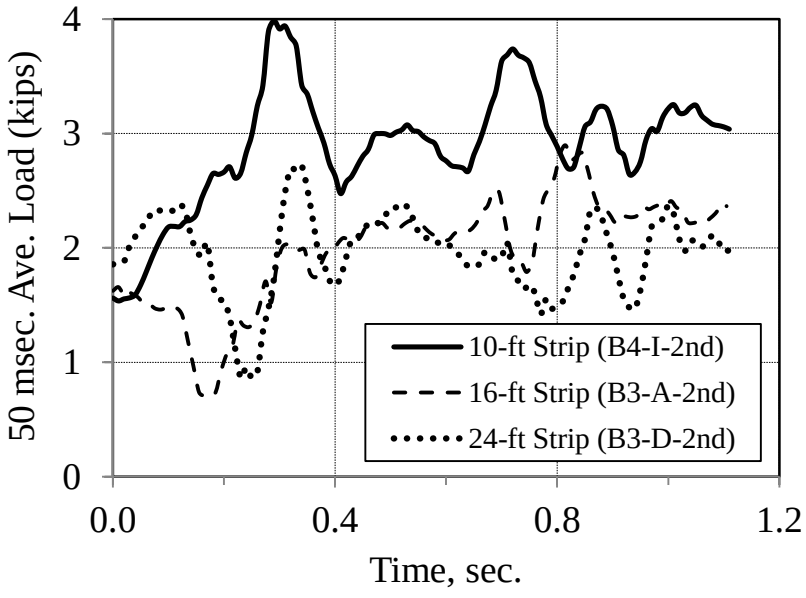

b) Second layer of soil reinforcement

Figure 6.28 Time-history of the total load in the maximum stressed strips (TL-5-2)

The maximum load in the reinforcing strips did not occur at the same location for the three analyses as shown in Table 6.8. This is associated with the overall kinematic behavior of the wall components when subjected to the impact load. As the strip length increases, the system becomes stiffer and little movement take place during impact. Therefore, the strip length also affects the soil-structure interaction of the system. However, the difference in load magnitude from the strips located at the impacted region is not significant.

The distribution of the total load in the highest stressed reinforcing strips is shown in Figure 7.32. These distributions are similar to the ones observed in the previous analyses for MASH TL-5-1. However, in this case the slope of the load distribution curve (friction) is larger than the MASH TL-5-1. This indicates that the apparent coefficient of friction (F*) developed during the impact loading increases dramatically due to the instantaneous nature of the impact load. The average skin friction developed at the interface soil-strip is 1.89 kip/ft^2 (90.5 kPa), 1.47 kip/ft^2 (70.4 kPa), and 0.84 kip/ft^2 (40.2 kPa) for the 10 ft (3.05 m), 16 ft (4.88 m) and 24 ft (7.32 m) long strip model, respectively.

In addition, the load in the element sections close to the wall panels experienced a high peak load and some bending due to the connection with the wall panels. After a short distance from the wall panels, the load dropped considerably. This behavior is associated with bending of the strips due to the rotational movement of the panels during impact. However, despite the high load in the reinforcing strips, the overall behavior of the wall is acceptable and the wall permanent movements are within tolerable limits.

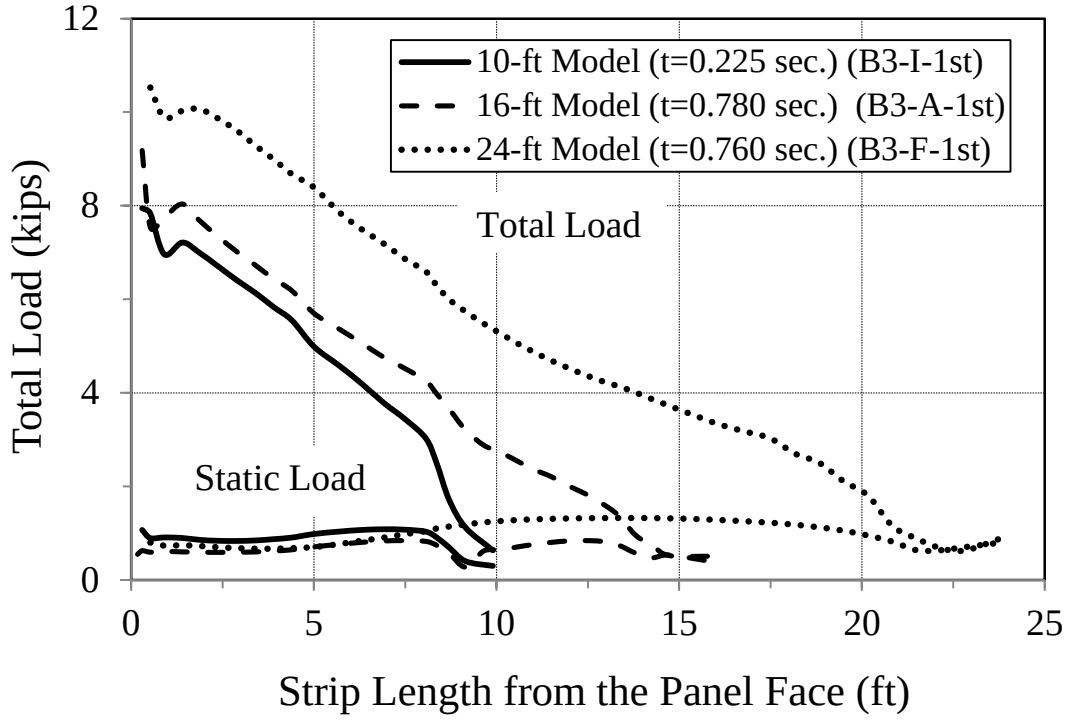

Figure 6.29 Distribution of the total load (TL-5-2)

6.4.3 Wall Panel Analyses

Similar to the analyses conducted for MASH TL-5-1, the wall panels located underneath the impact point (below B3) were significantly stressed at the level of the first layer of soil reinforcement. Therefore, they might experience light tension cracks due to excessive bending moment during impact.

The dynamic and permanent displacement of the wall panels for the three models is shown in (Figure 6.30). The maximum dynamic and permanent displacement at the top of the wall panels were 1.10 in. (27.9 mm) and 0.91 in. (23.1 mm), respectively.

The analyses conducted using the 16 ft (4.88 m) long strips indicated that the maximum dynamic and permanent displacements occurred at the half-section panel below B3 (B3_A). This area was directly impacted by the rear tandem axles of the trailer, and therefore, it produced the highest peak load and displacement in the strips. This information explains the inflection point shown in the displacement curve of the wall panels for the 16 ft (4.88 m) long strip model. These displacements were computed at section B3_D of the 10 ft (3.05 m) long strip model. For the longest strip model, the permanent displacement was minimal.

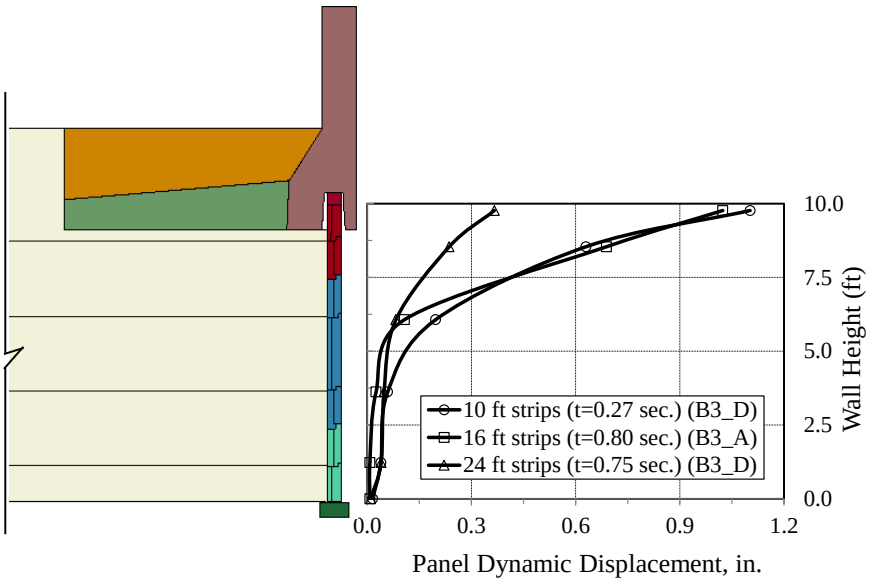

a) Dynamic displacement

Figure 6.30 Displacements at the wall panels (TL-5-2)

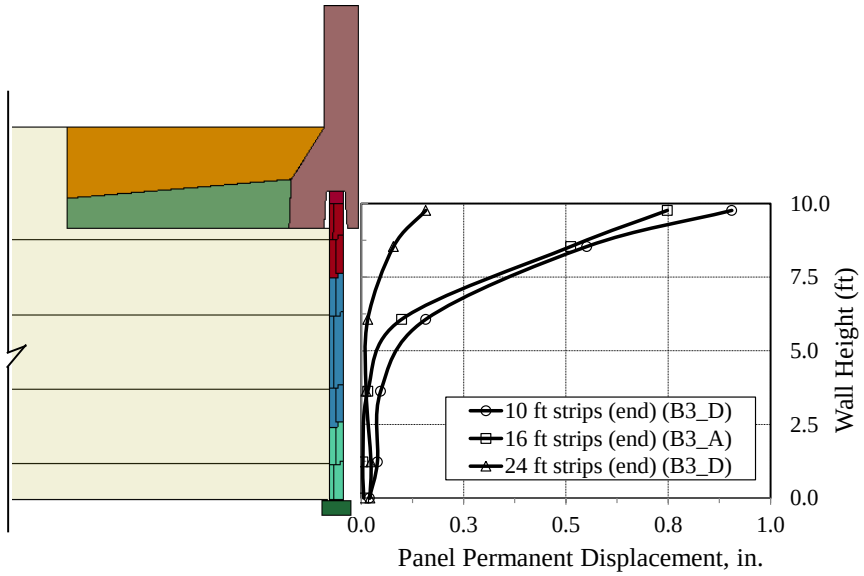

b) Permanent displacement

Figure 6.30 Continued

6.5 Conclusions

The following conclusions are based on and limited to the content of this chapter:

1. The impact loads in the barriers computed from the MASH TL-4, MASH TL-5-1 and MASH TL-5-2 impact simulation were similar in magnitude to the loads observed in the rigid barrier analyses conducted in section 3. This is because the levels of displacements associated with barrier-coping sections are significantly small. Therefore, the load levels are similar to those associated with rigid barriers.

2. The permanent displacement at the top of the barrier-coping section for MASH TL-4 and MASH TL-5 impact were within tolerable limits. The permanent displacement at the coping-section of the barrier for MASH TL-5-2 was on average 1.4 in. (35.6 mm) which overcome the threshold limit (1.0 in. (25.4 mm)). However, the overall behavior of the barriers, moment slabs and the wall components were acceptable indicating that no restoration is required for the underlying MSE wall.
3. The estimated width of moment slab to contain a MASH TL-5-2 impact with a permanent displacement limit of 1 in. (25.4 mm) at the coping section is approximately 10.3 ft (3.14 m). This information was estimated by simple interpolation between the analyses conducted on the 9 ft (2.74 m) and 12 ft (3.66 m) wide moment slab. However, since the behavior of the wall components using the 9 ft (2.74 m) wide moment slab was acceptable, the excess width of moment slab (1.3 ft (396.3 mm)) might not be required. This information will be verified using the results of the full-scale crash test.
4. The loads in the reinforcing strips were found to be larger than the static resistance for pullout. This means that the strips are at failure during the impact event (very short duration). During this short period of time, the strips and wall panels does not displace significantly and, therefore, the displacement are within acceptable limits.

5. The permanent displacement at the top of the wall panels for the MASH TL-4 and MASH TL-5-1 were within acceptable limits when using 10 ft (3.05 m) long strips sections. However, the MASH TL-5-2 impact simulation indicated that the wall panels could be subjected to excessive movement when using 10 ft (3.05 m) long strip. Therefore, recommendations for pullout pressure for MASH TL-5-2 impact will be based on a 16 ft (4.88 m) long strip. This will help to prevent excessive permanent movement of the wall component during a TL-5-2 impact.
6. The damage profile of the wall panels during the TL-5-1 and TL-5-2 impact simulation indicate that some of the wall panel might experience tension crack at the first layer of wall reinforcement due to impact load. However, thin hair-line cracks in the wall panels are acceptable as typically no restoration of the wall panels should be required.
7. Since the performance of the reinforcing strips was adequate for the different analyses, this indicates that the average design strip load in excess of static for each impact simulation can be used to develop the design guideline for pullout of the reinforcement. For example, for TL-5-1 the resistance (P) for the 10 ft (3.05 m) long strips was calculated to be 2.43 kips (10.8 kN) for the upper most layer and 3.78 kips (16.8 kN) for the second layer using Eq. (2-2) in Chapter 2 (AASHTO 11.10.6.3.2-1). The static load due to the earth pressure was 0.82 kips (3.65 kN). Therefore, the controlling design load in excess of the static load due to static earth pressures was calculated to be 1.61 kips (7.16 kN). Then, the pullout pressure design load for the uppermost layer for a density of three strips

per panel per layer with a tributary area of 3.07 ft^2 is approximately 525 psf (25.2 kPa) (1610 lb./3.07 ft^2=525 psf).

8. The pullout analyses at the second layer followed the procedure used at the first layer. The total dynamic load was 2.95 kips (13.12 kN) which is less than the calculated pullout resistance by AASHTO (3.8 kips (16.9 kN)). Therefore, the measured dynamic load in excess of the static load (1.60 kips (7.12 kN)) was used as the controlling dynamic load for pullout design. Then, the pullout pressure design load for the second layer for a density of three strips per panel per layer with a tributary area of 3.94 ft^2 is approximately 406 psf (19.34 kPa) (1600 lb./3.94 ft^2=406 psf).
9. The maximum total load experienced by the first layer of reinforcing strips was computed using the 24 ft (7.32 m) long strip model and it was 9.46 kips (42.1 kN). Therefore, it seems appropriate to use the actual load experienced by the strips to develop the guidelines for yielding analyses. Based on that, the controlling dynamic load for yielding design is 8.22 kips (36.6 kN) (total load minus static load). Then, the yielding pressure for a density of two strips per panel per layer with a tributary area of 4.60 ft^2 is 1786 psf (89.34 kPa) (8220 lb./4.6 ft^2=1786 psf).
10. The yielding analyses at the second layer followed the procedure used at the first layer. The maximum tension load in the reinforcing strip was 3.21 kips (14.28 kN) (maximum load at the second layer of 16 ft (4.88 m) long strip). The excess dynamic load is 1.86 kips (8.3 kN). Then, the yielding pressure for a density of

three strips per panel per layer with a tributary area 3.94 ft^2 (0.37 m^2) is 472 psf (22.6 kPa) (1860 lb./3.94 ft^2=472 psf).

11. The recommended dynamic pressure distribution for pullout and yielding analyses of the soil reinforcing strip will be revised after the TL-5-1 full-scale crash test. In addition, detail calculations of pullout and yielding pressure are presented in section 9.3.

7 TL-5 FULL-SCALE TEST ON A ROADSIDE BARRIER SYSTEM PLACED ON TOP OF A 10-FT HIGH MSE WALL

A TL-5 full-scale crash test was performed to validate the preliminary design guidelines and/or modify them as necessary. The FE analysis was performed using LS-DYNA to help plan and predict the outcome of the TL-5 crash test.

7.1 Description of the Barrier-Moment Slab and MSE Wall

The total length of the test installation is about 135.5 ft (41.3 ft). The first 90.4 ft (27.6 m) of barrier-moment slab are placed on top of a 9.8 ft (3 m) tall MSE wall. The remaining 45.1 ft (13.75 m) consist of similar roadside barrier and moment slab sections with no underlying MSE wall. This extension of the test installation has the purpose of helping to redirect the vehicle after impact and to guarantee continuity of the system.

The precast barrier section used for the crash test was a New-Jersey (NJ) Shape barrier of approximately 15 ft (4.57 m) long and 6.83 ft (2.08 m) tall. The barrier portion is 42 in. (1.07 m) height (measured from the roadway) and 11.75 in. (0.3 m) wide at the top. The coping section is 40 in. (3.3 m) depth embedded below the grade. According to AASHTO LRFD *(3),* the 42 in. (1.07 m) tall rail height is the minimum height required to contain and redirect a fully-loaded tractor trailer impacting the system at 50 mph (80 km/hr.) at 15 degrees angle.

A series of two-15 ft (4.57 m) long precast barrier units were attached to each of three moment slabs, 7 ft (2.13 m) wide (measured from the face of the wall panels) and 30 ft (9.15 m) long. The moment slabs were cast-in-place with a concrete strength (f'_c) of 4000 psi (27.6 MPa). The barrier sections and the moment slabs were connected using No.5 top bars and No.4 bottom bars at 8 in. (203.2 mm) on center. The three moment slab sections were connected to one another using three No.11 shear dowels across each joint.

The MSE wall on which the N.J. Shape barrier-coping sections were placed is approximately 9.8 ft (3 m) tall and 15 ft (4.57) wide. The wall is comprised of full and half-panel sections that are approximately 1.52 ft (5 ft) and 2.5 ft (0.76 m) wide, respectively. The bottom wall panels were placed on a 12 in. (304.8) wide × 6 in. (152.4 mm) thick concrete leveling pedestal with a compressive strength of 4000 psi (27.6 MPa). The MSE wall had three layers of reinforcement. The steel reinforcement strips were 10 ft (3.05 m) long. The wall panels were recessed inside the coping of the precast barrier-coping sections a distance of 10.5 in. (266.7 mm).

The AASHTO Manual for Assessing Safety Hardware (MASH) was used for the full-scale crash test. MASH test designation 5-12 involves a 79,200 lb. (36,000 kg) tractor-van-trailer (denoted 36000V) impacting the barrier at a speed of 50 mph (80 km/hr.) and an angle of 15 degrees.

7.1.1 Calculation of MSE Wall Capacity

The force expected in the 10 ft (3.05 m) long strips reinforcement due to the gravity load was computed according to AASHTO LRFD *(3)*. The preliminary design pressure distributions of MSE wall reinforcement recommended in section 6 were used to estimate the dynamic loads on the strips resulted from a TL-5 impact. The information obtained from these analyses is presented in Table 7.1 and it was ultimately compared to forces estimated through numerical simulation and measured in the TL-5 full-scale crash test. The detailed design calculation for designing the MSE test wall are provided in Appendix B.

Table 7.1 Pullout Unfactored resistance and force in the reinforcing strips for TL-5 MSE wall

Layer	Strips Length (ft)	Depth (ft)	T_{static} [1] (kips)	$T_{dynamic}$ [2] (kips)	$T_{total} = T_{static} + T_{dynamic}$ (kips)	P Resistance [3] of Pullout (kips)
Top	10	3.6	0.83	1.35	2.19	2.43 (F*=1.63)
Second	10	6.1	1.33	1.64	2.95	3.73 (F*=1.49)

(1) *AASHTO LRFD*

(2) Using the preliminary pullout pressure of 525 psf (first layer) and 410 psf (second layer) for TL-5-1 as recommended in section 6.

(3) *AASHTO LRFD* Eq. 11.10.6.3.2-1

7.1.2 Calculation of Barrier Capacity

The NJ shape barrier section was designed to contain an impact load of 160 kips (712 kN) located at an effective height of 34 in. (864 mm). Figure 7.1 shows the cross section detail of the precast NJ shape barrier used in the TL-5 crash test.

The ultimate load capacity of the 42 in. (1.07 m) tall NJ shape barrier was computed to be 163.1 kips (725.8 kN) using the end section yield line analyses procedure described in AASHTO LRFD *(3)*. The length of the failure mechanism calculated from the analyzed section (A-A) was 10.5 ft (3.2 m). The moment and shear capacity of the coping section (B-B) were 870 kip-ft (1175 kN-m) and 205 kips (912.3 kN), respectively. This indicates that the coping section has sufficient capacity to develop the strength of the barrier. Therefore, the 15 ft (4.57 m) section length selected for evaluation of the TL-5 impact is sufficient for developing the primarily failure mechanism of the barrier.

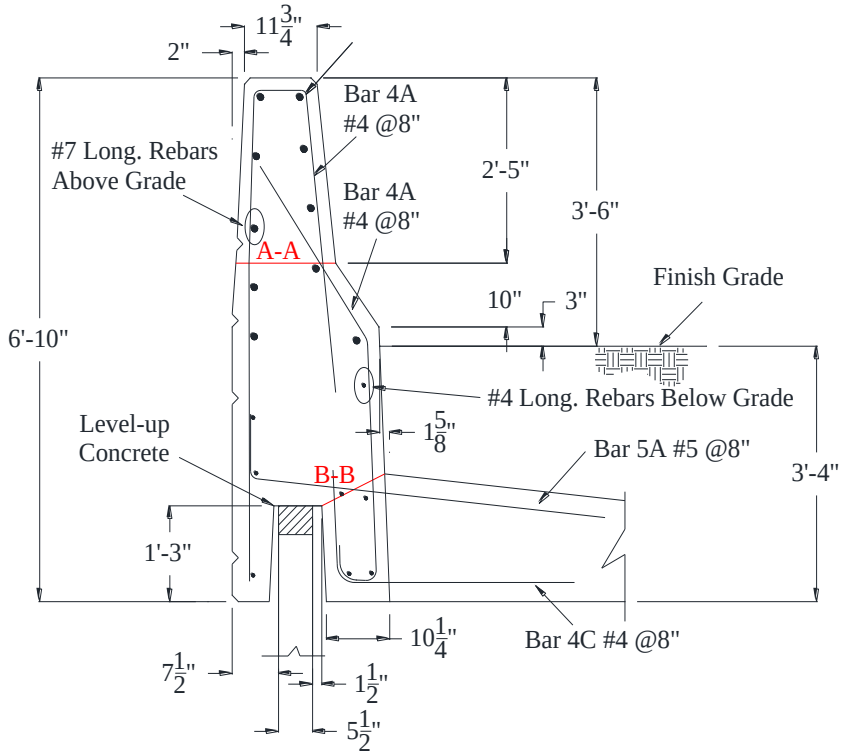

Figure 7.1 RECO N.J. shape concrete barrier details

7.2 Finite Element Analyses

The MSE wall model used to evaluate the TL-5 impact simulation was modified to model the proposed full-scale test installation. The modifications include:

1) Incorporation of the TL-5 N.J. shape barrier model with explicit reinforcement details as shown in Figure 7.1 and Figure 7.2.

2) The failure strain criteria of the U-bolt model of the tractor front tires were reduced from 16% to 12%. This modification causes failure of the U-bolts due to the front impact of the tractor model which resemble the kinematic behavior observed in full-scale crash tests associated with barrier shape similar to the test barrier (e.g., N.J. shape barrier)

.

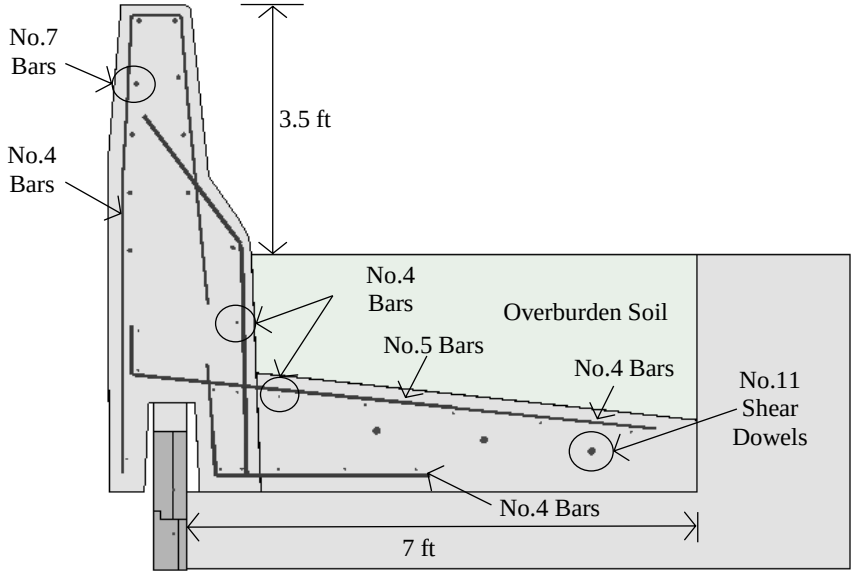

Figure 7.2 TL-5 barrier-moment slab system model of the TL-5 test installation

The first phase of the simulation process is to account for the steady-state conditions of the system due to gravitational load. The weight of the system is measured and used as a convergence criterion for the steady-state solution. The total weight of the

model for the 42 in. (1.07 m) tall N.J. shape barrier, the 7 ft (2.13 m) wide moment slab and the MSE wall is 2,791 kips (12,421 kN) using the mass of the finite element model and the acceleration of gravity.

Figure 7.3 shows the calculated and the measured weight of the system after accounting for gravitational loads. The result of the analysis indicates that there is a good agreement between the calculated weight and the measured weight. Then, the initialized model is set up with the tractor-van-trailer vehicle model in order to conduct the impact simulation, as shown in Figure 7.4 and Figure 7.5.

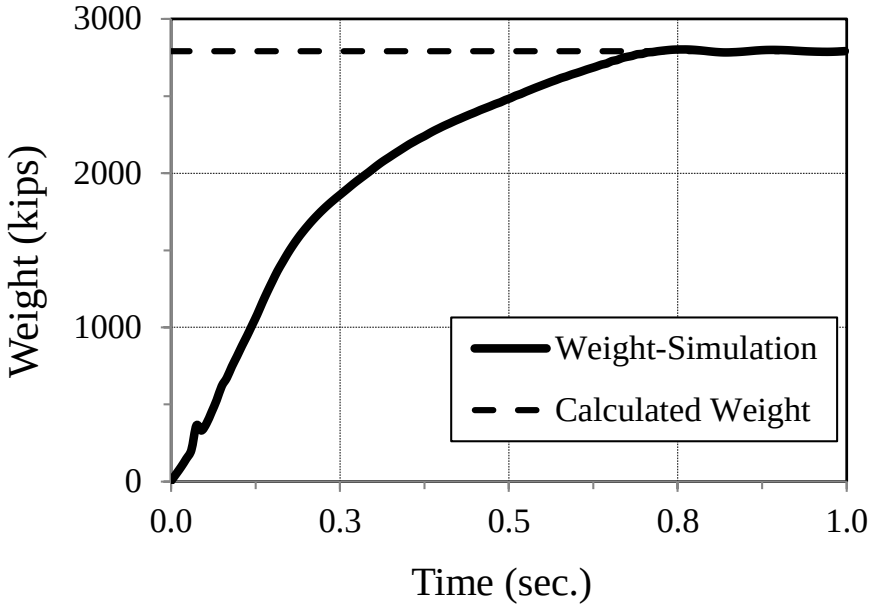

Figure 7.3 System reaction force of the TL-5 MSE wall test installation model

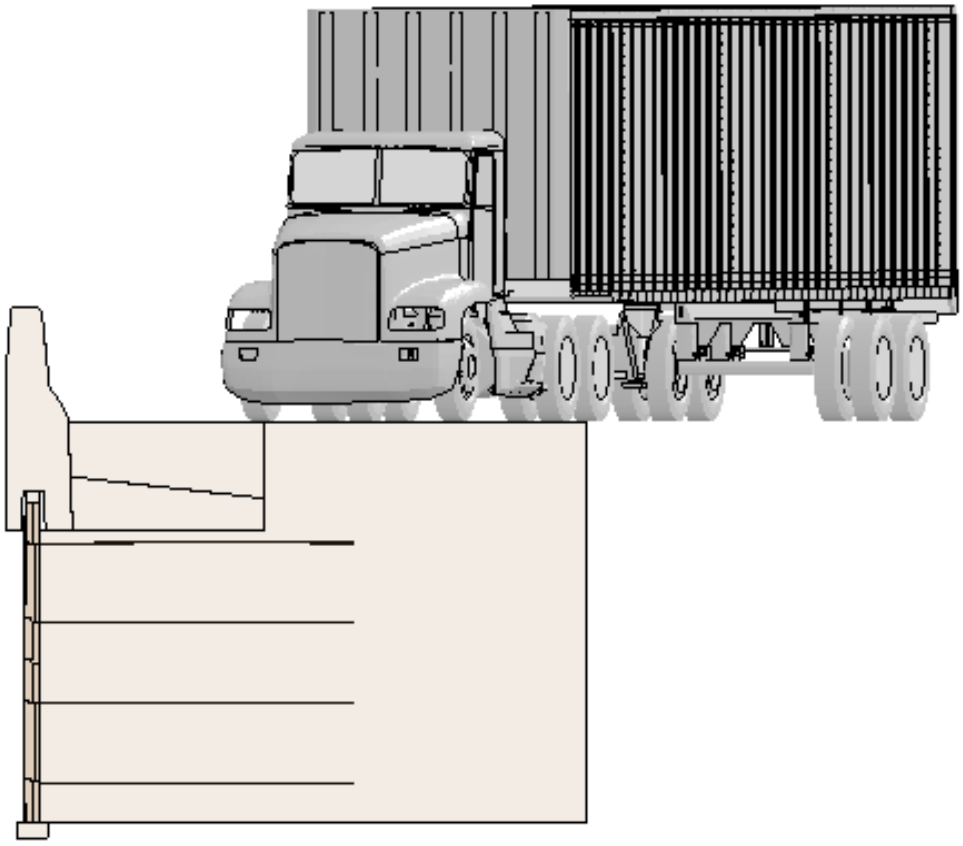

Figure 7.4 Downstream view of the TL-5 MSE wall model

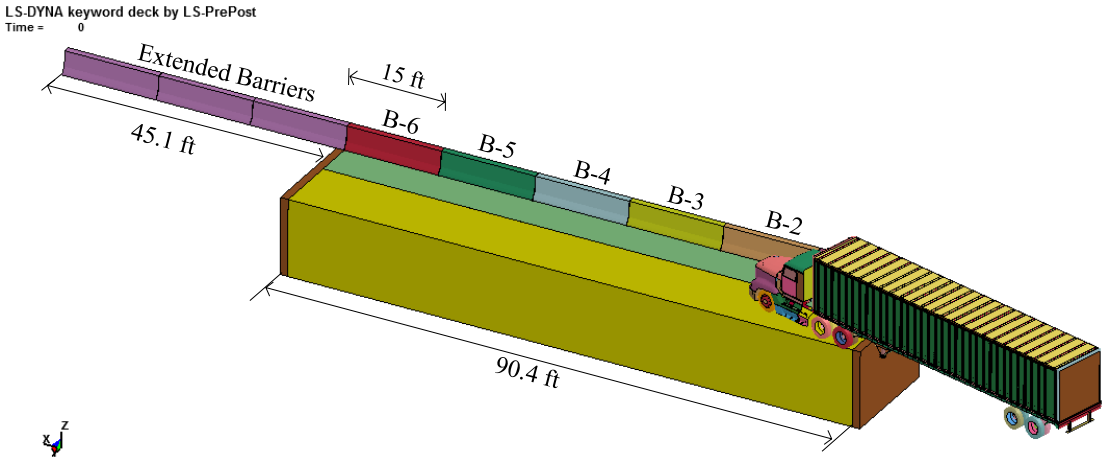

a) Three dimensional view of the test installation model (pre-impact time)

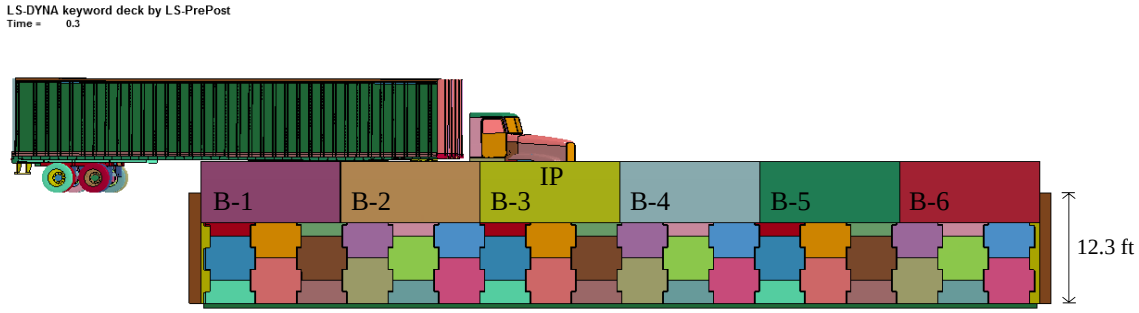

b) Elevation view of the test installation model (time of impact)

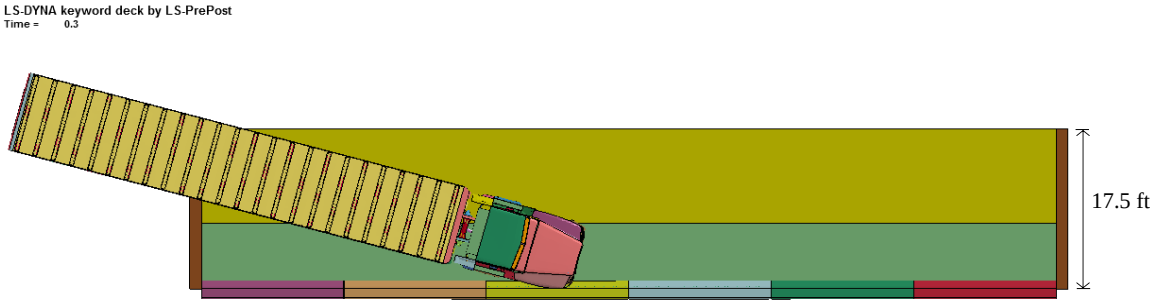

c) Top view of the test installation model (time of impact)

Figure 7.5 TL-5 MSE wall and tractor-van-trailer vehicle model

The TL-5 impact simulation was performed based on the nominal impact conditions specified in MASH for Test Level 5-12. The tractor-van-trailer vehicle model was given an initial velocity of 50 mph (80 km/hr.) and hit the third barrier (B-3) at its middle point at an angle of incidence of 15 degrees. This position of the impact point allows the 30 ft (9.15 m) long middle section to experience all forces associated with the impact of the tractor and the trailer models. The vehicle was positioned 22 ft (6.71 m) upstream the impact point in order to stabilize and settle under gravity loads. To enable comparison of forces and displacements, the barriers and selected strips locations were assigned an alphanumeric designator that describes their horizontal and vertical position as shown in Figure 7.6.

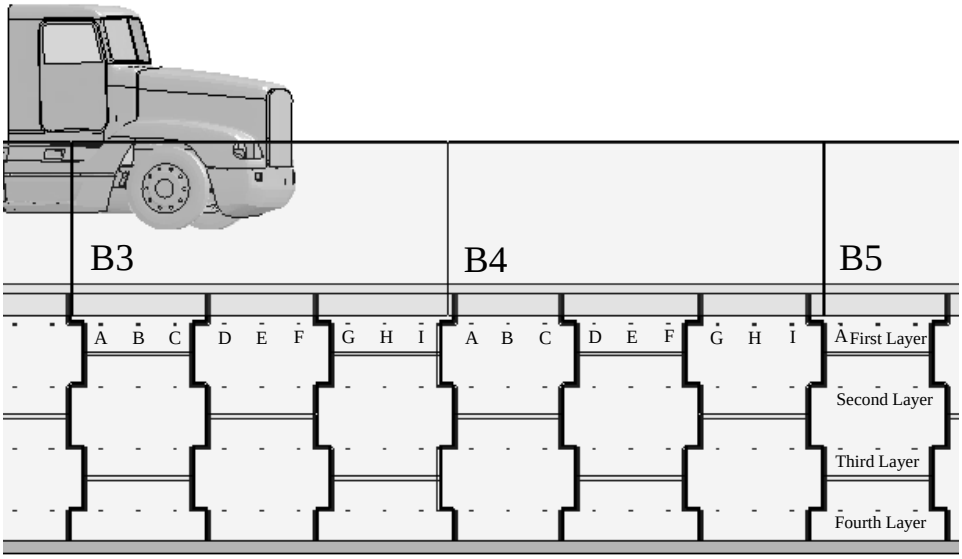

Figure 7.6 Elevation view of the test wall installation showing the distribution of the strips

The vehicle model was successfully contained and redirected by the barrier-moment slab system. The barriers and panels displacements were within the criterion limits. Figure 7.8 shows the sequential images of the vehicle model at each significant time.

7.2.1 Barrier Damage and Displacement

The magnitude of the lateral impact load for the three models is shown in Figure 7.7. The time history of the impact load indicates that, in average, the first peak load is 74.6 kips (332 kN), the second peak load is 103.1 kips (458.8 kN) and the third peak load is 167.4 kips (744.9 kN).

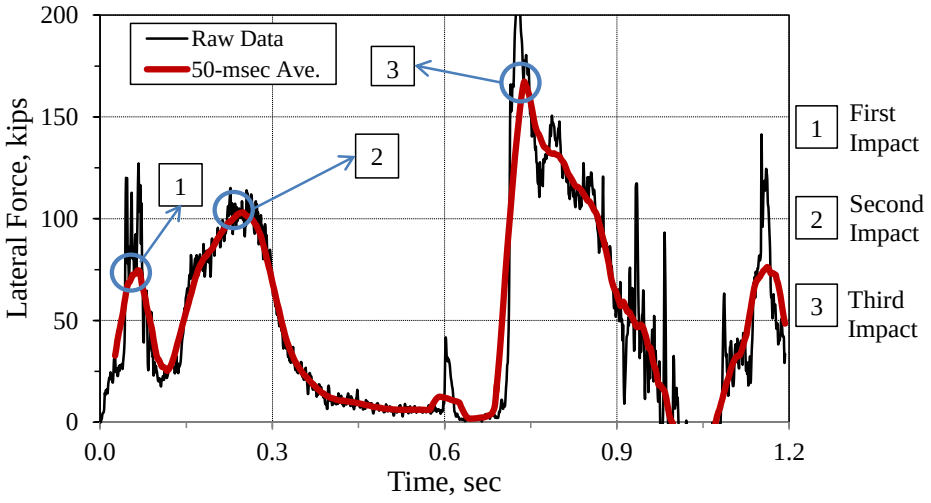

Figure 7.7 50 msec. average impact load on the N.J. barrier

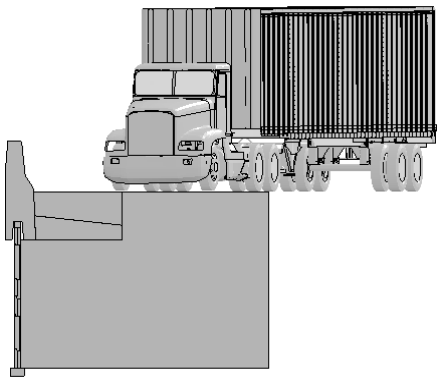

a) Pre-impact time position

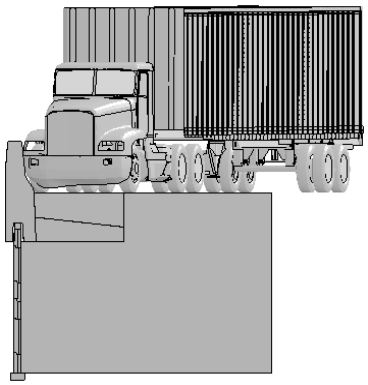

b) Initial impact (t=0 sec.)

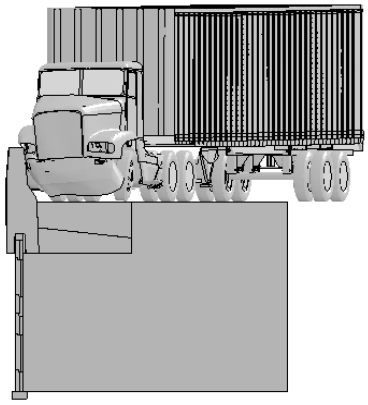

c) First peak load (t=0.066 sec.)

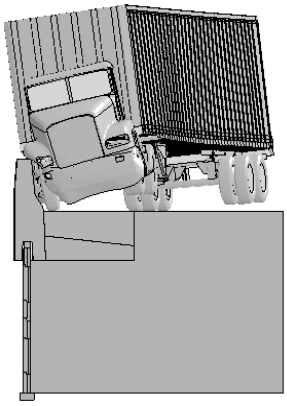

d) Second peak load (t=0.269 sec.)

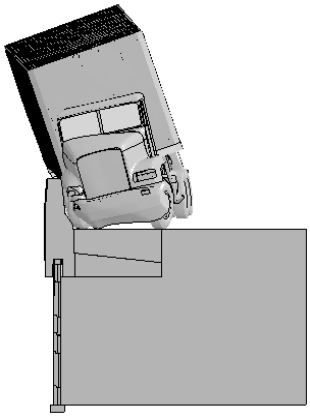

e) Third peak load (t=0.739 sec.)

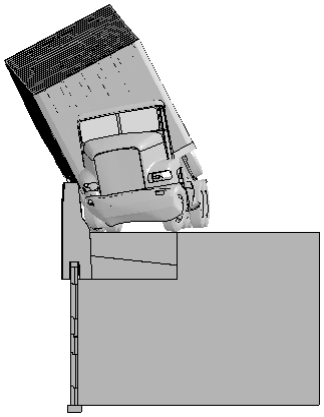

f) Max. strip load (t=0.845 sec.)

Figure 7.8 Vehicle position at each significant time for the test wall installation model

Damage to the 42 in. (1.07 m) tall N.J. shape barriers and the moment slab is shown in Figure 7.9. The barrier should not present any structural damage after impact and only cosmetic marks due to friction of the tires and the trailer should be observed.

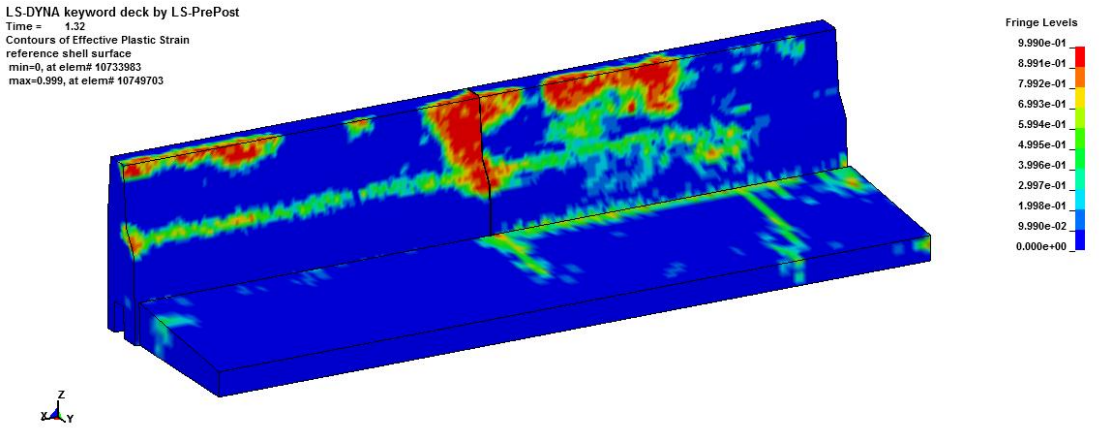

a) Front view of the barrier (impact of the rear axle of the trailer)

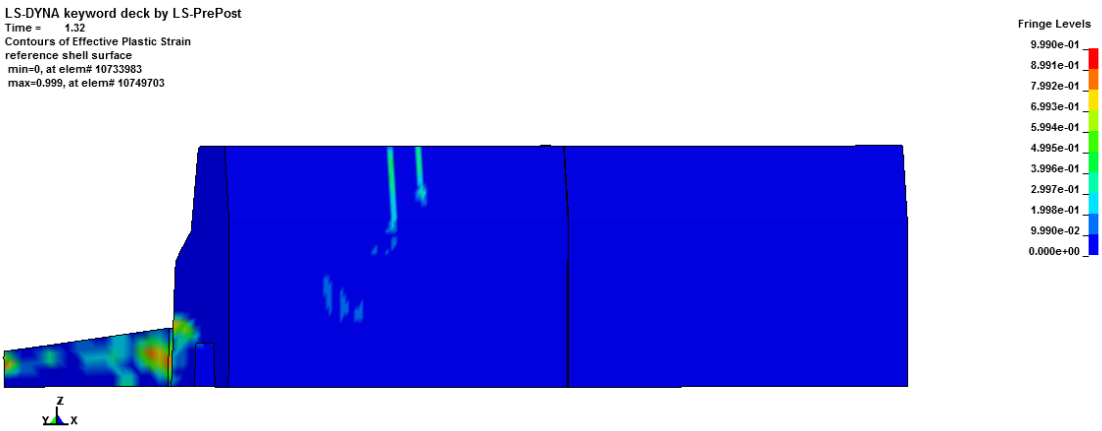

b) Back view of the barrier (impact of the rear axle of the trailer)

Figure 7.9 Damage profile of the N.J. shape barrier

The maximum displacements at the top and bottom of the 42 in. (1067 mm) tall barrier N.J. shape barrier were on average 1.43 in. (36.3 mm) and 0.85 in. (21.6 mm), respectively. The displacement time history is shown in Figure 7.10. The permanent displacement of the barrier at the top, ground level and bottom were 0.81 in. (20.6 mm), 0.65 in. (16.51 mm) and 0.53 in. (13.5 mm), respectively.

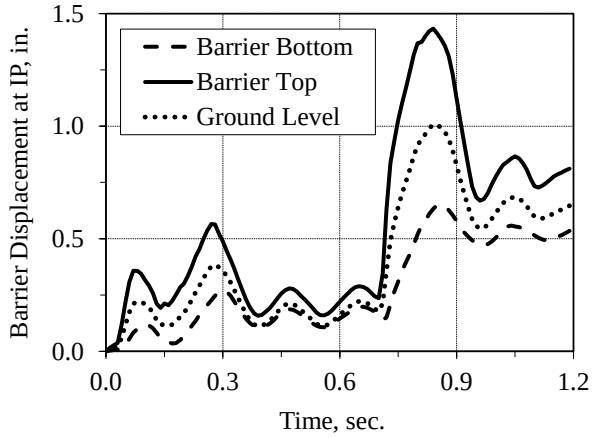

a) Displacement time history

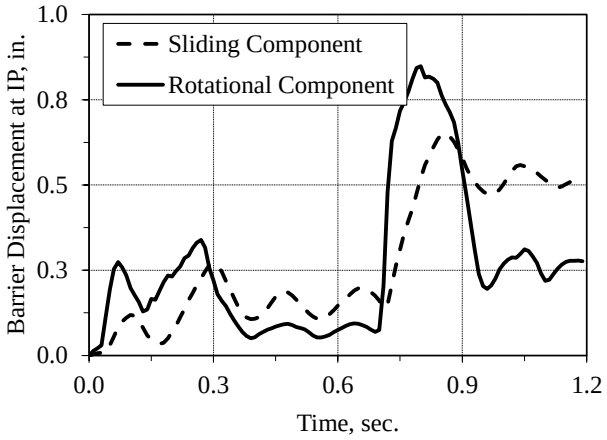

b) Rotation and sliding component of the displacement

Figure 7.10 Displacement of the N.J. shape barrier at the impact location

7.2.2 Loads and Displacements in the Reinforcing Strips

The load-time history for selected strips in the first and second layer is presented in Figure 7.12 and Figure 7.13, respectively. The total load and the excess dynamic in the first layer of soil reinforcing strips ranged from 2.97 kips (13.2 kN) to 5.85 kips (26.03 kN) and from 2.12 kips (9.43 kN) to 4.95 kips (22.02 kN), respectively. In the second layer, the total tension load and the excess dynamic load ranged was in strip section B3_B_2nd and it was 3.46 kips (15.4 kN) and 1.91 kips (8.5 kN), respectively.

The displacement in the reinforcing strips ranged from -0.1 in. (2.54 mm) to about 0.4 in. (10.2 mm) and it was around 0.84 sec. This impact time is associated with the impact of the trailer which imposed the largest load to the system. The inward movement of the strips is related to the kinematic behavior of the panels during impact. The wall panels are installed with a joint gap of 0.75 in. (19.05 mm) which permits them to behave as a flexible system. Due to computational time constraint, the permanent displacement from the FE model is difficult to determine since, at the end of the simulation run, the vehicle model had not left the MSE wall installation. However, it can be estimated that the permanent displacement ranged from 0.05 in. to about 0.20 in. (5.1 mm).

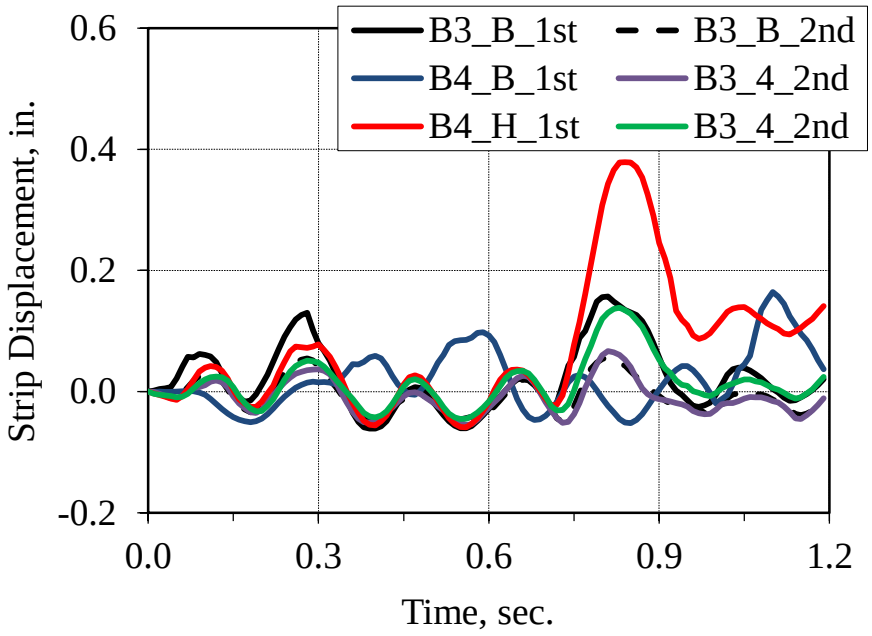

Figure 7.11 Displacement in the reinforcing strips from the FE model

7.2.3 Panels Analyses

The damage profile and the bending moment in the wall panels below the impact point was evaluated from the FE model, as shown in Figure 7.14 and Figure 7.15. The results showed that the wall panels located below the impact point are subjected to high bending moment at the level of the top layer of strips. This might indicate that the panel could be subjected to some tension cracks inside the traffic side of the wall since the simulation indicates that the bending moment overcome the moment resistance to cracking (M_{cr}=2.34 kip-ft/ft (10.41 kN-m/m)) (see appendix B). Yet, since the impact load occur

for a short period of time, the magnitude of the moment obtained from the simulation might not result in a structural failure of the wall panel.

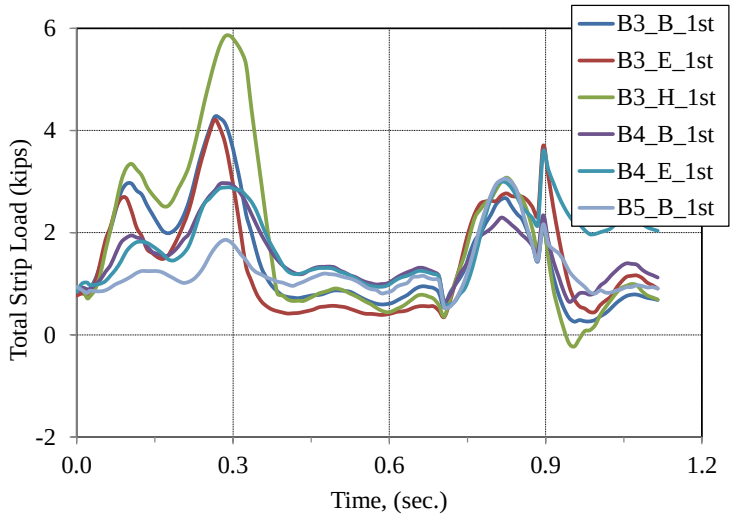

a) Total load

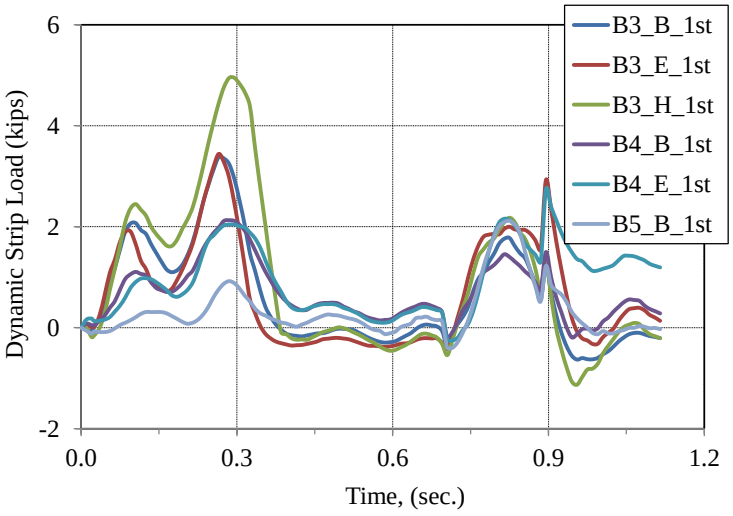

b) Dynamic load

Figure 7.12 Load for selected strip in the uppermost layer

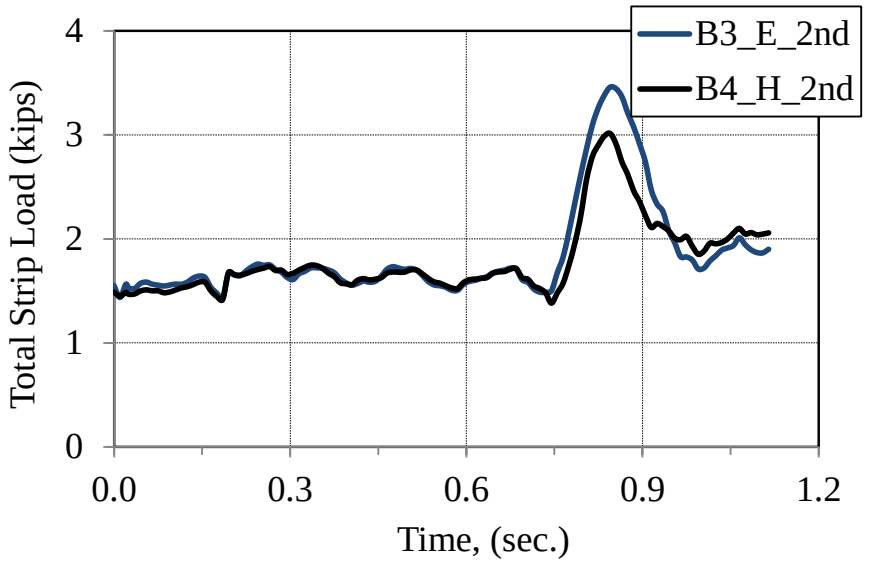

a) Total load

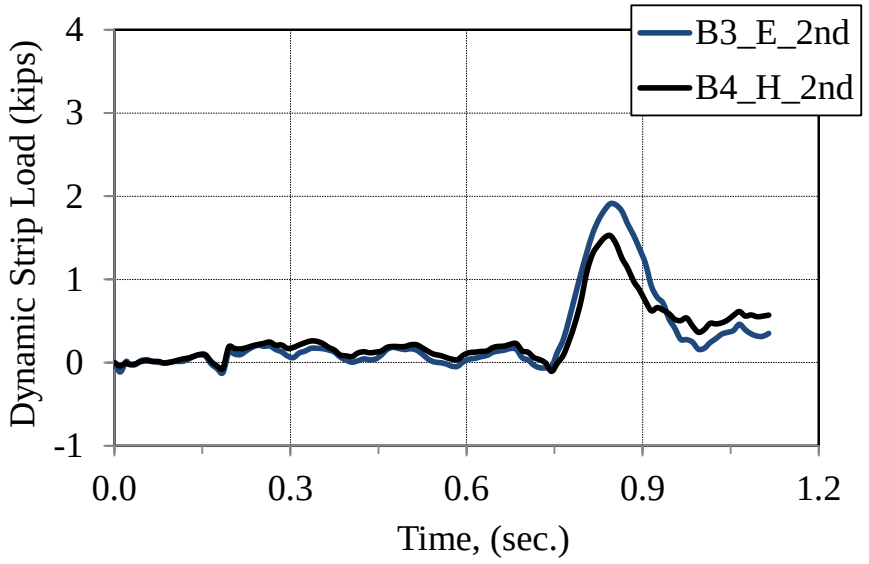

b) Dynamic load

Figure 7.13 Load for selected strip in the second layer

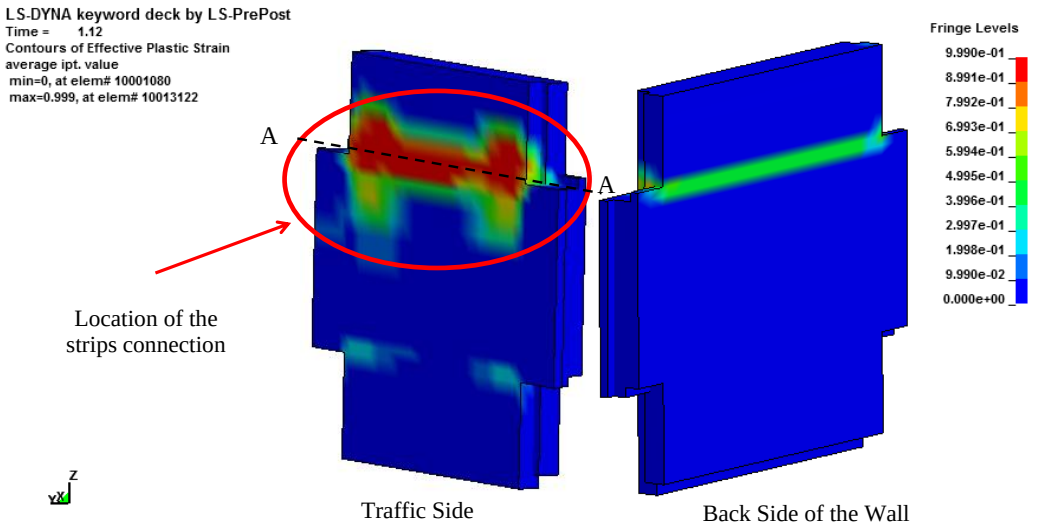

Figure 7.14 Damage profile of the test wall panel at B3 (below IP) for TL-5-1 impact on a N.J. barrier on top of the MSE Wall

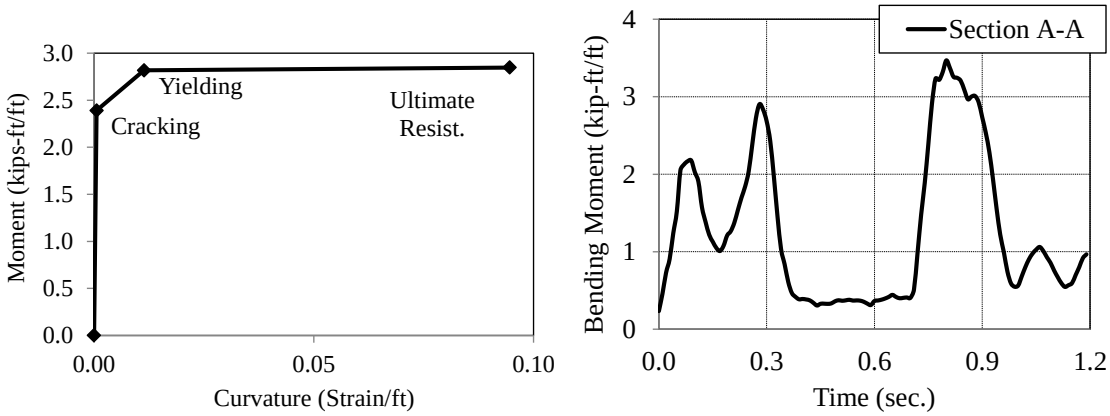

a) Theoretical moment resistance **b) Bending in the wall panel below IP**

Figure 7.15 Change in bending moment along section A-A of the wall panel

The dynamic and permanent displacement of the wall panels is shown in Figure 7.16. The maximum dynamic displacement was 0.58 in. (14.7 mm) at section B3_D. The permanent displacement at this section was 0.28 in. (7.1 mm). The results obtained from the FE analyses indicate that most of the displacement occurs at the top layer of panels and little movement was observed at the bottom row of panels.

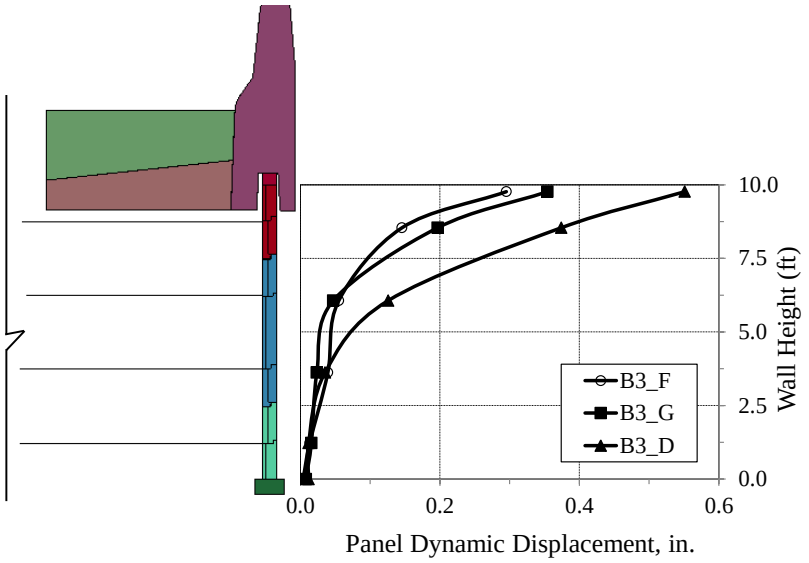

a) Dynamic displacement

Figure 7.16 Wall panel displacement from the FE test wall model

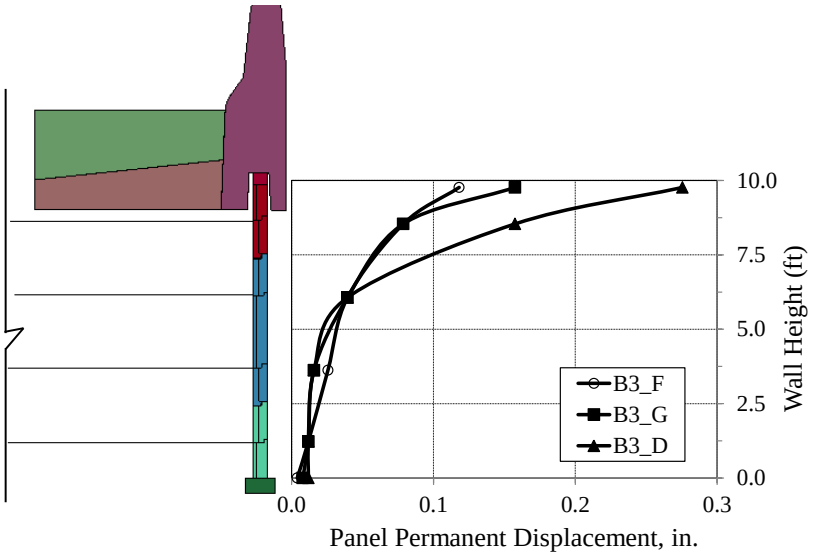

b) Permanent displacement

Figure 7.16 Continued

7.3 TL-5 Crash Test

7.3.1 TL-5 MSE Wall Construction and Test Installation

An overall layout of the TL-5 MSE wall test installation is shown in Figure 7.17 through Figure 7.19. The total length of the installation is about 135.5 ft (41.3 m) long. The first 90.4 ft (27.6 m) are placed on top of a 9.8 ft (3 m) tall instrumented MSE wall (Figure 7.18(a)) and the remaining 45.1 ft (13.8 m) are composed of the same barrier-moment slab system without wall installed to allow redirection of the vehicle downstream (Figure 7.18 (b)).

The wall section is comprised of full and half-panel sections that are approximately 5 ft (1.52 m) wide. The panels were installed with a $^{3}/_{4}$ in. (19 mm) wide vertical and horizontal joint to maximize the flexibility of the wall. Two bearing pads were positioned at the horizontal joint (typically at a quarter span points of the panels). Filter cloths were attached to each side of all joints to prevent migration of the backfill material. The bottom wall panels were placed on a 1 ft (304.8 mm) wide × 6 in. (152.4 mm) thick concrete leveling pedestal.

The MSE wall had three layers of reinforcement. The uppermost layer is at a depth of 3.7 ft (1128 mm) below the finished grade. The vertical spacing of the successive reinforcement layers is approximately 2.5 ft (760 mm). The steel reinforcement strips are 10 ft (3.05 m) long. The reinforcement had a density of three strips per layer per panel. The wall panels were 10.5 in. (266.7 mm) recessed inside the coping of the precast barrier-coping sections. The barrier-coping sections rested on a 4.5 in. (114 mm) layer of a level-up concrete placed on top of the wall panels.

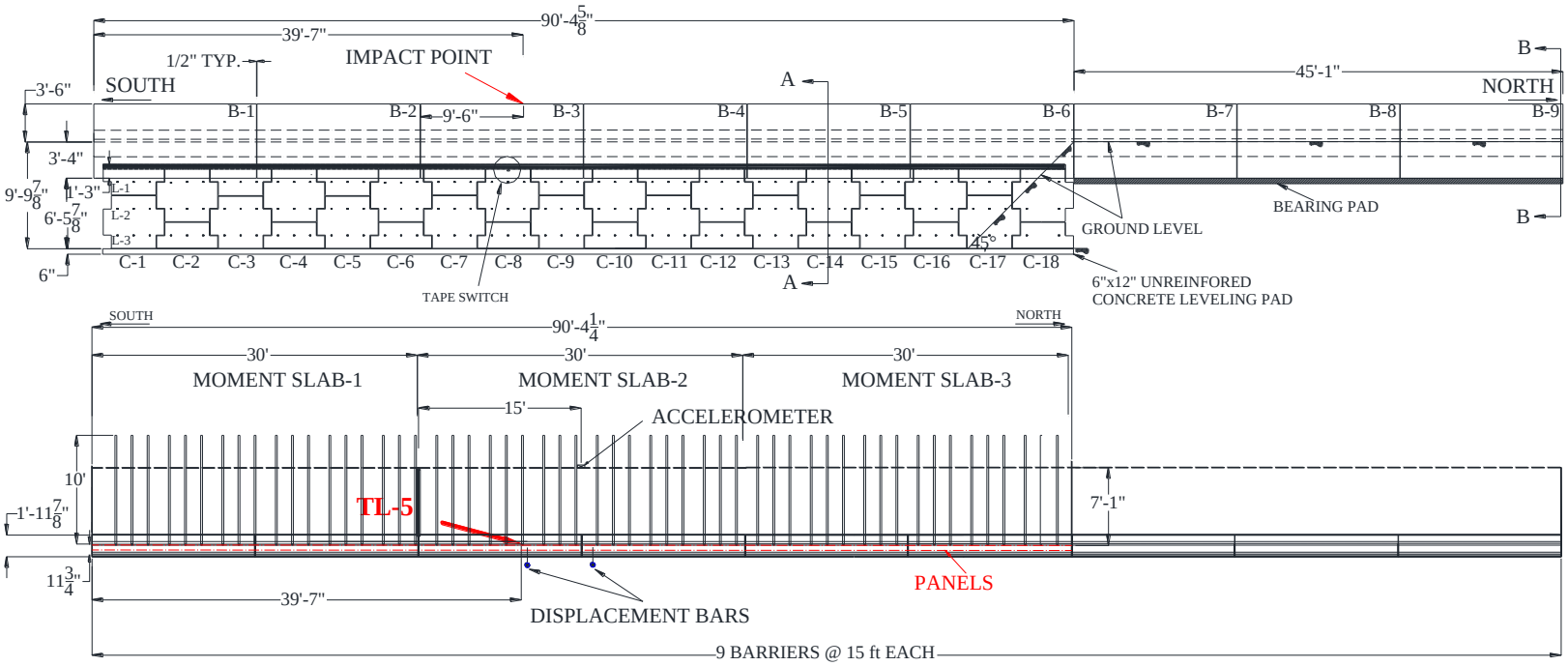

Figure 7.17 Overall layout of the TL-5 MSE wall test installation

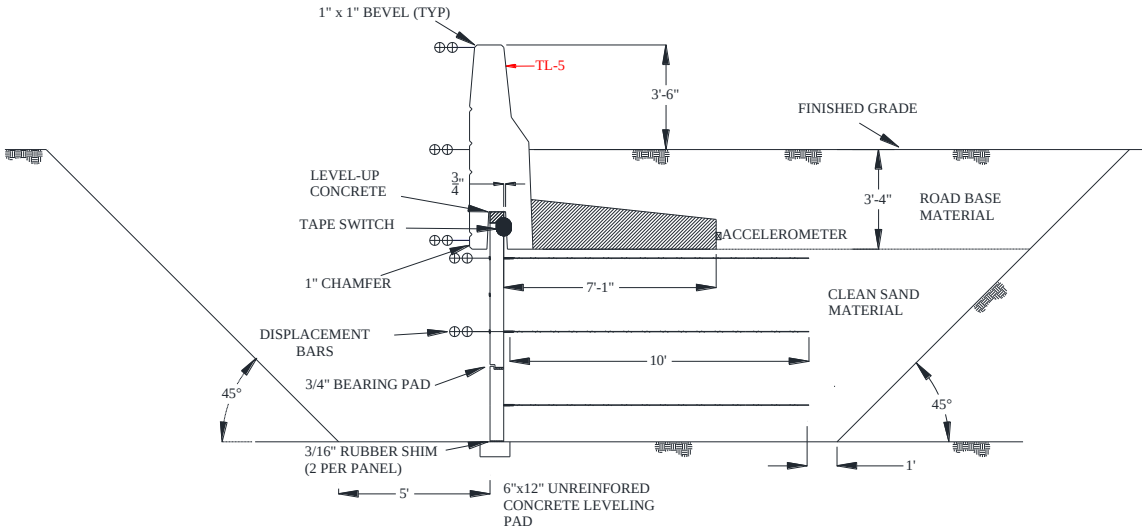

a) South section (SEC. A-A)

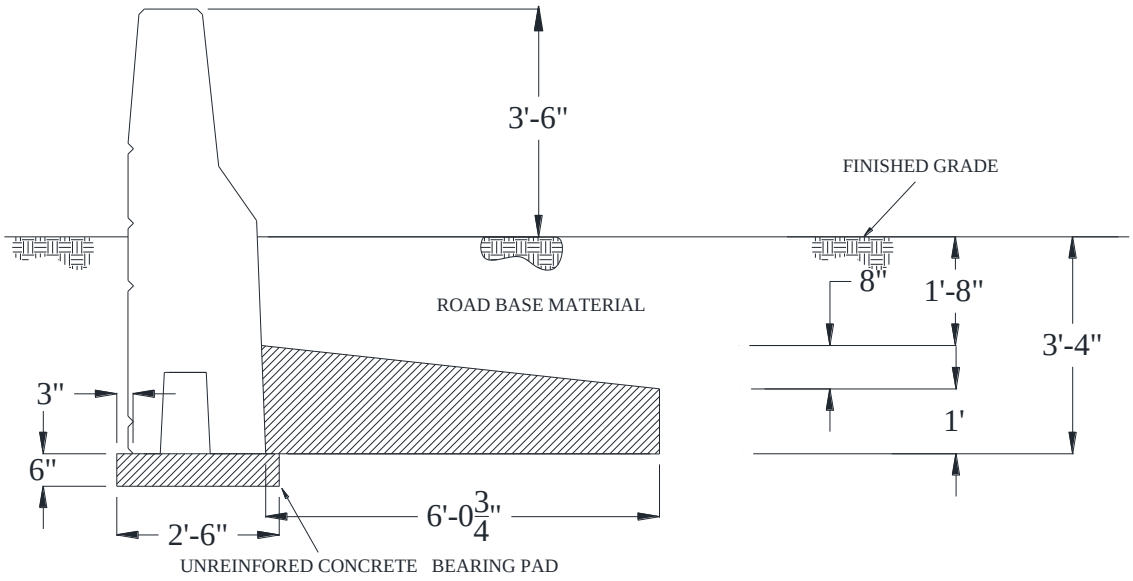

b) North section (SEC. B-B)

Figure 7.18 Side view of the TL-5 test wall installation with 42 in. (1.07 m) tall barrier

a) Three dimensional view of the installation

b) Set-up of the TL-5 full-scale showing the impact position

Figure 7.19 Full-scale MSE wall test installation and TL-5 crash-test set up

The wall section consists of a series of two-15 ft (4.57 m) long precast barrier units attached to each of the three 7 ft (2.13 m) wide × 30 ft (9.15 m) long moment slabs. The portion of the test installation without underlying wall consisted of three 15 ft (4.57 m) long precast barrier units attached to a 7 ft (2.13 m) wide × 45 ft (12.2 m) long moment slab. The moment slabs were cast-in-place with a concrete compressive strength of 4000 psi (27.6 MPa). The four moment slabs were connected to one another using three No.11 shear dowels across each joint. The tension members used to connect the barrier section to the moment slabs consist of No. 5 top bars and No. 4 bottom bars spaced at 8 in. (203.2 mm) on center.

The barrier portion of the precast barrier-coping sections consisted of a N.J. shape concrete. The capacity of the wall section is 163.1 kips (725.8 kN) with a failure length of 10.5 ft (3.2 m) computed using the AASHTO LRFD end section yield line procedure. The barrier portion is 3.5 ft (1067 mm) in height (measured from the roadway to the top of the barrier), 11.75 in. (298.5 mm) wide at the top and 23.9 in. (606.2 mm) wide at the roadway surface. The coping is 3.3 ft (1015 mm) in height (measured from the bottom of the coping to the roadway). Longitudinal reinforcement in the barrier-coping section consists of ten No. 7 bars above grade and eight No. 4 bars below grade. Transverse reinforcement consists of No. 4 bars at 8 in. (203 mm) on center at the barrier section and No. 6 bars at 8 in. (203 mm) on center at the coping section. Figure 7.20 shows photos of the instrumented MSE wall before the TL-5 crash test. The barriers and panels were assigned alphanumeric designators as described earlier. The precast barrier-

coping sections, concrete wall panels, and steel strip wall reinforcement were provided by RECO at no cost to the project.

a) Targets to measure dynamic displacements

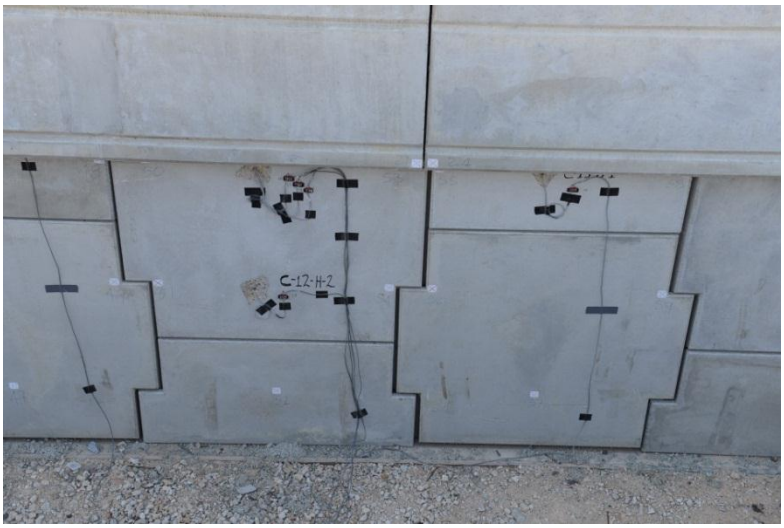

b) Strain gages in the panels

Figure 7.20 Instrumentation in the MSE wall test installation

The MSE wall backfill was made of two layers: a poorly graded (SP) clean sand from the bottom of the wall to the bottom of the moment slab (6.25 ft or 1.91 m) and a limestone road base from the bottom of the moment slab to the riding surface (3.3 ft or 1016 mm). The sand backfill and the road base satisfied the gradation limits of TxDOT Type B (Table 7.2 *(48))*.

Table 7.2 Gradation limits for TxDOT type A and B select backfill *(48)*

Type A		Type B	
Sieve Size	Percent Retained	Sieve Size	Percent Retained
3 in.	0	3 in.	0
½ in.	50-100	No. 4	See Note
No. 4	See Note	No. 40	40-100
No. 40	85-100	No. 200	85-100

Note: if 85% or more is material is retained in No. 4 sieve, the backfill will be considered rock backfill.

The index properties of the clean sand and limestone road base material are shown in Table 7.3. For the clean sand, the coefficient of curvature (C_c) and the coefficient of uniformity (C_u) were 0.84 and 3.85, respectively. The percent of fine passing the #200 sieve was 3.1% using the wet sieve analyses (ASTM D 2217-85). The clean sand was classified as a poorly-graded sand (SP) according to the Unified Soil Classification System (USCS). The road base is composed of a mix of gravel, sand and lime with a plasticity index of 3.3%. The percent passing the #200 sieve was 15% using

the wet sieve analyses (ASTM D 2217-85). The road base was classified as silty gravel (GM) according to the USCS. The particle size distribution curve of the clean sand and the limestone road base material are shown in Figure 7.21.

Table 7.3 Select index properties of the backfill soil material *(46)*

Property	Soil Sample	
	Clean Sand	Road Base
D_{10}[(1)] (mm)	0.20	0.03
D_{30}[(2)] (mm)	0.36	0.8
D_{50}[(3)] (mm)	0.51	4
D_{60}[(4)] (mm)	0.77	6.5
Perc. Fines (%)	3.1	15.0
C_c[(5)]	0.84	3.28
C_u[(6)]	3.85	216.7
w_L (%)	-	17.7
w_P (%)	-	14.4
w_{PI} (%)	-	3.3
Perc. gravel (%)	0.7	46
Perc. sand (%)		36.9
Max. void ratio (e_{max})	0.60	-
Min. void ratio (e_{min})[(7)]	0.43	-
Gs	2.64	-
USCS[(8)]	SP	GM

[(1)] Particle diameter at 10% finer; [(2)] particle diameter at 30% finer; [(3)] particle diameter at 50% finer;[(4)] particle diameter at 60% finer; [(5)] coefficient of curvature; [(6)] coefficient of uniformity; [(7)] estimated using non-standard procedures; [(8)] Unified Soil Classification System.

The modified Proctor curve and the stiffness curve of the backfill material are shown in Figure 7.22. The estimated maximum dry unit weight of the clean sand was 117.8 pcf (18.5 kN/m^3) with an optimum water content of 2.5%. For the road base, the estimated maximum dry unit weight was 136.8 pcf (21.5 kN/m^3) with an optimum water content of 6.6%. The stiffness curve presented in Figure 7.22 indicates that the modulus of the clean sand and the road base are very sensitive to the water content. Therefore, it was decided to achieve the maximum in-situ density by compacting the soil in the dry side of the optimum water content.

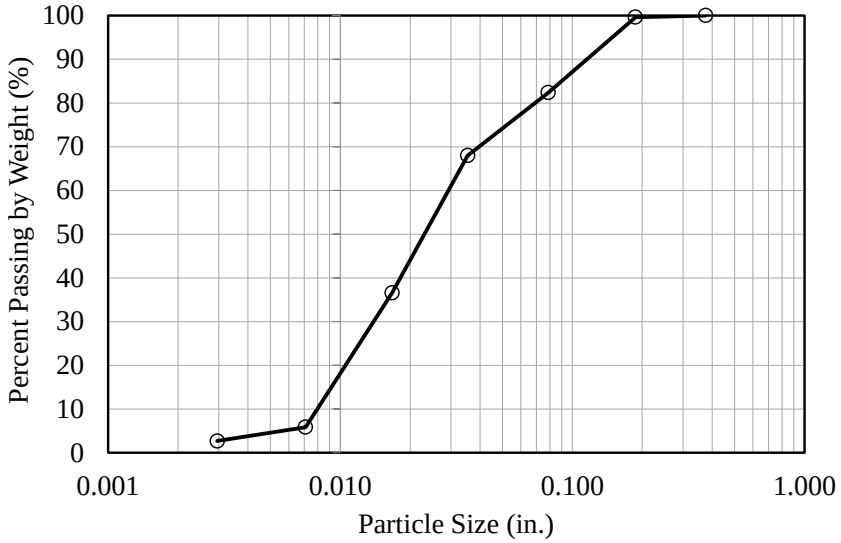

a) Clean sand (SP) (wet sieve analyses)

Figure 7.21 Particle size distribution curve of the backfill material for TL-5 crash test *(46)*

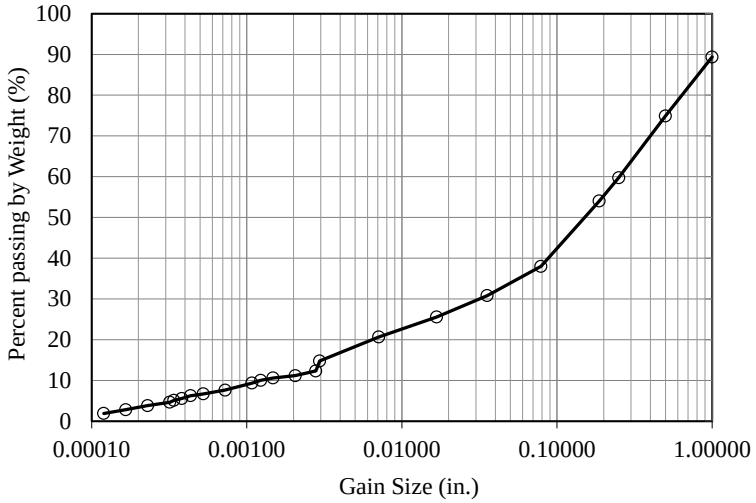

b) Limestone road base (GM) (wet sieve analyses + hydrometer analyses)

Figure 7.21 Continued

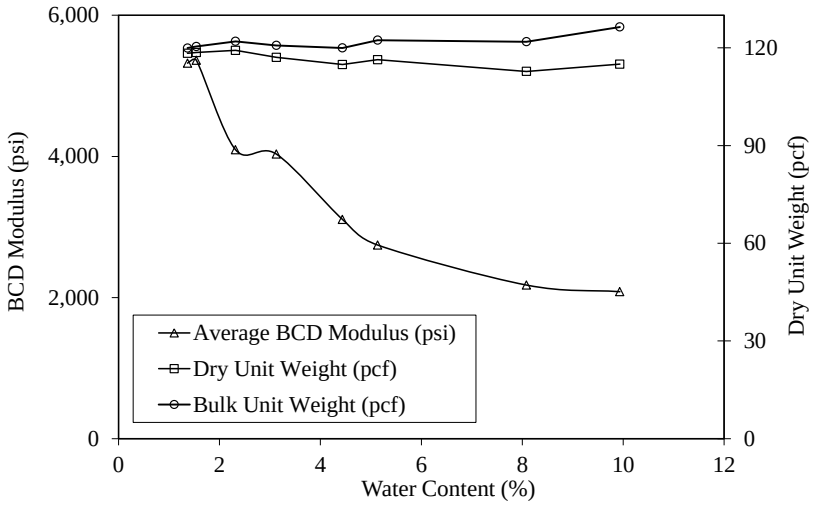

a) Clean sand (SP)

Figure 7.22 Modified Proctor curve and stiffness curve of the backfill material for TL-5 crash test *(46)*

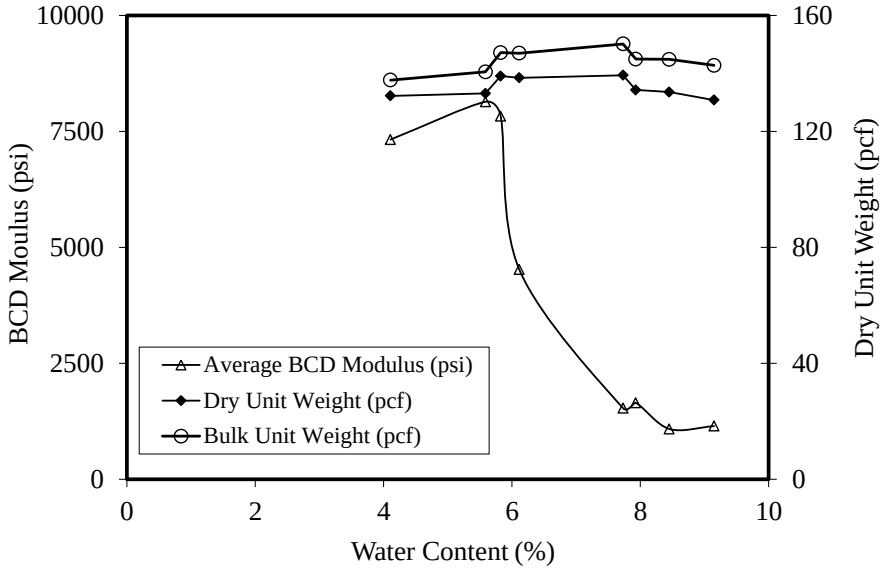

b) Limestone road base (GM)

Figure 7.22 Continued

The sand was compacted in loose lifts of 6 in. (152.4 mm) to 12 in. (304 mm) thick maximum with 6 passes of a 2,176 lb. (9.7 kN), 35 in. (890 mm) wide drum roller. The road base was compacted in loose lifts of 10 in. (254 mm) thick maximum with 6 passes of a 8 tons (8000 kg), 66 in. (1.68 m) wide drum roller The in situ dry density and the water content as compacted were measured using the nuclear density (ND) device. Two tests were conducted at the level of the bottom layer of strips. The average dry density and water content were 111.7 pcf (17.5 kN/m^3) and 3%, respectively. This dry density represents 95% of the maximum dry density obtained in the modified Proctor test for the sand. In addition, three in-situ nuclear density tests were conducted at the finished level of the sand backfill and the road base, as described in Figure 7.23. The

average in-situ dry density and the water content as compacted were 110.8 (17.4 kN/m^3) and 3.03% for the sand and 128.1 pcf (20.1 kN/m^3) and 5.81% for the road base. These dry densities represents, on average, 94.2% and 93.8% of the maximum dry densities obtained in the modified Proctor test for the sand and the road base, respectively. The friction angle of the sand was measured in the direct shear test by recompacting the sand at its maximum dry density; a value of 40 degrees was obtained together with an apparent cohesion of 0.73 psi (5 kPa) (*46*).

The friction angle of the road base was measured in a large triaxial cell by recompacting the road base to its maximum dry density; a value of 45 degrees was obtained with a cohesion intercept of 80 kPa (11.6 psi) (*46*). The modulus of the sand and the road base were measured with the Briaud Compaction Device (BCD) (*49*); the values obtained were, on average, 2147 psi (14.8 MPa) and 8003 psi (55.2 MPa), respectively. A summary of the nuclear density tests and the BCD modulus test in the sand backfill and the road base is presented in Table 7.4.

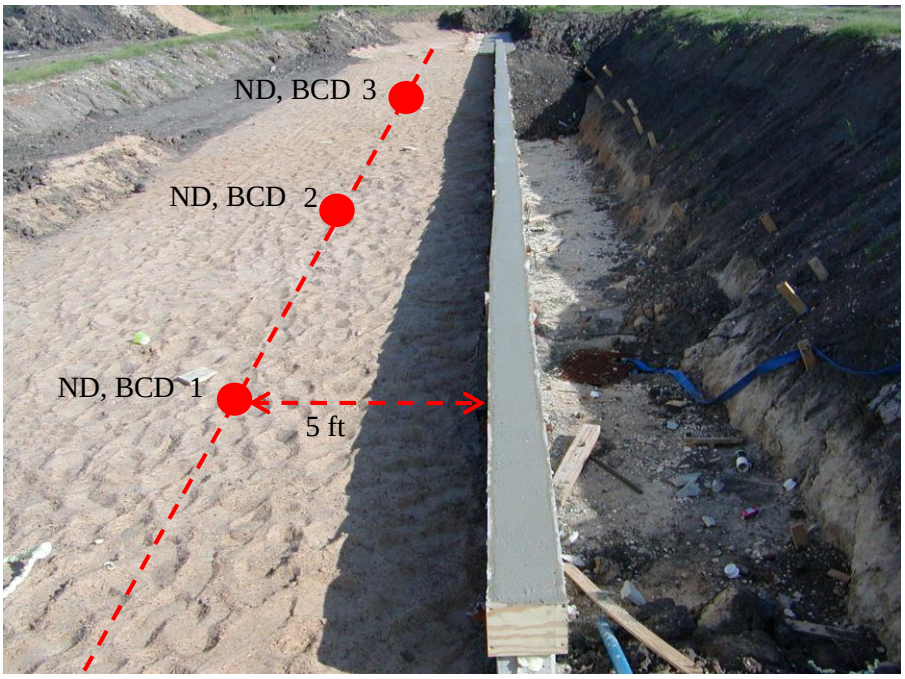

a) In-situ density tests in the clean sand

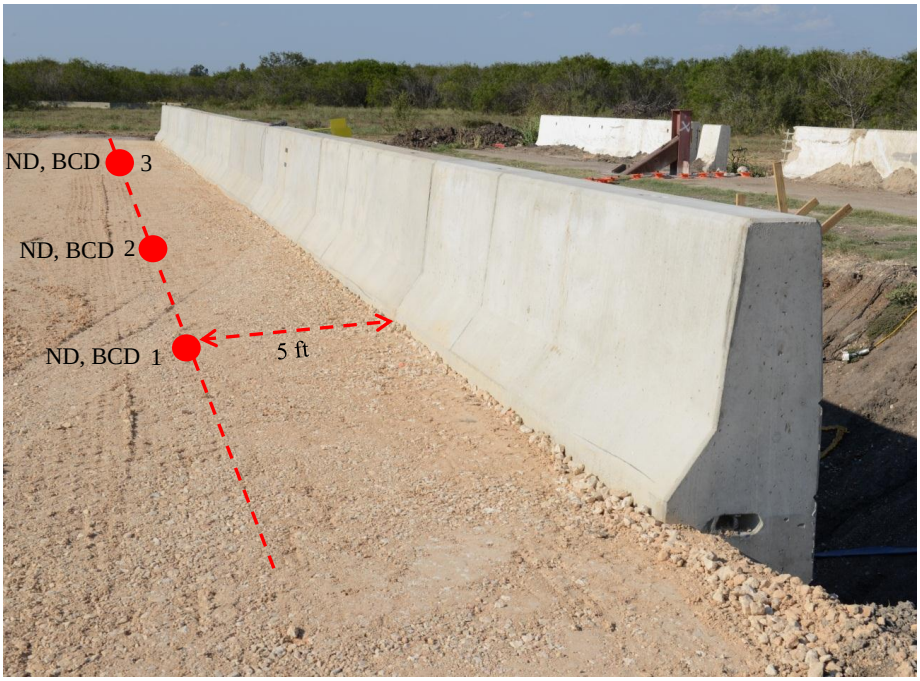

b) In-situ density tests in the clean sand

Figure 7.23 In-situ density tests conducted in the TL-5 MSE wall test installation

Table 7.4 Summary of the in-situ nuclear density tests and BCD modulus tests

Soil Material	Point No.	Location from upstream end (ft)	Wet Density (pcf)	Dry Density (pcf)	Water Content (%)	Relative Compaction (%)	Ave. BCD Modulus (psi)
Clean Sand	1	15	112.8	109	3.04	92.6	2147
	2	45	114.3	110.7	3.2	94.1	2060
	3	75	115.9	112.7	2.86	95.8	2234
Average			114.3	110.8	3.03	94.2	2147
Road Base	1	15	138.3	129.7	6.58	95.0	9000
	2	45	134	127.5	5.11	93.4	7540
	3	75	134.4	127.1	5.75	93.1	7469
Average			135.6	128.1	5.81	93.8	8003

Selected reinforcement strips in the MSE wall were instrumented with single active arm bridge strain gages to capture the tensile forces transmitted into the reinforcement during the full-scale crash test. A total of 14 full-bridge strain gages were installed as shown in Figure 7.24. The location of the strain gages is based on the location of maximum tensile forces in the reinforcements as determined by the FEA. Information obtained from this instrumentation is used to validate the recommended design loads and design procedures for designing barriers on top of MSE walls.

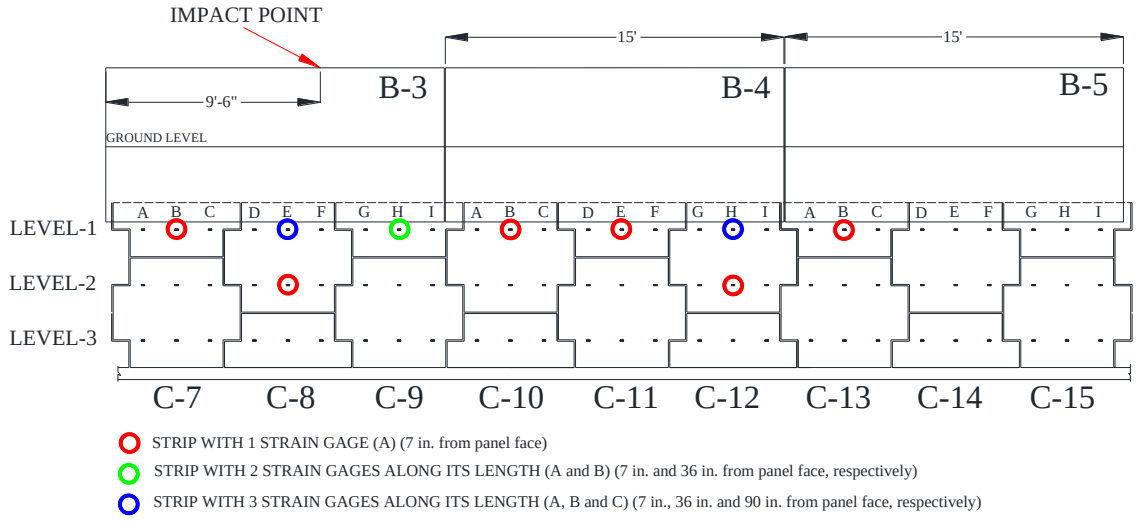

Figure 7.24 Selected strips with strain gage location for the TL-5 test wall

A contact switch was placed at the top edge of the traffic face (inside face) of the wall panels inside the coping recess. The location of the contact switch is close to the impact point as the simulation results predicts the maximum barrier movement. The switch indicates the time (referenced from impact) at which the barrier slides and/or rotates sufficiently for the coping to contact the wall panel. An accelerometer was placed at the longitudinal edge of the second moment slab (interface soil-concrete) to measure any vertical acceleration or motion imparted to the moment slab during impact. The accelerometer was located at the mid-point of the 30 ft (9.15 m) long moment slab.

Displacement and/or rotation of the barrier and wall panels were determined from high-speed video operating at 1000 frames/second. Displacement gages were placed at the top and bottom of the precast barrier-coping section and on the wall panels at heights corresponding to the first and second layer of soil reinforcement. The location

of the displacement gages is at the impact point and at 10 in. (254 mm) from the upstream end of barrier section 4 as shown in the south section view in Figure 7.17. Detailed drawings of the test installation and photographs of the construction procedure are presented in Appendix C and D, respectively.

7.3.2 Impact Conditions

MASH test 5-12 involves a 36000V tractor-van-trailer weighing 79,300 lb. ±1,100 lb. (36,000 kg ±500 kg) and impacting the N.J. shape barrier at an impact speed of 50 mph ±2.5 mph (80 km/hr. ±4 km/hr.) and an angle of 15 degrees ±1.5 degrees. The target impact point was 39.5 ft (12.04 m) from the upstream end, at barrier section 3 (B3). The 2000 Sterling TF tractor with the 1997 Strick van-trailer used in the test weighed 79,230 lb. (35,938 kg) and the actual impact speed and angle were 49.4 mph (79.5 km/hr.) and 15.1 degrees, respectively. The actual impact point was about 2 ft (609.6 mm) upstream of the target impact point, or 37.5 ft (11.43 m) from the upstream end. The impact severity was 432.6 kip-ft (586.9 kN-m), which was 2.5 % below target.

7.3.3 Test Vehicle

A 2000 Sterling TF with 1997 Strick 48 ft (14.63 m) van-trailer, shown in Figure 7.25, was used for the crash test. Test inertia weight of the vehicle was 79230 lb. (35938 kg), and its gross static weight was 79230 lb. (35938 kg). The height to the lower edge of the

vehicle front bumper was 23.5 in. (596.9 mm), and the height to the upper edge of the front bumper was 35.5 in. (901.7 mm). Additional dimensions and information on the vehicle are given in appendix E. The vehicle was directed into the installation using the cable reverse tow and guidance system, and was released to be free-wheeling and unrestrained just prior to impact.

a) Test vehicle for full-scale crash test

Figure 7.25 Test vehicle and test installation geometry

b) Installation geometry

Figure 7.25 Continued

7.3.4 Test Description

The 36000V vehicle, while traveling at an impact speed of 49.7 mph (80 km/hr.), impacted the N.J. shape barrier placed on top of the MSE wall at 37.5 ft (11.4 m) from the upstream end at an impact angle of 15.1 degrees. At approximately 0.10 sec. after impact, the cab of the test vehicle began to redirect, and at 0.20 sec., the lower right front corner of the van-trailer contacted near the top of the barrier. At 0.40 sec., the cab of the test vehicle was traveling parallel with the barrier. The van-trailer began traveling parallel with the barrier at 0.7 sec. At 0.697 sec., the lower right rear corner of the van-trailer contacted near the top of the barrier. As the test vehicle continued along the

barrier, it righted itself and rode off the end of the installation. The brakes on the test vehicle were applied right after the vehicle left the installation. The test vehicle came to rest about 100 ft (30.5 ft) downstream of the end of the MSE wall test installation and 6 ft (1.83 m) toward the field side.

7.3.5 Test Article and Vehicle Damage

Damage to the barrier was mostly cosmetic, as shown in Figure 7.26. In the soil forward of the face of the barrier, there was a sequential crack right at the edge of the moment slab (6 ft (1.83 m) from the N.J. barrier) (Figure 7.27). The soil crack was approximately 0.20 in. (5 mm) thick in some areas and 0.12 in. (3 mm) to 0.16 in. (4 mm) thick in others. It started at 3 ft (914.4 mm) upstream of the joint between barrier section 2 and barrier section 3 (B2-B3) and it moved downstream to approximately the middle point of barrier section 4 (B4). The approximately total length of the soil crack was 25 ft (7.62 m).

a) N.J shape barrier after test

b) Crack at the barrier joint (B2-B3) due to the trailer impact

Figure 7.26 Barrier and MSE wall installation after TL-5 crash test

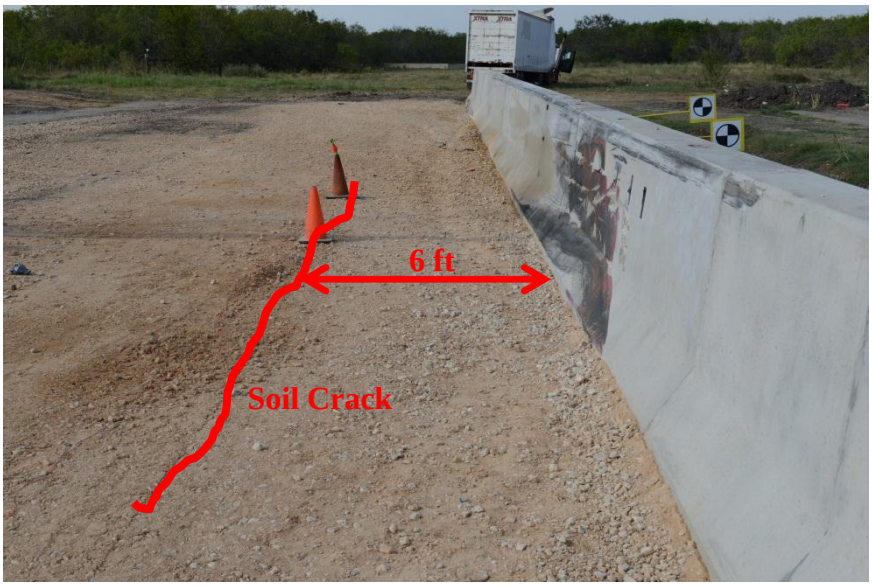

Figure 7.27 Crack in soil after impact

Damage to the 36000V is shown in Figure 7.28. The front axle, tie rods, right front spring, right front U-bolts, right front shock, right frame rail were deformed. Also damaged were the front bumper, hood, right front tire and wheel rim, right fuel tank, right door, fifth wheel mount, right outer tire and wheel rim. On the trailer, the right and left trailer jack, and rear outer tire were damaged and there were scuff marks along the right side of the trailer. Estimated maximum crush to the tractor was 18 in. (457.2 mm) at the right front corner of the tractor at bumper height.

a) Front view of the tractor

b) Side view of the trailer

Figure 7.28 Vehicle damage after impact

7.3.6 Occupant Risk

Occupant risk values are not applicable for MASH test 5-12. However, data from the accelerometers, located at the vehicle mid-position, were digitized for evaluation of occupant risk. In the longitudinal direction, the occupant impact velocity was 1.31 ft/sec. (0.4 m/sec.) at 0.232 sec., the highest 10-msec. occupant ridedown acceleration was -4.5 g's from 1.011 to 1.021 sec., and the maximum 50-msec. average acceleration was -1.4 g's. In the lateral direction, the occupant impact velocity was 13.12 ft/sec. (4 m/sec.) at 0.232 sec., the highest 10-msec. occupant ridedown acceleration was 12.4 g's from to 1.01 sec. to 1.02 sec., and the maximum 50 msec. average was -4.4 g's between 0.202 and 0.252 sec. The Theoretical Head Impact Velocity (THIV) was 13.12 ft/sec. (4 m/sec.) at 0.23 sec., the Post-Impact Head Decelerations (PHD) was 12.5 g's between 1.01 and 1.02 sec., and the Acceleration Severity Index (ASI) was 0.5 between 0.201 and 0.251 sec. A summary of the test data is presented in Figure 7.29.

7.3.7 Data from Accelerometers

The test vehicle was instrumented with a self-contained, on-board data acquisition system. The accelerometers, that measure the x, y, and z axis of vehicle acceleration, are strain gauge type with linear millivolt output proportional to acceleration. Angular rate sensors, measuring vehicle roll, pitch, and yaw rates, are ultra-small size, solid state units designs for crash test service.

≈0.01 sec.

≈0.25 sec.

≈0.50 sec.

≈0.90 sec.

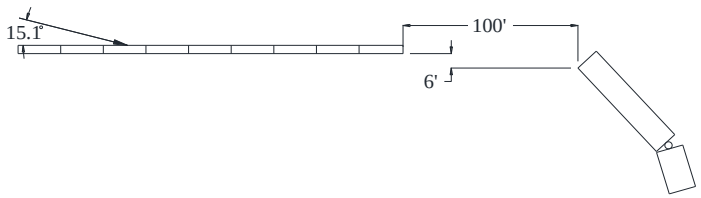

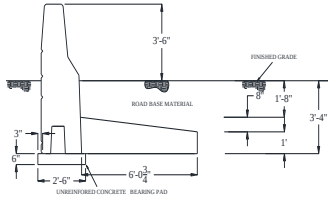

General Information
- Test Agency..... Texas Transportation Institute (TTI)
- Test Standard Test No. ..... MASH Test 5-12
- TTI Test No. ..... 478130-MSE wall
- Date..... 2012-09-26

Test Article
- Type ..... Barrier-coping system on top MSEW
- Name..... New Jersey Shape Barrier
- Installation Length..... 135.5 ft (41.3 m)
- Material or Key Elements....

Soil Type and Condition..... Clean sand and road base material

Test Vehicle
- Type/Designation 36000V
- Make and Model..... 2000 Sterling TF with 1997 Strick Van-Trailer
- Curb..... 29,800 lb. (13517 kg)
- Test Inertial ..... 79,230 lb. (35938 kg)
- Dummy..... No dummy
- Gross Static ..... 79,230 lb. (35938 kg)

Impact Conditions
- Speed .....49.4 mph (79.5 km/hr.)
- Angle .....15.1 degrees
- Location/Orientation .....37.5 ft (11.4 m) downstream of end

Impact Severity.....438.3 kip-ft

Exit Conditions
- Speed .....Not obtainable
- Angle .....Not obtainable

Occupant Risk Values
- Impact Velocity
- Longitudinal.....1.31 ft/s (0.4 m/s)
- Lateral.....13.12 ft/s (4 m/s)

Ridedown Accelerations
- Longitudinal.....-4.4 g's
- Lateral.....12.4 g's
- THIV.....13.12 ft/sec. (4m/sec.)
- PHD .....12.5 g's
- ASI.....0.50

Max. 0.050-s Average
- Longitudinal ..... -1.4 g's
- Lateral ..... -4.4 g's
- Vertical..... -3.2 g's

Post-Impact Trajectory
- Stopping Distance..... 200 ft

Vehicle Stability
- Maximum Yaw Angle ..... -15.7 degrees
- Maximum Pitch Angle..... -6.4 degrees
- Maximum Roll Angle..... 32.5 degrees
- Vehicle Snagging ..... No
- Vehicle Pocketing..... No

Test Article Deflections
- Dynamic ..... Not available
- Permanent..... 1.1 in. (27.9 mm)
- Working Width..... 15 ft (4.57 m)

Vehicle Damage
- CDC ..... (see text)
- Max. Exterior Deformation ..... 18 in. (457.2 mm)

Figure 7.29 Summary of results for MASH test 5-12 on the N.J. shape barrier on top of the MSE wall

Accelerometers and rate transducers were placed on the tractor frame close to the fifth wheel. The rear accelerometers were placed on the trailer frame. During the test, the data were recorded from each channel at a rate of 10,000 values per second. Initial contact of the pressure switch on the vehicle bumper provides a time zero mark as well as initiating the recording process. The raw data were then processed by the Test Risk Assessment Program (TRAP) software to produce detailed reports of the test results.

The results from the truck-mounted accelerometer are presented from Figure 7.30 through Figure 7.32. The maximum 50 msec. average acceleration measured close to the rear tandem axles of the tractor in the x, y and z direction were -1.4 g's, -4.4 g's and -3.2 g's, respectively. The maximum 50 msec. average acceleration measured close to the rear tandem axles of the trailer in the x and y direction were -3.4 g's and -10.8 g's, respectively. The acceleration in the z direction at the rear tandem axles of the trailer could not be recorded due to unknown problems in the data acquisition system. The maximum roll angle recorded at the rate transducer was 32.5 degrees.

Using the test inertial of the vehicle and the lateral acceleration measured at the central axles of the tractor-van-trailer and at the rear tandem axles of the trailer, the impact force can be approximated using the equation of motion, as described in section 3. The results show that the second and third peak load were approximately 140.8 kips (626.6 kN) and 201.2 kips (895.4 kN), respectively. These load values might not represent the true impose load by the vehicle as the acceleration data tends to overestimate the peak load. However, examination of the impact events helps explain that the largest load imposed to the barrier was due to the impact of the trailer.

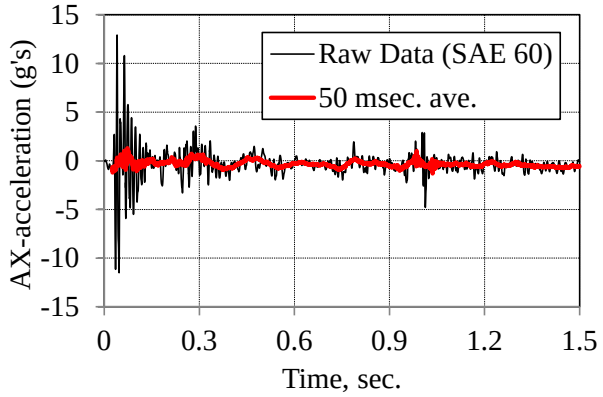

a) x-acceleration (close to the rear tandem axles of tractor)

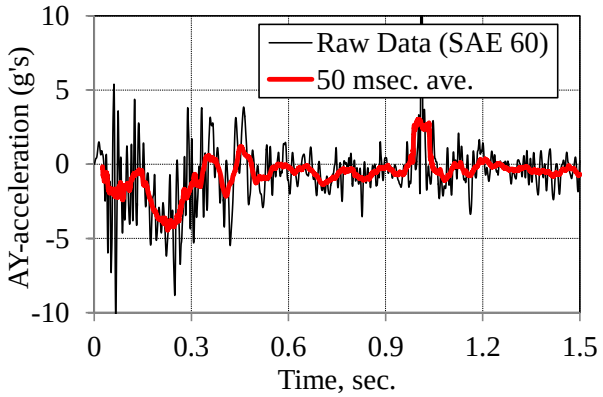

b) y-acceleration (close to the rear tandem axles of tractor)

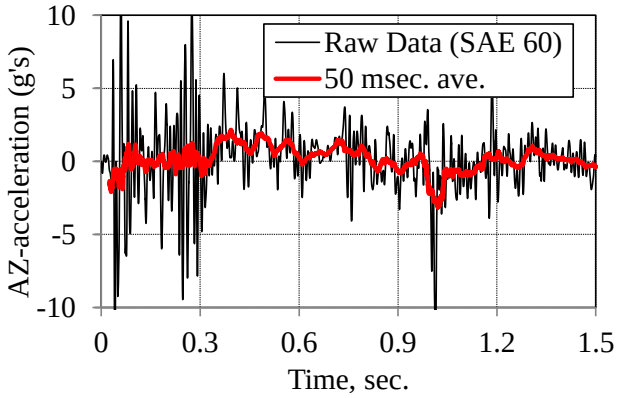

c) z-acceleration (close to the rear tandem axles of tractor)

Figure 7.30 Acceleration data from the tractor-mounted accelerometer

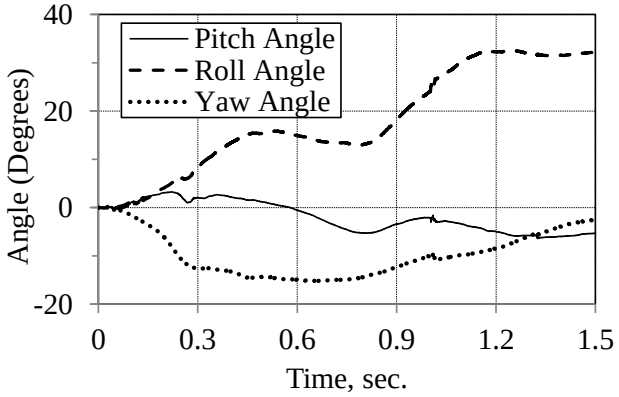

Figure 7.31 Roll, Pitch and yaw angle measure close to the vehicle fifth wheel

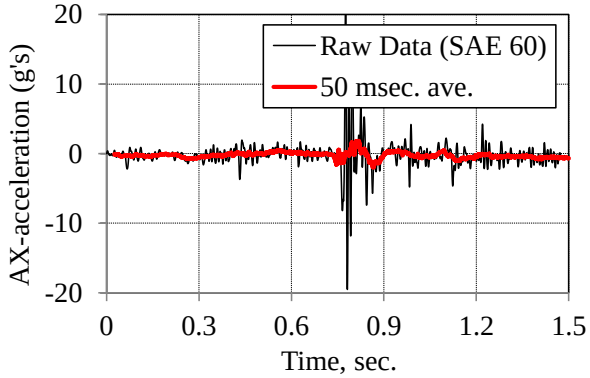

a) x-acceleration (rear tandem axles of trailer)

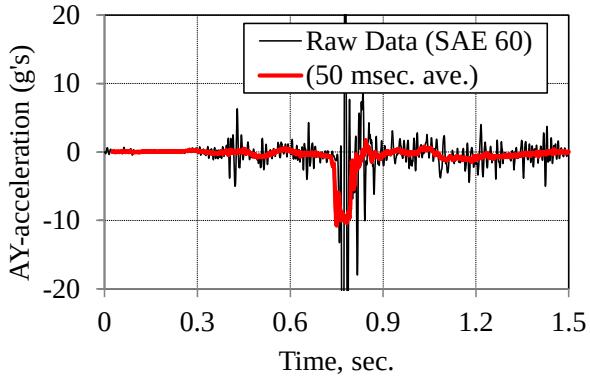

b) y-acceleration (rear tandem axles of trailer)

Figure 7.32 Acceleration data from the trailer-mounted accelerometer

The 50 msec. average vertical acceleration of the moment slab is presented in Figure 7.33. The time-history of the acceleration data shows two acceleration peaks which can be associated with the time of impact of the rear tandem axles of the tractor (t=0.2 sec.) and impact of the rear tandem axles of the trailer (t=0.7 sec.), respectively. The velocity and the vertical displacement were computed using double integration of the acceleration data. However, since the data was excessively noisy, the results inherent a significant error and seem to be unreasonable.

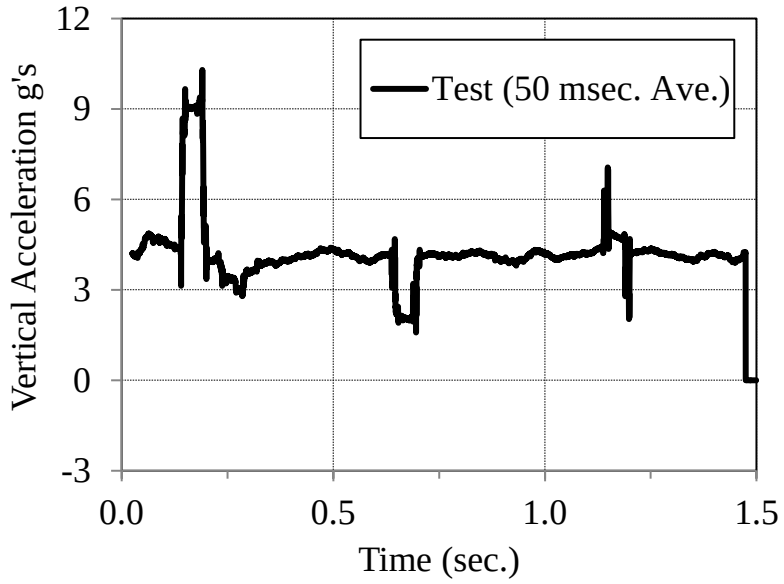

Figure 7.33 Acceleration of the moment slab during impact

7.3.8 Photographic Instrumentation

Targets affixed to the displacement bars attached to the top, ground level and bottom of the barrier-coping section (see Figure 7.34) were used as reference points to determine angular and translational displacement of the barrier from analysis of high-speed video. The displacement bars were located at the target impact point and 10 in. (254 mm) downstream the joint between barriers segment 3 and 4. In the wall panels, the displacement bars were located the level of the first and second layer of the strip reinforcement. Unfortunately, the high speed video camera was triggered too early before impact and no information of the impact was recorded.

Figure 7.34 Location of displacement bars affixed on the barrier and panels.

7.3.9 Loads in the Strips from the Strain Gages

A total of 14 wall reinforcement strips were instrumented with four strain gages (two at the top and two at the bottom) to capture the tensile forces transmitted into the reinforcement during the vehicle impact. To enable comparison of forces and displacements, barriers and selected strip locations have been assigned alphanumeric designators that describe their horizontal position and vertical reinforcement layer. For example, strip "B4-E-1st" is positioned beneath the downstream end of the fourth barrier in the first (i.e., upper) layer of reinforcement as shown in Figure 7.35.

Raw data obtained from the strain gages on the strips were analyzed and the results are presented in Figure 7.36. The maximum 50-msec. average of the raw data was analyzed to obtain design loads for the strips, and the results are presented in Figure 7.37. A summary of the maximum dynamic loads measured in the strips is shown in Table 7.5.

The static load in the strips was measured during the construction to allow computation of the total load in the strips during impact. The average static load in the uppermost layer of reinforcement was 0.79 kips (3.51 kN) and the average static load in the second layer of reinforcement was 0.9 kips (4.01 kN). A comparison of the measured static loads with those calculated by AASHTO LRFD is shown in Table 7.6.

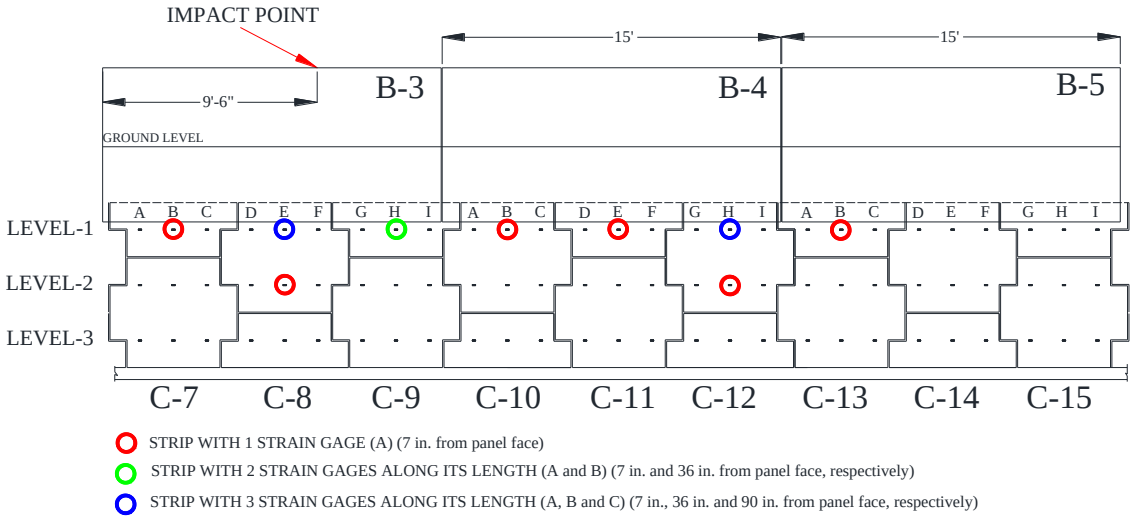

Figure 7.35 Location indicators for strain gages on the strips.

Table 7.7 shows the total measured load (measured static load + measured dynamic load) in the reinforcement strips in comparison to the calculated resistance of the strips using the AASHTO LRFD 11.10.6.3.2-1. The pullout resistance of the strip was calculated to 2.43 kips (10.8 kN) at uppermost layer of strips and 3.72 kips (16.55 kN) at the second layer.

Table 7.5 Measured dynamic loads on the soil reinforcing strips

Strip Section	Layer of soil reinforcement	Location from the panel face (in.)	Maximum load from raw data (kips)	Maximum load from 50 msec. ave data (kips)
B3_B_1st(A)	First	7	1.38	1.17
B3_E_1st(A)	First	7	1.61	1.47
B3_E_1st(B)	First	36	1.70	1.60
B3_E_1st(C)	First	90	1.45	1.30
B3_E_2nd(A)	Second	7	2.72	1.98
B3_H_1st(A)	First	7	1.44	1.35
B3_H_1st(B)	First	36	1.49	1.38
B4_B_1st(A)	First	7	0.44	0.38
B4_E_1st(A)	First	7	1.61	1.33
B4_H_1st(A)	First	7	0.44	0.42
B4_H_1st(B)	First	36	1.36	1.30
B4_H_1st(C)	First	90	1.29	1.23
B4_H_2nd(A)	Second	7	1.27	1.18
B5_B_1st(A)	First	7	1.56	1.51

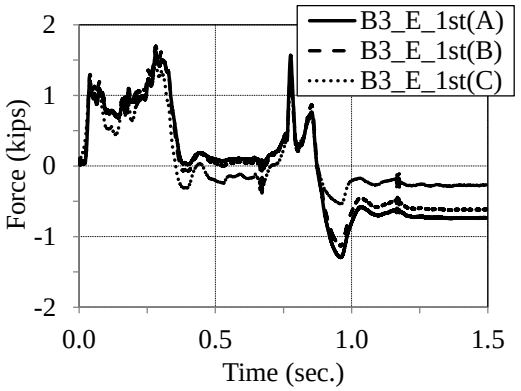

a) Strip section B3_E

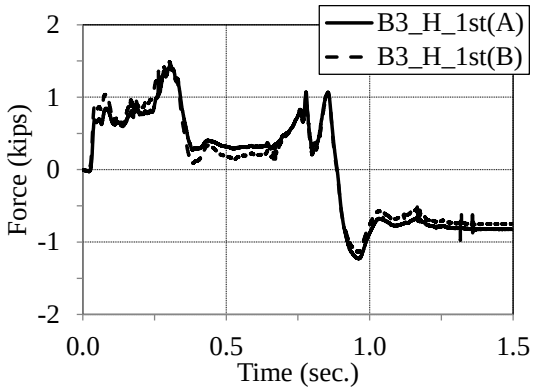

b) Strip section B3_H

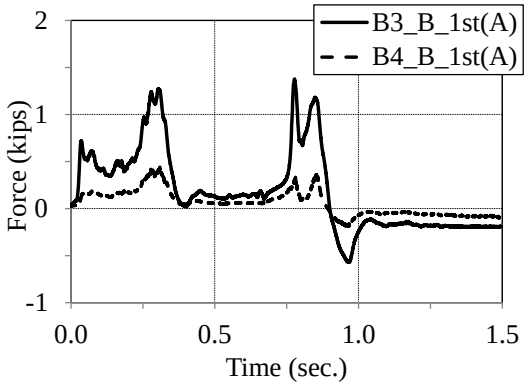

c) Strip section B3_B and B4_B

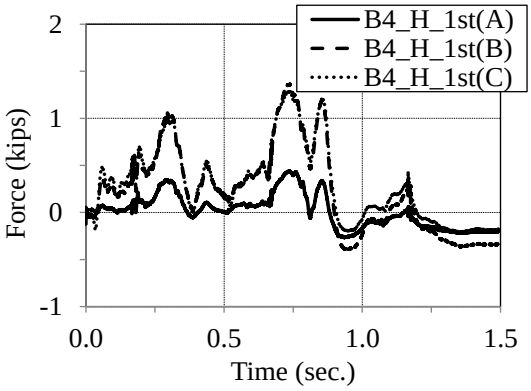

d) Strip section B4_H

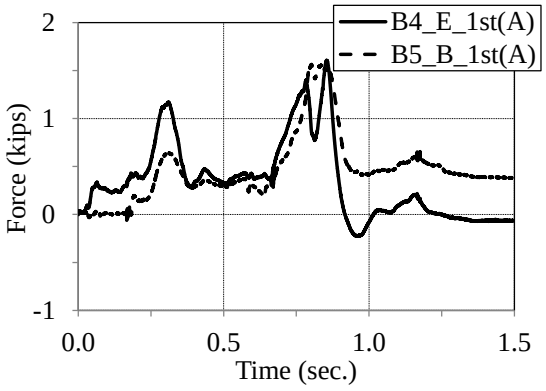

e) Strip section B4_E and B5_B

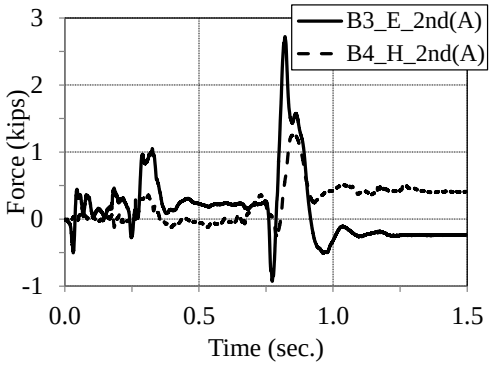

f) Second layer of strips

Figure 7.36 Dynamic load on the soil reinforcing strips (raw data)

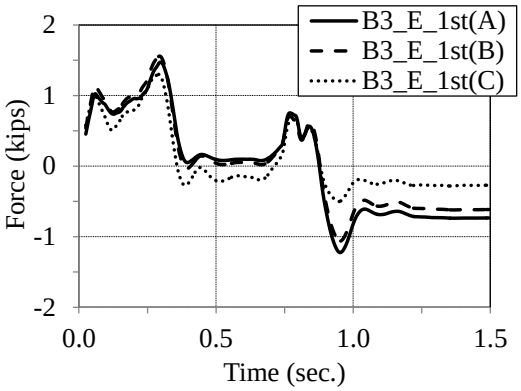

a) Strip section B3_E

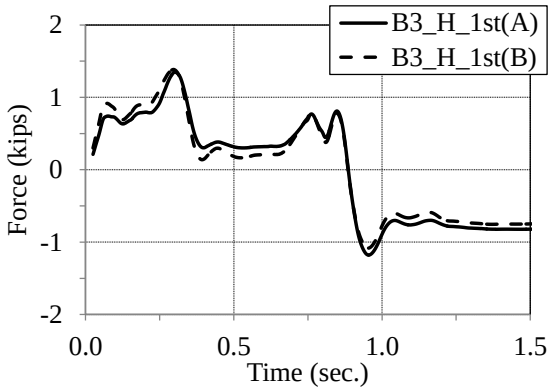

b) Strip section B3_H

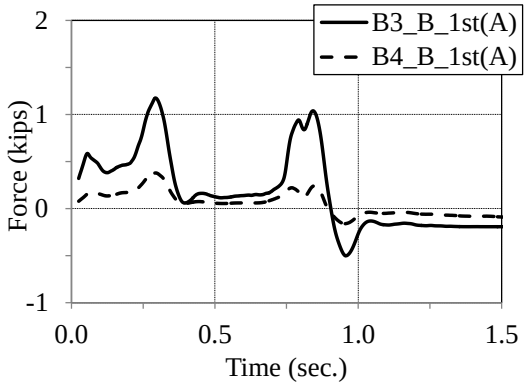

c) Strip section B3_B and B4_B

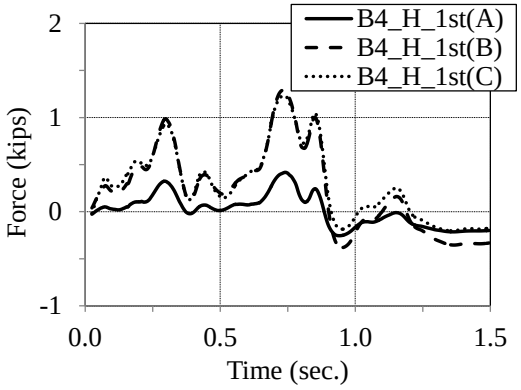

d) Strip section B4_H

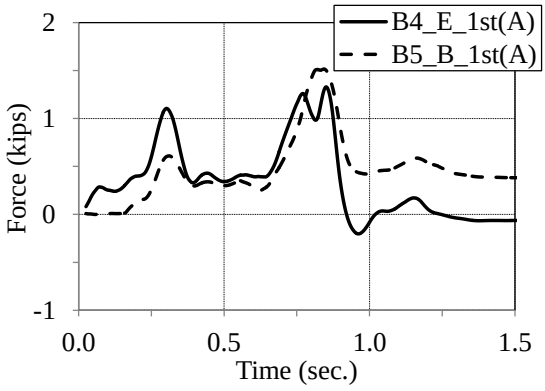

e) Strip section B4_E and B5_B

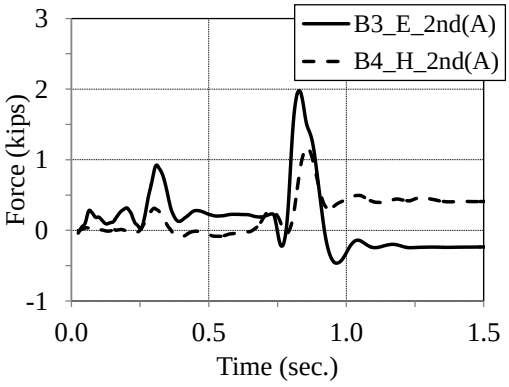

f) Second layer of strips

Figure 7.37 Dynamic load on the soil reinforcing strips (50 msec. average data)

Table 7.6 Static load on the soil reinforcing strips

	Static Load By measured (kips)	Static Load By AASHTO (kips)
Top Layer	0.79	0.82
Second Layer	0.90	1.35

Table 7.7 Total loads on the soil reinforcing strips

	Static Load By measured (kips)	Dynamic Load [(1)] By measured (kips)	Total Loads (kips)	Resistance By AASHTO[(2)] (kips)
Top Layer	0.79	1.60	2.39	2.43
Second Layer	0.90	1.98	2.88	3.72

[(1)] Maximum recorded load at the first layer (maximum 50-msec. average load).
[(2)] AASHTO LRFD 11.10.6.3.2-1

Two of the reinforcing strips were instrumented with three full-bridge strain gages located along its length at a distance of 7 in. (178 mm), 36 in. (914 mm) and 90 in. (2286 mm) from the face of the wall. Another strip was instrumented with two full-bridge strain gages located at a distance of 7 in. (178 mm) and 36 in. (914 mm) from the face of the wall. The objectives of these analyses were to determine the distribution of the dynamic load in the strips due to the TL-5 impact load. The results are shown in Figure 7.38. Notice that for strip sections B3_H and B4_H, the loads close to the wall panel and further down the strips were not significantly different. In strip section B4_H, the load close to the wall panel was very small when compare to the others. This may be

associated with bending of the strips during impact due to lose of contact between the coping of the barrier and the top of the sand layer.

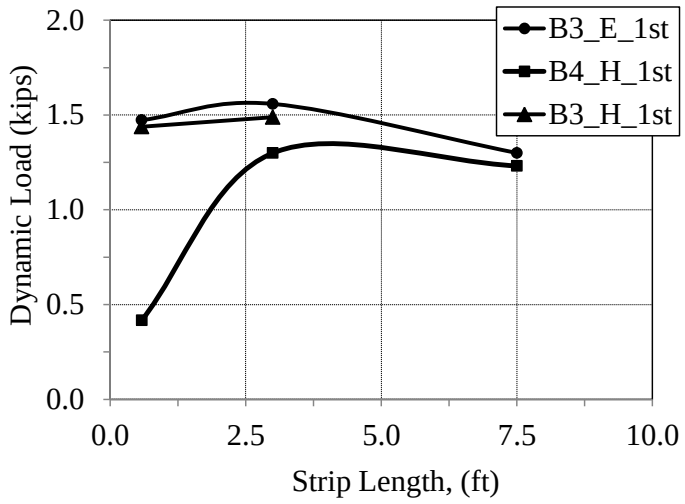

a) Measured Dynamic load

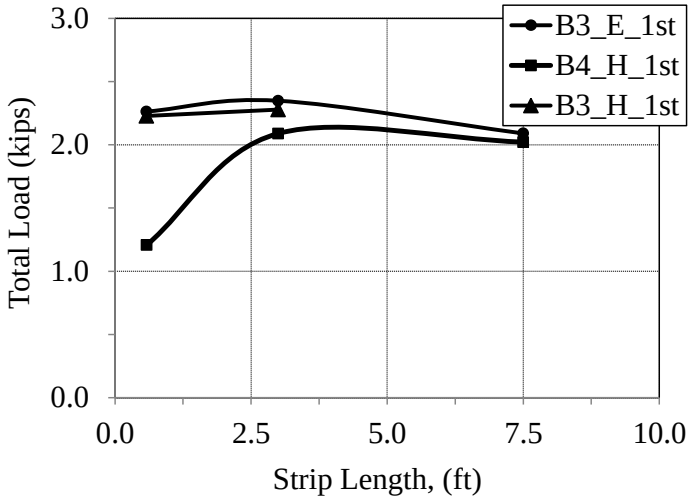

b) Measured dynamic load + measured static load

Figure 7.38: Dynamic load distribution in the strips by measured

7.3.10 Panel Analyses

The wall panels were not instrumented for the crash test. Upon completion of the test, a visual inspection was conducted to verify the structural integrity of the wall panels. Two of the full-section panels presented a hair-line crack at the level of the uppermost layer of strips, as shown in Figure 7.39.

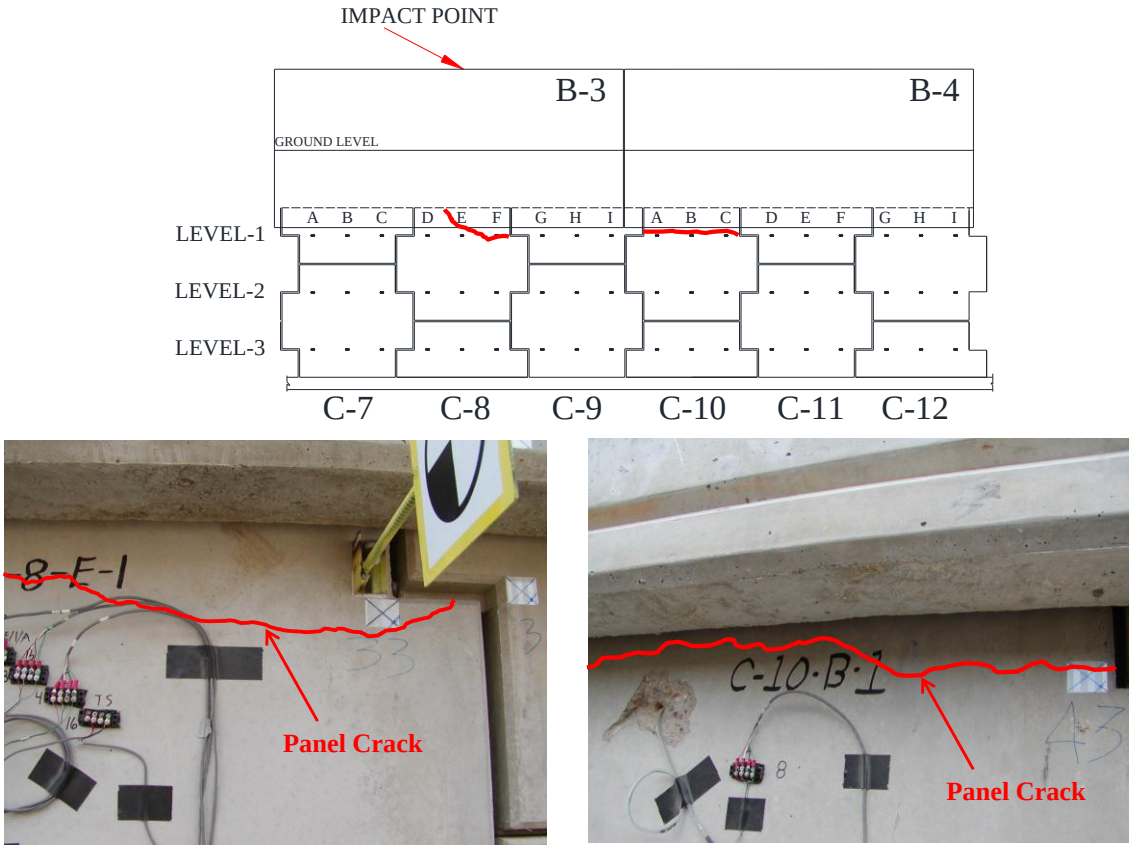

Figure 7.39 Hair-line crack in the panels after impact

In the full-panel section below barrier 3 (panel column C-8), the crack propagated from the edge of the panel to the coping section. In the full-panel section below barrier 4 (panel column C10), the crack propagated from one edge of the panel to the other and it was also close to the level of the first strip. However, the overall performance of the wall panels was satisfactory and no restoration will be required.

7.3.11 Other Instrumentation

Reflective targets were placed at different locations of the barriers (B2, B3, B4, and B5) and the wall panels to measure permanent deflection in the lateral, longitudinal and vertical direction after vehicle impact, as shown in Figure 7.40. The coordinates of each point, before and after impact, were determined using a total station. After vehicle impact, the lateral and total permanent deflection at the top of the barriers ranged from 0.12 in. (3 mm) to 1.17 in. (29.7 mm) and 0.18 in. (4.6 mm) to 1.22 in. (31 mm), respectively. At the bottom of the barriers, the lateral and total permanent deflection ranged 0.12 in. (3 mm) to 0.65 in. (16.5 mm) and 0.18 in. (4.6 mm) to 0.76 in. 19.3 mm), respectively. The maximum residual displacement occurred at the upstream end of barrier segment "B3", which was directly impacted by the vehicle. The magnitude of the displacement capture at each point is described from Figure 7.41 to Figure 7.44 and summarized in Table 7.8.

The lateral and total permanent defection of the wall panels ranged from 0.54 in. (13.7 mm) to 0.01 in. (0.25 mm) and 0.63 in. (16 mm) to 0.13 in. (3.3 mm), respectively.

The information is summarized in Figure 7.42 and Figure 7.43. Note that the wall panels, as well as the barriers, are moving in the longitudinal and vertical direction. Such movement may be the result of the barrier and the panels being loaded vertically and longitudinally while the vehicle was riding on top of the barrier during redirection. As described in section 3, the vertical load imposed by the tractor-van-trailer is significantly large due to deceleration imposed by the box of the trailer.

The barrier segments were positioned with a clear space of about ¾ in. (19.05 mm) to 1 in. (25.4 mm) between the through of the barrier and the wall panels to preclude transfer high impact loads into the wall panels. Therefore, the contact switch placed on the top edge of the level-up concrete on top of the wall panels inside the coping recess indicated that the coping did not contact the wall panel.

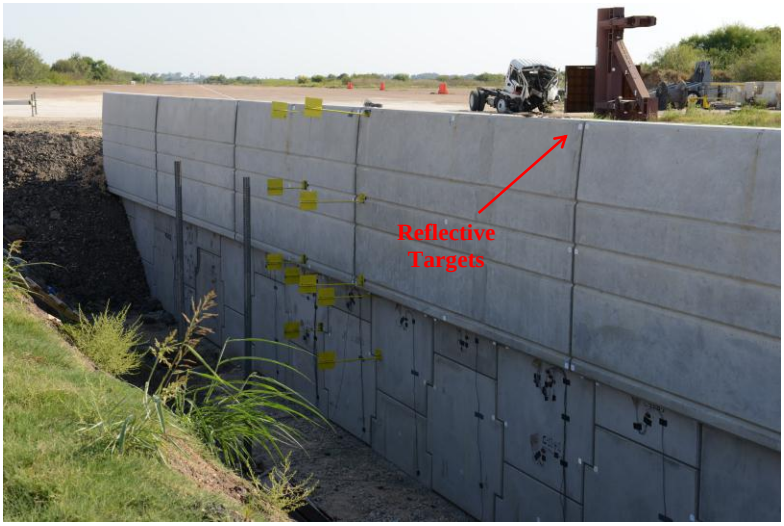

Figure 7.40 Reflective targets in the barrier and wall panel to measure permanent deflection

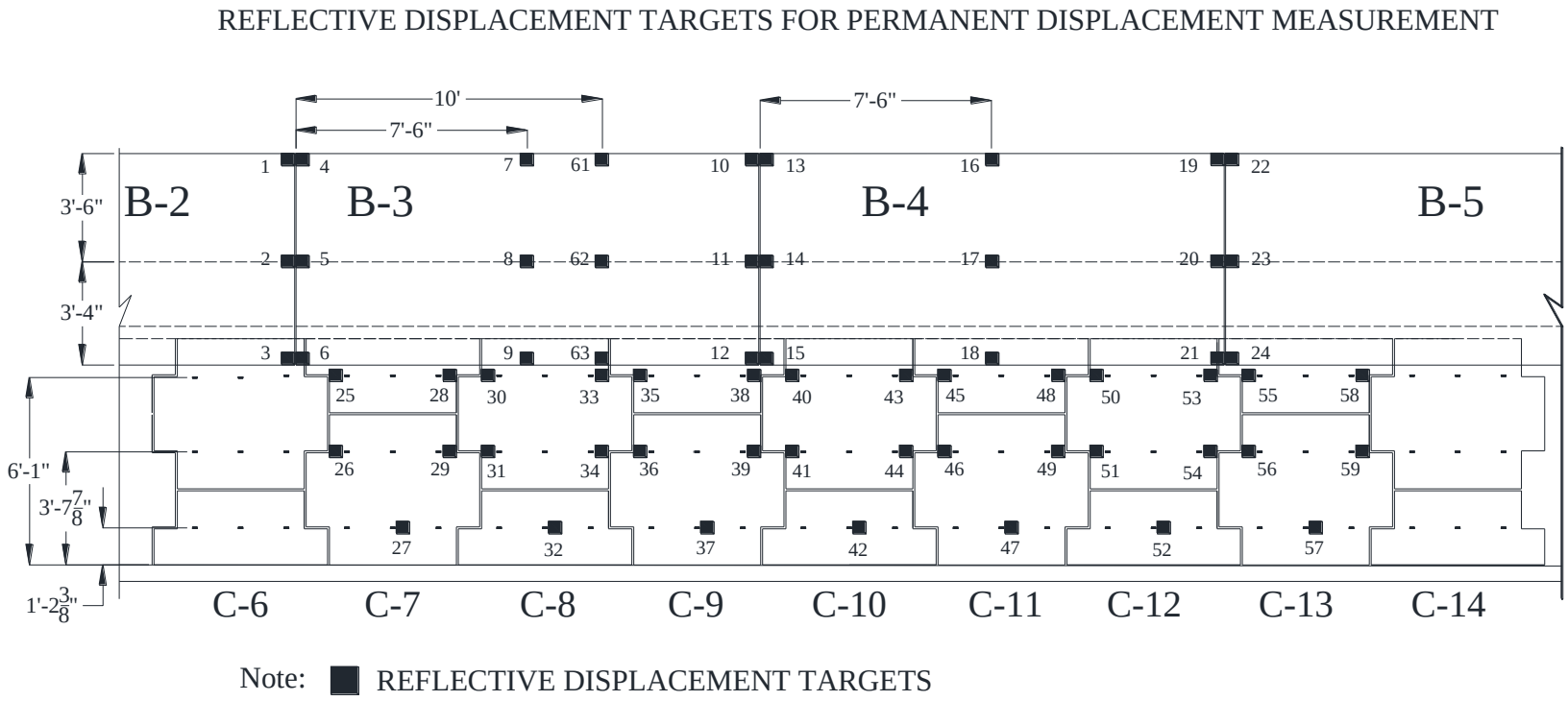

Figure 7.41 Location of the reflective displacement targets for measurement of permanent deflection

Table 7.8 Results of permanent deflection measurements

Permanent Displacement Measurement with Total Station									
Target Point	Δx (in.)	Δy (in.)	Δz (in.)	Total (in.)	Target Point	Δx (in.)	Δy (in.)	Δz (in.)	Total (in.)
1	0.1102	0.6680	0.1850	0.7018	32	0.0276	0.0682	0.2546	0.2650
2	0.1457	0.5748	0.1890	0.6224	33	0.0512	0.4094	0.3491	0.5405
3	0.1549	0.5341	0.1785	0.5841	34	0.0551	0.1509	0.3504	0.3855
4	0.0276	1.1732	0.3871	1.2358	35	0.0630	0.4265	0.3228	0.5386
5	0.0433	0.8858	0.3990	0.9725	36	0.0131	0.1286	0.2585	0.2891
6	0.0604	0.6549	0.3871	0.7631	37	0.0223	0.0866	0.2297	0.2465
7	0.0354	1.0564	0.3845	1.1248	38	0.0630	0.4698	0.2585	0.5399
8	0.0525	0.7428	0.4068	0.8485	39	0.0026	0.1247	0.2283	0.2602
9	0.0853	0.5394	0.3819	0.6664	40	0.0643	0.3228	0.2927	0.4405
10	0.0591	0.9291	0.3766	1.0043	41	0.0682	0.1614	0.2756	0.3266
11	0.0669	0.6063	0.4121	0.7361	42	0.0092	0.0420	0.2100	0.2143
12	0.0669	0.4134	0.3963	0.5766	43	0.0630	0.2428	0.3031	0.3935
13	0.0499	0.6654	0.3031	0.7329	44	0.0499	0.0997	0.2756	0.2973
14	0.0669	0.5551	0.3018	0.6354	45	0.0604	0.1890	0.2756	0.3396
15	0.0748	0.4423	0.2900	0.5341	46	0.0039	0.0433	0.1837	0.1888
16	0.0486	0.5276	0.2782	0.5984	47	0.0184	0.0276	0.1837	0.1867
17	0.0472	0.4003	0.2756	0.4883	48	0.0643	0.1168	0.2677	0.2991
18	0.0709	0.2375	0.2848	0.3775	49	0.0026	0.0315	0.1759	0.1787
19	0.0433	0.4331	0.2428	0.4984	50	0.0564	0.1903	0.2231	0.2986
20	0.0577	0.3123	0.2454	0.4014	51	0.0407	0.0971	0.2218	0.2455
21	0.0879	0.1601	0.2454	0.3059	52	0.0079	0.0105	0.1706	0.1711
22	0.0577	0.1168	0.1365	0.1887	53	0.0538	0.1352	0.2100	0.2555
23	0.0276	0.1430	0.1129	0.1843	54	0.0604	0.0223	0.2060	0.2159
24	0.0249	0.1299	0.1207	0.1791	55	0.0459	0.1483	0.2021	0.2548
25	0.0512	0.4199	0.3793	0.5682	56	0.0039	0.0354	0.1601	0.1640
26	0.0472	0.1417	0.2257	0.2707	57	0.0013	0.0289	0.1234	0.1267
27	0.0013	0.0446	0.2756	0.2792	58	0.0577	0.0801	0.1260	0.1600
28	0.0184	0.3793	0.3806	0.5376	59	0.0026	0.0328	0.1129	0.1176
29	0.0249	0.0984	0.2979	0.3147	61	0.0591	1.0276	0.3885	1.1001
30	0.0656	0.5367	0.3320	0.6345	62	0.0433	0.6732	0.4108	0.7898
31	0.0394	0.1706	0.3465	0.3882	63	0.0591	0.3924	0.4252	0.5816

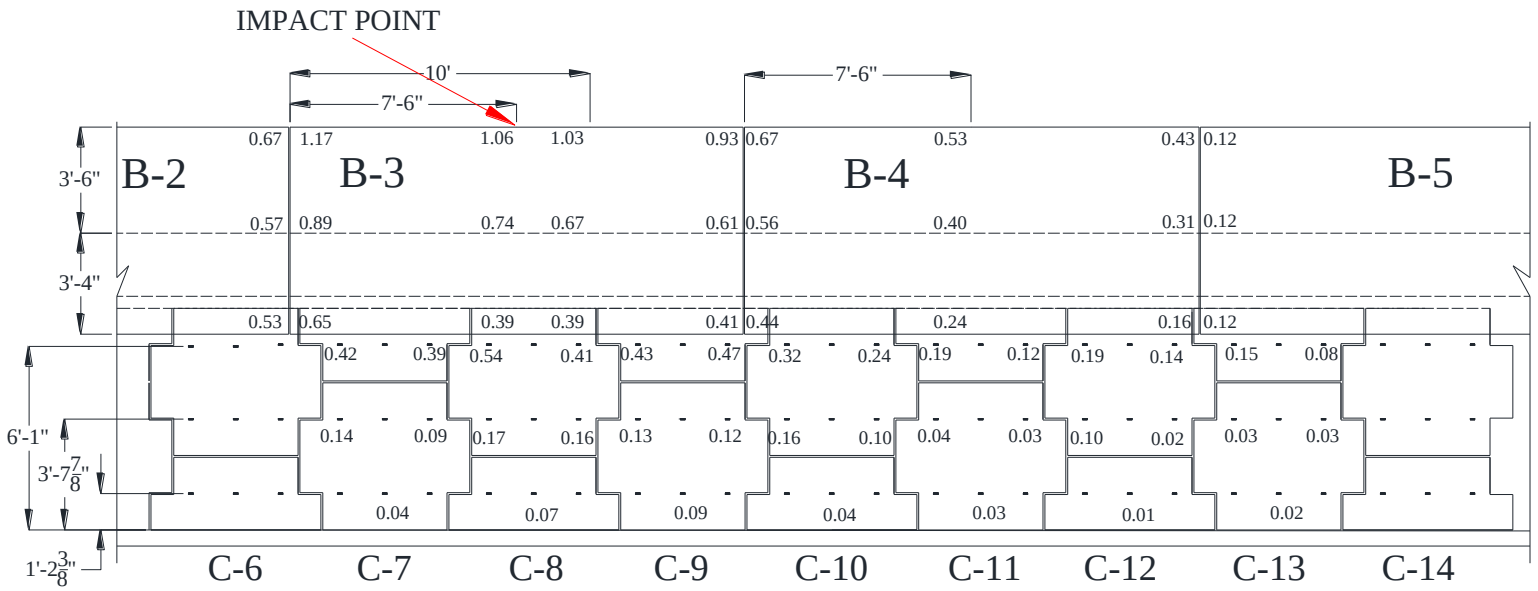

Note: Displacement in inches

Figure 7.42 Lateral permanent deflection at the selected targets

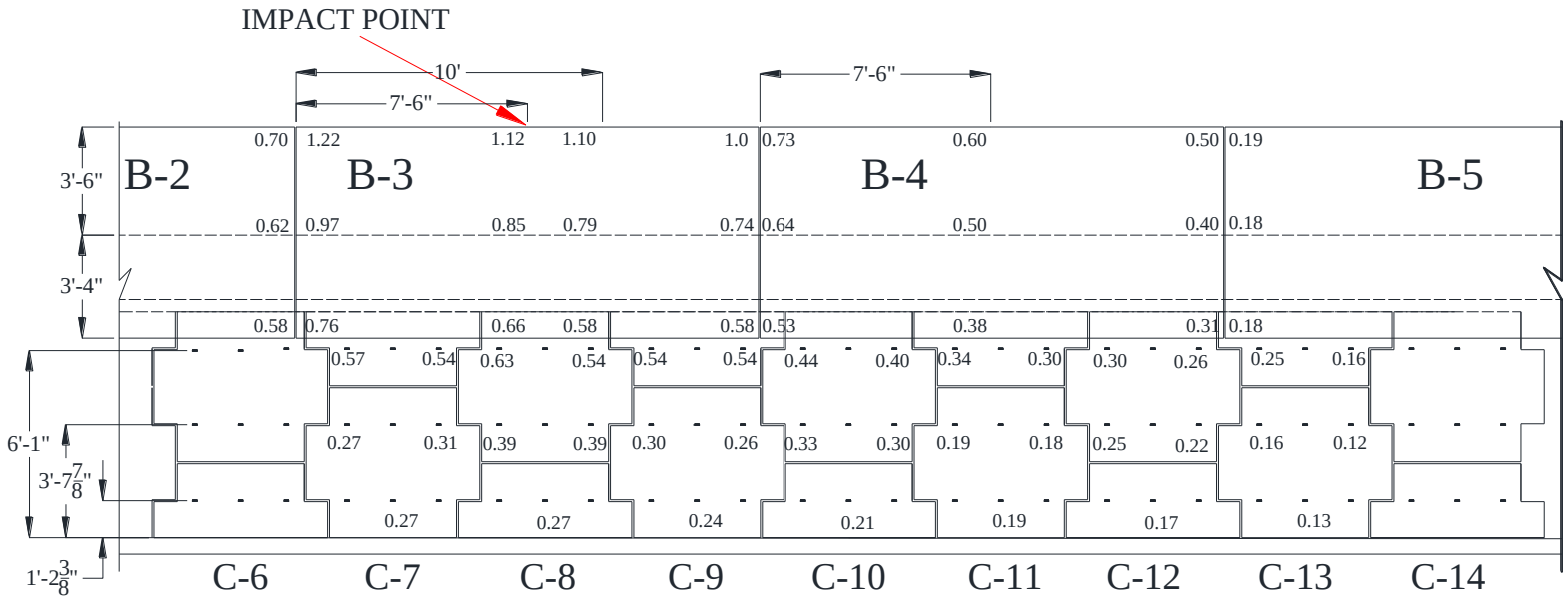

Note: Displacement in inches

Figure 7.43 Total permanent deflection at the selected targets

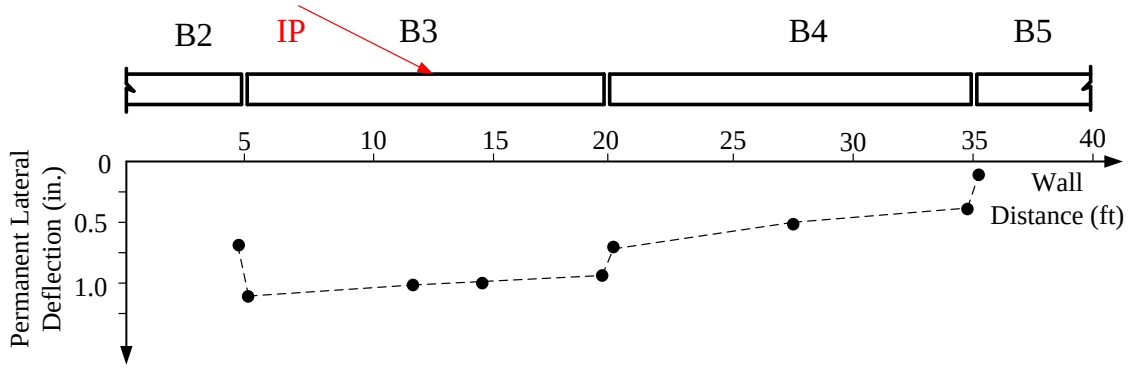

a) Top of the barriers

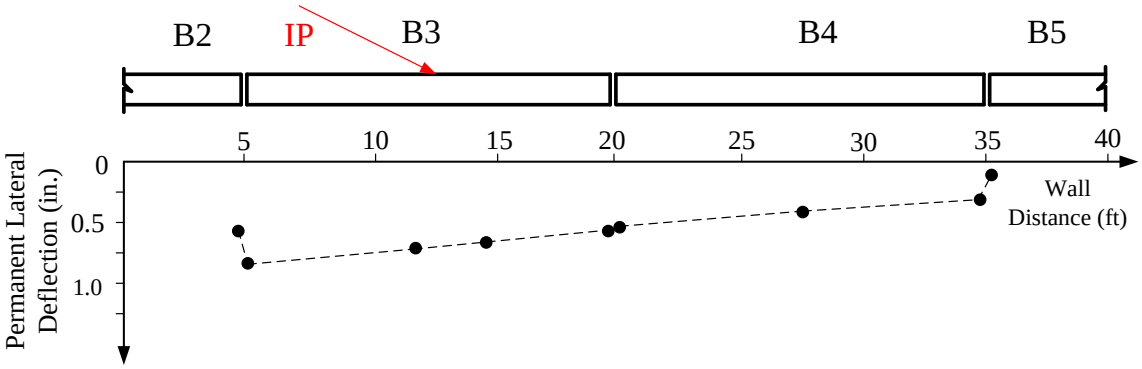

b) Ground level

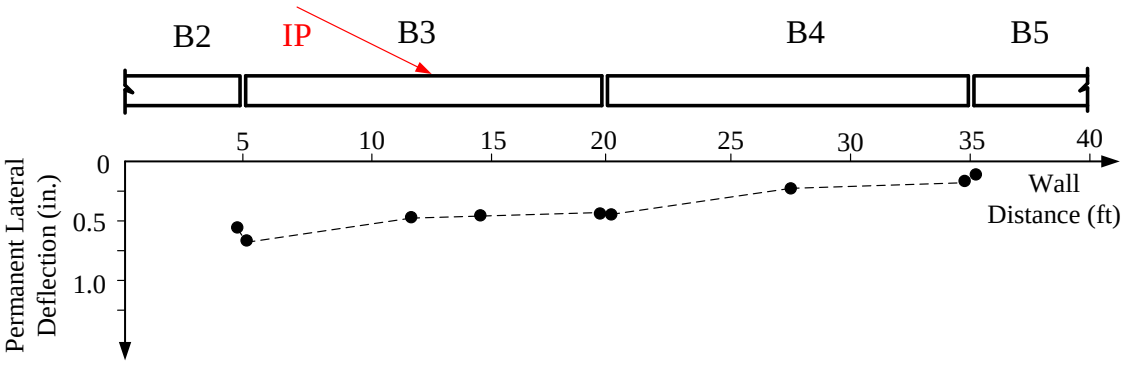

c) Bottom of the barriers

Figure 7.44 Sketch of lateral permanent deflection at the impacted area

7.3.12 Damage of Moment Slab After Test

After the crash test, the overburden soil was removed to permit inspection of the moment slab and the connection between the coping and moment slab. No structural cracks were observed during the inspection. However, there was loss of adherence at the connection between barrier segment 3 and the moment slab as shown in Figure 7.45.

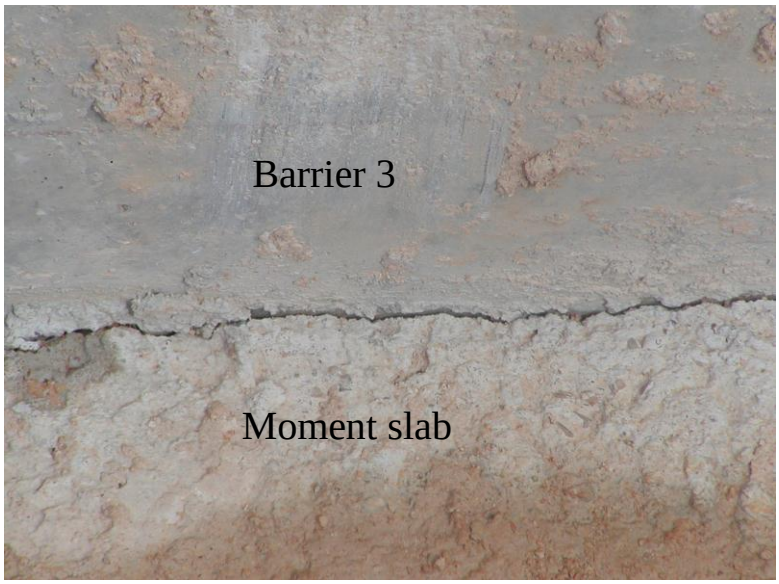

Figure 7.45 Structural integrity of the moment slab after impact

7.4 Conclusions

The roadside barrier mounted on the edge of the MSE wall performed acceptably according to the evaluation criteria specified for MASH test designation 5-12, as shown in Table 7.9. The roadside barrier on MSE wall contained and redirected the 36000V vehicle. The vehicle did not penetrate, underride, or override the installation. No significant lateral movement of the barrier was noted. No detached elements, fragments, or other debris was present to penetrate or show potential for penetrating the occupant compartment, or to present hazard to others in the area. The 36000V vehicle remained upright during and after the collision event.

Table 7.9 Performance evaluation summary for MASH Test 5-12 on the MSE Wall

Test Agency: Texas Transportation Institute Test No.: 478130 Test Date: 2012-09-26

MASH Evaluation Criteria	Test Results	Assessment
Structural Adequacy A. Test article should contain and redirect the vehicle or bring the vehicle to a controlled stop; the vehicle should not penetrate, underride, or override the installation although controlled lateral deflection of the test article is acceptable	The roadside barrier on MSE wall contained and redirected the 36000V vehicle. The vehicle did not penetrate, underride, or override the installation. No significant lateral movement of the barrier was noted.	Pass
Occupant Risk D. Detached elements, fragments, or other debris from the test article should not penetrate or show potential for penetrating the occupant compartment, or present an undue hazard to other traffic, pedestrians, or personnel in a work zone.	No detached elements, fragments, or other debris was present to penetrate or show potential for penetrating the occupant compartment, or to present hazard to others in the area.	Pass
Deformations of, or intrusions into, the occupant compartment should not exceed limits set forth in Section 5.3 and Appendix E of MASH.	No occupant compartment deformation occurred	Pass
G. It is preferable, although not essential, that the vehicle remain upright during and after collision.	The 36000V vehicle remained upright during and after the collision event.	Pass

7.5 Comparison of Test and Simulation

A comparison between the results of the full-scale TL-5 crash test and the numerical simulations was conducted to establish confidence in the simulation for use in the guideline development process. Since the numerical simulation was conducted prior to performing the TL-5 crash test, the differences between the TL-5 test and simulation are listed below. These items may explain some of the differences observed between the full-scale test and the full-scale numerical simulation.

1. The MSE wall model was two full panels high (10 ft or 3.05 m) while the test used a wall that was one and half panels high (7.5 ft (2.29 m)) as shown in Figure 7.46. However, the results of the simulation indicate that the load in the fourth layer of soil reinforcing strips was negligible.
2. The 36000V vehicle model used in the simulation has concrete barriers as ballast while the test vehicle used concrete channel-shaped blocks. This could affect the magnitude of the impact load imposed to the barrier between the test and vehicle model. However, the differences should not be significant.
3. The coping detail of the barrier differed between model and test installation. The horizontal gap between the throat of the precast barrier and the back face of the panels in the test was 0.75 in. (19.05 mm) while in the simulation was 1.5 in. (38.1 mm). However, this should not affect the results since the coping of the barrier did to contact the wall panels.

a) Full-scale MSE wall and vehicle set-up

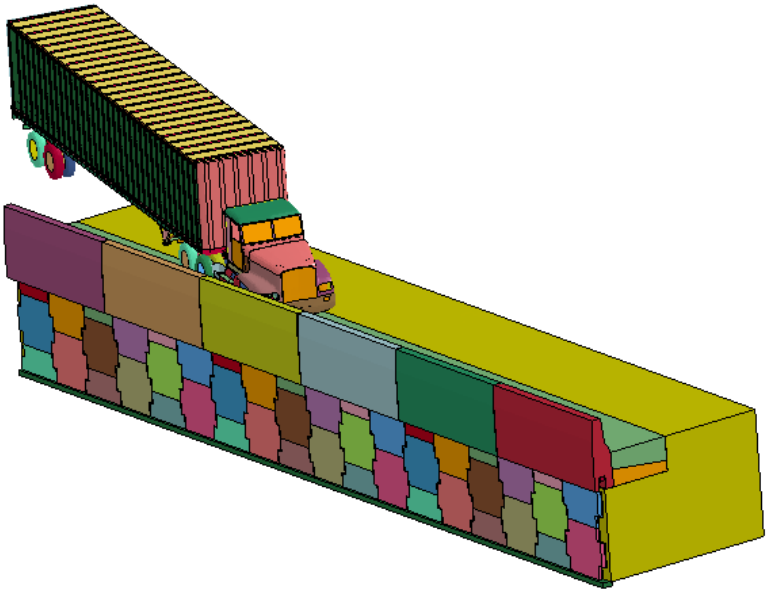

b) Full-scale MSE wall model and vehicle set-up

Figure 7.46 Comparison of the full-scale test installation and the full-scale FE model

4. The leveling concrete pad was modeled in accordance with standard practice using a weak material to allow it to break, or deform, in case the wall panels experience relative movements. However, in the test installation, the concrete leveling pad was built with a concrete compressive strength of 4000 psi (27.6 MPa). This may explain some of the difference between lateral movement in the simulation and in the test.
5. The tractor FE model and the trailer FE model were developed based on Freightliner FLD 120 and Stoughton (48 ft (14.63 m) long) model, respectively. The tractor and the trailer used in the test were a 2000 Sterling TF model and 1997 Strick (48 ft (14.63 m) long) van-trailer, respectively. Therefore, there were some differences in dimension between the test vehicle and the FE model.

A quantitative evaluation was conducted based on a comparison of the acceleration-time histories, loads and displacements collected in the model to those collected in full-scale crash test. In the qualitative assessment, the general response of the FE model compared reasonable well to the full-scale crash test. The model results replicated the basic timing and magnitudes of phenomenological events that occurred in the full-scale test. A comparison of sequential views of the test and simulation showed that the attitudes (e.g., roll and pitch) of both the tractor and the semitrailer models were consistent with the behavior of the vehicle in the full-scale crash test, as shown in Figure 7.47 .

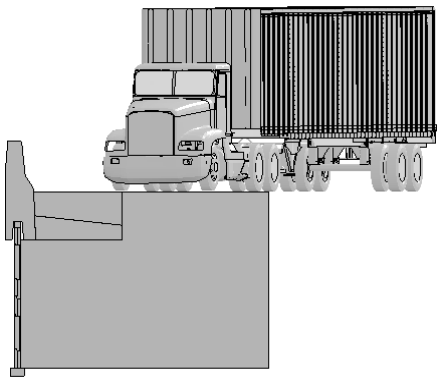

a) Pre-impact time position

b) Pre-impact time position

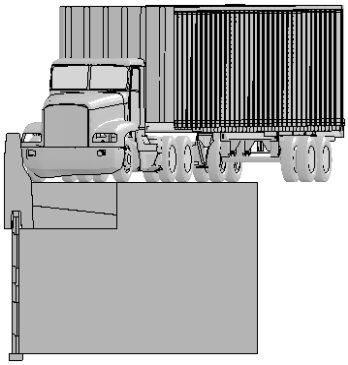

c) Initial impact (t=0 sec.)

d) Initial impact (t=0 sec.)

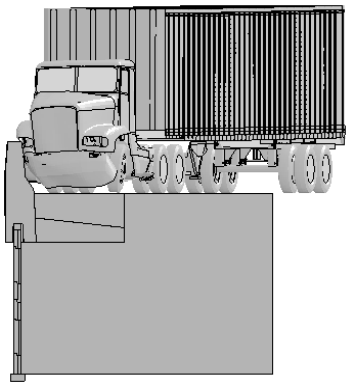

e) First peak load (t=0.07 sec.)

f) First peak load (t=0.07 sec.)

Figure 7.47 Comparison of vehicle position at each significant time

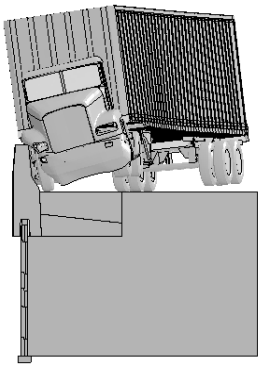

g) Second peak load (t=0.26 sec.) **h) Second peak load (t=0.26 sec.)**

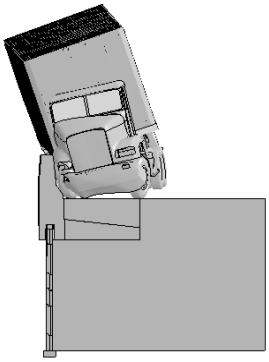

i) Third peak load (t=0.74 sec.) **j) Third peak load (t=0.74 sec.)**

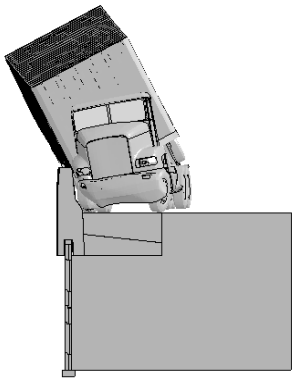

k) Max. strip load (t=0.84 sec.) **l) Max. strip load (t=0.84 sec.)**

Figure 7.47 Continued

The acceleration time-histories collected at the rear tandem location on the trailer and semitrailer model seemed to compare reasonably well to those from test, particularly regarding the maximum peak in the lateral acceleration-time-history of the trailer which corresponded to the highest lateral load on the barrier. However, the simulation showed significant peaks in the lateral acceleration time-history that did not appear in the test results. These peaks were related to the tire/suspension response of the trailer *(41)*. For example, at the rear tandem axles of the tractor, the maximum 50 msec. average acceleration in the longitudinal and lateral direction were -2.1 g's and -5.3 g's for the model and -1.4 g's and -4.4 g's for the test, respectively (Figure 7.48). At the rear tandem axles of the trailer, the maximum 50 msec. average acceleration in the longitudinal and lateral direction were -2.7 g's and -11.6 g's for the model and -3.4 g's and -10.8 g's for the test , respectively (Figure 7.49).

The time history of the impact load from the test vehicle was estimated using the results of the acceleration data and the test inertial measurements of the tractor and the trailer. The load was computed using the equation of motion, as described in section 3. The result was then compared with the contact force obtained from the numerical simulation, as shown Figure 7.50. Figure 7.50 shows that the times history compared reasonably well in timing and magnitude. The data from the test shows some peaks loads that did not appear in the simulation data.

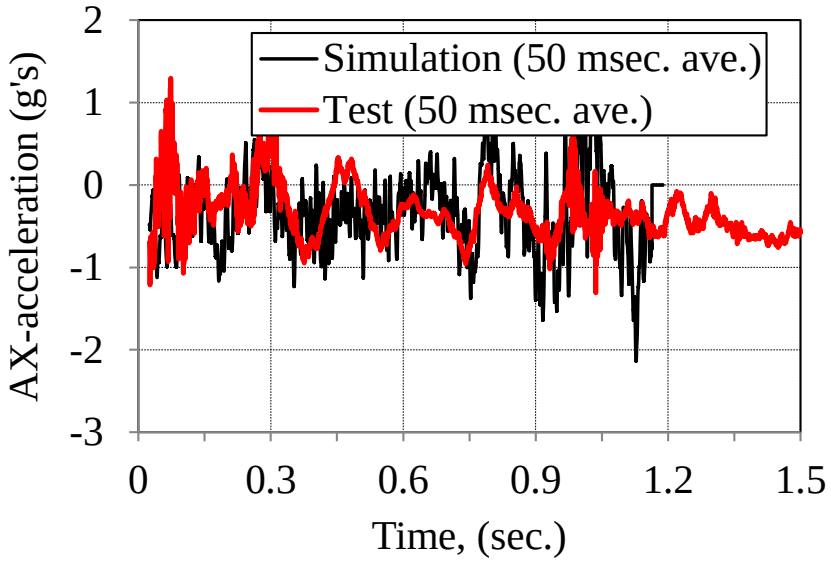

a) AX direction

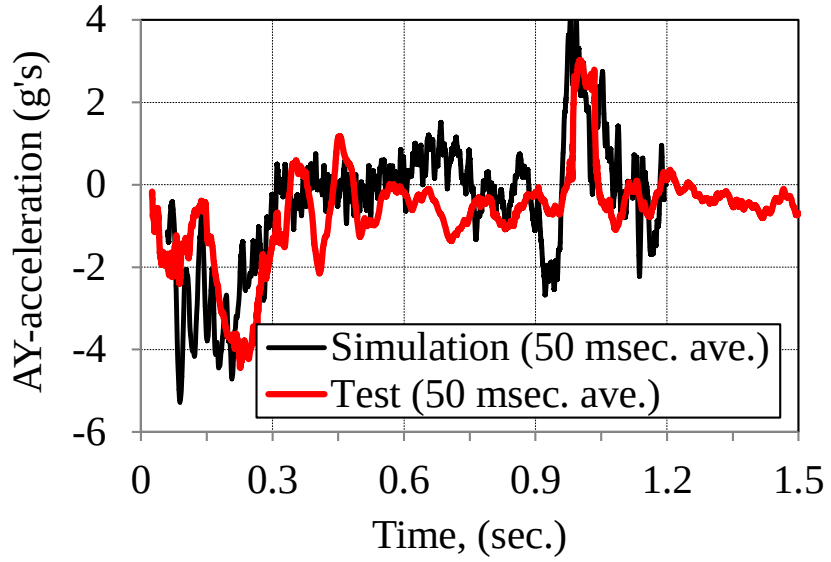

b) AY direction

Figure 7.48 Comparison of the tractor acceleration between test and simulation

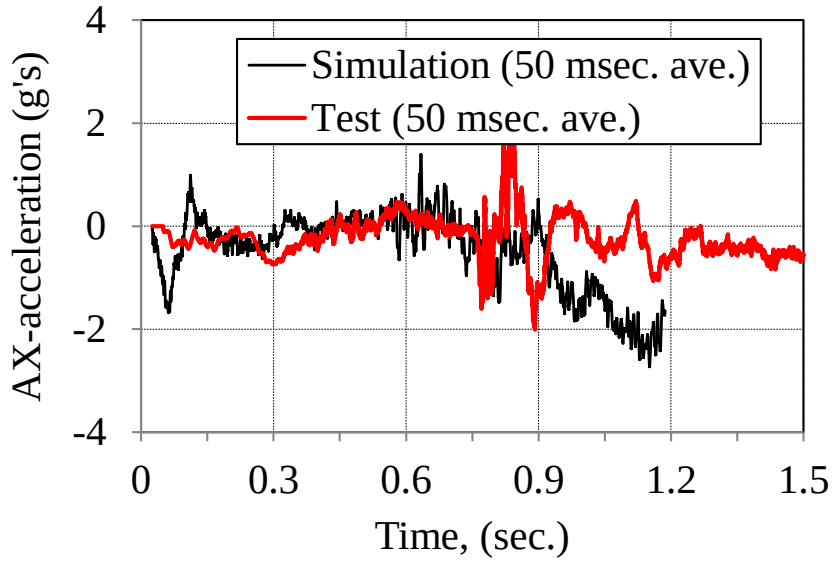

a) AX direction

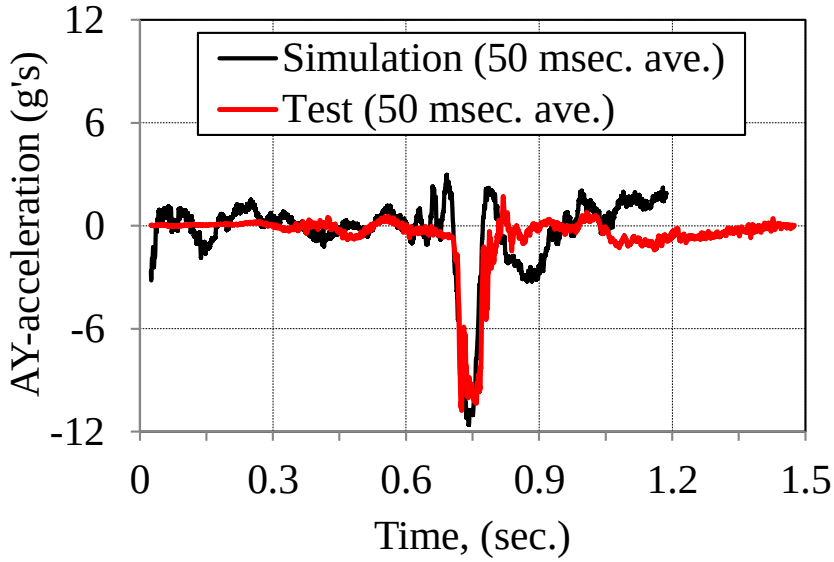

b) AY direction

Figure 7.49 Comparison of the trailer acceleration between test and simulation

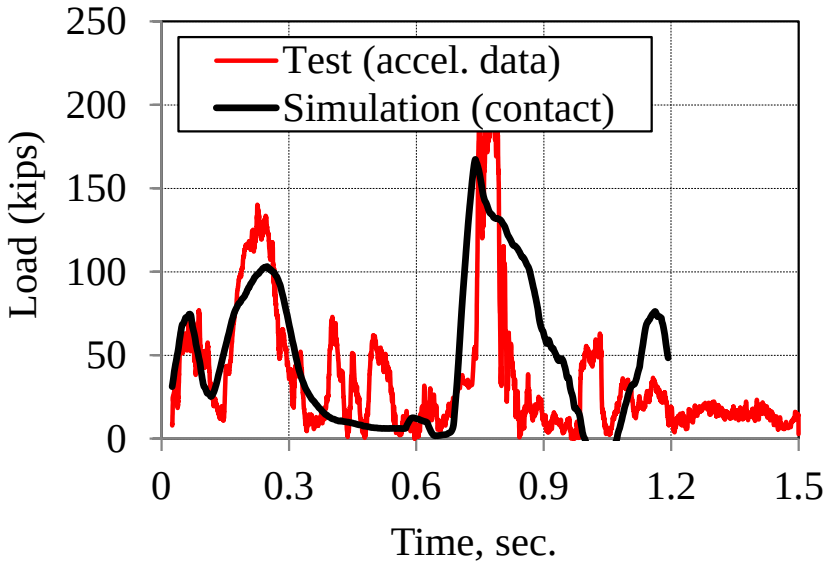

Figure 7.50 Comparison of time-history impact load in the test and simulation

The measured permanent displacements at the barriers were compared with the permanent displacement obtained from the numerical simulation. The information is summarized in Table 7.10. The simulation predict the permanent displacement of the barrier reasonable well except for the top of barrier segment 3 and the bottom of barrier segment 4 which were within 25% difference.

Table 7.10 Comparisons between measured and simulated displacement in the barriers

	Barrier 3 (Impact Point)			Barrier 4 (Joint)		
	Top (in.)	Ground Level (in.)	Bottom (in.)	Top (in.)	Ground Level (in.)	Bottom (in.)
Measured	1.06	0.74	0.40	0.67	0.56	0.44
Simulated	0.85	0.65	0.53	0.63	0.62	0.60

The dynamic displacements at the wall panels could not be measured due to problems in the instrumentation. The lateral permanent deflection, measured using a total station, ranged from 0.01 in. (0.25 mm) to 0.54 in. (13.72 mm). The dynamic and permanent deflection determined from the FE analyses ranged from .01 in. (0.25 mm) to 0.58 in. (14.73 mm) and from 0.01 in. (0.25 mm) to 0.28 in. (7.11 mm), respectively. The results of the simulation underpredict the permanent displacement in some wall panels but predict others reasonable well.

In addition, the simulation analyses predicted high bending stresses of the panels located underneath the impact point. After the test, the full-section panel located below the impact point (B3_DEF) and the full-panel section below barrier-segment 4 (B4_ABC) showed a thin hair-line crack across the section. These cracks were observed at the back side of the wall. No inspection was conducted at the traffic side of the panel but it is presumed that the crack propagated from the inside face of the panels.

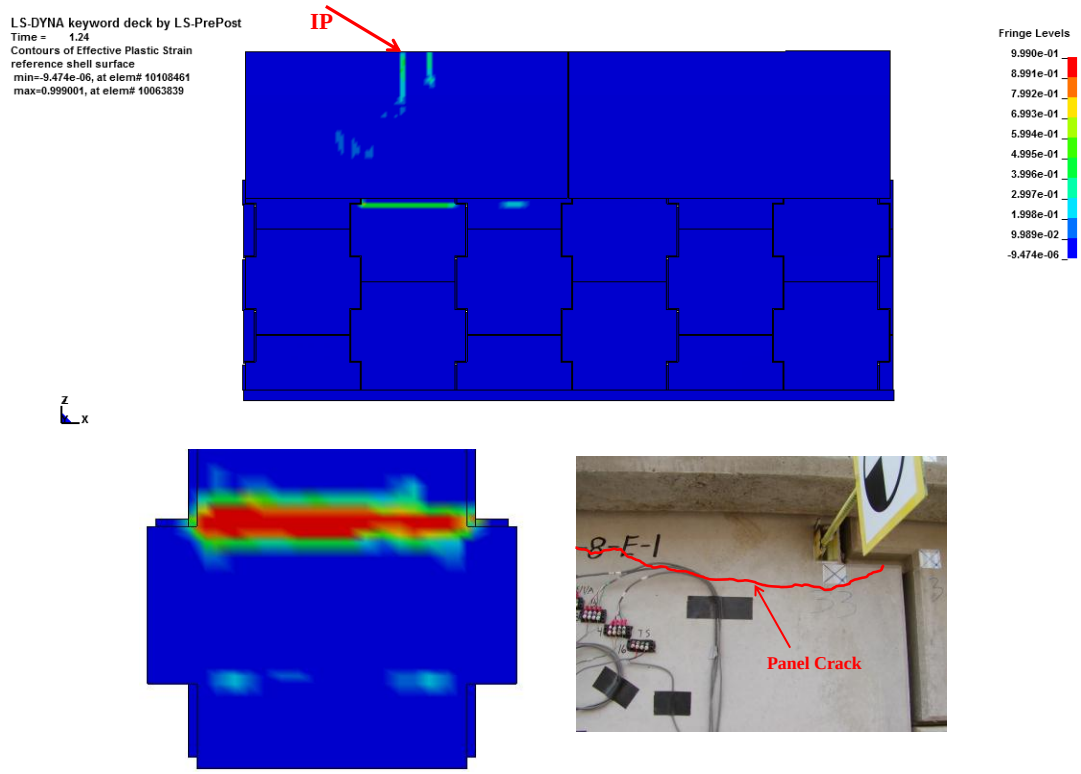

Figure 7.51 Comparison of panel analyses between test and simulation

The simulated average static load in the soil reinforcing strips was subtracted from the simulated total strip load to provide the dynamic load component due to the impact load. The simulation overpredicted the maximum strip load in the upper layer of reinforcement but captured the trends in the load-time history of the strip (Figure 7.52). Some peak loads shown in the simulation were not measured during the test. In the second layer of strips, the simulation results and the test results compared reasonable well, as shown in Figure 7.53.

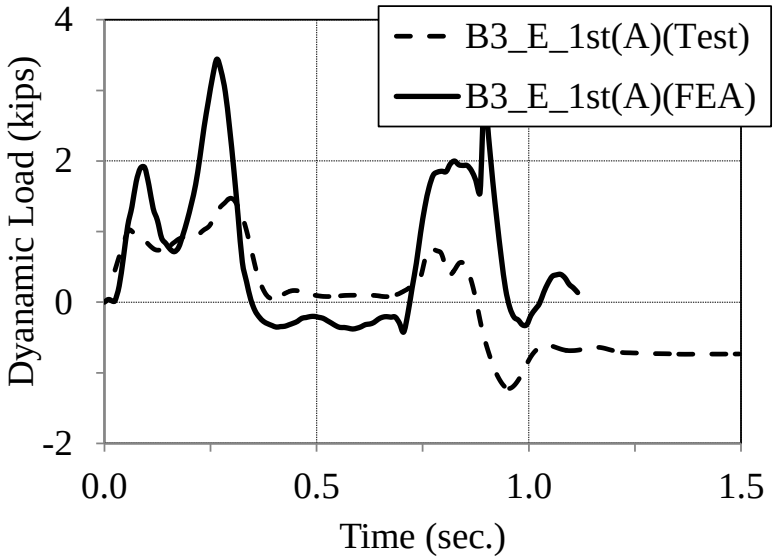

a) Strip section B3_E

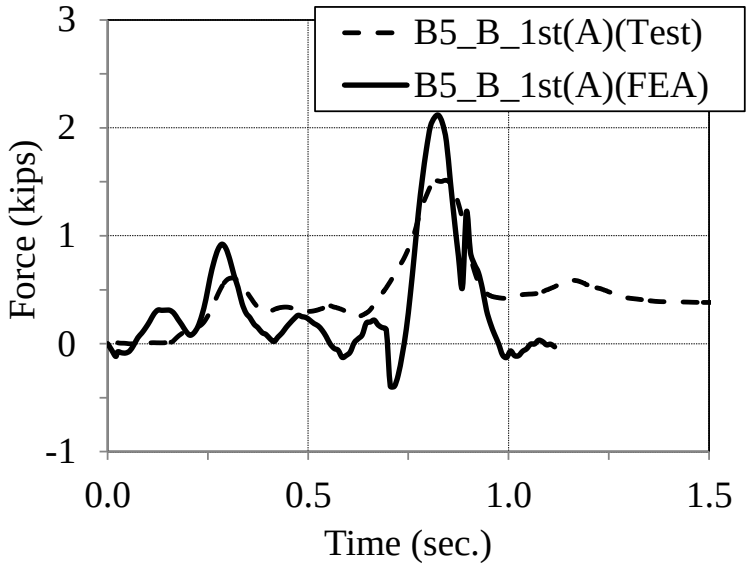

b) Strip section B5_B

Figure 7.52 Comparison of strips loads at the upper most layer of soil reinforcement

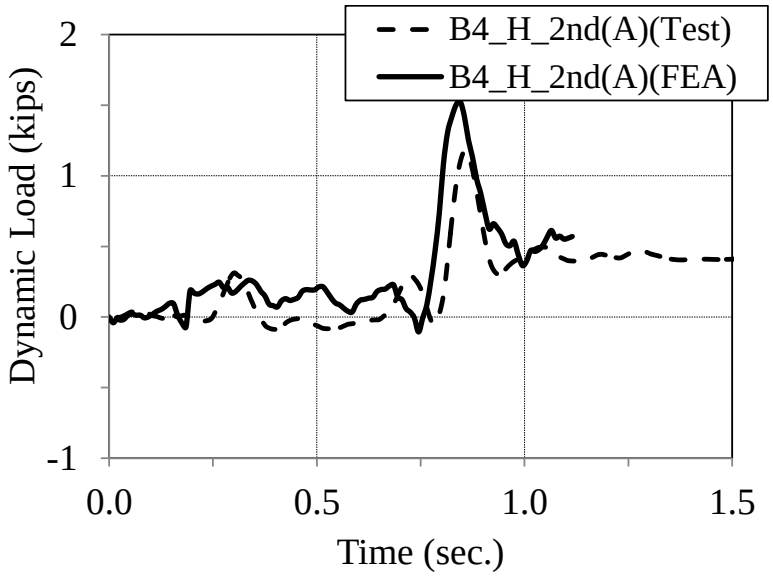

a) Strip section B4_H

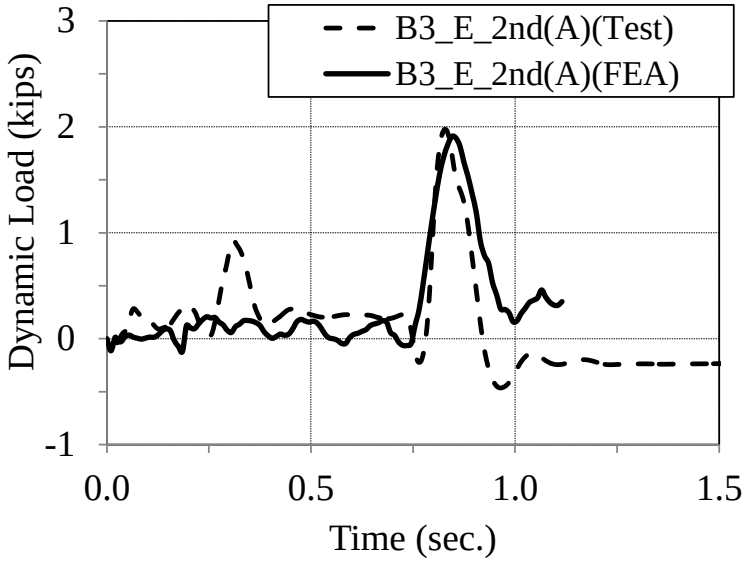

b) Strip section B4_E

Figure 7.53 Comparison of strips loads at the second layer of soil reinforcement

8 TL-5 STATIC LOAD TEST ON BARRIER-MOMENT SLAB SYSTEM

Upon completion of the full-scale crash test, a static load test was conducted on the barrier-moment slab system (section B5-B6) of the MSE wall test installation. The objective of the static test study was to assess the equivalent static load of the same TL-5 barrier-moment slab system used for the full-scale dynamic test.

8.1 Static Analytical Solution

The first part of the study was to estimate the force required to generate sliding (F_s) and overturning (F_o) of the barrier-moment slab system using equilibrium equations. These forces were computed using Eq. (8-1) for sliding and Eq. (8-2) for overturning, as described in section 4:

$$F_s = W \tan \phi_r + f_r A_s \tag{8-1}$$

$$F_o = \frac{Wl + f_r A_s \times x_s}{h} \tag{8-2}$$

The results of the analyses are summarized in Table 8.1. The analytical solution shows that the sliding and overturning resistance of the system, including the soil resistance, are similar in magnitude when the soil resistance is considered. Therefore, it is difficult to predict which failure mode will occur first.

Table 8.1 Results of the analytical solution of the TL-5 test barrier-moment slab system

Test Level	W (kips)	Moment Arms around Rotation Point B		Sliding Analyses		Overturning Analyses	
						Rotation Point B	
		l_B (in.)	h_B (in.)	F_S (kips)	F_{s+soil} (kips)[1]	F_o (kips)	F_{o+soil} (kips)
TL-5-1	128.6	34.5	59.3	86	90.5	74.8	93.3

[1] Strength of the soil was only considered at the side faces of the moment slab and not at the front. The value was 126 psf as backcalculated from NCHRP Report 663.

8.2 Quasi-Static FE Analyses

To further study of the static response of the system, a FE model analyses was conducted on the barrier-foundation portion of the MSE wall model. The shear dowels connecting the barrier-moment slab systems were removed to isolate the different sections. The interface between the soil and the moment slab were modeled using contact to capture the force generated between the soil and the moment slab. The analyses was conducted by applying a prescribed displacement to a wood block that was used as a means of providing distribution of the applied controlled quasi-static loading definition. The displacement was applied at a very low rate to reduce the inertia effects. The length of the wood block was 10 ft (3.05 m) as recommended in section 3 for the TL-5 load distribution in the longitudinal direction (Figure 8.1). The load was applied at an

effective height of 34 in. (864 mm) from the riding surface. The set-up of the quasi-static FE model is shown in. The analysis was conducted using as a reference the point of contact between the barriers and the panels (rotation point B).

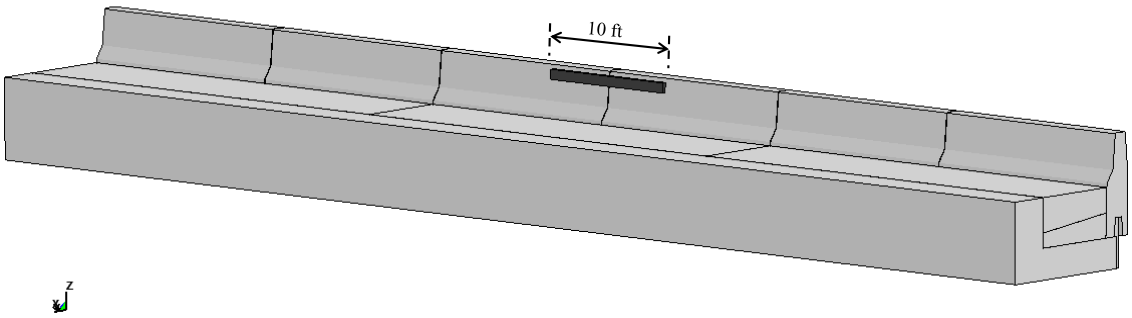

a) Longitudinal distribution of the quasi-static load

Figure 8.1 Quasi-static FE analyses set up for the test barrier-moment slab system

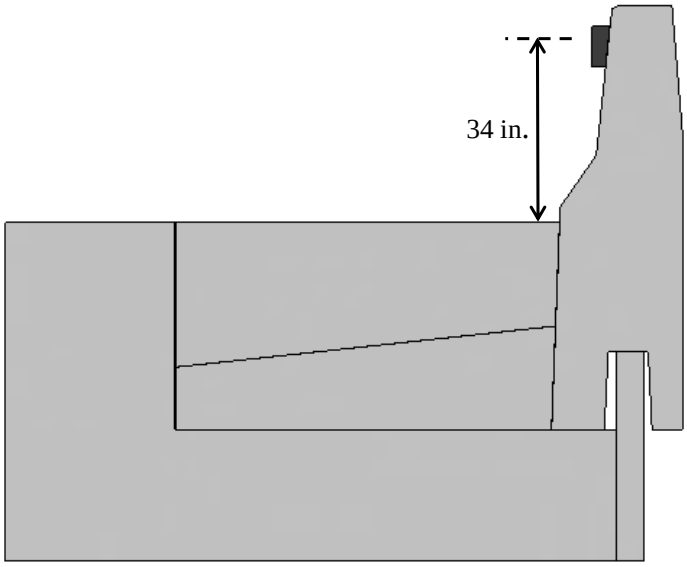

b) Application height of the quasi-static load

Figure 8.1 Continued

The result of the quasi-static FE analyses is presented in Figure 8.2. Although the primary failure mode of the barrier-foundation system is overturning, the system also slides considerable. This result is highly dependent in the friction developed at the interface between the coping and the concrete leveling pad. The simulation indicates that the ultimate load should be reached at about 100 kips (445 kN). At this load level, the displacement of the barrier at the top, ground surface level and bottom are 0.65 in. (16.51 mm), 0.43 in. (7.62 mm) and 5.84 mm), respectively.

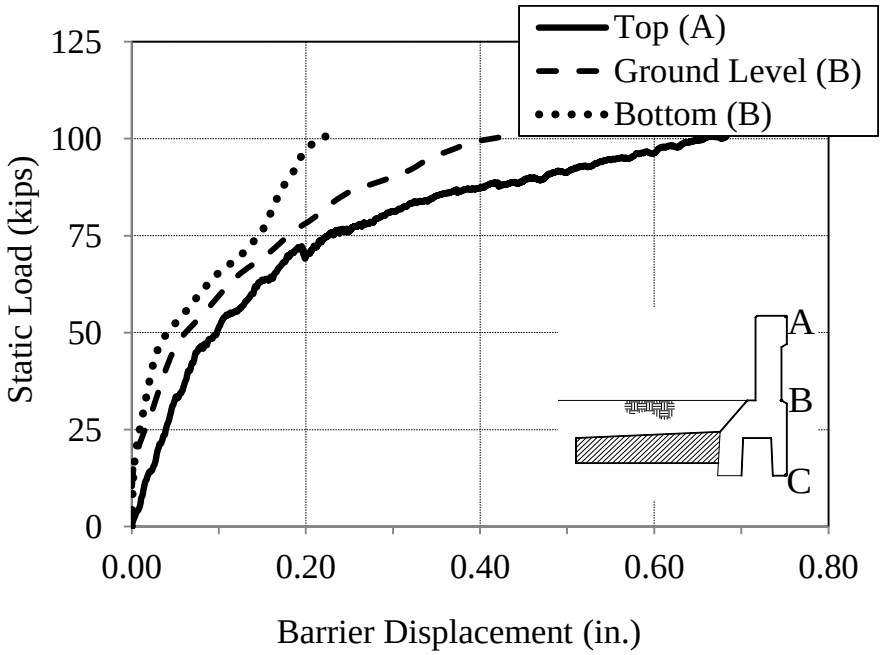

Figure 8.2 Results of the quasi-static FE analyses in the test barrier-foundation system

8.3 Full-Scale Static Load Test

The purpose of the static load test was to verify the magnitude of the load on the barrier required to initiate movement of the barrier-moment slab system. The setup for the static load test of the barrier system is illustrated in Figure 8.3 and Figure 8.4. A steel-reaction frame was anchored to an existing concrete deck. The load was applied at an effective height of 34 in. (864 mm) from the finished grade by means of a hydraulic cylinder. A spreader beam with a wood-block attached to its face was used to distribute the load over

a longitudinal barrier length of 10 ft (3.05 m). The applied pressure from the hydraulic cylinder was measured and converted into force. The load was applied continuously at a rate of 5 kips (22.25 kN) per minute in order to reduce the inertial effect of the system. Displacement of the barrier, coping, and moment slab was recorded digitally using calibrated string pot sensors. The string pots in the barrier were positioned behind and along the centerline of the barrier segments near its top edge, ground level and bottom. These three displacement measurement devices were secured to a steel frame located at the back side of the wall. At the moment slab, the string pots were positioned at each edge and at the center point of the 30 ft (9.15 m) moment slab section. When the lateral load applied to the top of the barrier reached about 80 kips (356 kN), the soil began to crack along the edges of the moment slab, as shown in Figure 8.5. The load test was stopped at a load of 100 kips (445 kN).

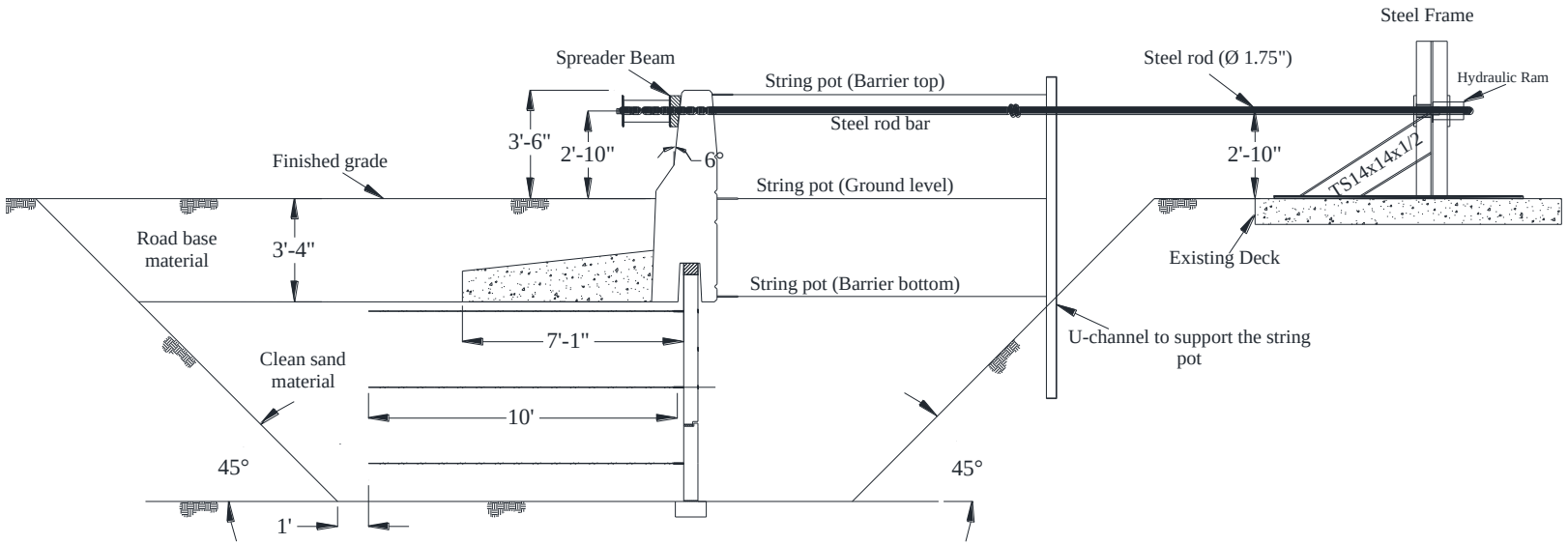

a) Croass section view

Figure 8.3 Details of the full-scale static test set-up on the barrier-foundation system

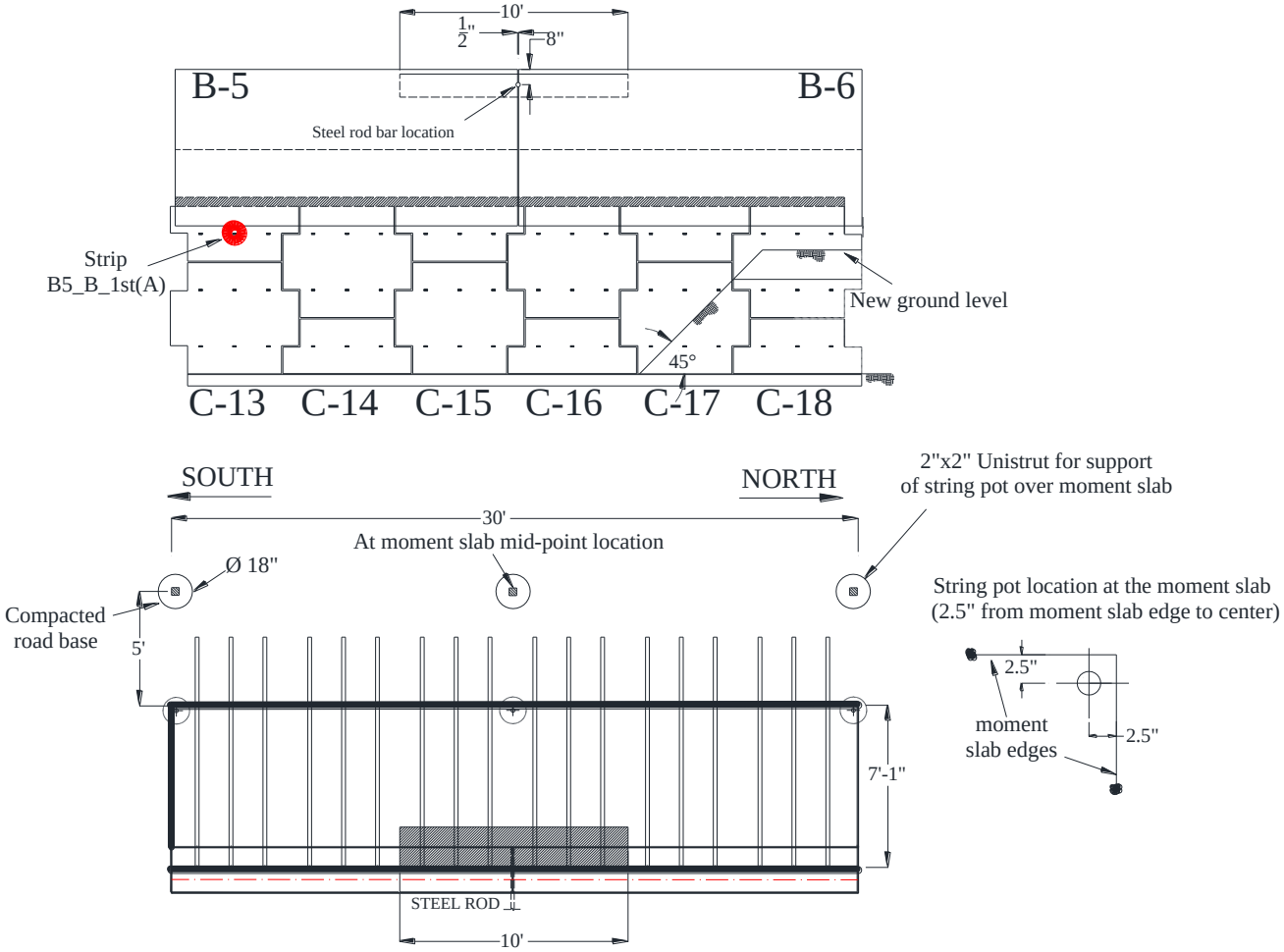

b) Elevation view

Figure 8.3 Continued

a) Side view of the static test set-up

b) Overall view of the static test set-up

Figure 8.4 Photograph of the full-scale static test set-up

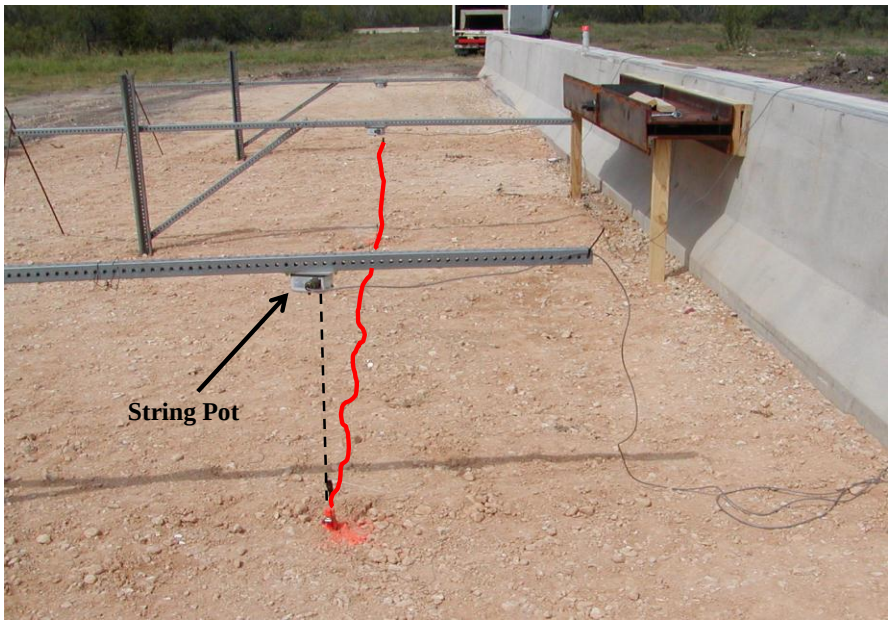

Figure 8.5 Crack in the soil during the static load test

The force-displacement curves generated from the test data are shown in Figure 8.6(a). The steps of the static test are described as follow:

a) The system was loaded up to 100 kips (445 kN). The displacement at the top of the barrier at this load level was about 0.5 in. (12.7 mm).

b) The system was unloaded (zero load). The residual displacement at the top of the barrier was 0.25 in. (6.35 mm).

c) The system was re-loaded from zero to 80 kips (356 kN). The displacement at the top of the barrier after re-load was 0.43 in. (10.92 mm).

d) The load was increased from 80 kips (kips) to 100 kips (445 kN) in steps of 5 kips (22.25 kN) per minute. The displacement at the top of the barrier was 0.50 in. (12.7 mm), and,

d) After the load reached 100 kips (445 kN), it was left applied to the system for a period of one minute. The displacement increased from 0.50 in. (12.7 mm) to 0.54 in. (13.7 mm).

The load-deflection response of the barrier-moment slab system was stiffer up to a load of 75 kips (190.5 kN). This load corresponds quite well with the load capacity of the 30 ft (9.15 m) long barrier-moment system based on the static equilibrium analysis shown previously in Table 8.1. Figure 8.6(b) indicates that the barrier had moved 0.15 in. (3.81 mm) at the top at a load of 75 kips (190.5 kN). Upon further loading beyond of 75 kips (190.5 kN), the displacement of the barrier increased in a nonlinear manner. The barrier system also shows movement in sliding at the bottom and at the ground level, as shown in Figure 8.6(b). At the load of 100 kips (445 kN), the displacement of the barrier at top, ground level and bottom were 0.54 in. (13.71 mm), 0.30 in. (7.62 mm) and 0.15 mm (3.81 mm), respectively. At the time the load test was stopped, the shear strength of the soil had been exceeded and the load-deflection curve was nearly asymptotic.

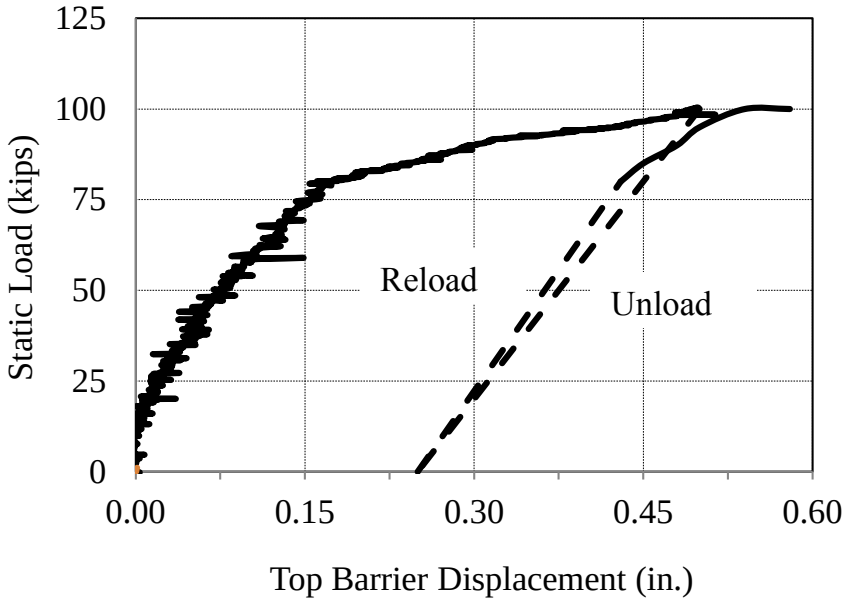

a) Load and re-load displacement curve

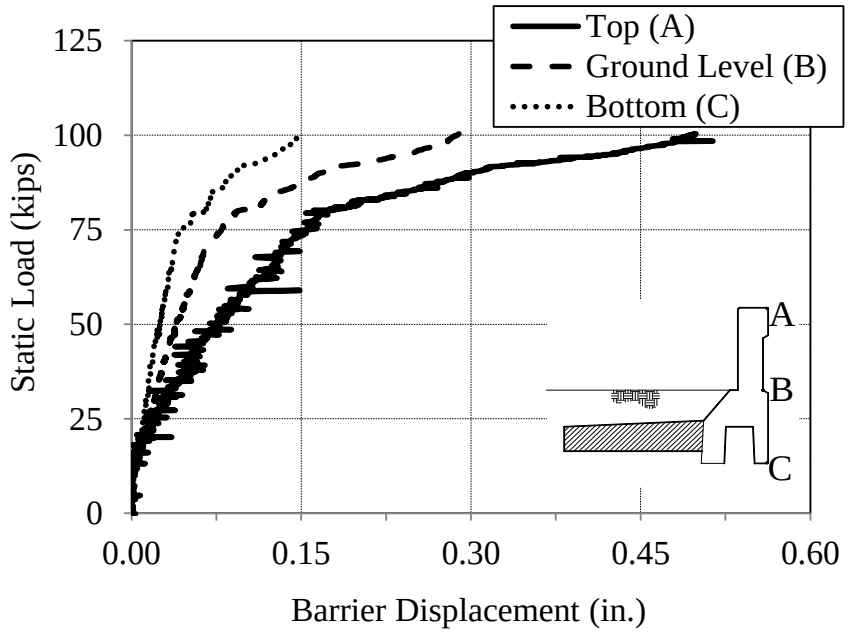

b) Load displacement curve at different location

Figure 8.6 Results of the full-scale static test on the barrier-foundation system

Figure 8.7 shows the variation of the displacement of the moment slab with the applied static load to the system. The displacement of the moment slab was measured by the string pot (SP) located at the upstream end (SP-A), center (SP-B) and downstream end (SP-C) of the moment slab. The maximum displacement of the moment slab was 0.17 in. (4.3 mm) at the upstream end section. However, the displacements at the three locations were, on average, similar. Figure 8.7 also show that the vertical displacement of the moment slab increases once the static load reaches the applied load of 75 kips (333.8 kN), which is associated with the static capacity of the system to overturning discounting the shear resistance of the soil.

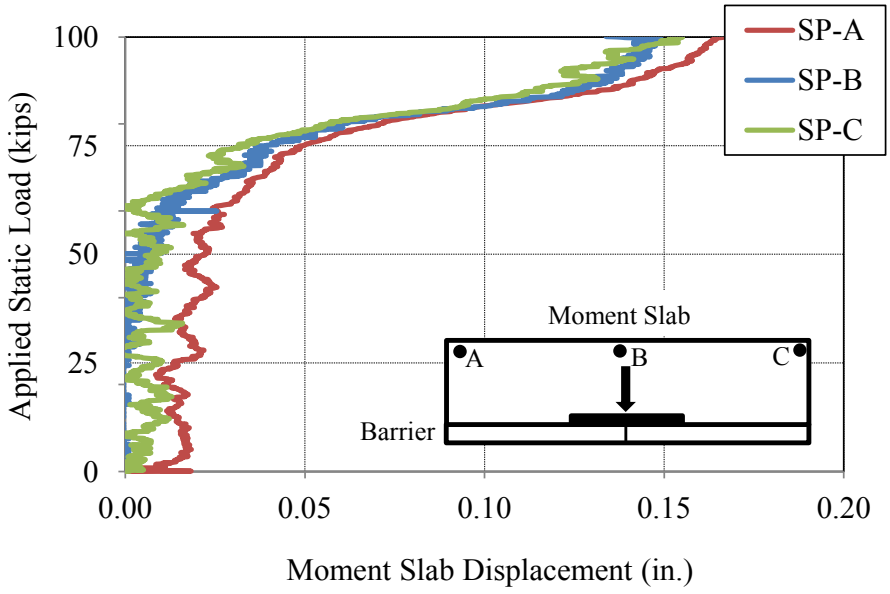

Figure 8.7 Vertical displacement of moment slab and applied static load

During the static test, the load in strip section B5_B_1st(A) was recorded at every load increment of 5 kips (22.25 kN) in the barrier. The strip was positioned below barrier segment 5 and the strain gage was located at a distance of 7 in. (177.8 mm) from the face of the panel. This strip was previously used to capture the dynamic load from the TL-5 full-scale crash test. The time-history load is presented in Figure 8.8. It is observed that the load in the strip increases more rapidly after the static load had reached 80 kips (356 kN), which correspond to the load that initiated excessive moment in the barrier.

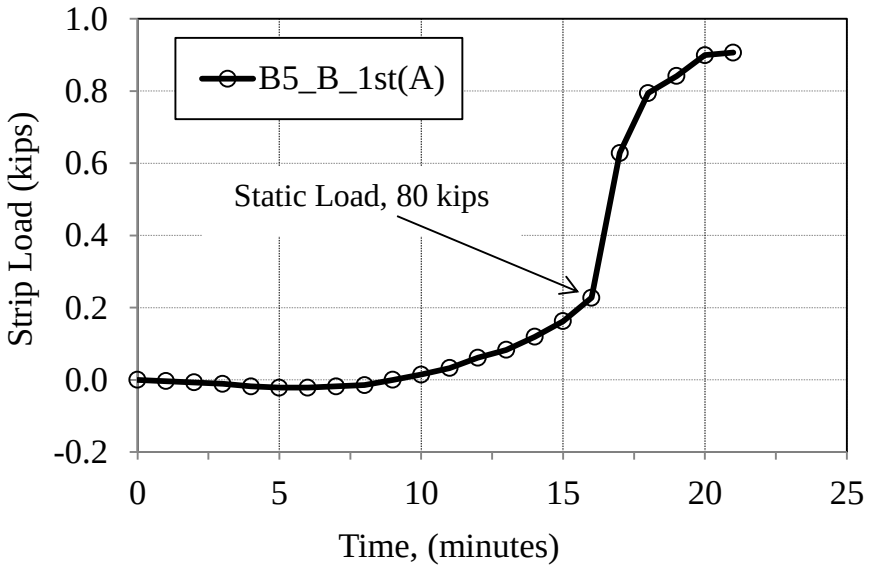

Static Load Rate in the Barrier, 5 kips/min.

Figure 8.8 Time history load of the strip during the static test

During the conduction of the static test, it was observed that the barrier system was not only rotating around its longitudinal axis but also around its vertical axis. This unexpected movement was associated with additional friction developed at the interface of the slabs joints between barrier segment 4 and 5. At the joint between barrier segment 6 and 7 (bottom section), the sliding component of the movement was around 0.5 in. (12.7), as shown in Figure 8.10. After the test, the bottom joint between barrier segment 6 and 7 was about 1.0 in. (25.4 mm). However, prior the test, this barrier joint was about 0.4 in. (10.2 mm) to 0.5 in. (12.7 mm) offset.

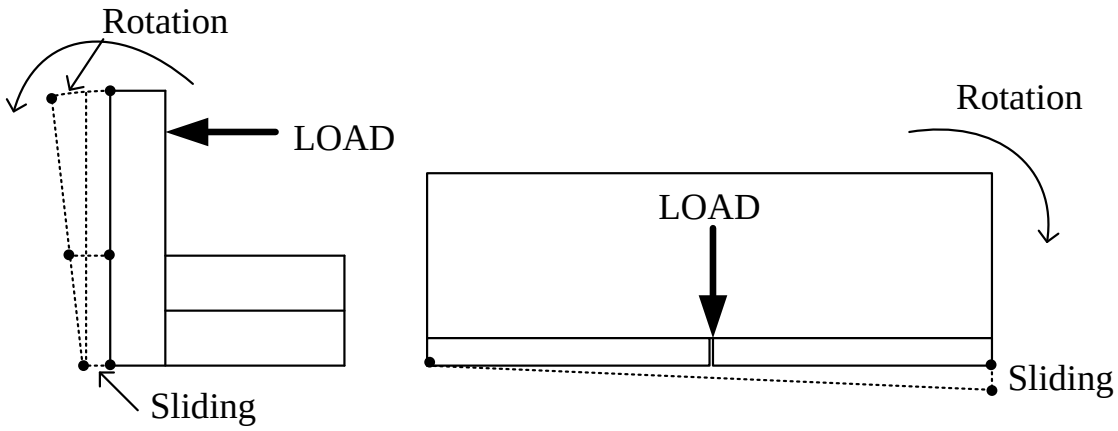

Figure 8.9 Sketch of movement of the barrier system during the static test

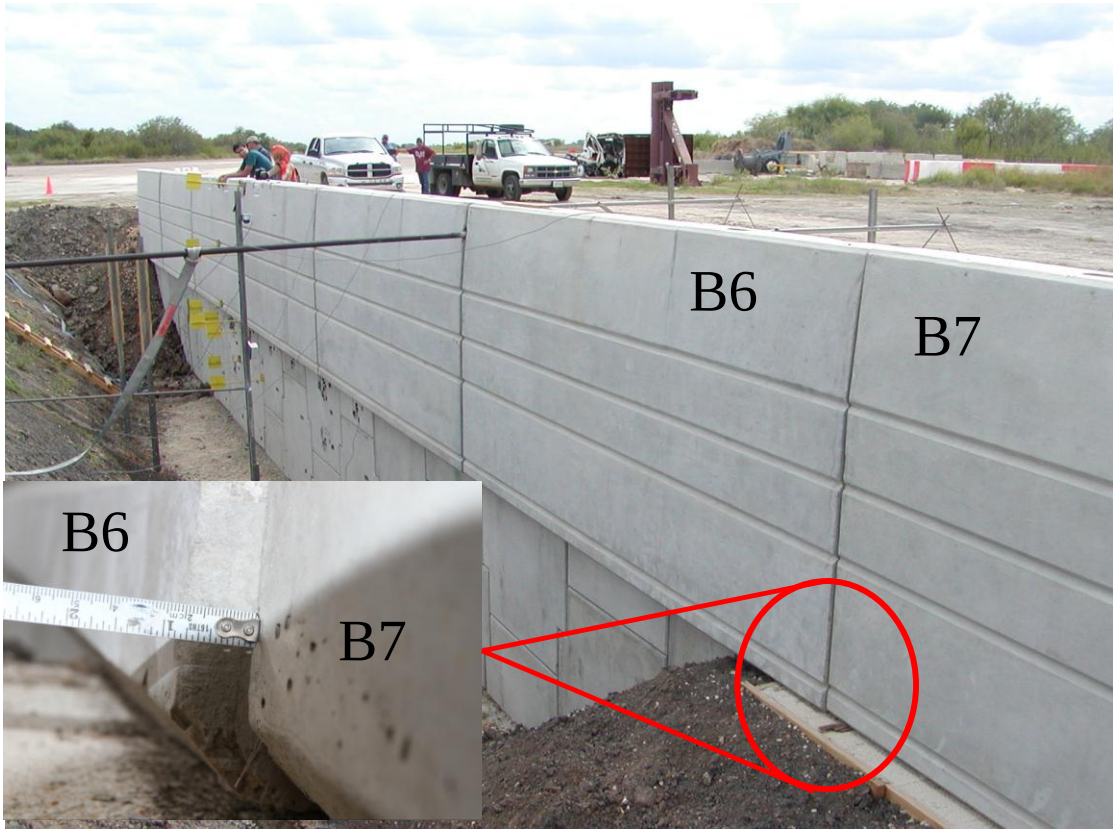

Figure 8.10 Relative movement at the bottom of barrier segment 6 and 7 during the during the static test

Upon completion of the static test, a visual inspection of the underlying MSE wall was conducted. Some of the wall panels located underneath barrier segments 5 and 6 experienced relative movement between them in the vertical and longitudinal direction. The wall panels were originally installed with a nominal joint gap of 0.75 in. (19.05 mm) ± 0.2 in. (5.1 mm). In addition, this portion of the wall was not significantly affected by

the impact test conducted prior the static load test as observed in the permanent deflection measurements described previously.

The vertical movement was minimal (less than 0.25 in. (6.35 mm) and it was associated with the high compressive load imposed by the barrier system during its rotation on top of the leveling concrete pad and wall panels. The relative movement in the longitudinal direction was more significant and it ranged between 0.2 in. (5.1 mm) to 0.5 in. (12.7 mm). The longitudinal movements of the panels were associated with the uneven deflection of system observed in the north section of the barrier-moment slab system.

8.4 Conclusion

The following conclusions are based on and limited to the content of this chapter:

The primary failure mode of the system was overturning since it occurred before sliding. This was shown analytically and confirmed in the full-scale static test However, there was significant sliding, especially in the north section area of the barrier system. Therefore, both criteria must be checked. The results of the test also validate the equivalent static load propose to size the moment barrier-moment slab system against TL-5-1 impact. In addition, it also give credibility to the FE analyses conducted for other test levels.

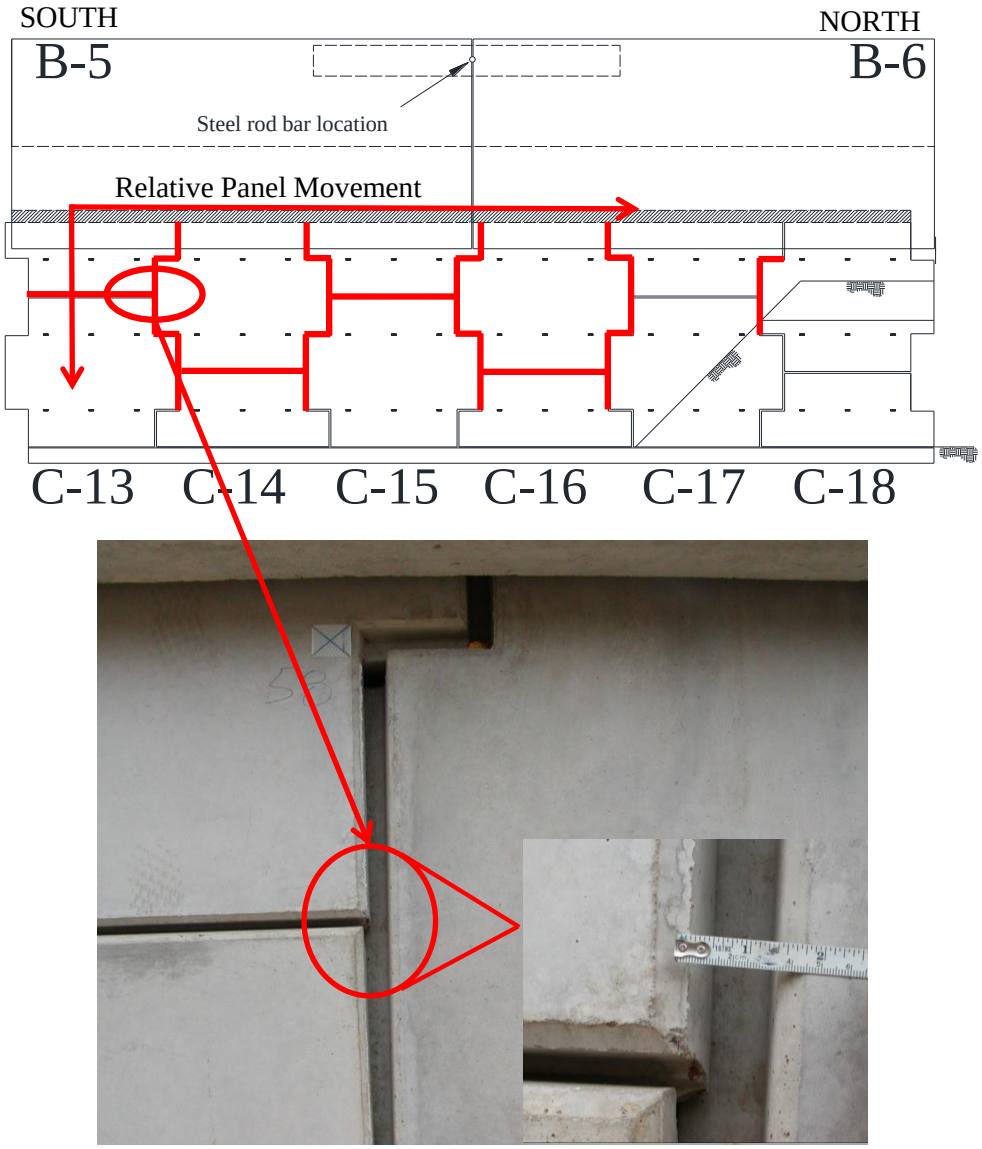

Figure 8.11 Relative panel movement observed during the static load test

8.5 Comparison of Test and Simulation

Figure 8.12 shows the load test results compared to the numerical simulation. The FE analyses estimated the load reasonable well (within 7% difference). Additional friction was developed at the interface of the test moment slab with its neighbor sections which may explain the difference between the test and the simulation beyond an applied load of 65 kips (289.3 kN).

This comparison between the test and simulation indicates that the static resistance is made of two components: the component due to the weight of the moment slab and overburden soil, and the component due to the friction between the moment slab-overburden soil and the surrounding soil. Back-calculations indicate that the average shear strength of the concrete soil interface at that shallow depth was or 266 psf (12.74 kPa) which is approximately 15% of the cohesion intercept estimated from the triaxial test. As explain before, the friction component might not be attributable only to the soil.

Similar to the previous analyses conducted in section 4, the results confirm that overturning is the likely mode of failure since sliding develops more resistance. This comparison also gives credibility to the numerical simulation.

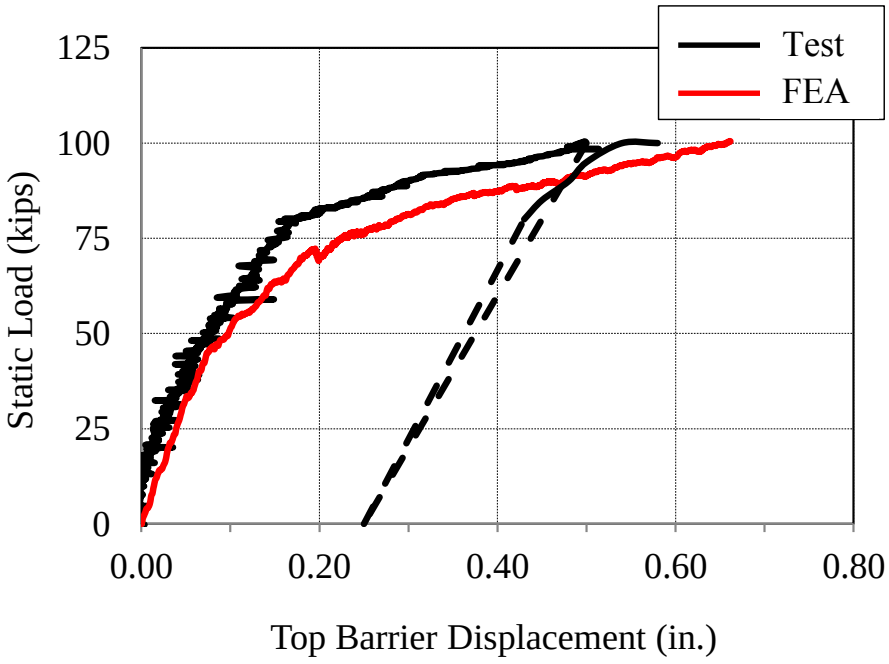

Figure 8.12 Comparison of static test and FE static model

9 DESIGN GUIDELINE FOR BARRIER MOMENT SLAB SYSTEM PLACED ON MSE WALL FOR TL-3 THROUGH TL-5 IMPACT

The format presented in this section follows chapter 7 of the NCHRP Report 663, "Design Guidelines" *(2).* The research conducted in that report was limited to TL-3 impact. The information contained herein extend the guidelines to TL-4 and TL-5 impact.

The design guidelines for TL-4 were developed based on the data collected from the full-scale impact simulation. The design guideline for TL-5 were developed based on data collected from the full-scale crash test, static test and the FE analyses. The FE analyses were conducted using vertical wall barriers. However, the results should be applicable to other common barrier types.

The design guidelines address three components:

- The barrier-moment slab system,
- The MSE wall reinforcement and
- The wall panel.

The guidelines are set in terms of AASHTO LRFD practice. The AASHTO LRFD format version of the design guidelines is shown in Appendix F. An example of the application of the preliminary design guidelines for the TL-5 crash test MSE wall is presented in Appendix B.

Depending on the design, two points of rotation are possible as shown in Figure 9.1. The point of rotation should be determined based on the interaction between the barrier coping and top of the wall panel. With reference to Figure 9.1 the point of rotation should be taken as Point A if the top of the wall panel is isolated from contact with the coping by presence of an air gap or sufficiently compressible material. The point of rotation should be taken as Point B if there is direct bearing between the bottom of the coping and the top of the wall panel or level up concrete.

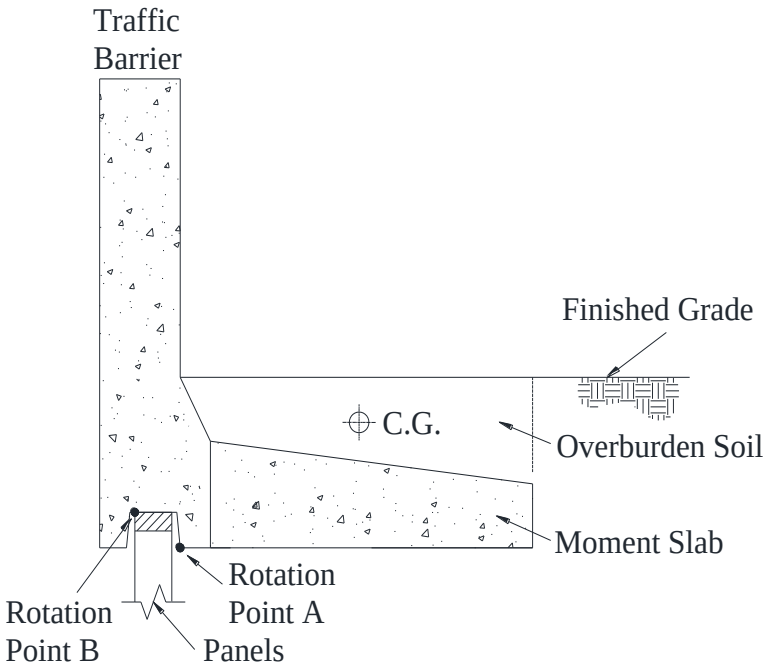

Figure 9.1 Barrier-moment slab system for design guideline

9.1 Guidelines for the Barrier

The barrier, the coping, and moment slab should be safe against structural failure. A barrier should be designed to resist the impact load recommended in this report according to the information presented in Table 9.1 . Any section along the coping and the moment slab should not fail in bending when the barrier is subjected to an impact load. Two modes of stability failure are possible in addition to structural failure of the barrier system. They are sliding and overturning of the barrier-moment slab system.

9.1.1 Sliding of the Barrier

The factored static resistance (φ P) to sliding of the barrier-moment slab system along its base should be greater than or equal to the factored equivalent static load (γ L_s) due to the dynamic impact force.

$$\varphi P \geq \gamma L_s \qquad (9\text{-}1)$$

The equivalent static load, L_s, is determined from Table 9.1, ϕ resistance factor is 0.8 (AASHTO LRFD Table 10.5.5-1), and γ load factor is 1.0 (extreme event).

Table 9.1 Recommended equivalent static load (L_s) for TL-3 through TL-5

Test Designation	Dynamic Load (kips)	Equivalent[1] Static Load (kips)	Equivalent[1] Static Load per unit length (kips/ft)	Minimum Barrier Height (in.)	Effective Height, H_e (in.)
TL-3[2]	54	18	0.8	32	24
TL-4	80	23	0.8	36	30
TL-5-1	160	60	2.0	42	34
TL-5-2	260	80	2.7	>42	43

[1] Equivalent static load based on a rotation point B
[2] NCHRP Report 663, Figure 7.1 *(1)*

The static force P should be calculated as:

$$P = W \tan\phi_r \tag{9-2}$$

where

W = weight of the monolithic section of barrier and moment slab plus any material laying on top of the moment slab

ϕ_r = friction angle of the soil -moment slab interface

The factored equivalent static load should be applied to the length of the moment slab between joints. Any coupling between adjacent moment slabs or friction that may exist between free edges of the moment slab and the surrounding soil should be neglected. If the soil – moment slab interface is rough (e.g., cast in place), ϕ_r is equal to

the friction angle of the soil ϕ_s. If the soil – moment slab interface is smooth (e.g., precast), ϕ_r should be reduced accordingly $\left(\frac{2}{3}\tan\phi_s\right)$.

9.1.2 Overturning of the Barrier

The factored static moment resistance (φM) to overturning of the barrier-moment slab system should be greater than or equal to the factored static load (γL_s) due to the impact force times the moment arm h_A or h_B. The moment arm is taken as the vertical distance from the point of impact due to the dynamic force (effective height, H_e) to the point of rotation A or B (Figure 9.2).

$$\varphi M \geq \gamma L_s (h_A \text{ or } h_B) \tag{9-3}$$

The static load, L_s, is determined from Table 9.1, φ resistance factor is 0.9, and γ load factor is 1.0 (extreme event).

M should be calculated as:

$$M = W (l_A \text{ or } l_B) \tag{9-4}$$

where

W= weight of the monolithic section of barrier and moment slab plus any material lying on top of the moment slab.

l_A *or* l_B = horizontal distance from the center of gravity (c.g.) of the weight W to the point of rotation A or B.

The moment contribution due to any coupling between adjacent moment slabs, shear strength of the overburden soil, or friction which may exist between the backside of the moment slab and the surrounding soil should be neglected.

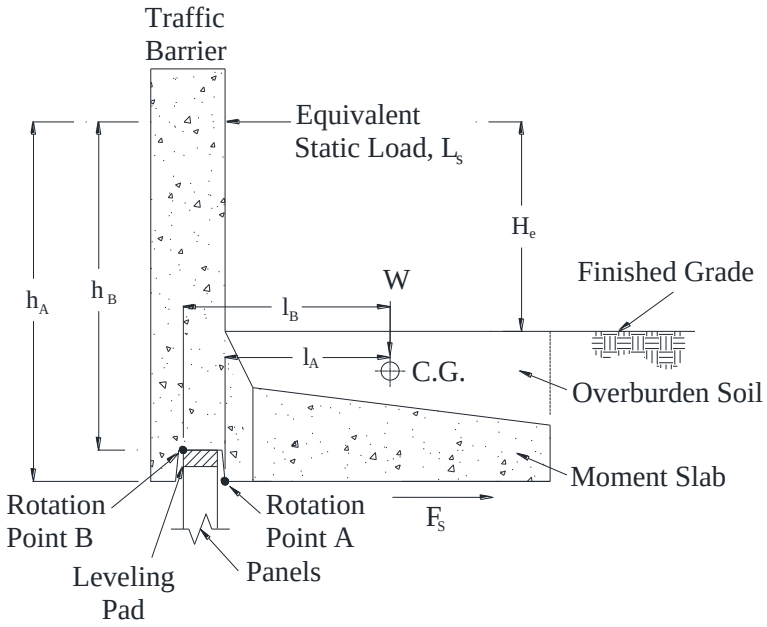

Figure 9.2 Barrier moment slab system for barrier design guideline (sliding and overturning).

9.1.3 Rupture of the Coping in Bending

The critical section of the coping must be designed to resist the applicable impact load conditions for the appropriate test level as defined in this report and Table 9.1 (Figure 9.3).

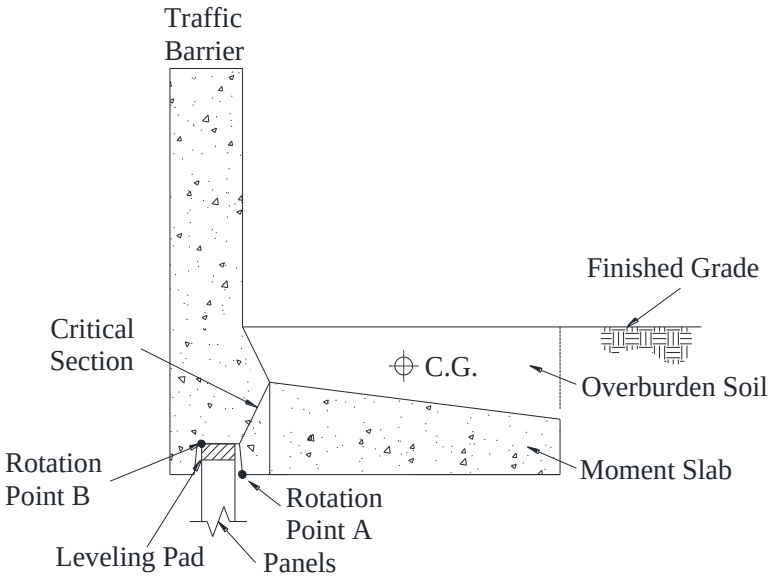

Figure 9.3 Coping and possible weakest section.

9.2 Guidelines for the Wall Reinforcement

The wall reinforcement guidelines should ensure that the reinforcement does not pullout or break during a barrier impact with the chosen design vehicle. The connection

between the reinforcement and the wall panel should be able to resist the pull out load or breaking load which ever controls.

9.2.1 Pullout of the Wall Reinforcement

a) Pressure Distribution Approach

The capacity of the reinforcement calculated by common static methods should be compared to the dynamic impact loads because no significant difference was found between the static capacity and the dynamic capacity of the reinforcement.

The factored static resistance (ϕ P) to pullout of the reinforcement should be greater than or equal to the sum of the factored static load (γ_s F_s) due to the earth pressure and the factored dynamic load (γ_d F_d) due to the impact. The static load F_s should be obtained from the static earth pressure p_s times the tributary area A_t of the reinforcement unit. The dynamic load F_d should be obtained from the pressure p_d of the pressure distribution (Table 9.2 and Figure 9.4) times the tributary area A_t of the reinforcement unit.

$$\phi P \geq \gamma_s F_s + \gamma_d F_d \quad (9\text{-}5)$$

$$\phi P \geq \gamma_s p_s A_t + \gamma_d p_d A_t \quad (9\text{-}6)$$

(For the load level TL-3 through TL-5 p_d is given in Table 9.2 and Figure 9.4, ϕ resistance factor is 1.0, γ_d load factor is 1.0, and γ_s load factor is 1.0.)

Table 9.2 Design pressure p_d for reinforcement pullout and tributary height

Test Designation	First Layer		Second Layer	
	p_{d-1} (psf)	h_1 (ft)	p_{d-2} (psf)	h_2 (ft)
TL-3[(1)]	315	1.8	230	2.5
TL-4	470	1.8	260	2.5
TL-5-1	625	1.6	500	2.5
TL-5-2	810	1.6	500	2.5

[(1)] NCHRP Report 663, Figure 7.4 (*1*)

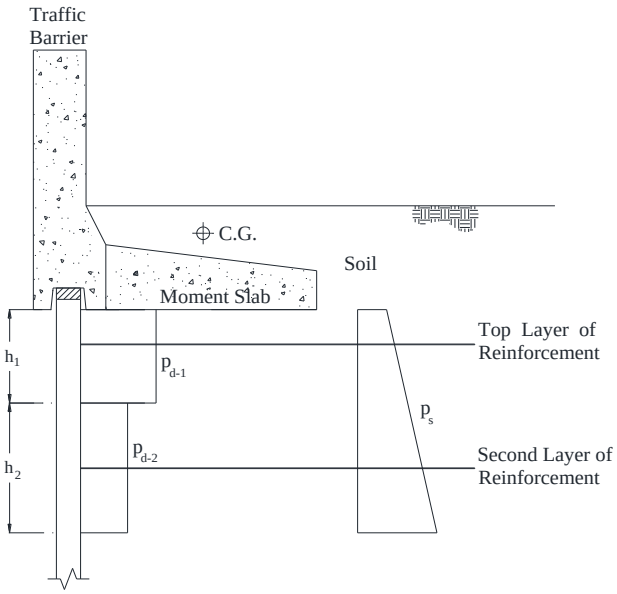

Figure 9.4 Pressure distribution p_d for reinforcement pullout.

The reinforcement resistance P for strips should be calculated as (AASHTO LRFD Eq. 11.10.6.3.2-1):

$$P = F^* \sigma_v 2b L \quad (9\text{-}7)$$

where

F*= resistance factor (sliding plus bearing) obtained from the current AASHTO LRFD (Figure 9.5).

σ_v= vertical effective stress on the reinforcement

b= width of the strip

L= full length of the reinforcement.

The reinforcement resistance P for bar mats should be calculated as:

$$P = F^* \sigma_v \pi D n L \quad (9\text{-}8)$$

where

D= diameter of the bar mats, and

n= is the number of longitudinal bars.

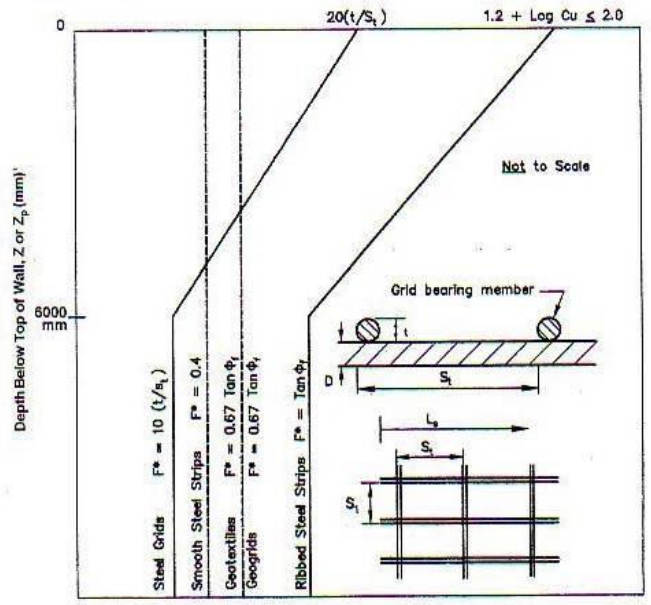

Figure 9.5 Default values for the pullout friction factor, *F (AASHTO LRFD Figure 11.10.6.3.2-1).**

b) Line Load Approach

The factored static resistance (ϕ P) to pullout of the reinforcement should be greater than or equal to the sum of the factored static load (γ_s F_s) due to the earth pressure and the factored dynamic load (γ_d F_d) due to the impact. The static load F_s should be obtained from the static earth pressure p_s times the tributary area A_t of the reinforcement unit. The dynamic impact load F_d should be obtained from the line load Q_d times the longitudinal spacing (S_L) of the reinforcement.

$$\varphi P \geq \gamma_s F_s + \gamma_d F_d \quad (9\text{-}9)$$

$$\varphi P \geq \gamma_s p_s A_t + \gamma_d Q_d S_L \quad (9\text{-}10)$$

(For the load level TL-3 through TL-5, Q_d is given by the line load shown in Table 9.3 and Figure 9.6; φ resistance factor is 1.0, γ_d load factor is 1.0, and γ_s load factor is 1.0.)

Table 9.3 Design line load Q_d for reinforcement pullout

Test Designation	Line Load (lb./ft)	
	First Layer, Q_{d-1}	Second Layer, Q_{d-2}
TL-3[(1)]	575	575
TL-4	850	650
TL-5-1	1000	1250
TL-5-2	1300	1250

[(1)] NCHRP Report 663, Figure 7.4 (*1*)

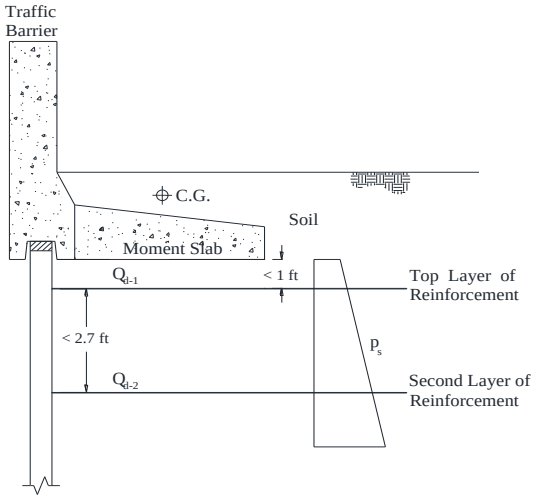

Figure 9.6 Line Load Q_d for reinforcement pullout.

The reinforcement resistance P for strips should be calculated as (AASHTO LRFD Eq. 11.10.6.3.2-1):

$$P = F^* \sigma_v 2b L \quad (9\text{-}11)$$

where

F*= resistance factor (sliding plus bearing), obtained from the current AASHTO LRFD guidelines *(3)* (Figure 9.5).

σ_v= vertical effective stress on the reinforcement

b= width of the strip

L= full length of the reinforcement

The reinforcement resistance P for bar mats should be calculated as:

$$P = F^* \sigma_v \pi D n L \quad (9\text{-}12)$$

where

D= diameter of the bar mats, and

n= number of longitudinal bars.

9.2.2 Yield of the Wall Reinforcement

a) Pressure Distribution

The factored resistance (ϕ R) to yield of the reinforcement should be greater than or equal to the sum of factored static load (γ_s F_s) due to the earth pressure and the factored dynamic load (γ_d F_d) due to the impact. The static load F_s should be obtained from the static earth pressure p_s times the tributary area A_t of the reinforcement unit. The dynamic load F_d should be obtained from the dynamic pressure p_d of the pressure distribution (Table 9.4 and Figure 9.7) times the tributary area A_t of the reinforcement unit. It is expressed as:

$$\varphi R \geq \gamma_s F_s + \gamma_d F_d \tag{9-13}$$

$$\varphi R \geq \gamma_s p_s A_t + \gamma_d p_d A_t \tag{9-14}$$

(For the load level TL-3 through TL-5, p_d is given by the pressure distribution shown in Table 9.4 and Figure 9.7, ϕ resistance factor is 1.0, and γ_d load factor is 1.0, and γ_s load factor is 1.0.)

Table 9.4 Design pressure p_d for reinforcement yield

Test Designation	First Layer		Second Layer	
	p_{d-1} (psf)	h_1 (ft)	p_{d-2} (psf)	h_2 (ft)
TL-3[(1)]	1200	1.8	230	2.5
TL-4	1450	1.8	260	2.5
TL-5-1	1790	1.9	500	2.5
TL-5-2	2410	1.6	500	2.5

[(1)] NCHRP Report 663, Figure 7.4 (*1*)

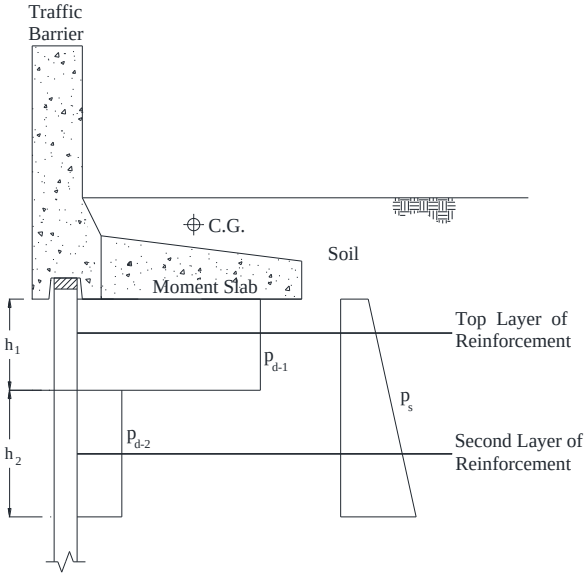

Figure 9.7 Pressure distribution p_d for reinforcement yield

The reinforcement resistance R for strips or bar mats should be calculated as:

$$R = \sigma_t A_s \tag{9-15}$$

where

σ_t= tensile strength of the reinforcement, and

A_s= cross section area of the reinforcement.

$$A_s = b \times E_c \ \ per\ Strip \tag{9-16}$$

where

E_c= strip thickness corrected for corrosion loss. (AASHTO LRFD Figure 11.10.6.4.1-1)

$$A_s = \frac{\pi D^{*2}}{4} \text{ for Bar mats} \tag{9-17}$$

where

D^*= diameter of bar or wire corrected for corrosion loss. (AASHTO LRFD Figure 1.10.6.4.1-1).

b) Line Load Approach

The factored resistance (φ R) to yield of the reinforcement should be greater than or equal to the sum of factored static load (γ_s F_s) due to the earth pressure and the factored dynamic load (γ_d F_d) due to the impact. The static load F_s should be obtained from the static earth pressure p_s times the tributary area A_t of the reinforcement unit. The dynamic load F_d should be obtained from the line load Q_d times the longitudinal spacing (S_L) of the reinforcement.

$$\varphi R \geq \gamma_s F_s + \gamma_d F_d \quad (9\text{-}18)$$

$$\varphi R \geq \gamma_s p_s A_t + \gamma_d Q_d S_L \quad (9\text{-}19)$$

(For the load level TL-3 through TL-5, Q_d is given by the line load shown in Table 9.5 and Figure 9.8, φ resistance factor is 1.0, and γ_d load factor is 1.0, and γ_s load factor is 1.0).

Table 9.5 Design line load Q_d for reinforcement yield

Test Designation	Line Load (lb./ft)	
	First Layer, Q_{d-1}	Second Layer, Q_{d-2}
TL-3[(1)]	2160	575
TL-4	2610	650
TL-5-1	3400	1250
TL-5-2	3860	1250

[(1)] NCHRP Report 663, Figure 7.4 (*1*)

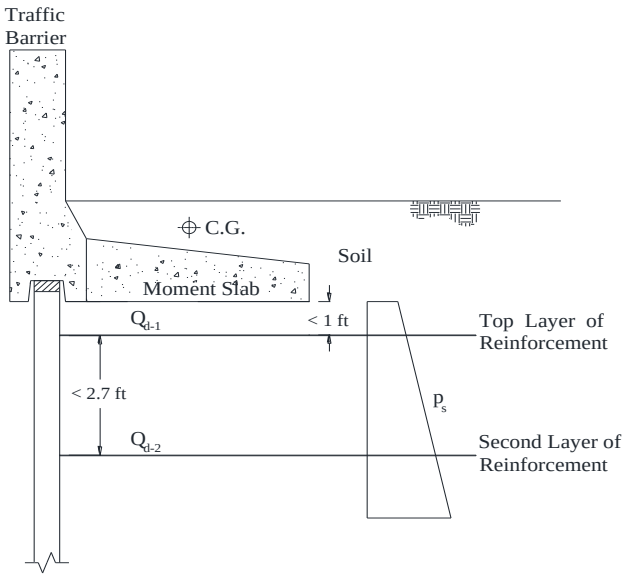

Figure 9.8 Line Load Q_d for reinforcement yield.

The reinforcement resistance R for strips or bar mats should be calculated as:

$$R = \sigma_t A_s \tag{9-20}$$

where

σ_t= tensile strength of the reinforcement, and

A_s= cross section area of the reinforcement.

$$A_s = b \times E_c \ \ per\ Strip \tag{9-21}$$

where

E_c= strip thickness corrected for corrosion loss (AASHTO LRFD Figure 11.10.6.4.1-1).

$$A_s = \frac{\pi D^{*2}}{4} \text{ for Bar mats} \tag{9-22}$$

where

D^*= diameter of bar or wire corrected for corrosion loss. (AASHTO LRFD Figure 11.10.6.4.1-1).

9.2.3 Guidelines for the Wall Panel

The wall panels must be designed to resist the dynamic pressure distributions as defined in Table 9.5. The wall panel should have sufficient structural capacity to resist the maximum design yielding load for the wall reinforcement. The static load is not included because it is not located at the panel connection.

9.3 Data to Back Up Guidelines for TL-4 and TL-5

The information presented in this section served as an evidence of the final recommended loads and pressures for design of the barrier, moment slab and wall reinforcement.

9.3.1 Data for TL-4

a) Barrier-Moment Slab System

The selected design load for MASH TL-4 impact is 80 kips (356 kN). This load was selected with consideration to both theoretical and FE analyses, and is considered to be representative of the upper bound lateral impact load imposed by the MASH TL-4 test vehicle. For stability of the MASH 10000S test vehicle, the minimum barrier height

required is 36 in. (914 mm). This barrier height was successfully crash-tested by TTI researchers *(19).*

The dimensions of the moment slab are determined using an equivalent static load of 23 kips (102.4 kN) around the point of rotation B. The point of application of the load is 30 in. (762 mm) measured from the finished grade. The calculation indicates that an approximately 4.5 ft (1.37 m) wide (measured from the face of the panel), 30 ft (9.14 m) long moment slab without the shear strength of the soil is capable to withstand a TL-4 impact. Therefore, the equivalent static load per unit length of wall is 0.77 kips/ft (11.24 kN/m). It was found that the overturning mode occurs before the sliding and is, therefore, the controlling failure mode.

The propose design load was based on the evidence presented below. A decision was made to aim for a barrier-moment slab system design that would generate about 1 in. (25.4 mm) permanent movement at the coping section during impact. This permanent movement is considered acceptable as it would likely require little or no repair of the underlying MSE wall, and should not affect the impact performance of the barrier system.

b) Wall Reinforcement

Three MASH TL-4 full-scale impact simulations with reinforcement lengths of 10 ft (3.05 m), 16 ft (4.88 m) and 24 ft (7.32 m) were conducted to design the guidelines for MASH TL-4 impact. The impact load was on average 74 kips (329.3 kN). The

maximum 50-msec. average dynamic loads, including the static load, and the wall displacement measured during the impact simulation is summarized in Table 9.6.

The loads presented in Table 9.6 were computed at 7 in. (178 mm) from the face of the wall where the load is expected to be the highest. Even though the reinforcement appears to have reached its maximum pull out resistance during impact simulation, the overall performance of the wall was satisfactory in the FE analyses. Therefore, it was decided that having the reinforcement working at maximum pull out resistance would be acceptable given that the load duration is so short and the displacements were tolerable. The design recommendations are based on a pressure diagram approach that prescribes the pressure due to impact (in excess of static load) that must be resisted by the reinforcement.

Table 9.6 Summary of the pullout resistance, maximum 50 msec. ave. strip load and wall displacement for MASH TL-4 impact simulation

Strip Length (ft)	AASHTO Pullout Resistance (kips)		Total Strip Load (kips)		Dynamic Wall Displacement (in.)			Approximate Permanent Wall Displacement (in.)		
	First Layer	Second Layer	First Layer	Second Layer	Top[(1)]	First Layer	Second Layer	Top[(1)]	First Layer	Second Layer
10	2.05	3.41	4.4	2.24	0.37	0.20	0.07	0.13	0.07	0.02
16	3.28	5.46	5.8	1.9	0.29	0.16	0.04	0.08	0.04	0.02
24	4.93	8.20	7.0	1.7	0.22	0.12	0.02	0.04	0.03	0.03

[(1)] Displacement measured at the coping level

- Pullout of the Wall Reinforcement:

The NCHRP Report 663 conducted several pullout tests at rates varying from quasi-static all the way to rates approaching impact loading rates. According to the conclusion stated in the report, no consistent rate effect was found; therefore, the recommended design guidelines require the pullout resistance of the reinforcement to be calculated according to common static methods and sized to resist the full dynamic loads *(2).*

The average design strip load in excess of static for the TL-4 impact simulation with 10 ft (3.05 m) long reinforcing strip was used to develop the design guideline for pullout of the reinforcement. This reinforcement length was selected for pullout analyses as it generated the largest wall displacement. The resistance (*P*) for the 10 ft (3.05 m) long strips was calculated to be 2.05 kips (9.1 kN) for the upper most layer and 3.41 kips (15.1kN) for the second layer using Eq. (2-2) in Chapter 2 (AASHTO 11.10.6.3.2-1). The pullout friction factor F* was 1.69 for the upper most layer and 1.52 for the second layer.

The total load (50-msec. average) in the strip at the upper most layer was 4.4 kips (19.6 kN). Although the measured total load in the strip was higher than the resistance (2.05 kips (9.1 kN)), the displacement of the strips and performance of the wall were considered acceptable. In other words, the analyses indicate that a 10 ft (3.05 m) long strip will perform acceptably for a TL-4 impact. Therefore, the resistance was used to obtain the dynamic design load in excess of the static load at the upper most layers. The controlling design load in excess of the static load due to static earth pressures was calculated to be 1.36 kips (6.05 kN). The value was found by calculating the total

resistance of the 10 ft (3.05 m) long strip at the depth of the first layer (2.05 kips (9.1 kN)) minus the calculated load due to static earth pressures from AASHTO LRFD (0.69 kips (3.07 kN)). This load represent a static load, equivalent to a dynamic load, which would indicate that the 10 ft (3.05 m) long strip perform well in the case of a TL-4 impact.At the second layer, the same process was followed. The total dynamic load was 2.24 kips (10 kN).

The static earth pressure load for the second layer was calculated to be 1.25 kips (5.6 kN) by AASHTO LRFD. The total load from the simulation (2.24 kips (10 kN) was therefore less than the calculated pullout load at that depth (3.48 kips (15.5 kN)). Therefore, the measured dynamic load in excess of the static load was used as the controlling dynamic load for pullout design. Table 9.6 shows the total measured dynamic load from the simulation, calculated static load, calculated pullout resistance, and the recommended design pressure for pullout resistance.

The dynamic pressure per strip was calculated as shown in Table 9.7. For the 10 ft (3.05 m) long strip with a density of 3 strips per panel per layer, the tributary area was 2.92 ft^2 (0.27 m^2) for the top layer and the tributary area was (3.94 ft^2) 0.37 m^2 for the second layer.

The dynamic design pressure was calculated as shown in Table 9.7. The dynamic design pressure in excess of the static earth pressure for pullout is recommended to be 470 psf (22.5 kPa) for the upper most layer and 260 psf (12.45 kPa) for the second layer.

Table 9.7 Simulation results and calculation of TL-4 design strip load for pullout

	(1) Total Load (kips)	(2) Static Load (kips)	(3) Dynamic Load (kips)	(4) Calculated Resistance [(a)] (kips)	Controlling Design Dynamic Load (kips)	Total Design Pressure (psf)
Top Layer	4.4	0.69	3.70	2.05	((3)-(2) = 1.36)	1360 kips / 2.92 ft^2 [(b)] = **466 psf (final 470 psf)**
Second Layer	2.24	1.25	0.99	3.48	((1)-(2) =0.99)	990 kips / 3.94 ft^2 [(c)] = **251 psf (final 260 psf)**

[(a)] Calculated from AASHTO 11.10.6.2 – 11.10.6.3

[(b)] Tributary area of the panel for the top layer (2.92 ft^2 = 4.87 ft × 1.8 ft / 3 strips per panel)

[(c)] Tributary area of a panel for the second layer (3.94 ft^2 = 4.87 ft × 2.43 ft / 3 strips per panel)

- Yielding of the Wall Reinforcement:

The reinforcement resistance to yielding (R) for a strip was calculated using Eq. (8-15). The tensile strength of the reinforcement (σ_t) was 60 ksi (414 MPa) and the thickness, after accounting for corrosion loss (E_c), was 0.102 in. (2.59 mm) for a 75-year design life. The R was computed to be 12.02 kips (53.5 kN).

To develop the design guideline against yielding of the reinforcement, the highest design load on the strip, computed from the full-scale impact simulation, was used. The maximum 50 msec. average total load on the strip located in the uppermost layer was 7 kips (31.2 kN) (24 ft (7.32 m) long strip). In the second layer, the total load was 2.24 kips (10 kN) and 1.9 kips (8.5 kN) for the 10 ft (3.05 m) and 16 ft long strip model, respectively. Therefore, the controlling dynamic design strip load for yielding of

the reinforcement is 6.31 kips (28.1 kN) for the uppermost layer and 0.99 kips (4.41 kN) for the second layer (Table 9.8).

Table 9.8 Simulation results for TL-4 impact and calculation of design strip load for yielding design

Strip Length (ft)	(1) Dynamic Load (kips)		(2) Static Load[(a)] (kips)		(3)= (1)+(2) Total Load (kips)		(4) Calculated Resistance[(b)] (kips)		Controlling Design Dynamic Load (kips)	
	First Layer	Second Layer	First Layer	Second Layer	First Layer	Second Layer	First Layer	Second Layer	First Layer	Second Layer
10	3.71	0.99	0.69	1.25	4.4	2.24	12.02	12.02		
16	5.11	0.65	0.69	1.25	5.8	1.9	12.02	12.02	6.31	0.99
24	6.31	0.45	0.69	1.25	7.0	1.7	12.02	12.02		

[(a)] Calculated from AASHTO 11.10.6.4.3
[(b)] Reinforcement steel ASTM Grade 60

The dynamic pressure per strip for yielding of the reinforcement was calculated as shown in Table 9.9. For 10 ft (3.05) long strip with a density of 3 strips per panel per layer, the tributary area was 3.94 ft^2 (0.37 m^2). For 24 ft (7.32 m) long strip with a density of 2 strips per panel per layer, the tributary area was 4.38 ft^2 (0.41 m^2). The dynamic design pressure in excess of static earth pressure to consider in the design against yielding of the reinforcement was calculated as shown in Table 9.9. The dynamic

design pressure for rupture of the reinforcement is recommended to be 1450 psf (69.42 kPa) for the uppermost layer and 260 psf (12.45 kPa) for the second layer.

Table 9.9 TL-4 design pressure for yielding of soil reinforcement based on simulation results

Layer	Total Design Load (kips)	Static Load (kips)	Dynamic Design Load (kips)	Total Design Pressure, *p*
Top	7.0	0.69	6.31	6310 lb. / 4.38 ft^{2}[(a)] = **1441 psf (final 1450 psf)**
Second	2.24	1.25	0.99	990 lb./3.94 ft^{2}[(b)] = **252 psf (final 260 psf)**

[(a)] Tributary area of the panel for the top layer (4.38 ft^2 = 4.87 ft × 1.8 ft / 2 strips per panel)
[(b)] Tributary area of a panel for the second layer (3.94 ft2 = 4.87 ft × 2.43 ft / 3 strips per panel).

9.3.2 Data for TL-5-1

a) Barrier-Moment Slab System

The final design impact load for MASH TL-5-1 impact is 160 kips (712 kN). This load was selected by using the results of the FE analyses. The load is considered to be representative of the upper bound lateral impact load imposed by the MASH 36000V test vehicle. It also includes the component of friction generated at the top of the barrier

due to the vehicle riding on top of it while it is being redirected. For stability of the MASH 36000V test vehicle, the minimum barrier height required is 42 in. (1.07 m). This barrier height has been successfully crash-tested by TTI researchers, as shown in Table 2.4.

To preclude any damage to the underlying MSE wall or relative displacement between barriers, the recommended length of a precast barrier section for TL-5-1 is 15 ft (4.57 m). This length will enable the barriers to develop their primarily failure mechanism (yield line) in the wall face provided the coping is sufficiently strong. This is the preferred failure mode of the barrier-coping-moment slab system because it reduces the cost of repair after a severe impact.

The dimensions of the moment slab are determined using an equivalent static load of 60 kips (267 kN) around the point of rotation B. The load is located at a height of 34 in. (864 mm) from the finished grade. The calculation indicates that an approximately 7 ft (2.13 m) wide (measured from the face of the panel), 30 ft (9.14 m) long moment slab without the shear strength of the soil is capable to withstand a TL-5-1 impact. Therefore, the equivalent static load per unit length of wall is 2 kips/ft (29.2 kN/m). It was found that the overturning mode occurs before the sliding and is, therefore, the controlling failure mode.

The equivalent static load was also verified using a full-scale static test in the same barrier-moment slab system used for TL-5 impact. The system was dimensioned using the equivalent static load of 60 kips (267 kN). The ultimate static resistance of the system, including the soil resistance, was 100 kips (445 kN). The unfactored and

factored static resistance to overturning were 74.8 kips (332.9 kN) and 67.3 kips (300 kN), respectively.

The propose design load was based on the evidence presented below. A decision was made to aim for a barrier-moment slab system design that would generate about 1 in. (25.4 mm) permanent movement at the coping section during impact. This permanent movement is considered acceptable as it would likely require little or no repair of the underlying MSE wall, and should not affect the impact performance of the barrier system.

b) Wall Reinforcement

The results of the MASH TL-5 full-scale crash test and the full-scale impact simulations with reinforcement lengths of 10 ft (3.05 m), 16 ft (4.88 m) and 24 ft (7.32 m) were used to design the guidelines for MASH TL-5 impact. The simulation results showed that the impact load was on average 167.3 kips (744.5 kN). The maximum 50-msec. average total loads, dynamic loads, and the wall displacement measured during the impact simulation are summarized in Table 9.6.

Table 9.10 Summary of the pullout resistance, maximum 50 msec. ave. strip load and wall displacement for MASH TL-5-1 impact simulation

Strip Length (ft)	AASHTO Pullout Resistance (kips)		Total Strip Load (kips)		Dynamic Wall Displacement (in.)			Approximate Permanent Wall Displacement (in.)		
	First Layer	Second Layer	First Layer	Second Layer	Top[(1)]	First Layer	Second Layer	Top[(1)]	First Layer	Second Layer
10	2.43	3.78	5.50	2.95	0.50	0.24	0.11	0.28	0.12	0.04
16	3.89	6.04	8.50	3.21	0.38	0.22	0.10	0.24	0.12	0.02
24	5.83	9.06	9.46	3.47	0.23	0.20	0.09	0.02	0.02	0.02

[(1)] Displacement measured at the coping level

The loads presented in Table 9.10 were computed at 7 in. (178 mm) from the face of the wall where the load is expected to be the highest. Even though the reinforcement appears to have reached its maximum pull out resistance during impact simulation, the overall performance of the wall was satisfactory in the FE analyses. Therefore, it was decided that having the reinforcement working at maximum pull out resistance would be acceptable given that the load duration is so short and the displacements were tolerable. The design recommendations are based on a pressure diagram approach that prescribes the pressure due to impact (in excess of static load) that must be resisted by the reinforcement.

The results of the MASH TL-5 full-scale crash test are summarized in Table 9.11. The total measured loads in the first and second of soil reinforcement were 2.39 kips

(10.64 kN) and 2.88 kips (12.82 kN), respectively. The maximum permanent displacement at the wall panels was 0.54 in. (13.7 mm).

Table 9.11 Summary of the dynamic design load on the strips for pullout resistance from the MASH TL-5 full-scale impact test

Strip Length (ft)	AASHTO Pullout Resistance (kips)		Total Strip Load (kips)		Static[(1)] Load (kips)		Dynamic[(1)] Load (kips)	
	First Layer	Second Layer	First Layer	Second Layer	Top Layer	Second Layer	Top Layer	Second Layer
10	2.43	3.78	2.40	2.88	0.79	0.90	1.60	1.98

[(1)] Measured loads

- Pullout of the Wall Reinforcement:

The results of the TL-5 full-scale test were used to develop the design guideline for pullout of the reinforcement. This reinforcement length was selected for the test as it generated the largest displacement in the soil reinforcing strip. The resistance (P) for the 10 ft (3.05 m) long strips was calculated to be 2.43 kips (10.8 kN) for the upper most layer and 3.78 kips (16.8 kN) for the second layer using Eq. (2-2) in Chapter 2 (AASHTO 11.10.6.3.2-1). The pullout friction factor F* was 1.63 for the upper most layer and 1.49 for the second layer.

The measured total load (50-msec. average) at the upper most layer of strips was 2.39 kips (10.64 kN). This load theoretically reached the strip resistance to pull out of

the test wall (2.43 kips (10.8 kN)). Therefore, the measured dynamic load will generate a similar equivalent dynamic pressure distribution than the resistance in excess of the static load to resist pull out failure of the strips for MASH TL-5.

The controlling design load in excess of the static load due to static earth pressures was calculated to be 1.60 kips (7.21 kN). The value was found by calculating the total resistance of the 10 ft (3.05 m) long strip at the depth of the first layer (2.43 kips (10.8 kN)) minus the calculated load due to static earth pressures from AASHTO LRFD (0.83 kips (3.69 kN)). This load represent a static load, equivalent to a dynamic load, which would indicate that the 10 ft (3.05 m) long strip perform well in the case of a TL-5 impact.

At the second layer, the same process was followed. The total measured dynamic load was 2.88 kips (12.82 kN). The static earth pressure load for the second layer was calculated to be 1.33 kips (5.92 kN) by AASHTO LRFD. The total measured load from the test (2.88 kips (12.82 kN) was therefore less than the calculated pullout load at that depth (3.48 kips (15.5 kN)). Therefore, the measured dynamic load in excess of the static load was used as the controlling dynamic load for pullout design. Table 9.12 shows the total measured dynamic load from the simulation, calculated static load, calculated pullout resistance, and the recommended design pressure for pullout resistance.

The dynamic pressure per strip was calculated as shown in Table 9.12. For the 10 ft (3.05 m) long strip with a density of 3 strips per panel per layer, the tributary area was 2.57 ft^2 (0.24 m^2) for the top layer and the tributary area was (3.94 ft^2) 0.37 m^2 for the second layer. The dynamic design pressure was calculated as shown in Table 9.12. The

dynamic design pressure in excess of the static earth pressure for pullout is recommended to be 625 psf (29.93 kPa) for the upper most layer and 500 psf (23.94 psf) for the second layer. The dynamic pressure at the first layer of reinforcement has a tributary height of 19 in. ft (482.5 mm). Therefore, the tributary working area is 2.57 ft^2 (0.24 m^2).

Table 9.12 Test results of the TL-5-1 impact and calculation of design strip load for pullout design

	(1) Total (kips)	(2) Static Load (kips)	(3)=(1)-(2) Dynamic Load (kips)	(4) Calculated Resistance[(a)] (kips)	Controlling Design Dynamic Load (kips)	Total Design Pressure (psf)
Top Layer (Measured)	2.39	0.79	1.60	2.43	(1)-(2) = 1.60	1600 lb./2.57 ft^2[(b)] = **623 psf (Final 625)**
Top Layer (Excess load from Resistance)	--	0.82	--	2.43	(4)-(2) = 1.61	1610 lb./2.57 ft^2 [(b)] = **626 psf (Final 625)**
Second Layer (Measured)	2.88	0.90	1.98	3.78	(1)-(2) = 1.98	1980 lb./3.94 ft^2 [(c)] = **502 psf (Final 500 psf)**

[(a)] Calculated from AASHTO 11.10.6.2 – 11.10.6.3

[(b)] Tributary area of the panel for the top layer (2.57 ft^2 = 4.87 ft × 1.583 ft / 3 strips per panel)

[(c)] Tributary area of a panel for the second layer (3.94 ft^2 = 4.87 ft × 2.43 ft / 3 strips per panel)

- Yielding of the Wall Reinforcement:

The reinforcement resistance to yielding (R) for a strip was calculated using Eq. (8-15). The tensile strength of the reinforcement (σ_t) was 60 ksi (414 MPa) and the thickness,

after accounting for corrosion loss (E_c), was 0.102 in. (2.59 mm) for a 75-year design life. The R was computed to be 12.02 kips (53.5 kN).

To develop the design guideline against yielding of the reinforcement, the highest average dynamic load on the strip, computed from the full-scale impact simulation, was used. The maximum 50 msec. average total load on the strip located in the uppermost layer was 9.46 kips (41.83 kN) (24 ft (7.32 m) long strip).

In the second layer, the higest excess dynamic load was at the 16 ft (4.88 m) long strip. Therefore, the controlling dynamic design strip load for yielding of the reinforcement is 8.22 kips (36.6 kN) for the uppermost layer and 1.86 kips (8.27 kN) for the second layer (Table 9.13).

Table 9.13 Simulation results for TL-5-1 impact and calculation of design strip load for yielding design

Strip Length (ft)	(1) Dynamic Load (kips)		(2) Static Load[(a)] (kips)		(3)=(1)+(2) Total Load (kips)		(4) Calculated Resistance[(b)] (kips)		Controlling Design Dynamic Load (kips)	
	First Layer	Second Layer	First Layer	Second Layer	First Layer	Second Layer	First Layer	Second Layer	First Layer	Second Layer
10	4.70	1.60	0.82	1.35	5.52	2.95	12.02	12.02		
16	7.70	1.86	0.82	1.35	8.52	3.21	12.02	12.02	8.22	1.86
24	8.22	1.44	1.24	2.03	9.46	3.47	12.02	12.02		

[(a)]Calculated from AASHTO 11.10.6.4.3
[(b)]Reinforcement steel ASTM Grade 60

The dynamic pressure per strip for yielding of the reinforcement was calculated as shown in Table 9.14. For 16 ft (4.88 m) long strip with a density of 3 strips per panel per layer, the tributary area was 4.60 ft^2 (0.43 m^2). For 24 ft (7.32 m) long strip with a density of 2 strips per panel per layer, the tributary area was 4.38 ft^2 (0.41 m^2). The dynamic design pressure in excess of static earth pressure to consider in the design against yielding of the reinforcement was calculated as shown in Table 9.14. The dynamic design pressure for rupture of the reinforcement is recommended to be 1790 psf (85.7 kPa) for the uppermost layer and 500 psf (23.94 kPa) for the second layer.

Table 9.14 TL-5-1 design pressure for yielding of soil reinforcement

Layer	Total Load (kips)	Static Load (kips)	Dynamic Design Load (kips)	Total Design Pressure, *p*
Top	9.46	1.24	8.22	8220 lb./ 4.60 ft^2 [(a)] = **1786 psf** **(Final 1790 psf)**
Second	3.21	1.35	1.86	1860 lb./ 3.94 ft^2 [(b)] **472 psf** **(Final 500 psf)** [(c)]

[(a)] Tributary area of the panel for the top layer (4.60 ft^2 = 4.87 ft × 1.89 ft / 2 strips per panel)
[(b)] Tributary area of a panel for the second layer (3.94 ft^2= 4.87 ft × 2.44 ft / 3 strips per panel).
[(c)] The design pressure for pullout is used since it is more critical.

9.3.3 Data for TL-5-2

a) Barrier-Moment Slab System

The final design load for MASH TL-5-2 impact is 260 kips (1157 kN). This load was selected by using the results of the FE analyses and it applies to any barrier higher than 42 in. (1067 mm) where the mass of the trailer is engaged during the impact. Barriers taller than 42 in. (1067 mm) have also been crash-tested by TTI researchers, as shown in Table 2.4.

To preclude any damage to the underlying MSE wall or relative displacement between barriers, the recommended length of the precast barrier section for TL-5-2 is 15 ft (4.57 m). This length will enable the barriers to develop their primarily failure mechanism (yield line) in the wall face provided the coping is sufficiently strong. This is the preferred failure mode of the barrier-coping-moment slab system because it reduces the cost of repair after a severe impact.

The dimensions of the moment slab are determined using an equivalent static load of 80 kips (356 kN) around the point of rotation B. The load is located at a height of 43 in. (1092 mm) from the finished grade. The calculation indicates that an approximately 9 ft (2.74 m) wide (measured from the face of the panel), 30 ft (9.14 m) long moment slab without the shear strength of the soil is capable to withstand a TL-5-2 impact. Therefore, the equivalent static load per unit length of wall is 2.67 kips/ft (39

kN/m). It was found that the overturning mode occurs before the sliding. However, the system also slides significantly as shown in the full-scale impact simulation.

The propose design load was based on the evidence presented below. A decision was made to aim for a barrier-moment slab system design that would generate about 1 in. (25.4 mm) permanent movement at the coping section during impact. However, the full-scale impact simulation showed that the permanent displacement of the barrier system overcome the displacement threshold. Yet, the results of the full-scale crash test allow estimating that even at those levels of displacements, the overall behavior of the system would be acceptable. Consequently, the design equivalent static load is based on the 9 ft (2.74 m) wide moment slab.

b) Wall Reinforcement

The results of the MASH TL-5-2 full-scale impact simulations with reinforcement lengths of 10 ft (3.05 m), 16 ft (4.88 m) and 24 ft (7.32 m) were used to design the guidelines for MASH TL-5-2 impact. The simulation results showed that the impact load was on average 257 kips (1144 kN). The maximum 50-msec. average dynamic loads, including the static load, and the wall displacement measured during the impact simulation is summarized in Table 9.15.

Table 9.15 Summary of the pullout resistance, maximum 50 msec. ave. strip load and wall displacement for MASH TL-5-2 impact simulation

Strip Length (ft)	AASHTO Pullout Resistance (kips)		Total Strip Load (kips)		Dynamic Wall Displacement (in.)			Approximate Permanent Wall Displacement (in.)		
	First Layer	Second Layer	First Layer	Second Layer	Top[(1)]	First Layer	Second Layer	Top[(1)]	First Layer	Second Layer
10	2.48	3.82	7.16	3.99	1.1	0.63	0.2	0.91	0.55	0.20
16	3.96	6.11	9.02	2.90	1.02	0.69	0.11	0.75	0.51	0.10
24	5.94	9.17	10.55	2.71	0.37	0.24	0.08	0.16	0.08	0.02

[(1)] Displacement measured at the coping level

The loads presented in Table 9.15 were computed at 7 in. (178 mm) from the face of the wall where the load is expected to be the highest. Even though the reinforcement appears to have reached its maximum pull out resistance during the impact simulation, the overall performance of the wall was satisfactory in the FE analyses. However, is observed that the wall might experience an excessive wall permanent displacement (>0.75 in. (19.05 mm) during a MASH TL-5-2 impact which could induce structural failure in the wall components. Therefore, it was decided that the design recommendations are based on a pressure diagram approach that prescribes the pressure due to impact (in excess of static load) that must be resisted by the 16 ft (4.88 m) long strip reinforcement with a density of two strips per panel in the first and

second layer. Such equivalent design pressure will prevent excessive movement of the wall.

- Pullout of the Wall Reinforcement:

The average design strip load in excess of static for the TL-5 impact simulation with 16 ft (4.88 m) long reinforcement strip was used to develop the design guideline for pullout of the reinforcement. The 10 ft (3.05 m) long strip reinforcement was not selected for pullout analyses as it generated excessive wall displacement. The resistance (P) for the 16 ft (4.88 m) long strips was calculated to be 3.96 kips (17.62 kN) for the upper most layer and 6.11 kips (27.2 kN) for the second layer using Eq. (2-2) in Chapter 2 (AASHTO 11.10.6.3.2-1). The pullout friction factor F* was 1.63 for the upper most layer and 1.49 for the second layer.

The total load (50-msec. average) in the strip at the upper most layer was 9.02 kips (40.14 kN). Although the measured total load in the strip was higher than the resistance (3.96 kips (17.62 kN)), the displacement of the strips and performance of the wall were considered acceptable. In other words, the analyses indicate that a 16 ft (4.88 m) long strip will perform acceptably for a TL-5-2 impact. Therefore, the resistance was used to obtain the dynamic design load in excess of the static load at the upper most layer. The controlling design load in excess of the static load due to static earth pressures was calculated to be 3.12 kips (13.88 kN). The value was found by calculating the total resistance of the 16 ft (4.88 m) long strip at the depth of the first layer (3.96 kips (17.62 kN)) minus the calculated load due to static earth pressures from AASHTO LRFD (0.84

kips (3.74 kN)). This load represent a static load, equivalent to a dynamic load, which would indicate that the 16 ft (4.88 m) long strip perform well in the case of a TL-5-2 impact.

At the second layer, the same process was followed. The total dynamic load was 2.90 kips (12.91 kN). The static earth pressure load for the second layer was calculated to be 1.37 kips (5.96 kN) by AASHTO LRFD. The total load from the simulation (2.90 kips (12.91 kN) was therefore less than the calculated pullout load at that depth (6.11 kips (15.5 kN)). Therefore, the measured dynamic load in excess of the static load was used as the controlling dynamic load for pullout design. Table 9.16 shows the total measured dynamic load from the simulation, calculated static load, calculated pullout resistance, and the recommended design pressure for pullout resistance.

The dynamic pressure per strip was calculated as shown in Table 9.16. For the 16 ft (4.88 m) long strip with a density of 2 strips per panel at the top layer, the tributary area was 3.86 ft^2 (0.36 m^2). For the second layer with a density of 2 strips per panel the tributary area was (5.94 ft^2) 0.55 m^2. The dynamic design pressure was calculated as shown in Table 9.16. The dynamic design pressure in excess of the static earth pressure for pullout is recommended to be 810 psf (38.78 kPa) for the upper most layer and 500 psf (24 kPa) for the second layer.

Table 9.16 Simulation results of the TL-5-2 impact and calculation of design strip load for pullout design

	(1) Total (kips)	(2) Static Load (kips)	(3)=(1)-(2) Dynamic Load (kips)	(4) Calculated Resistance [a] (kips)	Controlling Design Dynamic Load (kips)	Total Design Pressure (psf)
Top Layer	9.02	0.84	8.18	3.96	(4)-(2) = 3.12	3120 lb./3.86 ft^2 [b] = 808 **psf** **(Final 810 psf)**
Second Layer	2.90	2.03	0.87	6.11	(1)-(2) = 0.87	870 lb./5.94 ft^2 [c] = **145 psf** **(Final 500 psf)**[d]

[a] Calculated from AASHTO 11.10.6.2 – 11.10.6.3

[b] Tributary area of the panel for the top layer (3.86 ft^2 = 4.87 ft × 1.583 ft / 2 strips per panel)

[c] Tributary area of a panel for the second layer (5.94 ft^2 = 4.87 ft × 2.44 ft /2 strips per panel)

[d] Used design pressure for pullout as determined for MASH TL-5-1

- Yielding of the Wall Reinforcement:

The reinforcement resistance to yielding (R) for a strip was calculated using Eq. (8-15). The tensile strength of the reinforcement (σ_t) was 60 ksi (414 MPa) and the thickness, after accounting for corrosion loss (E_c), was 0.102 in. (2.59 mm) for a 75-year design life. The R was computed to be 12.02 kips (53.5 kN).

To develop the design guideline against yielding of the reinforcement, the highest design load on the strip, computed from the full-scale impact simulation, was used. The maximum 50 msec. average total load on the strip located in the uppermost layer was 10.55 kips (46.95 kN) (24 ft (7.32 m) long strip). In the second layer, the total load was 3.53 kips (15.71 kN) (24 ft long strip). Therefore, the controlling dynamic

design strip load for yielding of the reinforcement is 9.29 kips (41.34 kN) for the uppermost layer and 1.47 kips (6.54 kN) for the second layer (Table 9.17).

Table 9.17 Simulation results for TL-5-2 impact and calculation of design strip load for yielding design

Strip Length (ft)	(1) Dynamic Load (kips)		(2) Static Load[(a)] (kips)		(3)=(1)+(2) Total Load (kips)		(4) Calculated Resistance[(b)] (kips)		Controlling Design Dynamic Load (kips)	
	First Layer	Second Layer	First Layer	Second Layer	First Layer	Second Layer	First Layer	Second Layer	First Layer	Second Layer
10	6.32	2.62	0.84	1.37	7.16	3.99	12.02	12.02		
16	8.18	1.63	0.84	1.37	9.02	2.90	12.02	12.02	9.29	1.63
24	9.29	1.47	1.26	2.06	10.55	3.53	12.02	12.02		

[(a)] Calculated from AASHTO 11.10.6.4.3
[(b)] Reinforcement steel ASTM Grade 60

The dynamic pressure per strip for yielding of the reinforcement was calculated as shown in Table 9.18. For 16 ft (4.88) long strip with a density of 3 strips per panel per layer, the tributary area was 3.94 ft^2 (0.37 m^2) at the second layer. For 24 ft (7.32 m) long strip with a density of 2 strips per panel per layer, the tributary area was 3.85 ft^2 (0.36 m^2). The dynamic design pressure in excess of static earth pressure to consider in the design against yielding of the reinforcement was calculated as shown in Table 9.18. The dynamic design pressure for rupture of the reinforcement is recommended to be

2410 psf (115.4 kPa) for the uppermost layer and 500 psf (23.94 kPa) for the second layer.

Table 9.18 TL-5-2 design pressure for yielding of soil reinforcement

Layer	Total Design Load (kips)	Static Design Load (kips)	Dynamic Design Load (kips)	Total Design Pressure, *p*
Top	10.55	1.26	9.29	9290 lb./3.85 ft^2 [(a)] = **2413 psf** **(Final 2410 psf)**
Second	2.90	1.37	1.63	1630 kips/3.94 ft^2 [(b)] = **357 psf** **(Final 500 psf)**[(c)]

[(a)] Tributary area of the panel for the top layer (3.85 ft^2 = 4.87 ft × 1.583 ft / 2 strips per panel)
[(b)] Tributary area of a panel for the second layer (3.94 ft^2 = 4.87 ft × 2.43 ft / 3 strips per panel).
[(c)] Used design pressure for pullout as determined for MASH TL-5-1

10 SUMMARY AND CONCLUSION

10.1 Summary

10.1.1 Section 1

The problem statement and objective are presented in Chapter 1. The research plan for accomplishing the project objectives to develop procedures for designing roadside barrier systems placed on MSE retaining structures for TL-3 through TL-5 impact consisted of ten tasks.

10.1.2 Section 2

Design and construction methods of MSE walls are presented in term of LRFD. In addition, background regarding roadside barrier crash testing criteria, design impact loads for heavy vehicles and design practice of roadside barriers placed atop of MSE retaining wall are presented.

10.1.3 Section 3

MASH TL-4 and TL-5 impact load studies were performed on rigid barriers of different heights. The study was conducted using measured data from previous full-scale tests and

FE analyses. It was found that the magnitude, distribution and resultant height of the impact load are influenced by the height of the barrier.

The MASH TL-4 impact simulations were conducted using barrier heights ranging from 36 in. (914 m) to a very tall rigid wall. It was found that the lateral impact load increases with the height of the barrier. The selected design impact load was 80 kips (356 kN) located at 30 in. (762 mm) from the finished grade.

The MASH TL-5 impact simulations were conducted using barrier heights ranging from 42 in. (1067 mm) to a very tall rigid wall. A dramatic increase in the impact load was found between barriers of 42 in. (1067 mm) heights and taller barriers. This load increment was associated with the effect imposed by the trailer and the rigid ballast when it hits the barrier during redirection of the vehicle. Based on that, the MASH TL-5 analyses was divided into two: a) MASH TL-5-1 associated with a 42 in. (1067 mm) tall barrier and a design impact load of 160 kips (712 kN) located at 34 in. (864 mm) from the finished grade, and, b) MASH TL-5-2 associated with barriers taller than 42 in.(1067 mm) and a design impact load of 260 kips (1157 kN) located at 43 in. (1092 mm) from the finished grade.

10.1.4 Section 4

A set of full-scale impact simulations on barrier-moment slab systems were performed to evaluate their dynamic behavior when subjected to a MASH TL-4 and MASH TL-5 impact. The results indicates that the required width of moment slab for TL-4, TL-5-1,

and TL-5-2 are 4.5 ft (1.37 m), 7 ft (2.13 m) and 9 ft (2.74 ft), respectively. The analyses were conducted using a 30 ft long moment slab and a displacement threshold of 1.0 in. (25.4 mm) permanent at the barrier coping section.

Upon completion of the dynamic analyses, the same systems were used to perform a quasi-static FE analyses. The results indicate that the required static capacity of the system are 23 kips (102.4 kN), 60 kips (267 kN) and 80 kips (356 kN) for TL-4, TL-5-1, and TL-5-2, respectively. These loads are based on the point of rotation B, 1.0 in. (25.4 mm) permanent displacement threshold and discounting the shear strength of the soil.

10.1.5 Section 5

Several impact simulations were conducted using a prototype barrier-moment slab system. The objective of this section was to theoretically explain the ratio of dynamic to static load (DAF) in the design of a barrier-moment slab system. A generic diagram was developed to help predict the dynamic load using the static load when the impact conditions are different from the nominal values.

10.1.6 Section 6

The barrier moment slab systems analyzed in section 4 were placed on top of an MSE wall model to conduct the full-scale impact simulations. The analyses were conducted

using wall reinforcement of different lengths (10 ft (3.05 m), 16 ft (4.88 m) and 24 ft (7.32 m)). The results obtained from the shortest strips were used to develop the guideline for pullout resistance and the results from the longest strips were used to develop guidelines for yielding of the strip reinforcement.

10.1.7 Section 7

A TL-5 full-scale crash test on a roadside barrier system on top of an MSE Wall was designed and planned according to the results obtained from the full-scale impact simulation. The roadside barrier mounted on the edge of the MSE wall performed acceptably according to the evaluation criteria specified for MASH test designation 5-12 and the displacement criteria established in this report. The roadside barrier on top of the MSE wall contained and redirected the 36000V vehicle. The vehicle did not penetrate, underride, or override the installation. No detached elements, fragments, or other debris was present to penetrate or show potential for penetrating the occupant compartment, or to present hazard to others in the area. The 36000V vehicle remained upright during and after the collision event. Maximum roll was 32.5 degrees. Test results are presented in Figure 7.29.

10.1.8 Section 8

A full-scale static test was designed and planned according to the results of the quasi-static FE analyses. The test was conducted on the same roadside barrier-moment slab system used for the TL-5 full-scale crash test. The objective of the analysis was to verify the static load required to initiate movement of the system The ultimate load, determined from the test, was around 100 kips (445 kN) including the strength of the soil. The system failed by overturning, however, there was considerable sliding of the system. The results verified the load

10.1.9 Section 9

The resulting guidelines are presented in Chapter 9. They were developed following AASHTO LRFD design practices and followed the methodology presented in NSHCP Report 663 *(1)*. The design procedures for the barrier system address sliding, overturning, structural adequacy of the coping, and wall panel. Dynamic load and static load are also presented in the guidelines. The reinforcement design procedure considers pullout and rupture of the reinforcement. The dynamic design loads are specified using both a pressure distribution approach and line load approach.

10.2 Conclusion

The use of MSE wall structures has increased dramatically in recent years. Traffic barriers are frequently placed on top of the MSE wall to resist vehicular impact. The barriers are anchored to the concrete in case of rigid pavement. Nevertheless, in case of flexible pavement, the barriers are constructed in an L shape so that the impact load on the vertical part of the L can be resisted by the inertia force required to uplift the horizontal part of the L. The barrier must be designed to resist the full dynamic load but the size of the horizontal part of the L (moment slab) is determined using an equivalent static load.

Full scale impact simulations on rigid barriers of different heights were conducted for MASH TL-4 and MASH TL-5 impact. The results were used to help defined impact loads in the lateral, longitudinal, and vertical direction, and the longitudinal distribution and height of the resultant lateral load. These recommendations are selected to represent a practical design scenario associated with each impact level. For MASH TL-5, the final recommendations also address the effect of the trailer on the amount of load imposed to the barrier.

The full-scale dynamic impact simulations and the quasi-static FE analyses were used to develop design guidelines for stability of the barrier-moment slab system when subjected to vehicular impact. The guidelines define recommended design loads for barrier and coping section design and overall stability of the system against sliding and rotation. In addition, section 5 of this document provide a comprehensive analyses of the

relation between the dynamic and the static load component associated with each test level. The information was ultimately summarized in a diagram which helps to predict impact load given impact condition and system characteristic.

Guideline for the wall panels and wall reinforcements were developed on the basis of full scale impact simulation of barrier placed on top of an MSE wall. They address pullout and yielding of the MSE wall reinforcements and structural adequacy of the MSE wall panels. The guidelines for pullout were developed on the basis of minimal wall reinforcement (10 ft (3.05 m) long strip). The guidelines for yielding were developed on the basis of larger wall reinforcement (24 ft (7.32 m) long strip). The dynamic design loads for the reinforcement are specified using a pressure distribution approach and a line load approach.

A full-scale tractor-trailer (TL-5) crash test into a N.J. shape barrier mounted on the edge of a 9.8 ft (3 m) tall MSE wall was performed. Damage and displacement of the MSE wall panels and the barrier system were minimal and within tolerance. The barrier was made of 15 ft (4.57 m) long precast barrier-coping sections connected to a 7 ft (2.13 m) wide and 30 ft (9.15 m) long moment slabs and performed as well as the wall. This wall barrier system was designed according to the guidelines presented in section 6 of this document. The entire system behaved well and no repairs would be necessary. The results of the full-scale crash test were used to verify and modify the proposed guideline determined from full-scale impact simulation.

During the test, the load in the top level of reinforcement reached the maximum load calculated by AASHTO-LRFD Bridge Design Specifications. In the simulation

analyses, the load in the top layer of reinforcement were higher that the calculated by AASHTO-LRFD. This means that the reinforcement could have been at pull out failure during the impact. However, the overall behavior of the wall system was adequate. Therefore, it is acceptable and allowed in the guidelines to have the reinforcement of the soil at failure since the spikes (peak loads) in the time history load of the strips occurs for a short period of time such as the strips does not have time to displace considerably.

The final guidelines are presented in section 9 of this report. It address structural and stability design of the barrier-coping system, wall reinforcement analyses for pullout and yielding and structural adequacy of the MSE wall panels. They were developed following AASHTO LRFD design practices and the NCHRP Report 663 procedure *(1).* The analyses was conducted using a reference the point of rotation between the coping section and the wall panels (Rotation Point B) as it is the common mechanism observed in practice. However, the results are also applicable to the point of rotation A.

REFERENCES

1. Berg, R., B. Christopher and N. Samtani. *Design of Mechanically Stabilized Earth walls and Reinforced Soil Slopes – Volume I*. Ryan R. Berg & Associates, Inc. 2190 Leyland Alcove, MN 55125, National Highway Institute, Federal Highway Administration, U.S. Department of Transportation, Washington, D.C. November 2009.

2. Bligh, R.P., J.L. Briaud, K.M. Kim and A. Abu-Odeh. *Design of Roadside Barrier Systems Placed on MSE Retaining walls*. NCHRP Report 663, Transportation Research Board, National Research Council, Performed by Texas Transportation Institute, College Station, TX, 2009.

3. *AASHTO LRFD Bridge Design Specifications, Fourth Edition*. American Association of State Highway and Transportation Officials, Washington, D.C., 2010.

4. Ross, H.E., D.L. Sicking, R.A. Zimmer and J.D. Michie. Recommended Procedures for Safety Performance Evaluation of Highway Features. National Cooperative Research Program (NCHRP) Report No. 350, Transportation Research Board, Washington, D.C., 1993.

5. *AASHTO Manual for Assessing Safety Hardware (MASH), First Edition*. American Association of State Highway and Transportation Officials, Washington, D.C., 2009.

6. Hallquit, J.O. LS-DYNA: Keyword User's Manual, Version 971. Livermore Software Technology Corporation (LSTC), Livermore, CA, 2007.

7. *Minimum Embedment Requirements for MSE Structures: Technical Bulletin: MSE - 7*, The Reinforced Earth Company, October 1995.

8. Stuedlein, A.W., M. Bailey , D. Lindquist , J. Sankey and W.J. Neely. Design and Performance of a 46-m-High MSE Wall. *Journal of Geotechnical and Environmental Engineering*, ASCE, Vol. 136, No. 6, June 1, 2010, pp. 786–796.

9. Horpibulsuk, S. and A. Niramitkornburee. Pullout Resistance of Bearing Reinforcement Embedded in Sand. *In Soil and Foundation, Japanese Geotechnical Society*, Vol. 50, No. 2, April, 2010, pp. 215–226.

10. Huang, B., R. J. Bathurst and T. M. Allen. Load and Resistance Factor Design (LRFD) Calibration for Steel Strip Reinforced Soil Walls. *Journal of Geotechnical and Environmental Engineering*, ASCE, Vol. 138, No. 8, (in press).

11. Elias, V., B. Christopher and R. Berg. *Mechanically Stabilized Earth walls and Reinforced Soil Slopes Design and Construction Guidelines*. Ryan R. Berg & Associates, Inc. 2190 Leyland Alcove, Woodbury, MN 55125; National Highway Institute, Federal Highway Administration, U.S. Department of Transportation, Washington, D.C. March 2001.

12. Committee on Guardrails and Guide Posts. Proposed Full-Scale Testing Procedures for Guardrails. Highway Research Correlation Service Circular 482, Highway Research Board, Washington, D.C., 1962.

13. Beason, W.L. and T.J. Hirsch. Measurement of Heavy Vehicle Impact Forces and Inertia Properties. Research Report. Texas Transportation Institute, College Station, TX, 1989.

14. Noel, J.S., T.J. Hirsch, C.E., Buth and A. Arnold. *Loads on Bridge Railings.* Transportation Research Record 796, Transportation Research Board, Washington, D.C., 1981, pp 31-35.

15. Buth, C.E., A. Arnold, W. L. Camprise, T. J. Hircsh, D. L. Ivey and J. S. Noel. Safer Bridge Railings, Volume 1: Summary Report. Report No. FHWA/RD-82/072, Federal Highway Administration, U.S. Department of Transportation, Washington, D.C., 1984.

16. *AASHTO Standard Specifications for Highway Bridges, 17th Edition*. American Association of State Highway and Transportation Officials. Washington, D.C., 2002.

17. *AASHTO Standard Specifications for Highway Bridges, 9th Edition*. American Association of State Highway and Transportation Officials. Washington, D.C., 1965.

18. Bullard, D.L., R. Bligh, and W. Menges. *MASH08 TL-4 Testing and Evaluation of the New Jersey Safety Shape Bridge Rail.* Prepared for National Cooperative Highway Research Program Transportation Research Board National Research Council, Performed by the Texas Transportation Institute, Texas A&M University System, College Station, TX, November 2008.

19. Nauman, M.S., R. Bligh and W. Menges. *Development and Testing of MASH Test Level 4 Concrete Bridge Rail*. Texas Transportation Institute (TTI), College Station, TX, 2010.

20. Hirsch, T.J., and A. Arnold. *Bridge Rail to Restrain and Redirect 80,000 lb. Trucks.* Report No. FHWA/TX-81/16+230-4F, Performed for the Texas State Department of Highways and Public Transportation, Performed by the Texas Transportation Institute, Texas A&M University System, College Station, TX, November 1981.

21. Hirsch, T.J., and W.L. Fairbanks. *Bridge Rail to Contain and Redirect 80,000 lb. Tank Trucks.* Report No. FHWA/TX-84-911-1F, Performed for the Texas State Department of Highways and Public Transportation, Performed by the Texas Transportation Institute, Texas A&M University System, College Station, TX, February 1984.

22. Hirsch, T.J., W.L. Fairbanks and C.E. Buth. *Concrete Safety Shape with Metal Rail on Top to Redirect 80,000 lb. Trucks.* Texas Transportation Institute, Transportation Research Record No. 1065, pp. 79-87, 1986.

23. *AASHTO Roadside Design Guide, 4th Edition*. American Association of State Highway and Transportation Officials (AASHTO), Washington, D.C., 2011.

24. Buth, C.E and Campise, W. L. *Full-Scale Crash Tests of High-Performance Median Barrier*. Federal Highway Administration, U. S. Department of Transportation, Washington D.C., Prepared by the Texas Transportation Institute, College Station, TX, 1982.

25. Campise, W.L. and C.E. Buth. *Performance Limits of Longitudinal Barrier Systems, Volume III-Appendix B: Details of Full-Scale Crash Tests on Longitudinal Barriers.* Performed for the Federal Highway Administration, Performed by the Texas Transportation Institute, Texas A&M University System, College Station, TX, February 1986.

26. Alberson, D.C., R.A. Zimmer and W.L. Menges. *NCHRP Report 350 Compliance Test 5-12 of the 1.07 m Vertical wall Bridge Railing.* Report to Federal Highway Administration, Texas Transportation Institute, January 1997.

27. Polivka, K.A., R.K. Faller, J.C. Holloway, J.R. Rohde, and D.L. Sicking. *Development, Testing, and Evaluation of NDOR's TL-5 Aesthetic Open Concrete Bridge Rail.* MwRSF Report No. TRP-03-148-04, University of Nebraska-Lincoln, Lincoln, NE, 2005.

28. Rosenbaugh, S.K., D.L. Siking, and R.K. Faller. *Development of a TL-5 Vertical Faced Concrete Median Barrier Incorporating Head Ejection Criteria*. MwRSF Report No. TRP-03-194-07, University of Nebraska-Lincoln, Lincoln, NE, 200**7**.

29. Buth, C. E. and W.L. Menges. *MASH Test 5-12 of the Schöck ComBAR Parapet.* Performed for Competence Center ComBARSchöck Bauteile GmbH, Performed by the Texas Transportation Institute, Texas A&M University System, College Station, TX, March, 2011.

30. Buth, C. E. and W.L. Menges. *MASH Test 5-12 on the Ryerson Pultrall Parapet.* Performed for Ryerson University, Toronto, Canada, Performed by the Texas Transportation Institute, Texas A&M University System, College Station, TX, February, 2012.

31. Buth, C.E., T.J. Hirsh and W.L Menges. *Testing of New Bridge Rail and Transition Design-Volume XI: Appendix J: 42 in. (1.07 m) F-Shape Bridge Railing.* Report No. FHWA-RD-93-068, Pooled Funds Bridge Rail Study, Federal Highway Administration, Washington, D.C., September 1993.

32. Buth, C.E., T.J. Hirsh and W.L. Menges. *Testing of New Bridge Rail and Transition Design-Volume X: Appendix I: 42 in. (1.07 m) Concrete Parapet Bridge Railing.* Report No. FHWA-RD-93-067, Pooled Funds Bridge Rail Study, Federal Highway Administration, Washington, D.C., September 1993.

33. Olson, R., E. Post and W. McFarland. *Tentative Service Requirements for Bridge Rail Systems.* National Cooperative Highway Research Program (NCHRP) Report 86, Washington, D.C., 1970.

34. Hirsch, T.J. *Longitudinal Barriers for Buses and Trucks State of the Art*. Report No. FHWA/TX-86/32+416-2F, Performed for the Texas State Department of Highways and Public Transportation, Performed by the Texas Transportation Institute, Texas A&M University System, College Station, TX, February 1986.

35. *AASHTO Guide Specifications for Bridge Railings.* American Association of State Highway and Transportation Officials, Washington, DC, 1989.

36. Faller, R., D. Sicking, J. Larsen, J. Rohde, R. Bielenberg and K. Polivka. *TL-5 Development of 42 in. and 51 in. Tall, Single-Faced, F-Shape Concrete Barriers*. MwRSF Research Report No. TRP-03-149-04, University of Nebraska-Lincoln, Lincoln, NE, 2005.

37. National Crash Analysis Center (NCAC). *Finite Element Vehicle Models: Chevrolet C2500 Pickup.* George Washington University, VA. http://www.ncac.gwu.edu/vml/ models.html. , Accessed in June 2008.

38. National Transportation Research Center, Inc. (NTRCI). *Methodology for Validation and Documentation of Vehicle Finite Element Crash Models for Roadside Hardware Applications.* University Transportation Center, Knoxville, TN. http://single-unit-truck.model.ntrci.org/description/. Accessed in March 2011.

39. National Transportation Research Center, Inc. (NTRCI). *Finite Element Models for SemitrailerTrucks.* University Transportation Center, Knoxville, TN. http://thyme.ornl.gov/FHWA/TractorTrailer/index.cgi?model=1&navv=0. Accessed in February 2011.

40. Polaxico, C., J. Kennedy, B.S. Simunovic and N. Zisi. *Enhanced Finite Element Analysis Crash Model of Tractor-Trailers (Phase A).* National Transportation Research Center, Inc., University Transportation Center, Knoxville, TN., 2008.

41. Polaxico, C., J. Kennedy, B.S. Simunovic and N. Zisi. *Enhanced Finite Element Analysis Crash Model of Tractor-Trailers (Phase B).* National Transportation Research Center, Inc., University Transportation Center, Knoxville, TN., 2008.

42. Murray, Y.D. *User's Manual for LS-DYNA Concrete Material Model 159.* Publication FHWA-HRT-05-063, Federal Highway Administration, U.S. Department of Transportation, VA, 2007.

43. Abu-Odeh, A., K.M. Kim, W. Williams, E. Buth and C. Patten. *Crash Wall Design for Mechanically Stabilized Earth (MSE) Retaining Wall Phase I: Engineering Analysis and Simulation.* Sponsored by Roadside Safety Research Program Pooled Fund Study, Performed by the Texas Transportation Institute, Texas A&M University System, College Station, TX, November 2008.

44. Abu-Odeh, A. *Application of New Concrete Model to Roadside Safety Barriers*. The 9th International LS-DYNA User Conference, Dearborn, MI, June 04-06, 2006.

45. *Crash Testing of a Precast Concrete Atop of a Reinforced Earth Wall: Technical Bulletin: MSE -8*, The Reinforced Earth Company, October 1995.

46. Saez, D.O. *Determination of Soil Properties of Sandy Soils and Road Base at Riverside Campus Using Laboratory Testing and Numerical Simulation*. MS Thesis, Dept. of Civil Engineering, Texas A&M University, College Station, TX, May 2010, 229 p.

47. Elitok, K., Mehmet A.G., Bertan B. and Ulrich S. *An Investigation on the Roll-Over Crashworthiness of an Intercity Coach, Influence of Seat Structure and Passenger Weight*. The 9th International LS-DYNA User Conference, Dearborn, MI, June 04-06, 2006.

48. *Standard Specifications for Construction and Maintenance of Highways, Streets, and Bridges*, Texas Department of Transportation, 2004.

49. Briaud J.-L., Li Y. and Rhee K. BCD: A Soil Modulus Device for Compaction Control", *Journal of Geotechnical and Geoenvironmental Engineering*, ASCE, Reston, VA, Vol. 132, No. 1.

APPENDIX A

PRELIMINARY DESIGN OF MSE WALLS FOR TL-4, TL-5-1 AND TL-5-2 IMPACT

Note: the pullout and yielding pressures were scaled based on NCHRP Report 663. These values are only preliminary and, therefore, they will be revised upon completion of the FE analyses and the full-scale crash test.

Preliminary Design of MSE Wall for TL-4 Impact (10 ft and 16 ft long strip)

INPUT VALUES

1) Height of the Barrier=	42.0	in.	8) Static Load, F_s=	23.0	kips
2) Soil Unit Weight=	0.125	kcf	9) Steel Reinforcement Strength, f_y=	60.0	ksi
3) Concrete Unit Weight=	0.150	kcf	10) Concrete Compressive Strength, f_c=	4.0	ksi
4) Soil-Slab Fric. Angle, Φ_r=	34.0	deg.	11) Length of soil reinforcement=	10.0	ft
5) Length of Section =	30.0	ft	12) Dyn. Pres. for the first strip (Pullout)=	467.0	psf
6) Dynamic Load, F_d=	80.0	kips	13) Dyn. Pres. for the sec. strip (Pullout)=	341.0	psf
7) Panel Thickness, h=	5.50	in.	14) Dyn. Pres. for the sec. strip (Yielding)=	1778.0	psf
8) Strip Width=	1.97	in.	13) Dyn. Pres. for the sec. strip (Yielding)=	341.0	psf

1.0 Stability

1.1 Sliding of the Barrier

$$\varphi P \geq \gamma L_s$$

Where:
- ϕ= Resistance factor
- P= Resistance load ($P=W\tan\phi_r$)
- γ= Load factor
- L_s= Static load
- W= Weight the system above the moment slab base.
- ϕ_r= Interface friction angle between the concrete and the soil

a) Computing the Location of the Impact Force with Respect to the Rotation Point

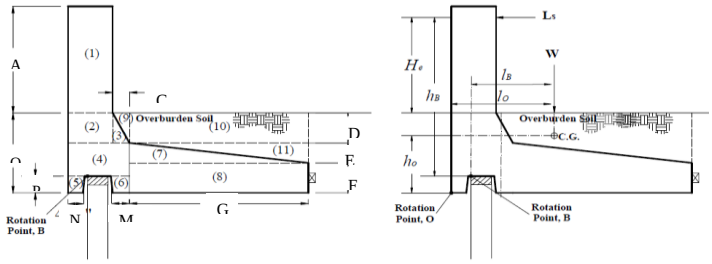

System Dimensions:

A=	42.00	in.	E=	6.00	in.	M=	4.75	in.	Q=	24.00	in.
C=	4.50	in.	F=	9.00	in.	N=	4.75	in.	$Slab_{bot.}$=	24.00	in.
D=	9.00	in.	G=	48.00	in.	P=	5.50	in.			

Concrete Unit Weight=	0.150	kcf	H_e=	30.00	in.
Soil Unit Weight=	0.125	kcf	L_{slab}=	24.00	ft
Length of Section =	30.00	ft	First Strip Loc.=	3.0	ft

	Section	x (in.)	y (in.)	Area ($in.^2$)	weight (kips)	x from O (in.)	y from O (in.)	y*weight (kips-in.)	x*weight (kips-in.)
	1	13.00	42.00	546.00	17.06	6.50	45.00	767.81	110.91
Barrier	2	12.00	9.00	108.00	3.38	6.00	19.50	65.81	20.25
Coping	3	4.50	9.00	20.25	0.63	13.50	18.00	11.39	8.54
	4	17.50	9.50	166.25	5.20	8.75	10.25	53.25	45.46
	5	4.75	5.50	26.13	0.82	2.38	2.75	2.25	1.94
	6	4.75	5.50	26.13	0.82	15.13	2.75	2.25	12.35
	7	48.00	6.00	144.00	4.50	33.50	11.00	49.50	150.75
M. Slab	8	48.00	9.00	432.00	13.50	41.50	4.50	60.75	560.25
	9	4.50	9.00	20.25	0.53	16.00	21.00	11.07	8.44
Soil	10	48.00	9.00	432.00	11.25	41.50	19.50	219.38	466.88
	11	48.00	6.00	144.00	3.75	49.50	13.00	48.75	185.63

Total	61.43		1292.21	1571.38
h_o and l_o in inches =			21.04	25.58

Distance from the C.G. to the Rotation Point in the x Direction, l_B = 20.08 in. ≈ 1.67 ft

Distance from the L_S to the Rotation Point in the y Direction, h_B = 48.50 in. ≈ 4.04 ft

b) Computing the Sliding Resistance

ϕ=	0.80		γ=	1.00		
P=	41.43	kips	L_s=	23.00	kips	
φP =	33.15	kips	φP	≥	γL_s	
γL_s=	23.00	kips	**33.1 (kips)**	≥	**23.0 (kips)**	**OK**

1.2 Overturning Moment of the Barrier

$$\varphi M \geq \gamma L_s h_B$$
$$\varphi W l_B \geq \gamma L_s h_B$$

ϕ=	0.90		γ=	1.00		
M=	1233.54	kips-in.	$L_s h_B$=	1115.50	kips-in.	
M=	102.80	kips-ft	$L_s h_B$=	92.96	kips-ft	
φM =	92.52	kips-ft	φM	≥	$\gamma L_s h_B$	
$\gamma L_s h_B$=	92.96	kips-ft	**93 (kips-ft)**	≥	**93.0 (kips-ft)**	**OK**

1.3 Rupture of the Coping in Bending (AASHTO LRFD Section 5)

1.3.1. Checking for Bending Moment

$$\phi M_{ult} \geq M_{impact},$$

h_c=	42.00	in.	γ=	1.0	(Extreme Event AASHTO LRFD)
f_y=	60.00	ksi			
f_c=	4.00	ksi			

a) Factored Moment due to the Impact Load

γM_d=	γ	×	L_d	×	h_c		
γM_d=	1.0	×	80.0	kips	×	42.0	in.
γM_d=	3360.0	kips-in.					
γM_d=	**280.0**	**kips-ft**					

b) Factored Ultimate Moment

ϕ=	0.90		(Resistance Factor for Flexure)
t_c=	10.62	in.	(Thickness of the critical section of the coping)

$$\varphi M_{ult} = \varphi [A_s f_y d (1-k/2)] \qquad k = \frac{A_s f_y}{0.85 f_c' b d}$$

Use #	5	bars @	8.00	in. o.c.	(Stirrups)
Use #	6	bars @	10.00	in. o.c.	(Connection bars between coping and moment slab)
d_b=	0.625	in.			
A_{b-1}=	0.307	$in.^2$			(Stirrups)
A_{b-2}=	0.247	$in.^2$			(Connection bars between coping and moment slab)

d=	10.62	in.	-	2	in.	-	0.3125	in.
d=	8.31	in.						
d=	**9.00**	**in.**						

Note: The impact is resisted by the 10 ft length of a barrier unit at the moment slab

$A_{s\text{-}1} = \frac{10.00\ \text{ft}}{0.667\ \text{ft}} \times 0.307\ \text{in.}^2$

$A_{s\text{-}1} = 4.60\ \text{in.}^2$

$A_{s\text{-}2} = \frac{10.00\ \text{ft}}{0.833\ \text{ft}} \times 0.247\ \text{in.}^2$

$A_{s\text{-}2} = 2.96\ \text{in.}^2$

$A_{s\text{-total}} = 7.57\ \text{in.}^2$

$$k = \frac{A_s f_y}{0.85 f_c' b d}$$

k= 0.1236

$M_{ult} = 7.57 \times 60.00 \times 9.00 \times 0.938$

$M_{ult} = 3833.31$ kips-in.

$M_{ult} = 319.44$ kips-ft

$\varphi M_{ult} = 0.90 \times 319.44$

φM_{ult} = 287.50 kips-ft

287.50 kips-ft ≥ 280.0 kips-ft OK (φM_{ult} ≥ M_{impact})

2.0 Guidelines for the Soil Reinforcement

2.1 Pullout of the Soil Reinforcement

$$\varphi P \geq \gamma_s F_s + \gamma_d F_d$$

$$\varphi P \geq \gamma_s P_s A_t + \gamma_d P_d A_t$$

φ= 1.00 (Resistance Factor for Pullout Analysis)

γ_s= 1.00 (Static Load Factor for Pullout Analysis)

γ_d= 1.00 (Dynamic Load Factor for Pullout Analysis)

2.1.1 Top Layer of Reinforcement

a) Computing the Pullout Resistance

$P = F^* \times \sigma_{V1} \times L \times 2b$

Note: α is equal to 1.0 and C is equal to 2.0

F^*= 1.668 (AASHTO LRFD)

σ_{V1}= 0.375 ksf

L= 10.00 ft

b= 0.1640 ft

P= 2.052 kips

ϕP= 2.052 kips

$\gamma_s F_s$ = γ_s × F_s

$\gamma_s F_s$ = 1.00 × 0.69 kips

$\gamma_s F_s$ = 0.69 kips

$\gamma_s P_s A_t$ = 0.69 kips

Location= 3 ft

σ_{V1}= 0.375 ksf

k_r= 0.459 (AASHTO LRFD)

A_t= 3.99 ft^2

$T_{max} = \sigma_{H1} \times A_t$

T_{max}= 0.172 × 3.99

T_{max}= 0.69 kips/strips

Panel Width=	4.87	ft	
Trib. Height=	1.80	ft	
P_d=	467.00	psf	(First Strip)
P_d=	341.00	psf	(Second Strip)

$\gamma_d F_d$ =	γ_s	×	F_d		
$\gamma_d F_d$ =	γ_s	×	P_d	×	A_t
$\gamma_d P_d A_t$=	1.00	×	467.00	×	2.92
$\gamma_d P_d A_t$=	**1.365**	**kips**			

$\phi P \geq \gamma_s F_s + \gamma_d F_d$

ϕP		≥		$\gamma_s P_s A_t$	+	$\gamma_d P_d A_t$	
2.052		≥		0.69	+	1.365	
2.05	**kips**	**≥**	**2.05**	**kips**		**OK**	10 ft Long Strip
3.28	**kips**	**≥**	**2.06**	**kips**		**OK**	16 ft Long Strip

2.1.2 Second Layer of Reinforcement

a) Computing the Pullout Resistance

P= F^* × σ_{V1} × L × $2b$ Note: α is equal to 1.0 and Cis equal to 2.0

F^*= 1.524 (AASHTO LRFD)

σ_{V1}=	0.683	ksf	Location=	5.46	ft
L=	10.00	ft	σ_{V1}=	0.683	ksf
b=	0.1640	ft			
			k_r=	0.442	(AASHTO LRFD)
P=	3.413	kips	A_t=	3.99	ft^2
ϕP=	**3.413**	**kips**			
			T_{max}=	σ_{H1} ×	A_t
$\gamma_s F_s$ =	γ_s	× F_s	T_{max}=	0.302 ×	3.99
$\gamma_s F_s$ =	1.00	× 1.20 kips	**T_{max}=**	**1.2**	**kips/strips**
$\gamma_s F_s$ =	1.20	kips			
$\gamma_s P_s A_t$ =	**1.204**	**kips**			

Panel Width=	4.87	ft	
Trib. Height=	2.46	ft	

$\gamma_d F_d$ =	γ_s	×	F_d		
$\gamma_d F_d$ =	γ_s	×	P_d	×	A_t
$\gamma_d P_d A_t$=	1.00	×	341	×	3.99
$\gamma_d P_d A_t$=	**1.362**	**kips**			

$\phi P \geq \gamma_s F_s + \gamma_d F_d$

ϕP		≥		$\gamma_s P_s A_t$	+	$\gamma_d P_d A_t$	
3.413		≥		1.20	+	1.362	
3.41	**kips**	**≥**	**2.57**	**kips**		**OK**	10 ft Long Strip
5.46	**kips**	**≥**	**2.57**	**kips**		**OK**	16 ft Long Strip

2.2 Yielding of the Soil Reinforcement

$\varphi R \geq \gamma_s F_s + \gamma_d F_d$

$\varphi R \geq \gamma_s P_s A_t + \gamma_d P_d A_t$

φ=	1.00	(Resistance Factor for Rupture Analysis)
γ_s=	1.00	(Static Load Factor for Rupture Analysis)
γ_d=	1.00	(Dynamic Load Factor for Rupture Analysis)

2.2.1 Top Layer of Reinforcement

a) Computing the Yielding Resistance of the Strips for 75 years Service Life

E_c=	0.10173	in.	(AASHTO LRFD)					
R=	σ_t	×	b	×	E_c			
R=	60	ksi	×	1.97	in.	×	0.1017	in.
R=	12.015	kips						
ϕR=	ϕ	×	R	kips				
ϕR=	1.00	×	12.015	kips				
ϕR=	**12.02**	**kips**						

$\gamma_s P_s A_t$ = 0.687 kips

Panel Width=	4.87	ft	
Trib. Height=	1.80	ft	
P_d=	1778	psf	(First Strip)
P_d=	341	psf	(Second Strip)

$\gamma_d F_d$ =	**γ_s**	×	**F_d**			
$\gamma_d F_d$ =	**γ_s**	×	P_d	×	A_t	
$\gamma_d P_d A_t$=	1.00	×	1778	×	2.92	
$\gamma_d P_d A_t$=	**5.20**	**kips**				

$\varphi R \geq \gamma_s F_s + \gamma_d F_d$

φR		≥		$\gamma_s P_s A_t$	+	$\gamma_d P_d A_t$
2.052		≥		0.69	+	5.195
12.02	**kips**	**≥**	**5.88**	**kips**		**OK**

2.2.1 Second Layer of Reinforcement

a) Computing the Yielding Resistance of the Strips for 75 years Service Life

E_c=	0.10173	in.	(AASHTO LRFD)					
R=	σ_t	×	b	×	E_c			
R=	60	ksi	×	1.97	in.	×	0.10	in.
R=	12.015	kips						
ϕR=	ϕ	×	R	kips				
ϕR=	1.00	×	12.015	kips				
ϕR=	**12.015**	**kips**						

$\gamma_s P_s A_t$ = 1.204 kips

Panel Width=	4.87	ft	
Trib. Height=	2.46	ft	
P_d=	1778.00	psf	(First Strip)
P_d=	341.00	psf	(Second Strip)

$\gamma_d F_d$ =	**γ_s**	×	**F_d**			
$\gamma_d F_d$ =	**γ_s**	×	P_d	×	A_t	
$\gamma_d P_d A_t$=	1.00	×	341	×	3.99	
$\gamma_d P_d A_t$=	**1.362**	**kips**				

$\varphi R \geq \gamma_s F_s + \gamma_d F_d$

φR		≥		$\gamma_s P_s A_t$	+	$\gamma_d P_d A_t$
2.052		≥		1.20	+	1.362
12.015	**kips**	**≥**	**2.565**	**kips**		**OK**

Preliminary Design of MSE Wall for TL-4 Impact (24 ft long strip)

INPUT VALUES

1) Height of the Barrier=	42.0	in.	8) Static Load, F_s=	23.0	kips
2) Soil Unit Weight=	0.125	kcf	9) Steel Reinforcement Strength, f_y=	60.0	ksi
3) Concrete Unit Weight=	0.150	kcf	10) Concrete Compressive Strength, f_c=	4.0	ksi
4) Soil-Slab Fric. Angle, Φ_r=	34.0	deg.	11) Length of soil reinforcement=	24.0	ft
5) Length of Section =	30.0	ft	12) Dyn. Pres. for the first strip (Pullout)=	467.0	psf
6) Dynamic Load, F_d=	80.0	kips	13) Dyn. Pres. for the sec. strip (Pullout)=	341.0	psf
7) Panel Thickness, h=	5.50	in.	14) Dyn. Pres. for the sec. strip (Yielding)=	1778.0	psf
8) Strip Width=	1.97	in.	13) Dyn. Pres. for the sec. strip (Yielding)=	341.0	psf

1.0 Stability

1.1 Sliding of the Barrier

$$\varphi P \geq \gamma L_s$$

Where:
- ϕ= Resistance factor
- P= Resistance load ($P=W\tan\phi_r$)
- γ= Load factor
- L_s= Static load
- W= Weight the system above the moment slab base.
- ϕ_r= Interface friction angle between the concrete and the soil

a) Computing the Location of the Impact Force with Respect to the Rotation Point

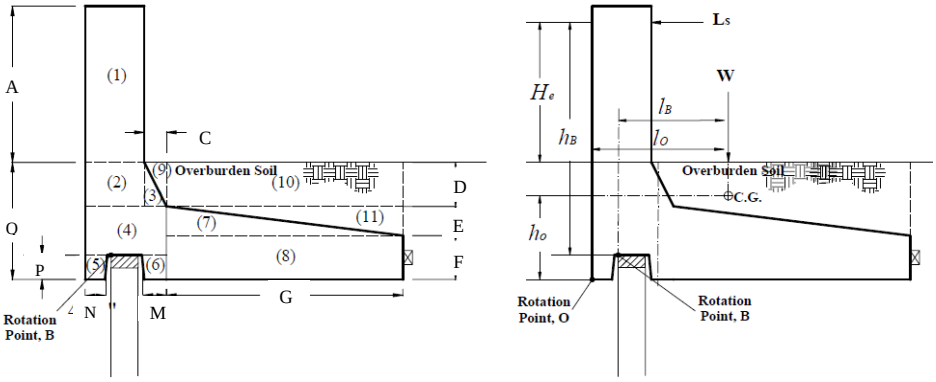

System Dimensions:

A=	42.00	in.	E=	6.00	in.	M=	4.75	in.	Q=	24.00	in.
C=	4.50	in.	F=	9.00	in.	N=	4.75	in.	$Slab_{bot.}$=	24.00	in.
D=	9.00	in.	G=	48.00	in.	P=	5.50	in.			

Concrete Unit Weight=	0.150	kcf	H_e=	30.00	in.
Soil Unit Weight=	0.125	kcf	L_{slab}=	24.00	ft
Length of Section =	30.00	ft	First Strip Loc.=	3.0	ft

	Section	x (in.)	y (in.)	Area ($in.^2$)	weight (kips)	x from O (in.)	y from O (in.)	y*weight (kips-in.)	x*weight (kips-in.)
	1	13.00	42.00	546.00	17.06	6.50	45.00	767.81	110.91
Barrier	2	12.00	9.00	108.00	3.38	6.00	19.50	65.81	20.25
Coping	3	4.50	9.00	20.25	0.63	13.50	18.00	11.39	8.54
	4	17.50	9.50	166.25	5.20	8.75	10.25	53.25	45.46
	5	4.75	5.50	26.13	0.82	2.38	2.75	2.25	1.94
	6	4.75	5.50	26.13	0.82	15.13	2.75	2.25	12.35
	7	48.00	6.00	144.00	4.50	33.50	11.00	49.50	150.75
M. Slab	8	48.00	9.00	432.00	13.50	41.50	4.50	60.75	560.25
	9	4.50	9.00	20.25	0.53	16.00	21.00	11.07	8.44
Soil	10	48.00	9.00	432.00	11.25	41.50	19.50	219.38	466.88
	11	48.00	6.00	144.00	3.75	49.50	13.00	48.75	185.63

Total	61.43		1292.21	1571.38
h_o and l_o in inches =			21.04	25.58

Distance from the C.G. to the Rotation Point in the x Direction, l_B = 20.08 in. ≈ 1.67 ft

Distance from the L_S to the Rotation Point in the y Direction, h_B = 48.50 in. ≈ 4.04 ft

b) Computing the Sliding Resistance

ϕ=	0.80			γ=	1.00		
P=	41.43	kips		L_s=	23.00	kips	
φP =	33.15	kips	φP	≥	γL_s		
γL_s=	23.00	kips	**33.1 (kips)**	≥	**23.0 (kips)**		**OK**

1.2 Overturning Moment of the Barrier

$$\varphi M \geq \gamma L_s h_B$$
$$\varphi W l_B \geq \gamma L_s h_B$$

ϕ=	0.90			γ=	1.00		
M=	1233.54	kips-in.		L_sh_B=	1115.50	kips-in.	
M=	102.80	kips-ft		L_sh_B=	92.96	kips-ft	
φM =	92.52	kips-ft	φM	≥	γL_sh_B		
γL_sh_B=	92.96	kips-ft	**93 (kips-ft)**	≥	**93.0 (kips-ft)**		**OK**

1.3 Rupture of the Coping in Bending (AASHTO LRFD Section 5)

1.3.1. Checking for Bending Moment

$$\phi M_{ult} \geq M_{impact},$$

h_c=	42.00	in.	γ=	1.0	(Extreme Event AASHTO LRFD)
f_y=	60.00	ksi			
f_c=	4.00	ksi			

a) Factored Moment due to the Impact Load

γM_d=	γ	×	L_d	×	h_c		
γM_d=	1.0	×	80.0	kips	×	42.0	in.
γM_d=	3360.0	kips-in.					
γM_d=	**280.0**	**kips-ft**					

b) Factored Ultimate Moment

ϕ=	0.90		(Resistance Factor for Flexure)
t_c=	10.62	in.	(Thickness of the critical section of the coping)

$$\varphi M_{ult} = \varphi [A_s f_y d (1\text{-}k/2)] \qquad k = \frac{A_s f_y}{0.85 f_c' b d}$$

Use #	5	bars @	8.00	in. o.c.	(Stirrups)
Use #	6	bars @	10.00	in. o.c.	(Connection bars between coping and moment slab)
d_b=	0.625	in.			
$A_{b\text{-}1}$=	0.307	$in.^2$			(Stirrups)
$A_{b\text{-}2}$=	0.247	$in.^2$			(Connection bars between coping and moment slab)

d=	10.62	in.	-	2	in.	-	0.3125	in.
d=	8.31	in.						
d=	**9.00**	**in.**						

Note: The impact is resisted by the 10 ft length of a barrier unit at the moment slab

$A_{s\text{-}1}$= 10.00 ft / 0.667 ft × 0.307 $in.^2$

$A_{s\text{-}1}$= 4.60 $in.^2$

$A_{s\text{-}2}$= 10.00 ft / 0.833 ft × 0.247 $in.^2$

$A_{s\text{-}2}$= 2.96 $in.^2$

$A_{s\text{-}total}$= 7.57 $in.^2$

$$k = \frac{A_s f_y}{0.85 f_c' b d}$$

k= 0.1236

M_{ult} = 7.57 × 60.00 × 9.00 × 0.938

M_{ult} = 3833.31 kips-in.

M_{ult} = 319.44 kips-ft

φM_{ult} = 0.90 × 319.44

φM_{ult} = 287.50 kips-ft

φM_{ult} ≥ M_{impact},

287.50 kips-ft ≥ 280.0 kips-ft OK

2.0 Guidelines for the Soil Reinforcement

2.1 Pullout of the Soil Reinforcement

$$\varphi P \geq \gamma_s F_s + \gamma_d F_d$$

$$\varphi P \geq \gamma_s P_s A_t + \gamma_d P_d A_t$$

φ= 1.00 (Resistance Factor for Pullout Analysis)

γ_s= 1.00 (Static Load Factor for Pullout Analysis)

γ_d= 1.00 (Dynamic Load Factor for Pullout Analysis)

2.1.1 Top Layer of Reinforcement

a) Computing the Pullout Resistance

P= $F^* \times \sigma_{V1} \times L \times 2b$ Note: α is equal to 1.0 and C is equal to 2.0

F^*= 1.668 (AASHTO LRFD)

σ_{V1}= 0.375 ksf

L= 24.00 ft

b= 0.1640 ft

P= 4.925 kips

ϕP= 4.925 kips

$\gamma_s F_s$ = γ_s × F_s

$\gamma_s F_s$ = 1.00 × 1.03 kips

$\gamma_s F_s$ = 1.03 kips

$\gamma_s P_s A_t$ = 1.03 kips

Location= 3 ft

σ_{V1}= 0.375 ksf

k_r= 0.459 (AASHTO LRFD)

A_t= 6.00 ft^2

T_{max}= σ_{H1} × A_t

T_{max}= 0.172 × 6.00

T_{max}= 1.03 kips/strips

Panel Width=	4.87	ft	
Trib. Height=	1.80	ft	
P_d=	467.00	psf	(First Strip)
P_d=	341.00	psf	(Second Strip)

$\gamma_d F_d$ =	γ_s	×	F_d			
$\gamma_d F_d$ =	γ_s	×	P_d	×	A_t	
$\gamma_d P_d A_t$=	1.00	×	467.00	×	4.38	
$\gamma_d P_d A_t$=	**2.047**	**kips**				

$\varphi P \geq \gamma_s F_s + \gamma_d F_d$

ϕP		≥		$\gamma_s P_s A_t$	+	$\gamma_d P_d A_t$	
4.925		≥		1.03	+	2.047	
4.93	**kips**	**≥**	**3.08**	**kips**		**OK**	24 ft Long Strip

2.1.2 Second Layer of Reinforcement

a) Computing the Pullout Resistance

P= F^* × σ_{V1} × L × $2b$ Note: α is equal to 1.0 and C is equal to 2.0

F^*= 1.524 (AASHTO LRFD)

σ_{V1}=	0.683	ksf	Location=	5.46	ft
L=	24.00	ft	σ_{V1}=	0.683	ksf
b=	0.1640	ft			
			k_r=	0.442	(AASHTO LRFD)
P=	8.190	kips	A_t=	6.00	ft^2
ϕP=	**8.190**	**kips**			

					T_{max}=	σ_{H1}	×	A_t
$\gamma_s F_s$ =	γ_s	×	F_s		T_{max}=	0.302	×	6.00
$\gamma_s F_s$ =	1.00	×	1.81	kips	**T_{max}=**	**1.8**	**kips/strips**	
$\gamma_s F_s$ =	1.81	kips						
$\gamma_s P_s A_t$ =	**1.810**	**kips**						

Panel Width=	4.87	ft					
Trib. Height=	2.46	ft					
$\gamma_d F_d$ =	γ_s	×	F_d				
$\gamma_d F_d$ =	γ_s	×	P_d	×	A_t		
$\gamma_d P_d A_t$=	1.00	×	341	×	5.99		
$\gamma_d P_d A_t$=	**2.043**	**kips**					

$\varphi P \geq \gamma_s F_s + \gamma_d F_d$

ϕP		≥		$\gamma_s P_s A_t$	+	$\gamma_d P_d A_t$	
8.190		≥		1.81	+	2.043	
8.19	**kips**	**≥**	**3.85**	**kips**		**OK**	

2.2 Yielding of the Soil Reinforcement

$\varphi R \geq \gamma_s F_s + \gamma_d F_d$

$\varphi R \geq \gamma_s P_s A_t + \gamma_d P_d A_t$

φ=	1.00	(Resistance Factor for Rupture Analysis)
γ_s=	1.00	(Static Load Factor for Rupture Analysis)
γ_d=	1.00	(Dynamic Load Factor for Rupture Analysis)

2.2.1 Top Layer of Reinforcement

a) Computing the Yielding Resistance of the Strips for 75 years Service Life

E_c=	0.10173	in.	(AASHTO LRFD)					
R=	σ_t	×	b	×	E_c			
R=	60	ksi	×	1.97	in.	×	0.1017	in.
R=	12.015	kips						
ϕR=	ϕ	×	R	kips				
ϕR=	1.00	×	12.015	kips				
ϕR=	**12.02**	**kips**						

$\gamma_s P_s A_t$ = 1.033 kips

Panel Width=	4.87	ft
Trib. Height=	1.80	ft
P_d=	1778	psf (First Strip)
P_d=	341	psf (Second Strip)

$\gamma_d F_d$ =	**γ_s**	×	**F_d**			
$\gamma_d F_d$ =	**γ_s**	×	P_d	×	A_t	
$\gamma_d P_d A_t$=	1.00	×	1778	×	4.38	
$\gamma_d P_d A_t$=	**7.79**	**kips**				

$\varphi R \geq \gamma_s F_s + \gamma_d F_d$

φR		≥		$\gamma_s P_s A_t$	+	$\gamma_d P_d A_t$
4.925		≥		1.03	+	7.793
12.02	**kips**	**≥**	**8.83**	**kips**		**OK**

2.2.1 Second Layer of Reinforcement

a) Computing the Yielding Resistance of the Strips for 75 years Service Life

E_c=	0.10173	in.	(AASHTO LRFD)					
R=	σ_t	×	b	×	E_c			
R=	60	ksi	×	1.97	in.	×	0.10	in.
R=	12.015	kips						
ϕR=	ϕ	×	R	kips				
ϕR=	1.00	×	12.015	kips				
ϕR=	**12.015**	**kips**						

$\gamma_s P_s A_t$ = 1.810 kips

Panel Width=	4.87	ft
Trib. Height=	2.46	ft
P_d=	1778.00	psf (First Strip)
P_d=	341.00	psf (Second Strip)

$\gamma_d F_d$ =	**γ_s**	×	**F_d**			
$\gamma_d F_d$ =	**γ_s**	×	P_d	×	A_t	
$\gamma_d P_d A_t$=	1.00	×	341	×	5.990	
$\gamma_d P_d A_t$=	**2.043**	**kips**				

$\varphi R \geq \gamma_s F_s + \gamma_d F_d$

φR		≥		$\gamma_s P_s A_t$	+	$\gamma_d P_d A_t$
4.925		≥		1.81	+	2.043
12.02	**kips**	**≥**	**3.85**	**kips**		**OK**

Preliminary Design of MSE Wall for TL-5-1 Impact (10 ft and 16 ft long strip)

INPUT VALUES

1) Height of the Barrier=	42.0	in.	8) Static Load, F_s=	60.0	kips
2) Soil Unit Weight=	0.125	kcf	9) Steel Reinforcement Strength, f_y=	60.0	ksi
3) Concrete Unit Weight=	0.150	kcf	10) Concrete Compressive Strength, f_c=	4.0	ksi
4) Soil-Slab Fric. Angle, Φ_r=	34.0	deg.	11) Length of soil reinforcement=	10.0	ft
5) Length of Section =	30.0	ft	12) Dyn. Pres. for the first strip (Pullout)=	930.0	psf
6) Dynamic Load, F_d=	160.0	kips	13) Dyn. Pres. for the sec. strip (Pullout)=	680.0	psf
7) Panel Thickness, h=	5.50	in.	14) Dyn. Pres. for the sec. strip (Rupture)=	3550.0	psf
8) Strip Width=	1.97	in.	13) Dyn. Pres. for the sec. strip (Rupture)=	680.0	psf

1.0 Stability

1.1 Sliding of the Barrier

$$\varphi P \geq \gamma L_s$$

Where:
- ϕ= Resistance factor
- P= Resistance load ($P=W\tan\phi_r$)
- γ= Load factor
- L_s= Static load
- W= Weight the system above the moment slab base.
- ϕ_r= Interface friction angle between the concrete and the soil

a) Computing the Location of the Impact Force with Respect to the Rotation Point

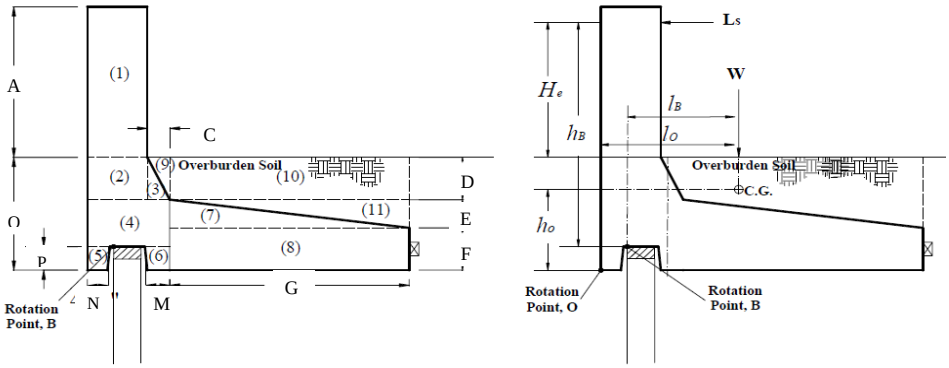

System Dimensions:

A=	42.00	in.	E=	7.50	in.	M=	11.00	in.	Q=	36.00	in.
C=	9.00	in.	F=	12.00	in.	N=	4.75	in.	$Slab_{bot.}$=	36.00	in.
D=	16.50	in.	G=	72.00	in.	P=	15.00	in.			

Concrete Unit Weight=	0.150	kcf	H_e=	34.00	in.
Soil Unit Weight=	0.125	kcf	L_{slab}=	7.00	ft
Length of Section =	30.00	ft	First Strip Loc.=	3.63	ft

	Section	x (in.)	y (in.)	Area ($in.^2$)	weight (kips)	x from O (in.)	y from O (in.)	y*weight (kips-in.)	x*weight (kips-in.)
	1	13.00	42.00	546.00	17.06	6.50	57.00	972.56	110.91
Barrier	2	12.00	16.50	198.00	6.19	6.00	27.75	171.70	37.13
Coping	3	9.00	16.50	74.25	2.32	15.00	25.00	58.01	34.80
	4	22.00	4.50	99.00	3.09	11.00	17.25	53.37	34.03
	5	4.75	15.00	71.25	2.23	2.38	7.50	16.70	5.29
	6	11.00	15.00	165.00	5.16	16.50	7.50	38.67	85.08
	7	72.00	7.50	270.00	8.44	46.00	14.50	122.34	388.13
M. Slab	8	72.00	12.00	864.00	27.00	58.00	6.00	162.00	1566.00
	9	9.00	12.00	54.00	1.41	19.00	27.50	38.67	26.72
Soil	10	72.00	16.50	1188.00	30.94	58.00	27.75	858.52	1794.38
	11	72.00	7.50	270.00	7.03	70.00	17.00	119.53	492.19
	Total			3799.50	110.86			2612.07	4574.64
	h_o and l_o in inches =							23.56	41.27

Distance from the C.G. to the Rotation Point in the x Direction, l_B =	35.8	in.	≈	2.98	ft	
Distance from the L_S to the Rotation Point in the y Direction, h_B =	55.0	in.	≈	4.58	ft	

b) Computing the Sliding Resistance

ϕ=	0.80		γ=	1.00	
P=	74.78	kips	L_s=	60.00	kips

φP =	59.82	kips	φP	≥	γL_s	
γL_s=	60.00	kips	**60**	**≥**	**60.0**	**OK**
			(kips)		**(kips)**	

1.2 Overturning Moment of the Barrier

$$\varphi M \geq \gamma L_s h_B$$
$$\varphi W l_B \geq \gamma L_s h_B$$

ϕ=	0.90		γ=	1.00	
M=	3964.91	kips-in.	L_sh_B=	3300.00	kips-in.
M=	330.41	kips-ft	L_sh_B=	275.00	kips-ft

φM =	297.37	kips-ft	φM	≥	γL_sh_B	
γL_sh_B=	275.00	kips-ft	**297.37**	**≥**	**275.00**	**OK**
			(kips-ft)		**(kips-ft)**	

1.3 Rupture of the Coping in Bending (AASHTO LRFD Section 5)

1.3.1. Checking for Bending Moment

$$\phi M_{ult} \geq M_{impact},$$

h_c=	54.25	in.	γ=	1.0	(Extreme Event AASHTO LRFD)
f_y=	60.00	ksi			
f_c=	4.00	ksi			

a) Factored Moment due to the Impact Load

γM_d=	γ	×	L_d	×	h_c		
γM_d=	1.0	×	160.0	kips	×	54.3	in.
γM_d=	8680.0	kips-in.					
γM_d=	**723.3**	**kips-ft**					

b) Factored Ultimate Moment

ϕ=	0.90		(Resistance Factor for Flexure)
t_c=	11.88	in.	(Thickness of the critical section of the coping)

$$\varphi M_{ult} = \varphi [A_s f_y d (1-k/2)] \qquad k = \frac{A_s f_y}{0.85 f_c' b d}$$

Use #	5	bars @	4.00	in. o.c.	(Stirrups)			
Use #	5	bars @	8.00	in. o.c.	(Connecting moment slab and coping section)			
d_b=	0.625	in.						
A_{b-1}=	0.307	$in.^2$			(Stirrups)			
A_{b-2}=	0.172	$in.^2$			(Connecting moment slab and coping section)			
d=	11.88	in.	-	2	in.	-	0.3125	in.
d=	9.57	in.						
d=	**10.00**	**in.**						

Note: The impact is resisted by the 15 ft length of a barrier unit at the moment slab

$A_{s\text{-}1}$= 15.00 ft / 0.333 ft × 0.307 in.^{2}

$A_{s\text{-}1}$= 13.81 in.^{2}

$A_{s\text{-}1}$= 15.00 ft / 0.667 ft × 0.172 in.^{2}

$A_{s\text{-}1}$= 3.86 in.^{2}

$A_{s\text{-}total}$= 17.67 in.^{2}

$$k = \frac{A_s f_y}{0.85 f_c' b d}$$

k= 0.1732

M_{ult} = 17.67 × 60.00 × 10.00 × 0.913

M_{ult} = 9681.64 kips-in.

M_{ult} = 806.80 kips-ft

φM_{ult} = 0.90 × 806.80

φM_{ult} = 726.12 kips-ft

φM_{ult} ≥ M_{impact}

726.12 kips-ft ≥ 723.3 kips-ft OK

2.0 Guidelines for the Soil Reinforcement

2.1 Pullout of the Soil Reinforcement

$$\varphi P \geq \gamma_s F_s + \gamma_d F_d$$

$$\varphi P \geq \gamma_s P_s A_t + \gamma_d P_d A_t$$

φ= 1.00 (Resistance Factor for Pullout Analysis)

γ_s= 1.00 (Static Load Factor for Pullout Analysis)

γ_d= 1.00 (Dynamic Load Factor for Pullout Analysis)

2.1.1 Top Layer of Reinforcement

a) Computing the Pullout Resistance

P= F^* × σ_{V1} × L × $2b$

Note: α is equal to 1.0 and C is equal to 2.0

F^*= 1.631 (AASHTO LRFD)

σ_{V1}= 0.454 ksf

L= 10.00 ft

b= 0.1640 ft

P= 2.428 kips

ϕP= 2.428 kips

$\gamma_s F_s$ = γ_s × F_s

$\gamma_s F_s$ = 1.00 × 0.82 kips

$\gamma_s F_s$ = 0.82 kips

$\gamma_s P_s A_t$ = 0.82 kips

Location= 3.63 ft

σ_{V1}= 0.454 ksf

k_r= 0.455 (AASHTO LRFD)

A_t= 3.99 ft^2

T_{max}= σ_{H1} × A_t

T_{max}= 0.206 × 3.99

T_{max}= 0.82 kips/strips

Panel Width= 4.87 ft

Trib. Height= 1.80 ft

P_d= 930.00 psf (First Strip)

P_d= 680.00 psf (Second Strip)

$\gamma_d F_d$ =	γ_s	×	F_d			
$\gamma_d F_d$ =	γ_s	×	P_d	×	A_t	
$\gamma_d P_d A_t$ =	1.00	×	930.00	×	2.92	
$\gamma_d P_d A_t$ =	**2.717**	**kips**				

$$\varphi P \geq \gamma_s F_s + \gamma_d F_d$$

ϕP		≥		$\gamma_s P_s A_t$	+	$\gamma_d P_d A_t$
2.428		≥		0.82	+	2.717
2.43	**kips**	**≥**	**3.54**	**kips**	**VERIFIED**	(10 ft long strip)
3.89	**kips**	**≥**	**3.54**	**kips**	**OK**	(16 ft long strip)

2.1.2 Second Layer of Reinforcement

a) Computing the Pullout Resistance

P= F^* × σ_{V1} × L × $2b$ Note: α is equal to 1.0 and Cis equal to 2.0

F^*= 1.488 (AASHTO LRFD)

σ_{V1}=	0.774	ksf	Location=	6.19	ft
L=	10.00	ft	σ_{V1}=	0.774	ksf
b=	0.1640	ft			
			k_r=	0.438	(AASHTO LRFD)
P=	3.776	kips	A_t=	3.99	ft^2
ϕP=	**3.776**	**kips**			

					T_{max}=	σ_{H1}	× A_t
$\gamma_s F_s$ =	γ_s	×	F_s		T_{max}=	0.339	× 3.99
$\gamma_s F_s$ =	1.00	×	1.35	kips	**T_{max}=**	**1.35**	**kips/strips**
$\gamma_s F_s$ =	1.35	kips					
$\gamma_s P_s A_t$ =	**1.352**	**kips**					

Panel Width=	4.87	ft
Trib. Height=	2.46	ft

$\gamma_d F_d$ =	γ_s	×	F_d			
$\gamma_d F_d$ =	γ_s	×	P_d	×	A_t	
$\gamma_d P_d A_t$ =	1.00	×	680.00	×	3.99	
$\gamma_d P_d A_t$ =	**2.716**	**kips**				

$$\varphi P \geq \gamma_s F_s + \gamma_d F_d$$

ϕP		≥		$\gamma_s P_s A_t$	+	$\gamma_d P_d A_t$
3.776		≥		1.35	+	2.716
3.78	**kips**	**≥**	**4.07**	**kips**	**VERIFIED**	
6.04	**kips**	**≥**	**4.07**	**kips**	**OK**	

2.2 Yielding of the Soil Reinforcement

$$\varphi R \geq \gamma_s F_s + \gamma_d F_d$$

$$\varphi R \geq \gamma_s P_s A_t + \gamma_d P_d A_t$$

φ=	1.00	(Resistance Factor for Rupture Analysis)
γ_s=	1.00	(Static Load Factor for Rupture Analysis)
γ_d=	1.00	(Dynamic Load Factor for Rupture Analysis)

2.2.1 Top Layer of Reinforcement

a) Computing the Yielding Resistance of the Strips for 75 years Service Life

E_c=	0.10	in.	(AASHTO LRFD)					
R=	σ_t	×	b	×	E_c			
R=	60.000	ksi	×	1.97	in.	×	0.10	in.
R=	12.016	kips						
ϕR=	ϕ	×	R	kips				
ϕR=	1.00	×	12.016	kips				
ϕR=	**12.02**	**kips**						

$\gamma_s P_s A_t$ =	**0.824**	**kips**

Panel Width=	4.87	ft	
Trib. Height=	1.80	ft	
P_d=	3550.00	psf	(First Strip)
P_d=	680.00	psf	(Second Strip)

$\gamma_d F_d$ =	**γ_s**	×	**F_d**			
$\gamma_d F_d$ =	**γ_s**	×	P_d	×	A_t	
$\gamma_d P_d A_t$=	1.00	×	3550.00	×	2.92	
$\gamma_d P_d A_t$=	**10.373**	**kips**				

$\varphi R \geq \gamma_s F_s + \gamma_d F_d$

φR		≥		$\gamma_s P_s A_t$	+	$\gamma_d P_d A_t$
2.428		≥		0.82	+	10.373
12.016	**kips**	**≥**	**11.197**	**kips**		**OK**

2.2.1 Second Layer of Reinforcement

a) Computing the Yielding Resistance of the Strips for 75 years Service Life

E_c=	0.10	in.	(AASHTO LRFD)					
R=	σ_t	×	b	×	E_c			
R=	60.000	ksi	×	1.97	in.	×	0.10	in.
R=	12.016	kips						
ϕR=	ϕ	×	R	kips				
ϕR=	1.00	×	12.016	kips				
ϕR=	**12.02**	**kips**						

$\gamma_s P_s A_t$ =	**1.352**	**kips**

Panel Width=	4.87	ft	
Trib. Height=	2.46	ft	
P_d=	3550.00	psf	(First Strip)
P_d=	680.00	psf	(Second Strip)

$\gamma_d F_d$ =	**γ_s**	×	**F_d**			
$\gamma_d F_d$ =	**γ_s**	×	P_d	×	A_t	
$\gamma_d P_d A_t$=	1.00	×	680.00	×	3.993	
$\gamma_d P_d A_t$=	**2.716**	**kips**				

$\varphi R \geq \gamma_s F_s + \gamma_d F_d$

φR		≥		$\gamma_s P_s A_t$	+	$\gamma_d P_d A_t$
2.428		≥		1.35	+	2.716
12.02	**kips**	**≥**	**4.07**	**kips**		**OK**

Preliminary Design of MSE Wall for TL-5-1 Impact (24 ft long strip)

INPUT VALUES

1) Height of the Barrier=	42.0	in.	8) Static Load, F_s=	60.0	kips
2) Soil Unit Weight=	0.125	kcf	9) Steel Reinforcement Strength, f_y=	60.0	ksi
3) Concrete Unit Weight=	0.150	kcf	10) Concrete Compressive Strength, f_c=	4.0	ksi
4) Soil-Slab Fric. Angle, Φ_r=	34.0	Degrees	11) Length of soil reinforcement=	24.0	ft
5) Length of Section =	30.0	ft	12) Dyn. Pres. for the first strip (Pullout)=	930.0	psf
6) Dynamic Load, F_d=	160.0	kips	13) Dyn. Pres. for the sec. strip (Pullout)=	680.0	psf
7) Panel Thickness, h=	5.50	in.	14) Dyn. Pres. for the sec. strip (Rupture)=	3550.0	psf
8) Strip Width=	1.97	in.	13) Dyn. Pres. for the sec. strip (Rupture)=	680.0	psf

1.0 Stability

1.1 Sliding of the Barrier

$$\varphi P \geq \gamma L_s$$

Where:
- ϕ= Resistance factor
- P= Resistance load (P=Wtanϕ_r)
- γ= Load factor
- L_s= Static load
- W= Weight the system above the moment slab base.
- ϕ_r= Interface friction angle between the concrete and the soil

a) Computing the Location of the Impact Force with Respect to the Rotation Point

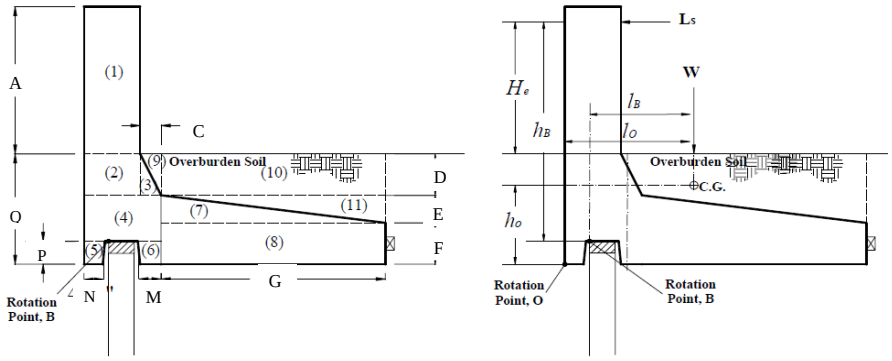

System Dimensions:

A=	42.00	in.	E=	7.50	in.	M=	11.00	in.	Q=	36.00	in.
C=	9.00	in.	F=	12.00	in.	N=	4.75	in.	$Slab_{bot.}$=	36.00	in.
D=	16.50	in.	G=	72.00	in.	P=	15.00	in.			

Concrete Unit Weight=	0.150	kcf	H_e=	34.00	in.
Soil Unit Weight=	0.125	kcf	L_{slab}=	7.00	ft
Length of Section =	30.00	ft	First Strip Loc.=	3.63	ft

	Section	x (in.)	y (in.)	Area ($in.^2$)	weight (kips)	x from O (in.)	y from O (in.)	y*weight (kips-in.)	x*weight (kips-in.)
	1	13.00	42.00	546.00	17.06	6.50	57.00	972.56	110.91
Barrier	2	12.00	16.50	198.00	6.19	6.00	27.75	171.70	37.13
Coping	3	9.00	16.50	74.25	2.32	15.00	25.00	58.01	34.80
	4	22.00	4.50	99.00	3.09	11.00	17.25	53.37	34.03
	5	4.75	15.00	71.25	2.23	2.38	7.50	16.70	5.29
	6	11.00	15.00	165.00	5.16	16.50	7.50	38.67	85.08
	7	72.00	7.50	270.00	8.44	46.00	14.50	122.34	388.13
M. Slab	8	72.00	12.00	864.00	27.00	58.00	6.00	162.00	1566.00
	9	9.00	12.00	54.00	1.41	19.00	27.50	38.67	26.72
Soil	10	72.00	16.50	1188.00	30.94	58.00	27.75	858.52	1794.38
	11	72.00	7.50	270.00	7.03	70.00	17.00	119.53	492.19
	Total			3799.50	110.86			2612.07	4574.64
	h_o and l_o in inches =							23.56	41.27

Distance from the C.G. to the Rotation Point in the x Direction, l_B =	35.8	in.	≈	2.98	ft
Distance from the L_S to the Rotation Point in the y Direction, h_B =	55.0	in.	≈	4.58	ft

b) Computing the Sliding Resistance

ϕ=	0.80			γ=	1.00		
P=	74.78	kips		L_s=	60.00	kips	
φP =	59.82	kips		φP	≥	γL_s	
γL_s=	60.00	kips		**60 (kips)**	**≥**	**60.0 (kips)**	**OK**

1.2 Overturning Moment of the Barrier

$$\varphi M \geq \gamma L_s h_B$$
$$\varphi W l_B \geq \gamma L_s h_B$$

ϕ=	0.90			γ=	1.00		
M=	3964.91	kips-in.		$L_s h_B$=	3300.00	kips-in.	
M=	330.41	kips-ft		$L_s h_B$=	275.00	kips-ft	
φM =	297.37	kips-ft		φM	≥	$\gamma L_s h_B$	
$\gamma L_s h_B$=	275.00	kips-ft		**297.4 (kips-ft)**	**≥**	**275.0 (kips-ft)**	**OK**

1.3 Rupture of the Coping in Bending (AASHTO LRFD Section 5)

1.3.1. Checking for Bending Moment

$$\phi M_{ult} \geq M_{impact},$$

h_c=	54.25	in.	γ=	1.0	(Extreme Event AASHTO LRFD)
f_y=	60.00	ksi			
f_c=	4.00	ksi			

a) Factored Moment due to the Impact Load

γM_d=	γ	×	L_d	×	h_c		
γM_d=	1.0	×	160.0	kips	×	54.3	in.
γM_d=	8680.0	kips-in.					
γM_d=	**723.3**	**kips-ft**					

b) Factored Ultimate Moment

ϕ=	0.90		(Resistance Factor for Flexure)
t_c=	11.88	in.	(Thickness of the critical section of the coping)

$$\varphi M_{ult} = \varphi [A_s f_y d (1-k/2)] \qquad k = \frac{A_s f_y}{0.85 f_c' b d}$$

Use #	5	bars @	4.00	in. o.c.	(Stirrups)				
Use #	5	bars @	8.00	in. o.c.	(Connecting moment slab and coping section)				
d_b=	0.625	in.							
A_{b-1}=	0.307	$in.^2$			(Stirrups)				
A_{b-2}=	0.172	$in.^2$			(Connecting moment slab and coping section)				
d=	11.88	in.	-	2	in.	-	0.3125	in.	
d=	9.57	in.							
d=	**10.00**	**in.**							

Note: The impact is resisted by the 15 ft length of a barrier unit at the moment slab

$A_{s\text{-}1} = \frac{15.00\ \text{ft}}{0.333\ \text{ft}} \times 0.307\ \text{in.}^2$

$A_{s\text{-}1} = 13.81\ \text{in.}^2$

$A_{s\text{-}1} = \frac{15.00\ \text{ft}}{0.667\ \text{ft}} \times 0.172\ \text{in.}^2$

$A_{s\text{-}1} = 3.86\ \text{in.}^2$

$A_{s\text{-total}} = 17.67\ \text{in.}^2$

$$k = \frac{A_s f_y}{0.85 f_c' b d}$$

k= 0.1732

$M_{ult} = 17.67 \times 60.00 \times 10.00 \times 0.913$

$M_{ult} = 9681.64$ kips-in.

$M_{ult} = 806.80$ kips-ft

$\varphi M_{ult} = 0.90 \times 806.80$

$\varphi M_{ult} = 726.12$ kips-ft

$\varphi M_{ult} \geq M_{impact}$

726.12 kips-ft ≥ 723.3 kips-ft OK

2.0 Guidelines for the Soil Reinforcement

2.1 Pullout of the Soil Reinforcement

$$\varphi P \geq \gamma_s F_s + \gamma_d F_d$$

$$\varphi P \geq \gamma_s P_s A_t + \gamma_d P_d A_t$$

φ= 1.00 (Resistance Factor for Pullout Analysis)

γ_s= 1.00 (Static Load Factor for Pullout Analysis)

γ_d= 1.00 (Dynamic Load Factor for Pullout Analysis)

2.1.1 Top Layer of Reinforcement

a) Computing the Pullout Resistance

$P = F^* \times \sigma_{V1} \times L \times 2b$

Note: α is equal to 1.0 and C is equal to 2.0

F^*= 1.631 (AASHTO LRFD)

σ_{V1}= 0.454 ksf

L= 24.00 ft

b= 0.1640 ft

P= 5.828 kips

ϕP= 5.828 kips

$\gamma_s F_s$ = γ_s × F_s

$\gamma_s F_s$ = 1.00 × 1.24 kips

$\gamma_s F_s$ = 1.24 kips

$\gamma_s P_s A_t$ = 1.24 kips

Location= 3.63 ft

σ_{V1}= 0.454 ksf

k_r= 0.455 (AASHTO LRFD)

A_t= 6.00 ft^2

$T_{max} = \sigma_{H1} \times A_t$

T_{max}= 0.206 × 6.00

T_{max}= 1.24 kips/strips

Panel Width=	4.87	ft				
Trib. Height=	1.80	ft				
P_d=	930.00	psf	(First Strip)			
P_d=	680.00	psf	(Second Strip)			

$\gamma_d F_d$ =	γ_s	×	F_d			
$\gamma_d F_d$ =	γ_s	×	P_d	×	A_t	
$\gamma_d P_d A_t$=	1.00	×	930.00	×	4.38	
$\gamma_d P_d A_t$=	**4.076**	**kips**				

$$\varphi P \geq \gamma_s F_s + \gamma_d F_d$$

ϕP		≥		$\gamma_s P_s A_t$	+	$\gamma_d P_d A_t$
5.828		≥		1.24	+	4.076
5.83	**kips**	**≥**	**5.31**	**kips**		**OK**

2.1.2 Second Layer of Reinforcement

a) Computing the Pullout Resistance

P= $F^* \times \sigma_{V1} \times L \times 2b$ Note: α is equal to 1.0 and Cis equal to 2.0

F^*=	1.488	(AASHTO LRFD)					
σ_{V1}=	0.774	ksf			Location=	6.19	ft
L=	24.00	ft			σ_{V1}=	0.774	ksf
b=	0.1640	ft					
					k_r=	0.438	(AASHTO LRFD)
P=	9.063	kips			A_t=	6.00	ft^2
ϕP=	**9.063**	**kips**					
					T_{max}=	σ_{H1}	× A_t
$\gamma_s F_s$ =	γ_s	×	F_s		T_{max}=	0.339	× 6.00
$\gamma_s F_s$ =	1.00	×	2.03	kips	**T_{max}=**	**2.03**	**kips/strips**
$\gamma_s F_s$ =	2.03	kips					
$\gamma_s P_s A_t$ =	**2.033**	**kips**					

Panel Width=	4.87	ft				
Trib. Height=	2.46	ft				

$\gamma_d F_d$ =	γ_s	×	F_d			
$\gamma_d F_d$ =	γ_s	×	P_d	×	A_t	
$\gamma_d P_d A_t$=	1.00	×	680.00	×	5.99	
$\gamma_d P_d A_t$=	**4.073**	**kips**				

$$\varphi P \geq \gamma_s F_s + \gamma_d F_d$$

ϕP		≥		$\gamma_s P_s A_t$	+	$\gamma_d P_d A_t$
9.063		≥		2.03	+	4.073
9.063	**kips**	**≥**	**6.107**	**kips**		**OK**

2.2 Yielding of the Soil Reinforcement

$$\varphi R \geq \gamma_s F_s + \gamma_d F_d$$
$$\varphi R \geq \gamma_s P_s A_t + \gamma_d P_d A_t$$

φ=	1.00	(Resistance Factor for Rupture Analysis)
γ_s=	1.00	(Static Load Factor for Rupture Analysis)
γ_d=	1.00	(Dynamic Load Factor for Rupture Analysis)

2.2.1 Top Layer of Reinforcement

a) Computing the Rupture Resistance of the Strips for 75 years Service Life

E_c=	0.10	in.	(AASHTO LRFD)					
R=	σ_t	×	b	×	E_c			
R=	60.000	ksi	×	1.97	in.	×	0.10	in.
R=	12.016	kips						
ϕR=	ϕ	×	R	kips				
ϕR=	1.00	×	12.016	kips				
ϕR=	**12.016**	**kips**						

$\gamma_s P_s A_t$ =	**1.239**	**kips**

Panel Width=	4.87	ft	
Trib. Height=	1.80	ft	
P_d=	3550.00	psf	(First Strip)
P_d=	680.00	psf	(Second Strip)

$\gamma_d F_d$ =	**γ_s**	×	**F_d**			
$\gamma_d F_d$ =	**γ_s**	×	P_d	×	A_t	
$\gamma_d P_d A_t$=	1.00	×	3550.00	×	4.38	
$\gamma_d P_d A_t$=	**15.560**	**kips**				

$\varphi R \geq \gamma_s F_s + \gamma_d F_d$

φR		≥		$\gamma_s P_s A_t$	+	$\gamma_d P_d A_t$
5.828		≥		1.24	+	15.560
12.016	**kips**	**≥**	**16.80**	**kips**	**VERIFIED**	

2.2.1 Second Layer of Reinforcement

a) Computing the Rupture Resistance of the Strips for 75 years Service Life

E_c=	0.10	in.	(AASHTO LRFD)					
R=	σ_t	×	b	×	E_c			
R=	60.000	ksi	×	1.97	in.	×	0.10	in.
R=	12.016	kips						
ϕR=	ϕ	×	R	kips				
ϕR=	1.00	×	12.016	kips				
ϕR=	**12.016**	**kips**						

$\gamma_s P_s A_t$ =	**2.033**	**kips**

Panel Width=	4.87	ft	
Trib. Height=	2.46	ft	
P_d=	3550.00	psf	(First Strip)
P_d=	680.00	psf	(Second Strip)

$\gamma_d F_d$ =	**γ_s**	×	**F_d**			
$\gamma_d F_d$ =	**γ_s**	×	P_d	×	A_t	
$\gamma_d P_d A_t$=	1.00	×	680.00	×	5.990	
$\gamma_d P_d A_t$=	**4.073**	**kips**				

$\varphi R \geq \gamma_s F_s + \gamma_d F_d$

φR		≥		$\gamma_s P_s A_t$	+	$\gamma_d P_d A_t$
5.828		≥		2.03	+	4.073
12.016	**kips**	**≥**	**6.11**	**kips**	**OK**	

Preliminary Design of MSE Wall for TL-5-2 Impact (10 ft and 16 ft long strip)

INPUT VALUES

1) Height of the Barrier=	48.0	in.	8) Static Load, F_s=	80.0	kips
2) Soil Unit Weight=	0.125	kcf	9) Steel Reinforcement Strength, f_y=	60.0	ksi
3) Concrete Unit Weight=	0.150	kcf	10) Concrete Compressive Strength, f_c=	4.0	ksi
4) Soil-Slab Fric. Angle, Φ_r=	34.0	deg.	11) Length of soil reinforcement=	10.0	ft
5) Length of Section =	30.0	ft	12) Dyn. Pres. for the first strip (Pullout)=	1517.0	psf
6) Dynamic Load, F_d=	260.0	kips	13) Dyn. Pres. for the sec. strip (Pullout)=	1107.0	psf
7) Panel Thickness, h=	5.50	in.	14) Dyn. Pres. for the sec. strip (yielding)=	5778.0	psf
8) Strip Width=	1.97	in.	13) Dyn. Pres. for the sec. strip (yielding)=	1107.0	psf

1.0 Stability

1.1 Sliding of the Barrier

$$\varphi P \geq \gamma L_s$$

Where:
- ϕ= Resistance factor
- P= Resistance load (P=Wtanϕ_r)
- γ= Load factor
- L_s= Static load
- W= Weight the system above the moment slab base.
- ϕ_r= Interface friction angle between the concrete and the soil

a) Computing the Location of the Impact Force with Respect to the Rotation Point

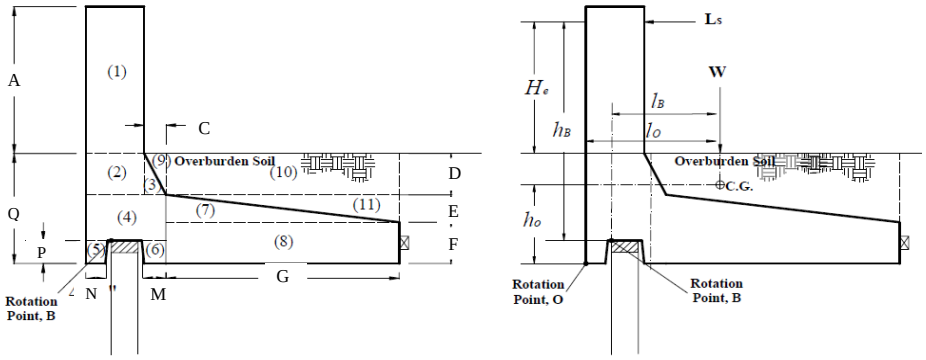

System Dimensions:

A=	48.00	in.	E=	7.50	in.	M=	14.50	in.	Q=	40.00	in.
C=	12.00	in.	F=	12.00	in.	N=	4.75	in.	$Slab_{bot.}$=	40.00	in.
D=	20.50	in.	G=	92.20	in.	P=	15.00	in.			

Concrete Unit Weight=	0.150	kcf	H_e=	43.00	in.
Soil Unit Weight=	0.125	kcf	L_{slab}=	9.00	ft
Length of Section =	30.00	ft	First Strip Loc.=	3.63	ft

	Section	x (in.)	y (in.)	Area ($in.^2$)	weight (kips)	x from O (in.)	y from O (in.)	y*weight (kips-in.)	x*weight (kips-in.)
	1	13.00	48.00	624.00	19.50	6.50	64.00	1248.00	126.75
Barrier	2	12.00	20.50	246.00	7.69	6.00	29.75	228.70	46.13
Coping	3	12.00	20.50	123.00	3.84	16.00	26.33	101.22	61.50
	4	25.00	4.50	112.50	3.52	12.50	17.25	60.64	43.95
	5	4.75	15.00	71.25	2.23	2.38	7.50	16.70	5.29
	6	14.50	15.00	217.50	6.80	17.75	7.50	50.98	120.64
	7	92.20	7.50	345.75	10.80	55.73	14.50	156.67	602.18
M. Slab	8	92.20	12.00	1106.40	34.58	71.10	6.00	207.45	2458.28
	9	12.00	12.00	72.00	1.88	21.00	27.50	51.56	39.38
Soil	10	92.20	20.50	1890.10	49.22	71.10	29.75	1464.34	3499.64
	11	92.20	7.50	345.75	9.00	86.47	17.00	153.07	778.54
	Total			5154.25	149.05			3739.32	7782.27
	h_o and l_o in inches =							25.09	52.21

Distance from the C.G. to the Rotation Point in the x Direction, l_B =	46.7	in.	≈	3.89	ft
Distance from the L_S to the Rotation Point in the y Direction, h_B =	68.0	in.	≈	5.67	ft

b) Computing the Sliding Resistance

ϕ=	0.80		γ=	1.00			
P=	100.54	kips	L_s=	80.00	kips		
φP =	80.43	kips	φP	≥	γL_s		
γL_s=	80.00	kips	**80 (kips)**	**≥**	**80.0 (kips)**	**OK**	

1.2 Overturning Moment of the Barrier

$$\varphi M \geq \gamma L_s h_B$$
$$\varphi W l_B \geq \gamma L_s h_B$$

ϕ=	0.90		γ=	1.00			
M=	6962.49	kips-in.	L_sh_B=	5440.00	kips-in.		
M=	580.21	kips-ft	L_sh_B=	453.33	kips-ft		
φM =	522.19	kips-ft	φM	≥	γL_sh_B		
γL_sh_B=	453.33	kips-ft	**522.19 (kips-ft)**	**≥**	**453.33 (kips-ft)**	**OK**	

1.3 Rupture of the Coping in Bending (AASHTO LRFD Section 5)

1.3.1. Checking for Bending Moment

$$\phi M_{ult} \geq M_{impact},$$

h_c=	67.25	in.	γ=	1.0	(Extreme Event AASHTO LRFD)
f_y=	60.00	ksi			
f_c=	4.00	ksi			

a) Factored Moment due to the Impact Load

γM_d=	γ	×	L_d	×	h_c		
γM_d=	1.0	×	260.0	kips	×	67.3	in.
γM_d=	17485.0	kips-in.					
γM_d=	**1457.1**	**kips-ft**					

b) Factored Ultimate Moment

ϕ=	0.90		(Resistance Factor for Flexure)
t_c=	15.18	in.	(Thickness of the critical section of the coping)

φM_{ult} = $\varphi [A_s f_y d (1-k/2)]$ $\quad k = \dfrac{A_s f_y}{0.85 f_c' b d}$

Use #	7	bars @	4.00	in. o.c.	(Stirrups)			
Use #	5	bars @	8.00	in. o.c.	(Connecting moment slab and coping section)			
d_b=	0.875	in.						
$A_{b\text{-}1}$=	0.601	$in.^2$			(Stirrups)			
$A_{b\text{-}2}$=	0.172	$in.^2$			(Connecting moment slab and coping section)			
d=	15.18	in.	-	2	in.	-	0.4375	in.
d=	12.74	in.						
d=	**13.00**	**in.**						

Note: The impact is resisted by the 15 ft length of a barrier unit at the moment slab

$A_{s\text{-}1} = \frac{15.00\ \text{ft}}{0.333\ \text{ft}} \times 0.601\ \text{in.}^2$

$A_{s\text{-}1} = 27.06\ \text{in.}^2$

$A_{s\text{-}1} = \frac{15.00\ \text{ft}}{0.667\ \text{ft}} \times 0.172\ \text{in.}^2$

$A_{s\text{-}1} = 3.86\ \text{in.}^2$

$A_{s\text{-}total} = 30.92\ \text{in.}^2$

$$k = \frac{A_s f_y}{0.85 f_c' b d}$$

k= 0.2332

$M_{ult} = 30.92 \times 60.00 \times 13.00 \times 0.883$

$M_{ult} = 21305.39$ kips-in.

$M_{ult} = 1775.45$ kips-ft

$\varphi M_{ult} = 0.90 \times 1775.45$

φM_{ult} = 1597.90 kips-ft

φM_{ult}		$\geq$	M_{impact}		
1597.90	**kips-ft**	**≥**	**1457.1**	**kips-ft**	**OK**

2.0 Guidelines for the Soil Reinforcement

2.1 Pullout of the Soil Reinforcement

$$\varphi P \geq \gamma_s F_s + \gamma_d F_d$$

$$\varphi P \geq \gamma_s P_s A_t + \gamma_d P_d A_t$$

φ= 1.00 (Resistance Factor for Pullout Analysis)

γ_s= 1.00 (Static Load Factor for Pullout Analysis)

γ_d= 1.00 (Dynamic Load Factor for Pullout Analysis)

2.1.1 Top Layer of Reinforcement

a) Computing the Pullout Resistance

$P = F^* \times \sigma_{V1} \times L \times 2b$

Note: α is equal to 1.0 and C is equal to 2.0

F^*= 1.631 (AASHTO LRFD)

σ_{V1}= 0.463 ksf

L= 10.00 ft

b= 0.1640 ft

P= 2.475 kips

ϕP= 2.475 kips

$\gamma_s F_s$ = γ_s × F_s

$\gamma_s F_s$ = 1.00 × 0.84 kips

$\gamma_s F_s$ = 0.84 kips

$\gamma_s P_s A_t$ = 0.84 kips

Location= 3.7 ft

σ_{V1}= 0.463 ksf

k_r= 0.455 (AASHTO LRFD)

A_t= 3.99 ft^2

$T_{max} = \sigma_{H1} \times A_t$

$T_{max} = 0.210 \times 3.99$

T_{max}= 0.84 kips/strips

Panel Width=	4.87	ft					
Trib. Height=	1.80	ft					
P_d=	1517.00	psf	(First Strip)				
P_d=	1107.00	psf	(Second Strip)				

$\gamma_d F_d$ =	γ_s	×	F_d			
$\gamma_d F_d$ =	γ_s	×	P_d	×	A_t	
$\gamma_d P_d A_t$=	1.00	×	1517.00	×	2.92	
$\gamma_d P_d A_t$=	**4.433**	**kips**				

$$\phi P \geq \gamma_s F_s + \gamma_d F_d$$

ϕP		≥		$\gamma_s P_s A_t$	+	$\gamma_d P_d A_t$		
2.475		≥		0.84	+	4.433		
2.48	**kips**	**≥**	**5.27**	**kips**	**VERIFIED**		(10 ft long strip)	
3.96	**kips**	**≥**	**5.27**	**kips**	**VERIFIED**		(16 ft long strip)	

2.1.2 Second Layer of Reinforcement

a) Computing the Pullout Resistance

P= F^* × σ_{V1} × L × $2b$ Note: α is equal to 1.0 and Cis equal to 2.0

F^*= 1.488 (AASHTO LRFD)

σ_{V1}=	0.783	ksf		Location=	6.26	ft	
L=	10.00	ft		σ_{V1}=	0.783	ksf	
b=	0.1640	ft					
				k_t=	0.438	(AASHTO LRFD)	
P=	3.819	kips		A_t=	3.99	ft^2	
ϕP=	**3.819**	**kips**					

					T_{max}=	σ_{H1}	×	A_t
$\gamma_s F_s$ =	γ_s	×	F_s		T_{max}=	0.343	×	3.99
$\gamma_s F_s$ =	1.00	×	1.37	kips	**T_{max}=**	**1.37**	**kips/strips**	
$\gamma_s F_s$ =	1.37	kips						
$\gamma_s P_s A_t$ =	**1.368**	**kips**						

Panel Width=	4.87	ft						
Trib. Height=	2.46	ft						
$\gamma_d F_d$ =	γ_s	×	F_d					
$\gamma_d F_d$ =	γ_s	×	P_d	×	A_t			
$\gamma_d P_d A_t$=	1.00	×	1107.00	×	3.99			
$\gamma_d P_d A_t$=	**4.421**	**kips**						

$$\phi P \geq \gamma_s F_s + \gamma_d F_d$$

ϕP		≥		$\gamma_s P_s A_t$	+	$\gamma_d P_d A_t$		
3.819		≥		1.37	+	4.421		
3.82	**kips**	**≥**	**5.79**	**kips**	**VERIFIED**		(10 ft long strip)	
6.11	**kips**	**≥**	**5.79**	**kips**	**OK**		(16 ft long strip)	

2.2 Yielding of the Soil Reinforcement

$$\varphi R \geq \gamma_s F_s + \gamma_d F_d$$
$$\varphi R \geq \gamma_s P_s A_t + \gamma_d P_d A_t$$

φ=	1.00	(Resistance Factor for Rupture Analysis)
γ_s=	1.00	(Static Load Factor for Rupture Analysis)
γ_d=	1.00	(Dynamic Load Factor for Rupture Analysis)

2.2.1 Top Layer of Reinforcement

a) Computing the Rupture Resistance of the Strips for 75 years Service Life

E_c=	0.10	in.	(AASHTO LRFD)					
R=	σ_t	×	b	×	E_c			
R=	60.000	ksi	×	1.97	in.	×	0.10	in.
R=	12.016	kips						
ϕR=	ϕ	×	R	kips				
ϕR=	1.00	×	12.016	kips				
ϕR=	**12.016**	**kips**						

$\gamma_s P_s A_t$ =	**0.840**	**kips**

Panel Width=	4.87	ft	
Trib. Height=	1.80	ft	
P_d=	5778.00	psf	(First Strip)
P_d=	1107.00	psf	(Second Strip)

$\gamma_d F_d$ =	**γ_s**	×	**F_d**			
$\gamma_d F_d$ =	**γ_s**	×	P_d	×	A_t	
$\gamma_d P_d A_t$=	1.00	×	5778.00	×	2.92	
$\gamma_d P_d A_t$=	**16.883**	**kips**				

$\phi R \geq \gamma_s F_s + \gamma_d F_d$

φR		≥	$\gamma_s P_s A_t$	+	$\gamma_d P_d A_t$		
2.475		≥	0.84	+	16.883		
12.016	**kips**	**≥**	**17.723**	**kips**	**REDISIGN**	(10 ft & 16 ft long strip)	

2.2.1 Second Layer of Reinforcement

a) Computing the Rupture Resistance of the Strips for 75 years Service Life

E_c=	0.10	in.	(AASHTO LRFD)					
R=	σ_t	×	b	×	E_c			
R=	60.000	ksi	×	1.97	in.	×	0.10	in.
R=	12.016	kips						
ϕR=	ϕ	×	R	kips				
ϕR=	1.00	×	12.016	kips				
ϕR=	**12.02**	**kips**						

$\gamma_s P_s A_t$ =	**1.368**	**kips**

Panel Width=	4.87	ft	
Trib. Height=	2.46	ft	
P_d=	5778.00	psf	(First Strip)
P_d=	1107.00	psf	(Second Strip)

$\gamma_d F_d$ =	**γ_s**	×	**F_d**			
$\gamma_d F_d$ =	**γ_s**	×	P_d	×	A_t	
$\gamma_d P_d A_t$=	1.00	×	1107.00	×	3.993	
$\gamma_d P_d A_t$=	**4.421**	**kips**				

$\phi R \geq \gamma_s F_s + \gamma_d F_d$

φR		≥	$\gamma_s P_s A_t$	+	$\gamma_d P_d A_t$		
2.475		≥	1.37	+	4.421		
12.02	**kips**	**≥**	**5.788**	**kips**	**OK**	(10 ft & 16 ft long strip)	

Preliminary Design of MSE Wall for TL-5-2 Impact (24 ft long strip)

INPUT VALUES

1) Height of the Barrier=	48.0	in.	8) Static Load, F_s=	80.0	kips
2) Soil Unit Weight=	0.125	kcf	9) Steel Reinforcement Strength, f_y=	60.0	ksi
3) Concrete Unit Weight=	0.150	kcf	10) Concrete Compressive Strength, f_c=	4.0	ksi
4) Soil-Slab Fric. Angle, Φ_r=	34.0	deg.	11) Length of soil reinforcement=	24.0	ft
5) Length of Section =	30.0	ft	12) Dyn. Pres. for the first strip (Pullout)=	1517.0	psf
6) Dynamic Load, F_d=	260.0	kips	13) Dyn. Pres. for the sec. strip (Pullout)=	1107.0	psf
7) Panel Thickness, h=	5.50	in.	14) Dyn. Pres. for the sec. strip (yielding)=	5778.0	psf
8) Strip Width=	1.97	in.	13) Dyn. Pres. for the sec. strip (yielding)=	1107.0	psf

1.0 Stability

1.1 Sliding of the Barrier

$$\varphi P \geq \gamma L_s$$

Where:
- ϕ= Resistance factor
- P= Resistance load (P=Wtanϕ_r)
- γ= Load factor
- L_s= Static load
- W= Weight the system above the moment slab base.
- ϕ_r= Interface friction angle between the concrete and the soil

a) Computing the Location of the Impact Force with Respect to the Rotation Point

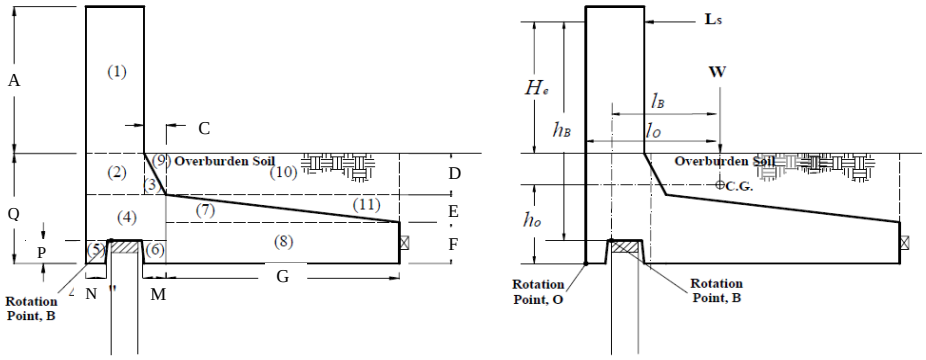

System Dimensions:

A=	48.00	in.	E=	7.50	in.	M=	14.50	in.	Q=	40.00	in.
C=	12.00	in.	F=	12.00	in.	N=	4.75	in.	$Slab_{bot.}$=	40.00	in.
D=	20.50	in.	G=	92.20	in.	P=	15.00	in.			

Concrete Unit Weight=	0.150	kcf	H_e=	43.00	in.
Soil Unit Weight=	0.125	kcf	L_{slab}=	9.00	ft
Length of Section =	30.00	ft	First Strip Loc.=	3.63	ft

	Section	x (in.)	y (in.)	Area ($in.^2$)	weight (kips)	x from O (in.)	y from O (in.)	y*weight (kips-in.)	x*weight (kips-in.)
	1	13.00	48.00	624.00	19.50	6.50	64.00	1248.00	126.75
Barrier	2	12.00	20.50	246.00	7.69	6.00	29.75	228.70	46.13
Coping	3	12.00	20.50	123.00	3.84	16.00	26.33	101.22	61.50
	4	25.00	4.50	112.50	3.52	12.50	17.25	60.64	43.95
	5	4.75	15.00	71.25	2.23	2.38	7.50	16.70	5.29
	6	14.50	15.00	217.50	6.80	17.75	7.50	50.98	120.64
	7	92.20	7.50	345.75	10.80	55.73	14.50	156.67	602.18
M. Slab	8	92.20	12.00	1106.40	34.58	71.10	6.00	207.45	2458.28
	9	12.00	12.00	72.00	1.88	21.00	27.50	51.56	39.38
Soil	10	92.20	20.50	1890.10	49.22	71.10	29.75	1464.34	3499.64
	11	92.20	7.50	345.75	9.00	86.47	17.00	153.07	778.54
	Total			5154.25	149.05			3739.32	7782.27
	h_o and l_o in inches =							25.09	52.21

Distance from the C.G. to the Rotation Point in the x Direction, l_B =	46.7	in.	≈	3.89	ft
Distance from the L_S to the Rotation Point in the y Direction, h_B =	68.0	in.	≈	5.67	ft

b) Computing the Sliding Resistance

ϕ=	0.80		γ=	1.00			
P=	100.54	kips	L_s=	80.00	kips		
φP =	80.43	kips	φP	≥	γL_s		
γL_s=	80.00	kips	**80 (kips)**	**≥**	**80.0 (kips)**	**OK**	

1.2 Overturning Moment of the Barrier

$$\varphi M \geq \gamma L_s h_B$$
$$\varphi W l_B \geq \gamma L_s h_B$$

ϕ=	0.90		γ=	1.00			
M=	6962.49	kips-in.	L_sh_B=	5440.00	kips-in.		
M=	580.21	kips-ft	L_sh_B=	453.33	kips-ft		
φM =	522.19	kips-ft	φM	≥	γL_sh_B		
γL_sh_B=	453.33	kips-ft	**522.19 (kips-ft)**	**≥**	**453.33 (kips-ft)**	**OK**	

1.3 Rupture of the Coping in Bending (AASHTO LRFD Section 5)

1.3.1. Checking for Bending Moment

$$\phi M_{ult} \geq M_{impact},$$

h_c=	67.25	in.	γ=	1.0	(Extreme Event AASHTO LRFD)
f_y=	60.00	ksi			
f_c=	4.00	ksi			

a) Factored Moment due to the Impact Load

γM_d=	γ	×	L_d	×	h_c		
γM_d=	1.0	×	260.0	kips	×	67.3	in.
γM_d=	17485.0	kips-in.					
γM_d=	**1457.1**	**kips-ft**					

b) Factored Ultimate Moment

ϕ=	0.90		(Resistance Factor for Flexure)
t_c=	15.18	in.	(Thickness of the critical section of the coping)

$$\varphi M_{ult} = \varphi [A_s f_y d (1-k/2)] \qquad k = \frac{A_s f_y}{0.85 f_c' bd}$$

Use #	7	bars @	4.00	in. o.c.	(Stirrups)			
Use #	5	bars @	8.00	in. o.c.	(Connecting moment slab and coping section)			
d_b=	0.875	in.						
$A_{b\text{-}1}$=	0.601	$in.^2$			(Stirrups)			
$A_{b\text{-}2}$=	0.172	$in.^2$			(Connecting moment slab and coping section)			
d=	15.18	in.	-	2	in.	-	0.4375	in.
d=	12.74	in.						
d=	**13.00**	**in.**						

Note: The impact is resisted by the 15 ft length of a barrier unit at the moment slab

$A_{s\text{-}1} = \frac{15.00\ \text{ft}}{0.333\ \text{ft}} \times 0.601\ \text{in.}^2$

$A_{s\text{-}1} = 27.06\ \text{in.}^2$

$A_{s\text{-}1} = \frac{15.00\ \text{ft}}{0.667\ \text{ft}} \times 0.172\ \text{in.}^2$

$A_{s\text{-}1} = 3.86\ \text{in.}^2$

$A_{s\text{-total}} = 30.92\ \text{in.}^2$

$$k = \frac{A_s f_y}{0.85 f_c' b d}$$

k= 0.2332

$M_{ult} = 30.92 \times 60.00 \times 13.00 \times 0.883$

$M_{ult} = 21305.39$ kips-in.

$M_{ult} = 1775.45$ kips-ft

$\varphi M_{ult} = 0.90 \times 1775.45$

φM_{ult} = 1597.90 kips-ft

$\varphi M_{ult} \geq M_{impact}$

1597.90 kips-ft ≥ 1457.1 kips-ft OK

2.0 Guidelines for the Soil Reinforcement

2.1 Pullout of the Soil Reinforcement

$$\varphi P \geq \gamma_s F_s + \gamma_d F_d$$

$$\varphi P \geq \gamma_s P_s A_t + \gamma_d P_d A_t$$

φ= 1.00 (Resistance Factor for Pullout Analysis)

γ_s= 1.00 (Static Load Factor for Pullout Analysis)

γ_d= 1.00 (Dynamic Load Factor for Pullout Analysis)

2.1.1 Top Layer of Reinforcement

a) Computing the Pullout Resistance

$P = F^* \times \sigma_{V1} \times L \times 2b$

Note: α is equal to 1.0 and C is equal to 2.0

F^*= 1.631 (AASHTO LRFD)

σ_{V1}= 0.463 ksf

L= 24.00 ft

b= 0.1640 ft

P= 5.941 kips

ϕP= 5.941 kips

$\gamma_s F_s$ = γ_s × F_s

$\gamma_s F_s$ = 1.00 × 1.26 kips

$\gamma_s F_s$ = 1.26 kips

$\gamma_s P_s A_t$ = 1.26 kips

Location= 3.7 ft

σ_{V1}= 0.463 ksf

k_r= 0.455 (AASHTO LRFD)

A_t= 6.00 ft^2

$T_{max} = \sigma_{H1} \times A_t$

$T_{max} = 0.210 \times 6.00$

T_{max}= 1.26 kips/strips

Panel Width=	4.87	ft			
Trib. Height=	1.80	ft			
P_d=	1517.00	psf	(First Strip)		
P_d=	1107.00	psf	(Second Strip)		

$\gamma_d F_d$ =	γ_s	×	F_d		
$\gamma_d F_d$ =	γ_s	×	P_d	×	A_t
$\gamma_d P_d A_t$=	1.00	×	1517.00	×	4.38
$\gamma_d P_d A_t$=	**6.649**	**kips**			

$$\phi P \geq \gamma_s F_s + \gamma_d F_d$$

ϕP		≥		$\gamma_s P_s A_t$	+ $\gamma_d P_d A_t$
5.941		≥		1.26	+ 6.649
5.94	**kips**	≥	**7.91**	**kips**	**VERIFIED**

2.1.2 Second Layer of Reinforcement

a) Computing the Pullout Resistance

$P = F^* \times \sigma_{V1} \times L \times 2b$ Note: α is equal to 1.0 and Cis equal to 2.0

F^*=	1.488	(AASHTO LRFD)					
σ_{V1}=	0.783	ksf			Location=	6.26	ft
L=	24.00	ft			σ_{V1}=	0.783	ksf
b=	0.1640	ft					
					k_r=	0.438	(AASHTO LRFD)
P=	9.165	kips			A_t=	6.00	ft^2
ϕP=	**9.165**	**kips**					
					T_{max}=	σ_{H1} ×	A_t
$\gamma_s F_s$ =	γ_s	×	F_s		T_{max}=	0.343 ×	6.00
$\gamma_s F_s$ =	1.00	×	2.06	kips	**T_{max}=**	**2.06**	**kips/strips**
$\gamma_s F_s$ =	2.06	kips					
$\gamma_s P_s A_t$ =	**2.056**	**kips**					

Panel Width=	4.87	ft			
Trib. Height=	2.46	ft			

$\gamma_d F_d$ =	γ_s	×	F_d		
$\gamma_d F_d$ =	γ_s	×	P_d	×	A_t
$\gamma_d P_d A_t$=	1.00	×	1107.00	×	5.99
$\gamma_d P_d A_t$=	**6.631**	**kips**			

$$\phi P \geq \gamma_s F_s + \gamma_d F_d$$

ϕP		≥		$\gamma_s P_s A_t$	+ $\gamma_d P_d A_t$
9.165		≥		2.06	+ 6.631
9.17	**kips**	≥	**8.69**	**kips**	**OK**
6.11	**kips**	≥	**8.69**	**kips**	**VERIFIED**

2.2 Yielding of the Soil Reinforcement

$$\phi R \geq \gamma_s F_s + \gamma_d F_d$$
$$\phi R \geq \gamma_s P_s A_t + \gamma_d P_d A_t$$

φ=	1.00	(Resistance Factor for Rupture Analysis)
γ_s=	1.00	(Static Load Factor for Rupture Analysis)
γ_d=	1.00	(Dynamic Load Factor for Rupture Analysis)

2.2.1 Top Layer of Reinforcement

a) Computing the Rupture Resistance of the Strips for 75 years Service Life

E_c=	0.10	in.	(AASHTO LRFD)					
R=	σ_t	×	b	×	E_c			
R=	60.000	ksi	×	1.97	in.	×	0.10	in.
R=	12.016	kips						
ϕR=	ϕ	×	R	kips				
ϕR=	1.00	×	12.016	kips				
ϕR=	**12.016**	**kips**						

$\gamma_s P_s A_t$ =	**1.263**	**kips**

Panel Width=	4.87	ft	
Trib. Height=	1.80	ft	
P_d=	5778.00	psf	(First Strip)
P_d=	1107.00	psf	(Second Strip)

$\gamma_d F_d$ =	**γ_s**	×	**F_d**			
$\gamma_d F_d$ =	**γ_s**	×	P_d	×	A_t	
$\gamma_d P_d A_t$=	1.00	×	5778.00	×	4.38	
$\gamma_d P_d A_t$=	**25.325**	**kips**				

$\varphi R \geq \gamma_s F_s + \gamma_d F_d$

φR		≥		$\gamma_s P_s A_t$	+	$\gamma_d P_d A_t$
5.941		≥		1.26	+	25.325
12.016	**kips**	**≥**	**26.6**	**kips**	**REDISIGN**	

2.2.1 Second Layer of Reinforcement

a) Computing the Rupture Resistance of the Strips for 75 years Service Life

E_c=	0.10	in.	(AASHTO LRFD)					
R=	σ_t	×	b	×	E_c			
R=	60.000	ksi	×	1.97	in.	×	0.10	in.
R=	12.016	kips						
ϕR=	ϕ	×	R	kips				
ϕR=	1.00	×	12.016	kips				
ϕR=	**12.02**	**kips**						

$\gamma_s P_s A_t$ =	**2.056**	**kips**

Panel Width=	4.87	ft	
Trib. Height=	2.46	ft	
P_d=	5778.00	psf	(First Strip)
P_d=	1107.00	psf	(Second Strip)

$\gamma_d F_d$ =	**γ_s**	×	**F_d**			
$\gamma_d F_d$ =	**γ_s**	×	P_d	×	A_t	
$\gamma_d P_d A_t$=	1.00	×	1107.00	×	5.990	
$\gamma_d P_d A_t$=	**6.631**	**kips**				

$\varphi R \geq \gamma_s F_s + \gamma_d F_d$

φR		≥		$\gamma_s P_s A_t$	+	$\gamma_d P_d A_t$
5.941		≥		2.06	+	6.631
12.02	**kips**	**≥**	**8.69**	**kips**	**OK**	

APPENDIX B

DESIGN OF TL-5 MSE WALL TEST INSTALLATION USING

RECOMMENDED DESIGN PARAMETERS

Note= the caclutation presented in this section were performed following the recommendation of impact loads for traffic barrier and MSE wall reinforcement presented in section 3 (impact load), section 4 (equivalent static load) and section 6 (soil reinforcing loads).

INPUT PARAMETERS

1) Height of the Barrier=	42.0	in.	8) Static Load, F_s=	60.0	kips
2) Soil Unit Weight=	0.12	kcf	9) Steel Reinforcement Strength, f_y=	60.0	ksi
3) Concrete Unit Weight=	0.15	kcf	10) Concrete Compressive Strength, f_c=	4.0	ksi
4) Soil-Slab Fric. Angle, Φ_r=	34.0	deg.	11) Length of the barrier Units=	15.0	ft
5) Length of Section =	30.0	ft	12) Dyn. Pres. for the first strip (Pullout)=	525.0	psf
6) Dynamic Load, F_d	160.0	kips	13) Dyn. Pres. for the first strip (Pullout)=	410.0	psf
7) Panel Thickness, h=	5.50	in.	14) Dyn. Pres. for the sec. strip (Yielding)=	1790.0	psf
8) Strip Width=	1.97	in.	13) Dyn. Pres. for the sec. strip (Yielding)=	475.0	psf

1.0 Stability

1.1 Sliding of the Barrier

$$\varphi P \geq \gamma L_s$$

Where:
- ϕ= Resistance factor
- P= Resistance load ($P=W\tan\phi_r$)
- γ= Load factor
- L_s= Static load
- W= Weight the system above the moment slab base.
- ϕ_r= Interface friction angle between the concrete and the soil

a) Computing the Location of the Impact Force with Respect to the Rotation Point

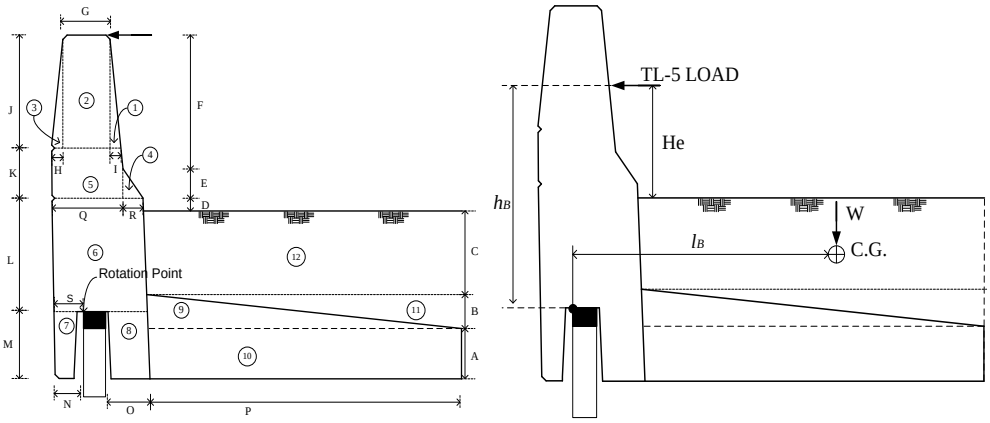

System Dimensions:

A=	12.00	in.	F=	29.00	in.	K=	13.75	in.	P=	72.50	in.
B=	8.00	in.	G=	11.75	in.	L=	27.75	in.	Q=	17.00	in.
C=	20.00	in.	H=	2.00	in.	M=	15.00	in.	R=	5.00	in.
D=	3.00	in.	I=	3.25	in.	N=	6.00	in.	S=	6.25	in.
E=	10.00	in.	J=	25.75	in.	O=	10.25	in.			

Concrete Unit Weight=	150.00	kcf	H_e=	34.00	in.
Soil Unit Weight=	115.00	kcf	L_{slab}=	3.33	ft (Bottom of mom. slab)
Length of Section =	30.00	ft			

	Section	x (in.)	y (in.)	Area (in.^{2})	weight (kips)	x from O (in.)	y from O (in.)	y*weight (kips-in.)	x*weight (kips-in.)
Barrier	1.0	3.3	25.8	41.8	1.3	8.58	50.08	65.49	11.22
	2.0	11.8	25.8	302.6	9.5	1.63	54.38	514.12	15.36
	3.0	2.0	25.8	25.8	0.8	-4.92	50.08	40.30	-3.96
	4.0	5.0	10.0	25.0	0.8	12.42	31.08	24.28	9.70
	5.0	17.0	13.8	233.8	7.3	2.25	34.63	252.92	16.44
	6.0	22.0	27.8	610.5	19.1	4.75	13.88	264.71	90.62
	7.0	6.0	15.0	90.0	2.8	-3.25	-7.50	-21.09	-9.14
	8.0	10.3	15.0	153.8	4.8	10.63	7.50	36.04	51.05
Mom. Slab	9.0	78.0	8.0	312.0	9.8	39.92	0.33	3.25	389.19
	10.0	72.5	12.0	870.0	27.2	52.00	9.00	244.69	1413.75
Soil	11.0	72.5	8.0	290.0	6.9	64.08	2.33	16.21	445.25
	12.0	72.5	20.0	1450.0	34.7	52.00	15.00	521.09	1806.46
	Total			2665.2	125.0			1962.0	4235.9
	h_o and l_o in inches =							15.70	33.89

Distance from the C.G. to the Rotation Point in the x Direction, l_B = **33.89** **in.** ≈ **2.82** ft

Distance from the L_S to the Rotation Point in the y Direction, h_B = **59.25** **in.** ≈ **4.94** ft

b) Computing the Sliding Resistance

ϕ=	0.80		γ=	1.00		
P=	84.30	kips	L_s=	60.00	kips	
φP =	67.44	Kips	φP	≥	γL_s	
γL_s=	60.00	Kips	**67.44 (kips)**	≥	**60.0 (kips)**	**OK**

1.2 Overturning Moment of the Barrier

$$\varphi M \geq \gamma L_s h_B$$
$$\varphi W l_B \geq \gamma L_s h_B$$

ϕ=	0.90		γ=	1.00		
M=	4235.94	kips-in	$L_s h_B$=	3555.00	kips-in.	
M=	352.99	kips-ft	$L_s h_B$=	296.25	kips-ft	
φM =	317.70	kips-ft	φM	≥	$\gamma L_s h_B$	
$\gamma L_s h_B$=	296.25	kips-ft	**317.70 (kips-ft)**	≥	**296.25 (kips-ft)**	**OK**

1.3 Rupture of the Coping in Bending (*AASHTO LRFD* Section 5)

1.3.1. Checking for Bending Moment

$$\phi M_{ult} \geq M_{impact},$$

h_c=	56.50	in.	γ=	1.0	(Extreme Event *AASHTO LRFD*)
f_y=	60.00	ksi			
f_c=	4.00	ksi			

a) Factored Moment due to the Impact Load

γM_d=	γ	×	L_d	×	h_c		
γM_d=	1.0	×	160.0	kips	×	56.5	in.
γM_d=	9040.0	kips-in.					
γM_d=	**753.3**	**kips-ft**					

b) Factored Ultimate Moment

ϕ=	0.90		(Resistance Factor for Flexure)
t_c=	10.86	in.	(Thickness of the critical section of the coping)

$\varphi M_{ult} = \varphi [A_s f_y d (1-k/2)]$ $\quad k = \dfrac{A_s f_y}{0.85 f_c' bd}$

Use #	6	bars @	4.00	in. o.c.	(Stirrups Vertical)
Use #	5	bars @	8.00	in. o.c.	(Connection Bars between Moment Slabs and Barriers)
d_b=	0.75	in.			
A_b=	0.442	$in.^2$			
t=	10.86	in.	- 2	in.	- 0.375 in.
d=	8.48	in.			
d=	**9.00**	**in.**			

Note: The impact is resisted by the 9.8 ft length of a barrier unit at the moment slab

$A_s = \dfrac{15.00 \text{ ft}}{0.333 \text{ ft}} \times 0.442 \text{ in.}^2$ $\quad A_s = \dfrac{15.00 \text{ ft}}{0.667 \text{ ft}} \times 0.442$

A_s= 19.88 $in.^2$ $\quad A_s$= 9.94 $in.^2$

A_s= 5.56 $in.^2$

$k = \dfrac{A_s f_y}{0.85 f_c' bd}$ $\quad$ **$A_{s\text{-total}}$= 25.44 $in.^2$**

k= 0.2771

M_{ult} =	25.44	×	60.00	×	9.00	×	0.861
M_{ult} =	11833.65	kips-in.					
M_{ult} =	986.14	kips-ft					
φM_{ult} =	0.90	×	986.14				
φM_{ult} =	**887.52**	**kips-ft**					

φM_{ult}		≥	M_{impact}		
887.52	**kips-ft**	**≥**	**753.3**	**kips-ft**	**OK**

2.0 Guidelines for the Soil Reinforcement

2.1 Pullout of the Soil Reinforcement

$\varphi P \geq \gamma_s F_s + \gamma_d F_d$

$\varphi P \geq \gamma_s P_s A_t + \gamma_d P_d A_t$

φ=	1.00	(Resistance Factor for Pullout Analysis)
γ_s=	1.00	(Static Load Factor for Pullout Analysis)
γ_d=	1.00	(Dynamic Load Factor for Pullout Analysis)

2.1.1 Top Layer of Reinforcement

a) Computing the Pullout Resistance

P= $F^* \times \sigma_{V1} \times L \times 2b$ Note: α is equal to 1.0 and C is equal to 2.0

F^*= 1.631 (AASHTO LRFD)

σ_{V1}=	0.455	ksf
L=	10.00	ft
b=	0.1640	ft
P=	2.435	kips
ϕP=	**2.435**	**kips**

$\gamma_s F_s$ =	**γ_s**	×	**F_s**	
$\gamma_s F_s$ =	1.00	×	0.83	kips
$\gamma_s F_s$ =	0.83	kips		
$\gamma_s P_s A_t$ =	**0.83**	**kips**		

Panel Width=	4.87	ft	
Trib. Height=	1.58	ft	
P_d=	525.00	psf	(First Strip)
P_d=	410.00	psf	(Second Strip)

$\gamma_d F_d$ =	γ_s	×	F_d			
$\gamma_d F_d$ =	γ_s	×	P_d	×	A_t	
$\gamma_d P_d A_t$=	1.00	×	525.00	×	2.57	
**$\gamma_d P_d A_t$=	**1.349**	**kips**				

$\phi P \geq \gamma_s F_s + \gamma_d F_d$

ϕP		≥		$\gamma_s P_s A_t$	+	$\gamma_d P_d A_t$
2.435		≥		0.83	+	1.349
2.435	**kips**	**≥**	**2.176**	**kips**		**OK**

2.1.2 Second Layer of Reinforcement

a) Computing the Pullout Resistance

P= F^* × σ_{V1} × L × $2b$ Note: α is equal to 1.0 and Cis equal to 2.0

F^*=	1.490	(AASHTO LRFD)
σ_{V1}=	0.7625	Ksf
L=	10.00	ft
b=	0.1640	ft
P=	3.727	kips
ϕP=	**3.727**	**kips**

$\gamma_s F_s$ =	γ_s	×	F_s		
$\gamma_s F_s$ =	1.00	×	1.33	kips	
$\gamma_s F_s$ =	1.33	kips			
**$\gamma_s P_s A_t$ =	**1.332**	**kips**			

Panel Width=	4.87	ft				
Trib. Height=	2.46	ft				
$\gamma_d F_d$ =	γ_s	×	F_d			
$\gamma_d F_d$ =	γ_s	×	P_d	×	A_t	
$\gamma_d P_d A_t$=	1.00	×	410.00	×	3.99	
**$\gamma_d P_d A_t$=	**1.637**	**kips**				

$\phi P \geq \gamma_s F_s + \gamma_d F_d$

ϕP		≥		$\gamma_s P_s A_t$	+	$\gamma_d P_d A_t$
3.727		≥		1.33	+	1.637
3.73	**kips**	**≥**	**2.97**	**kips**		**OK**

2.2 Rupture of the Soil Reinforcement

$\phi R \geq \gamma_s F_s + \gamma_d F_d$

$\phi R \geq \gamma_s P_s A_t + \gamma_d P_d A_t$

φ=	1.00	(Resistance Factor for Yielding Analysis)
γ_s=	1.00	(Static Load Factor for Yielding Analysis)
γ_d=	1.00	(Dynamic Load Factor for Yielding Analysis)

2.2.1 Top Layer of Reinforcement

a) Computing the Rupture Resistance of the Strips for 75 years Service Life

E_c=	0.10	in.	(AASHTO LRFD)					
R=	σ_t	×	b	×	E_c			
R=	60.000	ksi	×	1.97	in.	×	0.10	in.
R=	12.016	kips						
ϕR=	ϕ	×	R	kips				
ϕR=	1.00	×	12.016	kips				
**ϕR=	**12.02**	**kips**						

$\gamma_s P_s A_t$ =	**0.827**	**kips**							
Panel Width=	4.87	ft							
Trib. Height=	1.58	ft							
P_d=	1790.00	psf	(First Strip)						
P_d=	475.00	psf	(Second Strip)						
$\gamma_d F_d$ =	γ_s	×	**F_d**						
$\gamma_d F_d$ =	γ_s	×	P_d	×	A_t				
$\gamma_d P_d A_t$=	1.00	×	1790.00	×	2.57				
$\gamma_d P_d A_t$=	**4.60**	**kips**							

$\varphi R \geq \gamma_s F_s + \gamma_d F_d$

φR		≥		$\gamma_s P_s A_t$	+	$\gamma_d P_d A_t$			
2.435		≥		0.83	+	4.600			
12.016	**kips**	**≥**	**5.426**	**kips**		**OK**			

a) Computing the Rupture Resistance of the Strips for 100 years Service Life

E_c=	0.08	in.		(AASHTO LRFD)					
R=	σ_t	×	b	×	E_c				
R=	60.000	ksi	×	1.97	in.	×	0.08	in.	
R=	9.226	kips							
ϕR=	ϕ	×	R	kips					
ϕR=	1.00	×	9.226	kips					
ϕR=	**9.226**	**kips**							

$\varphi R \geq \gamma_s F_s + \gamma_d F_d$

φR		≥		$\gamma_s P_s A_t$	+	$\gamma_d P_d A_t$			
2.435		≥		0.83	+	4.600			
9.226	**kips**	**≥**	**5.426**	**kips**		**OK**			

2.2.1 Second Layer of Reinforcement

a) Computing the Rupture Resistance of the Strips for 75 years Service Life

E_c=	0.10	in.	(AASHTO LRFD)						
R=	σ_t	×	b	×	E_c				
R=	60.000	ksi	×	1.97	in.	×	0.10	in.	
R=	12.016	kips							
ϕR=	ϕ	×	R	kips					
ϕR=	1.00	×	12.016	kips					
ϕR=	**12.016**	**kips**							
$\gamma_s P_s A_t$ =	**1.332**	**kips**							
Panel Width=	4.87	ft							
Trib. Height=	2.46	ft							
P_d=	1790.00	psf	(First Strip)						
P_d=	475.00	psf	(Second Strip)						
$\gamma_d F_d$ =	γ_s	×	**F_d**						
$\gamma_d F_d$ =	γ_s	×	P_d	×	A_t				
$\gamma_d P_d A_t$=	1.00	×	475.00	×	3.993				
$\gamma_d P_d A_t$=	**1.897**	**kips**							

$\varphi R \geq \gamma_s F_s + \gamma_d F_d$

φR		≥		$\gamma_s P_s A_t$	+	$\gamma_d P_d A_t$			
2.435		≥		1.33	+	1.897			
12.016	**kips**	**≥**	**3.229**	**kips**		**OK**			

a) Computing the Rupture Resistance of the Strips for 100 years Service Life

E_c=	0.08	in.	(AASHTO LRFD)						
R=	σ_t	×	b	×	E_c				
R=	60.000	ksi	×	1.97	in.	×	0.08	in.	

R=	9.226	kips			
ϕR=	ϕ	×	R	kips	
ϕR=	1.00	×	9.226	kips	
ϕR=	**9.226**	**kips**			

$\varphi R \geq \gamma_s F_s + \gamma_d F_d$

φR		≥		$\gamma_s P_s A_t$	+	$\gamma_d P_d A_t$
2.435		≥		1.33	+	1.897
9.226	**kips**	**≥**	**3.229**	**kips**		**OK**

3. Guidelines for the Wall Panel

$\varphi M_u \geq \gamma_s M_i$

3.1 Compute the Ultimate Capacity of the Wall Panel (M_u)

Data:

b=	**12.0**	in. (Unit Length)	f_y=	**60000**	psi
h=	**5.50**	in.	E_y=	**3.E+07**	psi
f'_c=	**4000.0**	psi	d=	**2.75**	in.
A_s=	**0.22**	$in.^2$			
A_c=	**66.00**	$in.^2$			

a) Checking for cracking

$M_{cr} = \frac{I_g f_r}{c_b}$

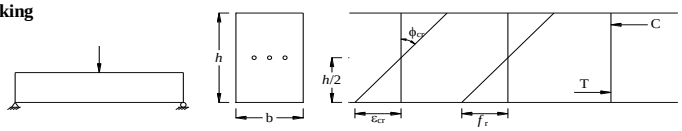

$I_g = \frac{b \times h^3}{12}$ (Moment of Inertia or Second Moment of Area)

$I_g = \frac{12.0 \times 166.375}{12}$

I_g = 166.38 $in.^4$

f_r = 7.5 × $(f'_c)^{1/2}$ (Maximun Tension Stress)

f_r = 7.5 × 63.25

f_r = 474.34 *psi*

c_b= y= 2.75 in

$M_{cr} = \frac{I_g \times f_r}{c_b}$

$M_{cr} = \frac{166.38 \times 474.34}{2.75}$

M_{cr}= 28697.67 lb-in./ft

M_{cr}= 2.391 kips-ft/ft

E_{cr} = 57000 × $(f'_c)^{1/2}$

E_{cr} = 57000 × 63.246

E_{cr} = 3604996.5 psi

E_{cr} = 3605.0 ksi

$\varepsilon_{cr} = \frac{fr}{E_{cr}}$

$\varepsilon_{cr} = \frac{474.34}{3604996.5}$

ε_{cr} = 0.000132 strain

$\phi_{cr} = \frac{\varepsilon_{cr}}{y}$

ϕ_{cr}= 4.785E-05 strain/in

ϕ_{cr}= 5.742E-04 strain/ft

b) Checking Yielding

$$M_n = A_s f_y d\left(1-\frac{k}{3}\right)$$

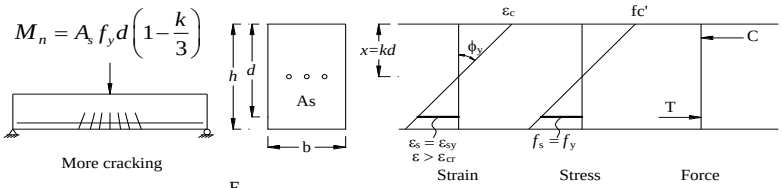

More cracking

$$\rho = \frac{A_s}{A_c} \qquad n = \frac{E_y}{E_c}$$

$\rho = \frac{0.22}{66.00}$ $\qquad n = \frac{2.9E+07}{3604997}$ psi

ρ= 0.00333 **n= 8.04**

ρ= 0.33333 %

$$k = \sqrt{(n\rho)^2 + (2n\rho)} - n\rho$$

***k*= 0.206**

$$M_n = A_s f_y d\left(1-\frac{k}{3}\right)$$

M_n = 0.22 × 60000.0 × 2.75 × 0.93123

M_n = 33803.62 lb-in/ft

M_n = 2.82 kips-ft/ft

M_y = 2.82 kips-ft/ft

$$\varepsilon_s = \frac{f_y}{E_s}$$

$\varepsilon_s = \frac{60000.00}{29000000.0}$

ε_s = 0.002069 strain

$$\phi_y = \frac{\varepsilon_s}{(d-kd)}$$

$\phi_y = \frac{2.069E-03}{2.182640}$

ϕ_y= 0.00095 **strain/in**

ϕ_y= 0.01138 strain/ft

c) Checking Ultimate Resistance

$$M_n = A_s f_y d\left(1-\frac{k}{2}\right) \qquad C = T \rightarrow 0.85 f_c' kdb = A_s f_y$$

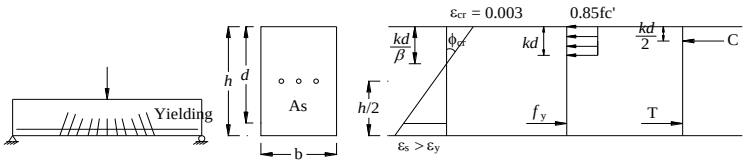

More cracking

φM_{ult} = $[A_s f_y d\ (1-k/2)]$

φM_{ult} = 34164.71 lb-in./ft

φM_{ult} = 2.8471 kips-ft/ft

$$k = \frac{A_s f_y}{0.85 f_c' bd}$$

$k = \frac{0.22}{0.85} \times \frac{60000.0}{4000.0 \times 33.0}$

***k*= 0.118**

ε_{cu}= 0.003 strain

β_1 = 0.85

$$\phi_n = \frac{\varepsilon_{cu}}{(kd/\beta_1)}$$

$\phi_n = \frac{0.003}{0.381}$

ϕ_n= 0.00788 strain/in.

ϕ_n= 0.09458 strain/ft

Cracking		Yielding		Ultimate Resist.	
M_{cr}	ϕ_{cr}	M_y	ϕ_y	M_u	ϕ_n
2.39147	**0.0006**	**2.817**	**0.0114**	**2.847**	**0.095**

φM_{ult}= 0.9 × 2.847 kips-ft/ft

φM_{ult}= 2.562 kips-ft/ft

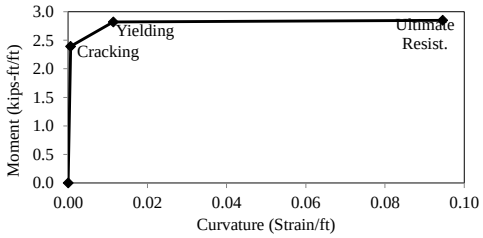

3.2 Compute the Impact Moment Produced to the Wall Panel (M_i)

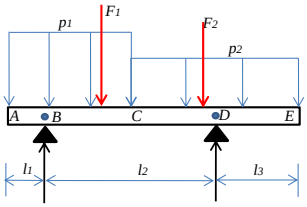

Data=

p_1=	1790.0	psf	l_1=	0.540	ft
p_2=	475.0	psf	l_2=	2.500	ft
			l_3=	1.200	ft
F_1=	3.2041	kips	R_1=	2.761	kips
F_2=	1.16375	kips	R_2=	1.607	kips

R_1= 2.761 kips R_2= 1.607 kips

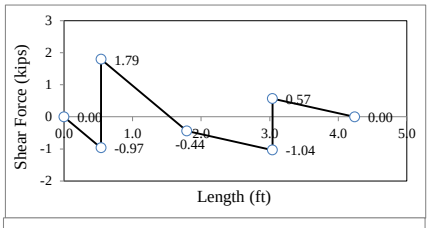

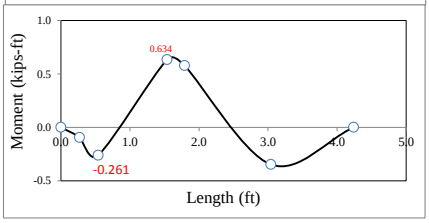

Section A-B

V_A=	0	kips	M_A=	0	kips-ft/ft
V_{B1}=	-0.9666	kips	M_{B1}=	-0.261	kips-ft/ft
V_{B2}=	1.7942	kips			

Section B-C

V_C=	-0.443	kips	M_C=	0.578	kips-ft/ft
V=	0.0	kips	x_{max}=	0.998	ft
			M_{max}=	0.634	kips-ft/ft

Section C-D

V_{D1}=	-1.037	kips	M_D=	-0.347	kips-ft/ft
V_{D2}=	0.57	kips			

Section D-E

V_E=	0.0	kips	M_E=	0.0	kips-ft/ft

M_i= 0.634 kips-ft/ft

γM_i= 1.00 × 0.634 **kips-ft/ft**

γM_i= 0.634 kips-ft/ft

(Max. Positive Moment)

φM_{ult}		**γM_i**	
2.56	**kips-ft/ft** ≥	**0.634**	**kips-ft/ft** **OK**

3.2 Checking Shearing **$1/2\phi V_{ult} \geq V_{impact}$,**

$$\phi V_{ult} = \phi 2\sqrt{f_c'} b_w d$$

ϕ = 0.90 (for shear)

V_{ult} = 2.0 × 63.2456 × 12.0 × 2.75

V_{ult} = 4174.21 lbs

V_{ult} = 4.174 kips

ϕV_{ult} = 0.90 × 4.174

ϕV_{ult} = 3.757 kips

$1/2\ \phi V_{ult}$		**V_{imp}**	
1.878	**kips/ft** ≥	**1.794**	**kips/ft** **OK**

(Max. Positive Shear)

APPENDIX C

DETAILS DRAWINGS OF THE TL-5 TEST WALL INSTALATION

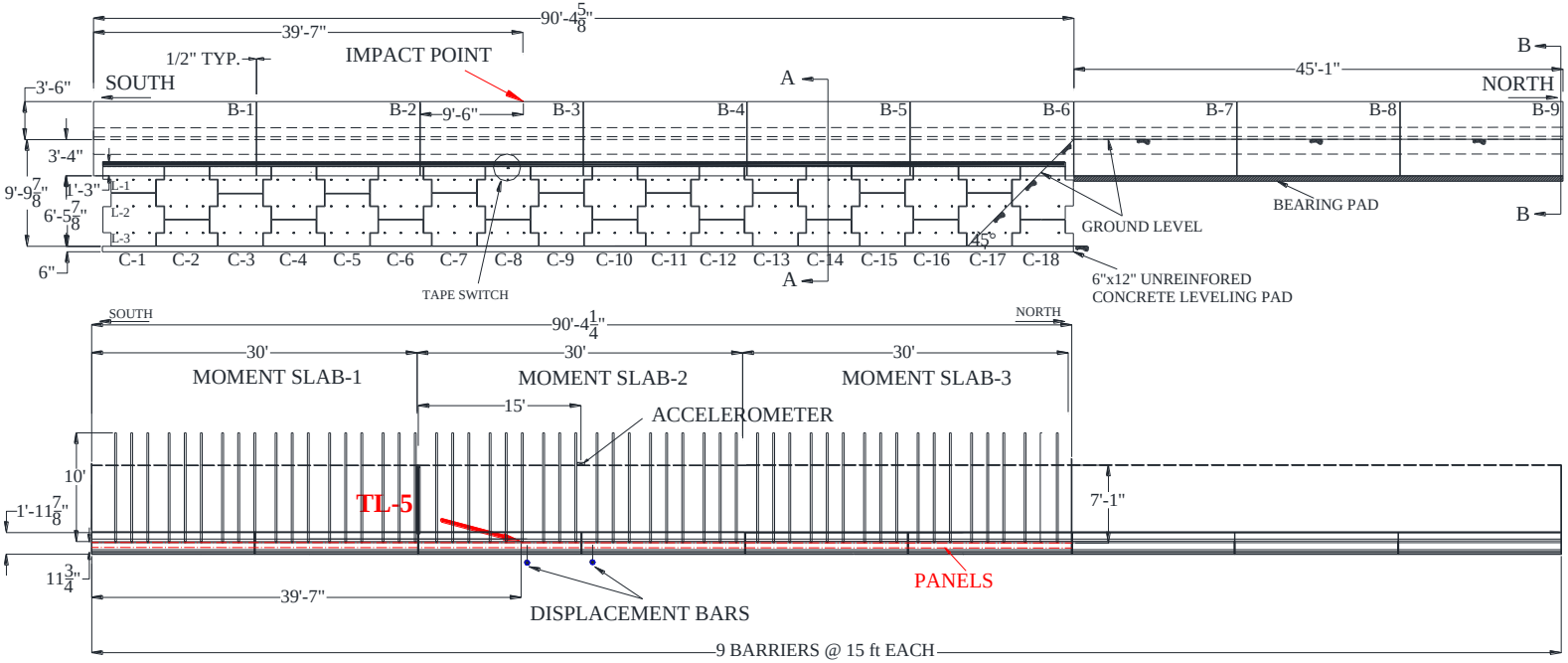

Figure C.1 Elevation view of the TL-5 full-scale test installation

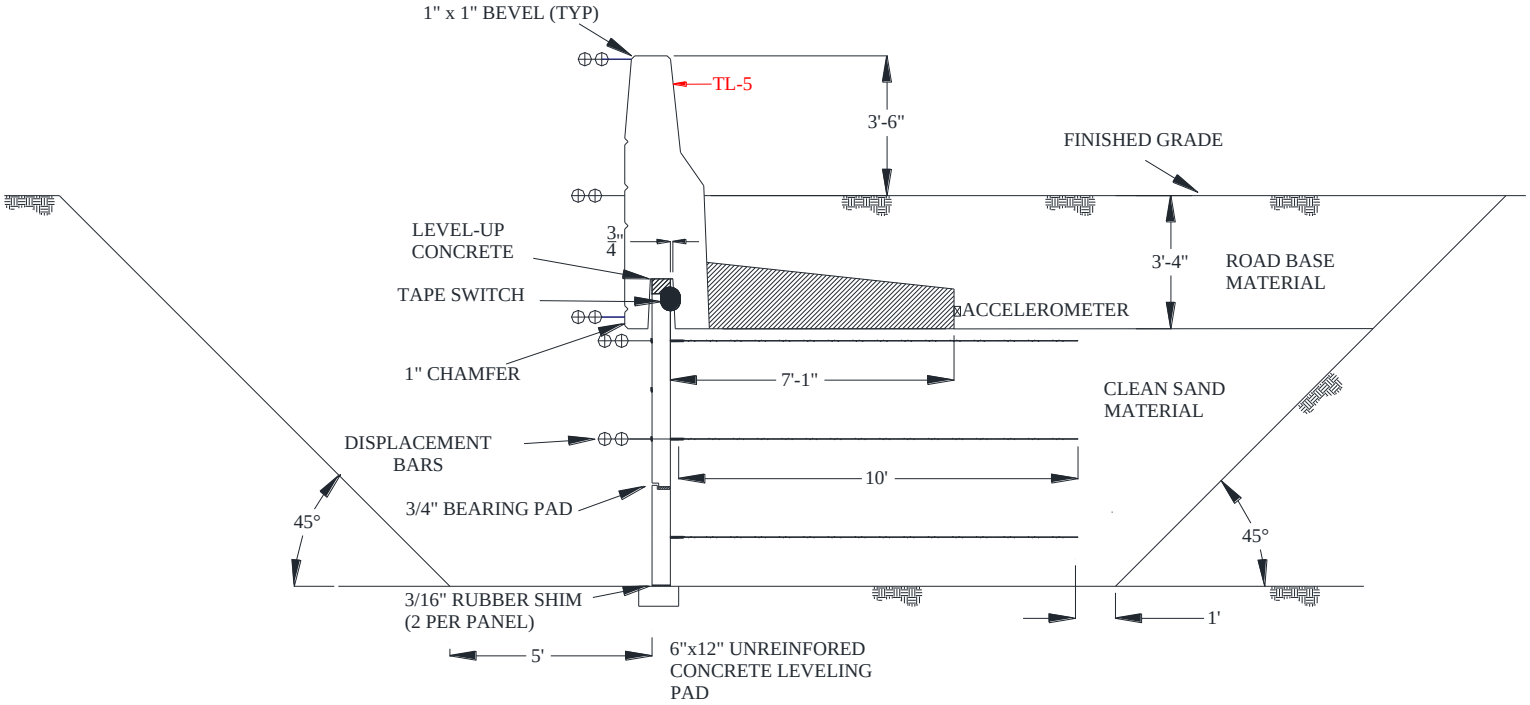

Figure C.2 Side view of the TL-5 full-scale test installation (cross section A)

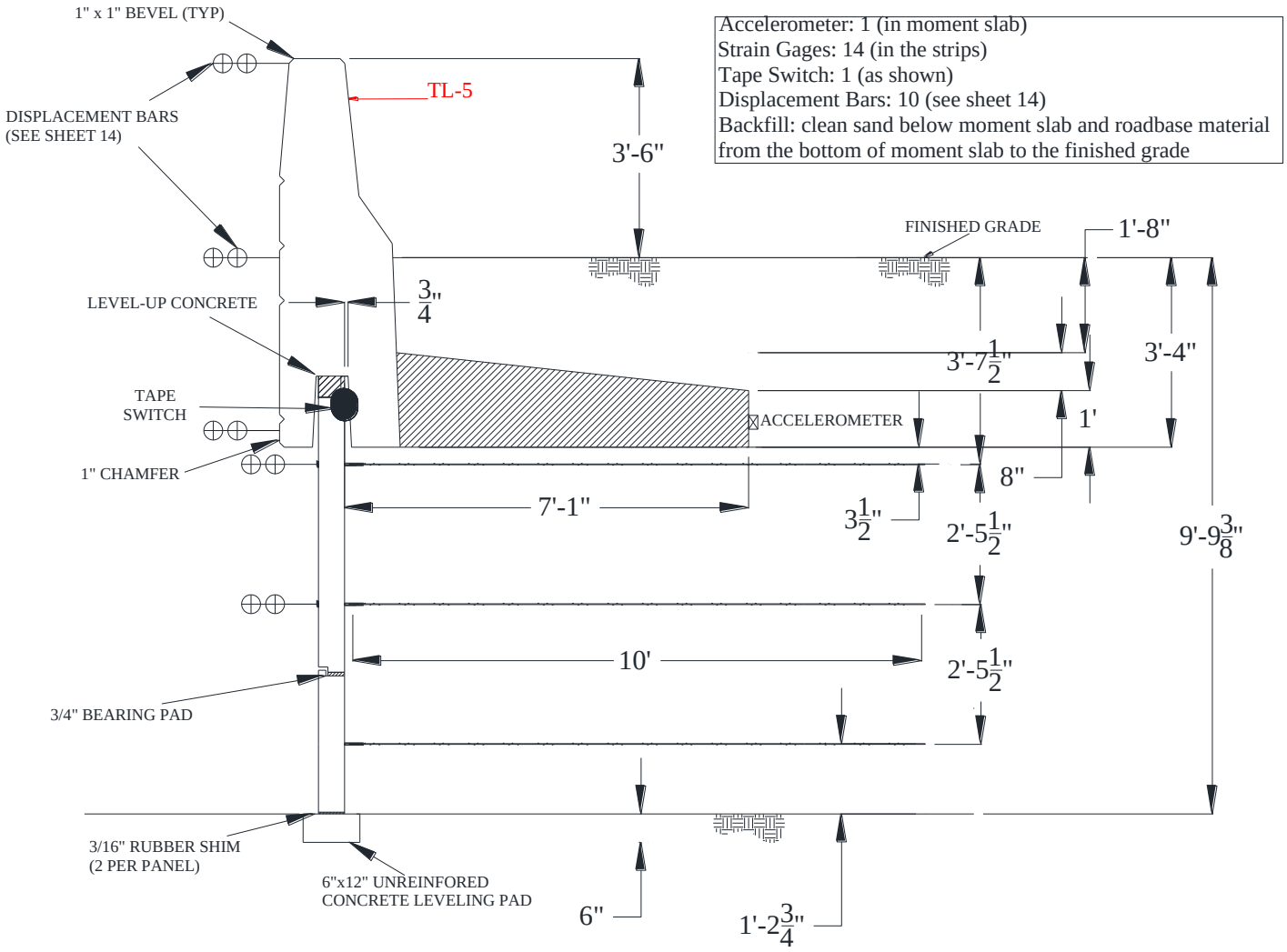

Figure C.3 Side view of the TL-5 full-scale test installation and description of the instrumentation

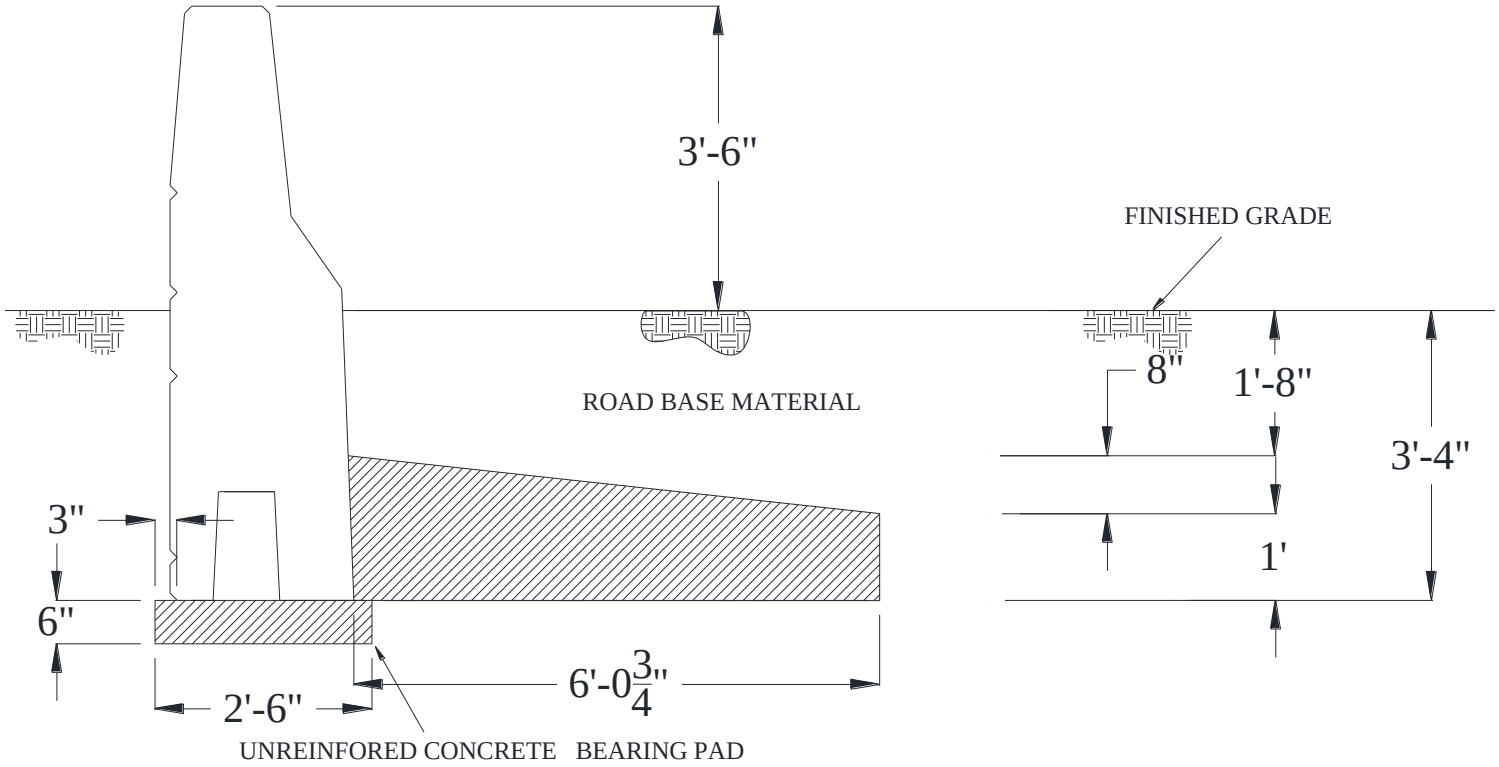

Figure C.4 Side view of the TL-5 full-scale test installation (cross section B)

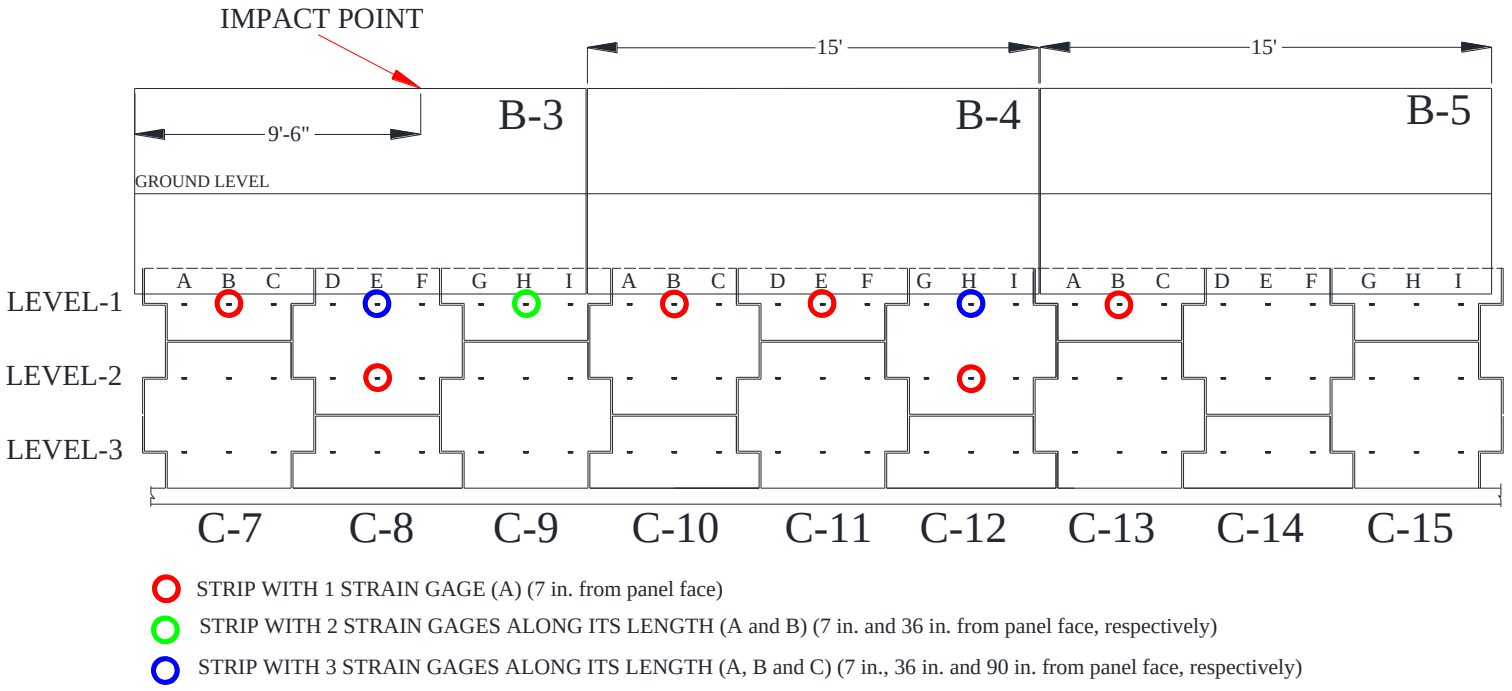

Figure C.5 Location of the strain gages in the panels

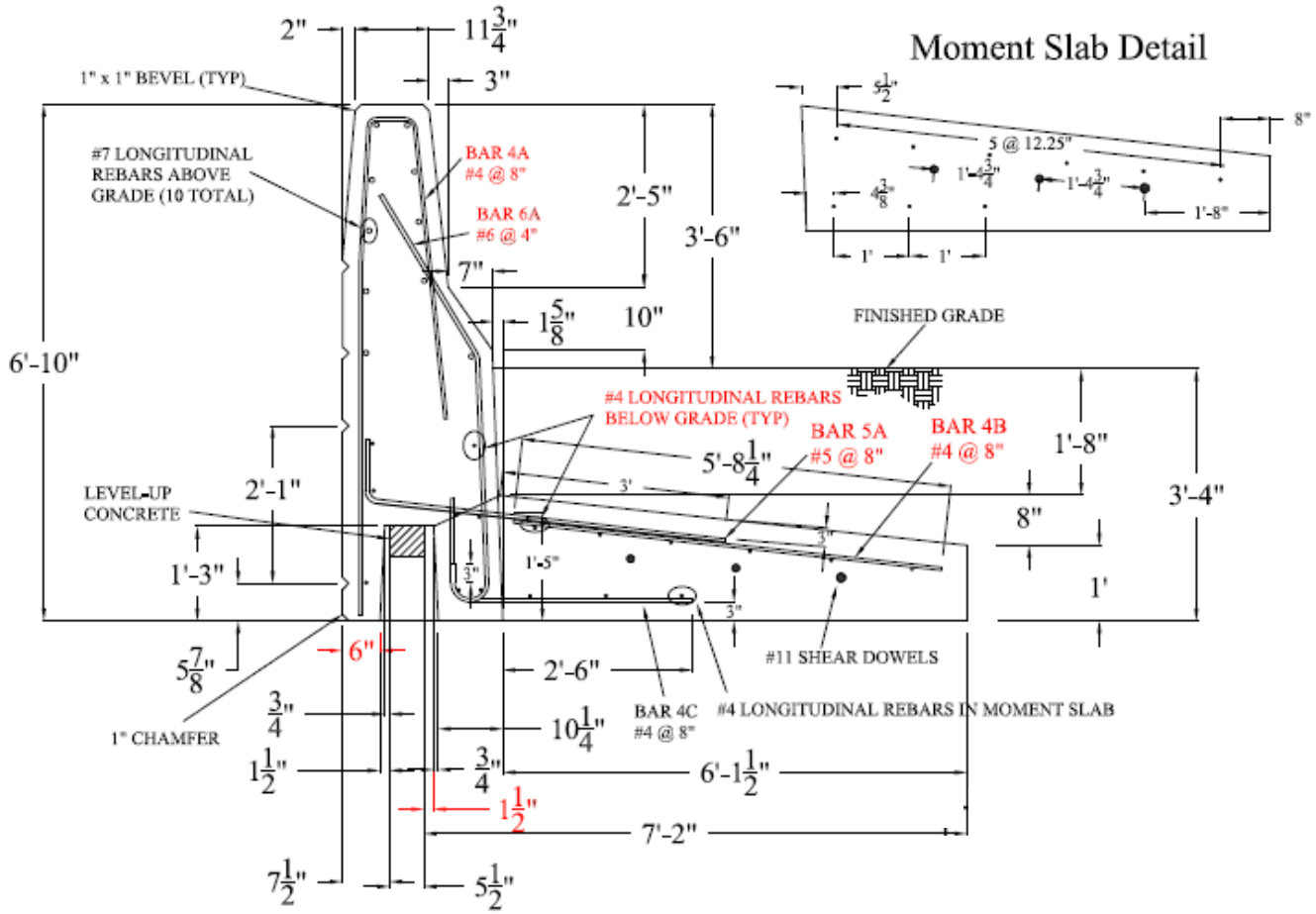

Figure C.6 TL-5 barrier-moment sab system details

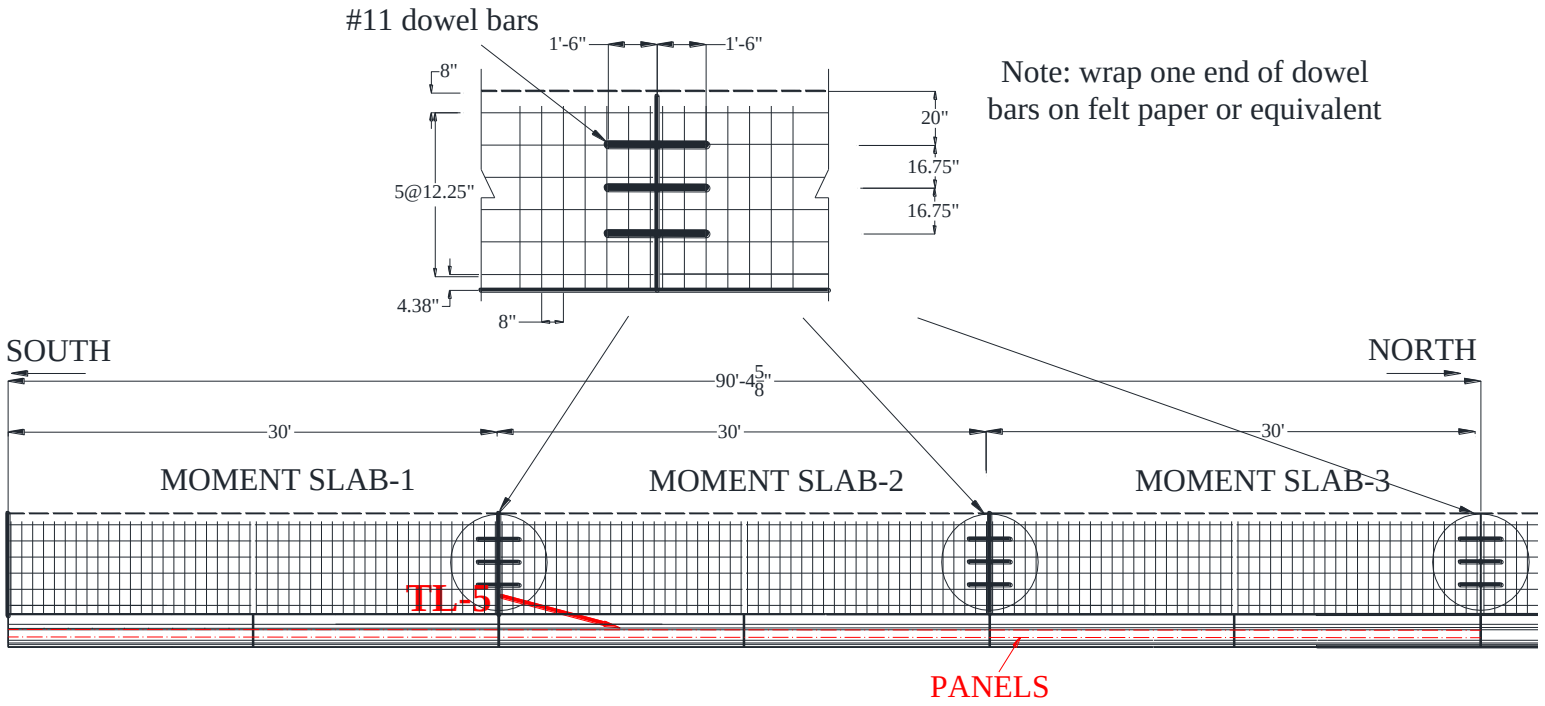

Figure C.7 Moment slab reinforcement details

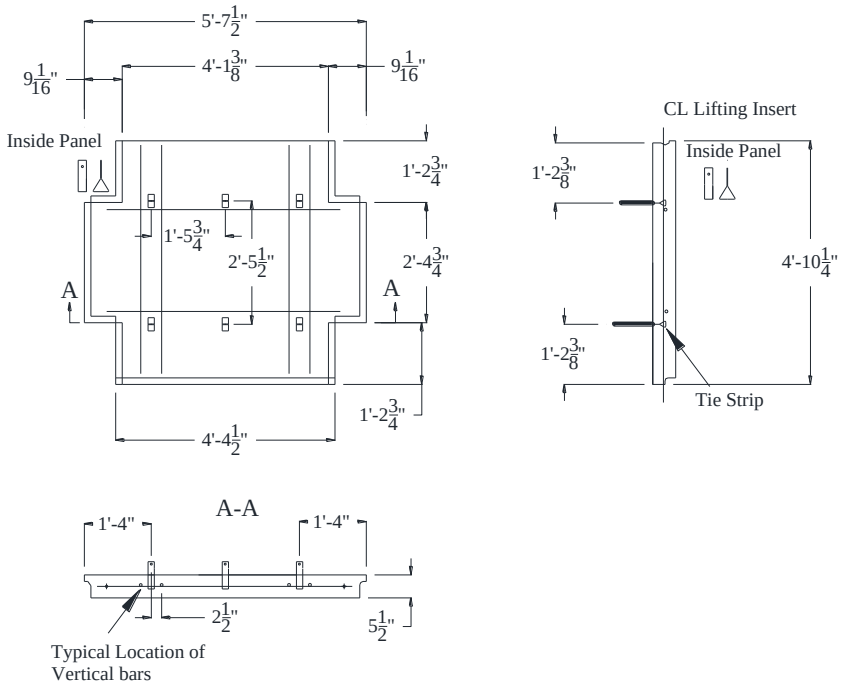

a) Typical full-panel details

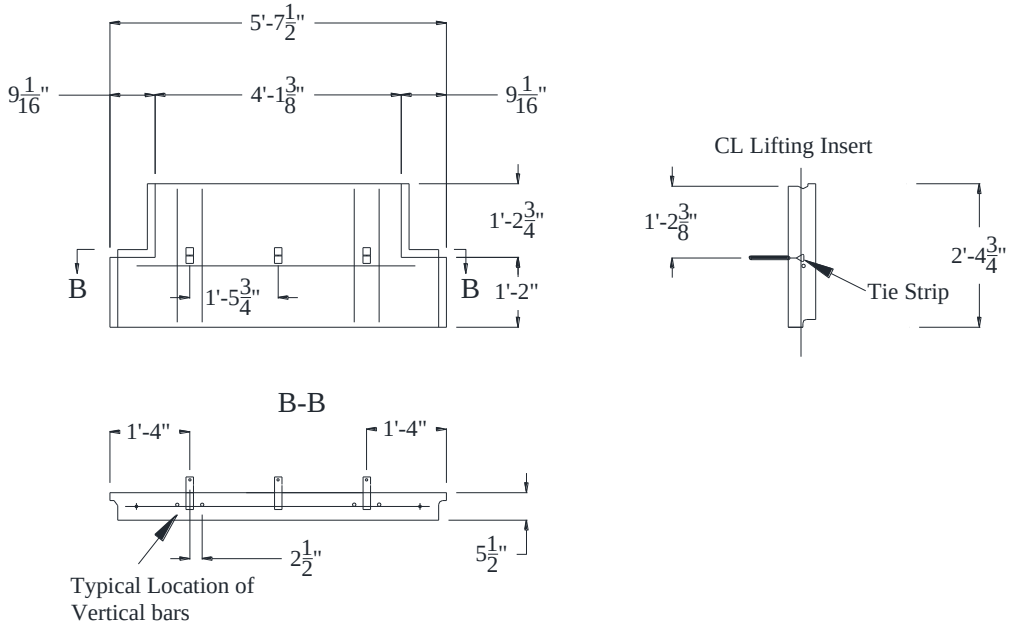

b) Typical half panel details

Figure C.8 Details of precast concrete panels

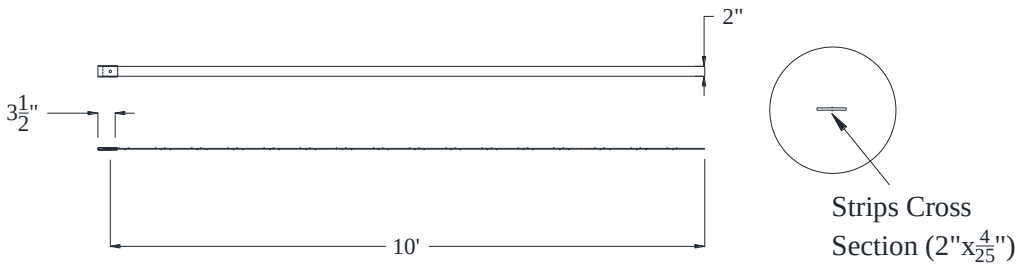

a) Typical reinforcing strip cross section

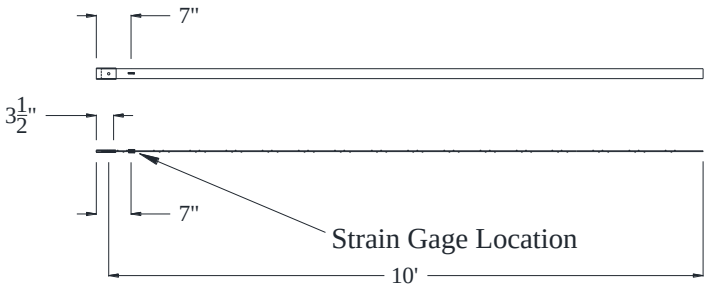

b) Strain gage location detail (SG-A)

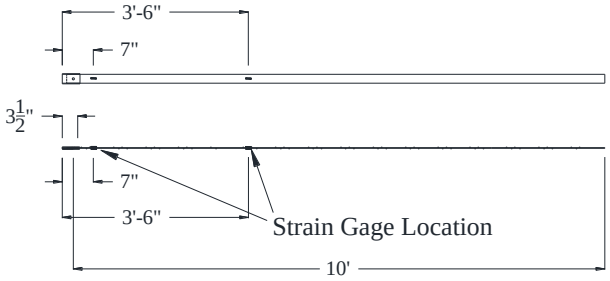

c) Strain gage location detail (SG-B)

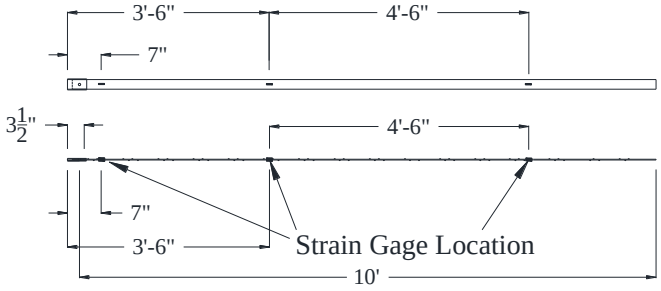

d) Strain gage location detail (SG-C)

Figure C.9 Details of reinforcing strips

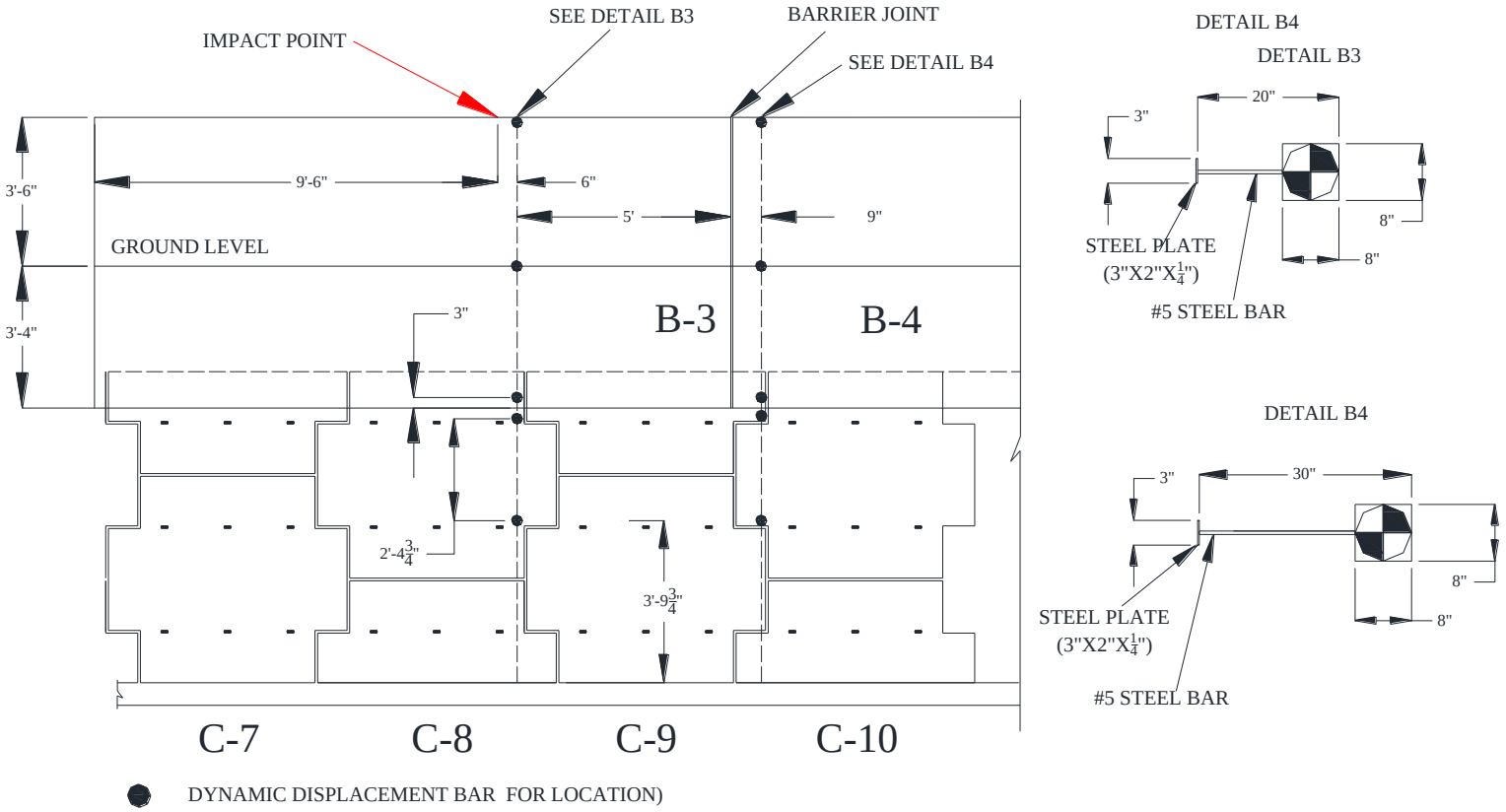

Figure C.10 Location of the dynamic displacement targets.

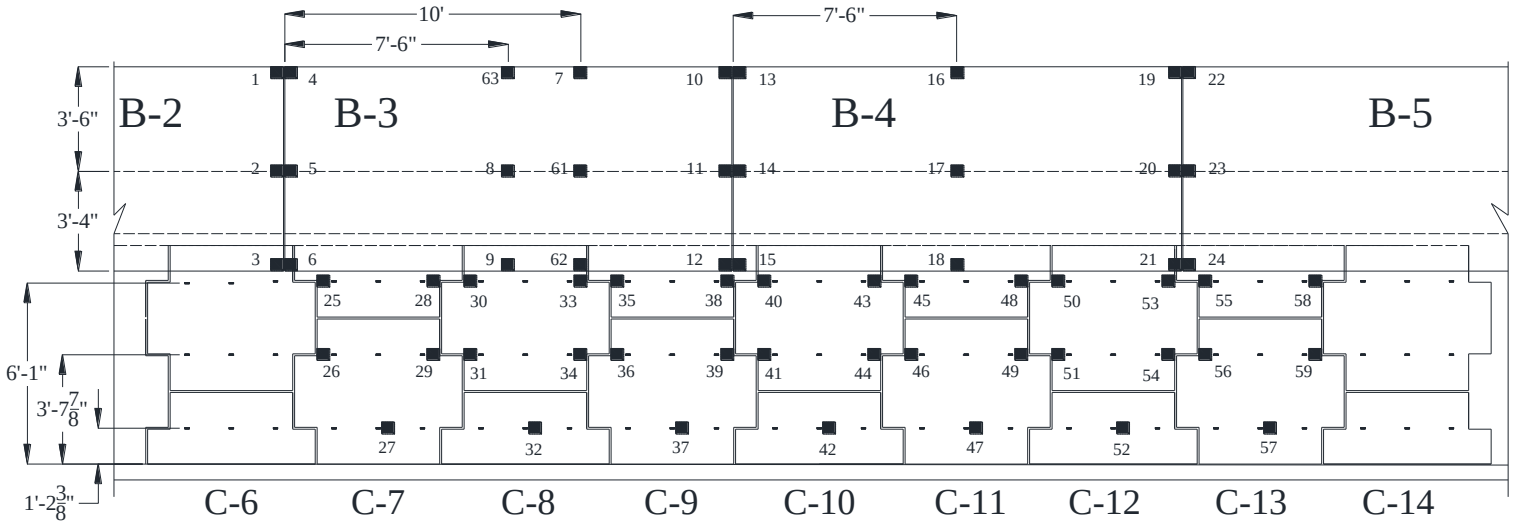

Note: ■ REFLECTIVE DISPLACEMENT TARGETS (2"x1.5") (62 IN TOTAL)
(ADHERED TO BARRIERS AND WALL PANELS)

Figure C.11 Location of the permanent displacement targets.

APPENDIX D

CONSTRUCTION SEQUENCE OF TL-5 MSE WALL TEST INSTALLATION

Sequences of pictures of the construction of the TL-5 MSE wall test installation are shown from Figure D.1 through Figure D.7. The precast concrete panels and the precast concrete barriers were fabricated and donated by RECO in conjunction with the reinforcing strips and accessories. Figure D.1 and Figure D.2 show the delivery of the precast concrete panels and the excavation process where the MSE wall test installation was built, respectively.

Figure D.1 Precast concrete panels of the TL-5 MSE wall test installation

Figure D.2 Excavation for construction of the TL-5 MSE wall test installation

Figure D.3 shows when the concrete of the leveling pedestal is being poured. The bottom wall panels are resting on the 12 in. (304.8 mm) wide × 6 in. (152.4 mm) thick concrete leveling pedestal, as shown in Figure D.4. The panels were installed with a $^{3}/_{4}$ in. (19 mm) wide vertical and horizontal joint to maximize the flexibility of the wall. Two rubber pads were positioned at the horizontal joint (typically at a quarter span points of the panels) to help maintain the vertical joint.

Figure D.3 Construction of the leveling pad where the first layer of panel will rest

Figure D.4 Installation of the bottom layer of panels

Figure D.5 shows the compaction process of the sand backfill material. The backfill was compacted in loose lifts of 6 in. (152.4 mm) to 12 in. (304 mm) thick maximum with 6 passes of a 2,176 lb. (9.7 kN), 35 in. (890 mm) wide drum roller. The maximum dry density of the backfill below the moment slab is 117.8 pcf (18.5 kN/m^3), as determined by the modified compaction Proctor test. Figure D.6 shows the filter cloths attached to each side of all joints to prevent migration of the backfill material and the bottom layer of soil reinforcement strips.

Figure D.5 Compaction of the backfill material below the bottom layer of strips

Figure D.6 Placement of the bottom layer of strips

Two nuclear density tests were conducted at the level of the bottom layer of strips (Figure D.7). The average dry density and water content were 111.7 pcf (17.5 kN/m^3) and 3%, respectively. This dry density represents 95% of the maximum dry density obtained in the modified Proctor test for the backfill material. Figure D.8 the first raw of panels braced and the preparation to place the second raw of panel.

Figure D.7 Nuclear density test to determine the in-situ dry unit weight and water content

Figure D.8 Placement of the second row of panels

Figure D.9 shows the location of the strain gages in the strips section B3_E_1st. The first, second and third strain-gage were located at 7 in. (178 mm), 36 in. (914 mm) and 8 ft (2.44 m) from the face of the wall, respectively. Figure D.10 shows the finished level of backfill material. At this stage, another nuclear density test was conducted at a distance of 39.6 ft (12.1 m) from the upstream end. The results of the test indicated that the dry density and water content were 109 pcf (17.1 kN/m^3) and 3.04%, respectively. This dry density represents 93% of the maximum dry density obtained in the modified Proctor test for the backfill material. In addition, a series of BCD tests were conducted to estimate the average BCD modules of the clean sand. The tests were conducted at a distance of 15 ft (4.57 m), 39.6 ft (12.1 m) and 75 ft (22.9 m) from the upstream end. The results of the three test were 1.94 ksi (13.4 MPa), 2.15 ksi (14.8 MPa) and 2.23 ksi (15.4 MPa), respectively.

Figure D.9 Location of strain gages in the strip

Figure D.10 Placement of the last layer of backfill material

Figure D.11 shows the un-reinforced leveling pad on top of the wall panels and the un-, reinforced pedestal where barriers 7, 8 and 9 are going to rest. Figure D.12 shows the location of the tape switch which will indicate if there is contact between the coping section of the barriers and the wall panels.

Figure D.11 Un-reinforced leveling pad and pedestal

Figure D.12 Tape switch located at the impact point

Figure D.13 shows the installation of the 15 ft (4.57 m) long precast concrete barrier. The barriers were fabricated by RECO. Figure D.14 shows the longitudinal, transverse and shear dowels at the moment slab joint. The shear dowels were wrapped in one end in order to prevent any stress due to expansion and contraction of the concrete.

Figure D.13 Installation of the TL-5 precast concrete barriers

Figure D.14 Reinforcement and shear dowels at the moment slab joint

Figure D.15 shows when the concrete of the moment slab is being poured. The final compressive strength of moment slab concrete was 4000 psi (27.5 MPa). Figure D.16 shows the placement of the road base material from the bottom of the moment slab to the finished grade.

Figure D.15 Construction of the moment slab sections

Figure D.16 Placement of road base material above the moment slab

Figure D.17 shows the compaction process of the road base material. The backfill was compacted in loose lifts of to 10 in. (254 mm) thick maximum with 6 passes of an 8 tons (8000 kg), 66 in. (1.68 m) wide drum roller. The maximum dry density of the road base material 136.7 pcf (21.5 kN/m^3), as determined by the modified compaction Proctor test. The Briaud Compaction Device (BCD) Test is shown in Figure D.18

Figure D.17 Compaction process of the road base material

Figure D.18: BCD Modulus test in the road base material

APPENDIX E

TEST VEHICLE PROPERTIES

Vehicle Properties for Test 478130.

DATE: 2012-09-26 **TEST NO.:** 478130-MSE Wall

TRACTOR
YEAR: 2000 MAKE: Sterling MODEL: TF

VIN No.: 2FWYHXYB4YAF5544 ODOMETER: 104713

TRAILER
YEAR: 1997 MAKE: STRI TRAILER MODEL: 48 ft

VIN No.: 1S12E9485VE422459

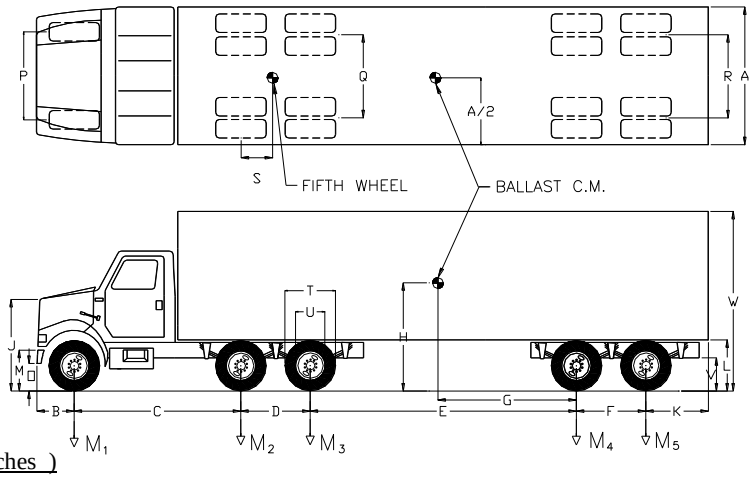

GEOMETRY (inches)

A	102	D	52	G	-	K	47.5	N	-	Q	74	U	23
B	48	E	417	H	73	L	48.5	O	23.5	R	77.5	V	32
C	157	F	48	J	71.5	M	35.5	P	82.5	T	40	W	159.5

Allowable Range: C = 200 inches max.; L = 52 ±2 inches; Overall Trailer Length = 600 inches max.; Overall Combination Length = 780 inches max.; Trailer Overhang = 87 inches max.; Ballast Center of Mass H_t = 73 ±2 inches above ground;

MASS (lb)	CURB		TEST INERTIAL	
M_1	9400		9960	
M_2	5770		15150	
M_3	5750		16860	
M_4	4700		16880	
M_5	4180	Allowable Range	20380	Allowable Range
M_{Total}	29800	29,000 ±3100 lb.	79230	79,300 ±1100 lb.

APPENDIX F

AASHTO LRFD FORMAT DESIGN GUIDELINE

Note: The format presented in this section follows Appendix I of the NCHRP Report 663, "Design of Roadside Barrier System Placed on MSE Retaining Walls" and the AASHTO LRFD format. The information contained herein apply for TL-3 through TL-5 impact.

SECTION 1

DESIGN GUIDELINES

1.1 SCOPE

This section provides guidelines to design three components: the barrier-moment slab, the MSE wall reinforcement, and the wall panel.

The guidelines are applicable for TL-3 through TL-5 criteria as defined in Section 13 of AASHTO LRFD *Bridge Design Specifications*, and for inextensible MSE wall reinforcement (e.g., strips, bar mats)

Depending on the design, two points of rotation are possible as shown in Figure 1.1-1. The point of rotation should be determined based on the interaction between the barrier coping and top of the wall panel. With reference to Figure 1.1-1, the point of rotation should be taken as Point A if the top of the wall panel is isolated from contact with the coping by the presence of an air gap or a sufficiently compressible material. The point of rotation should be taken as Point B if there is direct bearing between the bottom of the coping and the top of the wall panel or level up concrete.

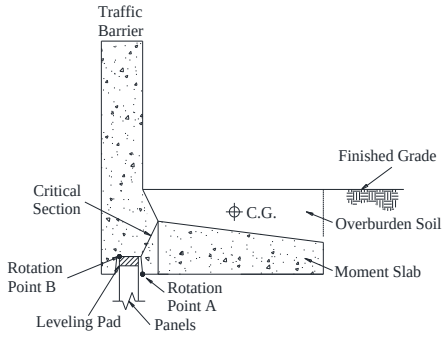

Figure 1.1-1 Barrier-moment slab system for design guideline.

1.2 DEFINITIONS

Rotation Point A—The rotation point of a barrier-moment slab system if the top of the wall panel is isolated from contact with the coping by the presence of an air gap or a sufficiently compressible material as shown in Figure 1.1-1.

Rotation Point B—The rotation point of a barrier-moment slab system if there is direct bearing between the bottom of the coping and the top of the wall panel or level up concrete as shown in Figure 1.1-1.

1.3 NOTATION

TL5-1 = refers to test level 5, as defined in AASHTO LRFD *Bridge Design Specifications*, with a barrier height of 42 in.
TL5-2 = refers to test level 5, as defined in AASHTO LRFD *Bridge Design Specifications*, with a barrier height greater than 42 in.
H = height of the barrier measured from the finished grade (in.)
h_a = moment arm taken as the vertical distance between the point of impact of the dynamic force and the point of rotation A (ft)
h_b = moment arm taken as the vertical distance between the point of impact of the dynamic force and the point of rotation B (ft)
h_1 = tributary height of the first layer of the soil reinforcements (ft)
h_2 = tributary height of the second layer of the soil reinforcements (ft)
h_c = moment arm taken as the vertical distance between the point of impact of the dynamic force and the middle of the weakest section of the coping (ft)
L_d = dynamic load (kips)
F_t = impact load in the lateral direction of the barrier (kips)
F_L = impact load in the longitudinal direction of the barrier (kips)
F_v = impact load in the longitudinal vertical of the barrier (kips)
L_L = longitudinal distribution of the impact load in the lateral direction (ft)
L_v = vertical distribution of the impact load in the lateral direction (ft)
L_s = static load equivalent to the dynamic impact force (kips)
l_A = horizontal distance from the center of gravity of the weight to the point of rotation A (ft).
l_B = horizontal distance from the center of gravity of the weight to the point of rotation B (ft).
M = static moment resistance to overturning of the barrier-moment slab system (kips-ft)
F_s = static resistance to sliding of the barrier-moment slab system (kips)
P = static resistance to pullout of the reinforcement (kips)
p_{d-1} = dynamic pressure diagram for pullout or yielding of the first layer of soil reinforcement (psf)
p_{d-2} = dynamic pressure diagram for pullout or yielding of the second layer of soil reinforcement (psf)
Q_{d-1} = dynamic line load diagram for pullout or yielding of the first layer of soil reinforcement (lb/ft)
Q_{d-2} = dynamic line load diagram for pullout or yielding of the first layer of soil reinforcement (lb/ft)
R = resistance for yielding of the reinforcement (kips)
W = weight of the monolithic section of barrier and moment slab per unit length plus any material laying on top of the moment slab (kips/ft)
γ = load factors
ϕ = resistance factors
ϕ_r = friction angle of the soil – moment slab interface (°)
ϕ_s = friction angle of the soil (°)
σ_v = vertical soil stress (ksf)

1.4 GUIDELINES FOR THE BARRIER

1.4.1 General

The barrier, the coping, and moment slab should be safe against structural failure. Any section along the coping and moment slab should not fail in bending when the barrier is subjected to the design impact load. Two modes of stability failure are possible in addition to structural failure of the barrier system. They are sliding and overturning of the barrier-moment slab system.

The equivalent static load defined in this section should be used for sizing the moment slab. The design for structural capacity of the barrier, coping, and moment slab should be designed to contain the impact load defined in Table 1.4.1 and follow the design recommended procedure described in Section 13 of the AASHTO LRFD *Bridge Design Specification*.

Width of moment slabs should range between 4.5 ft to 10 ft. Length of moment slabs should range between 20 ft to 60 ft with steel shear dowels across the joints. Dimensions outside these ranges can be used provided it is shown that sufficiently rigid body behavior is achieved.

C1.4.1

Much of the knowledge and experience with MSE structures and traffic barriers have been with design as specified in Section 11 and Section 13 *AASHTO LRFD Bridge Design Specifications*.

In these recommendations it is assumed that a barrier-moment slab design would generate 1 in. permanent movement or less at the coping section of the system. This 1 inch movement is considered acceptable as it would likely require little or no repair and should not affect the impact performance of the barrier system.

1.4.2 Sliding of the Barrier

C1.4.2

The factored static resistance (ϕP) to sliding of the barrier-moment slab system along its base should satisfy the following condition (Figure 1.4.2-1):

$$\phi P \geq \gamma L_s \qquad (1.4.2\text{-}1)$$

L_s = equivalent static load per unit length (Table 1.4.2-1)

ϕ = resistance factor (0.8) (*AASHTO LRFD Bridge Design Specifications* Table 10.5.5-1)

γ = load factor (1.0) [extreme event]

P = static resistance per unit length (kips/ft)

The static force P should be satisfy the following condition:

$$P = W \tan \phi_r \qquad (1.4.2\text{-}2)$$

where:

W = weight of the monolithic section per unit length of barrier and moment slab between joints plus any material laying on top of the moment slab

ϕ_r = friction angle of the soil–moment slab

If the soil – moment slab interface is rough (e.g. cast in place), ϕ_r is equal to the friction angle of the soil ϕ_s. If the soil – moment slab interface is smooth (e.g. precast), ϕ_r should be reduced accordingly $\left(\frac{2}{3}\tan\phi_s\right)$.

interface(°)

Table 1.4.2-2 Equivalent static loads for moment slab design

Test Designation	TL-3	TL-4	TL-5-1	TL-5-2
Rail Height, H (in.)	27	≥36	42	>42
L_s (kips/ft)	0.8	0.8	2.0	2.7
H_e (in.)	24	30	34	43

The equivalent static loads presented in Table 1.4.2-2 are defined with reference to rotation point B.

1.4.3 Overturning of the Barrier

C1.4.3

The factored static moment resistance (ϕM) of the barrier-moment slab system to overturning should satisfy the following condition (Figure 1.4.4-1):

$$\phi M \geq \gamma L_s (h_A \text{ or } h_B) \qquad (1.4.3\text{-}1)$$

where:

L_s = equivalent static load per unit length (Table 1.4.2-1)

ϕ = resistance factor (0.9)

γ = load factor (1.0) [extreme event]

h = moment arm taken as the vertical distance from the point of impact due to the dynamic force to the point of rotation A

h_b = moment arm taken as the vertical distance from the point of impact due to the dynamic force to the point of rotation B

M = static moment resistance per unit length (kips-ft/ft)

M should be calculated as:

$$M = W (l_A \text{ or } l_B) \qquad (1.4.3\text{-}2)$$

where:

W = weight of the monolithic section per unit length of barrier and moment slab plus any material laying on top of the moment slab

l_A = horizontal distance from the center of gravity of the weight W to the point of rotation A

The moment contribution due to any coupling between adjacent moment slabs, shear strength of the overburden soil, or friction which may exist between the backside of the moment slab and the surrounding soil should be neglected.

l_B = horizontal distance from the center of gravity of the weight W to the point of rotation B

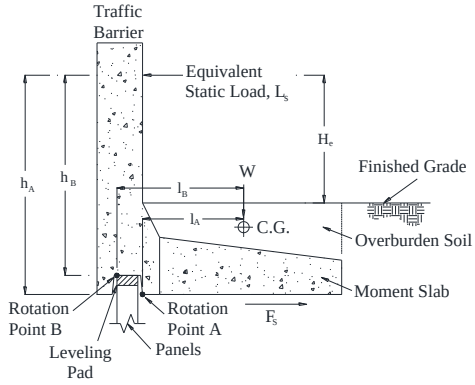

Figure 1.4.4-1 Barrier-moment slab system for barrier design guideline (sliding and overturning).

1.4.4 Design of the Coping

The critical section of the coping must be designed to resist the applicable impact load conditions for the appropriate test level as defined in Table 1.4.4-1 (Figure 1.4.4-1).

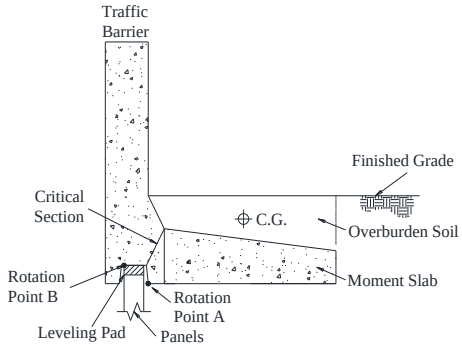

Figure 1.4.4-1 Coping and possible critical section.

Table 1.4.4-1 Dynamic loads for barrier design

Design Forces and Designations	TL-3	TL-4	TL-5-1	TL-5-2
Rail Height, H (in.)	27	≥36	42	>42
F_t Transverse (kips)	54	80	160	260
F_L Longitudinal (kips)	18	27	75	75
F_v Vertical (kips)	4.5	38	160	80
L_L (ft)	4	4	10	10
L_v (ft)	18	18	40	40
H_e (in.)	24	30	34	43

1.5 GUIDELINES FOR THE SOIL REINFORCEMENT

1.5.1 General

The reinforcement guidelines should ensure that the reinforcement does not pullout or break during the impact of the chosen vehicle.

C1.5.1

In this section, the recommendations for the load in the reinforcement due to the impact are based on a pressure diagram and line load diagram back calculated by using the design loads in excess of static earth pressure loads recorded in the tests.

The design load for pull out is different from the design load for yielding. The reason is that the design load for pullout is an equivalent static load while the design load for yielding is a measured dynamic load.

1.5.2 Pullout of the Soil Reinforcement

1.5.2.1 Pressure distribution approach

C1.5.2.1

The factored ultimate static resistance (ϕ P) to pullout of the reinforcement should satisfy the following condition:

$$\phi P \geq \gamma_s p_s A_t + \gamma_d p_d A_t \qquad (1.5.2.1\text{-}1)$$

where,

ϕ = resistance factor (1.0)

γ_s = load factor for static load (1.0)

p_s = static earth pressure

A_t = the tributary area of the reinforcement unit

p_d = dynamic pressure distribution to pullout of the reinforcement (Table 1.5.2.1-1 and Figure 1.5.2.1-1)

γ_d = load factor for dynamic load (1.0)

The reinforcement resistance P should be calculated by the equation shown in AASHTO 11.10.6.3.2-1.

The traffic surcharge should not be added as it is already include in the measured load during the experiments.

Table 1.5.2.1-1 Pressure, line load distribution and tributary height for reinforcement pullout

Test Designation	First Layer			Second Layer		
	p_{d-1} (psf)	h_1 (ft)	Q_{d-1} (lb./ft)	p_{d-2} (psf)	h_2 (ft)	Q_{d-2} (lb./ft)
TL-3	315	1.8	575	230	2.5	575
TL-4	470	1.8	850	260	2.5	650
TL-5-1	625	1.6	1000	500	2.5	1250
TL-5-2	810	1.6	1300	500	2.5	1250

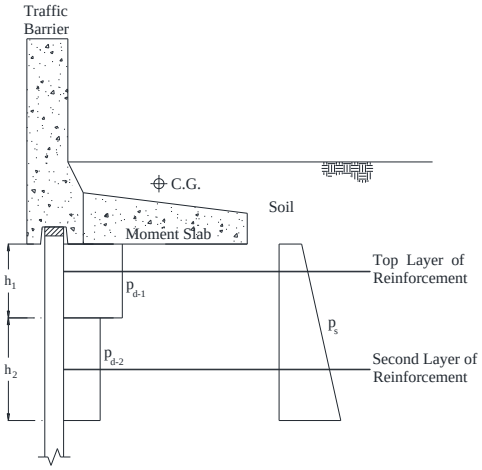

Figure 1.5.2.1-1 Pressure distribution p_d for reinforcement pullout.

1.5.2.2 Line load approach

C1.5.2.2

The reinforcement resistance P should be calculated by the equation shown in AASHTO 11.10.6.3.2-1.

The factored static resistance (ϕP) to pullout of the reinforcement should satisfy the following condition:

$$\phi P \geq \gamma_s p_s A_t + \gamma_d Q_d S_L \qquad (1.5.2.2\text{-}1)$$

where,

ϕ = resistance factor (1.0)

γ_s = load factor for static load (1.0)

p_s = static earth pressure

A_t = the tributary area of the reinforcement unit

γ_d = load factor for dynamic load (1.0)

Q_d = dynamic line load to pullout of the reinforcement (Table 1.5.2.1-1 and Figure 1.5.2.2-1)

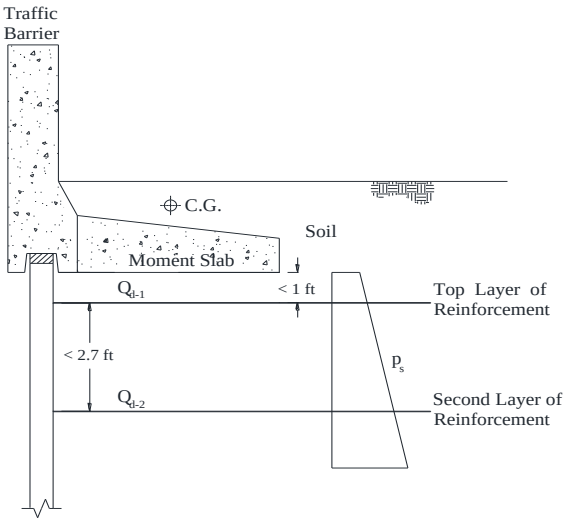

Figure 15.2.2.-1 Line load p_d for reinforcement pullout.

1.5.3 Yielding of the Soil Reinforcement

1.5.3.1 Pressure distribution approach

The factored resistance (ϕR) to yielding of the reinforcement should satisfy the following condition :

$$\phi R \geq \gamma_s p_s A_t + \gamma_d p_d A_t \qquad (1.5.3.1\text{-}1)$$

where,

ϕ = resistance factor (1.0)

γ_s = load factor for static load (1.0)

p_s = static earth pressure

A_t = the tributary area of the reinforcement unit

p_d = dynamic pressure distribution to yielding of the reinforcement (Table 1.5.3.1-1 and Figure 1.5.3.1-1)

γ_d = load factor for dynamic load (1.0)

C1.5.3

In this section, the recommendations for the load in the reinforcement due to the impact are based on a pressure diagram and line load diagram back calculated by using the design loads in excess of static earth pressure loads recorded in the tests.

C1.5.3.1

The factored resistance ϕR to yielding of the reinforcement is specified in Article 11.10.6.4.

The cross section of the reinforcement can be subject to corrosion in the long term, depending on the expected time of burial and the composition of the soil, sand, or aggregate. (AASHTO LRFD 11.10.6.4.2).

Table 1.5.3.1-1 Pressure, line load distribution and tributary height for reinforcement yielding

Test Designation	First Layer			Second Layer		
	p_{d-1} (psf)	h_1 (ft)	Q_{d-1} (lb./ft)	p_{d-2} (psf)	h_2 (ft)	Q_{d-2} (lb./ft)
TL-3	1200	1.8	2160	230	2.5	575
TL-4	1450	1.8	2610	260	2.5	650
TL-5-1	1790	1.6	2860	500	2.5	1250
TL-5-2	2410	1.6	3860	500	2.5	1250

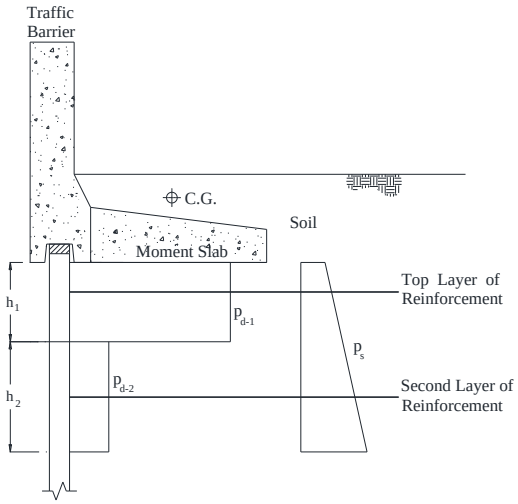

Figure 1.5.3.1-1 Pressure diagram p_d for reinforcement yielding.

1.5.3.2 Line load approach

The factored resistance (ϕR) to yielding of the reinforcement should satisfy the following condition:

$$\phi R \geq \gamma_s p_s A_t + \gamma_d Q_d S_L \qquad (1.5.3.2\text{-}1)$$

where,

ϕ = resistance factor (1.0)

γ_s = load factor for static load (1.0)

p_s = static earth pressure

A_t = the tributary area of the reinforcement unit

C1.5.3.2

The resistance ϕR to yielding of the reinforcement should be calculated by the equation shown in Article 11.10.6.4.

The cross section of the reinforcement can be subject to corrosion in the long term, depending on the expected time of burial and the composition of the soil, sand, or aggregate. (AASHTO LRFD 11.10.6.4.2).

γ_d = load factor for dynamic load (1.0)

Q_d = dynamic line load to yielding of the reinforcement (Table 1.5.3.1-1 and Figure 1.5.3.2-1)

S_L = longitudinal spacing of the reinforcement unit

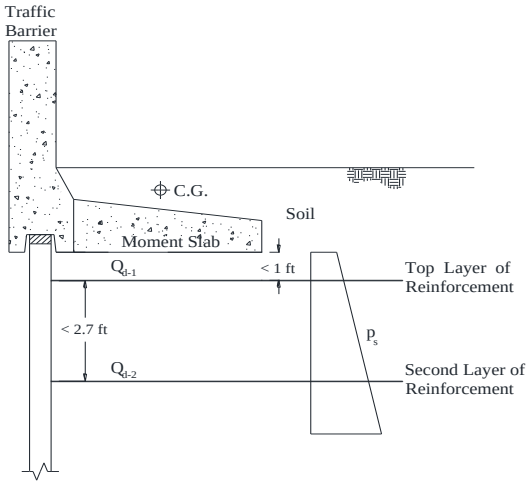

Figure 1.5.3.2-1 Line load Q_d for reinforcement yielding.

1.6 GUIDELINES FOR THE WALL PANEL

The wall panels must be designed to resist the dynamic pressure distributions defined in Table 1.5.3.1-1, Section 1.5.3.1.

The wall panel should have sufficient structural capacity to resist the maximum design yielding load for the wall reinforcement.

The static load is not included because it is not located at panel connection.